United States
Environmental
Protection
Agency

Office of Air Quality
Planning and Standards
Research Triangle Park, NC 27711

EPA-450/4-90-006B
APRIL 1990

AIR

EPA

URBAN AIRSHED MODEL STUDY OF FIVE CITIES

Demonstration of Low-Cost Application of the Model to the City of Atlanta and the Dallas-Fort Worth Metroplex Region

EPA-450/4-90-006B

URBAN AIRSHED MODEL STUDY OF FIVE CITIES

Demonstration of Low-Cost Application of the Model to the City of Atlanta and the Dallas-Fort Worth Metroplex Region

By

Ralph E. Morris
Thomas C. Myers
Edward L. Carr
Marianne C. Causley

Systems Applications, Inc.
101 Lucas Valley Road
San Rafael, CA 94903

EPA Project Officers:

Richard D. Scheffe, Office of Air Quality Planning and Standards
John C. Chamberlin, Office of Policy Planning and Evaluation

OFFICE OF AIR QUALITY PLANNING AND STANDARDS

U. S. ENVIRONMENTAL PROTECTION AGENCY

RESEARCH TRIANGLE PARK, NC 27711

APRIL 1990

Disclaimer

This material has been funded wholly or in part by the United States Environmental Protection Agency. It has been subject to the agency's review, and it has been approved for publication as an EPA document. Mention of trade names or commercial products does not constitute endorsement or recommendation for use.

Contents

List of Figures iv

List of Tables vii

1 INTRODUCTION 1

Use of the Urban Airshed Model 1

The "Five Cities" UAM Study 2

2 PLANR PROCEDURES FOR PREPARING UAM INPUTS 4

Episode Selection 6

Data Assessment and Meteorological Characterization 7

Preparation of UAM Input Files 7

Diagnostic Simulations to Define the Base Case 21

3 APPLICATION OF THE UAM TO THE CITY OF ATLANTA 25

Episode Selection 25

Meteorological Characterization 27

Modeling Domain Definition 28

Routine Data Available for Atlanta 28

Preparation of UAM Input Files 32

Definition of Base Case 43

4 APPLICATION OF THE UAM TO THE DALLAS-FORT WORTH MEXTROPLEX AREA 56

Episode Selection 56

Meteorological Characterization 57

Modeling Domain Definition 68

Routine Data Available for Dallas-Fort Worth 68

Emissions Preparation 71

Preparation of UAM Input Files 74

Tracer Simulation 95

Evaluation Simulations 96

5 SUMMARY AND CONCLUSIONS 174

Twice-Daily Upper-Air Soundings 174

Surface Wind Speeds 176

Air Quality Data 177

Emissions 177

Conclusions 179

References 180

Appendix A: Percent Contribution of Initial Concentrations, Boundary Conditions (Four Lateral Faces Plus Top Boundary) Anthropogenic Area Source Emissions, Point Source Emissions, and Biogenic Emissions to Hourly Tracer, NO_x, and VOC Concentrations for Atlanta on 4 June 1984

Appendix B: Hourly Predicted Ozone Concentrations for Atlanta Diagnostic Run 1

Appendix C: Hourly Predicted Ozone Concentrations for Atlanta Diagnostic Run 2

Appendix D: Sensitivity Analysis of the Calculations of Ozone Concentrations to Wind Speed Specification

Appendix E: Memorandum of 10 May 1989 on the Selection of a UAM Modeilng Episode for the Dallas-Fort Worth Metroplex Area

Appendix F: Initial Condition Tracer Simulation for Dallas-Fort Worth

Appendix G: Predicted Hourly Ozone Concentrations for Dallas-Fort Worth Diagnostic Run 1

Appendix H: Predicted Hourly Ozone Concentrations for Dallas Fort Worth Diagnostic Run 2

Figures

2-1 PLANR procedures for applying UAM 5

2-2 Flow diagram for creating the UAM CHEMPARAM input file 10

2-3 Flow diagram for creating the UAM TERRAIN input file 12

2-4 Flow diagram for creating the UAM DIFFBREAK and REGIONTOP input files 13

2-5 Flow diagram for creating the UAM METSCALARS input files 15

2-6 Flow diagram for creating the UAM TEMPERATUR input file 18

2-7 Flow diagram for creating the UAM WIND input files 19

2-8 Flow diagram for creating the UAM 1985 base case low-level emissions (EMISSIONS) and elevated emissions (PTSOURCE) files 22

3-1 UAM modeling domain for Atlanta 29

3-2 Emissions for the Atlanta 1984 base case 37

3-3 Observed and predicted ozone concentrations for the Atlanta diagnostic run 1 45

3-4 Observed and predicted ozone concentrations for the Atlanta evaluation run 2 48

3-5 Observed and nearest-neighbor predicted ozone concentrations for the Atlanta diagnostic run 2 49

3-6 Observed and nearest-neighbor predicted ozone concentrations for the Atlanta diagnostic run 2 50

3-7 Scatterplot residual analysis and model performance statistics for predicted and observed hourly ozone concentrations for the Atlanta diagnostic run 2 51

4-1 Constant pressure heights on 30 August 1985 58

89104n1.1

4-2 Constant pressure heights at 0600 on 31 August 1985 60

4-3 Constant pressure heights at 1800 on 31 August 1985 62

4-4 Observed daily maximum ozone concentrations in the Dallas-Fort Worth area 64

4-5 Locations of upper-air meteorological observation sites and UAM modeling domain for the Dallas-Fort Worth metroplex area 69

4-6 Estimated diurnal emissions of monoterpenes and isoprene in Tampa, Florida, for an average of summer days 75

4-7 1985 emissions for Dallas-Fort Worth 76

4-8 Time series of predicted and observed hourly ozone concentrations for the Dallas-Fort Worth diagnostic run 1 97

4-9 Scatterplot, residual analysis, and model performance statistics for predicted and observed hourly ozone concentrations on 30 August 1985 in Dallas-Fort Worth for diagnostic run 1 103

4-10 Scatterplot, residual analysis, and model performance statistics for predicted and observed hourly ozone concentrations on 31 August 1985 in Dallas-Fort Worth for diagnostic run 1 105

4-11 Time series of predicted and observed hourly NO concentrations in Dallas-Fort Worth for diagnostic run 1 108

4-12 Time series of predicted and observed hourly NO_2 concentrations in Dallas-Fort Worth for diagnostic run 1 113

4-13 Time series of predicted and observed hourly CO concentrations in Dallas-Fort Worth for diagnostic run 1 118

4-14 Isopleths of predicted daily maximum ozone concentrations with superimposed observations on 30 August 1985 for the Dallas-Fort Worth diagnostic run 2 124

4-15 Time series of predicted and observed hourly ozone concentrations for the Dallas-Fort Worth diagnostic run 2 125

4-16 Scatterplot, residual analysis, and model performance statistics for predicted and observed hourly ozone concentrations on 30 August 1985 in Dallas-Fort Worth for diagnostic run 2 131

4-17 Isopleths of predicted daily maximum ozone concentrations with superimposed observations on 31 August 1985 for diagnostic run 2 133

4-18 Scatterplot, residual analysis, and model performance statistics for predicted and observed hourly ozone concentrations on 31 August 1985 in Dallas-Fort Worth for diagnostic run 2 134

4-19 Time series of predicted and observed hourly NO concentrations in Dallas-Fort Worth for diagnostic run 2 137

4-20 Time series of predicted and observed hourly NO_2 concentrations in Dallas-Fort Worth for diagnostic run 2 142

4-21 Time series of predicted and observed hourly CO concentrations in Dallas-Fort Worth for diagnostic run 2 147

4-22 Time series of predicted and observed hourly ozone concentrations for the Dallas-Fort Worth diagnostic run 2 using a one-cell search nearest neighbor analysis 153

4-23 Time series of predicted and observed hourly NO concentrations (ppb) for the Dallas-Fort Worth diagnostic run 2 using a one-cell search nearest neighbor analysis 157

4-24 Time series of predicted and observed hourly NO_2 concentrations (ppb) for the Dallas-Fort Worth diagnostic run 2 using a one-cell search nearest neighbor analysis 160

4-25 Time series of predicted and observed hourly ozone concentrations for the Dallas-Fort Worth diagnostic run 2 using a two-cell search nearest neighbor analysis 163

4-26 Time series of predicted and observed hourly NO_2 concentrations (ppb) for the Dallas-Fort Worth diagnostic run 2 using a two-cell search nearest neighbor analysis 167

4-27 Time series of predicted and observed hourly ozone concentrations for the Dallas-Fort Worth diagnostic run 2 using a two-cell search nearest neighbor analysis 170

Tables

2-1 Surface roughness and deposition factors based on studies by Argonne National Laboratories 11

2-2 Exposure class (CE) classification based on cloud cover and solar zenith angle 16

3-1 Highest ozone days in Atlanta, 1984-1987 26

3-2 Surface meteorological observation sites, locations, and variables in the Atlanta region 30

3-3 Upper-air observation sites, locations, and distance from Atlanta used in this study 31

3-4 Ozone monitor names and locations 31

4-1 Surface meteorological observation sites at the continuous air monitoring stations 70

4-2 Upper-air meteorological observation sites in the vicinity of Dallas-Fort Worth 72

4-3 Surface air quality monitors in the Dallas-Fort Worth area in operation during 21-31 August 1988 73

4-4 Summary of emission totals for the Dallas-Fort Worth modeling domain 90

1 INTRODUCTION

The job of reducing ozone concentrations to levels below the National Ambient Air Quality Standard (NAAQS) has proven to be far more difficult than was thought when the Clean Air Act was passed and amended. The level of ozone precursor emissions remains too high; either emission reductions have been too small or have been required of the wrong sources, or both.

A plethora of technical explanations has been offered for failure to attain the ozone standard. These include perceived weaknesses in the attainment planning process (Federal Registrar, Vol. 52, No. 226, November 24, 1987; OTA 1988a,b,c), incomplete understanding or recognition of the anthropogenic and natural factors that cause elevated tropospheric ozone levels (Science, 1988), the failure to consider the effects of natural emissions (Chameides et al., 1988; Morris et al., 1989), use of a simplistic modeling approach (OTA, 1988a; Seinfeld, 1988a; Burton, 1988), and failure to reduce the amount of emissions intended, either through overestimates of the effectiveness of control technology or failure to account for certain categories of emission sources. The EPA, after lengthy consideration, has proposed a comprehensive policy that includes major changes in the planning process for reducing ozone concentrations (Federal Registrar, Vol. 52, No. 226, November 24, 1987). These changes include improvements in modeling practices and requirements for improving the data to support improved modeling practices. The EPA is now evaluating public comments on the proposed policy.

USE OF THE URBAN AIRSHED MODEL

The EPA recommends that states use the Urban Airshed Model (UAM) for the modeling of ozone and photochemical reactive pollutants in urban areas (EPA, 1986). An alternative approach, the Empirical Kinectics Modeling Approach (EKMA), has been accepted for demonstrating attainment of the ozone standard in most State Implementation Plans (Federal Registrar, Vol. 52, No. 226, 1987). The UAM and EKMA are quite different types of models; the UAM is a three-dimensional grid model while the EKMA is a trajectory box model.

A reluctance to use the UAM in the past is based on the perception that it requires using data from costly intensive measurement studies and requires extensive computational resources. Most of the cost of applying the UAM is attributed to the practice of conducting an extensive evaluation of UAM performance, which usually

entails many diagnostic simulations. This evaluation enables us to understand why the UAM performs as it does for a particular application and, if deemed necessary, to take actions to improve model performance. Historically, it has been expected that the UAM will calculate hourly ozone concentrations to within approximately 15 to 20 percent of the observed peak value (Seinfeld, 1988a; Burton, 1988). More recent applications of the UAM to the Los Angeles basin have used routinely available meteorological data and predicted observed ozone levels with a high degree of skill (Seinfeld, 1988a; Burton, 1988; Hogo, Mahoney, and Yocke 1988). A recent application of the UAM to the New York metropolitan area used simple inputs, i.e., constant wind fields and mixing depths (Rao 1987).

This simplified use of the UAM, relying on routinely available data and reducing the requirement for strict evaluations of model performance, offers air quality managers a practical air quality assessment tool for identifying emission control strategies that demonstrate attainment of the ozone NAAQS. This simplified approach is called Practice-for-Low-Cost-Airshed-Application-for-Nonattainment-Regions (PLANR). The PLANR use of the UAM requires almost the same quantity and quality of inputs as EKMA, and the overall application cost is substantially reduced. The possible exception is the emissions inventory, which in PLANR applications should contain the same spatially (horizontally and vertically) and temporally varying emissions used in standard UAM applications (such detail is necessary to account for the differing reactivities of VOC emissions). However, local agencies generally have emissions inventories at hand; in addition, UAM input inventories can be readily estimated from existing national emissions inventories (e.g., the National Acid Precipitation Program 1980 and 1985 inventories). Knowledge of current emission rates is needed to estimate the emission controls required to achieve attainment of the ozone NAAQS.

The PLANR use of the UAM may not be appropriate for all nonattainment regions. When attainment is expected to be imminent, improved methods for using EKMA may be adequate. In other, more complex situations, such as the Los Angeles basin, the Houston region, and the New York Metropolitan area among others, the complexity of meteorological conditions and the emissions distribution and the severity of the ozone attainment problem probably require a more detailed application of the UAM. The application of UAM to these more complex situations, called Practice-of-Airshed-Application-in-Complex-Regions (PACR), would involve more extensive model performance requirements and hence more diagnostic simulations, and a resultant increase in costs. However, even for a complex nonattainment region, the PLANR approach would probably be more comprehensive and reliable than EKMA for estimating the controls needed to achieve ozone attainment.

THE "FIVE CITIES" UAM STUDY

The EPA has funded a study of the PLANR approach in five urban areas in the U.S. (New York, St. Louis, Atlanta, Philadelphia, and Dallas-Ft. Worth). The main objectives of this "Five Cities" study are to:

(1) Demonstrate the usefulness of PLANR for air quality planning;

(2) Determine the effects of alternative fuels and alternative Reid vapor pressure values for fuels on urban ozone concentrations;

(3) Demonstrate the use of PLANR to evaluate SIP control strategies; and

(4) Transfer the UAM model, modeling data bases, and applications technology to the states for use in future SIPs.

In addition, the study includes two city-specific analyses:

(1) For the St. Louis and Philadelphia areas, comparison of the PLANR use of the UAM (i.e., using only routinely available data) with applications of the UAM that use an extensive data base; and

(2) The effects of biogenic emissions on anthropogenic emission reductions in the Atlanta area.

Previous reports on the "Five Cities" study have documented the PLANR use of UAM and the evaluation of alternative fuel emission scenarios for the New York metropolitan area and the city of St. Louis (Morris et al., 1989a); analyses of the effects of biogenic emissions on the anthropogenic VOC emission reductions required to meet attainment of the ozone NAAQS for the city of Atlanta (Morris et al., 1989c); and an evaluation of the PLANR use of the UAM for the city of St. Louis (Morris, Myers, and Carr, 1989).

This report describes the PLANR application of the UAM to the city of Atlanta and the Dallas-Fort Worth metroplex area.

2 PLANR PROCEDURES FOR PREPARING UAM INPUTS

The Urban Airshed Model (UAM) is a three-dimensional grid model designed to calculate the concentrations of both inert and chemically reactive pollutants by simulating the physical and chemical processes in the atmosphere that affect pollution concentration. The basis for the UAM is the atmospheric diffusion or species continuity equation. This equation represents a mass balance in which all of the relevant emissions, transport, diffusion, chemical reactions, and removal processes are expressed in mathematical terms. The model is usually applied to an 8- to 72-hour period during which adverse meteorological conditions result in elevated pollutant concentrations of the species of interest.

The basic UAM model formulation is discussed elsewhere (Ames et al., 1985a,b; Reynolds, Tesche, and Reid 1979). The version of the UAM employed in this study differs from the previous versions in that it includes the latest version of the Carbon Bond mechanism, the CB-IV (Gery, Whitten, and Killus 1988), and the advection/diffusion algorithm has been updated (Smolarkiewicz, 1983). The description of these updates to the UAM are discussed elsewhere (Hogo, Mahoney, and Yocke, 1988; Morris et al., 1989a,b).

Since the release of the first version of the UAM in 1979-1980, there have been various improvements not only in the UAM itself but in the procedures used to develop UAM inputs. The 1979-1980 UAM preprocessors rely on extensive measurement data and then interpolate the measured data to provide the gridded fields of input data required by the UAM. More recently, procedures have been developed for generating fields of meteorological inputs for air quality models using limited data availability (Morris et al., 1988, 1989a,b,c). These routines have been incorporated into the PLANR procedures for preparing UAM inputs.

As shown in Figure 2-1, the PLANR procedures for applying the UAM involves the following activities:

(1) Identification of the modeling episode.

(2) Assessment of available data (meteorological and air quality) for the episode.

(3) Characterization of the meteorological conditions during the episode to develope a conceptual picture of the conditions that led to the elevated ozone concentrations.

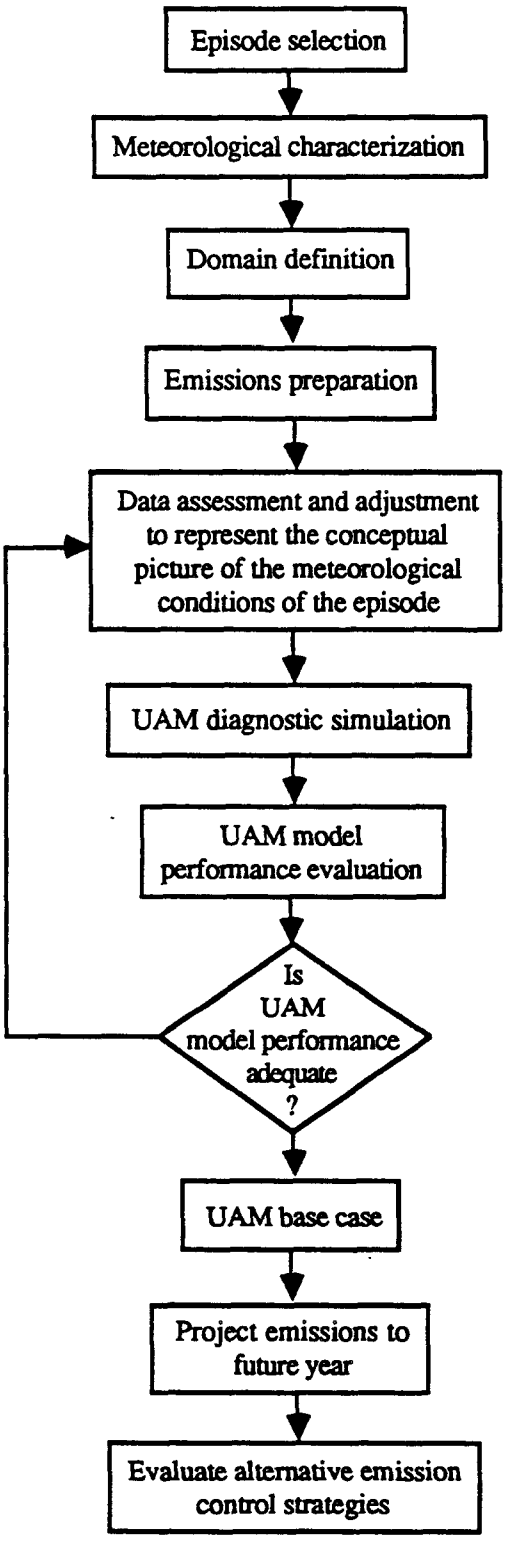

FIGURE 2-1. PLANR procedures for applying UAM.

(4) Definition of the modeling domain, including spatial extent, horizontal grid spacing, and number of vertical layers.

(5) Preparation of the TERRAIN UAM input file.

(6) Preparation of the base case emissions inventory (the EMISSIONS file and input to the PTSOURC preprocessor of UAM)

(7) Adjustment of the UAM preprocessor meteorological and air quality input data to represent the conceptual picture of the meteorological conditions.

(8) Preparation of the UAM meteorological input files.

(9) Simulation of an inert tracer simulation to define starting time (optional).

(10) Run the point source emissions preprocessor to prepare the PTSOURCE file and exercise the UAM for a diagnostic simulation.

(11) Evaluate whether the diagnostic simulation is deemed adequate as a base case. If model performance is considered inadequate, go back to (7).

(12) Project emissions to future year(s) (optional)

(13) Analyze alternative emission control strategies.

EPISODE SELECTION

The first activity of any UAM modeling study is to select an episode of high pollution levels. The model's ability to replicate the measured pollutant levels will then serve as a test of its ability to simulate accurate pollutant levels under the same conditions but with different emission parameters. The episode for an ozone analysis should satisfy the following criteria:

High and widespread ozone concentrations

No atypical meteorological conditions

Completeness of routine data

Recent occurrence of one of the highest observed ozone concentrations

The selection of a UAM modeling episode consists of the following activities:

Ranking of the days from several recent years based on the maximum ozone concentration for each day with ozone concentrations greater than the ozone NAAQS;

Definition of possible modeling episodes (one day or several days) from groupings of the highest observed ozone days;

Examination of the number of station-hours (i.e., total number of hours at any station) within each possible modeling episode and number of ozone monitors exceeding the ozone NAAQS for each episode. Elimination of days without widespread elevated ozone conditions (i.e., those episodes with isolated localized ozone peaks);

Examination of the meteorological conditions for each candidate episode, and elimination of those episodes experiencing atypical meteorological conditions;

Assessment of data availability, and elimination of candidate episodes for which sufficient routine data are not available;

Consideration of other factors, such as other motivations for the study;

Conferring with state, local, and federal agencies for the final selection.

DATA ASSESSMENT AND METEOROLOGICAL CHARACTERIZATION

After a modeling episode has been selected, the next activity is the assessment and acquisition of all surface meteorological data in the vicinity of the region and upper-air data within about 500 km of the area of interest. By analyzing this data and daily weather maps, a conceptual picture of the meteorological conditions that led to the elevated ozone concentrations is developed. This meteorological characterization is necessary because this conceptual picture will ultimately decide how the routine meteorological data will be interpreted and interpolated for input into the UAM preprocessors.

PREPARATION OF UAM INPUT FILES

The following 13 input files are required for UAM modeling analyses.

DIFFBREAK contains the daytime mixing height or nighttime inversion height for each column of cells at the beginning and end of each hour of the simulation.

REGIONTOP contains the height of each column of cells at the beginning and end of each hour of the simulation. If this height is greater than the mixing height, the cell or cells above the mixing height are assumed to be within an inversion.

WIND contains the x and y components of the wind velocity for every grid cell for each hour of the simulation. The maximum wind speed for the entire grid and average wind speeds at each boundary for each hour are also included in this file.

METSCALARS contains the hourly values of the meteorological parameters that do not vary spatially. These scalars are the NO_2 photolysis rate constant, the concentration of water vapor, the temperature gradient above and below the inversion base, the atmospheric pressure, and the exposure class.

AIRQUALITY contains the initial concentrations of each species for each grid cell at the start of the simulation.

BOUNDARY contains the location of the modeling region boundaries. This file also contains the concentration of each species that is used as the boundary condition along each boundary segment at each vertical level.

TOPCONC contains the concentration of each species for the area above the modeling region. These concentrations are the boundary conditions for vertical integration.

TEMPERATUR contains the hourly temperature for each surface layer grid cell.

EMISSIONS contains the ground-level emissions of NO, NO_2, seven carbon bond categories, and CO for each grid square for each hour of the simulation.

PTSOURCE contains the point source information (stack height, temperature and flow rate, the plume rise, the grid cell into which the emissions are emitted) and the emissions rates for NO, NO_2, seven carbon bond categories, and CO for each point source for each hour.

TERRAIN contains the value of the surface roughness and deposition factor for each grid square.

CHEMPARAM contains information about the chemical species to be simulated, including reaction rate constants, upper and lower bounds, activation energy, and reference temperature.

SIMCONTROL contains the simulation control information, such as the time of the simulation, file option information, default information, and information on integration and chemistry time steps.

Each of these files is explained in detail below.

CHEMPARAM

The CHEMPARAM file contains the information required by the numerical algorithms used to solve the Carbon Bond IV chemical kinetics mechanism in the UAM(CB-IV). The file only needs to be created once for all UAM simulations. It is created by the chemistry preprocessor program (cprep.f) using the CHEMCB4.INP file as input (see Figure 2-2).

TERRAIN

Information in the TERRAIN file is created by analyzing USGS topographical maps and/or land-use maps if available. Each grid cell of the modeling domain is assigned an integer between 1 and 13 that represents the most dominant land use category as listed in Table 2-1. This two-dimensional array of integers is then processed by the UAM terrain preprocessor (creter.f), which assigns to each grid cell a surface roughness and vegetation factor based on one of the 13 land use categories and is formatted into the proper format for the UAM (see Figure 2-3).

DIFFBREAK and REGIONTOP

The preparation of the DIFFBREAK file is a three-step procedure that uses surface meteorological data and a representative upper-air sounding and excercising three preprocessor programs (see Figure 2-4): (1) the mixing height program (e.g., mixht.f), which calculates the maximum daily mixing height at the location of each surface meteorological observation site; (2) the RAMMET program (rammet.f), which calculates hourly mixing heights at each surface meteorology site based on the maximum daily mixing height at the site, the height of the base of the nocturnal inversion from the morning sounding, and the surface data at the site; and (3) the UAM diffusion break preprocessor (dfnsbk.f), which spatially interpolates the mixing heights from each surface meteorology site to form the gridded field required by the UAM for each hour of the simulation. The REGIONTOP for the PLANR applications performed to date is defined as 50 - 100 meters above the maximum mixing height.

Some care must be taken in chosing a representative upper-air sounding for the calculation of mixing heights. The location of the sounding should not be separated from the modeling region by a large terrain feature or by such meteorological conditions as fronts. In addition, since ozone episodes usually occur during limited mixing conditions, the calculated mixing heights should be compared with climatological mixing heights for the region interest. If the calculated mixing heights greatly exceed the average summer season maximum mixing height for the region, and a UAM diagnostic simulation tends toward underprediction of the observed peak ozone,

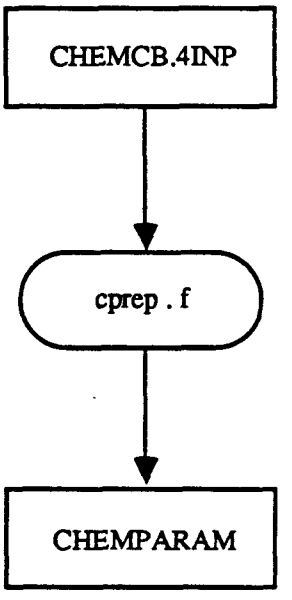

FIGURE 2-2. Flow diagram for creating the UAM CHEMPARAM input file.

TABLE 2-1. Surface roughness and deposition factors based on studies by Argonne National Laboratories.

	Land Use Category	Surface Roughness (meters)	Deposition Factor
1	Urban	3.00	0.2
2	Agricultural	0.25	0.5
3	Range	0.05	0.4
4	Deciduous Forest	1.00	0.4
5	Coniferous Forest including wetland	1.00	0.3
6	Mixed Forest	1.00	0.3
7	Water	0.0001	0.03
8	Barren land	0.002	0.2
9	Nonforest Wetlands	0.15	0.3
10	Mixed Agricultural and range	0.10	0.5
11	Rocky (low shrubs)	0.10	0.3

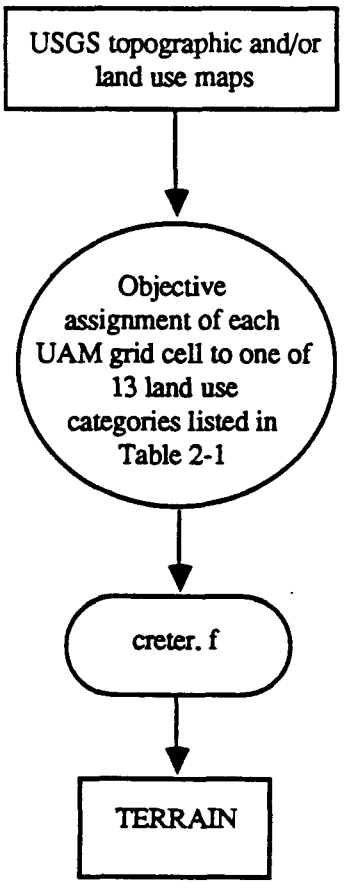

FIGURE 2-3. Flow diagram for creating the UAM TERRAIN input file.

EEE89104

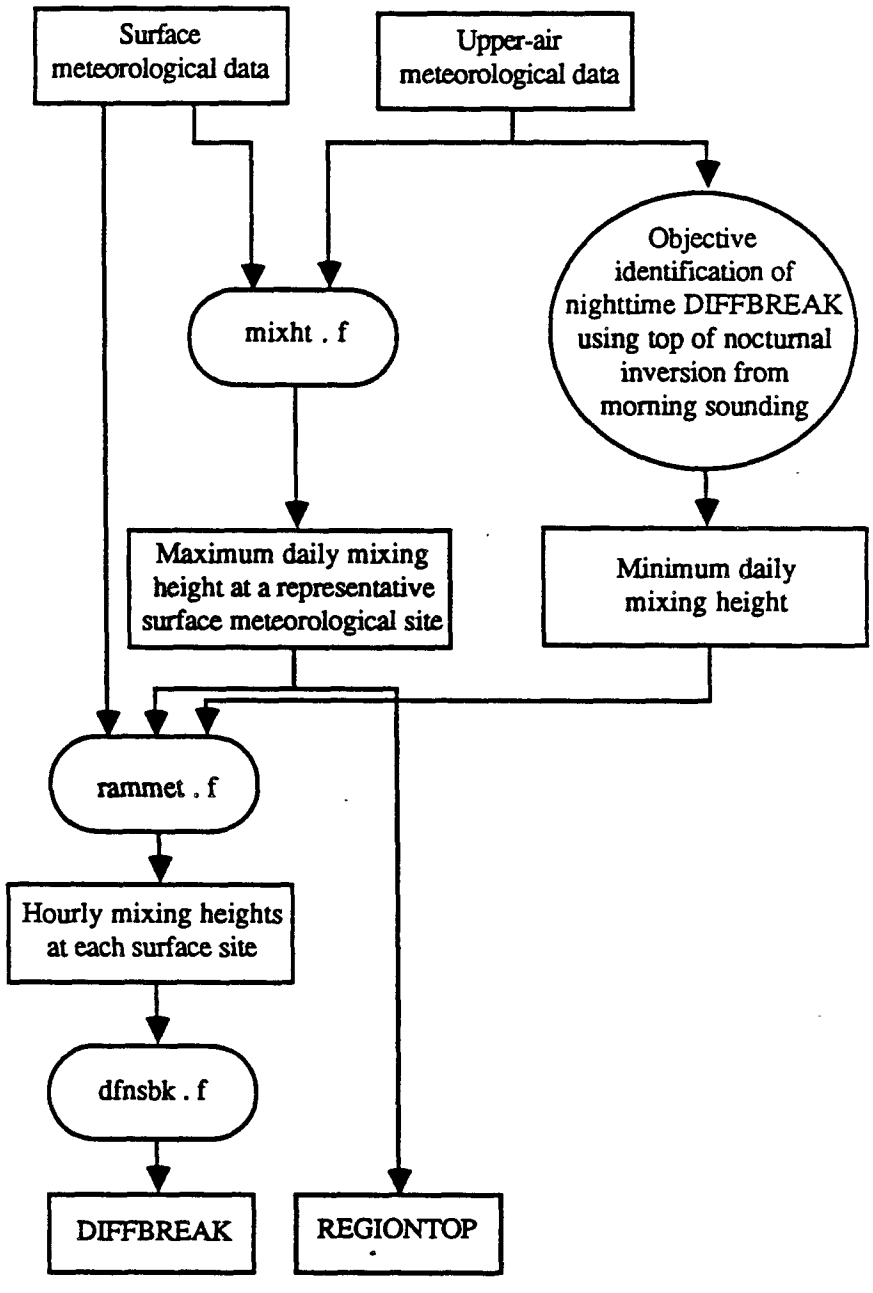

FIGURE 2-4. Flow diagram for creating the UAM DIFFBREAK and REGIONTOP input files.

then the mixing heights should be adjusted downward. In the PLANR applications performed to date, the mixing height algorithm of Kelley (1981) (mixht.t) was used, although other algorithms may be used at the user's discretion.

METSCALARS

Several hourly varying but spatially invariant meteorological parameters need to be defined. The atmospheric pressure in atm (ATMOSPRESS) and water vapor concentrations (CONCWATER) are defined as the average value of the hourly observations from all of the surface meteorological sites. Note that if atmospheric pressure is not reported then a value of 1.0 is adequate.

The NO_2 photolysis rate (RADFACTOR) is usually calculated based on the solar zenith angle for the location (latitude/longitude) and time (hour and day) of interest using the sunfunc.f program (see Figure 2-5). Adjustments for the attenuation of solar radiation and consequently the NO_2 photolysis rate due to clouds can also be accounted for. The NO_2 photolysis rate can also be directly estimated from measured insolation data, but this data is usually not routinely available. The exposure class (EXPCLASS) is calculated from cloud cover observations and the solar zenith angle, which is also given in the sunfunc.f program following the procedures given in Table 2-2.

The temperature gradients below (TGRADBELOW) and above (TGRADABOVE) the inversion (mixing height) are estimated from the representative upper-air soundings and the observed surface temperatures. An interpretation of the upper-air sounding and surface temperatures must be made to determine the temperature gradient inputs. This interpretation is especially difficult when using only the twice-daily routine upper-air data. The need to represent the typically complex vertical structure of the atmosphere with just two temperature gradients will demand some compromises in determining their values. First, the modeling episode is split into two regimes: a daylight regime, during which DIFFBREAK represents the convective mixed-layer, and a nightime regime, when the DIFFBREAK represents the top of a surface-based inversion.

For the daylight regime, TGRADBELOW is based on the afternoon sounding of the day to be modeled and the exposure class. For example, for the Atlanta episode the temperature gradient from the surface to the mixing height ranged from -0.0096 to -0.0107 (K/m). Thus for exposure class 2 and 3 (most unstable) a value of -0.0105 was used for TGRADBELOW. An exposure class of zero represents neutral conditions, thus TGRADBELOW was set to -0.0098 during zero exposre class. Finally, during periods of exposure class of 1 an intermediate value of -0.010 was used for TGRADBELOW.

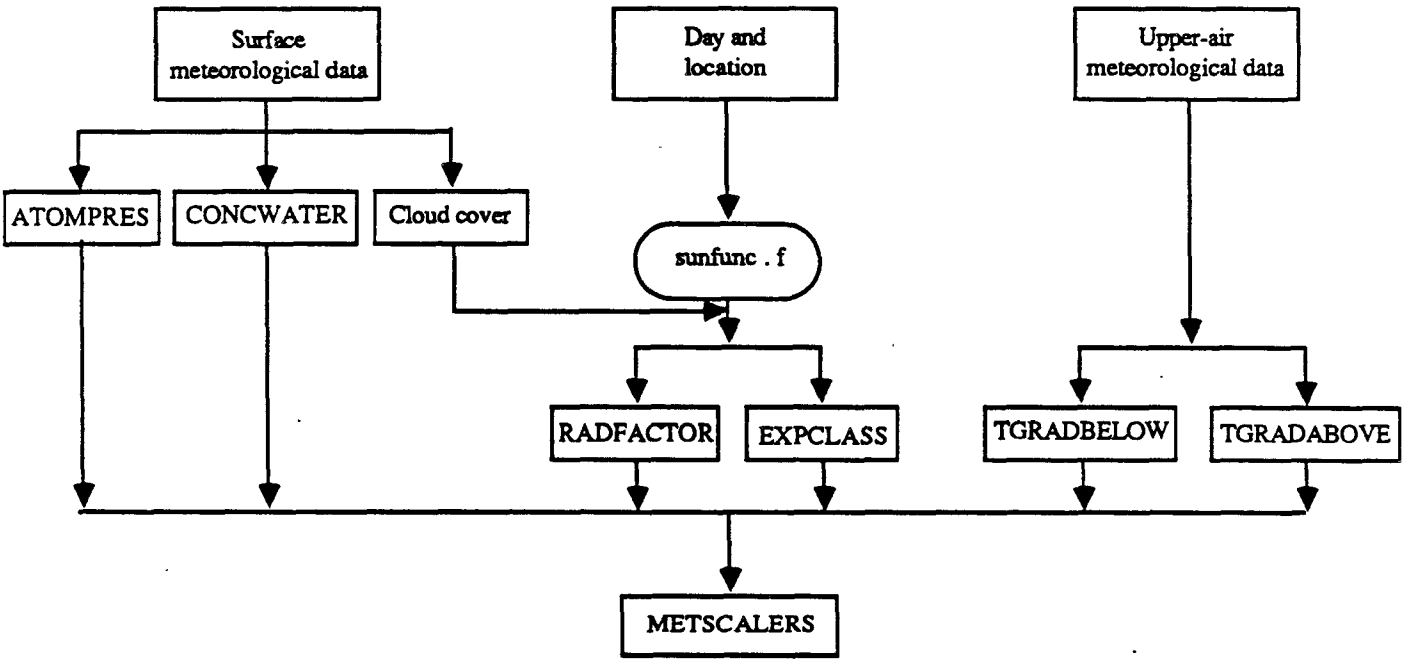

FIGURE 2-5. Flow diagram for creating the UAM METSCALERS input files.

EEE89104

TABLE 2-2. Exposure class (CE) classification based on cloud cover and solar zenith angle.

Solar Zenith Angle (degrees)	Cloud Cover (percent)	CE
	≥ 90	0
> 85	≤ 50	-2
> 85	> 50	-1
≤ 30	≤ 50	3
≤ 30	> 50	2
30 < θ ≤ 55	≤ 50	2
30 < θ ≤ 55	> 50	1
55 < θ ≤ 85	≤ 50	1
55 < θ ≤ 55	> 50	0

89104 3

To estimate TGRADABOVE during the daylight hours, the temperature at the top of the region (T_{top}) is obtained from the afternoon sounding and is assumed to be constant during the daylight regime. Then, for each hour of the day the temperature at the mixing height (T_{mix}) is estimated from the surface temperature (T_{surf}) and TGRADBELOW as follows:

$$T_{mix} = T_{surf} + \text{DIFFBREAK} * \text{TGRADBELOW}$$

The TGRADABOVE can be calculated:

$$\text{TGRADABOVE} = (T_{top} - T_{mix}) / (\text{REGIONTOP} - \text{DIFFBREAK})$$

During the nighttime regime the DIFFBREAK is fairly constant, ranging from 100 to 500 meters. It is usually assumed that the temperature at the DIFFBREAK will remain constant at night. Thus, using the temperature at the DIFFBREAK from the morning sounding (T_{mix}) and the surface temperature of the hour in question (T_{surf}), the temperature gradient below the inversion can be estimated as follows:

$$\text{TGRADBELOW} = (T_{mix} - T_{surf}) / \text{DIFFBREAK}$$

As an additional constraint, TGRADBELOW is not allowed to exceed the temperature gradient from the surface to the DIFFBREAK from the morning sounding. During the nighttime regime the value for TGRADABOVE is assumed to be constant and is obtained using the temperature gradient from the DIFFBREAK to the REGIONTOP from the morning sounding (following the night in question).

TEMPERATUR

The hourly varying fields of surface temperatures needed by the UAM are obtained by interpolating the hourly measured surface temperatures to the modeling grid using the tmprtr.f UAM preprocessor (Figure 2-6). The tmprtr.f preprocessor is excercised using the "stat interp" option (i.e., 1/r interpolation); a large radius of influence is specified so that each grid cell is influenced by all of the surface measurements weighted by the inverse distance from the station to the grid cell in question.

WIND

When only routinely available data are used in the UAM, the wind fields are one of the most uncertain inputs. The wind fields are created by exercising the Diagnostic Wind Model (DWM) (Douglas and Kessler 1988; Morris et al., 1988) to obtain 14 vertical levels of winds at constant heights above ground. The winds are then vertically averaged to the UAM vertical layer structure and the O'Brien adjustment scheme is used to eliminate the vertical velocity through the top (REGIONTOP) of the modeling domain. This last operation is accomplished using the uamwnd.f program (see Figure 2-7).

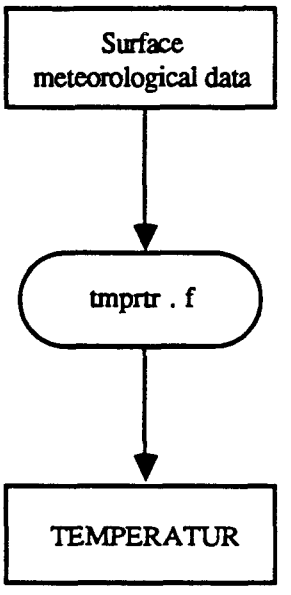

FIGURE 2-6. Flow diagram for creating the UAM TEMPERATUR input file.

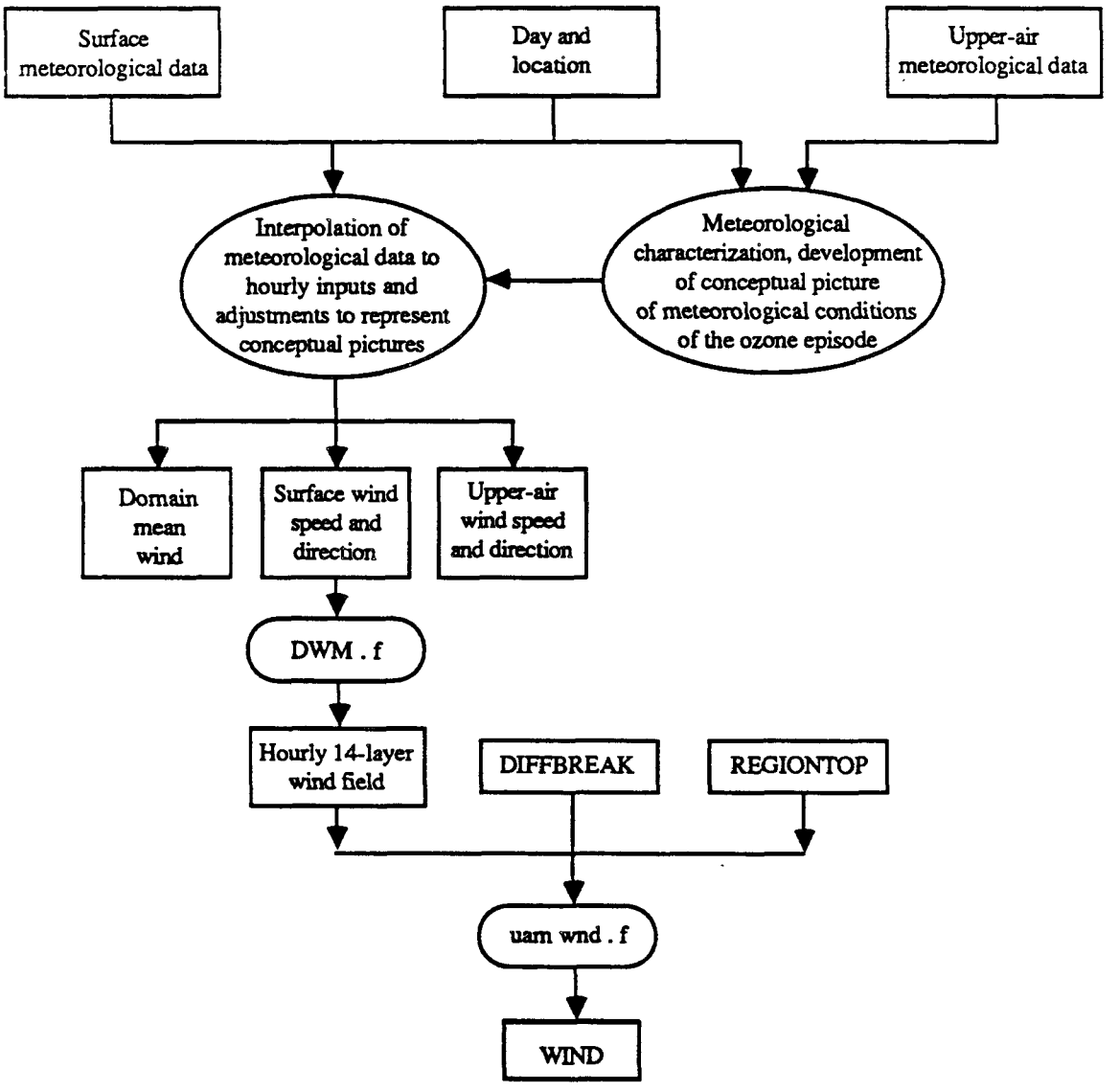

FIGURE 2-7. Flow diagram for creating the UAM WIND input files.

EEE89104

An important component of the PLANR use of the UAM is how the observed wind data is input into the DWM so that it represents the conceptual picture of the meteorological conditions of the episode. The DWM creates an hourly wind field in two steps. (1) A domain-mean wind representative of synoptic air flows of that hour is modified by the model to account for the presence of the terrain to create the multilevel wind fields: (2) The observations are objectively combined with the wind field created in step 1. Since routine data tend to be sparse, the domain-mean wind will have a large influence on the resultant wind field and must be selected with care.

Typically only the twice-daily upper-air soundings from one or two sites within approximately 400 km of the modeling domain and a handful of surface meteorological sites within and in the immediate vicinity of the modeling domain will be available for generating wind fields for the PLANR UAM. As a first guess, the hourly varying domain-mean wind is usually defined by linearly interpolating the twice-daily soundings from the nearest upper-air site. When a high-pressure system or front passes through the modeling domain, the domain-mean wind must be chosen more carefully. The timing of the passage of weather system can usually be obtained by examining when the wind shifts in the hourly surface wind observations. Examples of this more creative use of the routinely available upper-air data will be given in the discussion of the PLANR application of the UAM for Atlanta (Section 3).

Ozone episodes for an urban area are typically characterized by hot stagnant meteorological conditions with limited mixing. There are usually two types of surface meteorological observations: hourly average values from a state or local agency network, or instantaneous (one-minute averages) collected by observers at Federal Aviation Administration (FAA) sites. Recent analysis of collocated hourly average and instantaneous FAA wind observations in the South Central Coast Air Basin of California have indicated that, under stagnant conditions, the hourly average wind speeds are only 44 to 98 percent of the concurrent FAA values (depending on the site) (see Appendix D). Based on seven collocated FAA and hourly average wind speed monitoring sites, the FAA wind speeds were on average a factor of 1.8 times the hourly average wind speeds. This result is not surprising for two reasons.

First, as noted by Killus and Gutfreund (1984), vector averaging over an hour to obtain an hourly average wind observation inherently results in a lower wind speed than is obtained from an instantaneous or one-minute average. This fact is especially true during periods of light and variable winds, which typically occur during ozone episodes. Second, FAA observations are mainly used to advise pilots of any adverse wind conditions and wind directions during take-offs and landings. The pilots need information concerning the possibility of cross runway winds, not information concerning the hourly average wind. The UAM, on the other hand, requires information concerning the vector average transport conditions of the hour. Thus, if initial diagnostic UAM simulations that use FAA data without adjustments indicate that the predicted ozone peak is too low and occurs too far down

wind, then elimination of the unrepresentative FAA wind observations should be considered. Reduced FAA wind speeds might be used for model application in the absence of more representative data.

AIRQUALITY, BOUNDARY, and TOPCONC

The initial concentrations (AIRQUALITY) and boundary conditions for the lateral boundaries (BOUNDARY) and aloft (TOPCONC) are assumed to be "clean" unless higher concentrations are known or expected. This can be determined through measured air quality data or from knowledge that the area is known to be affected by transported pollutants. The effects of both anthropogenic and biogenic emissions need to be reflected in the initial and boundary concentrations. The "clean" values recommended for use in the PLANR UAM are as follows:

VOC = 25 ppbc (using EKMA default speciation)

ISOP = 0.0001 ppb

NO_x = 1 ppb (3/4 NO_2, 1/4 NO)

O_3 = 40 ppb

CO = 200 ppb

The UAM is usually initiated well before the ozone episode of interest to minimize the effects of initial concentrations. Thus "clean" values are usually sufficient for initializing the model. The first diagnostic simulations for Atlanta and Dallas both used these "clean" values for boundary conditions. However, because of the presence of large amounts of biogenic emissions in the vicinity of Atlanta, the VOC lateral boundary conditions were increased in subsequent diagnostic simulations for Atlanta.

EMISSIONS and PTSOURCE

The emission inventories for the PLANR application of the UAM to Atlanta and Dallas-Fort Worth were developed from the 1985 NAPAP annual continental U.S. emissions data base in several steps (Figure 2-8). Since the PLANR base cases for Atlanta and Dallas both used 1985 emission inventories, the creation of the inventories is more straight forward than if data for a different base year were needed. Thus there was no need to make adjustments for growth, effects of Reid Vapor Pressure, and any possible emission controls (e.g., Stage I and II). The reader is referred to SAI (1989) for more details on the procedures for preparing emission files for use in the UAM.

DIAGNOSTIC SIMULATIONS TO DEFINE THE BASE CASE

An important feature of the PLANR use of UAM is that the number of diagnostic simulations for improving model performance to an acceptable level is limited. As

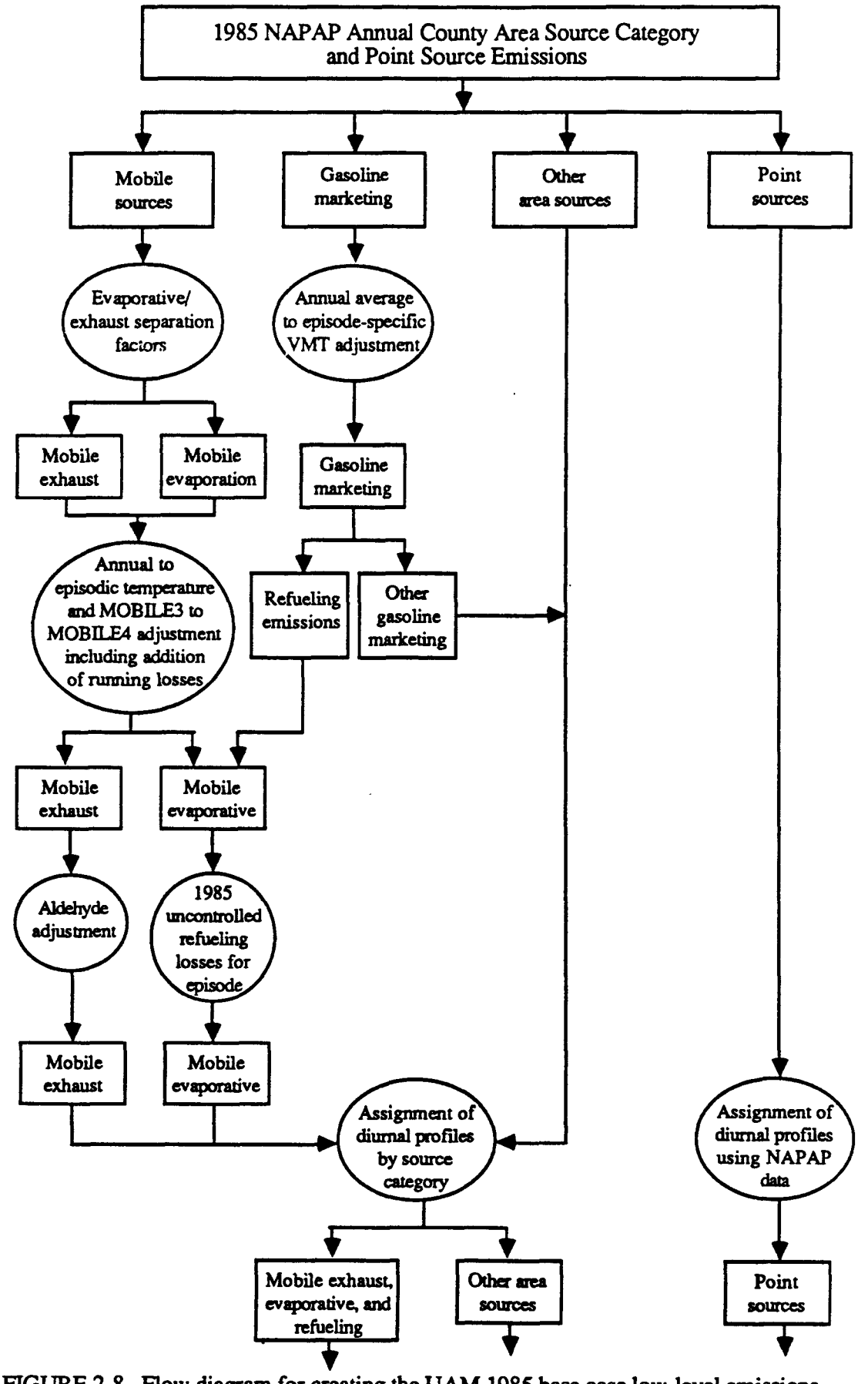

FIGURE 2-8. Flow diagram for creating the UAM 1985 base case low-level emissions (EMISSIONS) and elevated emissions (PTSOURC) files.

EEE89104

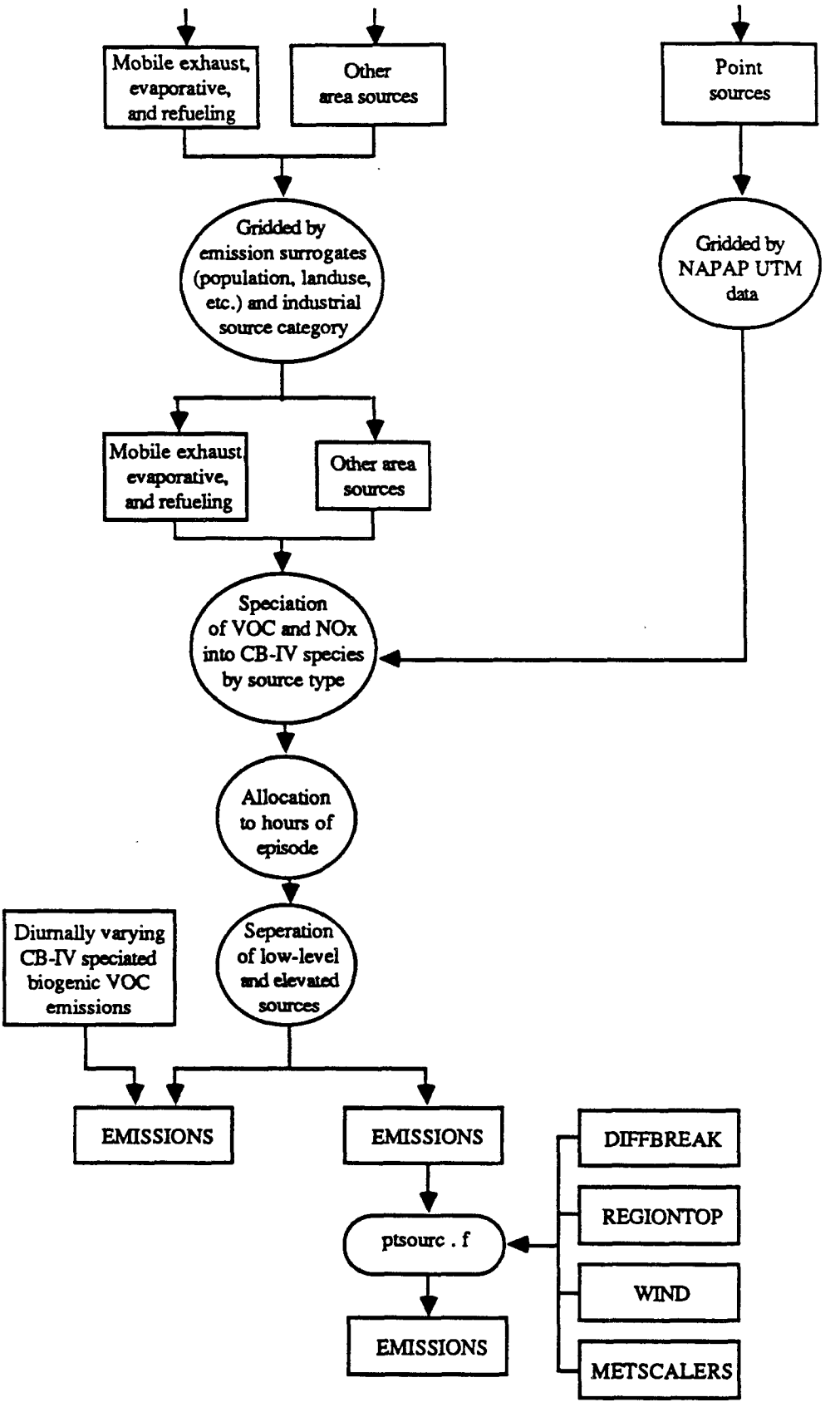

FIGURE 2-8. Concluded.

EEE89104

will be seen, the diagnostic simulations usually differ in the methods used in the interpolation of the meteorological data and how it is input into the UAM preprocessors so that they represent the conceptual picture of the meteorological conditions of the ozone episode. For the Atlanta application, one diagnostic simulation was carried out with only biogenic emissions in order to determine the level of background VOC concentrations due to only biogenic emissions for use in the boundary conditions.

Diagnostic simulations are an integral part of any UAM application, not only for improving model performance but also for obtaining indications that the model is getting the right answer for the right reasons. Adjustments to the UAM inputs were based on interpretation of the observed data so that the UAM inputs better reflected our conceptual picture of the meteorological conditions of the episode. Thus, adjustments to the UAM inputs to improve model performance should be based on reasonable physical interpretation of the observed data rather than random modifications of the data.

3 APPLICATION OF THE UAM TO THE CITY OF ATLANTA

There were two main objectives in the PLANR application of the UAM to the city of Atlanta: (1) demonstration of the PLANR use of the UAM for Atlanta; and (2) analysis of the effects of biogenic emissions on VOC emission control scenarios in the Atlanta region. In this report we discuss the demonstration PLANR application of UAM to Atlanta. The analysis of the effects of biogenic emissions on VOC emission control strategies in Atlanta is described in another report (Morris et al., 1989b).

As discussed in Section 2, PLANR involves the following steps: episode selection, meteorological characterization, domain definition, emissions preparation, UAM model input development, and performance of diagnostic simulations to achieve a statisfactory base case. The following sections discuss these activities.

EPISODE SELECTION

Table 3-1 lists all days from the years 1984 to 1987 in Georgia (either Atlanta or Columbus) in which the maximum daily ozone concentration at any monitor in the AIRS data base exceeds the National Ambient Air Quality Standard of 120 ppb. Of the 62 days where ozone concentrations in Georgia are greater than or equal to 120 ppb, 61 occur in Atlanta and one (18 March 1984) in Columbus (note that on other days Columbus may have an exceedence of the ozone standard but the ozone concentrations are less than recorded in Atlanta). The most striking feature in the ozone record for Atlanta are the months of July and August, 1987, where in a 21-day period (19 July to 7 August 1987) there were 15 exceedences of ozone NAAQS. This period also included the very highest observed ozone concentration in Atlanta (201 ppb on 31 July 1987). On most days during this period, most ozone monitors in Georgia, including Columbus, recorded high ozone concentrations. This seems to indicate a region-wide buildup of ozone concentrations over an extended length of time and area. Thus, the elevated ozone concentrations in Atlanta during July and August, 1987 may be attributable to regional-scale as well as urban-scale ozone formation.

The UAM analysis of Atlanta analyzed the effects of biogenic emissions on urban ozone formation and on the effectiveness of anthropogenic VOC emissions strategies designed to reduce ozone. A previous study on the effects of biogenic emissions for Atlanta used the EKMA model to analyze ozone formation on 4 June 1984

TABLE 3-1. Highest ozone days in Atlanta, 1984 - 1987.

Rank	Peak O3	Monitor	Date	Maximum Daily Ozone 130890002 Panthers. DKLB	130970002 Sweetwat. SWTR	131210053 MLK MLKM	132150008 Columbus COLO	132470001 Conyers CNYR
1	201.	130890002	7/31/87	201.	98.	141.	118.	163
2	169.	130890002	8/ 1/87	169.	130.	138.	80.	158
3	168.	130970002	7/24/87	140.	168.	155.	113.	90.
4	165.	132470001	6/26/86	163.	-99.	-99.	95.	165.
5	164.	130890002	7/18/86	164.	-99.	-99.	90.	142.
6	164.	130890002	7/23/86	164.	-99.	-99.	92.	111.
7	160.	130890002	6/27/86	160.	-99.	-99.	67.	131.
8	157.	132470001	8/ 2/87	138.	88.	128.	70.	157.
9	155.	132470001	7/10/84	115.	-99.	-99.	53.	155.
10	155.	130970002	7/23/87	154.	155.	153.	100.	85.
11	155.	130970002	7/25/87	113.	155.	118.	90.	94.
12	152.	132150008	3/18/84	60.	-99.	-99.	152.	-99.
13	151.	130890002	7/31/86	151.	-99.	-99.	108.	114.
14	150.	132470001	6/ 9/87	129.	73.	103.	75.	150.
15	150.	130970002	7/30/87	112.	150.	113.	93.	93.
16	149.	131210053	7/26/87	129.	100.	149.	98.	88.
17	147.	132470001	6/ 4/84	130.	-99.	-99.	83.	147.
18	147.	132470001	8/22/84	118.	-99.	-99.	78.	147.
19	146.	130890002	8/ 3/87	146.	118.	128.	80.	129.
20	145.	132470001	6/26/85	115.	-99.	-99.	72.	145.
21	145.	132470001	7/12/85	118.	-99.	-99.	65.	145.
22	144.	132470001	6/10/87	137.	95.	115.	85.	144.
23	142.	130890002	4/26/86	142.	-99.	-99.	100.	105.
24	140.	130970002	8/21/87	99.	140.	104.	68.	98.
25	140.	132470001	6/16/86	118.	-99.	-99.	108.	140.
26	137.	130890002	7/22/86	137.	-99.	-99.	80.	84.
27	137.	132470001	8/ 2/86	112.	-99.	-99.	103.	137.
28	136.	130890002	8/ 4/87	136.	100.	113.	75.	116.
29	136.	130890002	8/ 5/87	136.	95.	103.	100.	120.
30	136.	130890002	6/28/84	136.	-99.	-99.	55.	122.
31	135.	130890002	6/ 6/85	135.	-99.	-99.	67.	122.
32	135.	130890002	7/29/87	135.	128.	118.	88.	132.
33	133.	130970002	6/11/87	103.	133.	103.	120.	86.
34	133.	130970002	9/ 3/87	91.	133.	95.	78.	80.
35	133.	132470001	9/14/84	105.	-99.	-99.	103.	132.
36	132.	132470001	6/ 2/87	109.	68.	86.	63.	132
37	132.	132470001	9/ 2/87	108.	88.	89.	90.	132.
38	131.	132470001	8/ 1/86	114.	-99.	-99.	85.	131.
39	131.	130890002	5/13/85	131.	-99.	-99.	83.	72.
40	130.	132470001	6/ 4/85	120.	-99.	-99.	-99.	130.
41	130.	130890002	6/24/87	130.	75.	104.	53.	118.
42	130.	132150008	7/27/87	108.	108.	94.	130.	120.
43	130.	132470001	8/ 7/87	129.	78.	107.	63.	130.
44	129.	132470001	8/ 4/86	114.	-99.	-99.	103.	129
45	129.	130890002	7/19/86	129.	-99.	-99.	90.	112.
46	128.	132470001	6/ 3/87	103.	65.	72.	75.	128.
47	127.	130890002	8/18/84	127.	-99.	-99.	83.	100.
48	127.	132470001	6/ 5/85	92.	-99.	-99.	67.	127.
49	126.	130890002	7/19/87	126.	115.	109.	73.	75.
50	125.	132470001	8/23/87	115.	78.	96.	83.	125.
51	125.	132470001	6/ 1/84	97.	-99.	-99.	75.	125.
52	125.	132470001	6/ 3/84	105.	-99.	-99.	70.	125.
53	125.	132470001	7/11/85	118.	-99.	-99.	63.	125.
54	125.	130890002	7/ 8/86	125.	-99.	-99.	60.	123.
55	123.	130890002	8/16/86	123.	-99.	-99.	78.	93.
56	123.	130890002	7/21/86	123.	-99.	-99.	90.	110.
57	122.	132470001	7/20/85	115.	-99.	-99.	83.	122.
58	122.	132470001	8/ 1/85	95.	-99.	-99.	85.	122.
59	122.	130890002	7/26/86	122.	-99.	-99.	78.	74.
60	121.	130890002	6/22/86	121.	-99.	-99.	78.	85.
61	120.	130890002	7/22/87	120.	98.	116.	68.	82.
62	120.	130970002	8/20/87	100.	120.	108.	75.	96.

89104

axis of the high pressure system moved near the modeling region, a slight easterly component to the wind field developed (a result of the circulation about the high-pressure system). This flow was first seen in the upper levels (> 600m) on the morning of the 4th, but by mid morning was seen in the surface layer. After the passage of the high-pressure system, the winds became southwesterly. The weather conditions during the modeling period were clear, hot, and humid. Maximum temperatures were in the upper 80s and dew point temperatures in the low 60s.

MODELING DOMAIN DEFINITION

The modeling domain for the 3-4 June 1984 modeling episode should include a fairly large fetch upwind of Atlanta to account for sufficient amounts of biogenic emissions upwind of the urban core of Atlanta. The modeling domain should also include enough area downwind of Atlanta to capture the maximum ozone concentrations that will be formed. Grid spacing should be sufficiently small in order to resolve the anthropogenic emission distribution in Atlanta. To determine the modeling domain, synoptic weather maps along with upper-air data from Athens and Waycross, Georgia; Nashville, Tennessee; and Centreville-Brent, Alabama, and surface data from South Dekalb were analyzed to determine the mean flow conditions that existed on 3-4 June 1984.

Figure 3-1 gives a region-wide perspective of the modeling domain for Atlanta. This modeling domain consists of a 40 by 40 array of 4 km square grid cells. The domain origin is located at UTM coordinates 660 km easting, 3665 km northing in zone 16 and extends 160 km in the east and north direction. As discussed in the modeling protocol (SAI, 1988) five vertical layers were used in the UAM: two below the mixing height and three above. The region top was based on the maximum mixing height occurring during the modeling episode.

To accommodate the analysis of the effects of biogenic emissions on urban ozone formation in Atlanta, there is a region 75 to 100 km wide upwind of Atlanta. This allows for a 4 to 12 hour loading of biogenic emissions into the atmosphere upwind from the outskirts of Atlanta.

ROUTINE DATA AVAILABLE FOR ATLANTA

On 3-4 June 1984 there were six surface meteorological observation sites operating in and around the city of Atlanta (Table 3-2). There were no upper-air observation sites located within the modeling domain. Thus, we made use of upper-air observations from five sites that surround the modeling domain for generating wind and mixing height inputs (Table 3-3). The closest upper-air site to Atlanta is Athens, Georgia, approximately 100 km to the east-north-east. Air quality data in and around Atlanta during June 1984 consisted of three monitoring sites (Table 3-4).

(Chameides et al., 1988). It was highly desirable that this day also be chosen for the present analysis as long as no other reasons, such as excessive wind shear or other unusual meteorological phenomena, precluded its selection. On 4 June 1984 the maximum daily ozone concentration was 147 ppb at Conyers, Georgia. For the two-day period of 3-4 June 1984, winds are predominantly from the northwest, with some southwesterlies late on 4 June. Maximum daily ozone concentrations on 4 June are 78 ppb at Dallas upwind of Atlanta, and 130 ppb at DeKalb and 147 ppb at Conyers, at distances of 15 km (DKLB) and 40 km (CNYR) downwind of Atlanta (see Figure 3-1). Thus, it appears that there is not a large amount of transported ozone into the Atlanta region on 4 June 1984 and the ozone exceedence is predominantly due to emissions from the Atlanta area.

Since the 4 June 1984 ozone event is not overly influenced by transported ozone and, as will be shown, does not contain any unusual meteorological conditions, it appears to be an appropriate day for the analysis of biogenic emissions and a demonstration of the PLANR use of the UAM. Since it is desirable to minimize the effects of initial conditions in any UAM simulation, the UAM modeling episode was initialized on 3 June 1984 and terminated the evening of 4 June 1984. Thus, UAM modeling inputs were prepared for 3 and 4 June 1984 with the actual starting time on 3 June determined from an inert tracer simulation. This type of inert tracer simulation starts with an initial concentration of 100 and zero boundary conditions and emissions. The inert model is exercised with several different starting times; the starting time of the inert model simulation that eliminates the initial condition inert tracer concentrations from the region of interest on the morning of 4 June is the starting time chosen for the photochemical model simulation.

It should be noted that other days listed in Table 3-1 may be more appropriate for demonstrating ozone attainment in a State Implementation Plan (SIP). Generally, it would be desirable for a SIP to pick a day with a higher ozone concentration, a more recent episode, a day in which the elevated ozone concentrations can be attributed to Atlanta, and a day that represents typical meteorological conditions that produces ozone exceedences in Atlanta. The very highest ozone concentration in Table 3-1 (201 ppb observed on 31 July 1987) appears to be an anomalous event since it is almost 20 percent higher than any of the other high ozone events over the four year period.

METEOROLOGICAL CHARACTERIZATION

On 3 and 4 June 1984 a high-pressure system passed over the Atlanta region. The 500 mb height contours at 0700 EST on 4 June 1984 shows the high-pressure ridge approaching Atlanta. This high-pressure ridge passed through the region during the evening of the 4th of June; the axis of the surface high-pressure system passed through the modeling region during the afternoon of the 4th. On the 3rd of June, daytime low-level winds (<600m) were from the west at 3-6 ms^{-1} throughout the modeling region, while winds aloft were in the same direction, but stronger. As the

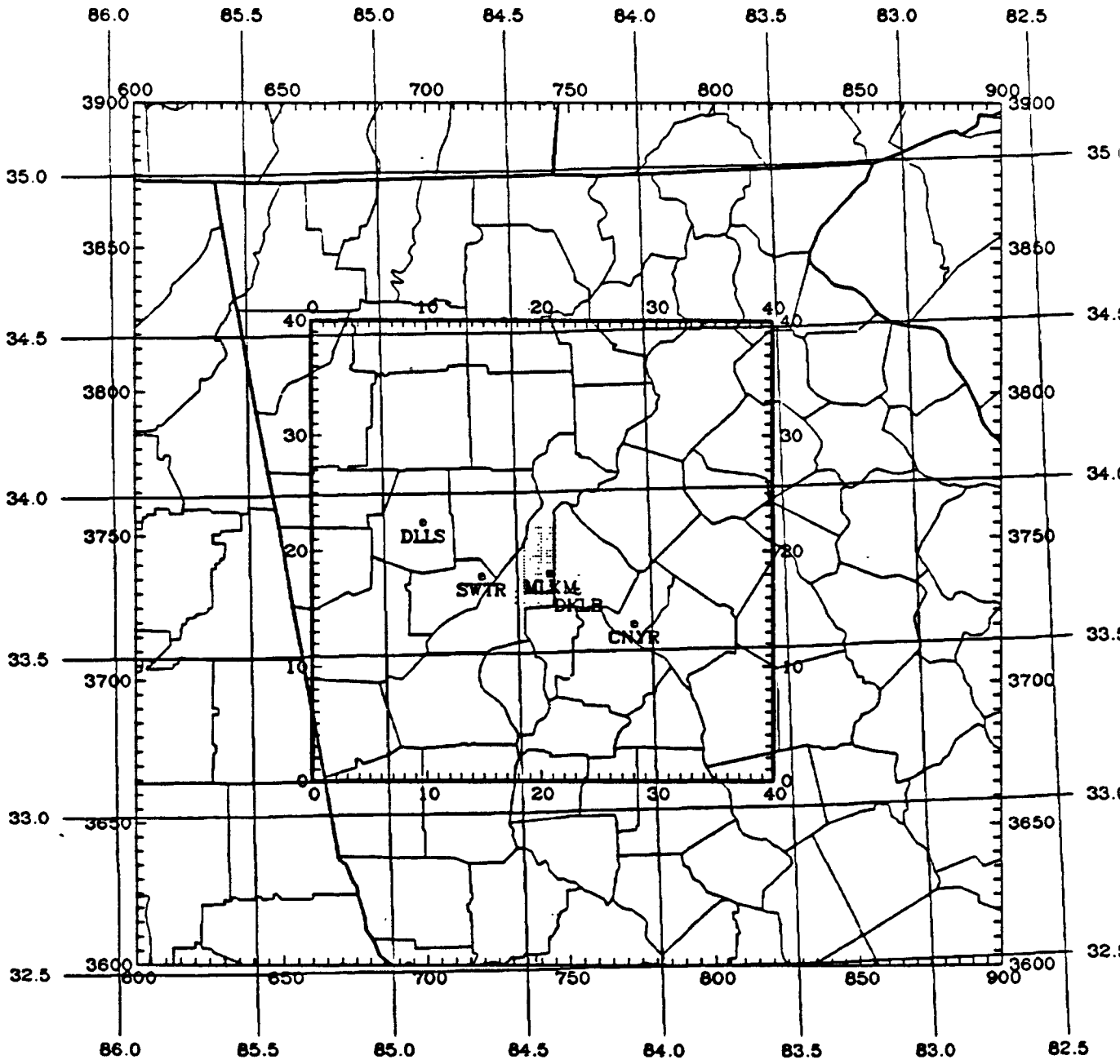

FIGURE 3-1. UAM modeling domain for Atlanta. Modeling domain consists of 40 by 40 array of 4 km grid cells with an origin at UTM coordinates 660 km easting, 3665 km northing, zone 16.

TABLE 3-2. Surface meteorological observation sites, locations, and variables in the Atlanta region.

Site Name	Location UTM (Zone 16) UTMX	UTMY	Variables Measured
Atlanta Hartsfield International Airport	739.580	3726.148	WS, WD, T, T_D, P
Dobbins Naval Air Station	729.590	3755.498	WS, WD, T, T_D, P
Fulton County (Charlie Brown) Airport	729.947	3740.709	WS, WD, T, T_D
Dekalb Peachtree Airport	749.724	3752.306	WS, WD, T, T_D
Conyers Monastery Monitor	772.248	3719.869	WS, WD
South Dekalb Panthersville Monitor	752.780	3730.991	WS, WD, T, T_D

TABLE 3-3. Upper-air observation sites, locations, and distance from Atlanta used in this study.

Site Name	Location Lat	Location Long	UTM Coordinates (Zone 16) UTMX	UTM Coordinates (Zone 16) UTMY	Distance from Atlanta (km)
Athens, GA	35° 57'	83° 19'	839.644	3763.429	109
Nashville, TN	36° 15'	86° 34'	538.182	4012.482	199
Greensboro, NC	36° 5'	79° 57'	1134.426	4016.946	491
Waycross, GA	31° 15'	82° 24'	937.394	3467.152	328
Centerville-Brent, AL	32° 54'	87° 15'	475.841	3640.638	275

TABLE 3-4. Ozone monitor names and locations.

Monitor JD	Monitor Name	UTM Location (Zone 16) UTMX	UTM Location (Zone 16) UTMY	Years Available (1984 - 1987)
130890002	DeKalb Jr. College (DKLB)	752.78	3730.99	1984 - 1987
130970002	Sweetwater Creek State Park (SWTR)	719.28	3736.10	1987
131210053	MLK Marta Station (MLKM)	743.10	3737.15	1987
132150008	Columbus Airport (COLO)	693.15	3799.91	1984 - 1987
132470001	Conyers Monastery (CNYR)	772.25	3719.87	1984 - 1987

There were no air quality data available near the boundaries of the modeling domain for use in prescribing boundary conditions.

PREPARATION OF UAM INPUT FILES

The following paragraphs describe how the UAM input files were prepared for the PLANR application of the UAM to Atlanta.

DIFFBREAK

This file contains the daytime mixing height or nighttime inversion height for each column of cells at the beginning and end of each hour of the simulation. Hourly mixing heights were estimated at several surface meteorological sites through use of the hourly surface measurements of temperature and the twice-daily upper-air observations from a representative upper-air site (Athens, Georgia). For three of the surface meteorological observation sites that recorded temperature (Fulton County Airport, Dobbins Air Force Base, and South Dekalb) the diurnal variations in mixing heights were calculated using the RAMMET meteorological processor. These hourly values were then input into the standard UAM mixing height interpolation program, DFSNBK (Ames et al., 1985b) using the 1/r interpolation option to produce the hourly spatially varying fields of mixing heights. The maximum daily mixing height varied from approximately 1200 to 1350 meters above ground across the region. Two of the surface observation sites that recorded temperature were not used in the generation of the DIFFBREAK file; one (Dekalb Peachtree Airport) had missing temperature data for 4 June 1984 and data from the other site (Atlanta Hartsfield International Airport) were not available in time to perform the mixing height analysis.

REGIONTOP

This file contains the height of each column of cells at the beginning and end of each hour of the simulation. If this height is greater than the mixing height, the cell or cells above the mixing height are assumed to be within an inversion. For the application of the UAM(CB-IV) to Atlanta a constant 1,400 m AGL region top was used. This value was picked because it is 50 m above the maximum mixing height; thus all five vertical layers of the UAM are contained within the well mixed layer, offering the maximum vertical resolution possible with the five-layer UAM configuration.

WIND

This file contains the x and y components of the wind velocity for every grid cell for each hour of the simulation. There are two steps in creating the wind fields for Atlanta: (1) application of the Diagnostic Wind Model (DWM) (Morris et al., 1988,

1989a; Douglas and Kessler, 1988) using 15 vertical levels and data from the six surface and five upper-air meteorological observation sites; and (2) vertical interpolation of the 15-layer hourly wind fields into the five-layer UAM configuration used for the Atlanta application (see Morris et al., 1989a).

The DWM creates an hourly 15-layer wind field by first creating a wind field by adjusting a domain-mean wind (based on upper-air observations) for terrain effects (kinematic effects, thermodynamically generated slope flows, blocking, and deflection). Then the observational information is added to the wind field by weighting the initial wind field heavily away from the observations and the observed winds heavily in the vicinity of the observations.

The 15-layer wind fields created by the DWM are then vertically averaged into the UAM five-layer configuration. Since the surface observations provide a more detailed representation of the air flows in the vicinity of Atlanta and their presence is only felt within the lowest layer of the DWM, the first UAM vertical layer was assumed to have the same wind field as the first DWM layer. The DWM first layer is also weighted 50 percent in the second UAM vertical layer. The wind fields for the remainder of the UAM vertical layers were obtained from the DWM wind fields using weighted averaging. The resultant five-layer wind field was then modified using the procedure suggested by O'Brien (1970), which minimizes the vertical velocity out of the top of the region. In this manner the boundary concentration assumed to exist above the region top (TOPCONC) does not greatly influence concentrations within the modeling domain.

For the application of the UAM to Atlanta, three separate wind fields were created for use in diagnostic simulations 1 and 2 and a sensitivity test reported in Appendix D. As will be discussed later, these wind fields were created using the procedures described above but differed in definition of the domain-mean wind and the surface observation sites used.

METSCALARS

This file contains the hourly values of the meteorological parameters that do not vary spatially. The NO_2 photolysis rates were calculated for the CB-IV mechanism using procedures described by Schere and Demerjian (1977) and actinic flux data collected by Bass and co-workers (1980). The concentration of water was based on measurements of temperature and dewpoint at three of the surface meteorological observation sites. These three values were averaged to obtain the hourly input for the UAM. Water concentrations ranged from approximately 14,000 to 18,000 ppm. An atmospheric pressure value of 1 atm was used.

Exposure class is a measure of near surface stability: +3 during high solar intensity to -2 at night with no clouds. Exposure class was assigned based on the solar intensity: a value of -2 at night and daytime values of from 0 (one hour day/night transi-

tion period) to 3. The temperature gradients below (TGRADBELOW) and above (TGRADABOVE) the inversion were based on the twice-daily upper-air soundings taken at Athens, Georgia, and hourly surface temperatures observed at Charlie Brown Airport. Values for TGRADBELOW from the surface to the mixing height (approximately 1300 m AGL) from the Athens evening sounding (1900 LST) are -0.0096, -0.0103, and -0.0107 K/m for June 2 through 4, respectively. Based on these measurements, values for TGRADBELOW were -0.0105 K/m for exposure classes 2 and 3, -0.01 K/m for exposure class 1, and -0.098 for exposure class 0.

The Athens morning sounding (0700 LST) measured values for TGRADBELOW of 0.018 and 0.030 K/m on June 3 and 4 respectively, assuming a mechanical mixing height of 250 m AGL. Observed temperatures at 250 m on 3 and 4 June were, respectively, 295.6 and 297.8 K. Nighttime hourly values for TGRADBELOW were then calculated for June 3 and 4 based on the surface temperature at the Charlie Brown Airport and the measured value at 250 m from the 0700 LST sounding.

For predawn hours, the temperature gradient from 250 m to the region top (1,400 m) from the 0700 sounding at Athens was used, resulting in values for TGRADABOVE of -0.0025 and -0.0075 °K/m for June 3 and 4, respectively. For daytime hours a temperature at the mixing height was calculated for each hour of the day using the surface measurement at the Charlie Brown Airport and the value for TGRADBELOW. Then the hourly temperature gradient between the mixing height and the region top was estimated using the calculated value at the mixing height and the measured temperature from the 0700 sounding at Athens at 1,400 m AGL (290.8 and 290.7 K on June 3 and 4, respectively)

AIRQUALITY

This file contains the initial concentrations of each species for each grid cell at the start of the simulation. Since the UAM was initiated at 12 noon on 3 June 1984, most of the material from the initial conditions were advected out of the region by the morning of 4 June; thus, initial concentrations do not influence ozone formation on 4 June. Accordingly, initial concentrations were assigned "clean values" as follows:

VOC	25 ppbc (using EKMA default speciation)
ISOP	0.001 ppb
NO_x	1 ppb (split 3/4 NO_2, 1/4 NO)
O_3	40 ppb
CO	200 ppb

BOUNDARY

This file contains the location of the modeling region boundaries. It also contains the concentration of each species that is used as the boundary condition along each boundary segment at each vertical level. For the first application of the UAM to Atlanta (diagnostic run 1), the minimum of a one-cell buffer of unsimulated cells was used (i.e., the boundary conditions), resulting in a simulation region of 152 km by 152 km. After examining the predicted ozone concentrations in diagnostic run 1 and the emissions distribution, we determined that the computational region for Atlanta could be reduced by about one-third without affecting the results. Thus for diagnostic run 2 and the sensitivity test (Appendix D) an 8-, 4-, 1-, and 3-cell buffer was used on the north, south, east, and west boundaries, respectively.

As will be discussed, two sets of boundary conditions were derived for evaluation runs number 1 and 2. For evaluation run number 1, "clean" values (listed previously) were specified for boundary conditions. However, these clean values may underestimate background concentrations because of the biogenic emissions which increase background VOC and ISOP (isoprene) concentrations above the clean background level. Thus in order to determine a better estimate of background conditions, a UAM simulation was carried out with no anthropogenic emissions (i.e., biogenic emissions and clean boundary concentrations only). During the day, isoprene and VOC concentrations ranged from approximately 0.5 to 2.0 ppb and 35 to 75 ppbC, respectively. Thus for the second diagnostic simulation, a 1 ppb ISOP boundary condition was prescribed and VOC boundary conditions were set at 40 ppbC; the increase from the clean value of 25 ppb was mainly (92%) due to the lower reactive PAR species and the remainder of the increase was due to increases in OLE. Boundary conditions for ozone (40 ppb) and NO_x (1 ppb) were the same as used in diagnostic run 1.

TOPCONC

This file contains the concentration of each species for the area above the modeling region. Since the wind fields are processed to eliminate the vertical velocity through the region top, the model results are not sensitive to TOPCONC. Accordingly, the clean concentration values listed previously were used.

TEMPERATUR

This file contains the hourly temperature for each surface layer grid cell. Hourly spatial varying temperatures were obtained by using 1/r interpolation from the surface meteorological observations.

EMISSIONS

This file contains the ground-level emissions of NO, NO_2, CB-IV VOC species categories, and CO for each grid square for each hour of the simulation. Anthropogenic emission estimates were obtained from the 1985 NAPAP county-wide emissions inventory through a multistep process that includes updating mobile source emissions from MOBILE-3 to MOBILE-4 based emission factors, applying summer weekday and episodic temperature adjustments, gridding of data using a known surrogate distribution, and speciation of the VOC and NO_x emissions into the CB-IV mechanism species (see Figure 2-8).

The NAPAP motor vehicle emission categories were split into exhaust and evaporative emissions using splitting factors from the MOBILE-3 emissions program and the same average temperature as was used in generating the NAPAP inventory. The MOBILE-4 emissions program was then exercised for the temperature conditions on 4 June 1984 to obtain day-specific evaporative and exhaust emissions. Estimates of running loss emissions (which are not included in the NAPAP inventory) were then obtained by applying the ratio of the running loss and exhaust emission factors to the mobile exhaust VOC emission rate from the NAPAP inventory.

The county-wide area source emissions were then mapped to the gridded modeling domain by assigning each area source Source Classification Code (SCC) to a known surrogate distribution (see SAI, 1989). Known surrogate distributions include: agriculture, urban, rural, and water from the national Geographical Information Services (GIS) land-use data base; population from the 1980 census; airports and limited access roadways based on digitizing the locations of airports and freeways from standard USGS maps; and spatial coverage based on the fractional coverage of each grid cell in each county. The gridded area source emissions were then adjusted to hourly emissions for a summer weekday and speciated into CB-IV species based on their SCC codes.

Estimates of biogenic VOC emissions were obtained from EPA's Atmospheric Research and Exposure Assessment Laboratory (EPA/AREAL) on a 1/4° longitude by 1/6° latitude grid for the entire Southeast. The EPA/AREAL had biogenic emission estimates for the entire Southeast for a two-week period during 1980. These emission estimates consider the effects of episodic temperature and solar intensity on the biogenic emission estimates. Based on analysis of surface temperatures, it was determined that 26 August 1980 provided the best match with episodic temperature and light intensity conditions of 4 June 1984. The biogenic emissions from the 1/4° by 1/6° grid were gridded onto the 4 km square grid cells used in the UAM modeling based on spatial covering of grid cells. The biogenic emissions from EPA/AREAL were already speciated into CB-IV species.

The final EMISSIONS file was obtained by merging the gridded NAPAP area source emissions with the low-level point sources and the biogenic emissions. The distribution of the resultant anthropogenic and biogenic emissions are given in Figure 3-2.

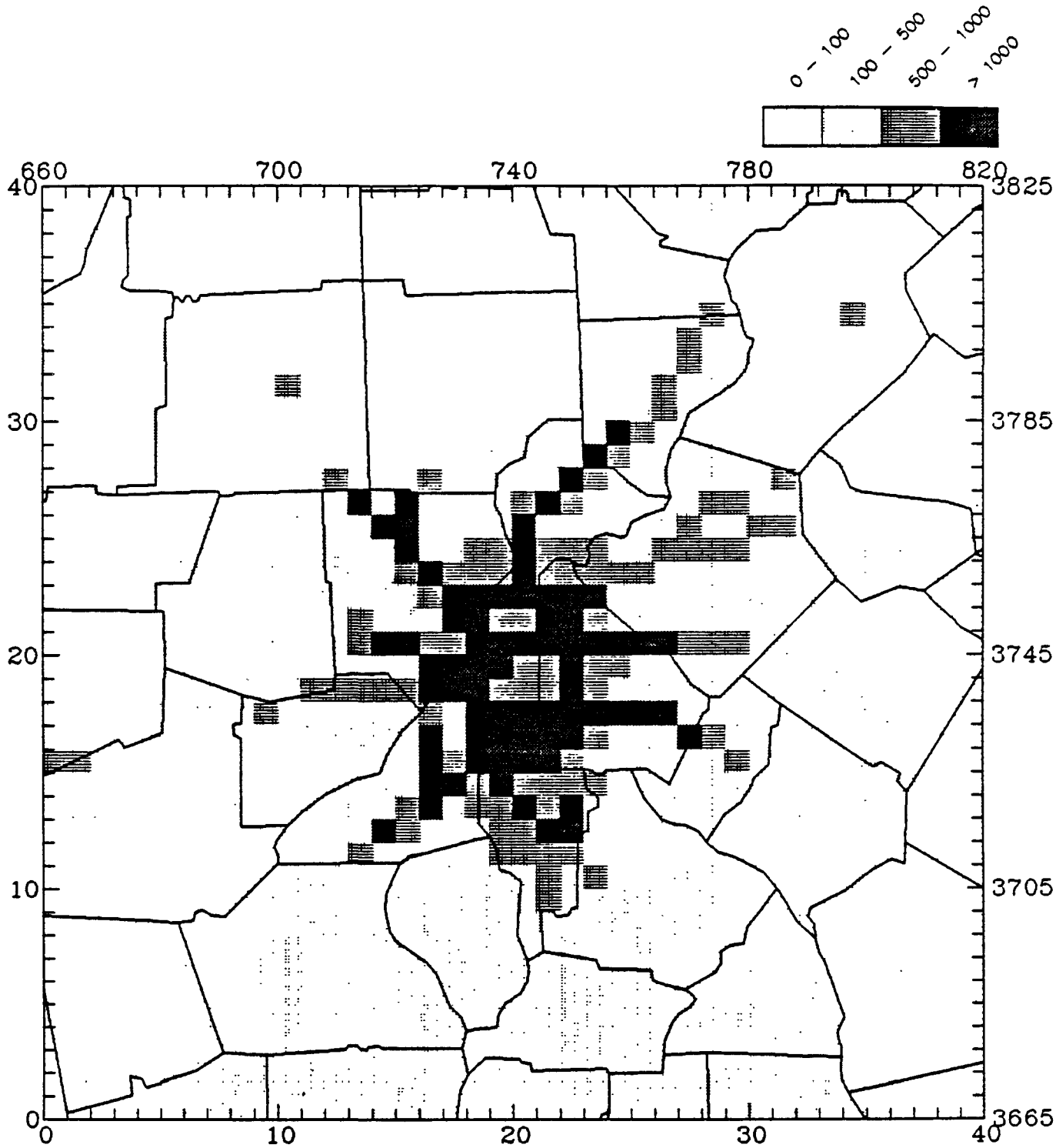

FIGURE 3-2a. Anthropogenic area source and low-level point source NO_x emissions (kg/day) for the Atlanta 1984 base case.

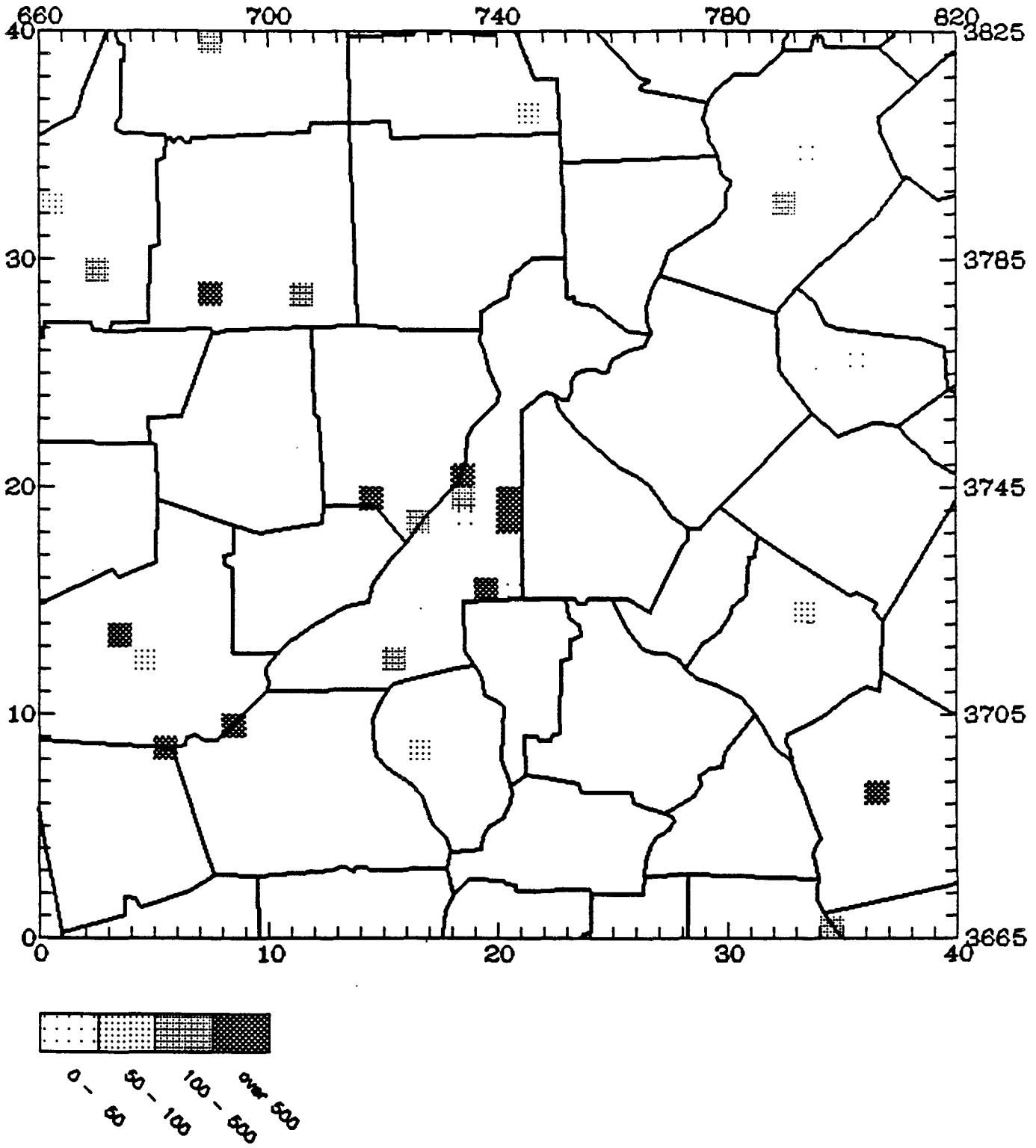

FIGURE 3-2b. Anthropogenic point source NO_x emissions (kg/day) for the Atlanta 1984 base case.

89104

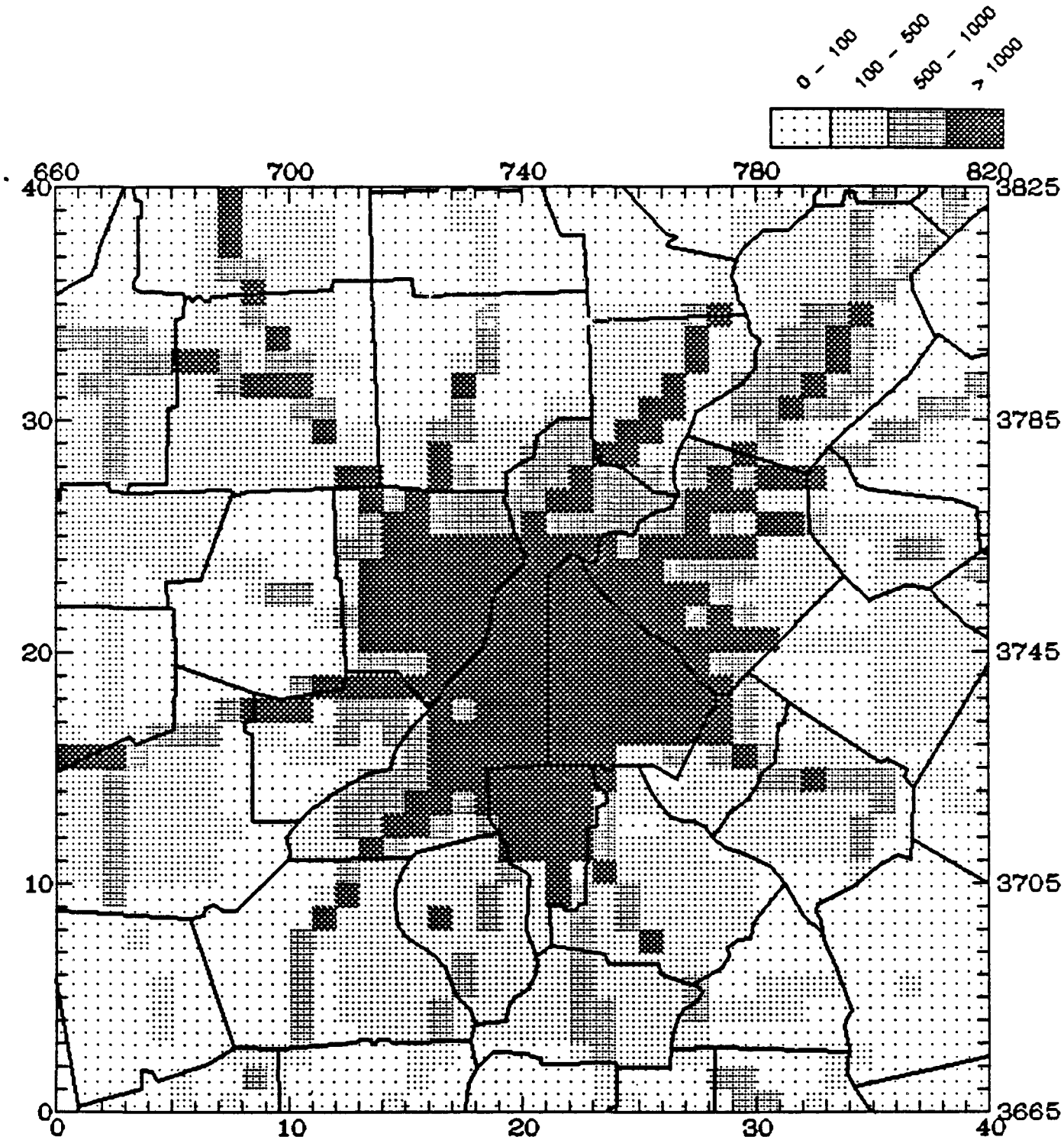

ATLANTA -- 1985 base -- anthropogenic only
RHC
(Kg/day)

FIGURE 3-2c. Anthropogenic area source and low-level point source VOC emissions (kg/day) for the Atlanta 1984 base case.

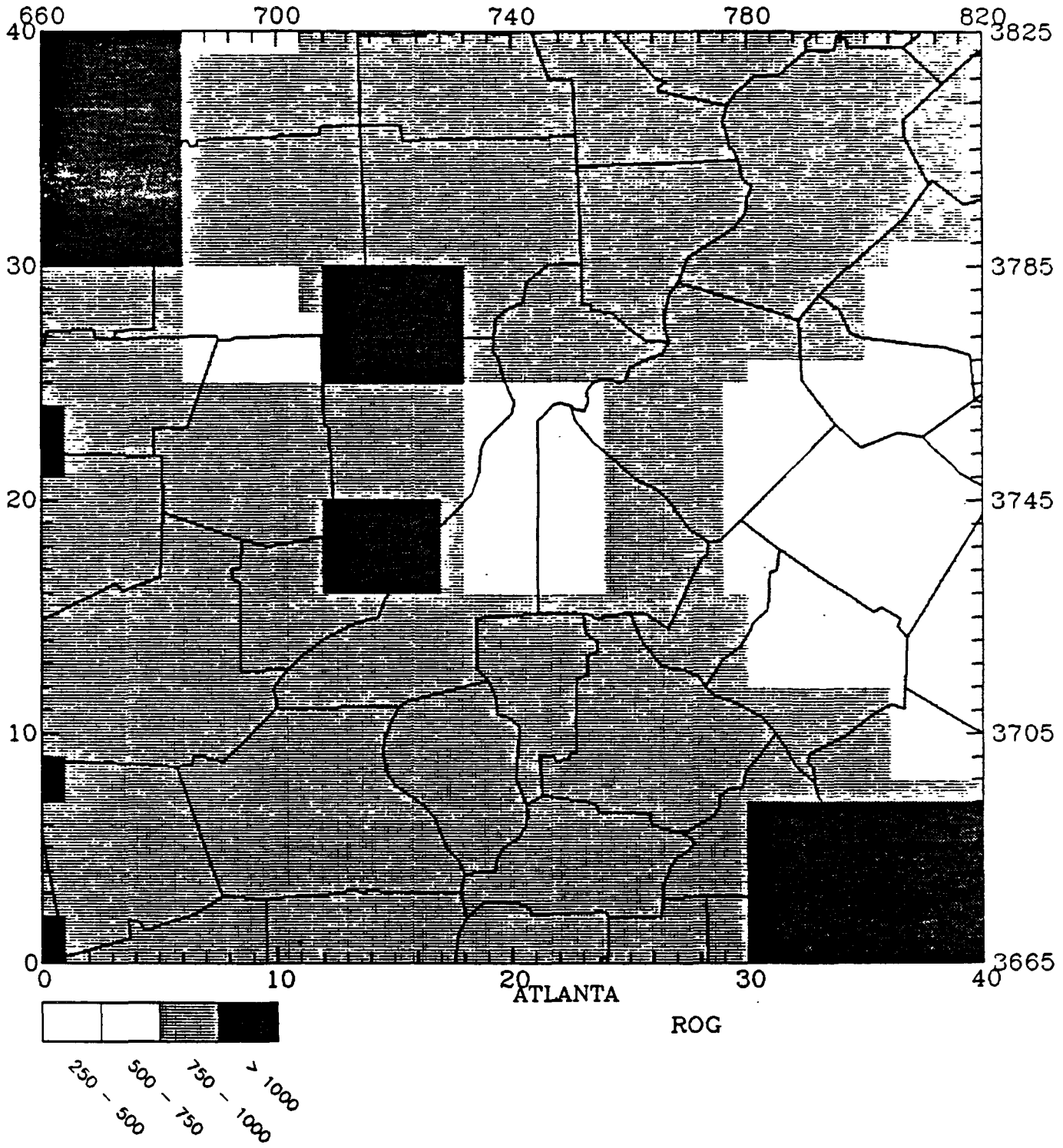

FIGURE 3-2d. Biogenic VOC emissions (kg/day) for the Atlanta 1984 base case.

89104

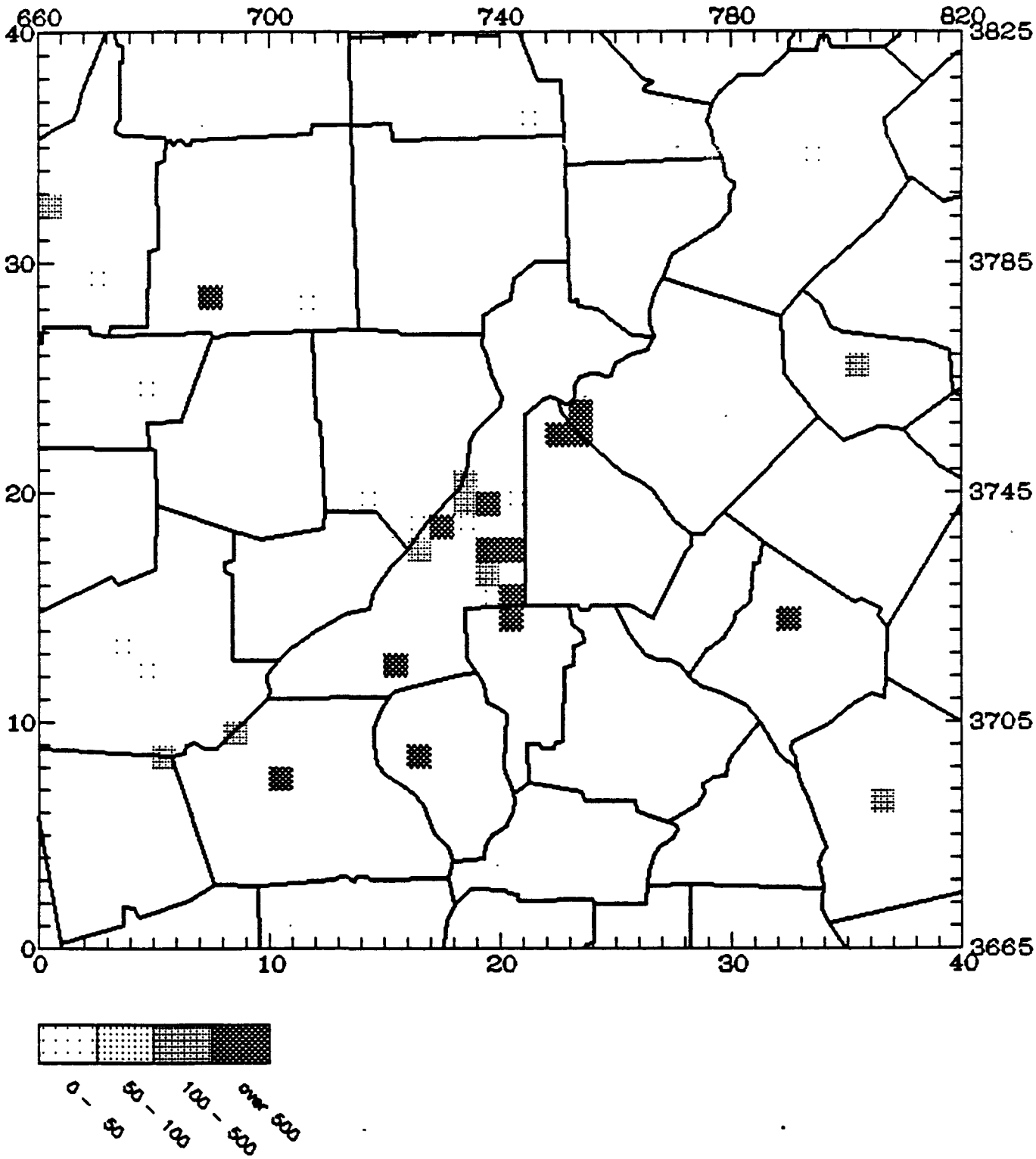

FIGURE 3-2e. Anthropogenic point source VOC emissions (kg/day) for the Atlanta 1984 base case.

89104

Of particular note is that biogenic VOC emissions account for approximately 60 percent of the VOC emissions within the modeling domain.

PTSOURCE

This file contains the point source information (stack height, temperature and flow rate, plume rise), the grid cell into which the emissions are emitted, and the emissions rates for NO, NO_2, CB-IV VOC categories, and CO for each point source for each hour. The 1985 NAPAP point source emissions file was separated into low-level and elevated points based on plume rise estimates. Those point sources whose plume rise was less than 25 m for typical atmospheric conditions were considered low-level sources and were merged with the EMISSIONS file after applying the summer weekday and diurnal emission profiles supplied as part of the NAPAP point source inventory.

Elevated point sources from the 1985 NAPAP point source file were adjusted to summer episodic conditions with diurnal variation using the adjustments given in the point source file. The emissions were then speciated into CB-IV species based on their SCC and SIC codes. The resultant data was run through the UAM point source preprocessor for input to the UAM. Of particular note is that point source NO_x (including electrical utilities) emissions account for almost 50 percent of the total NO_x emissions within the modeling domain.

TERRAIN

This file contains the value of the surface roughness and deposition factor for each grid square. Each 4 km^2 grid cell was assigned to a land-use category based on a digitized standard USGS map of the modeling region. The land-use categories were then converted to roughness lengths and vegetation factors according to data published by Argonne National Laboratory (see Morris et al., 1989a).

CHEMPARAM

This file contains information regarding the chemical species to be simulated, including reaction rate constants, upper and lower bounds, activation energy, and reference temperature. Reaction rate constants correspond to those given in the report documenting the CB-IV mechanism (Gery, Whitten, and Killus, 1988), except that reactions for methanol (MEOH) and ethanol (ETOH) have also been added to the mechanism (see Morris et al., 1989a).

DEFINITION OF BASE CASE

One of the key components of the PLANR use of the UAM is the development of a statisfactory base case simulation within a limited number of diagnostic simulations. However, the UAM base case must show some skill in replicating the observations, otherwise one would not have confidence in the model's responses to alternative emission control strategies. A minimal performance goal in the past was to have the predicted regional maximum ozone concentration be within 30 percent and in the general location of the peak observed value. Model performance has been considered good if the predicted peak ozone is within 15 percent. Clearly, when model inputs are based only on sparse routine data, rather than intensively measured data as in the past, model performance cannot be expected to always be as good in the past. However, there should be some minimal expectations of model performance since incorrect characterization of base case ozone concentrations may lead to incorrect calculations of ozone reductions due to alternative emission inputs.

The protocols for several recent UAM studies of the impacts of California offshore drilling emissions (Haney et al., 1986; Yocke et al., 1985) defined a minimal model performance standard as follows: (1) the UAM-predicted regional maximum ozone concentration should be within 20 percent and in the general location of the observed maximum, and (2) the UAM predicted maximum at the location of the observed maximum should be within 30 percent of the observed value.

We adopted this model performance standard as a performance goal for the PLANR application of the UAM for Atlanta and Dallas-Fort Worth. However, model evaluation should always include consideration of whether the right answer is being obtained for the right reason. Here we will also discuss approaches that may improve UAM performance but which also may deviate slightly from the demonstration of the PLANR use of the UAM. The PLANR use of the UAM for Atlanta involved three diagnostic simulations before a base case was obtained that satisfied the minimal performance goal. A sensitivity test was also performed (Appendix D).

Diagnostic Run 1

In the first diagnostic simulation, the UAM was exercised with clean boundary conditions (i.e., 40 ppb ozone, 25 ppbc VOC, 0.001 ppb ISOP, and 1 ppb NO_x), anthropogenic and biogenic emissions, and a first estimate of the wind field. The wind field was created using the DWM: the vertically varying domain-mean wind was defined as the vector average from the five upper-air soundings surrounding the modeling domain. The upper-air data obtained from the National Climatic Data Center (NCDC) on the TD9743 format was missing data from the lowest 1,500 m AGL of the 0700 June 4 sounding at Athens, Georgia. In addition, surface wind data was used from all of the surface sites, except Atlanta Hartsfield Airport, which was inadvertently left out of the initial analysis.

Hourly average predicted ozone concentrations for diagnostic run 1 are contained in Appendix B. A comparison of predicted versus observed hourly ozone concentrations for the three monitors within the UAM modeling domain is shown in Figure 3-3. As seen in Appendix B and Figure 3-3, the regional maximum predicted ozone concentration is 13.54 pphm, within 8 percent of the observed maximum of 14.7 which was recorded at the Conyers Monastery (CNYR) ozone monitor. However, the predicted regional maximum is approximately 28 km (7 grid cells) to the north-north-west of the observed value. The maximum predicted ozone at the CNYR site for diagnostic run 1 is 8.79 pphm, an approximate 40 percent underprediction of the observed maximum at that site. Model performance is better at the South Dekalb ozone monitor, where the maximum daily observed value of 13.0 pphm is reproduced to within 15 percent (11.1 pphm). However, concentrations are underpredicted at the Dallas (DLLS) ozone monitor, which lies upwind of the city of Atlanta. The maximum daily observed ozone concentration at DLLS of 7.8 pphm is underpredicted by about 60 percent (4.6 pphm).

Diagnostic Run 2

Improvements Over Diagnostic Run 1

An analysis of the observed ozone features for 4 June 1984 indicates two major deviations of the predictions from the observations for diagnostic run 1: (1) the gross underprediction of the upwind monitor indicates that the ozone and ozone precursor loadings upwind of Atlanta are too low; and (2) the predicted cloud of elevated ozone concentrations appears to be too far north during the afternoon of 4 June 1984.

The fact that diagnostic run 1 is underpredicting the ozone at the upwind (DLLS) monitor is not surprising since clean background concentrations were used for the upwind boundary conditions. In particular, given the presence of biogenic VOC emissions in the area, the boundary VOC concentrations used in diagnostic run 1 (25 ppbc VOC; 0.001 ppb ISOP) are probably too low. In order to determine the magnitudes of VOC concentrations to use as boundary conditions, a UAM simulation without the anthropogenic emissions (i.e., biogenic emissions and clean boundary conditions only) was performed. This simulation of biogenic emissions only produced a maximum buildup of ISOP and VOC concentrations that ranged across the modeling domain from, respectively, 0.5 to 2.0 ppb and 35 to 75 ppbC. Thus we chose values a little lower than the midpoint of the maximum buildup, 1 ppb for ISOP and 40 ppbC for VOC, as boundary conditions in diagnostic run 2.

An examination of the observed ozone concentrations at the DLLS monitor on 4 June 1984 (see Figure 3-3) reveals that the observed maximum daily ozone concentration of 7.8 pphm occurs fairly early in the day (12 noon). This suggests that the peak observed ozone concentration at DLLS is mainly due to entrainment of ozone concentrations aloft as the mixing height rises rather than to local production of ozone

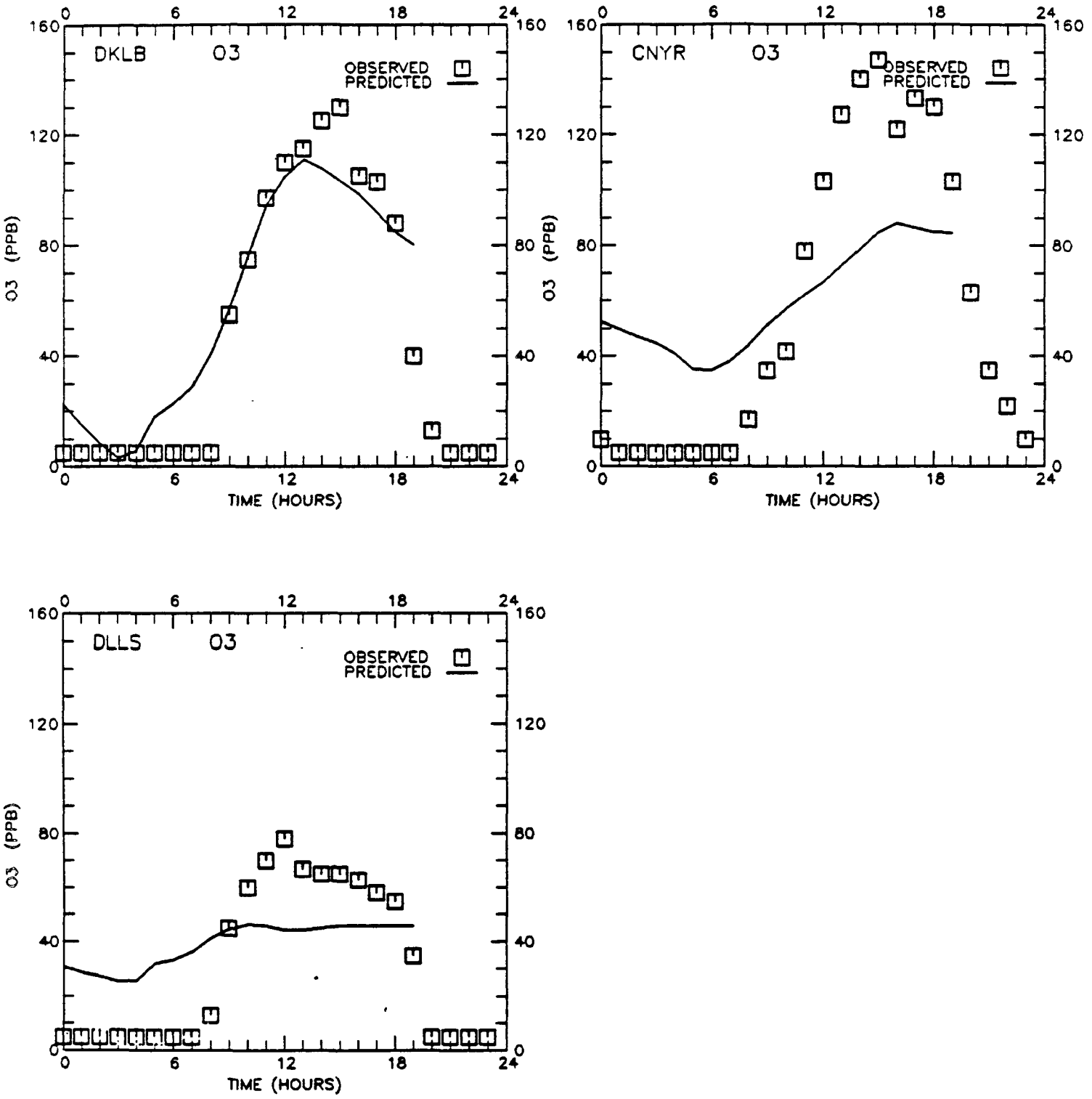

FIGURE 3-3. Observed and predicted ozone concentrations (ppb) . for the Atlanta diagnostic run 1.

due to local sources. Thus the boundary concentrations for ozone, and possibly NO_x, could justifiably be increased. However, we elected to keep the fairly low values for ozone and NO_x boundary conditions (40 and 1 ppb, respectively) for diagnostic run 2.

An examination of the observed winds, the predicted wind fields in diagnostic run 1 (see Morris et al., 1989b), and patterns of predicted hourly ozone concentrations (Appendix B) indicates that a southerly component in the wind field may occur too early in the afternoon. The persistence of a more northerly component in the winds in the late morning and early afternoon would result in the predicted cloud of elevated ozone concentrations impacting the CNYR monitor, producing a higher peak at that site. However, the wind measurements at the CNYR site observed southerly winds from about noon on. To determine whether this southerly wind was due to local effects or larger-scale flow features, the Georgia State meteorologist was consulted. The CNYR wind observation site is located near a grove of trees and may not be representative of mesoscale wind flows, and the Atlanta Hartsfield Airport wind observation site (which was inadvertently left out of the original analysis) was better sited (D. Kemmerick, personal communication, 1989). Thus, the CNYR wind measurement was eliminated and the Atlanta Hartsfield Airport winds added for the next diagnostic run.

A new definition of the domain-mean wind was also used for the diagnostic run 2. Instead of a linear interpolation to the hour in question of a vector average of the five twice-daily upper-air soundings that surround Atlanta, most of which are over 200 km away, the Athens Georgia upper-air sounding alone was used to define the domain mean wind. Wind data for the lowest 1,500 m of the 4 June sounding at 1900 LST was supplied by the state of Georgia.

A further modification was made on the boundary definition in diagnostic run 2. An examination of the spatial distribution of emissions (Figure 3-2) and the predicted hourly ozone concentrations from diagnostic run 1 (Appendix B) indicated that portions of the northern, southern, and western portions of the modeling domain could be eliminated without affecting the results. The boundary was thus modified and diagnostic run 1 was rerun to verify that the new boundary did not affect the computations.

Results of the Simulation

Diagnostic run 2 differed from run 1 in that (1) a higher VOC value was used (40 compared to 25 ppbC) and higher ISOP boundary conditions were used (1 compared to 0.001 ppb); (2) the domain-mean wind for the DWM came from the Athens upper-air sounding rather than a vector average from the five upper-air soundings; (3) the CNYR surface wind measurement was eliminated and the Atlanta Hartsfield wind measurement added to the analysis; (4) a minor mistake in the emissions inventory was corrected; and (5) the boundary was modified. The new UAM layer 1 wind fields generated for diagnostic run 2 is discussed in Morris et al., (1989b). The resulting

predicted hourly ozone concentrations for evaluation run 2 are given in Appendix C. The predicted regional maximum ozone concentration is 13.2 pphm, within approximately 10 percent of the observed maximum. The predicted maximum ozone is approximately 22 km to the north of the observed maximum ozone. However, as shown in Figure 3-4, at the location of the peak observed ozone, the maximum observation is replicated to within less than 30 percent. In addition, the daily maximum observed ozone concentrations at the DKLB and DLLS monitor are reproduced to within, respectively, 18 and 36 percent.

Comparison of UAM grid cell-average concentrations with the point observations at the site of the observed ozone is a particularly stringent test. A slight incorrect characterization of the wind field, as is very likely when sparse data sets are used, will result in the placement of the elevated ozone plume away from the ozone monitor resulting in poor model performance statistics. However, this displacement of the ozone plume may not affect the model's response to emission control requirements. Thus it has been suggested that concentrations in adjacent grid cells (i.e., nearest neighbor) also be compared with the observed value in order to determine whether the ozone cloud is just slightly displaced (Seinfeld, 1988a; Burton, 1988). Figures 3-5 and 3-6 compare the observed and predicted hourly ozone concentrations resulting from a one-cell and two-cell search of the predicted concentrations closest to the observed values. At the CNYR monitor the predicted maximum daily ozone concentrations for the point, a one-cell search, and a two-cell search match the observed value of 14.7 pphm to within, respectively, 29, 25, and 22 percent. However, at the other two monitors (DKLB and DLLS), the nearest-neighbor analysis also produced improvements in model performance; the point, one-cell search, and two-cell search match the peak observed observation to within 18, 8, and 5 percent for the DKLB monitor, and 36, 32, and 23 prcent for the DLLS monitors. For the CNYR monitor, it appears the elevated cloud of ozone concentrations is too far north. At the DKLB monitor the predicted ozone concentrations in the general vicinity (i.e., within two grid cells) are in very good agreement with the observed maximum values.

Figure 3-7 shows a scatter plot and model performance statistics between predicted and observed hourly ozone concentrations for diagnostic Run 2. Also contained in Figure 3-7 are analyses of the residuals of the predicted and observed ozone concentrations. As indicated in Figure 3-7 and the time series plots in Figure 3-4, diagnostic run 2 tends to overpredict the nighttime ozone concentrations and underpredict the peak daytime values. As a result, the bias of predicted hourly ozone concentrations is very low (less than 1 percent). However, the gross error (average absolute error) is fairly high (43 percent). The predicted hourly ozone concentrations for diagnostic run 2 follow the diurnal and spatial variations of the observations well, as indicated by the high correlation coefficient of 0.9. Nevertheless, even when all time and space constraints are removed, the simulated peak ozone value (13.2 pphm) is 10 percent less than the observed peak (14.7 pphm).

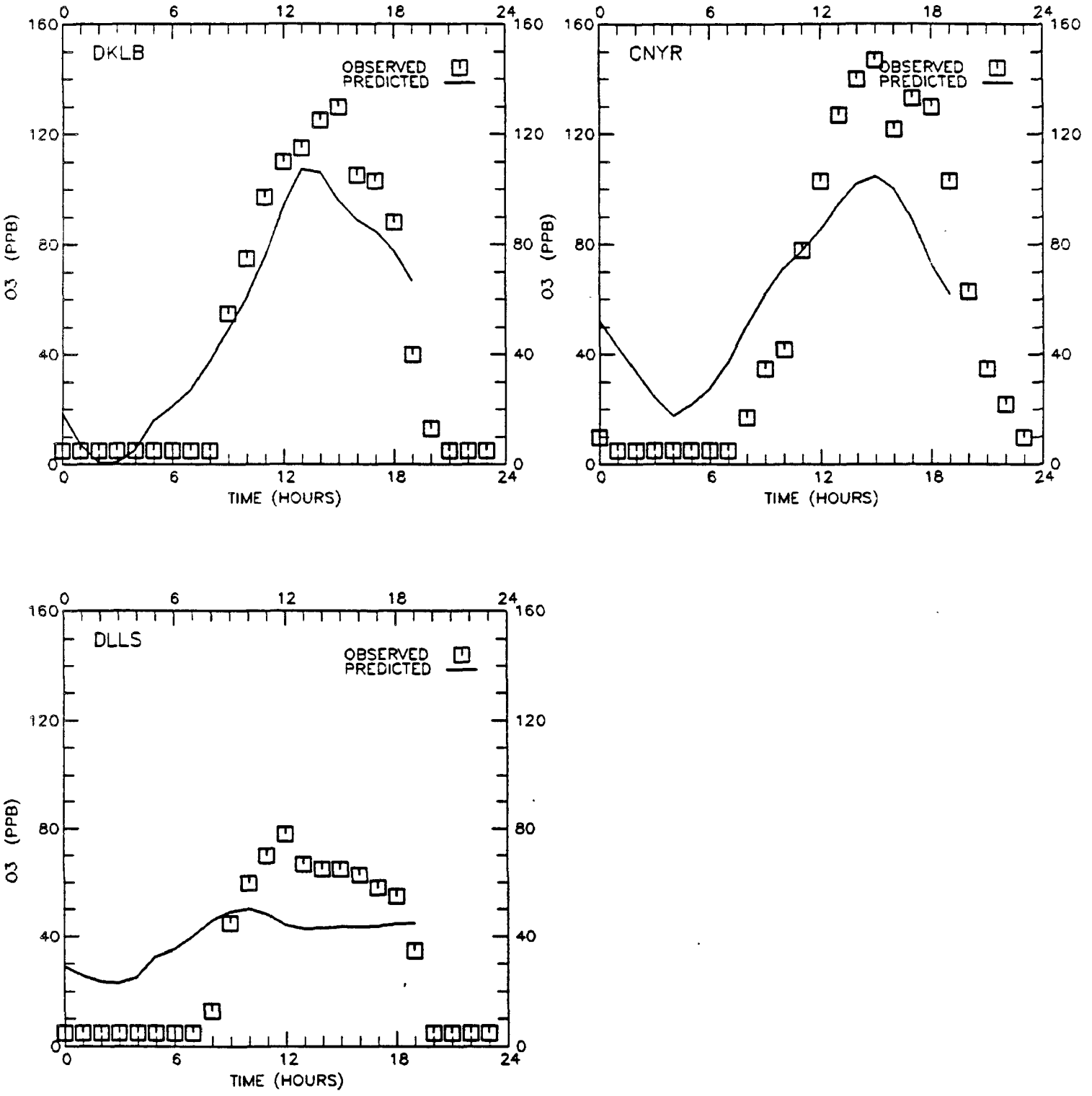

FIGURE 3-4. Observed and predicted ozone concentrations (ppb) for the Atlanta diagnostic run 2.

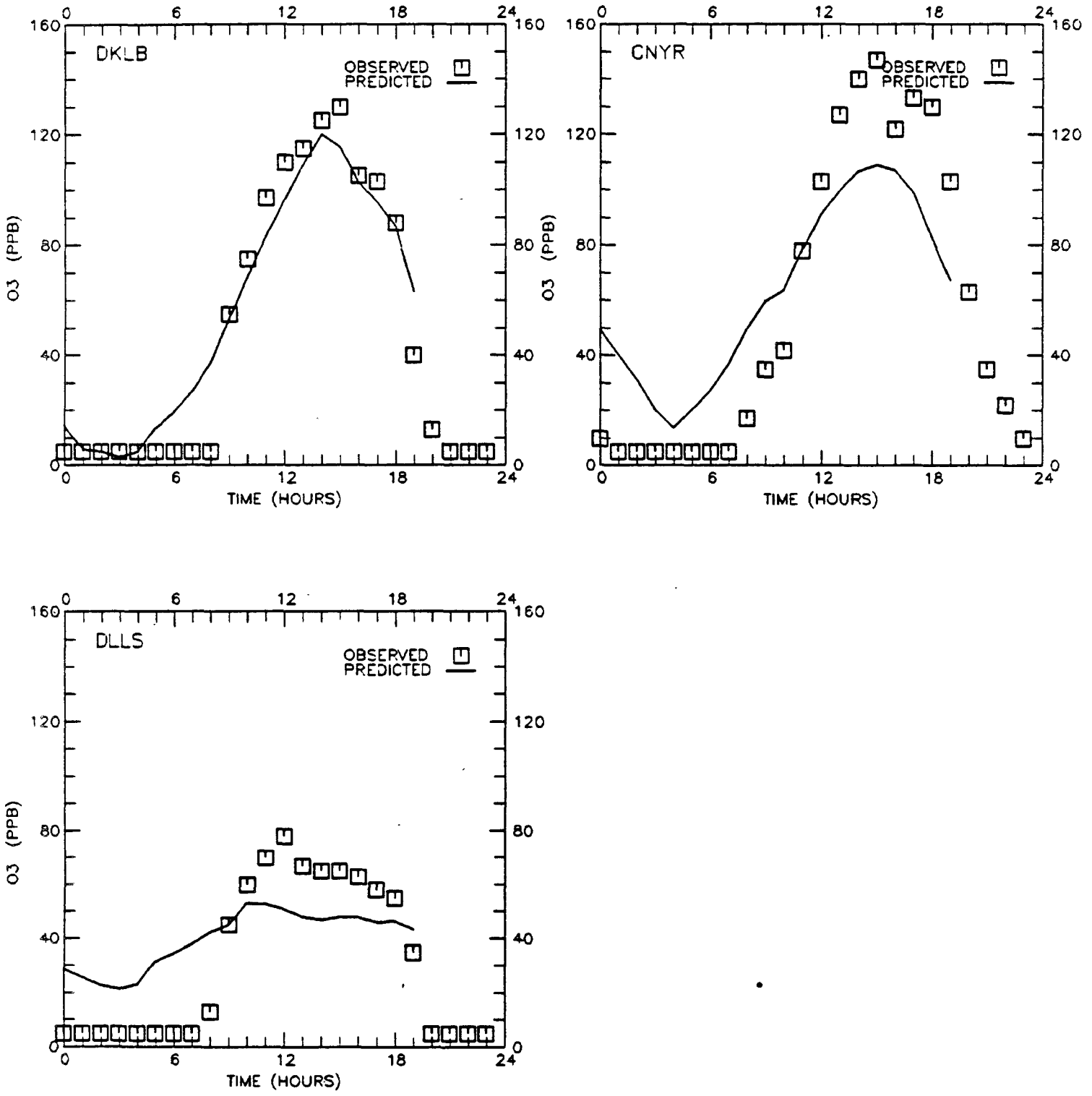

FIGURE 3-5. Observed and nearest-neighbor predicted (one-cell search) ozone concentrations (ppb) for the Atlanta diagnostic run 2.

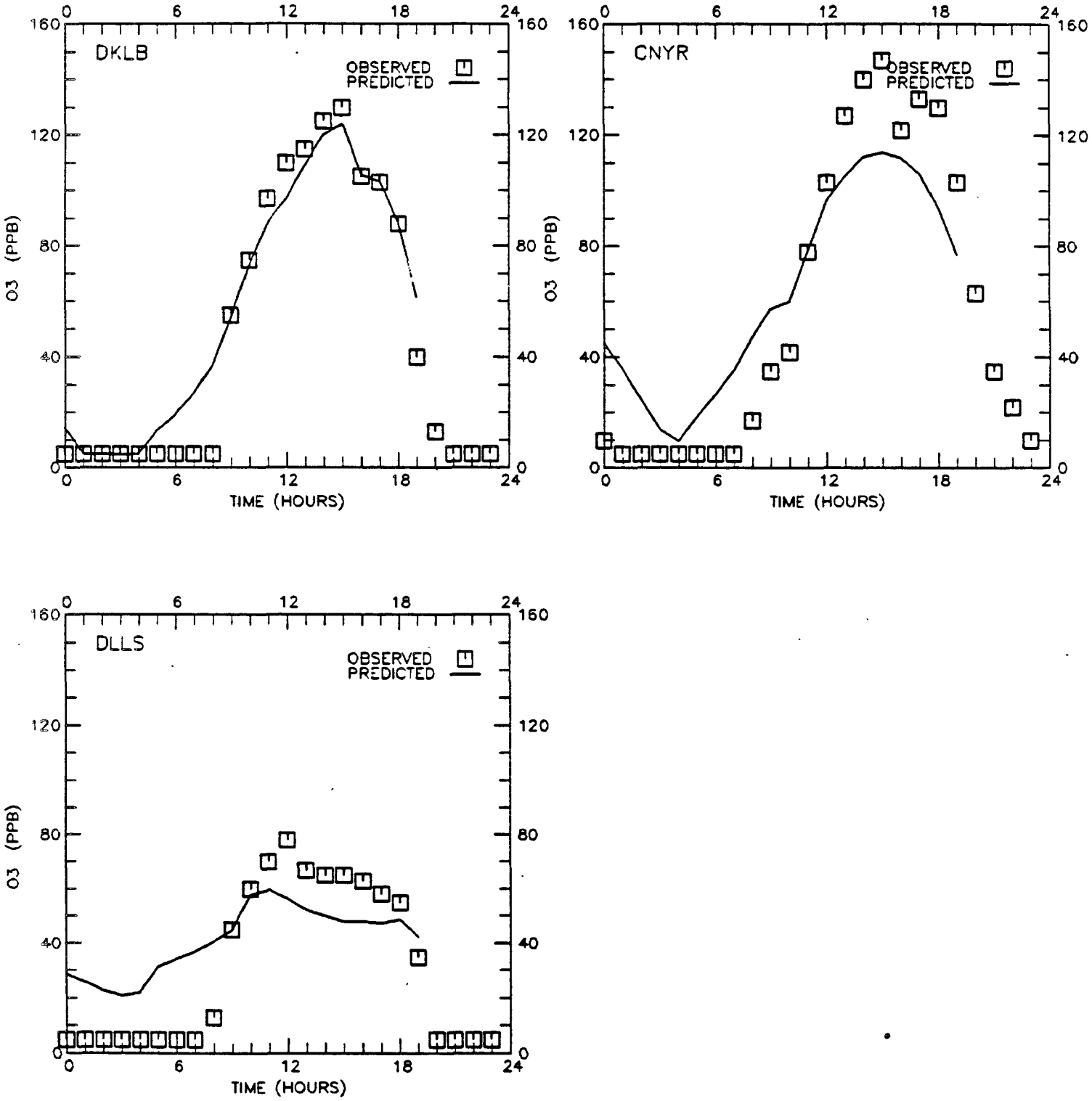

FIGURE 3-6. Observed and nearest-neighbor predicted (two-cell search) ozone concentration (ppb) for the Atlanta diagnostic run 2.

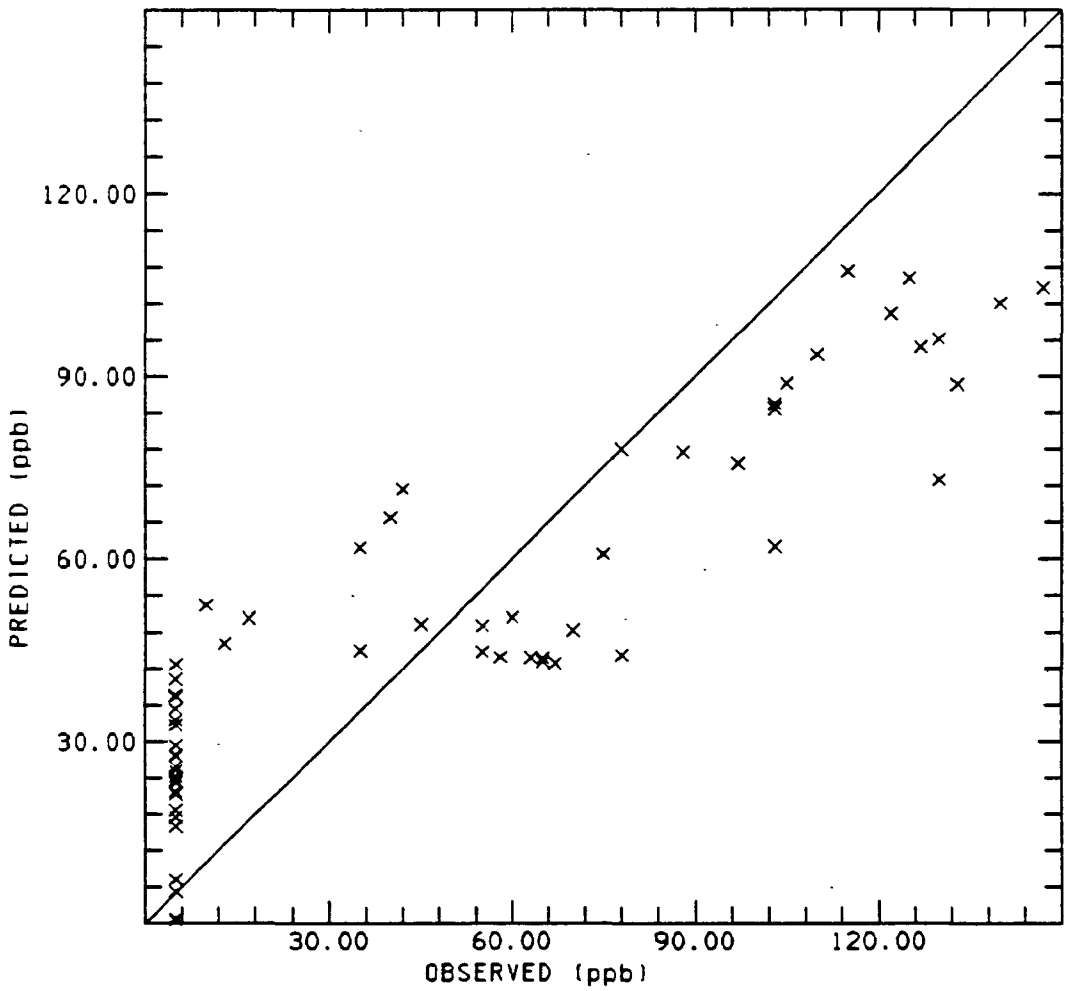

MOMENTS OF THE PROBABILITY DENSITY FUNCTION

	OBSERVED	PREDICTED
AVERAGE	50.39999	50.88372
STANDARD DEVIATION	47.63355	29.03820
SKEWNESS	0.51320	0.36600
KURTOSIS	-1.22432	-0.88317
OTHER MEASURES		
MEDIAN	40.00000	44.24000
UPPER QUARTILE	88.00000	72.92999
LOWER QUARTILE	5.00000	27.54000
MINIMUM VALUE	5.00000	0.53000
MAXIMUM VALLE	147.00000	107.30000

SKILL OF PREDICTION PARAMETERS

CORRELATION COEFFICIENT OF PREDICTED VERSUS OBSERVED 0.896
THE BOUNDS OF THE CORRELATION AT THE CONFIDENCE LEVEL OF 0.050 ARE
LOW BOUND 0.831 HIGH BOUND 0.937
RATIO OF OVER TO UNDER PREDICTIONS 1.069
PERCENT OF OVER PREDICTIONS GREATER THAN 200 PERCENT OF THE OBSERVED 38.333
PERCENT OF UNDER PREDICTIONS LESS THAN 50 PERCENT OF THE OBSERVED 3.333

FIGURE 3-7a. Scatterplot and model performance statistics for predicted and observed hourly ozone concentrations for the Atlanta diagnostic run 2 (N = 60).

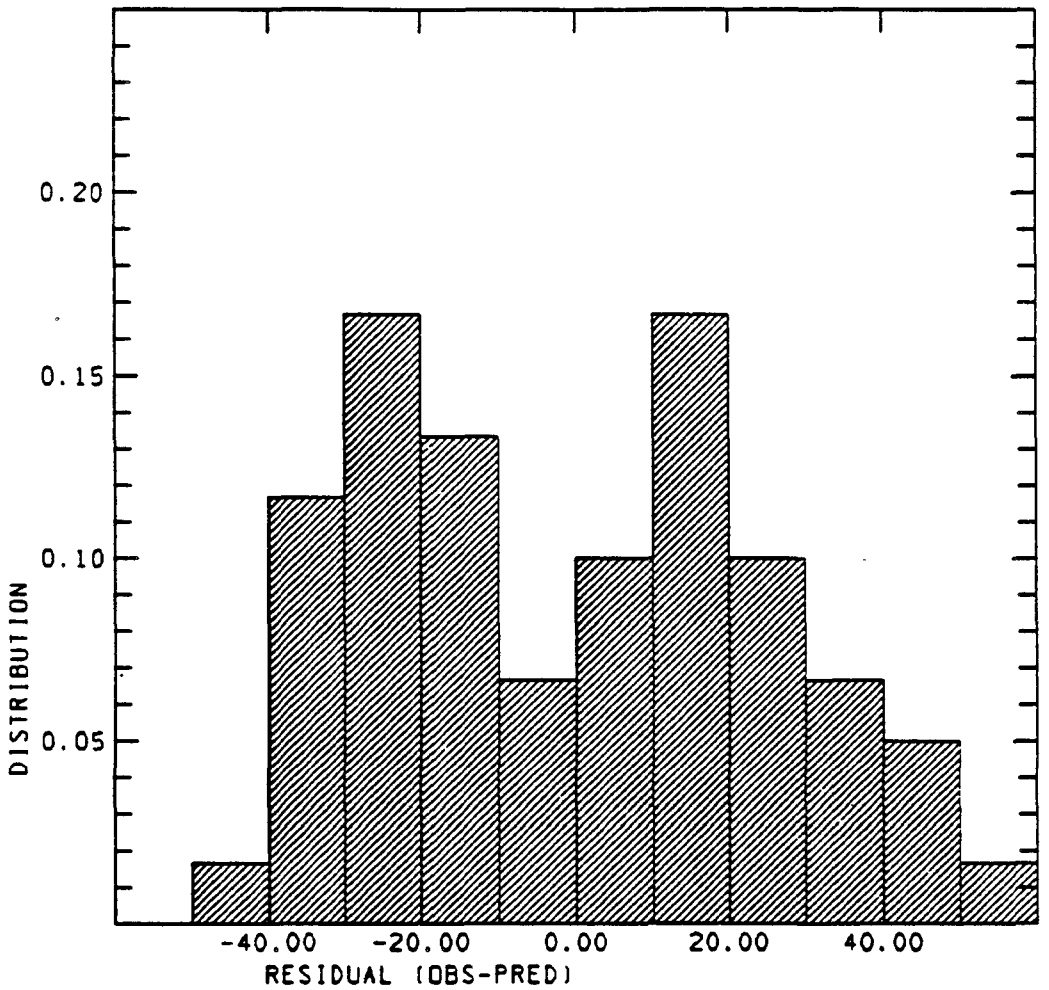

THE BINSIZE EQUALS 10.000

RESIDUAL ANALYSIS

AVERAGE	-0.48384
STANDARD DEVIATION	25.16143
SKEWNESS	0.20968
KURTOSIS	-1.08769
OTHER MEASURES	
MEDIAN	-0.21000
UPPER QUARTILE	18.80000
LOWER QUARTILE	-22.82000
MINIMUM VALUE	-42.45000
MAXIMUM VALUE	57.07001

BIAS CONFIDENCE INTERVAL
AT THE 0.0500 LEVEL
LOWER BOUND -12.5186
UPPER BOUND 11.5509

STD RESIDUAL CONFIDENCE INTERVAL
AT THE 0.0500 LEVEL
LOWER BOUND 480.3294
UPPER BOUND 879.6230

THE MEASURES OF GROSS ERROR
THE ROOT MEAN SQUARE ERROR IS 24.96
THE AVERAGE ABSOLUTE ERROR IS 21.88

VARIOUS MEASURES OF RELATIVE VARIABILITY
OBSERVATION COEFFICIENT OF VARIATION
0.9451
RESIDUAL COEFFICIENT OF VARIATION
0.4992
RATIO OF RESIDUAL TO OBSERVED ST. DEV.
- 0.5282

FIGURE 3-7b. Residual analysis of observed minus predicted hourly ozone concentrations for evaluation run 2 (N = 60).

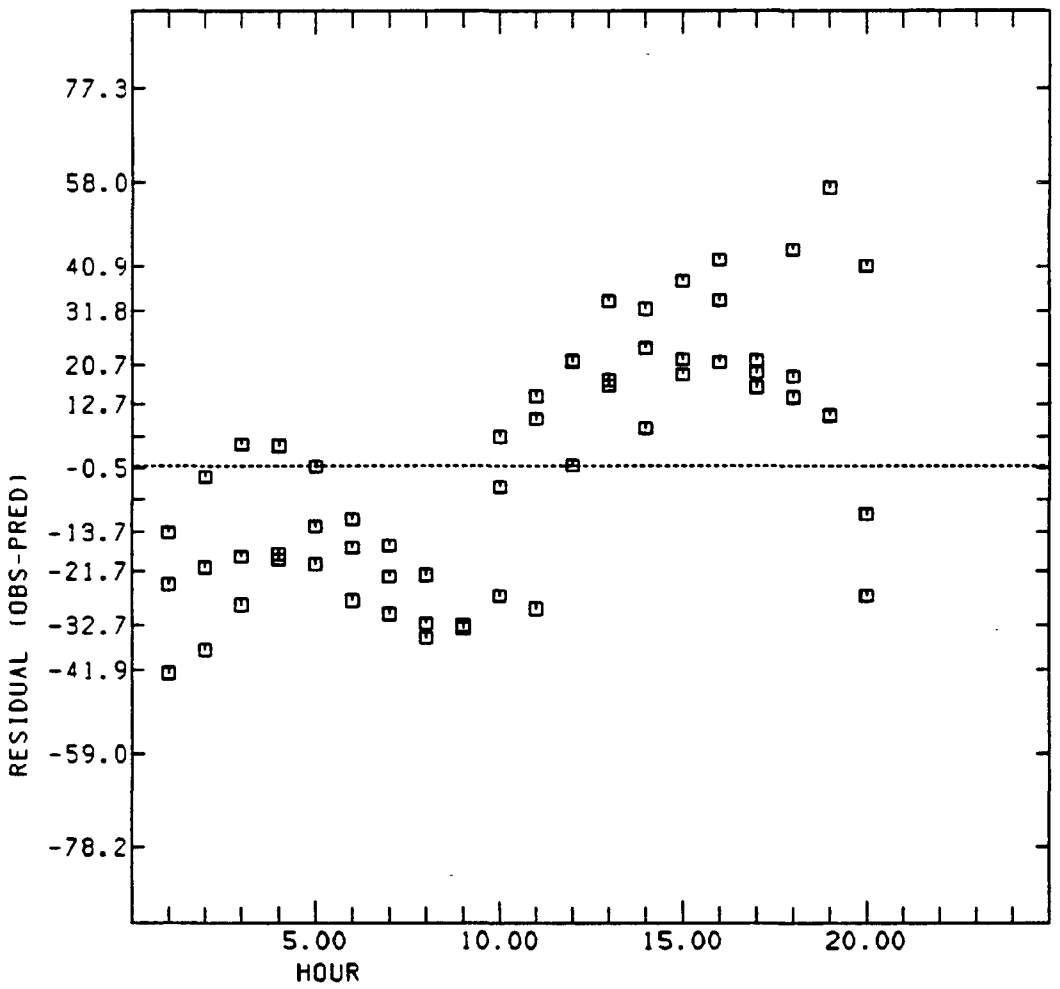

THE LINEAR MODEL PARAMETERS
THE CORRELATION IS 0.6804
THE LOWER BOUND IS 0.5155
THE UPPER BOUND IS 0.7967
AT THE 0.0500 PERCENT LEVEL
THE Y-X LINEAR MODEL INTERCEPT IS 10.576
THE Y-X LINEAR MODEL SLOPE IS 0.157
THE X-Y LINEAR MODEL INTERCEPT IS -31.398
THE X-Y LINEAR MODEL SLOPE IS 2.944

FIGURE 3-7c. Plot of residuals versus time of day for evaluation run 2 (N = 60).

89104

Possible Improvements to Diagnostic Run 2

Improvements in model performance from diagnostic run 2 could be obtained by raising the VOC, NO_x, and ozone boundary conditions, which may be justified based on the underprediction of the ozone at the upwind monitor (DLLS) and the low values current being used. The peak observed ozone concentration at the upwind monitor occurs fairly early in the day (12 noon), which indicates it is probably due to entrainment of an elevated ozone concentration aloft rather than local chemistry.

Improvements can also be made in the wind field. The wind field still has a significant southerly component in the late morning and afternoon, which appears to advect the elevated ozone cloud away from the CNYR monitor. Some wind shear is also present between UAM layers 1 and 2, which broadens the ozone peak from the urban emissions, resulting in a lower predicted regional maximum ozone concentration. Since in the afternoon UAM layers 1 and 2 are both contained within the well-mixed layer, one would not expect there to be significant amounts of wind shear between these layers. As noted earlier, during 4 June 1984 a high-pressure ridge passed across Atlanta, which resulted in a turning of the winds from the NNE to the SSW. This turning is present in the 0700 and 1900 LST upper-air soundings at Athens, but the exact hours of the turning of the upper-level winds cannot be determined from the hourly surface wind measurements, which are subjected to local influences. The use of linear interpolation of the 0700 and 1900 LST soundings at Athens results in a continuous turning of the wind throughout the day, when in actuality it probably occurs within a few hours as the high-pressure ridge passes through. If the upper-level winds persist with a more northerly component during the morning hours, as is present in the 0700 Athens sounding, and then turns to the SSW in the afternoon, the elevated ozone cloud could then possibly impact the CNYR monitor at the proper time. In addition, use of identical wind fields in layers 1 and 2 during periods of rapid vertical mixing to eliminate the wind shear below the mixing height may result in a sharper predicted peak concentration; the Athens upper-air sounding does support the presence of some wind shear in the mixed-layer.

Another possible explanation for the underprediction of the observed ozone peak at Conyers is that the 1985 NAPAP inventory may underestimate the amount of VOC emissions. There are still many uninventoried sources whose individual emissions may be small, but when combined together may produce a significant impact. In addition, there is a very large uncertainty in the mass amount of biogenic emissions, the speciation (reactivity) of the biogenic emissions, and the chemistry of biogenic species. A further possible reason for the underprediction is that the wind speeds are too high. There has been some discussion that wind speeds reported at FAA sites (instantaneous 1-minute averages) tend to be higher than the hourly integrated values. Thus, as a sensitivity simulation, all observed wind speeds at FAA sites were reduced 50 percent and new UAM wind fields were created. The results of this sensitivity test are discussed in Appendix D.

Although implementation of some of the above changes to the boundary conditions and wind fields would probably improve model performance, the use of those procedures may not be consistent with some of the objectives of this study, namely the demonstration of the PLANR use of the UAM. Thus, since model performance from diagnostic run 2 satisfies the model performance goal, it was deemed a suitable base case. Nevertheless we recommend that when the UAM(CB-IV) and associated preprocessor programs are delivered to the state of Georgia, they should carry out sensitivity studies like those discussed above (and presented in Appendix D), which may improve the UAM inputs data bases and model performance. This exercise will also help them gain experience with the causes and effects of UAM inputs on predicted ozone concentrations.

4 APPLICATION OF THE UAM TO THE DALLAS-FORT WORTH METROPLEX AREA

In this section we discuss the PLANR application of the UAM to the Dallas-Fort Worth metroplex area. As discussed in Section 2, the PLANR application of the UAM involves the following activities: episode selection, meteorological characterization, modeling domain definition, emissions preparation, preparation of the UAM modeling inputs, and a limited number of diagnostic simulations designed to obtain a base case with statisfactory model performance. These topics are discussed in the following sections.

EPISODE SELECTION

Ozone and meteorological data from the Dallas-Fort Worth area for 1984 through 1987, and parts of 1988 at some stations, were analyzed to determine an ozone episode suitable for demonstrating the PLANR use of the UAM. From 106 days of ozone exceedences in this period, three candidate days of high observed ozone concentrations were identified as possible modeling days. A memorandum was prepared for the Texas Air Control Board (TACB), EPA Region VI, and EPA Office of Air Quality and Planning Standards (OAQPS) on 10 May 1989 that documented the meteorological conditions, observed ozone concentrations, and appropriateness for using each of the candidate days for UAM modeling. This memorandum is presented in Appendix E. The three candidate UAM modeling days and their daily maximum observed ozone concentrations are as follows:

June 25, 1984	Dallas 150 ppb, Fort Worth 150 ppb
August 31, 1985	Dallas 170 ppb, Fort Worth 130 ppb
August 1, 1986	Dallas 170 ppb, Fort Worth 120 ppb

Based on the information provided in the memorandum in Appendix E, 31 August 1985 was selected for UAM modeling by the TACB, EPA OAQPS, and EPA Region VI. The episode on 31 August 1985 recorded the second highest observed ozone (170 ppb) in the period studied, contained exceedences in both Dallas and Fort Worth, and had meteorological conditions that are fairly typical of those that produce ozone exceedences in the Dallas-Fort Worth area.

The winds on 31 August 1985 were light and variable. Observed daily maximum ozone concentrations in Fort Worth on 30 August 1985 were quite high (140 ppb). In order to simulate the high ozone concentrations in Dallas on 31 August it was necessary to model August 30 and 29 as well. Thus, UAM modeling inputs were prepared for the three-day period 29-31 August 1985. The exact starting time on 29 August was determined after performing an inert tracer simulation, which indicates how long it takes to flush the initial conditions out of the modeling domain.

METEOROLOGICAL CHARACTERIZATION

The meteorological conditions of 31 August 1985 were characterized by examining daily weather maps, observed surface and upper-air meteorological data, and observed ozone concentrations. Data from the twice-daily upper-air soundings were used to estimate the heights of the 950, 900, and 850 mb constant pressure surfaces. Some of the analyses for 1900 August 30, 0700 August 31, and 1900 August 31 are given in Figures 4-1 through 4-3.

On 30 August a high-pressure system is the dominant feature at both 950 and 900 mb, centered west of the Dallas-Fort Worth area (Figure 4-1). This high-pressure persisted and continued to influence the region through 1 September (Figures 4-2 and 4-3). The surface winds were light and variable for the three-day period spanning 30 August through 1 September 1985. At 0700 LST on 31 August, surface winds were light and from the northwest and, as indicated in Figure 4-2, winds aloft had a southerly component. By 1900 LST the surface winds and winds aloft were light and from the south (Figure 4-3). The daily maximum temperature increased steadily during the episode with maximum surface values of 96, 100, and 103 °F measured on August 29, 30, and 31, respectively. No frontal systems passed through the area during this period. Under the influences of a high-pressure system a region may experience subsidence (large-scale downward motion) that can limit vertical mixing. Thus, the combination of high pressure, light winds, high temperature, and limited vertical mixing allowed ozone and ozone precursors to build up during the three-day period.

The distribution of observed daily maximum ozone concentrations for 29 August through 1 September 1985 in the Dallas-Fort Worth area are displayed in Figure 4-4. On 29 August the observed daily maximum ozone concentrations range from 5 to 9 pphm. By 30 August high ozone concentrations are observed in Fort Worth (14 pphm) while in Dallas the daily maximum ozone concentrations remain fairly low (5 to 7 pphm). On August 31 there are very high observed daily maximum ozone concentrations in Dallas and north of Dallas (17 pphm), and fairly high observed ozone concentrations in Fort Worth (13 pphm). Daily maximum ozone concentrations are still fairly high on 1 September (8 to 13 pphm), however there is only one exceedence of the ozone NAAQS and that occurs in Fort Worth. It appears that the light winds from the east on 30 August combined emissions from Dallas and Fort Worth to cause exceedences of the ozone standard in Fort Worth while Dallas remained fairly

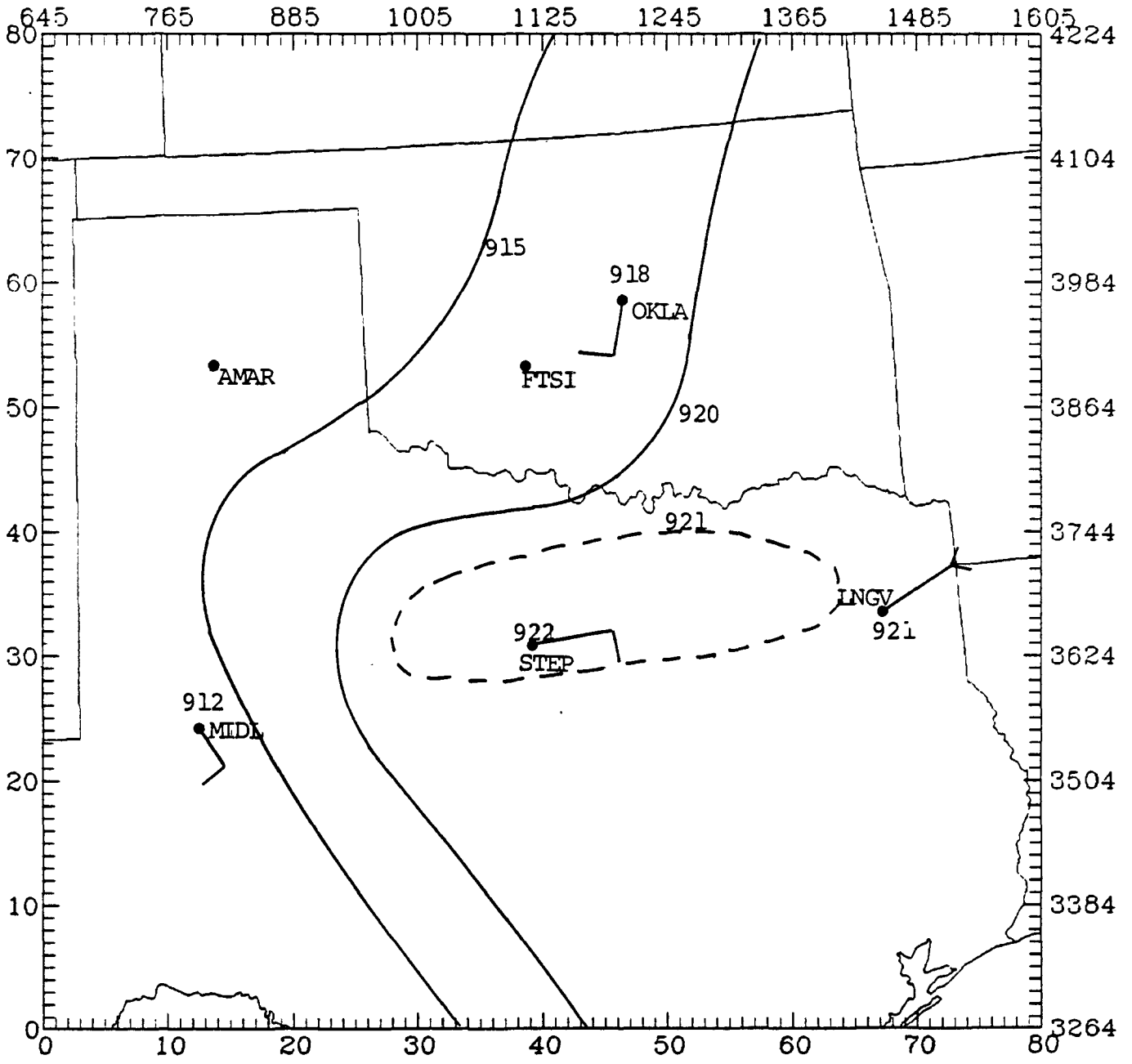

FIGURE 4-1a. 950 mb constant pressure heights at 1800 on 30 August 1985 (H denotes estimated center of high pressure).

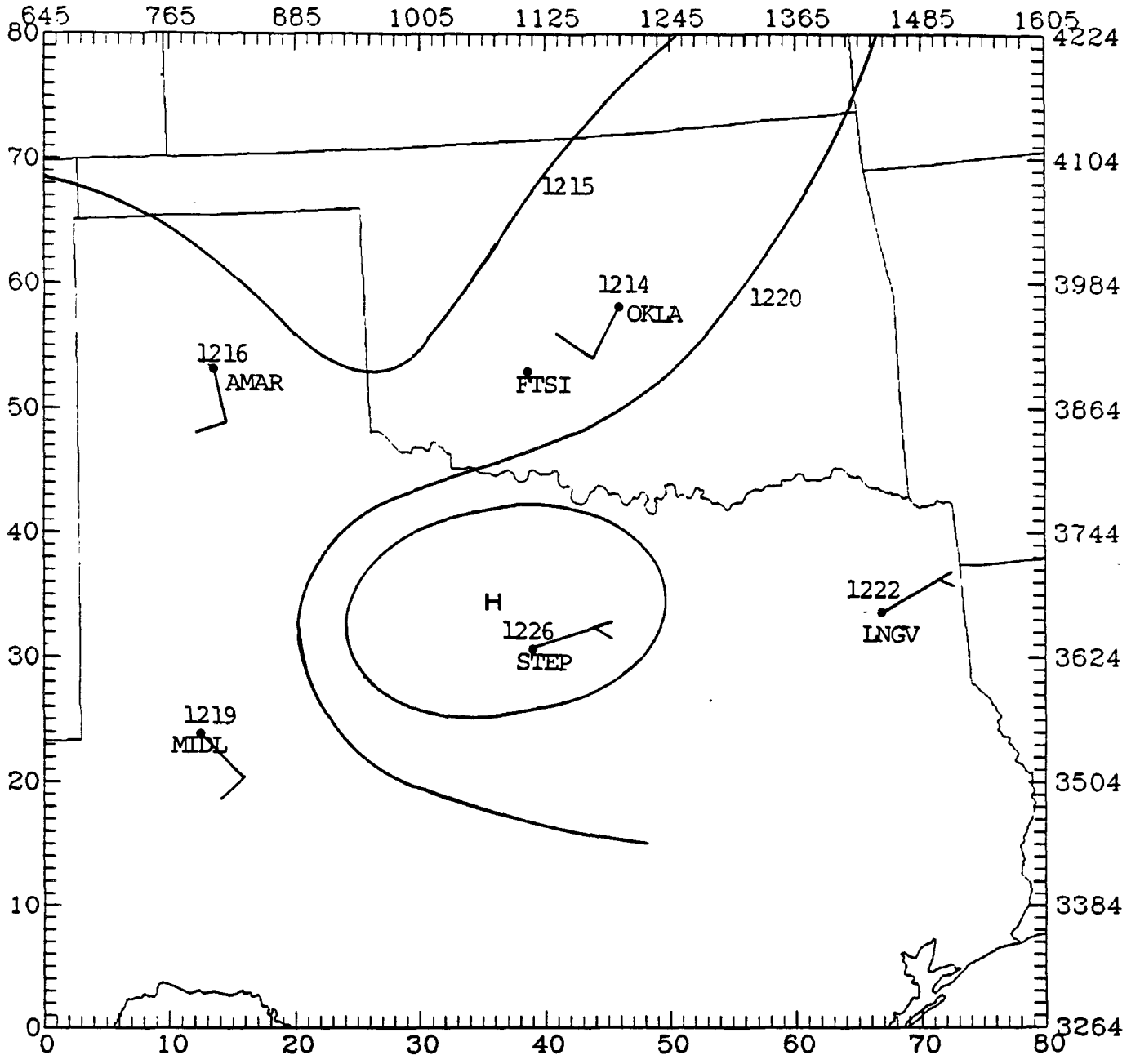

FIGURE 4-1b. 900 mb constant pressure heights at 1800 on 30 August 1985 (H denotes estimated center of high pressure).

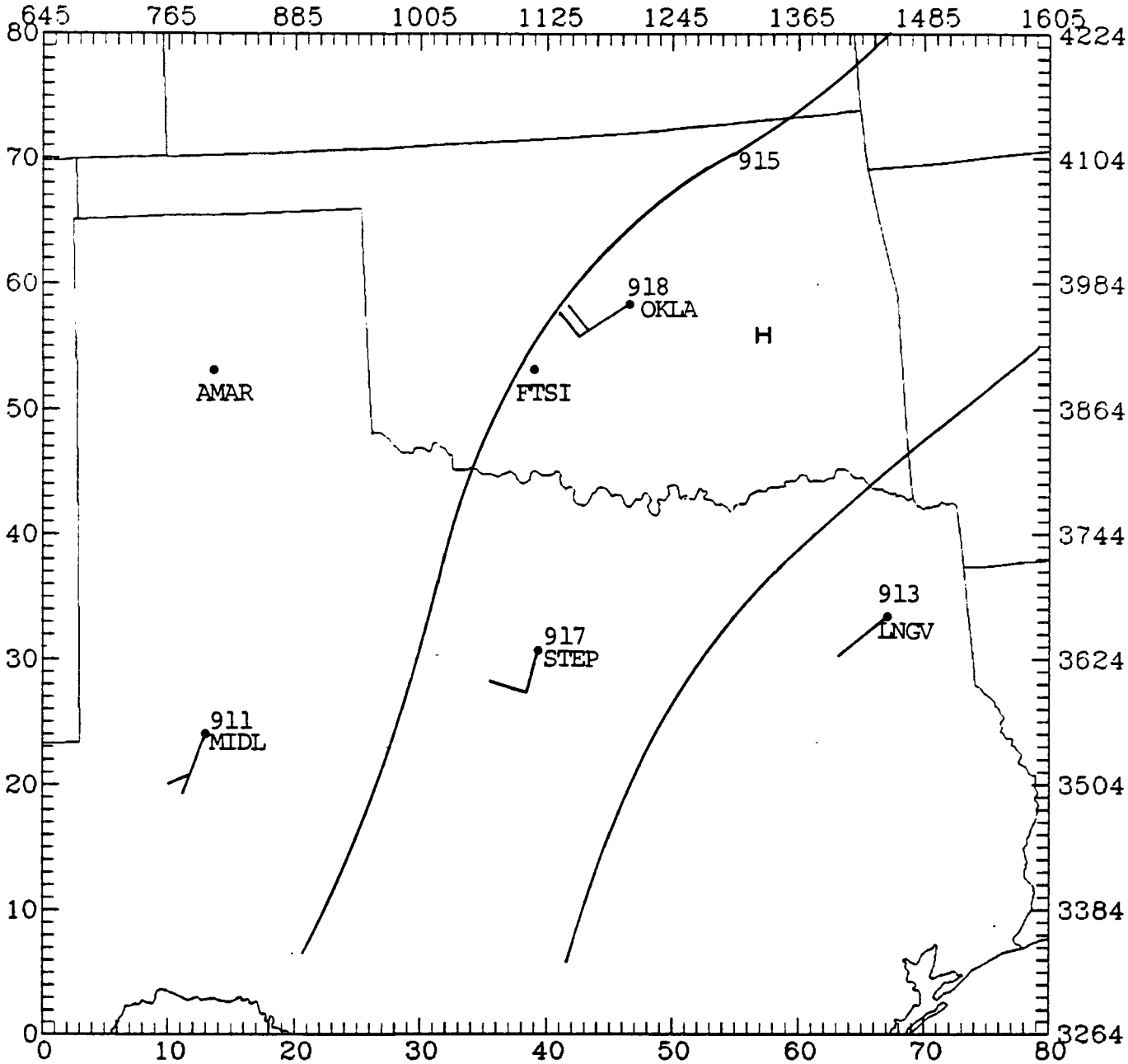

FIGURE 4-2a. 950 mb constant pressure heights at 0600 on 31 August 1985 (H denotes estimated center of high pressure).

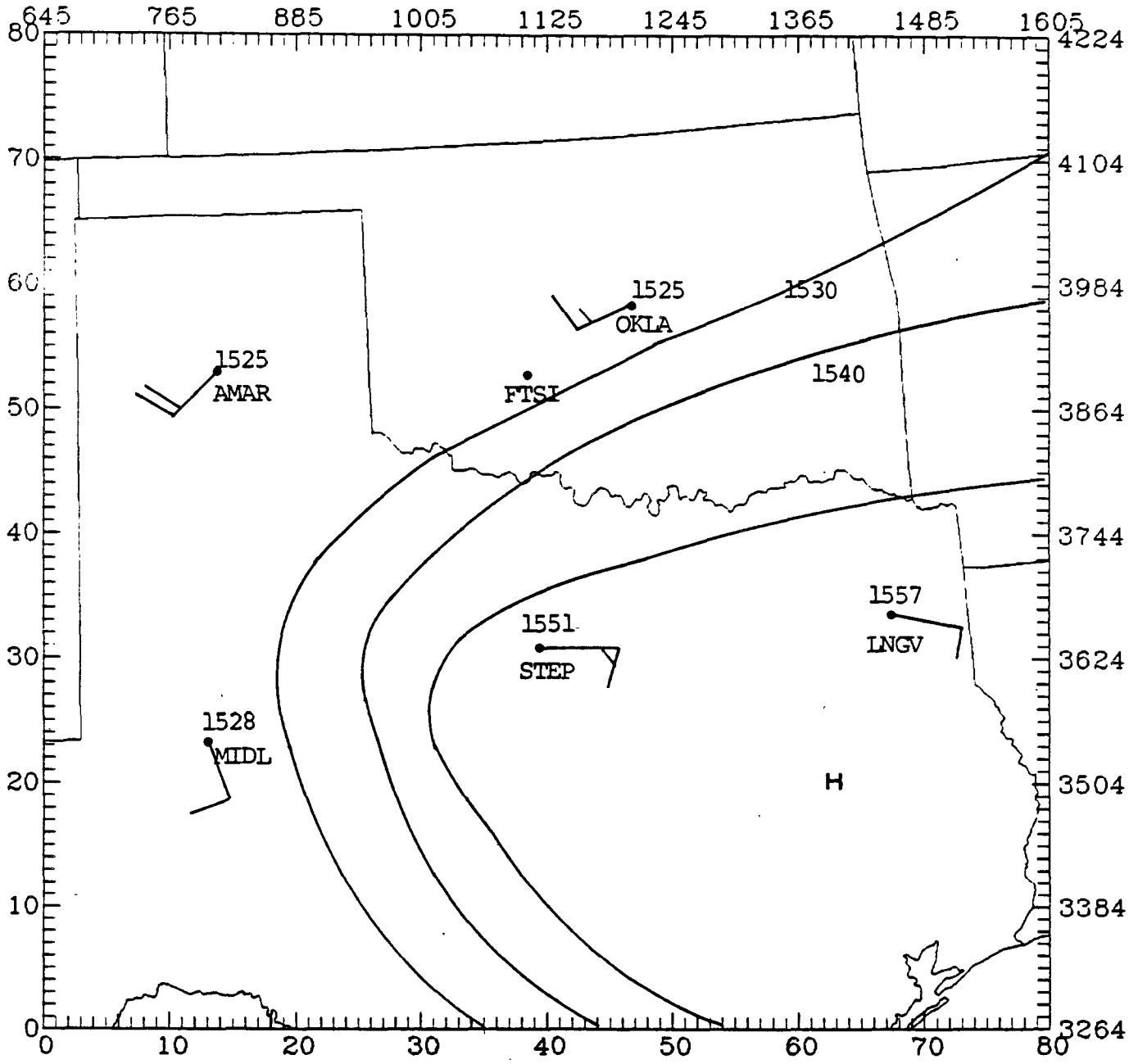

FIGURE 4-2b. 850 mb constant pressure heights at 0600 on 31 August 1985 (H denotes estimated center of high pressure).

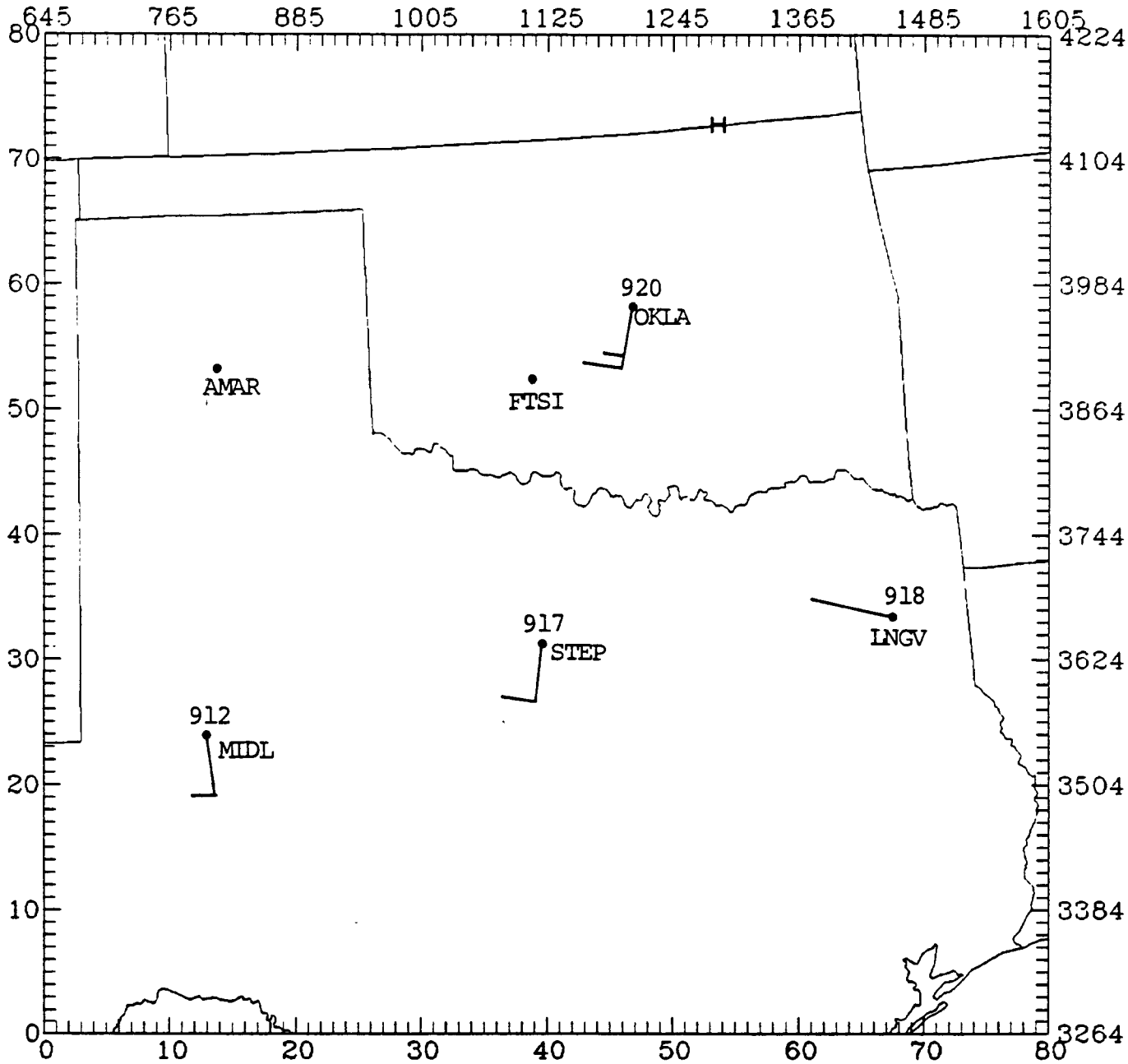

FIGURE 4-3a. 950 mb constant pressure heights at 1800 on 31 August 1985 (H denotes estimated center of high pressure).

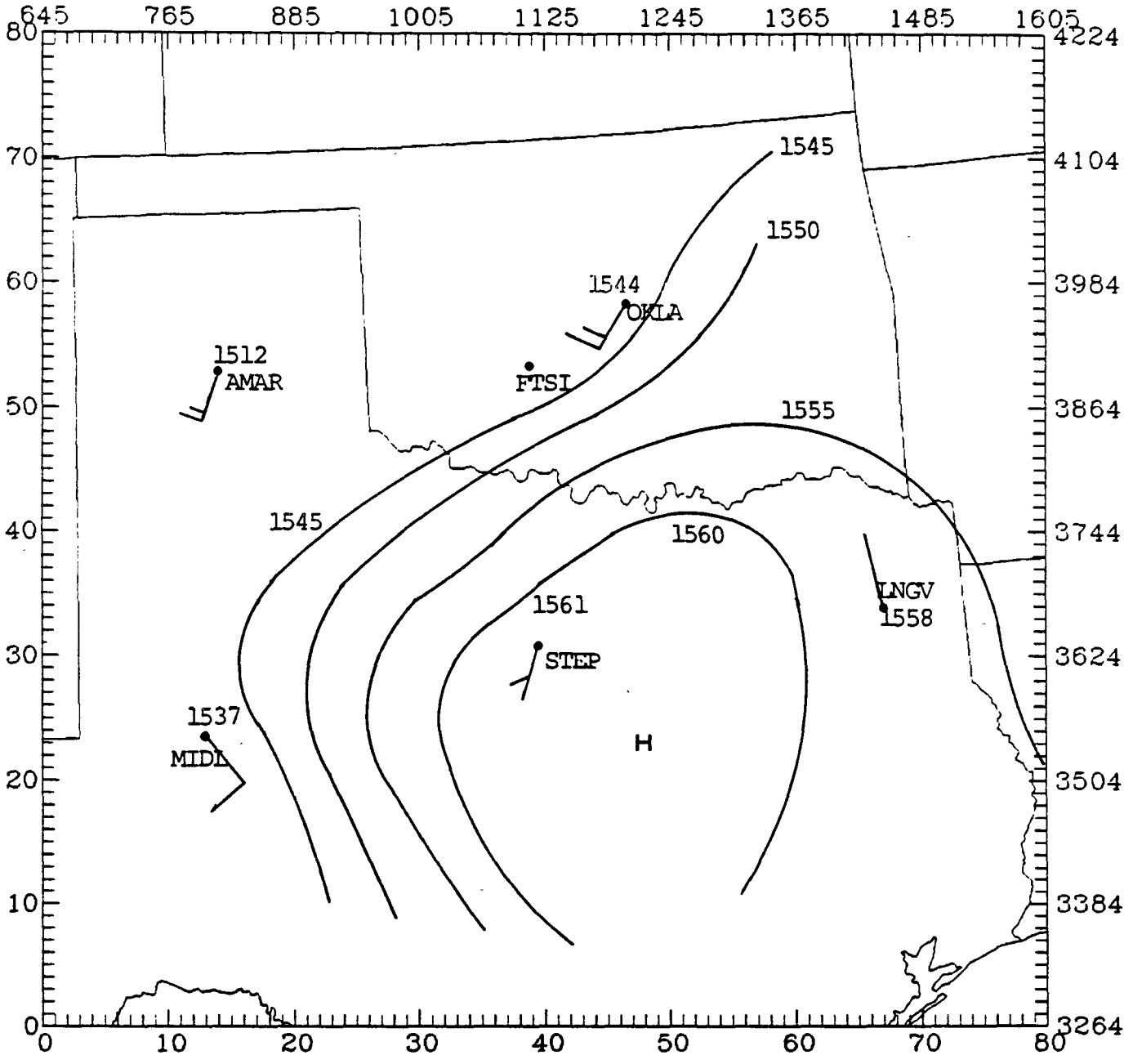

FIGURE 4-3b. 850 mb constant pressure heights at 1800 on 31 August 1985 (H denotes estimated center of high pressure).

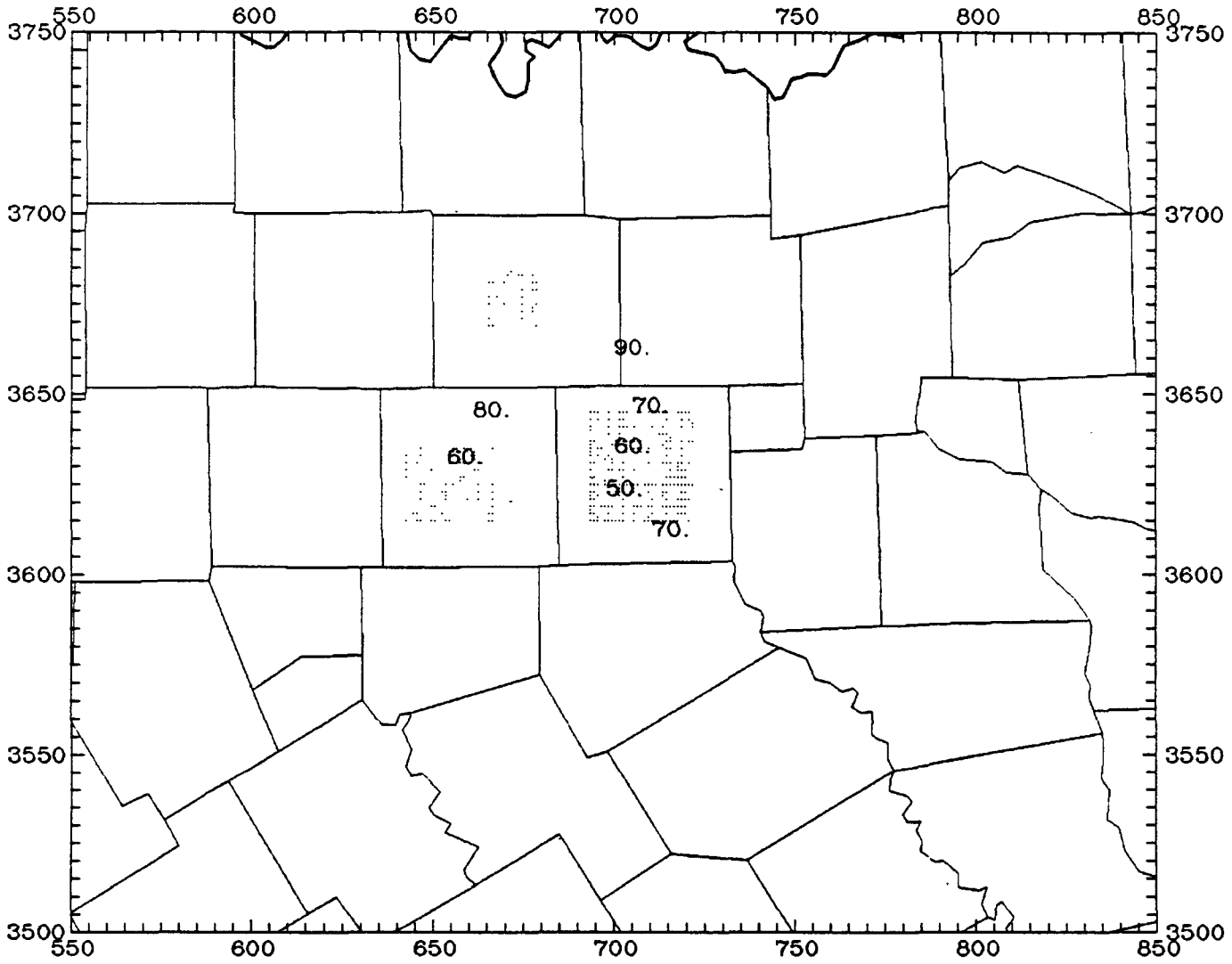

FIGURE 4-4a. Observed daily maximum ozone concentrations (ppb) in the Dallas-Fort Worth area, 29 August 1985.

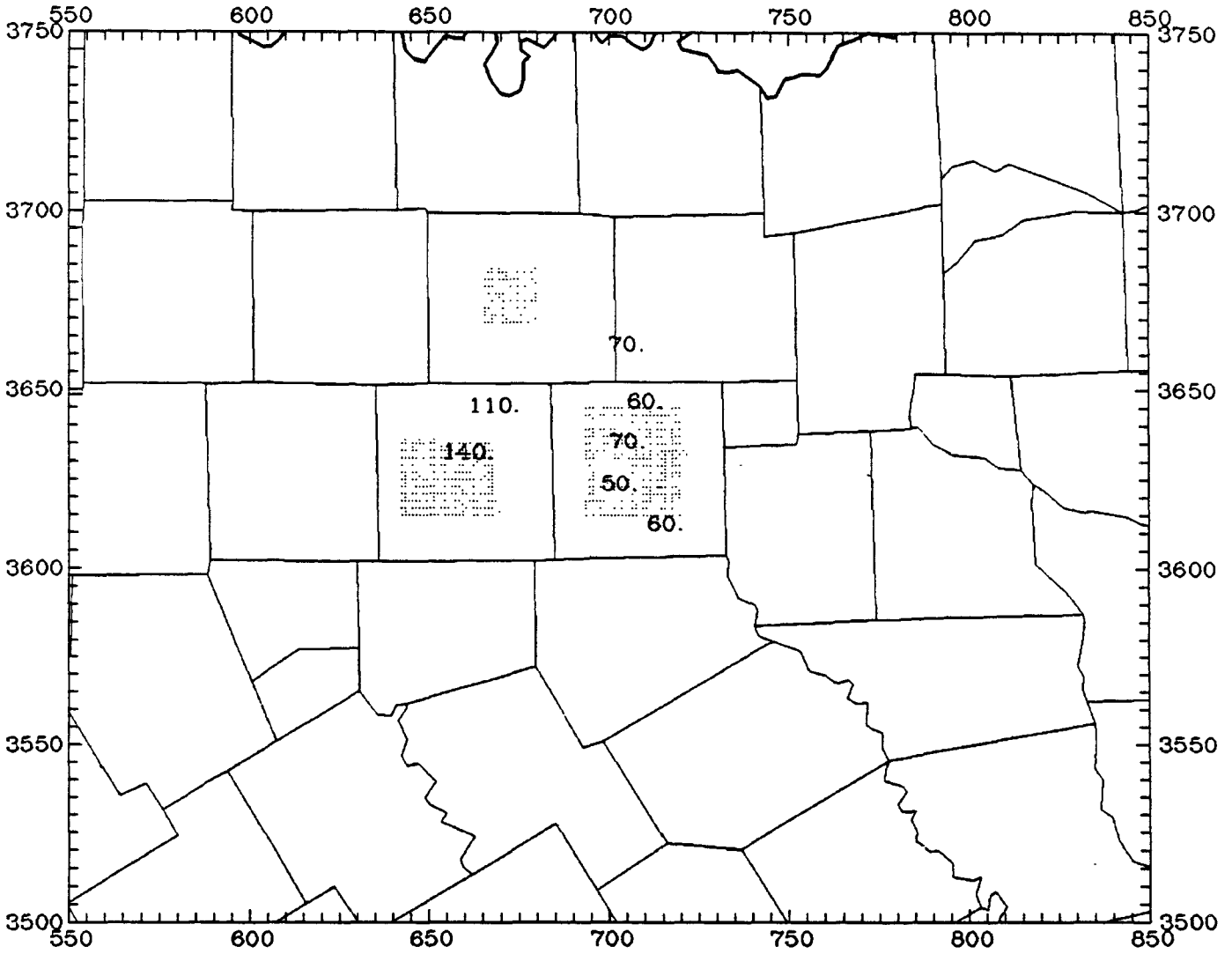

FIGURE 4-4b. 30 August 1985.

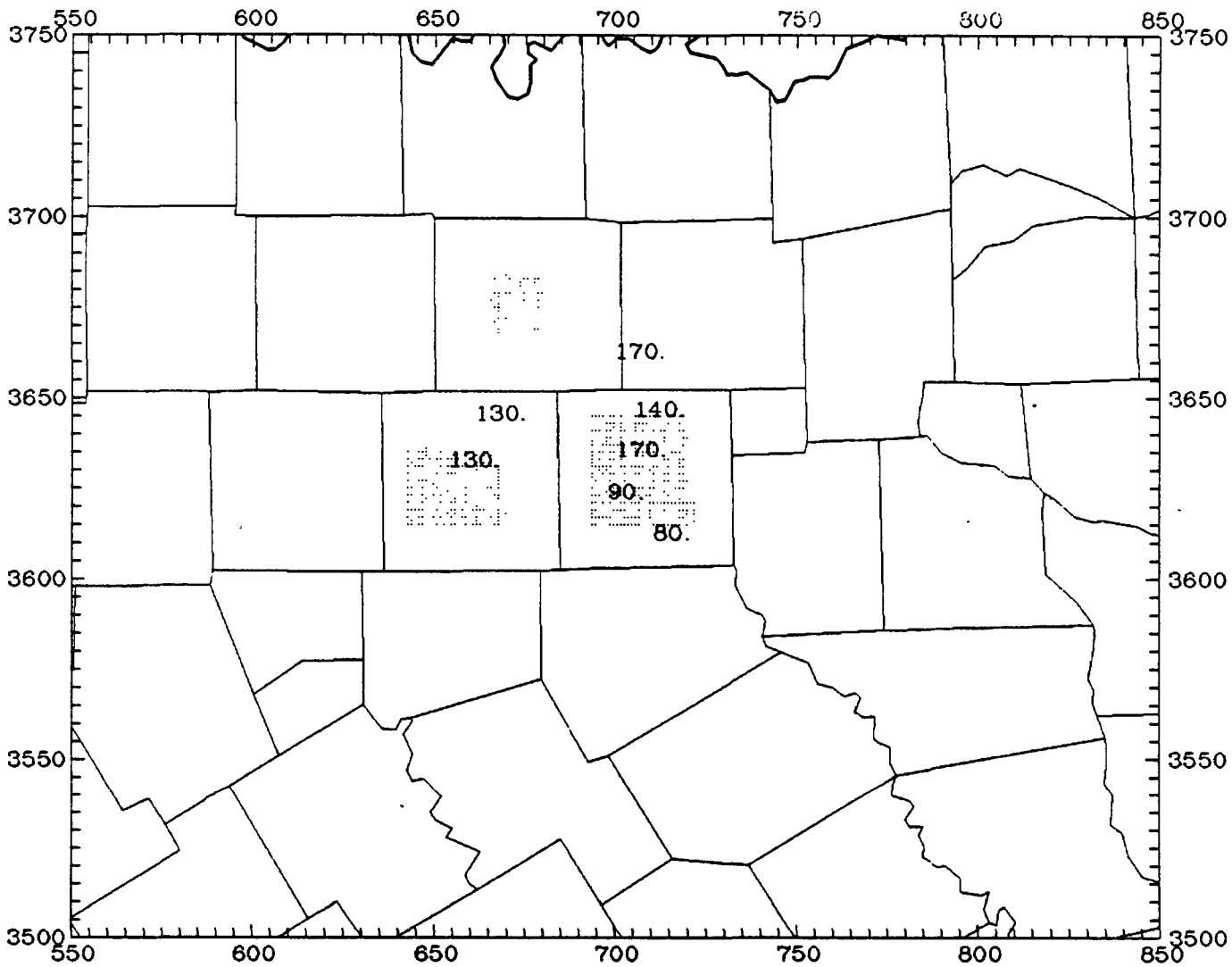

FIGURE 4-4c. 31 August 1985.

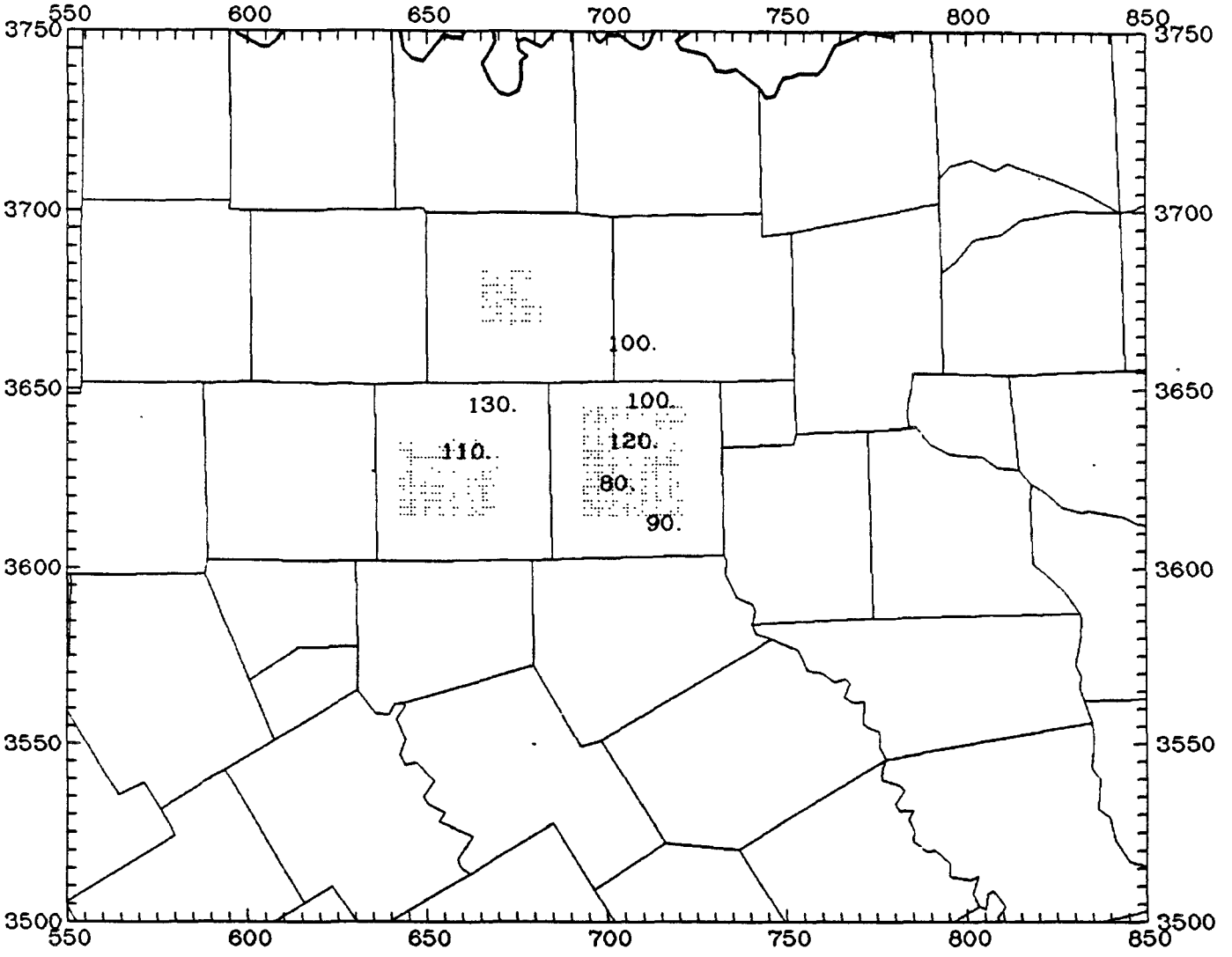

FIGURE 4-4d. 1 September 1985.

clean. As the surface winds shifted from the east to the northwest to the south the elevated cloud of ozone moved east to Dallas and then north of the city to cause the high ozone concentrations in Dallas on 31 August.

Winds were still fairly calm on 1 September, yet the only ozone exceedence was 13 pphm recorded in Fort Worth. Although observed daily maximum ozone concentrations were fairly high on 1 September (8 to 13 pphm), one might expect higher ozone on this day because of the calm conditions and high observed ozone concentrations on previous days. Possible explanations for this are that high ozone concentrations occurred but the monitoring network did not pick them up, or the lower emissions on Saturday (31 August) and Sunday (1 September) did not emit enough ozone precursors to cause a high exceedence despite the indications that meteorological conditions were favorable for ozone formation. The exceedences recorded on 31 August (Saturday) are most likely a combination of the emissions on Friday (30 August) and Saturday.

MODELING DOMAIN DEFINITION

Because of the stagnant meteorological conditions of 29-31 August 1985 it is difficult to determine how large a modeling domain is required to contain the predicted ozone peaks. The meteorological data indicate that there will be a sloshing of emissions from the Dallas-Fort Worth area to the west on 30 August and back to the northeast on 31 August. Thus an overly large modeling domain was selected, with an origin at UTM zone 14 coordinates of 600 km easting and 3560 km northing, spanning 180 km in the east-west direction and 160 km in the north-south direction (see Figure 4-5). As stated in the Dallas-Fort Worth modeling protocol, and to be consistent with other PLANR applications of the UAM, a horizontal grid spacing of 4 km was used and the vertical structure consisted of two layers below and three layers above the mixing height.

Meteorological and emission inputs were prepared for the entire modeling domain. However, after performing inert tracer simulations and examining the emissions distribution, the computational grid was reduced by defining new boundaries in the UAM BOUNDARY input file. This reduction in the computational grid is to reduce unnecessary computations.

ROUTINE DATA AVAILABLE FOR DALLAS-FORT WORTH

Surface meteorological data (hourly average wind speed, wind direction and temperature) collected at Continuous Air Monitoring Stations (CAMS) were obtained from EPA Region VI. These eight surface CAMS sites are listed in Table 4-1. Additional surface meteorological data from FAA sites at the Dallas-Fort Worth airport, Redbird, Love Field, Addison, and Meacham were also available.

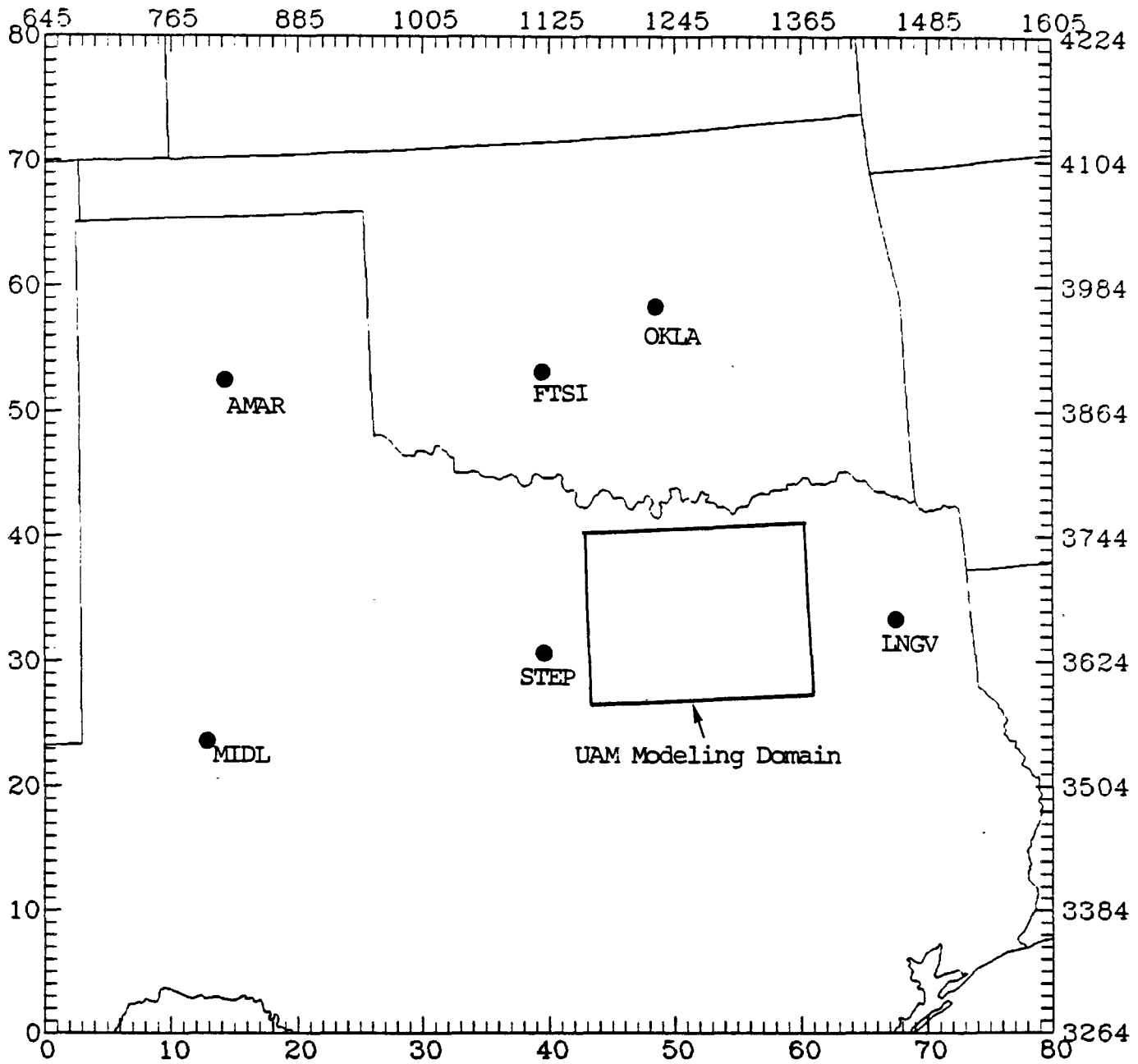

FIGURE 4-5. Locations of upper-air meteorological observation sites and UAM modeling domain for the Dallas-Fort Worth metroplex area.

TABLE 4-1. Surface meteorological observation sites at the continuous air monitoring stations (CAMS).

Site ID	Site Code	Site Location
MOCK	451310044H01	1500 West Mockingbird, Dallas
NTRA	451310045F01	12532 Nuestra Drive, Dallas
HNTN	451310069H01	1415 Hinton Drive, Dallas
BNVW	451310055H01	10501 Bonnie View, Dallas
DNTN	451420054H01	Quarter Mile Road off Highway 121, Denton County
ROSS	451880002F01	Ross Avenue, between Long and 34th Street, Fort Worth
PECN	451880003F01	100 N. Pecan, Fort Worth
KLLR	455070003F01	FAA site off Alta Vista Road, Fort Worth

Upper-air measurements at Longview, Stephenville, Midland, and Amarillo, Texas, and Oklahoma City and Fort Sill, Oklahoma, were also obtained (see Table 4-2). The locations of these upper-air sites and their relationship with the modeling domain is shown in Figure 4-4.

There were eight air quality monitor sites in operation during 29-31 August 1985. The locations and parameters measured at these eight sites are given in Table 4-3. One site was in Fort Worth (ROSS) and another just north of Fort Worth (KLLR). The remaining sites were in or around Dallas: one was located south of the city (BNVW), four were roughly within the city (MOCK, NSTA, ILLI, and NRTH), and one was north of the city (DNTN). There were no air quality monitors located near the modeling domain boundaries from which boundary conditions could be based.

EMISSIONS PREPARATION

Two separate emission files are required by the UAM: an area source emission file (EMISSION) whose emissions are injected into the lowest layer of the UAM; and a point source emission file (PTSOURC) whose emissions are injected into the appropriate vertical layers depending on plume rise calculations. The 1985 base case emissions data files were based on the 1985 NAPAP anthropogenic emission inventory (Zimmerman et al., 1989) and biogenic emissions estimates obtained from Washington State University (Lamb et al., 1986, 1987).

Anthropogenic Emissions

The anthropogenic emission inventory for the 1985 base case was created from the 1985 NAPAP point and area source anthropogenic emission data. The procedures for converting the 1985 NAPAP anthropogenic emissions into the UAM format were the same as those used for the Atlanta application and followed the methodology given in Figure 2-8 using software documented in "User's Manual for Preparing Emission Files for use in the Urban Airshed Model" (SAI, 1989).

Biogenic Emissions

The biogenic emissions inputs for the UAM application to Dallas-Fort Worth were prepared using different data sources and techniques than used for the Atlanta application. Biogenic emissions for Atlanta were originally generated for the EPA Regional Oxidant Model (ROM) and were obtained from the EPA. However, similar estimates for Dallas were not available because the ROM southeast modeling domain did not include Dallas. Thus the WSU monthly average, county-wide biogenic emissions data were used in the Dallas application.

TABLE 4-2. Upper-air meteorological observation sites in the vicinity of Dallas-Fort Worth.

Site ID	Site Name	Longitude	Latitude	Elevation (m)	UTM Zone 14 x(km)	UTM Zone 14 y(km)	Distance to Dallas-Fort Worth Airport (km)
LNGV	Longview, TX	94.630	32.330	124	911	3585	212
STEP	Stephenville, TX	98.170	32.220	399	578	3565	139
MIDL	Midland, TX	102.170	31.930	873	200	3567	506
OKLA	Oklahoma City, OK	97.580	35.380	392	629	3916	300
AMAR	Amarillo, TX	101.680	35.220	1094	256	3901	525
FTSI	Fort Sill, OK	98.400	34.650	362	554	3834	257

TABLE 4-3. Surface air quality monitors in the Dallas-Fort Worth area in operation during 21-31 August 1988.

Site ID	Site Description	UTM Zone 14 x(km)	UTM Zone 14 y(km)	Parameters Measured
MOCK	1500 West Mockingbird, Dallas	699.961	3633.841	O_3, NO, NO_2, CO
NSTA	12532 Nuestra Drive, Dallas	704.893	3645.068	O_3, NO, NO_2
ILLI	Illinois and Cockrell Hill, Dallas	697.673	3621.962	O_3, CO
BNVW	10501 Bonnie View, Dallas	710.465	3610.823	O_3, NO, NO_2
DNTN	Quarter Mile Road off Highway 121	699.641	3661.105	O_3
ROSS	Ross Avenue between Long and 34th Street, Fort Worth	653.810	3630.705	O_3, NO, NO_2, CO
KLLR	FAA site off Alta Vista Road, Fort Worth	660.907	3643.787	O_3
NRTH	North Ervay at Bryan, Dallas	706.301	3629.225	CO

Spatial Allocation

The monthly average biogenic emissions data obtained from WSU consisted of county-wide emissions of alpha-pinene, isoprene, and other NMHC by six land use categories. The biogenic emissions were allocated to the modeling grid cells based on the distribution of a surrogate. An examination of the available surrogates (population, roadways, area, and the 11 GIS land cover categories) identified only two appropriate surrogates that matched the WSU land use categories: alpha-pinene emissions from scrub and coniferous forest. Thus the county-wide alpha-pinene emissions were allocated to the UAM modeling grid cells based on these two land use categories, whereas the isoprene and other NMHC biogenic emissions were allocated to the modeling grid based on fractional area covered.

Speciation

The speciation of the biogenic emissions followed the recommendations of Hogo and Gery (1988). Isoprene is an explict species (ISOP) in the UAM(CB-IV) and was assigned to the CB-IV TSOP category. Alpha-pinene was split into the CB-IV species as 0.5 OLE, 6 PAR, and 1.5 ALD2. The catgory of other NMHC in the WSU biogenic emission estimates were assumed to be monoterpenes and were split into 1 OLE and 8 PAR.

Temporal Allocation

The diurnal variation of the biogenic emissions was based on the analysis of biogenic emission rates reported by Tingey and co-workers (1978a,b). As illustrated in Figure 4-6a, the diurnal variation of the alpha-pinene and other NMHC biogenic emissions was based on measured variations for five monoterpenes for slash pine in Tampa, Florida. The diurnal variation for isoprene emissions was based on emission rates from oak leaves assuming shaded leaves with one-half ambient sunlight (curve B in Figure 4-6b).

Results

Figure 4-7 displays the spatial distribution of the emissions used in the Dallas-Fort Worth diagnostic simulations. The emission totals for the entire modeling domain are summarized in Table 4-4.

PREPARATION OF UAM INPUT FILES

The following paragraphs describe how the UAM input files were prepared for the PLANR application of the UAM to Dallas-Fort Worth. A definition of the parameters contained in each file is discussed in Section 2.

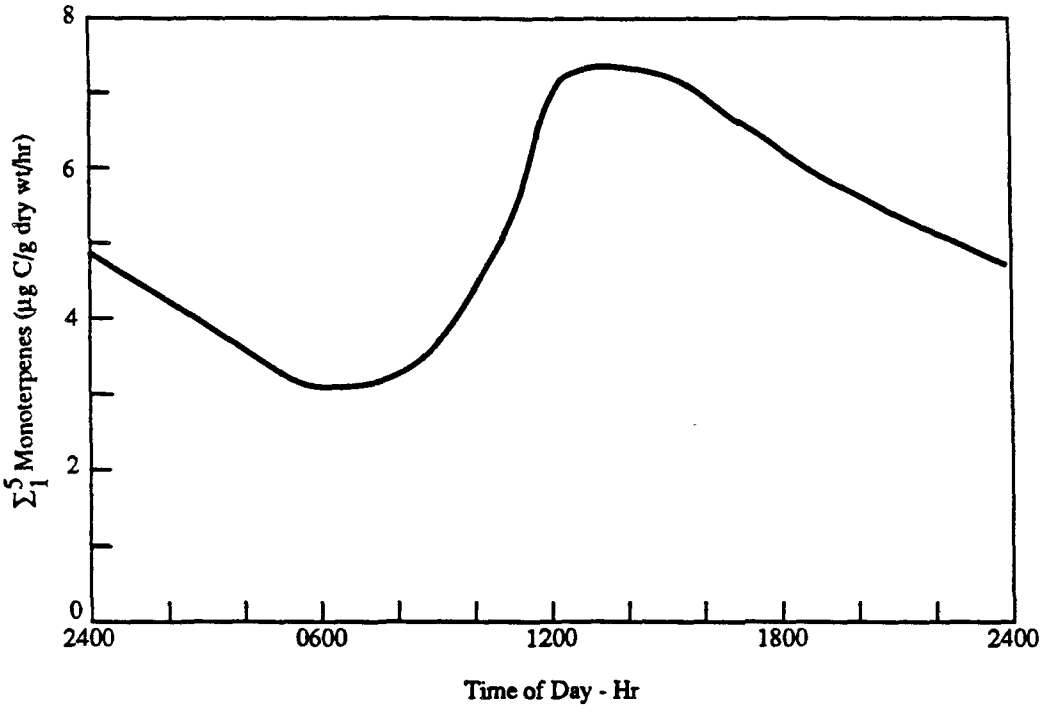

FIGURE 4-6a. Estimated diurnal emissions of five monoterpenes for slash pine in Tampa, Florida, for an average of summer days. (Adapted from Tingey et al. 1978b)

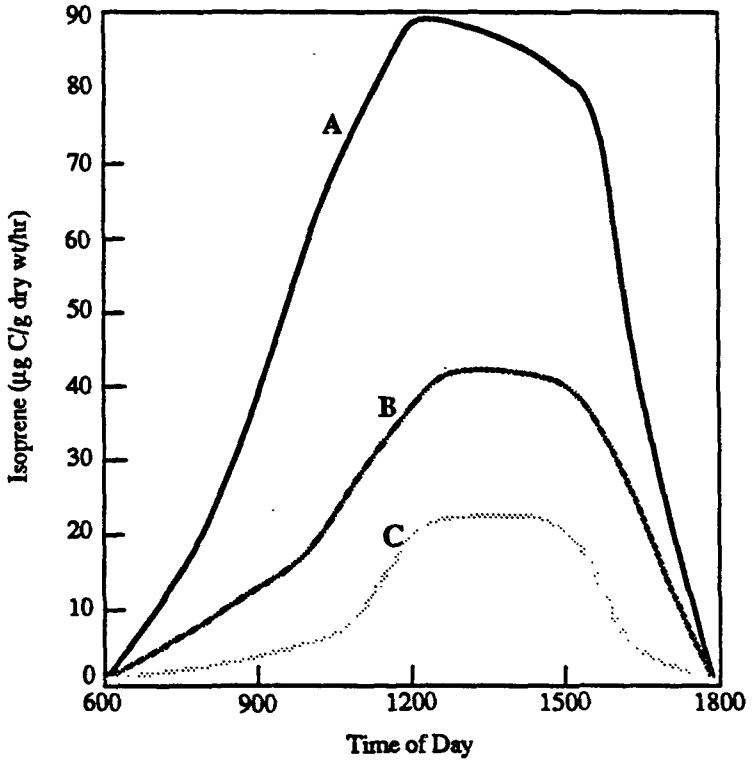

FIGURE 4-6b. Estimated diurnal emissions of isoprene for oak leaves in Tampa, Florida, for an average of summer days. A - sunlit leaves; B - shaded leaves (one-half ambient sunlight); C - shaded leaves (one-fourth ambient sunlight). (Adapted from Tingey et al., 1978b)

EEE89104

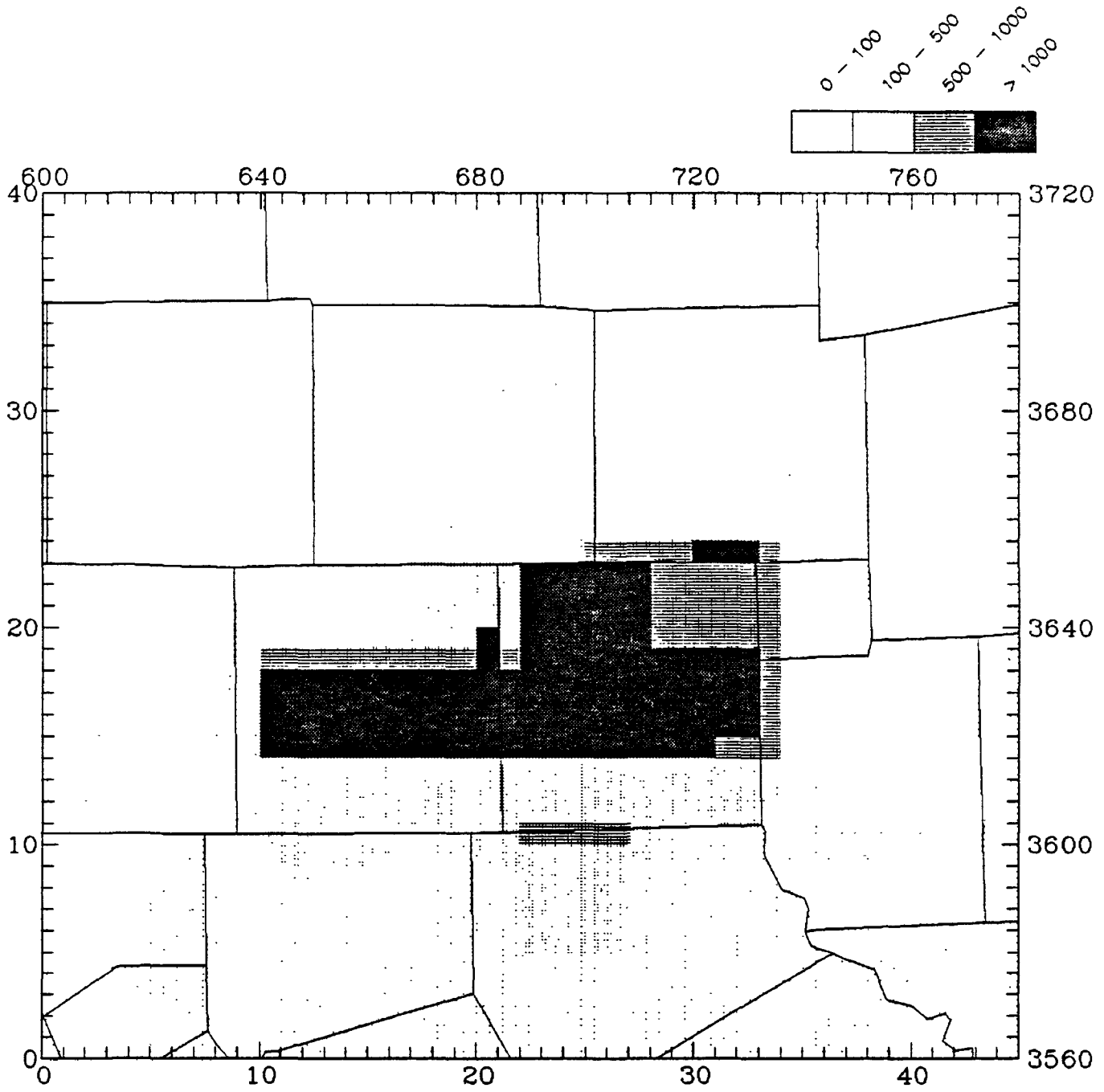

DALLAS -- '85 Area Weekday
NOx
Total: 280130 (Kg/day)

FIGURE 4-7a. 1985 emissions for Dallas-Fort Worth.

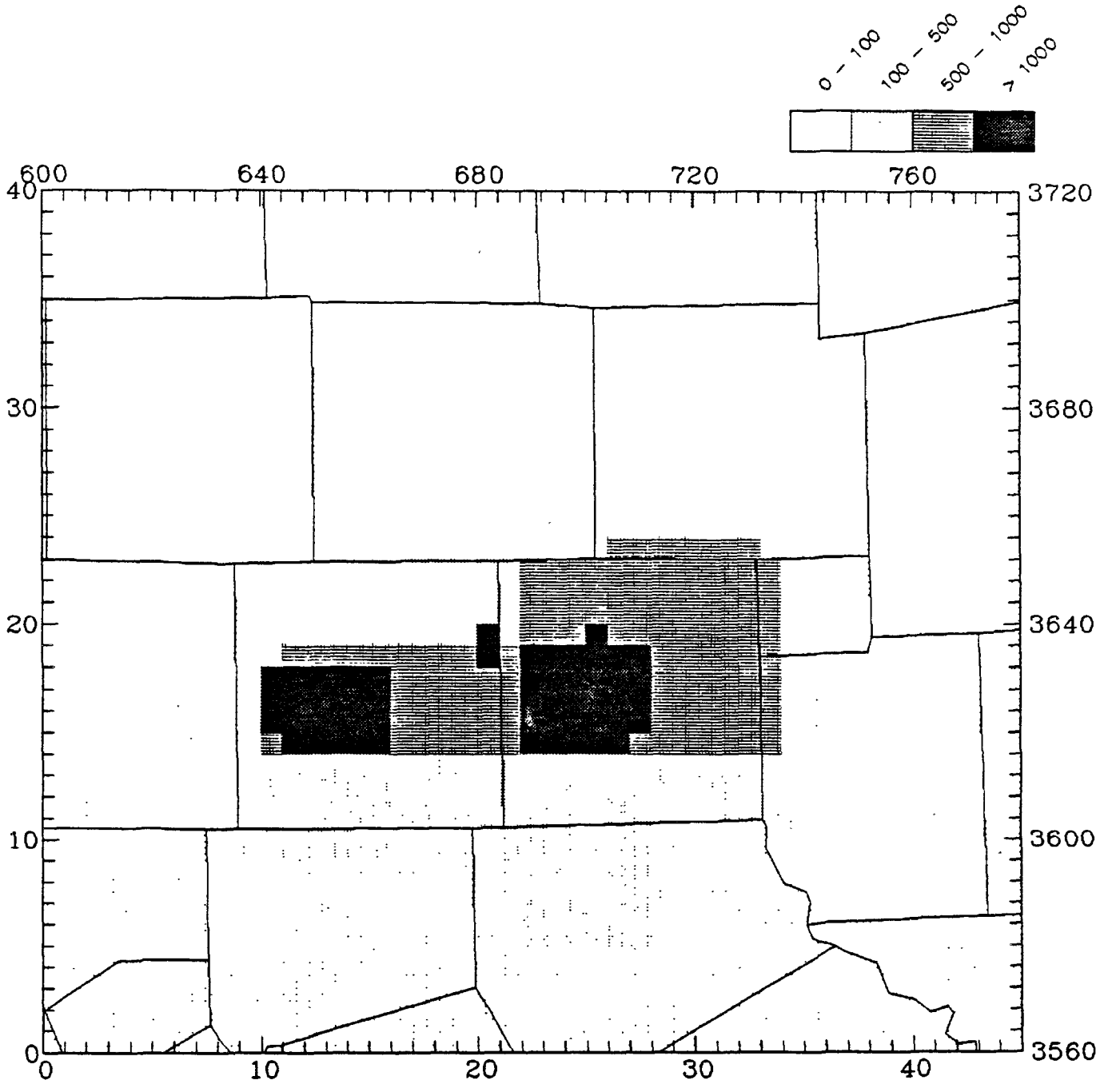

DALLAS -- '85 Area Weekend
NOx
Total: 237061 (Kg/day)

FIGURE 4-7b.

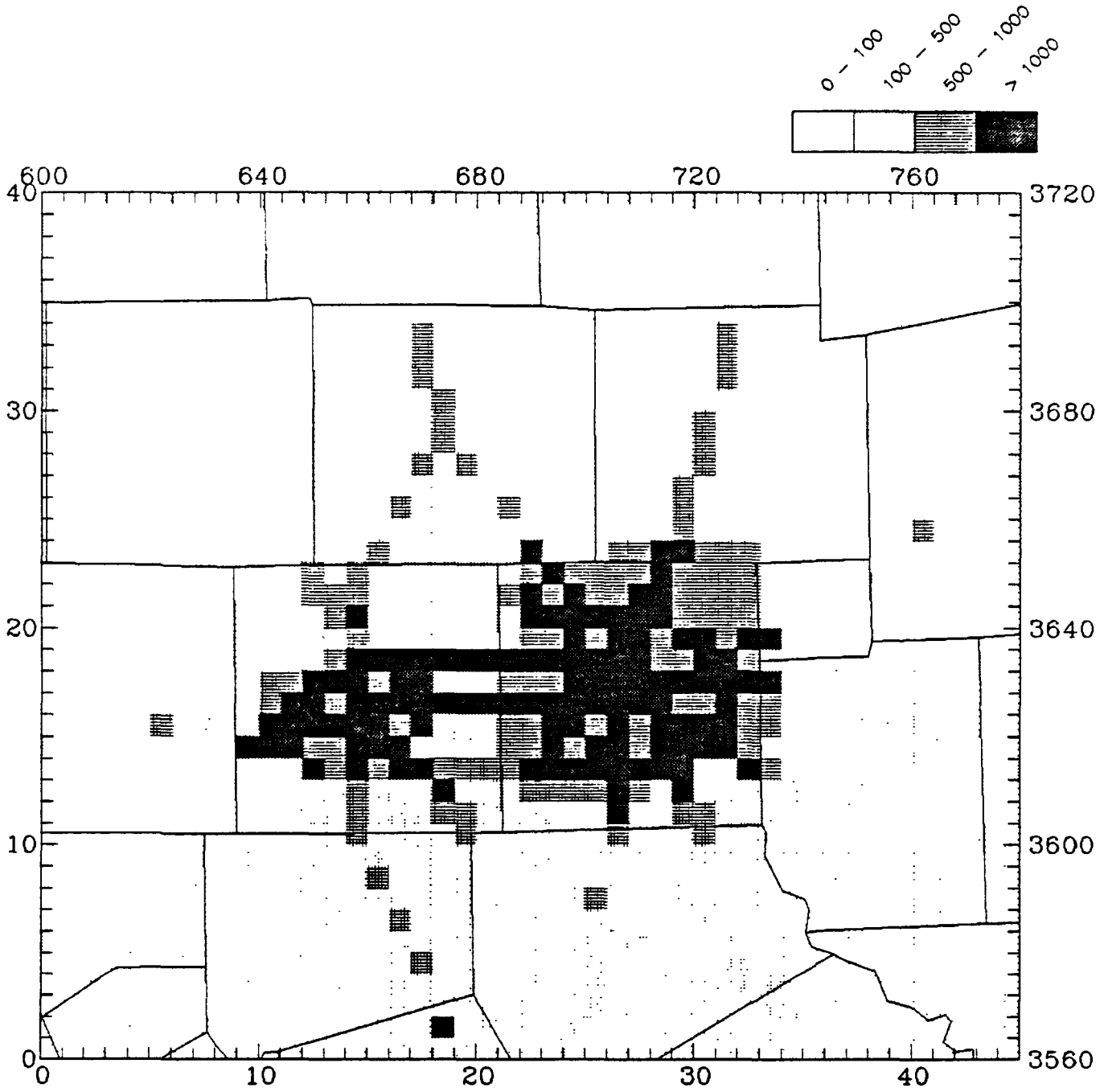

DALLAS -- '85 Motor Vehicle Weekday
NOx
Total: 346986 (Kg/day)

FIGURE 4-7c.

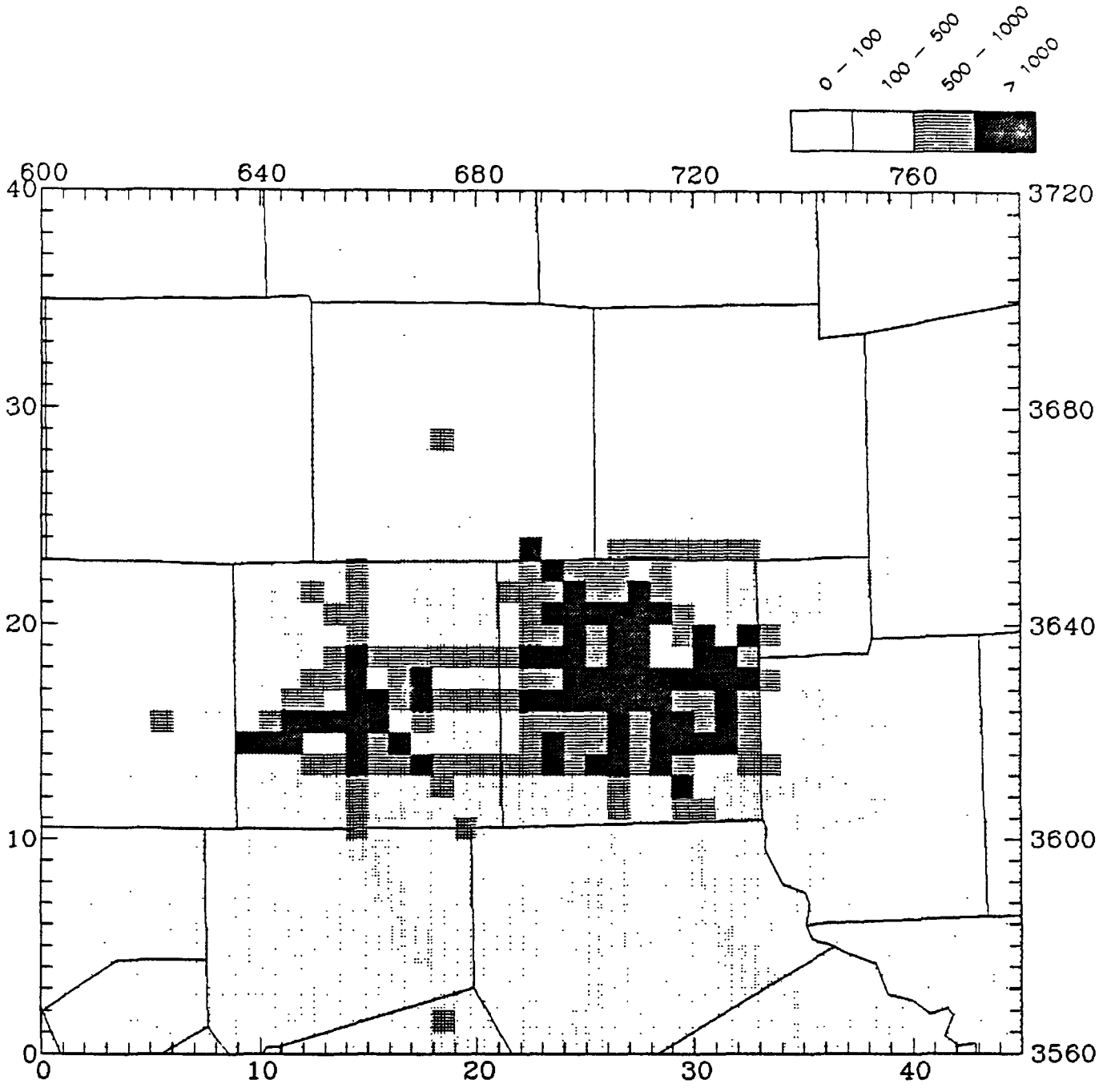

DALLAS -- '85 Motor Vehicle Weekend
NOx
Total: 260239 (Kg/day)

FIGURE 4-7d.

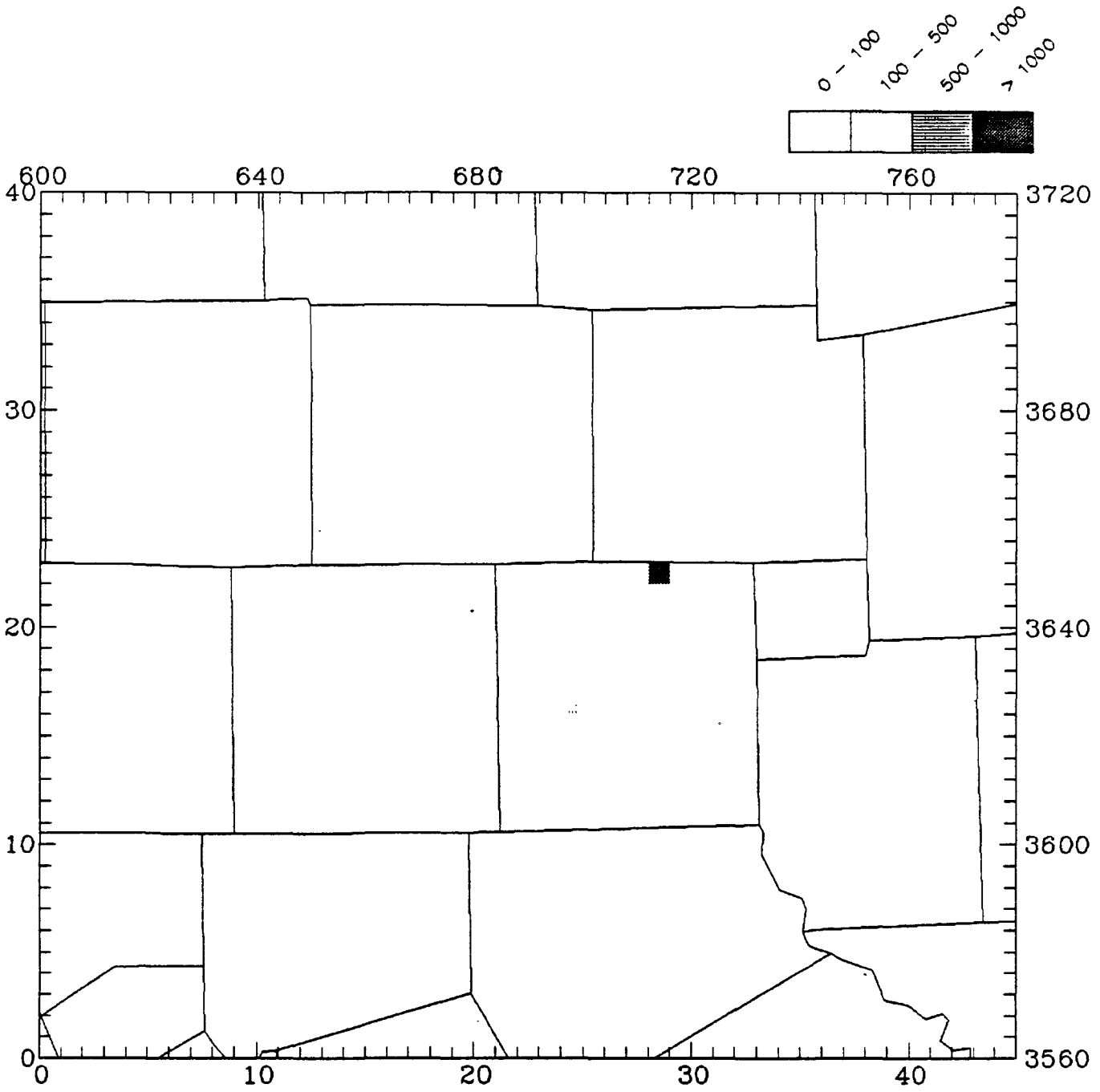

DALLAS -- '85 Low Level Points Weekday
NOx
Total: 18153 (Kg/day)

FIGURE 4-7e.

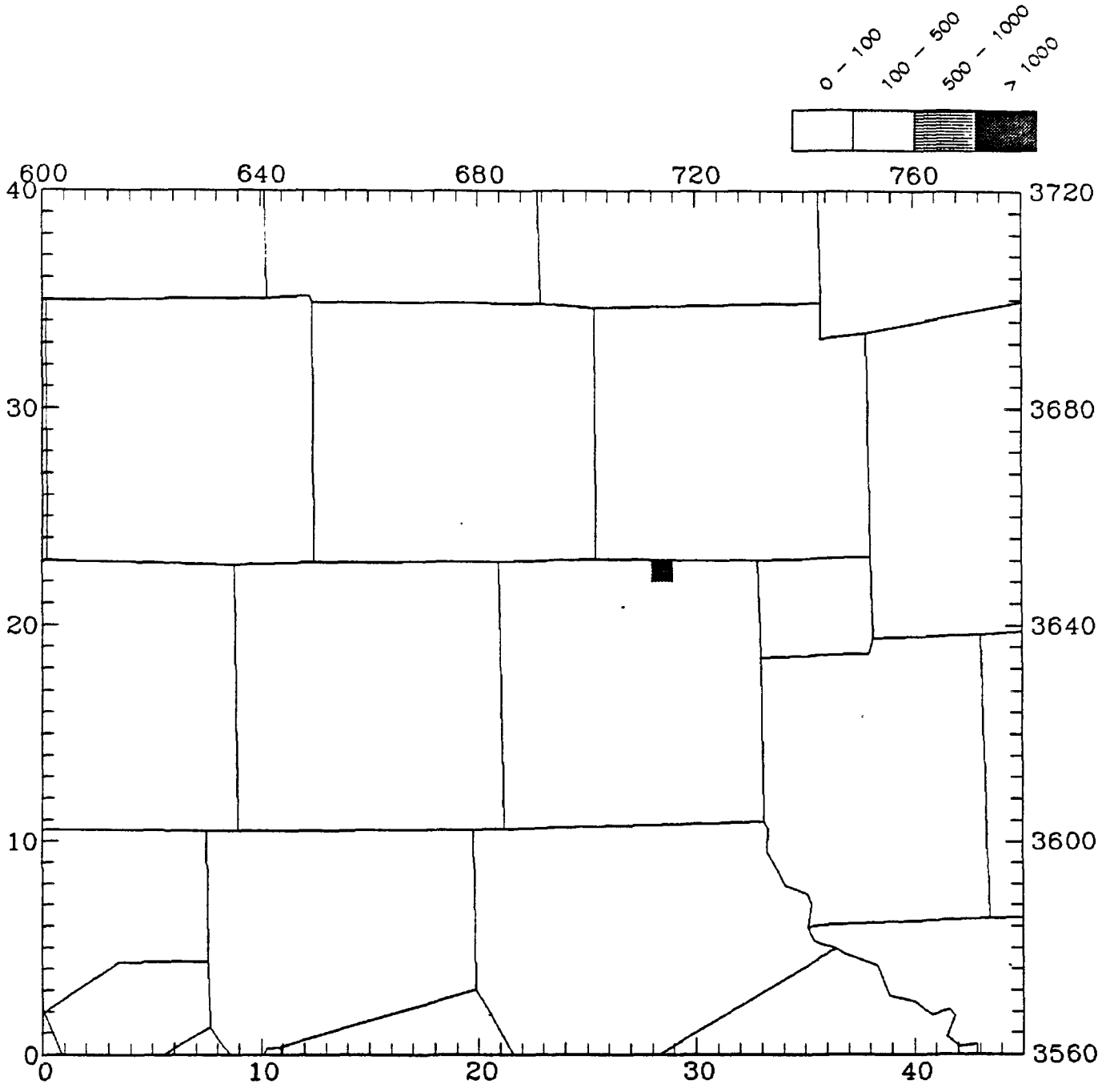

DALLAS -- '85 Low Level Points Weekend
NOx
Total: 17661 (Kg/day)

FIGURE 4-7f.

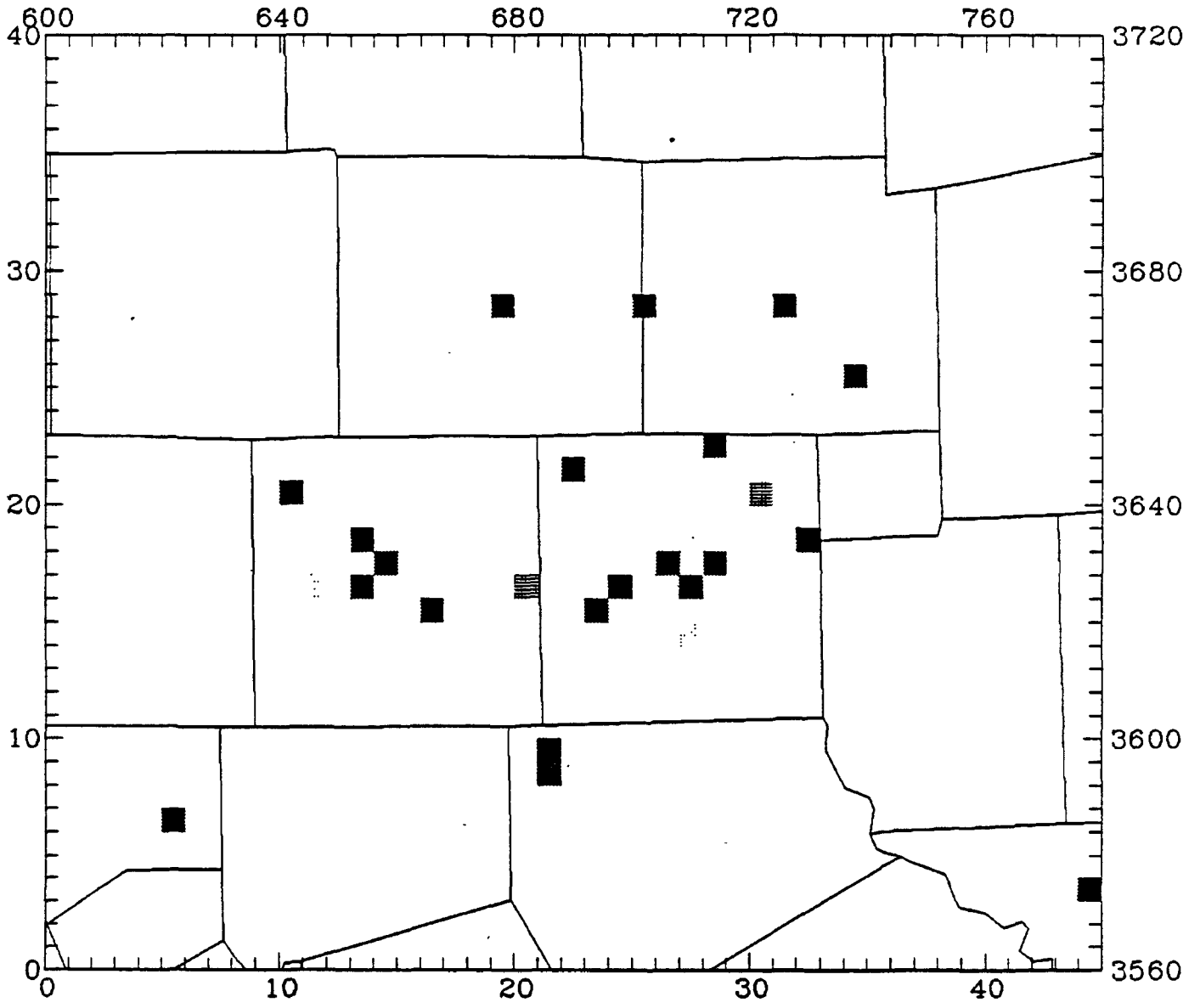

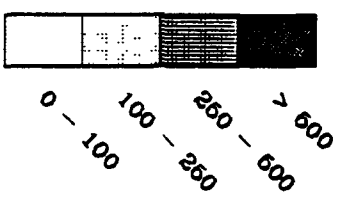

Dallas 85 Base Elevated Point Sources
NOx (kg/day)
Total = 162761.90

FIGURE 4-7g.

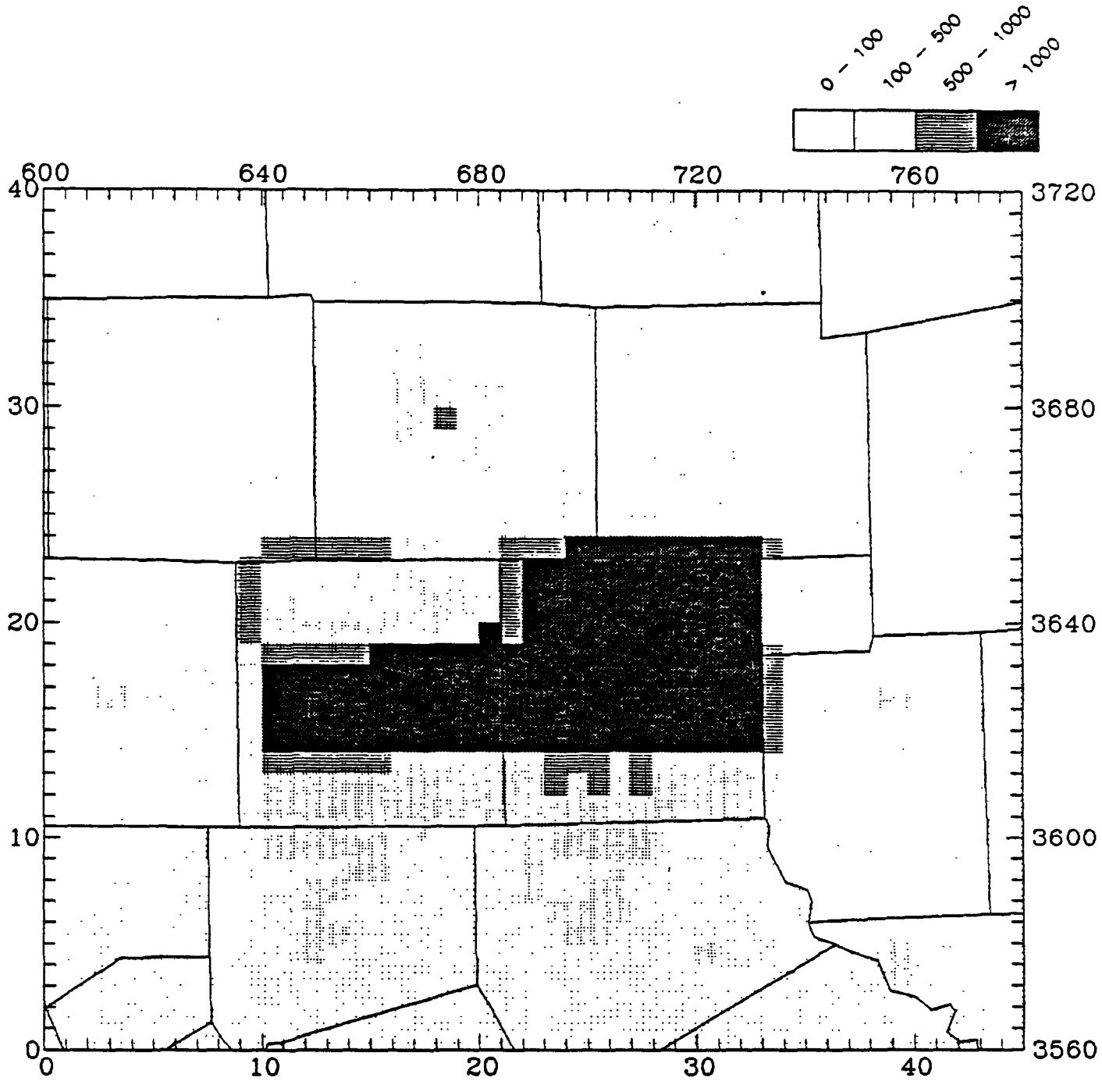

DALLAS -- '85 Area Weekday
RHC
Total: 400017 (Kg/day)

FIGURE 4-7h.

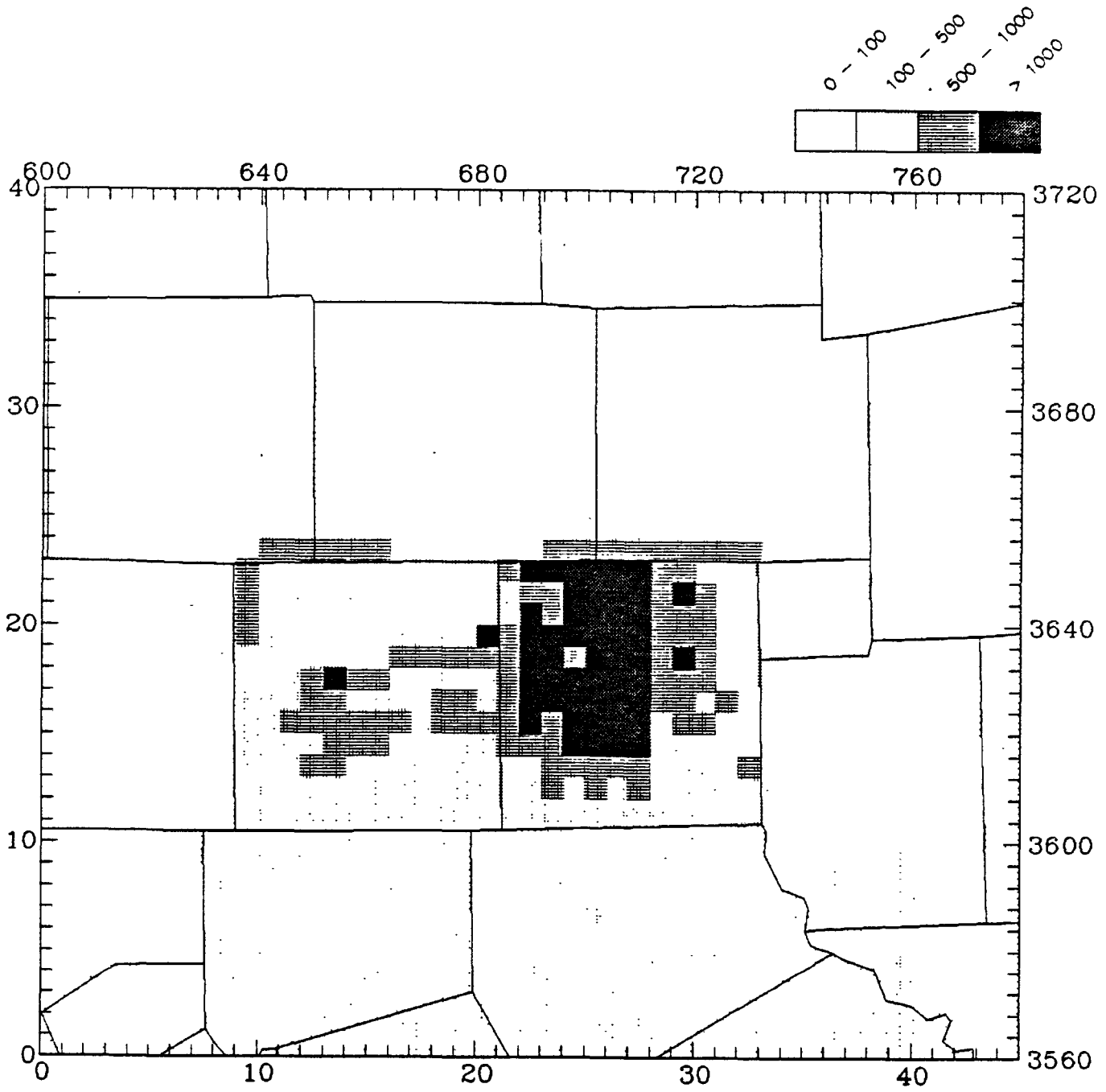

DALLAS -- '85 Area Weekend
RHC
Total: 221166 (Kg/day)

FIGURE 4-7i.

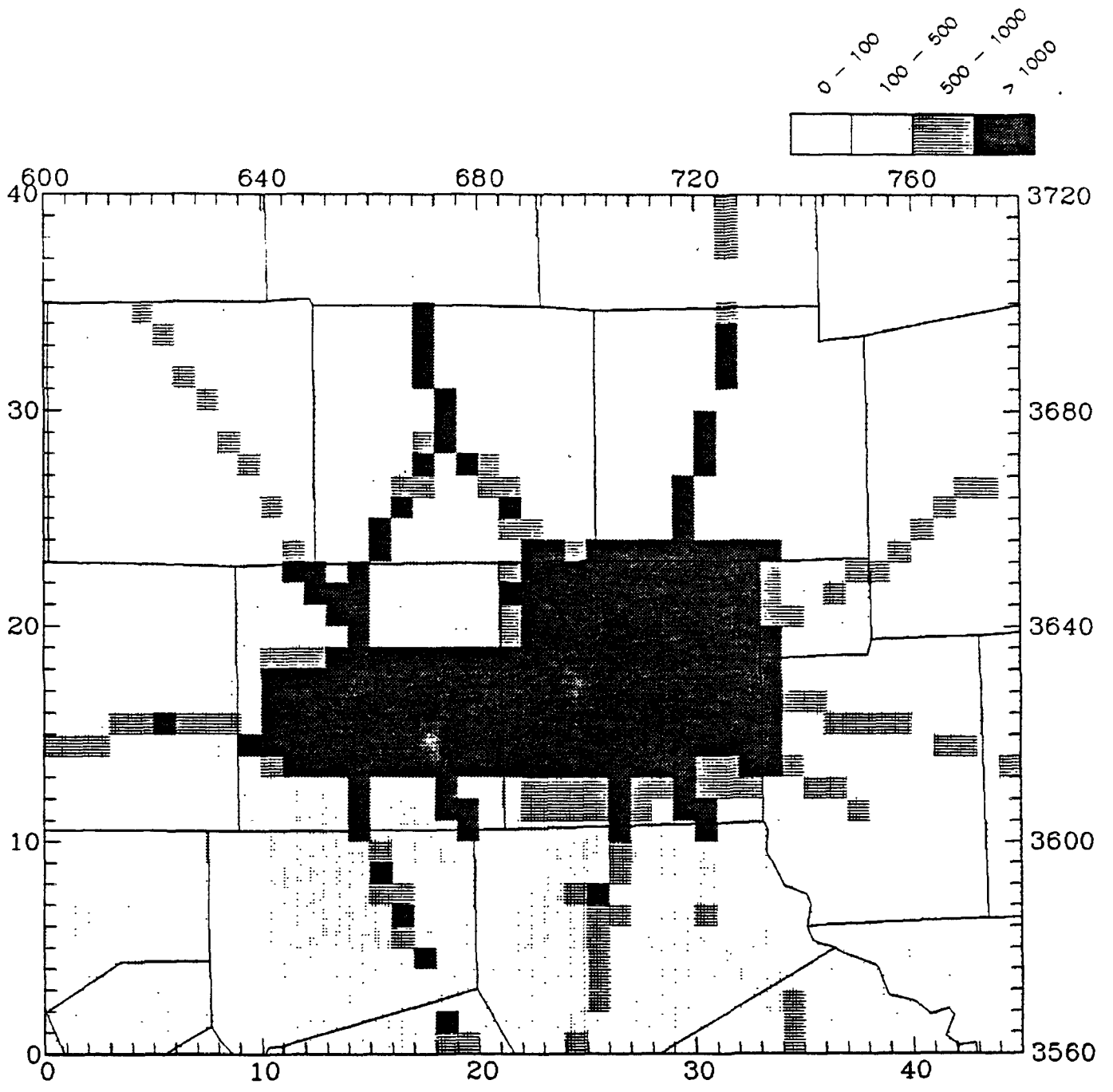

DALLAS -- '85 Motor Vehicle Weekday
RHC
Total: 831840 (Kg/day)

FIGURE 4-7j.

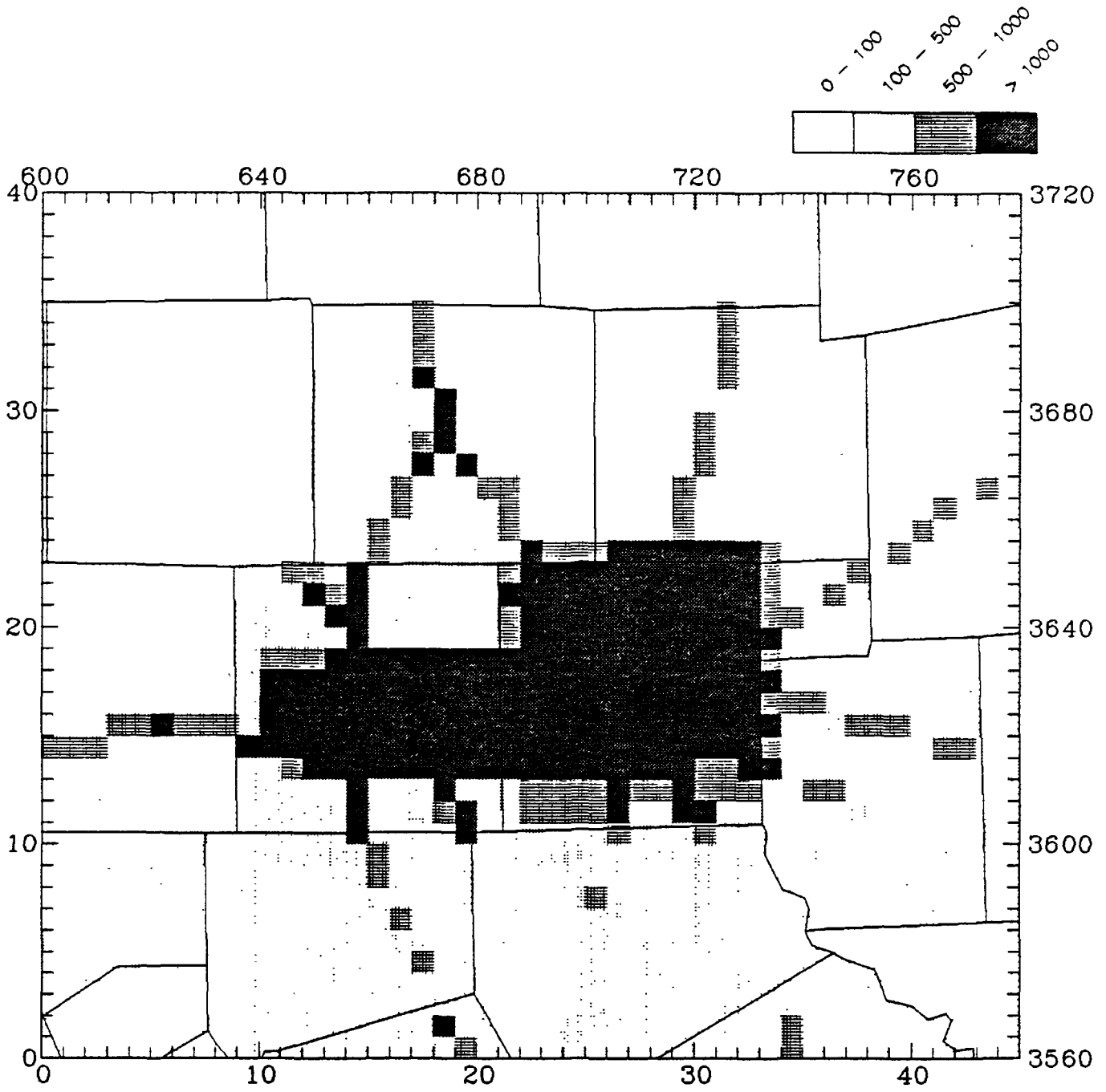

DALLAS -- '85 Motor Vehicle Weekend
RHC
Total: 623882 (Kg/day)

FIGURE 4-7k.

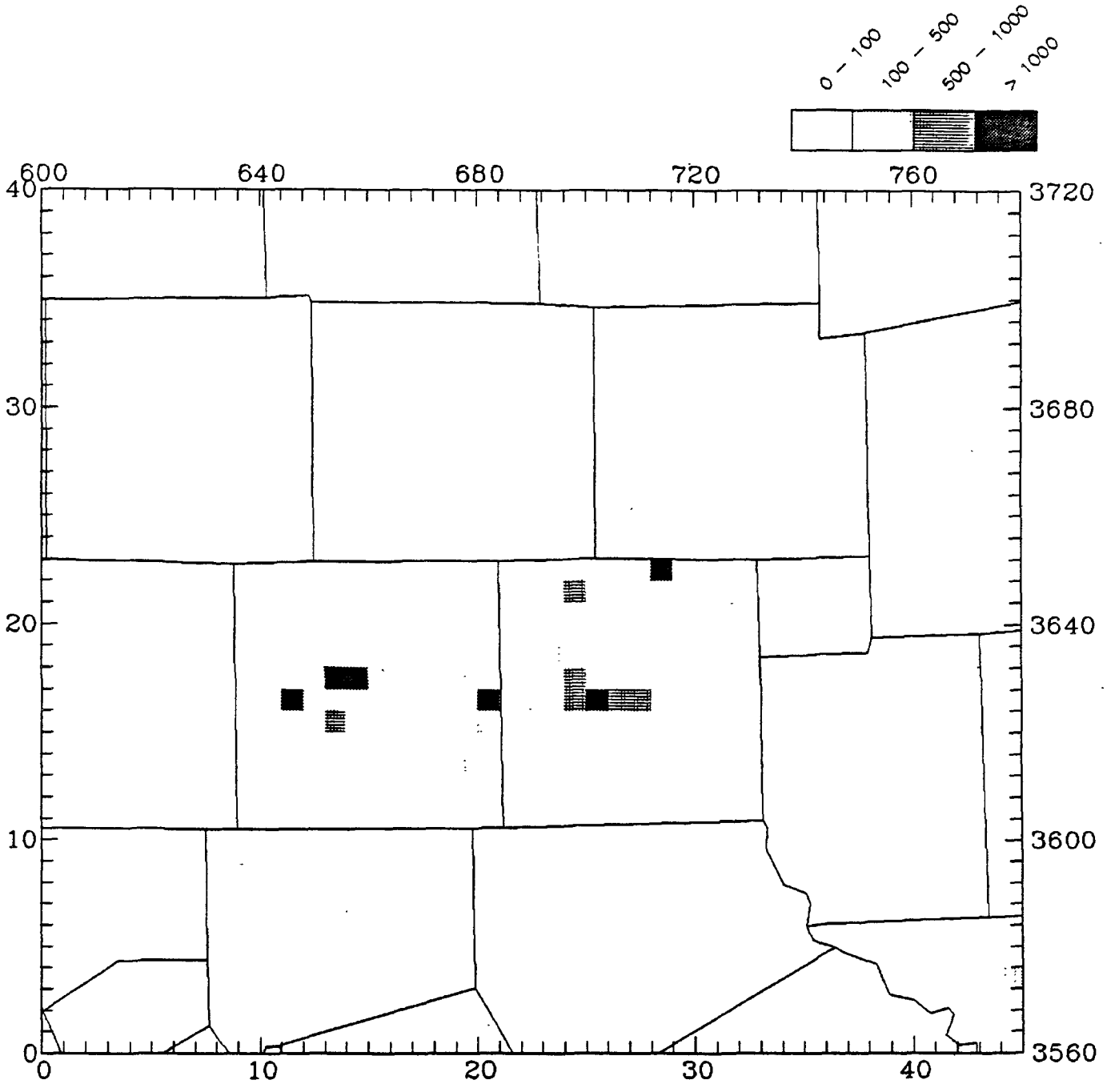

DALLAS -- '85 Low Level Points Weekday
RHC
Total: 23393 (Kg/day)

FIGURE 4-71.

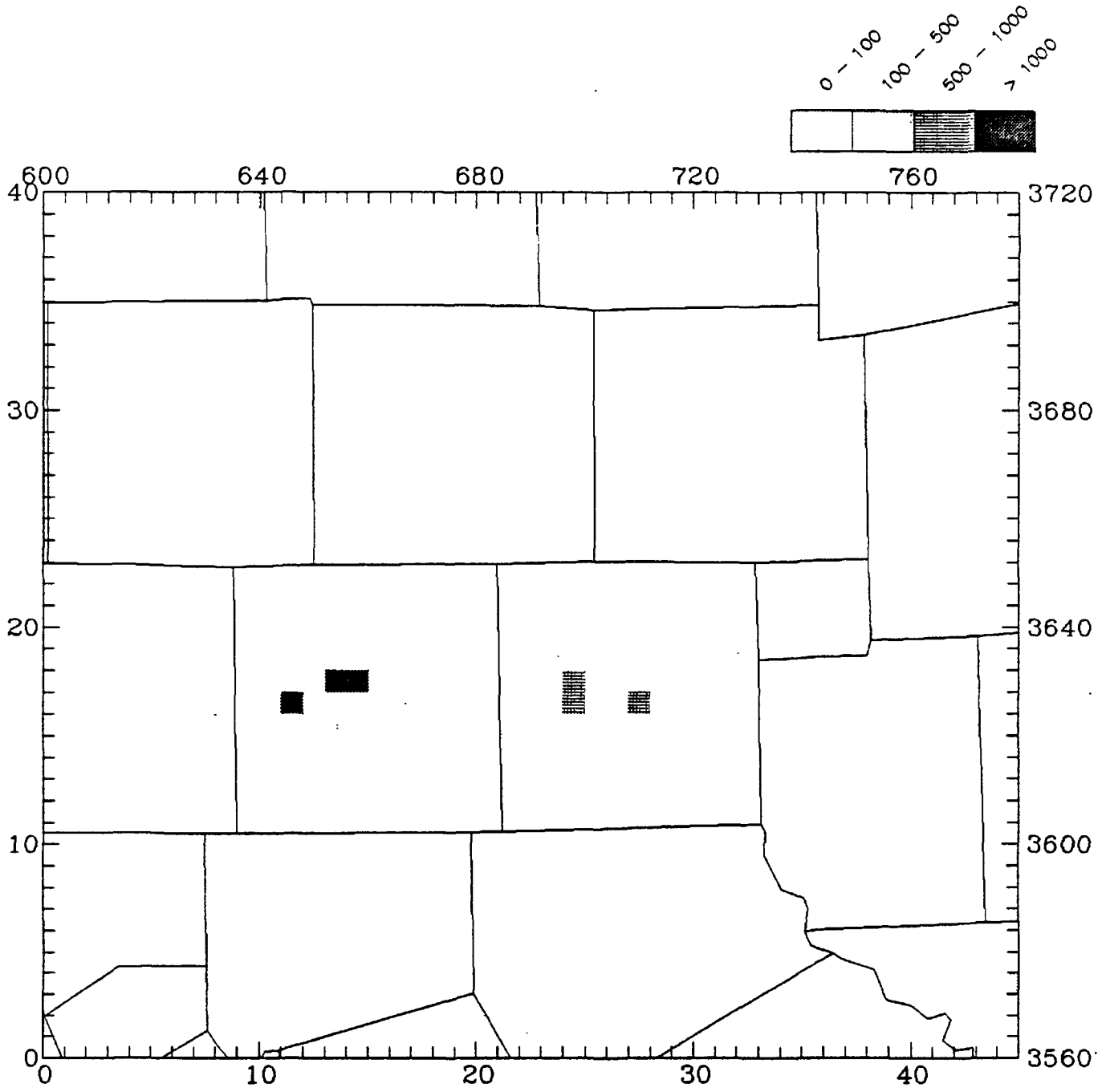

DALLAS -- '85 Low Level Points Weekend
RHC
Total: 10429 (Kg/day)

FIGURE 4-7m.

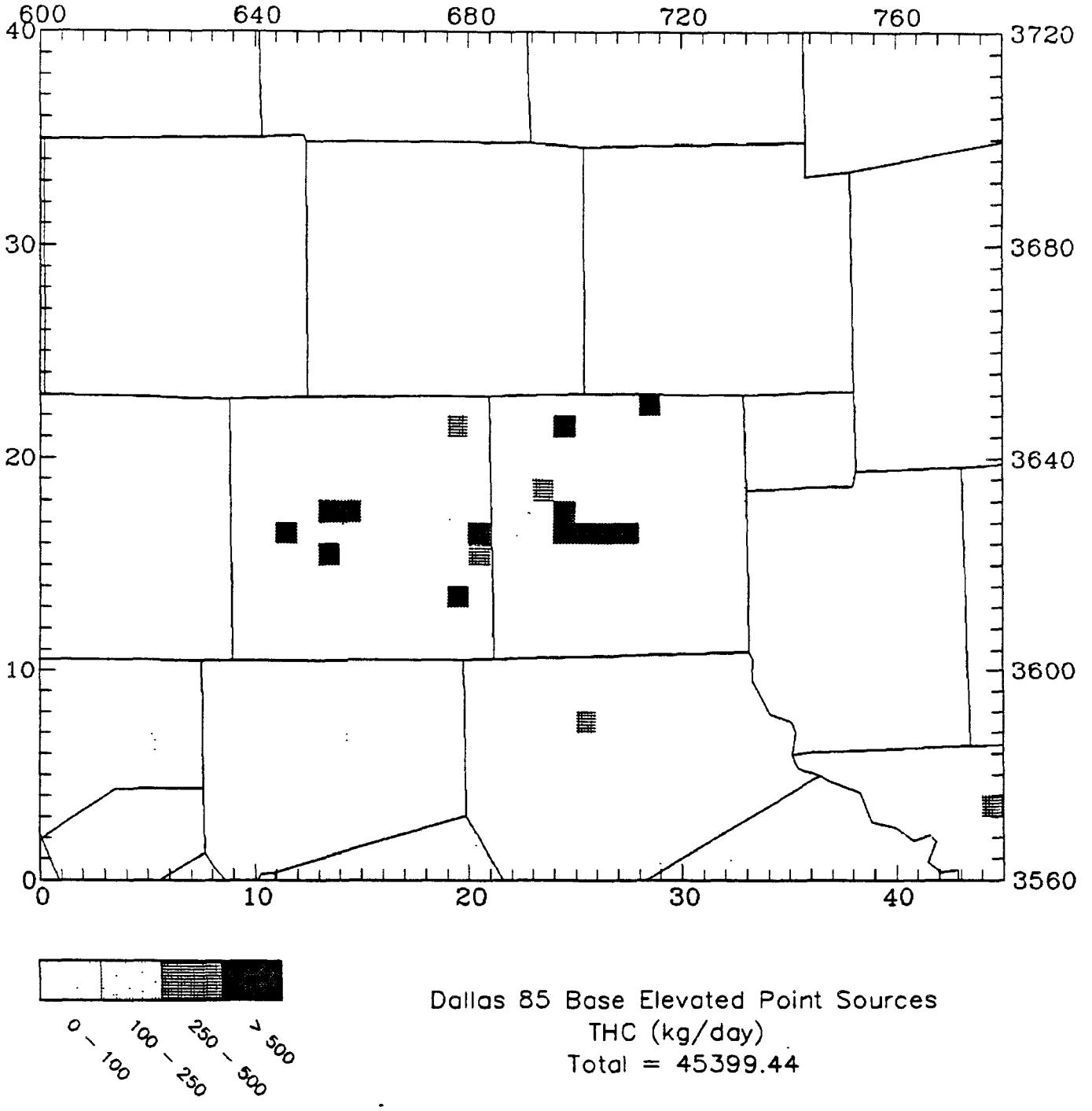
600
640
680
720
760
40
30
20
10
0
3720
3680
3640
3600
3560
0
10
20
30
40
0 - 100
100 - 250
250 - 500
> 500
Dallas 85 Base Elevated Point Sources
THC (kg/day)
Total = 45399.44

FIGURE 4-7n.

TABLE 4-4. Summary of emission totals (tons per day) for the Dallas-Fort Worth modeling domain.

	Weekday			Weekend		
	VOC	NO_x	CO	VOC	NO_x	CO
Motor vehicle	926	430	3174	734	344	2701
Other anthropogenic	454	439	193	190	382	184
Total anthropogenic	1380	869	3367	924	726	2885
Biogenic	631	0	0	631	0	0
Total anthropogenic and biogenic	2011	869	3367	1555	726	2885

89104 3

DIFFBREAK

This file contains the daytime mixing height or nighttime inversion height for each column of cells at the beginning and end of each hour of the simulation. Hourly mixing heights were estimated at several surface meteorological sites through use of the hourly surface measurements of temperature and the twice-daily upper-air observations from a representative upper-air site. The Longview, Texas upper-air site was felt to be most representative of upper-air conditions in Dallas-Fort Worth because it is closer to Dallas, the location of the observed maximum ozone concentration on 31 August (note that the Stephenville, Texas upper-air site is closer to Fort Worth). However, both the Longview and Stephenville sites yielded similar maximum mixing heights on the days selected for modeling. The diurnal variation in mixing heights at the eight CAMS surface meteorological observation sites (Table 4-1) was calculated using the RAMMET meteorological processor. These hourly values were then input into the standard UAM mixing height interpolation program, DFSNBK (Ames et al., 1985b) using the 1/r interpolation option to produce the spatially varying hourly fields of mixing heights. The maximum mixing height in diagnostic run 1 on 31 August was approximately 3,100 m AGL. Because it was believed that mixing heights lower than 3,100 m AGL actually existed in Dallas-Fort Worth on 31 August, diagnostic run 2 used a maximum mixing height of 2,000 m AGL. This is discussed later in this chapter.

REGIONTOP

This file contains the height of each column of cells at the beginning and end of each hour of the simulation. If this height is greater than the mixing height, the cell or cells above the mixing height are assumed to be within an inversion. For the Dallas-Fort Worth application a constant 3,000 m AGL region top was initially used. However, in diagnostic run 2, with the reduced maximum mixing height, a region top of 2,000 m AGL was specified.

WIND

This file contains the x and y components of the wind velocity for every grid cell for each hour of the simulation. There are two steps in creating the wind fields for Dallas-Fort Worth: (1) application of the Diagnostic Wind Model (DWM) (Morris et al., 1988, 1989a; Douglas and Kessler, 1988) using 15 vertical levels and data from the eight surface CAMS and two upper-air meteorological observation sites (Longview and Stephenville, Texas); and (2) vertical interpolation of the 15-layer hourly wind fields into the five-layer UAM configuration used for the Dallas-Fort Worth application (see Morris et al., 1989a).

The DWM creates an hourly 15-layer wind field by first creating a wind field by adjusting a domain-mean wind (based on upper-air observations) for terrain effects (kinematic effects, thermodynamically generated slope flows, blocking, and deflection). Then the observational information is added to the wind field by weighting the initial wind field heavily away from the observations and the observed winds heavily in the vicinity of the observations.

The 15-layer wind fields created by the DWM are then vertically averaged into the UAM five layer configuration. Since the surface observations provide a more detailed representation of the air flows in the vicinity of Dallas-Fort Worth and their presence is only felt within the lowest layer of the DWM, the first UAM vertical layer was assumed to have the same wind field as the first DWM layer. The DWM first layer is also weighted 50 percent in the second UAM vertical layer. The wind fields for the remainder of the UAM vertical layers were obtained from the DWM wind fields using weighted averaging. The resultant five-layer wind field was then modified using the procedure suggested by O'Brien (1970), which minimizes the vertical velocity out of the top of the region. In this manner, the boundary concentration assumed to exist above the region top (TOPCONC) does not greatly influence concentrations within the modeling domain.

For the application of the UAM to Dallas-Fort Worth, the hourly varying domain-mean wind input to the DWM was defined by averaging the winds from the two twice-daily upper-air soundings and then linearly interpolating these average soundings in time to the hour in question. Surface wind observations from the eight CAMS sites (Table 4-1) were also used in the DWM. Note that no instantaneous FAA/NWS wind observations were used in the generation of the wind fields because it was felt that they may overestimate the wind speeds of the stagant episode of 29-31 August 1985 (see Appendix D).

METSCALARS

This file contains the hourly values of the meteorological parameters that do not vary spatially. The NO_2 photolysis rates were calculated for the CB-IV mechanism using procedures described by Schere and Demerjian (1977) and actinic flux data collected by Bass and co-workers (1980) (see Gery, Whitten, and Killus, 1988). The concentration of water was based on measurements of temperature and dew point at the NWS surface site at Dallas. Water vapor concentrations ranged from approximately 13,000 to 23,000 ppm. Atmospheric pressure values of 0.98 atmosphere were used based on the data from the NWS site.

Exposure class is a measure of near surface stability: +3 during high solar intensity to -2 at night with no clouds. Exposure class was assigned based on the solar intensity: a value of -2 at night and daytime values of from 0 (one hour day/night transition period) to 3. The temperature gradients below (TGRADBELOW) and above

(TGRADABOVE) the inversion were based on the twice-daily upper-air soundings taken at Longview, Texas, and hourly surface temperatures observed at the NWS surface site in Dallas. Values for TGRADBELOW from the surface to the mixing height from the Longview evening sounding (1800 LST) are -0.0091, -0.0107, and -0.0113 K/m for August 29 through 31, respectively. Based on these measurements, values for TGRADBELOW were -0.0110 K/m for exposure classe 3, -0.0105 for exposure class 2, -0.01 K/m for exposure class 1, and -0.098 for exposure class 0.

The Longview morning sounding (0600 LST) measured values for TGRADBELOW of 0.012, 0.008, and 0.017 K/m on the mornings of August 29 to 31, respectively, assuming that the top of the surface based inversion was 250 m AGL. Observed temperatures at 250 m on August 29 through 31 were, respectively, 297.8, 297.4, and 301.3 K. Nighttime hourly values for TGRADBELOW were then calculated for 29-31 August based on the surface temperature at the Dallas NWS surface site and the measured value at 250 m from the 0600 LST sounding.

For predawn hours, the temperature gradient from 250 m to the original region top (3,000 m) from the 0600 sounding at Longview was used, resulting in values for TGRADABOVE of -0.0061, -0.0055, and -0.0062 K/m for August 29 through 31, respectively. For daytime hours a temperature at the mixing height was calculated for each hour of the day using the surface measurement at the Dallas NWS site and the value for TGRADBELOW. Then the hourly temperature gradient between the mixing height and the region top was estimated using the calculated value at the mixing height and the measured temperature from the 0600 sounding at Longview at 3,000 m AGL (281.8, 284.1, and 283.4 K for August 29 through 31, respectively)

AIRQUALITY

This file contains the initial concentrations of each species for each grid cell at the start of the simulation. Since the UAM was initiated at 12 noon on 29 August 1985, most of the material from the initial conditions was advected out of the region by the morning of 31 August; thus, initial concentrations do not influence ozone formation on 31 August. In the majority of the region the initial concentrations were assigned "clean values" as follows:

VOC	25 ppbc (using EKMA default speciation)
ISOP	0.001 ppb
NO_x	1 ppb (split 3/4 NO_2, 1/4 NO)
O_3	40 ppb
CO	200 ppb

Air quality measurements for ozone, NO, NO_2, and CO were available at up to eight sites in the Dallas-Fort Worth region (Table 4-3). Initial conditions were set according to the measured air quality data in the neighborhood of the sites.

BOUNDARY

This file contains the location of the modeling region boundaries. It also contains the concentration of each species that is used as the boundary condition along each boundary segment at each vertical level. For the application of the UAM to Dallas-Fort Worth the minimum of a one-cell buffer of unsimulated cells was used in the tracer simulation, resulting in a simulation region of 172 km by 152 km. The "clean" values listed previously were specified for boundary conditions. The tracer simulation showed that the stagnant conditions of the episode resulted in little transport of pollutants away from the urban areas. Therefore for the photochemical diagnostic simulations 3-, 4-, 7-, and 1-cell buffer zones were specified for respectively the north, south, east, and west boundaries, resulting in a 148 km by 124 km computational modeling domain.

TOPCONC

This file contains the concentration of each species for the area above the modeling region. Since the wind fields are processed to eliminate the vertical velocity through the region top, the model results are not sensitive to TOPCONC. Accordingly, the clean concentration values listed previously were used.

TEMPERATUR

This file contains the hourly temperature for each surface layer grid cell. Hourly spatial varying temperatures were obtained by using 1/r interpolation from the eight CAMS surface meteorological observations.

TERRAIN

This file contains the value of the surface roughness and deposition factor for each grid square. Each 4 km by 4 km grid cell was assigned to a land-use category based on a digitized USGS map of the modeling region. The land-use categories were then converted to roughness lengths and vegetation factors according to data published by Argonne National Laboratory (see Morris et al., 1989a).

CHEMPARAM

This file contains information regarding the chemical species to be simulated, including reaction rate constants, upper and lower bounds, activation energy, and reference temperature. Reaction rate constants correspond to those given in the

report documenting the CB-IV mechanism (Gery, Whitten, and Killus, 1988), except that reactions for methanol (MEOH) and ethanol (ETOH) have also been added to the mechanism (see Morris et al., 1989a).

TRACER SIMULATION

In order to determine the starting time and the computational modeling region for the UAM simulation, an inert tracer simulation was performed using an initial concentration field of all 100 and zero boundary conditions and emissions (Appendix F). Similarly, an inert boundary condition tracer simulation (100 on boundaries, zero initial concentrations and emissions) and emission tracer (constant emission rate with zero initial and boundary conditions) were performed (not shown). The tracer simulation was initiated at noon on 29 August. Note that these tracer simulations differ substantially from the weighted tracer simulation performed for Atlanta (Appendix A). In the tracer simulation for Atlanta the inert species were used to represent VOC and NO_x pollutant fluxes, whereas the inert tracer simulations performed for Dallas-Fort Worth were used only to determine how much of the initial conditions are present and gross flow aspects of the modeling inputs.

After 12 hours of simulation (0100 on 30 August) the initial concentrations still dominate about half of the region in the upper-northwest sector of the modeling domain. By noon on 30 August the initial condition tracer ranges from 5 to 30 in the upper northwestern portion of the region. At midnight on 30 August, after 36 hours of simulation, the initial condition tracer is still in the northwestern portion of the modeling domain with concentrations as high as 11. By 0800 on 31 August the maximum initial condition tracer is reduced to 4 and located in the northwestern corner of the modeling domain, well away from Fort Worth and Dallas.

The inert initial concentration tracer analysis indicates that if a starting time of noon on 29 August is used, the initial concentrations will not have any influence on the predicted concentrations on 31 August but will influence concentrations in the upper-northwest sector of the modeling domain on 30 August. The initial concentrations will also have a little influence on predicted concentrations in Fort Worth on 30 August but will not affect concentrations in Dallas on that day.

The inert initial, boundary, and emission tracer simulations also provided insight on how the computational modeling domain could be reduced without affecting the predicted concentrations. Because pollutants tend to slosh to the west on 30 August, the western boundary condition was not adjusted downward. It appears that pollutants travel somewhat eastward on 31 August, but then turn more toward the northeast. Since the wind speeds are so low on 31 August, pollutants are not expected to travel too far eastward from Dallas; thus eight grid cells (32 km) from the eastern boundary were eliminated from the computational grid. Finally, five grid cells from the southern boundary and four grid cells from the northern boundary were also eliminated in the computational grid.

EVALUATION SIMULATIONS

Two diagnostic simulations were performed before an adequate base case was obtained. As discussed above, the modeling period began at noon on 29 August 1985 and ended at 2000 on 31 August. All meteorological inputs were based on the six CAMS surface sites and the two upper-air meteorological observation sites. The first 12 hours of the simulation on 29 August was used to initialize the model and the model was evaluated against hourly average ozone, NO, NO_2, and CO concentrations at the surface air quality monitoring sites on August 30 and 31.

Diagnostic Run 1

For the first diagnostic simulation the observed meteorological data were used "as is" in the wind field model and other UAM preprocessors. The maximum mixing height on 31 August exceeded 3,000 m AGL. As noted in the tracer simulation, there is still significant amounts of initial conditions within the modeling domain on 30 August (see Appendix F). Since the model was initialized with "clean" concentrations, it is expected that the model may underpredict the peak observed ozone concentrations on 30 August.

30 August 1985

A comparison of predicted and observed hourly average ozone concentrations for diagnostic run 1 at the air quality monitoring sites are given in Figure 4-8. (Isopleths of hourly average ozone concentrations for diagnostic run 1 are shown in Appendix G.) As seen in Figure 4-4b, the observed peak ozone concentration on 30 August is 14 pphm and occurs in Fort Worth (ROSS). The predicted region-wide maximum ozone concentration on 30 August is 12.4 pphm (within 11 percent) and occurs approximately 40 km west of ROSS (Appendix G). Predicted daily maximum ozone concentrations in Fort Worth range from approximately 7 to 10 pphm on 30 August. At the location of the observed peak ozone concentration on 30 August (ROSS) the model predicts the observed peak (14 pphm) to within only 43 percent (7.9 pphm) At the other ozone site in Fort Worth operating on this day (KLLR) the observed maximum ozone concentration for 30 August (11 pphm) is replicated by the model to within 7 percent (10.2 pphm).

In the Dallas area the observed maximum ozone concentrations on 30 August range from 5 to 7 pphm (Figure 4-4b) while maximum model predictions range from 7 to 10 pphm (Appendix G). It appears that for 30 August in Dallas the model overpredicts the observed peak ozone concentrations (MOCK, NSTR, ILLI), while to the north (DNTN) and south (BNVW) the model replicates the observations quite well.

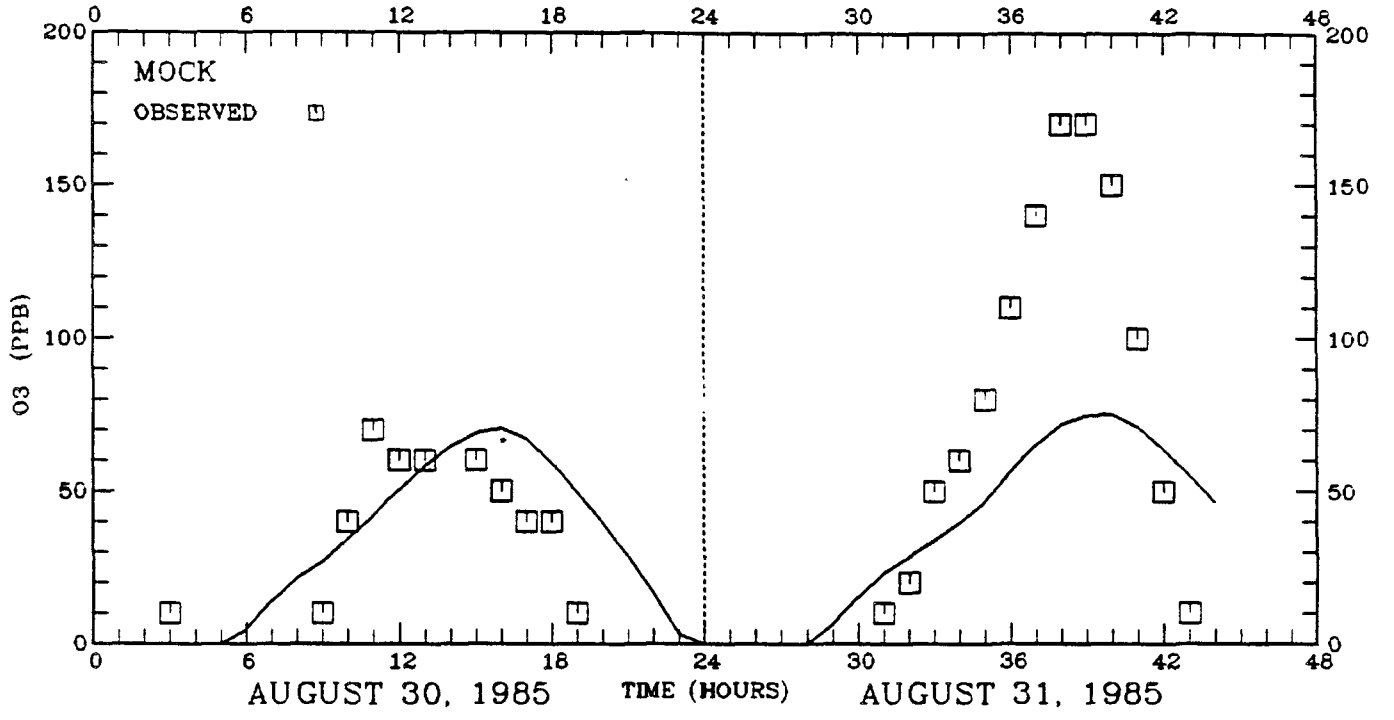

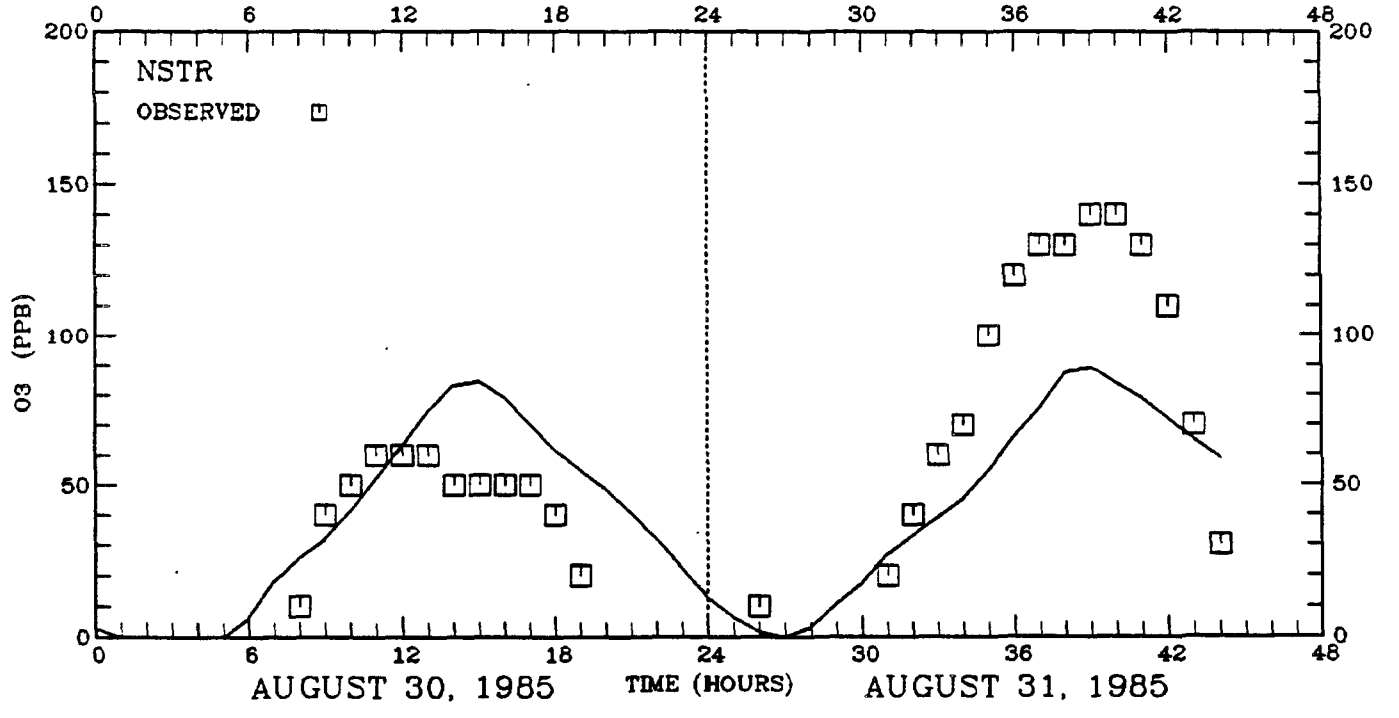

FIGURE 4-8. Time series of predicted and observed hourly ozone concentrations (ppb) for the Dallas-Fort Worth diagnostic run 1.

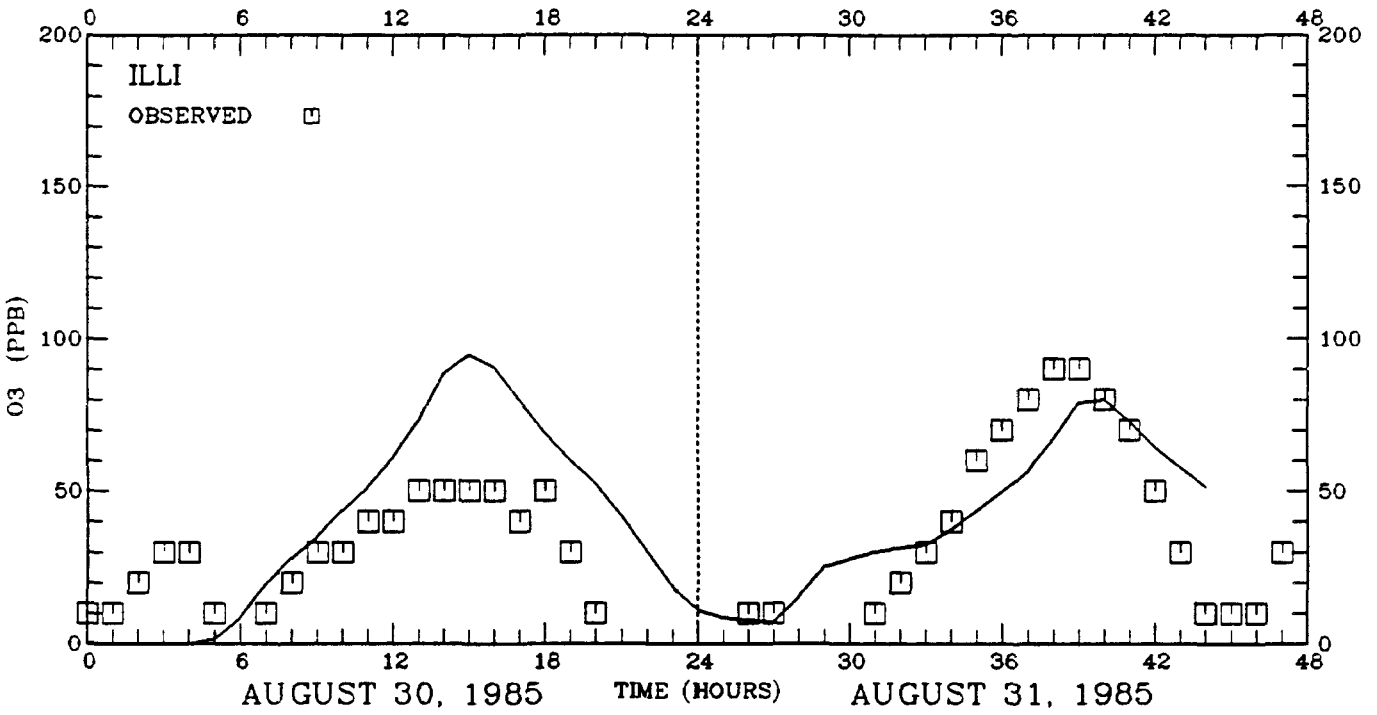

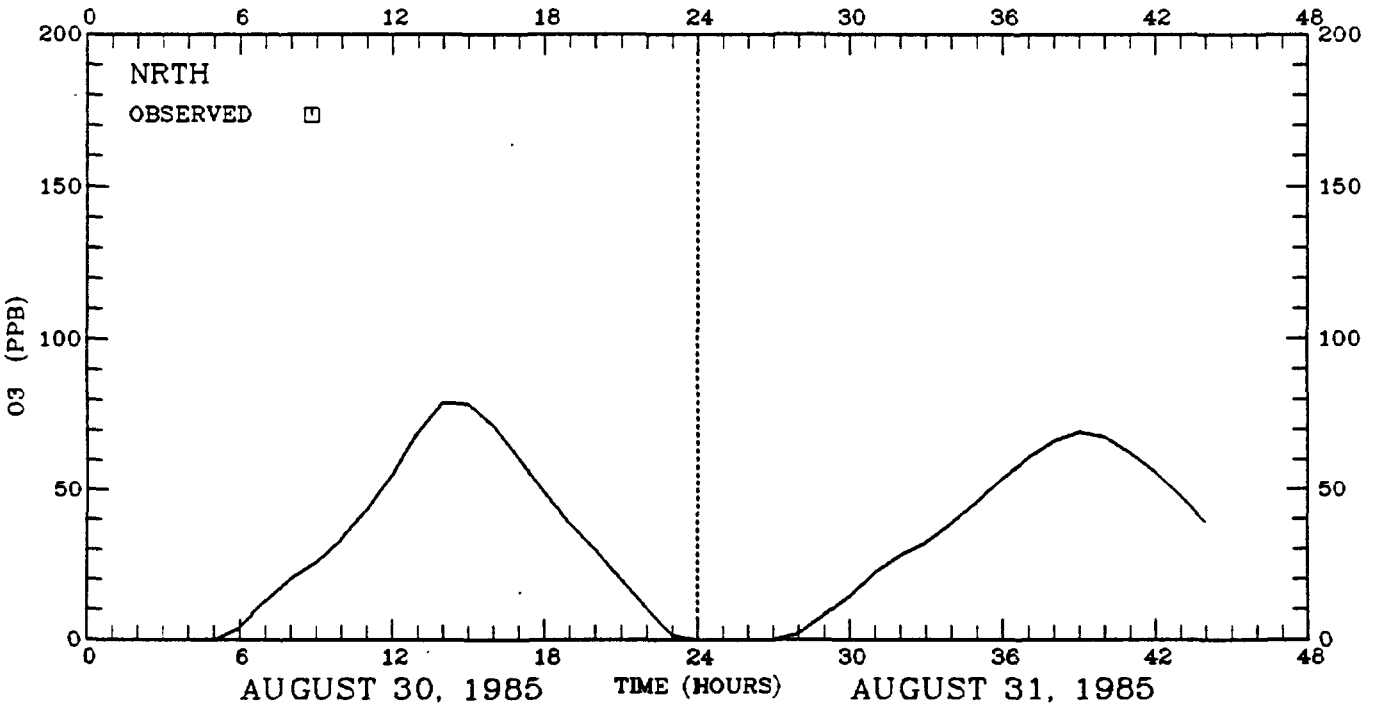

FIGURE 4-8 continued.

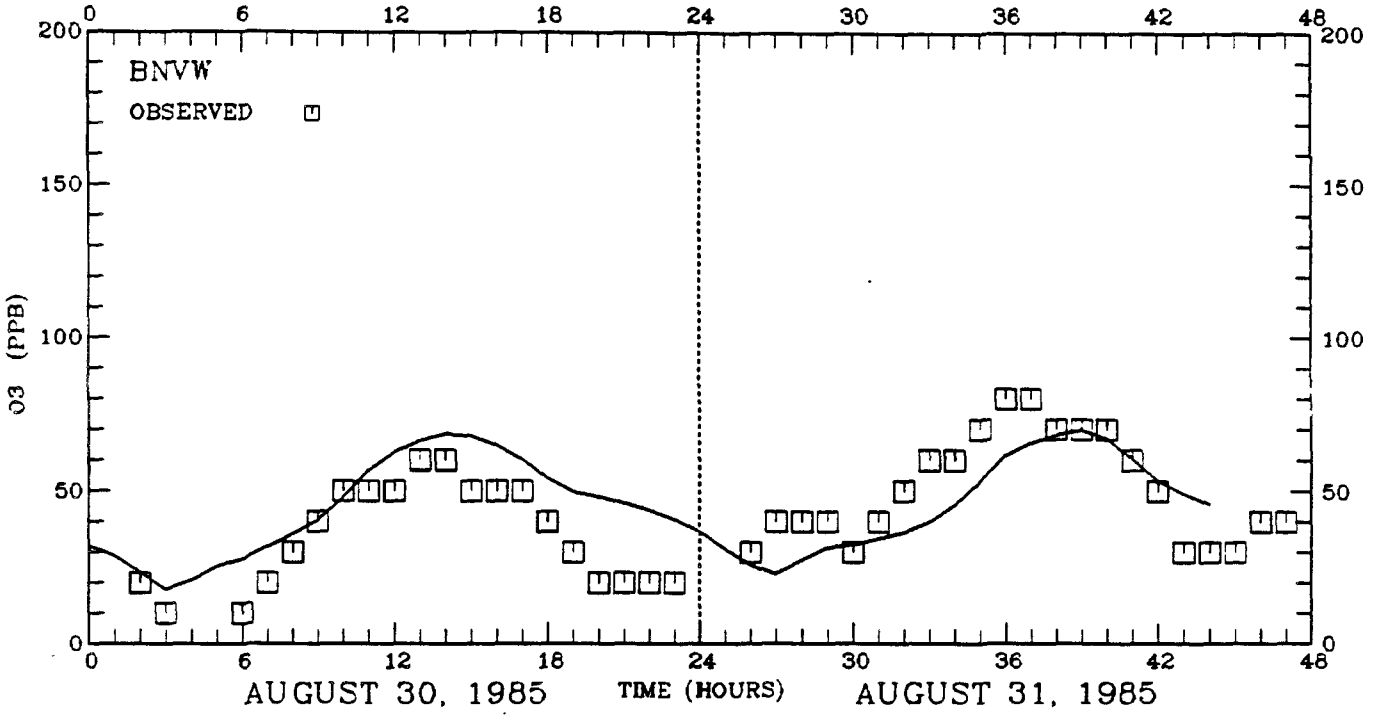

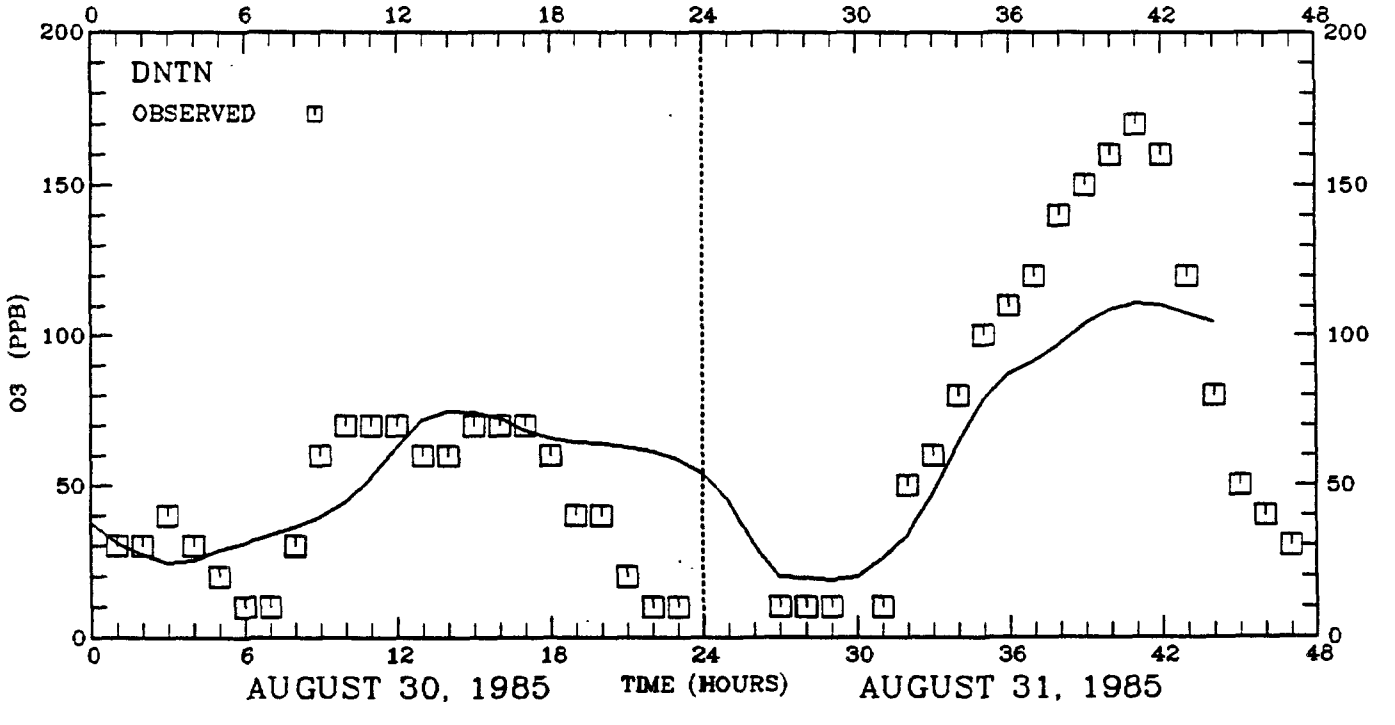

FIGURE 4-8 continued.

SYSTEMS APPLICATIONS, INC.

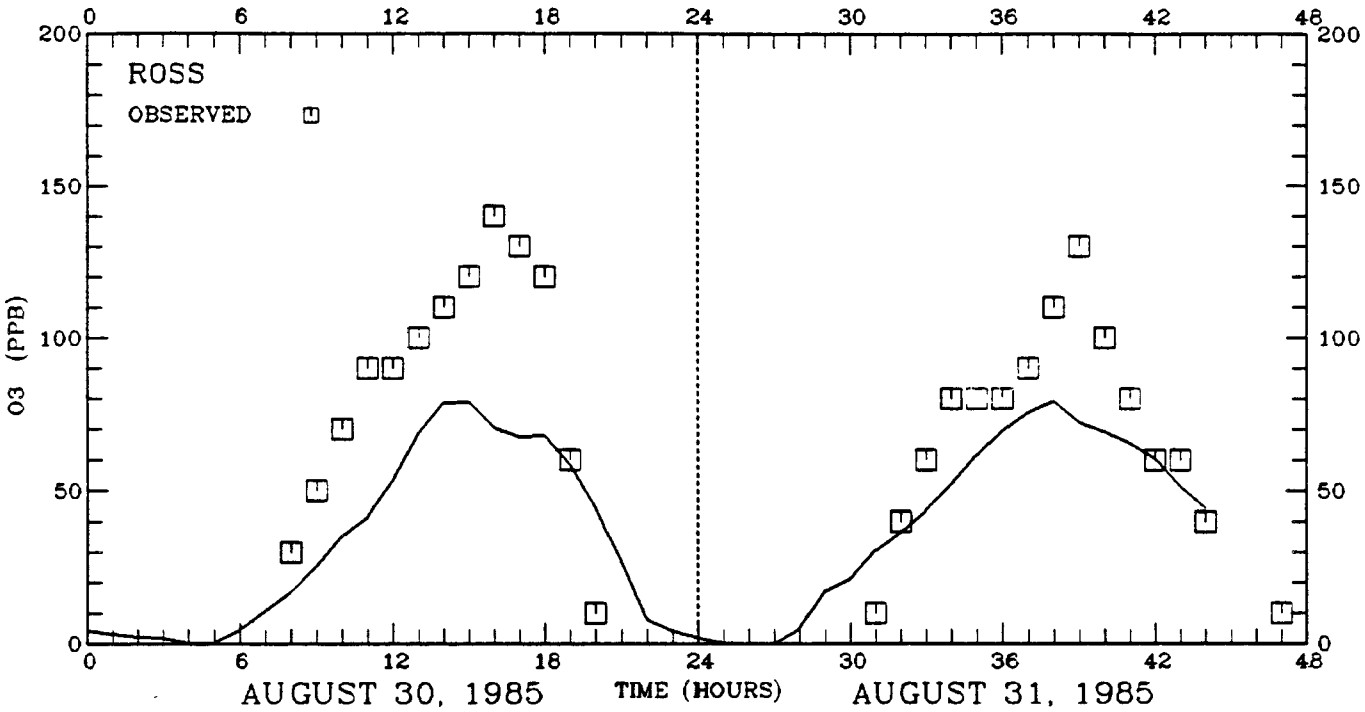

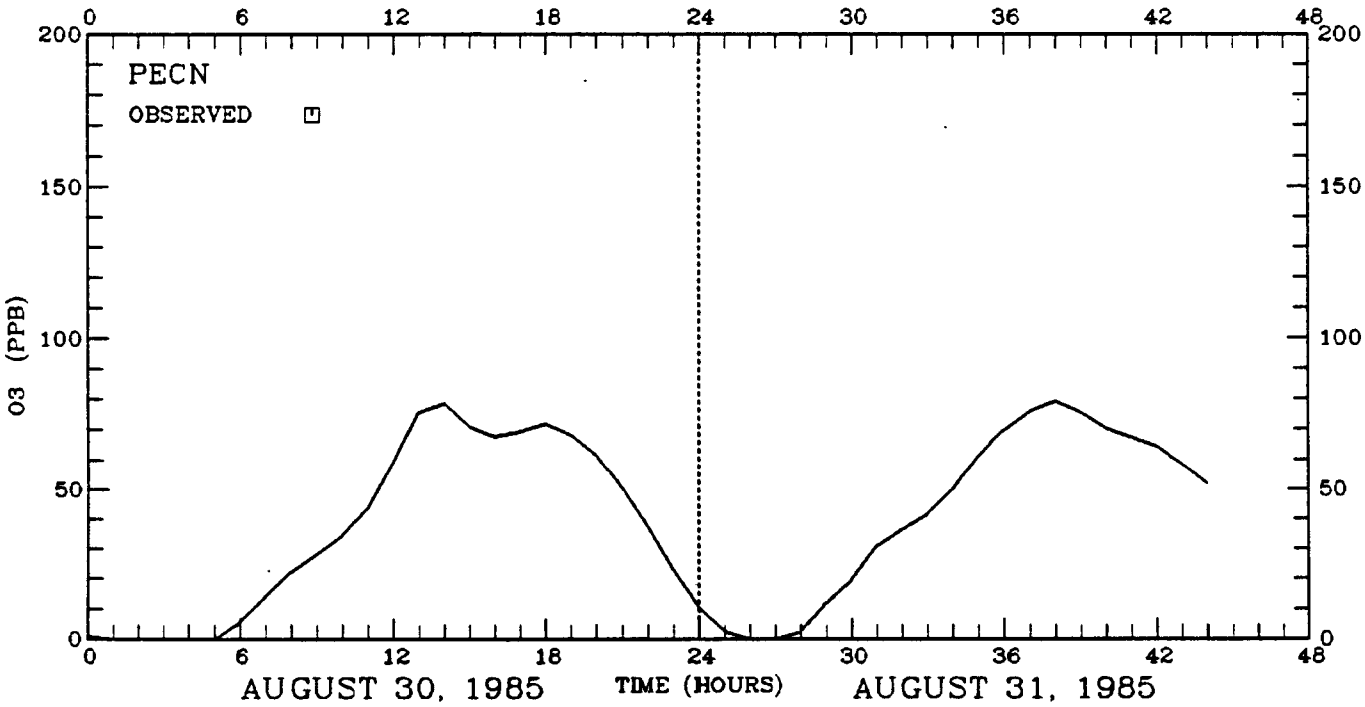

FIGURE 4-8 continued.

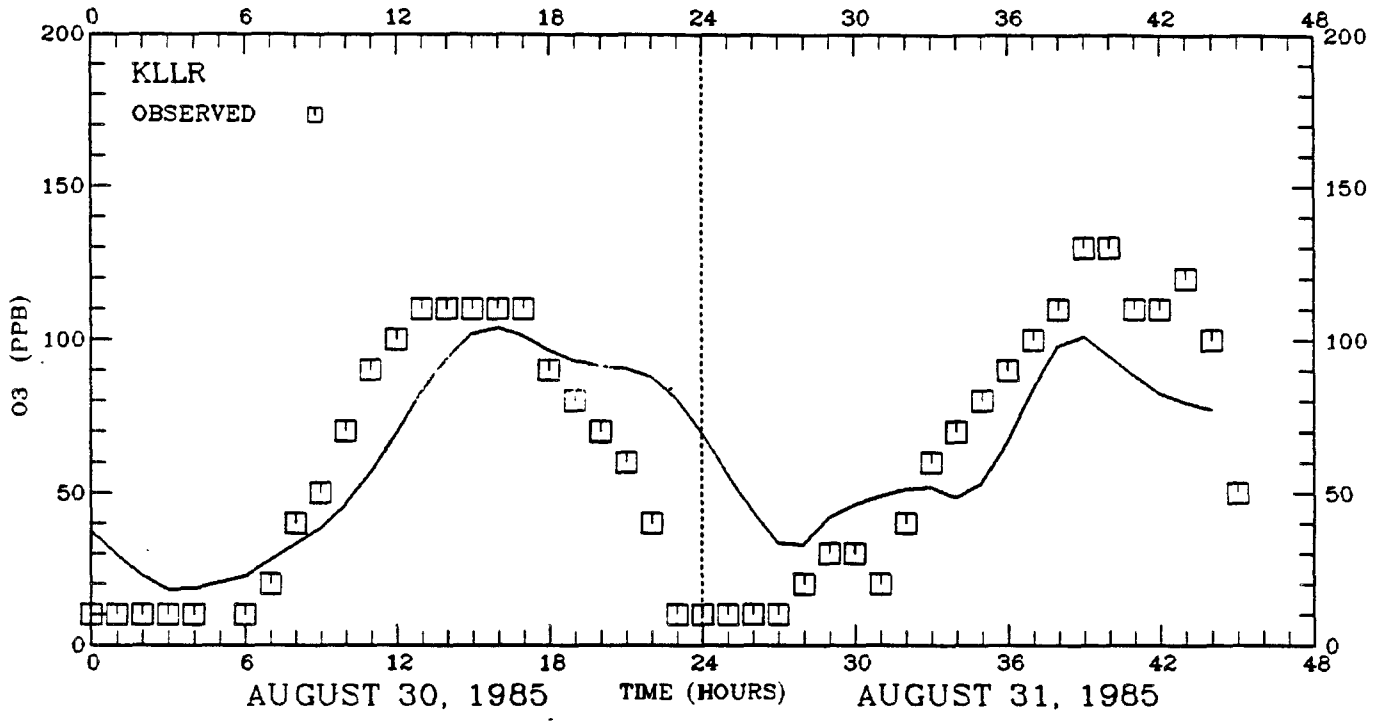

FIGURE 4-8 concluded.

Figure 4-9 presents a scatterplot along with model performance statistics for hourly ozone concentrations on 30 August. Over all hours and sites the model predictions have a bias of about 12 percent (-0.54 pphm) tending toward overprediction and a gross (average absolute error) of about 43 percent (2.0 pphm). The correlation coefficient between predicted and observed hourly ozone concentrations on 30 August for diagnostic run 1 is 0.64.

For diagnostic run 1 on 30 August the model predicts higher concentrations in Fort Worth than in Dallas. This ozone distribution is verified by the observations. The model underpredicts the observed peak ozone concentrations in Fort Worth and slightly overpredicts the observed daily maximum ozone concentrations in Dallas.

31 August 1985

On 31 August the observed peak (17 pphm) occurred at two sites: one in Dallas (MOCK) and another north of Dallas (DNTN). As seen in Appendix G, the predicted region-wide maximum ozone concentrations for diagnostic run 1 was 14.5 pphm (within 15 percent of the peak observation) and occurred in north Dallas between the two monitors that recorded the maximum observed value. At the location of one of the observed peaks in Dallas (MOCK) the model underpredicts the peak (17 pphm) by approximately 56 percent (7.5 pphm), whereas at the site north of Dallas (DNTN) the observed peak (17 pphm) is underpredicted by about 35 percent (11.1 pphm). At the only other site in Dallas that recorded a violation of the ozone NAAQS (14 pphm) on 31 August (NSTR) the model underpredicts by 36 percent (8.9 pphm).

Both of the sites in Fort Worth also recorded violations of the ozone NAAQS on 31 August (13 pphm). At these two sites the predicted maximum ozone concentrations on 31 August were within 39 (7.9 pphm at ROSS) and 22 (10.2 pphm at KLLR) percent of the peak observation.

Figure 4-10 displays a scatterplot and model performance statistics for predicted and observed hourly ozone concentrations on 31 August 1985 and diagnostic run 1. Over all hours the model has a bias of 18 percent tending toward underprediction (1.3 pphm) and a gross error of 33 percent (2.3 pphm). The hourly ozone predictions follow the observations well, as evidenced by the lack of excessive scatter in the scatterplot (Figure 4-10a) and the fairly high correlation coefficient (0.83).

NO, NO_2, and CO

Hourly observations of NO and NO_2 were available at four of the air quality monitoring sites: MOCK, NSTR, BNVW, and ROSS. CO observations were also available at four sites: MOCK, ILLI, NRTH, and ROSS. Historically, the performance of air quality simulation models for primary species, such as NO, NO_2, and CO, has been much worse than for secondary species, such as ozone. This is because the effects of

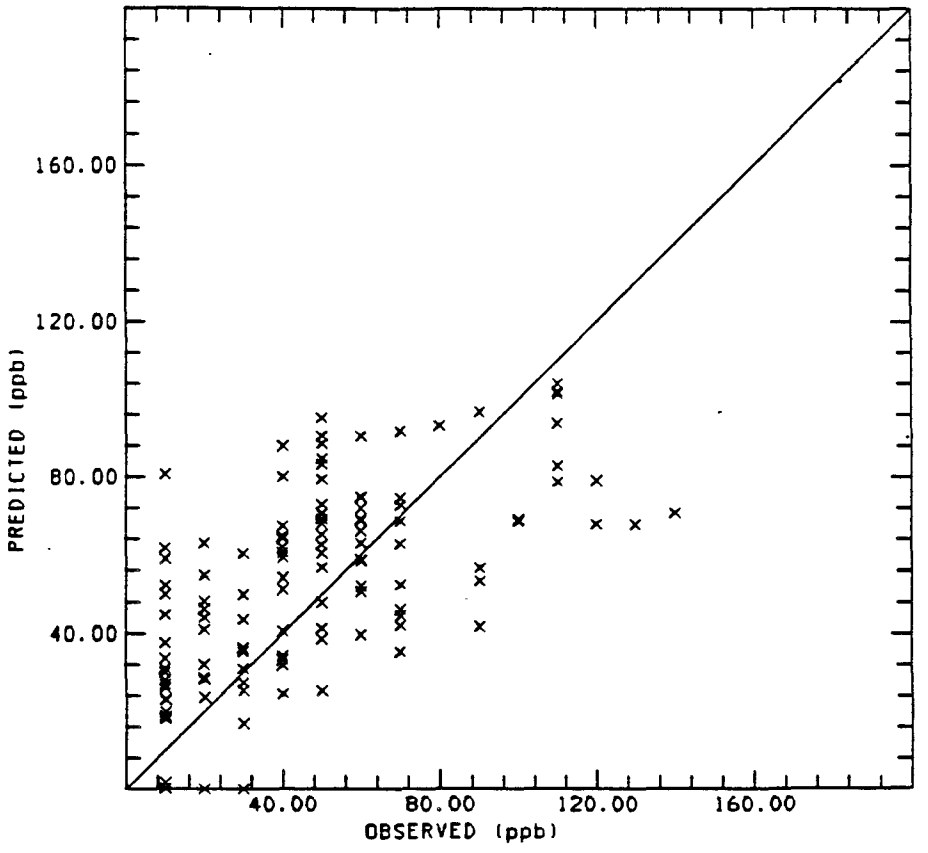

MOMENTS OF THE PROBABILITY DENSITY FUNCTION

	OBSERVED	PREDICTED
AVERAGE	46.96721	52.43745
STANDARD DEVIATION	31.01291	25.12773
SKEWNESS	0.82584	-0.13819
KURTOSIS	0.17512	-0.60323
OTHER MEASURES		
MEDIAN	40.00000	53.49000
UPPER QUARTILE	60.00000	69.10001
LOWER QUARTILE	20.00000	31.96000
MINIMUM VALUE	10.00000	0.01000
MAXIMUM VALUE	140.00000	104.00000

SKILL OF PREDICTION PARAMETERS

CORRELATION COEFFICIENT OF PREDICTED VERSUS OBSERVED 0.635
THE BOUNDS OF THE CORRELATION AT THE CONFIDENCE LEVEL OF 0.050 ARE
LOW BOUND 0.515 HIGH BOUND 0.730
RATIO OF OVER TO UNDER PREDICTIONS 1.711
PERCENT OF OVER PREDICTIONS GREATER THAN 200 PERCENT OF THE OBSERVED 19.672
PERCENT OF UNDER PREDICTIONS LESS THAN 50 PERCENT OF THE OBSERVED 6.557

FIGURE 4-9a. Scatterplot and model performance statistics for predicted and observed hourly ozone concentrations (ppb) on 30 August 1985 in Dallas-Fort Worth for diagnostic run 1 (N=122).

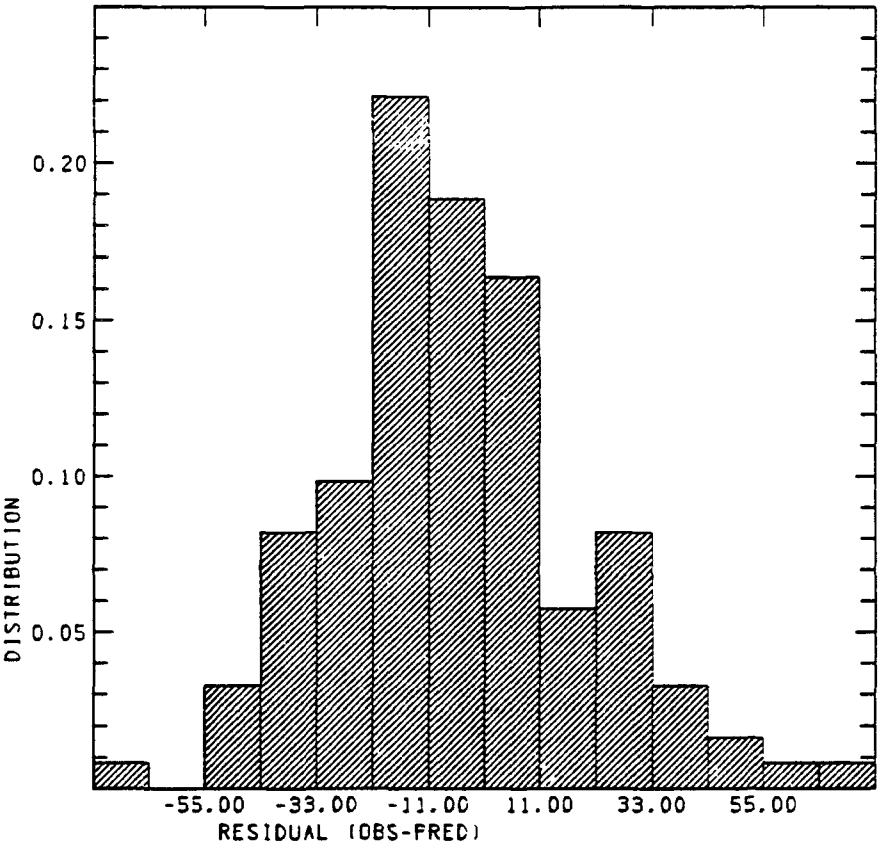

THE BINSIZE EQUALS 11.000

RESIDUAL ANALYSIS

AVERAGE	-5.47053
STANDARD DEVIATION	24.57855
SKEWNESS	0.41158
KURTOSIS	0.30432
OTHER MEASURES	
MEDIAN	-8.36000
UPPER QUARTILE	8.22000
LOWER QUARTILE	-21.04000
MINIMUM VALUE	-70.71001
MAXIMUM VALUE	69.17000

BIAS CONFIDENCE INTERVAL
AT THE 0.0500 LEVEL
LOWER BOUND -11.4614
UPPER BOUND 0.5203

STD RESIDUAL CONFIDENCE INTERVAL
AT THE 0.0500 LEVEL
LOWER BOUND 495.3563
UPPER BOUND 755.9985

THE MEASURES OF GROSS ERROR
THE ROOT MEAN SQUARE ERROR IS 25.08
THE AVERAGE ABSOLUTE ERROR IS 20.23

VARIOUS MEASURES OF RELATIVE VARIABILITY
OBSERVATION COEFFICIENT OF VARIATION
0.6603
RESIDUAL COEFFICIENT OF VARIATION
0.5233
RATIO OF RESIDUAL TO OBSERVED ST. DEV.
0.7925

FIGURE 4-9b. Residual analysis and model performance statistics for predicted and observed hourly ozone concentrations (ppb) on 30 August 1985 in Dallas-Fort Worth for diagnostic run 1 (N=122).

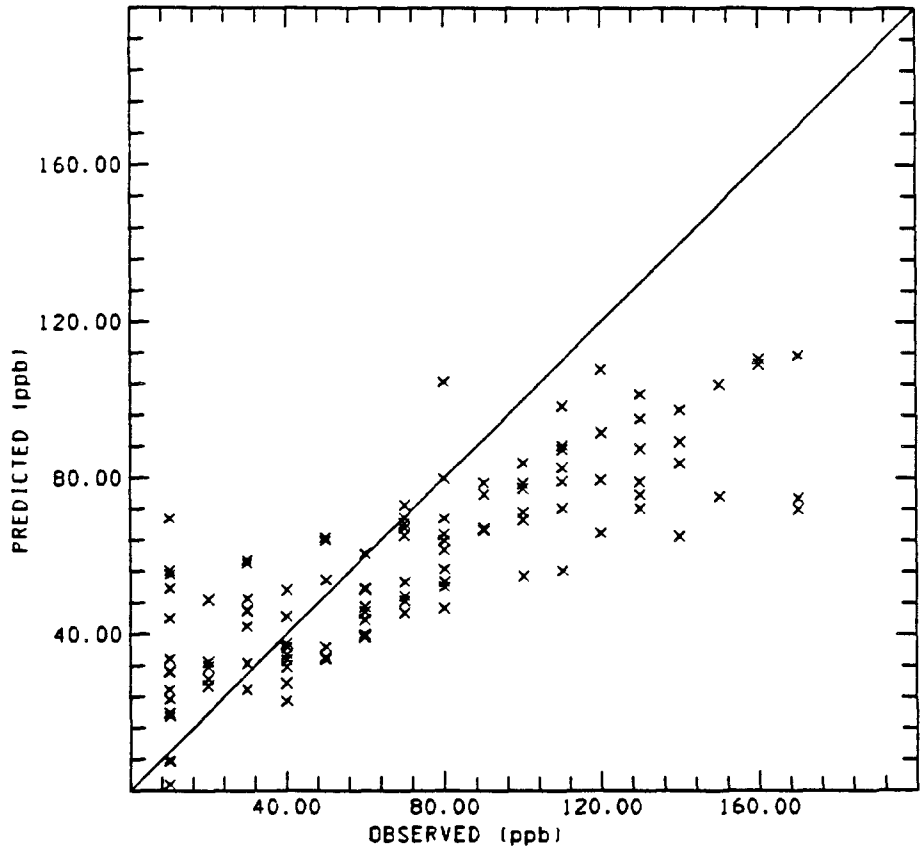

MOMENTS OF THE PROBABILITY DENSITY FUNCTION

	OBSERVED	PREDICTED
AVERAGE	70.60869	57.81913
STANDARD DEVIATION	44.49103	24.27184
SKEWNESS	0.38833	0.15263
KURTOSIS	-0.79089	-0.49933
OTHER MEASURES		
MEDIAN	70.00000	56.25000
UPPER QUARTILE	100.00000	73.11000
LOWER QUARTILE	30.00000	37.64000
MINIMUM VALUE	10.00000	1.63000
MAXIMUM VALUE	170.00000	111.39990

SKILL OF PREDICTION PARAMETERS

CORRELATION COEFFICIENT OF PREDICTED VERSUS OBSERVED 0.828
THE BOUNDS OF THE CORRELATION AT THE CONFIDENCE LEVEL OF 0.050 ARE
LOW BOUND 0.761 HIGH BOUND 0.878
RATIO OF OVER TO UNDER PREDICTIONS 0.438
PERCENT OF OVER PREDICTIONS GREATER THAN 200 PERCENT OF THE OBSERVED 9.565
PERCENT OF UNDER PREDICTIONS LESS THAN 50 PERCENT OF THE OBSERVED 3.478

FIGURE 4-10a. Scatterplot and model performance statistics for predicted and observed hourly ozone concentrations (ppb) on 31 August 1985 in Dallas-Fort Worth for diagnostic run 1 (N=115).

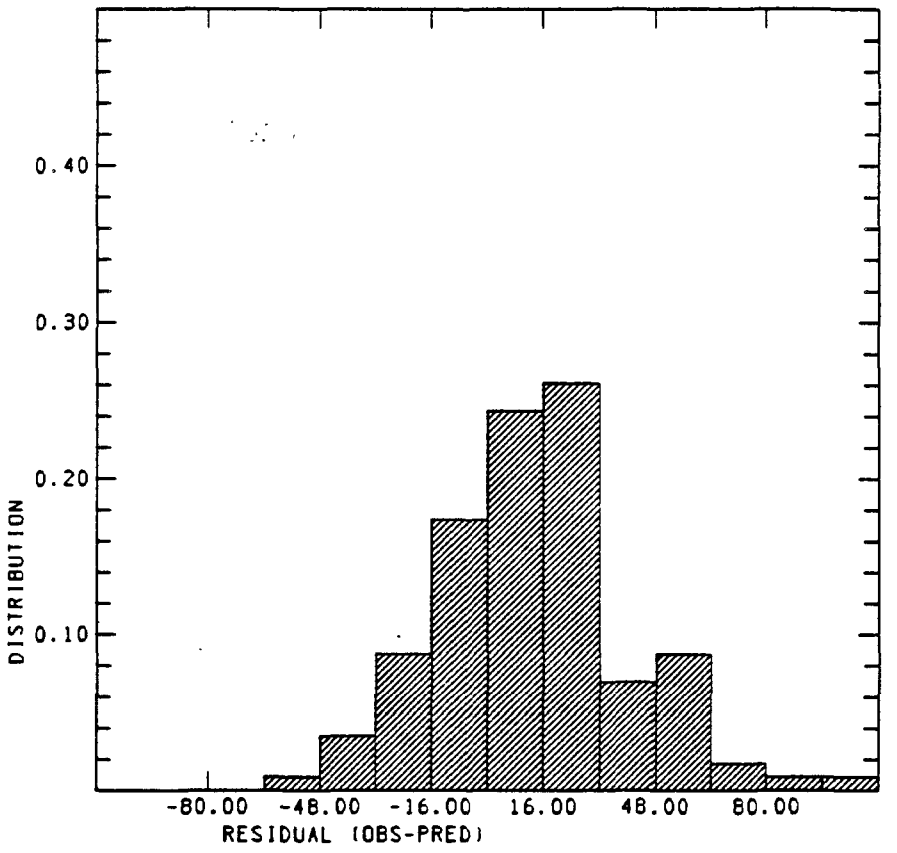

THE BINSIZE EQUALS 16.000

RESIDUAL ANALYSIS

AVERAGE	12.78924
STANDARD DEVIATION	27.91764
SKEWNESS	0.32808
KURTOSIS	0.58592
OTHER MEASURES	
MEDIAN	12.89000
UPPER QUARTILE	26.61000
LOWER QUARTILE	-6.91000
MINIMUM VALUE	-59.66000
MAXIMUM VALUE	98.00000

BIAS CONFIDENCE INTERVAL
AT THE 0.0500 LEVEL
LOWER BOUND 4.9507
UPPER BOUND 20.6277

STD RESIDUAL CONFIDENCE INTERVAL
AT THE 0.0500 LEVEL
LOWER BOUND 635.5250
UPPER BOUND 982.3846

THE MEASURES OF GROSS ERROR
THE ROOT MEAN SQUARE ERROR IS 30.60
THE AVERAGE ABSOLUTE ERROR IS 23.61

VARIOUS MEASURES OF RELATIVE VARIABILITY
OBSERVATION COEFFICIENT OF VARIATION
0.6301
RESIDUAL COEFFICIENT OF VARIATION
0.3954
RATIO OF RESIDUAL TO OBSERVED ST. DEV.
0.6275

FIGURE 4-10b. Residual analysis and model performance statistics for predicted and observed hourly ozone concentrations (ppb) on 31 August 1985 in Dallas-Fort Worth for diagnostic run 1 (N=115).

subgrid-scale variability (due to local emission sources) is much more pronounced in primary species. However, it is always useful to compare model predictions with observations of these primary species in order to determine whether the model is getting the right answer for the right reason.

As seen in Figure 4-11, the model tends to underpredict NO observations at all four sites. At the two sites in Dallas (MOCK and NSTR) the model predicts a primary NO peak at around 0300 and a secondary peak at 0700, whereas the observations only support an NO peak at 0700. The NO peak at 0700 is most likely due to increased emissions for that period. The model-predicted peak at 0300 may be due to a wind shift. At the monitor located south of Dallas (BNVW) the observations are at the lower threshold of the NO instrument (1 pphm) or zero. The model predictions for NO at BNVW are also very low. In Fort Worth (ROSS) the model does an excellent job replicating the pattern of the observed NO concentrations, however it appears to underpredict the peak NO observations by over a factor of two.

Diagnostic run 1 displays better agreement with hourly NO_2 observations than for NO as evidenced in Figure 4-12. The diurnal variations in the hourly observed NO_2 concentrations are replicated by the model quite well.

As is usually the case for a grid model like the UAM, the model has difficulty in reproducing the scatter in the hourly CO concentrations (Figure 4-13). In general it appears that the model underpredicts the observed CO concentrations during most hours and sites. The model does pick up some of the trends of the observations such as the peak around midnight; however, the scatter in the observations makes it difficult to evaluate model performance for CO concentrations.

Summary

The peak ozone observations on 30-31 August are replicated by the predicted region-wide maximum on these days to within 11 and 15 percent and is in the general vicinity of the peak observation. However, there is much spatial variation in the predicted ozone concentrations, resulting in predicted daily maximum ozone concentrations at the location of the peak observations that are only within 43 percent on 31 August and 56 and 35 percent (two sites) on 31 August. The model also tends to underpredict primary emitted species (NO, NO_2, and CO)

Diagnostic run 1 statisfies the primary model performance goal, that the predicted region-wide maximum ozone concentration be within 20 percent and in the general vicinity of the peak observation. However, it does not statisfy the secondary goal because the predicted daily maximum ozone concentration at the location of the observed region-wide maximum is only within 35 percent rather than the goal of 30 percent. The model predicts a high amount of spatial variation in the ozone concentrations. Thus a slight displacement of the ozone cloud, which is very likely under stagnant conditions, will result in poor model performance. Because the model

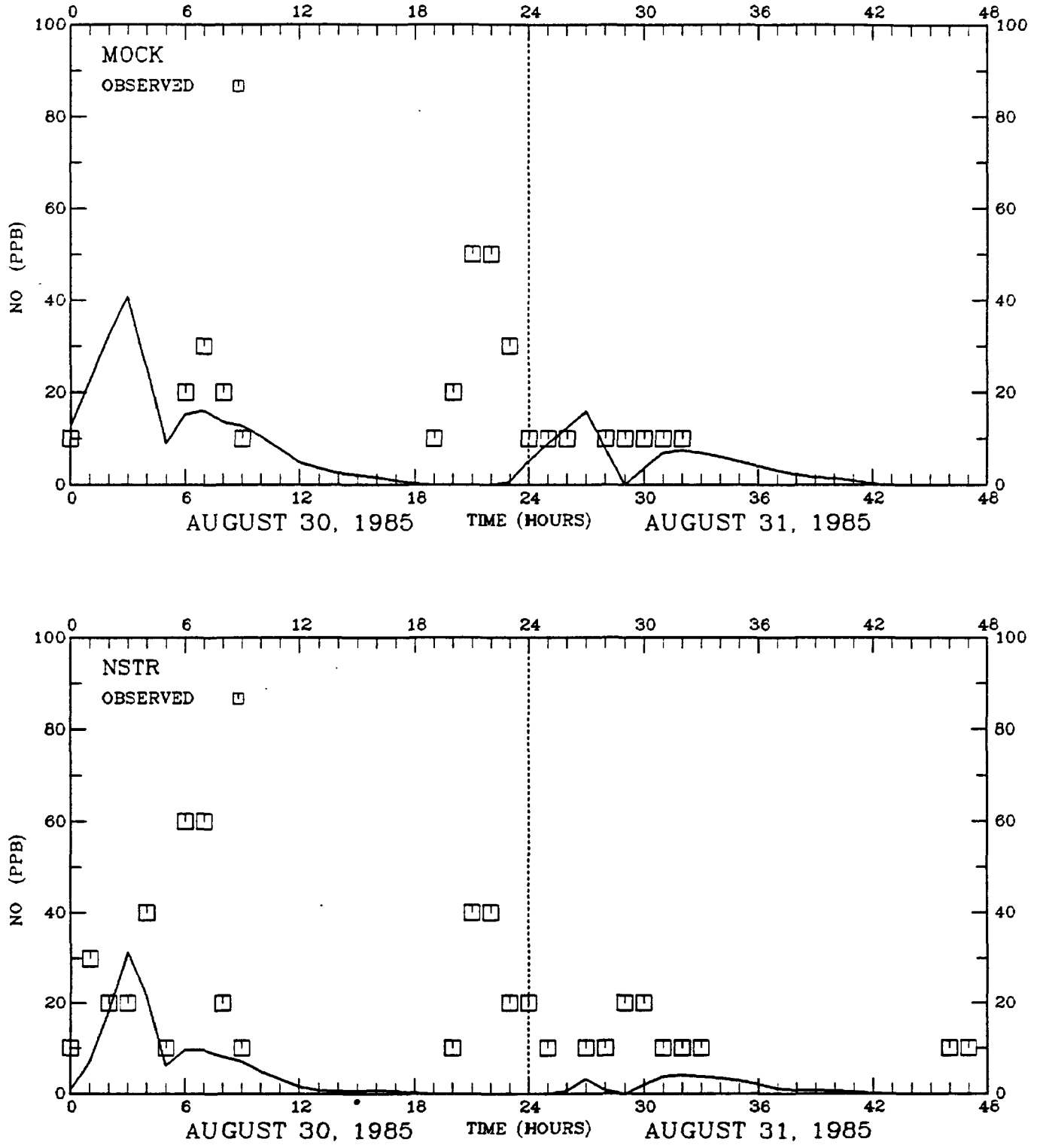

FIGURE 4-11. Time series of predicted and observed hourly NO concentrations (ppb) in Dallas-Fort Worth for diagnostic run 1.

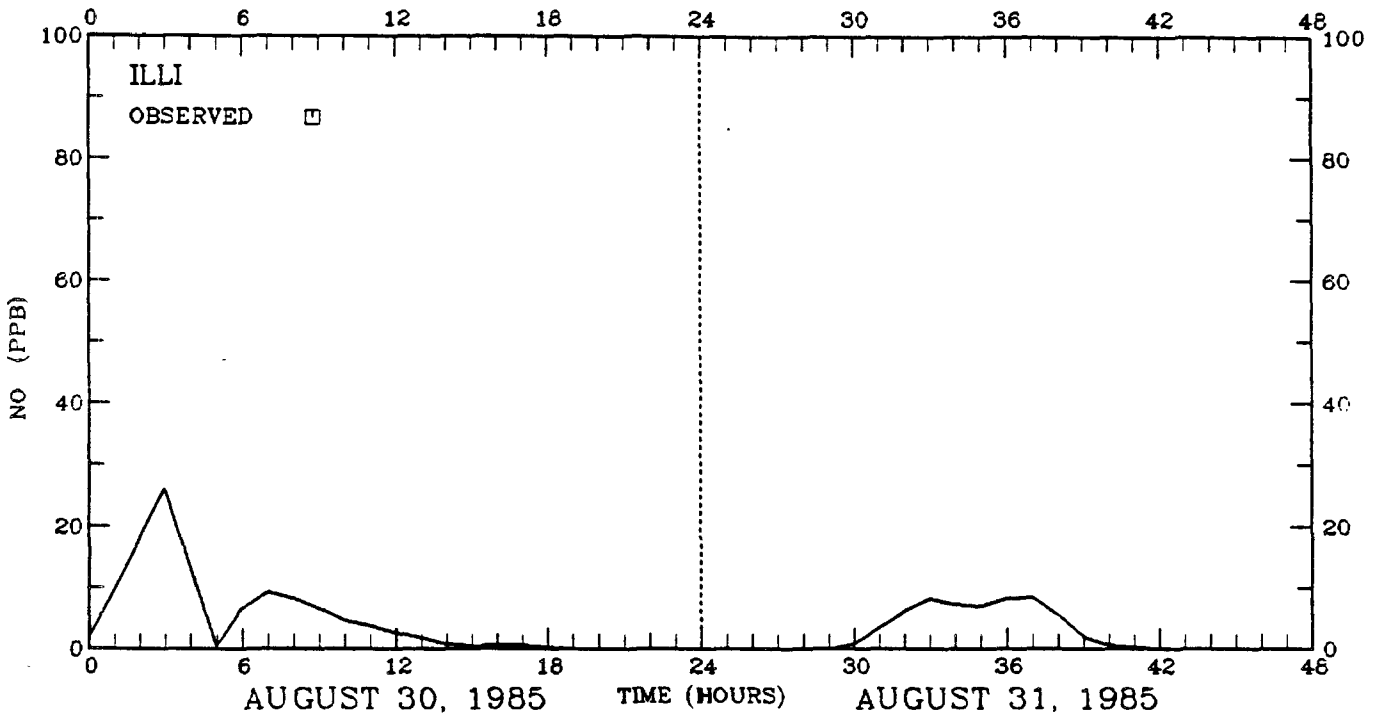

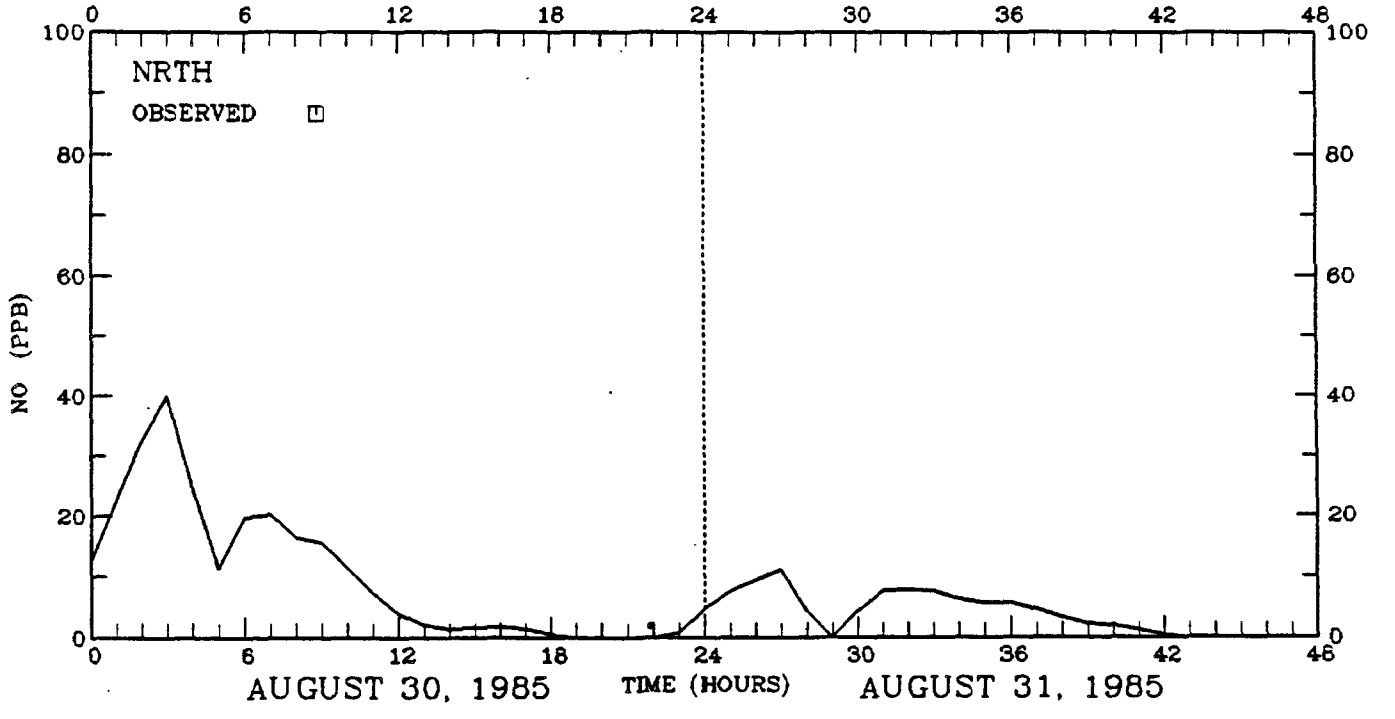

FIGURE 4-11 continued.

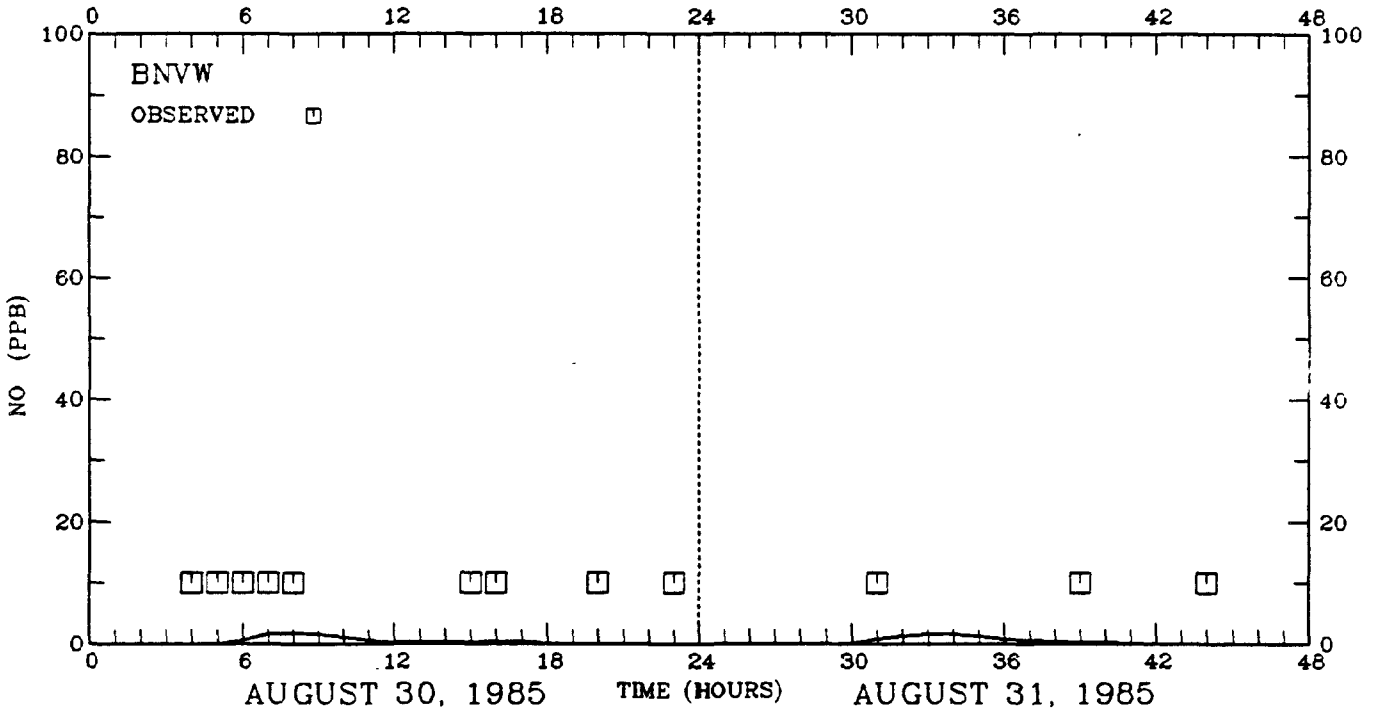

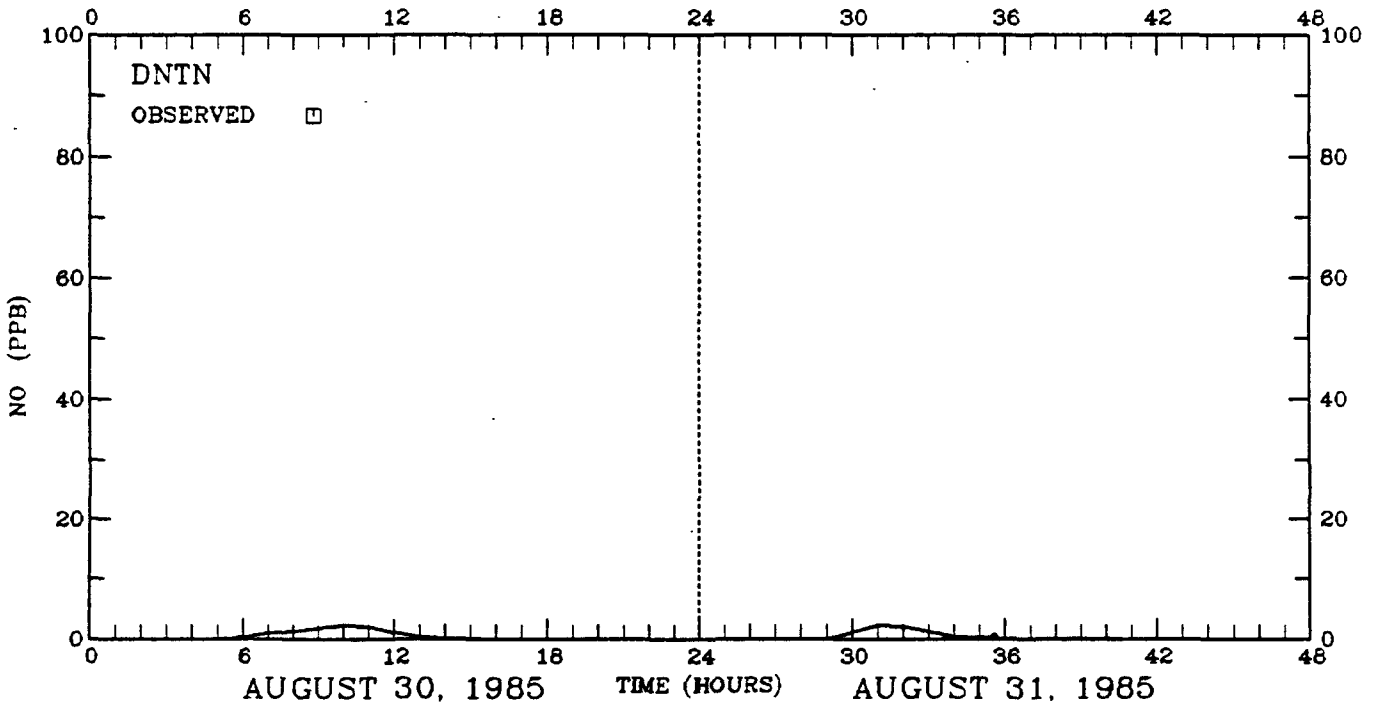

FIGURE 4-11 continued.

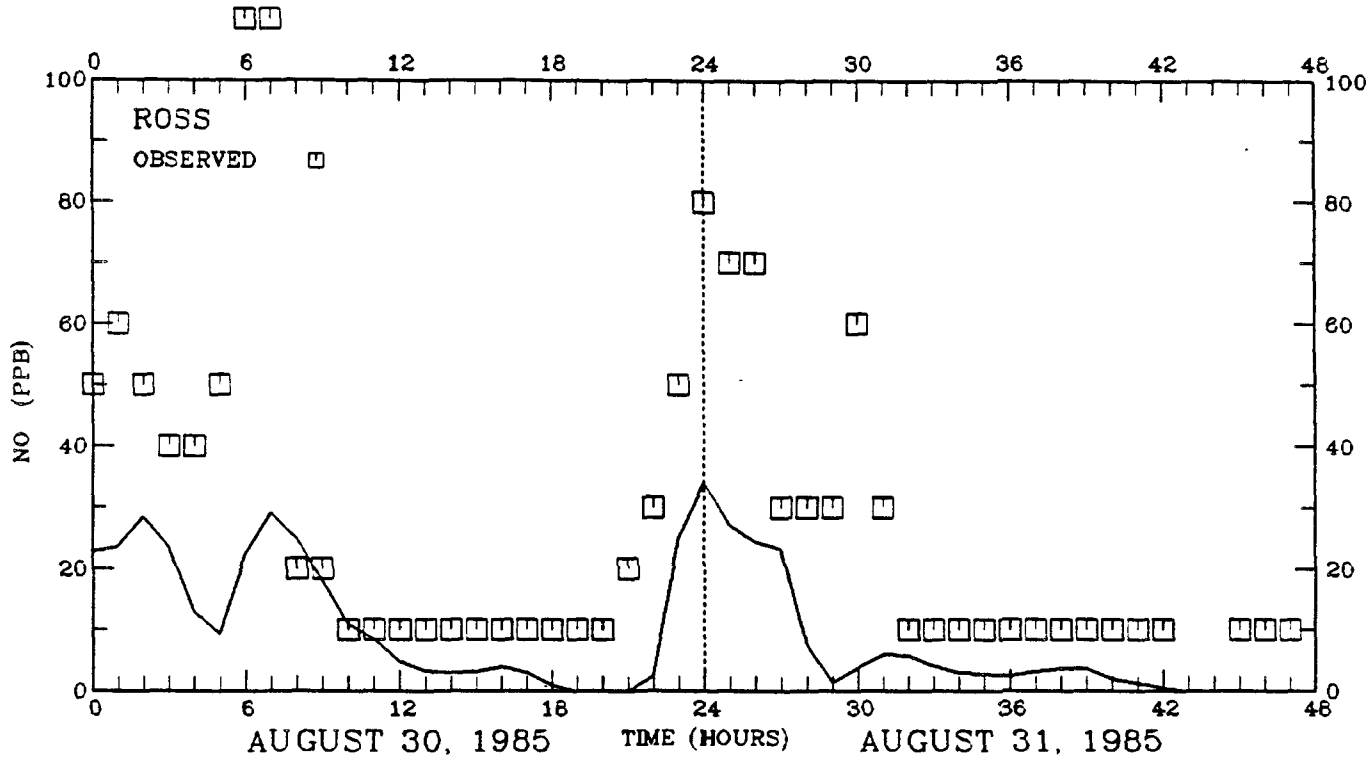

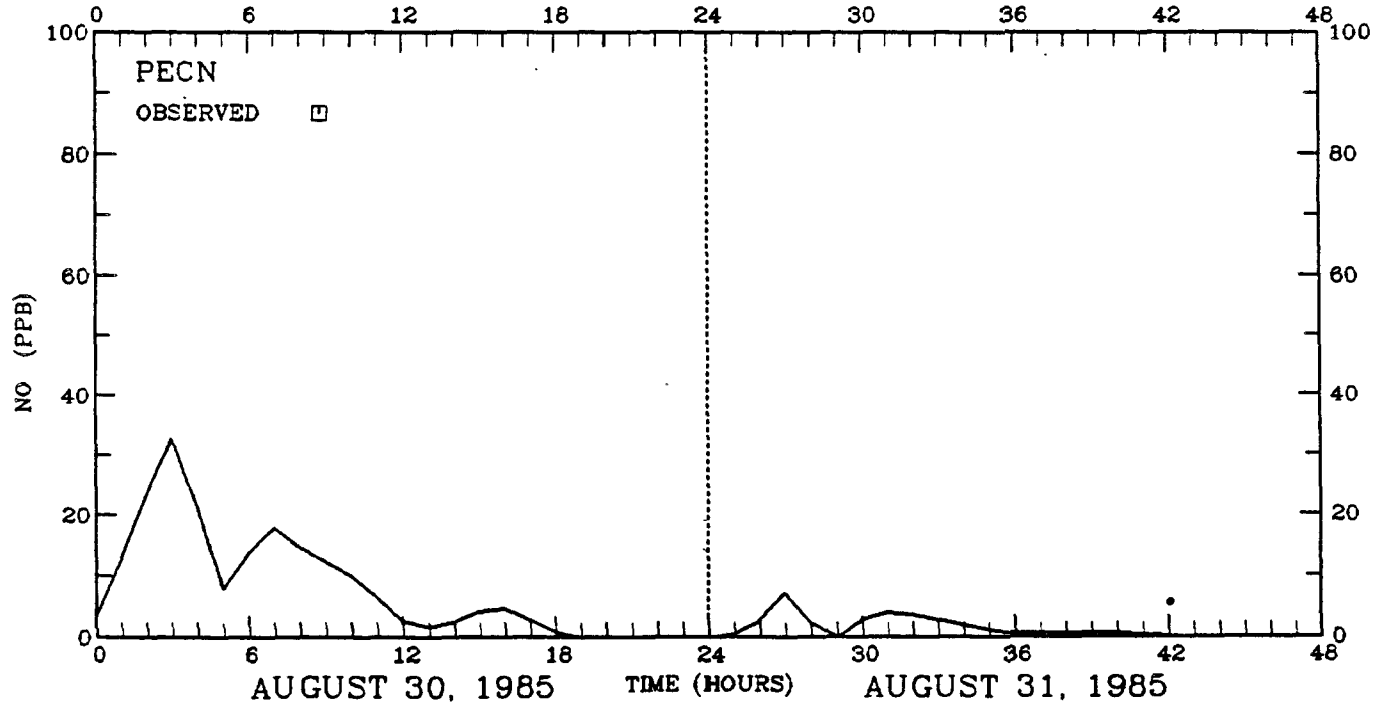

FIGURE 4-11 continued.

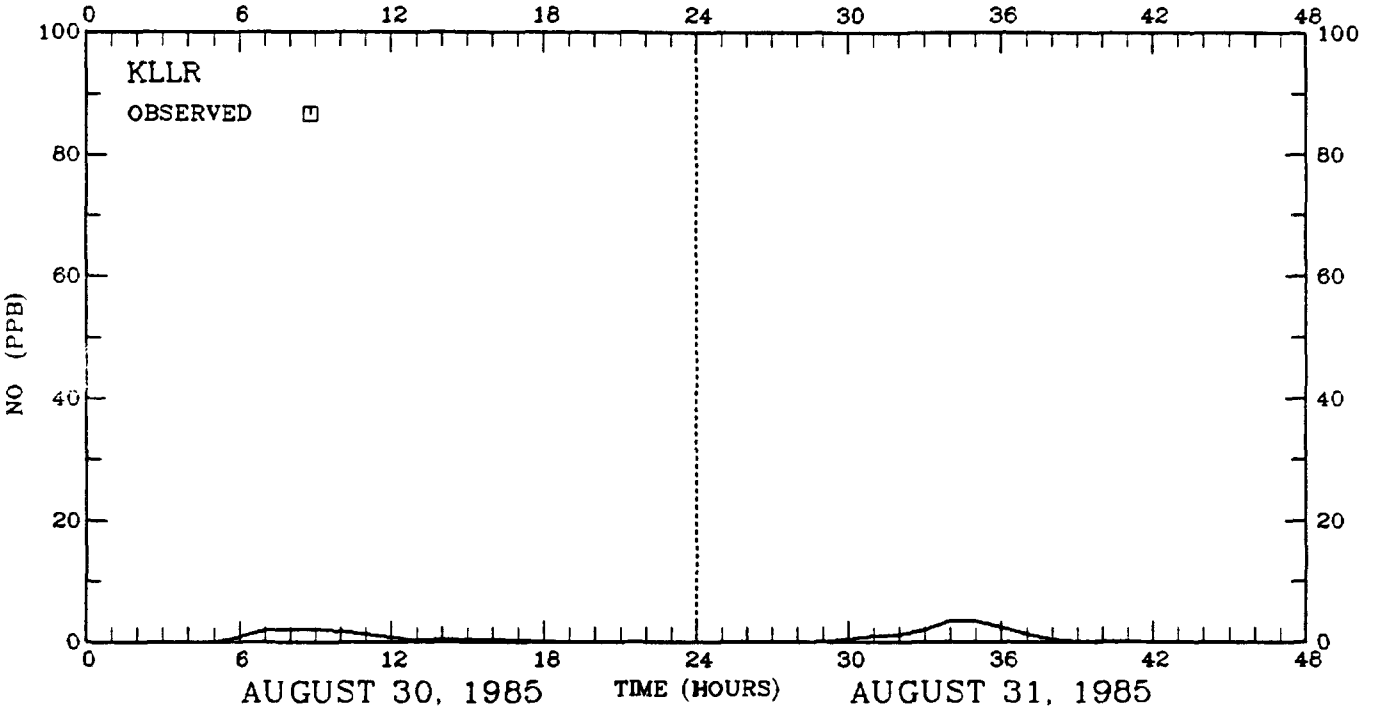

FIGURE 4-11 concluded.

SYSTEMS APPLICATIONS, INC.

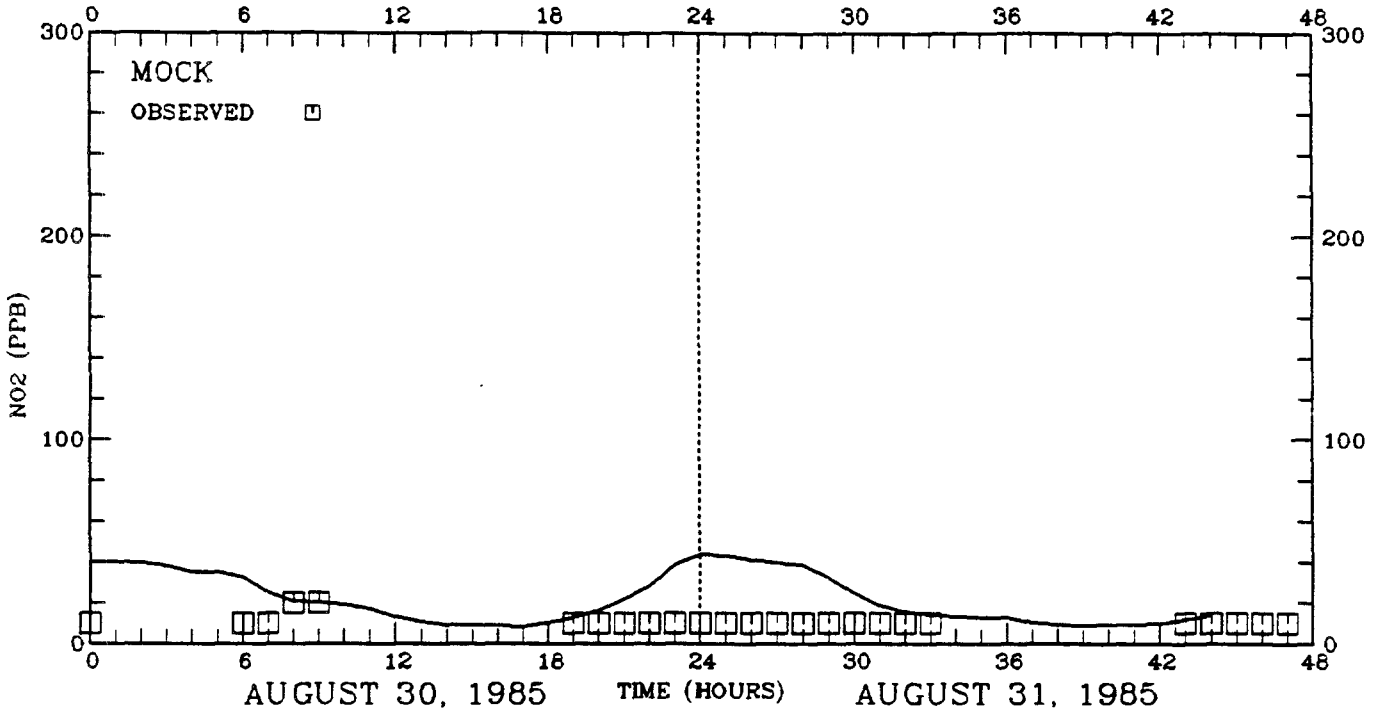

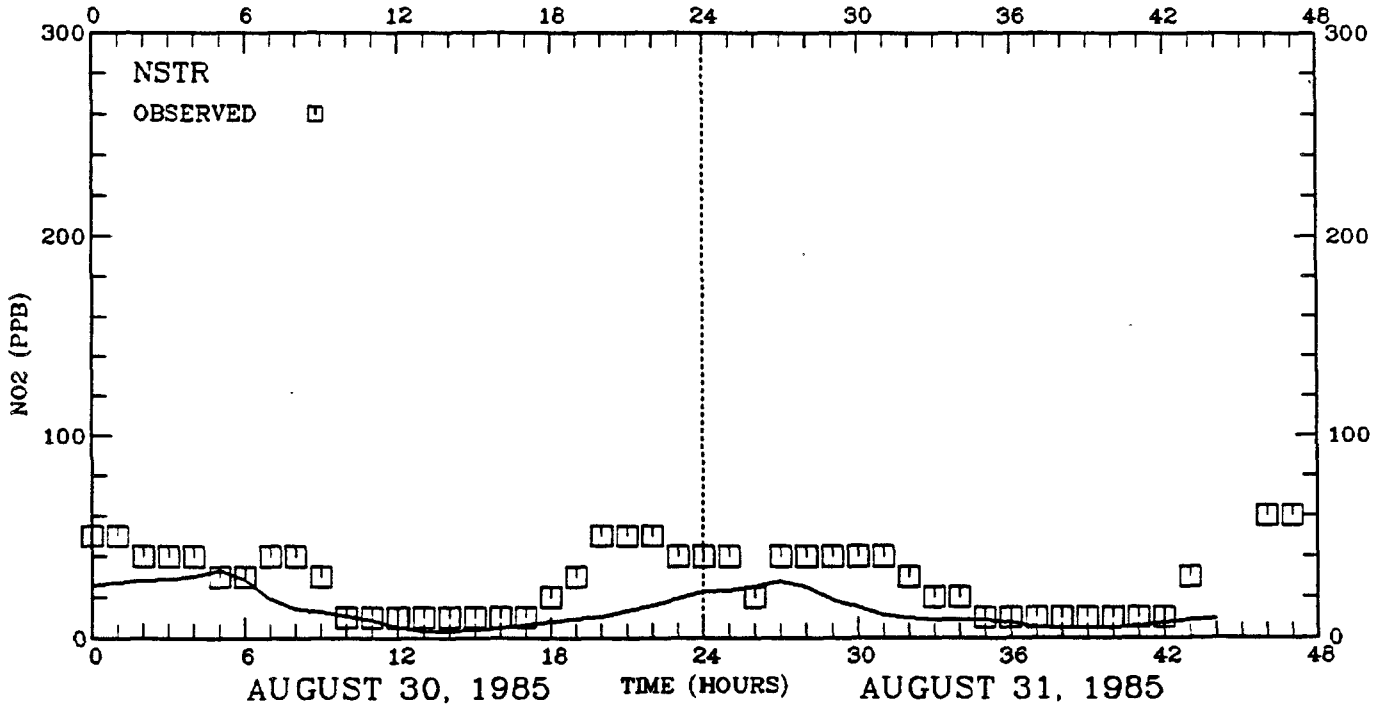

FIGURE 4-12. Time series of predicted and observed hourly NO_2 concentrations (ppb) in Dallas-Fort Worth for diagnostic run 1.

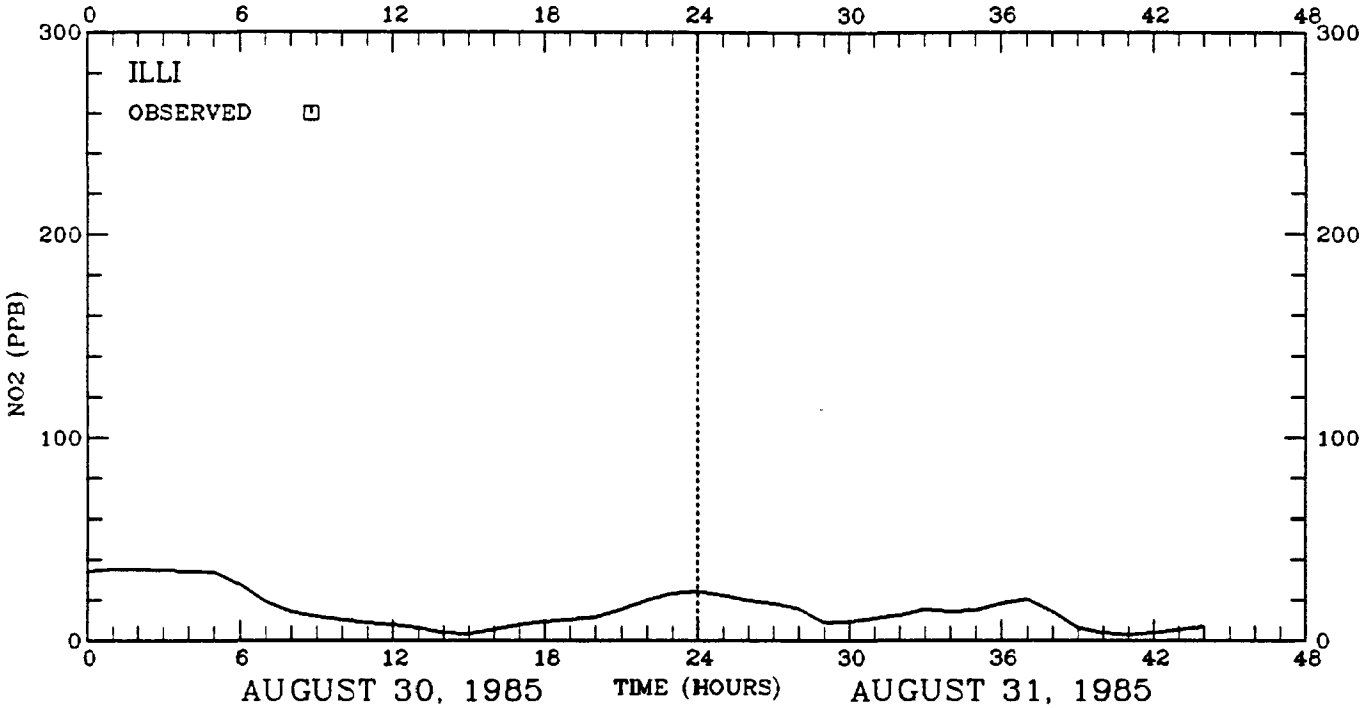

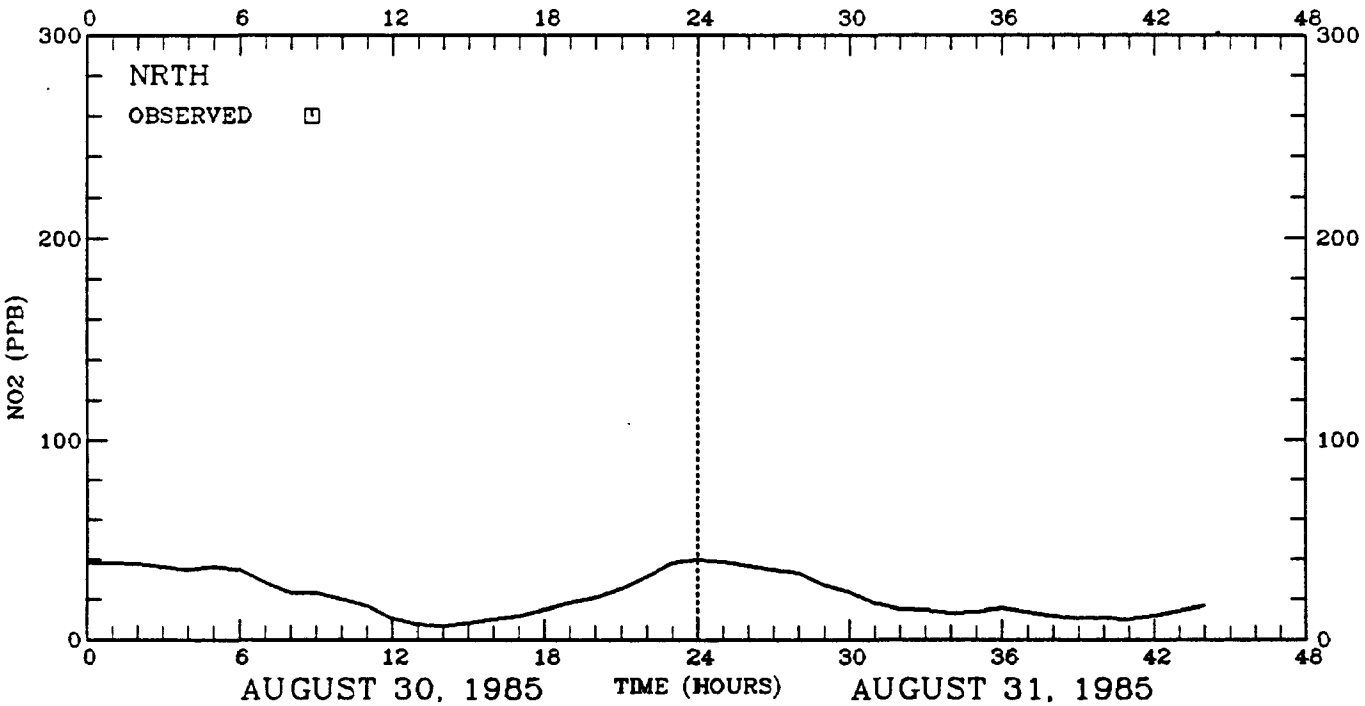

FIGURE 4-12 continued.

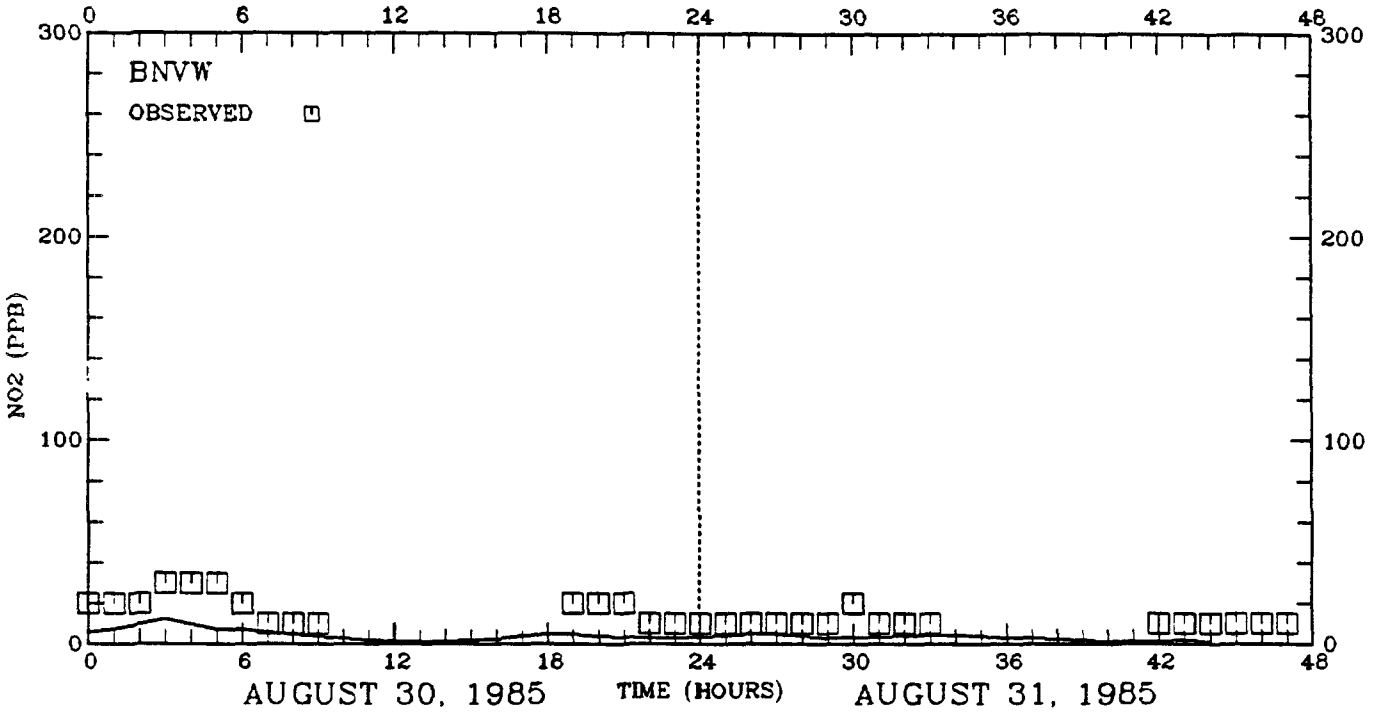

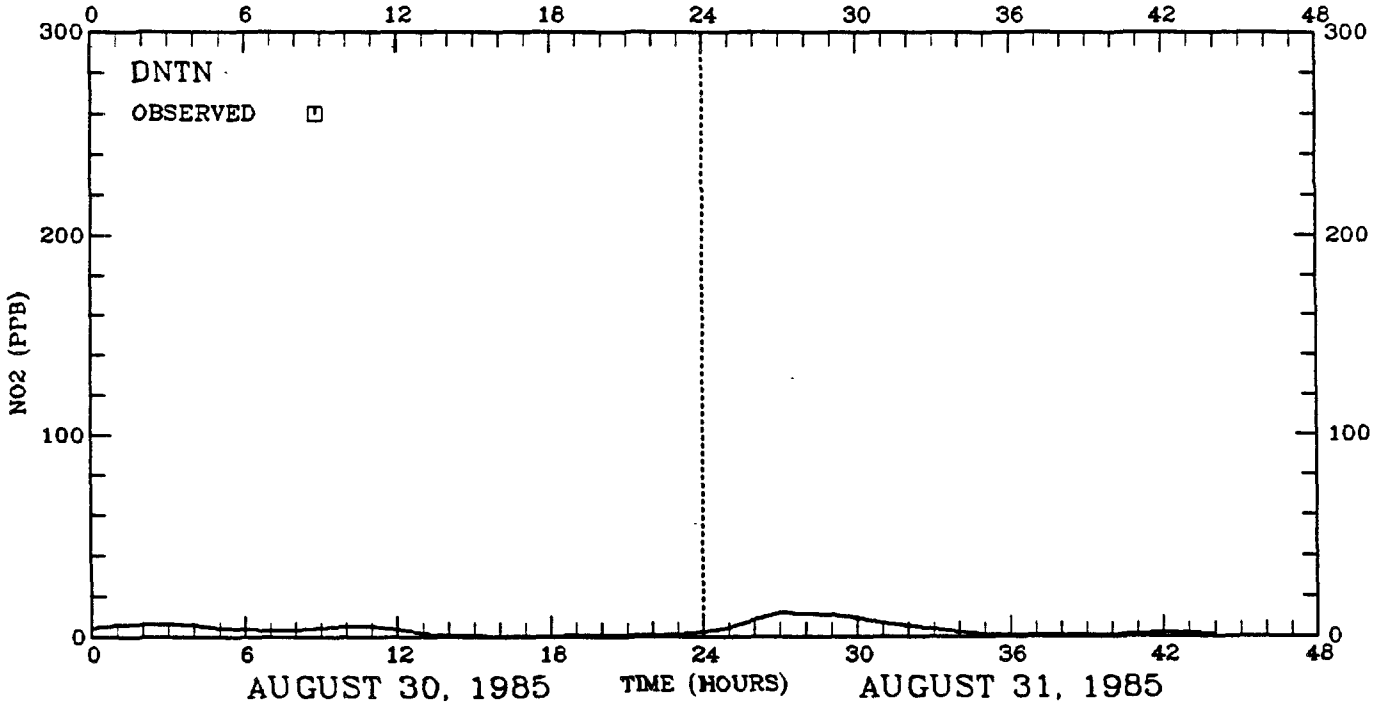

FIGURE 4-12 continued.

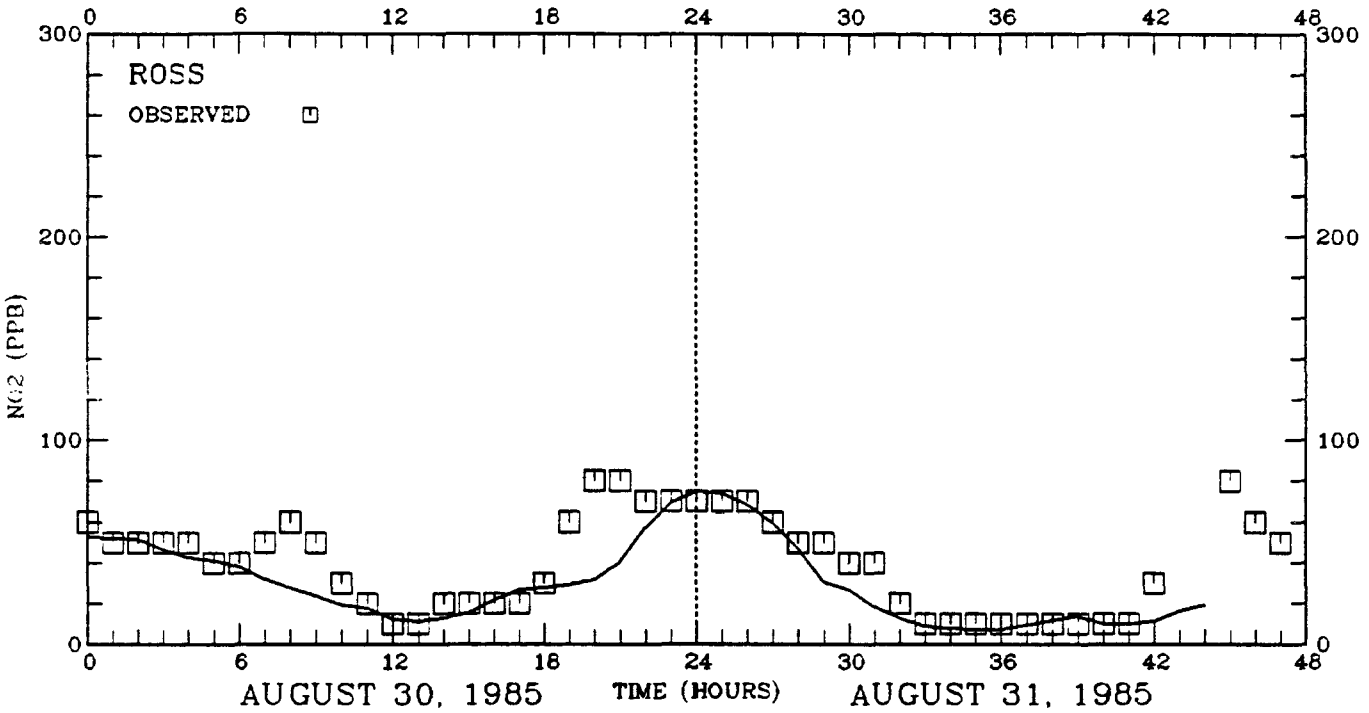

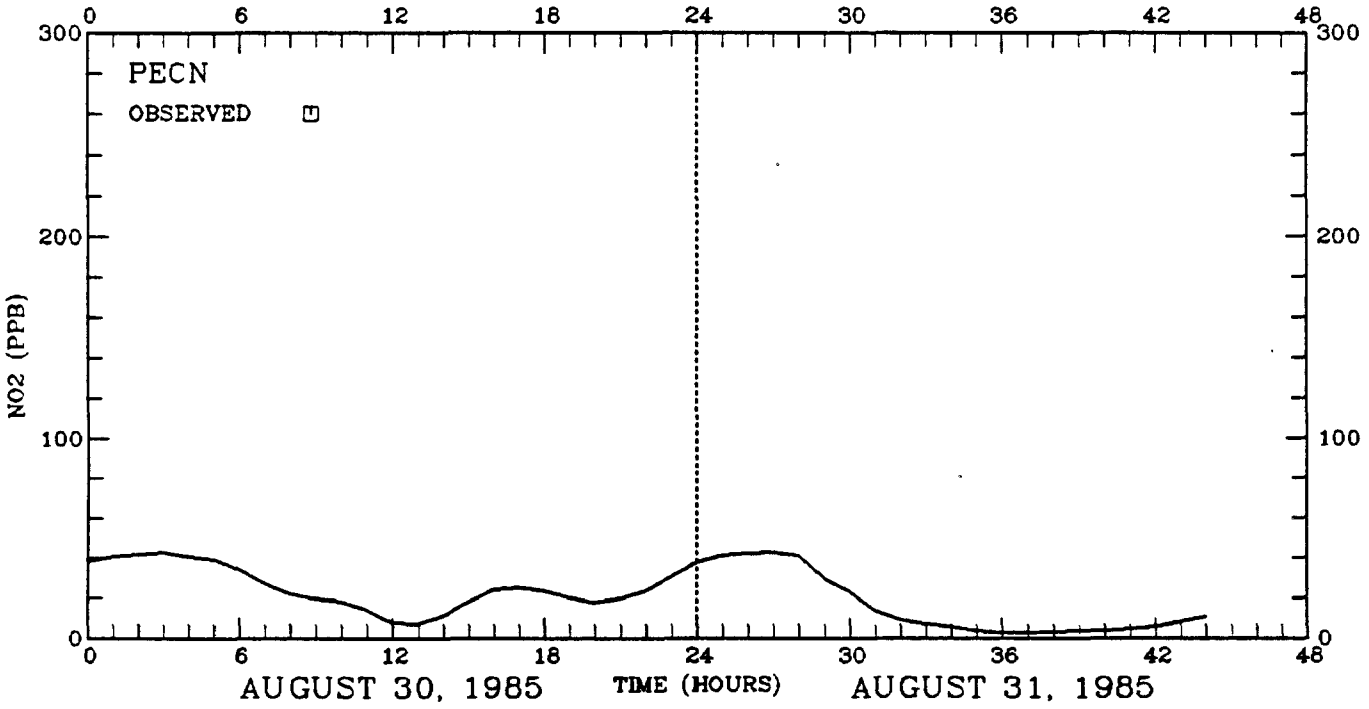

FIGURE 4-12 continued.

SYSTEMS APPLICATIONS, INC.

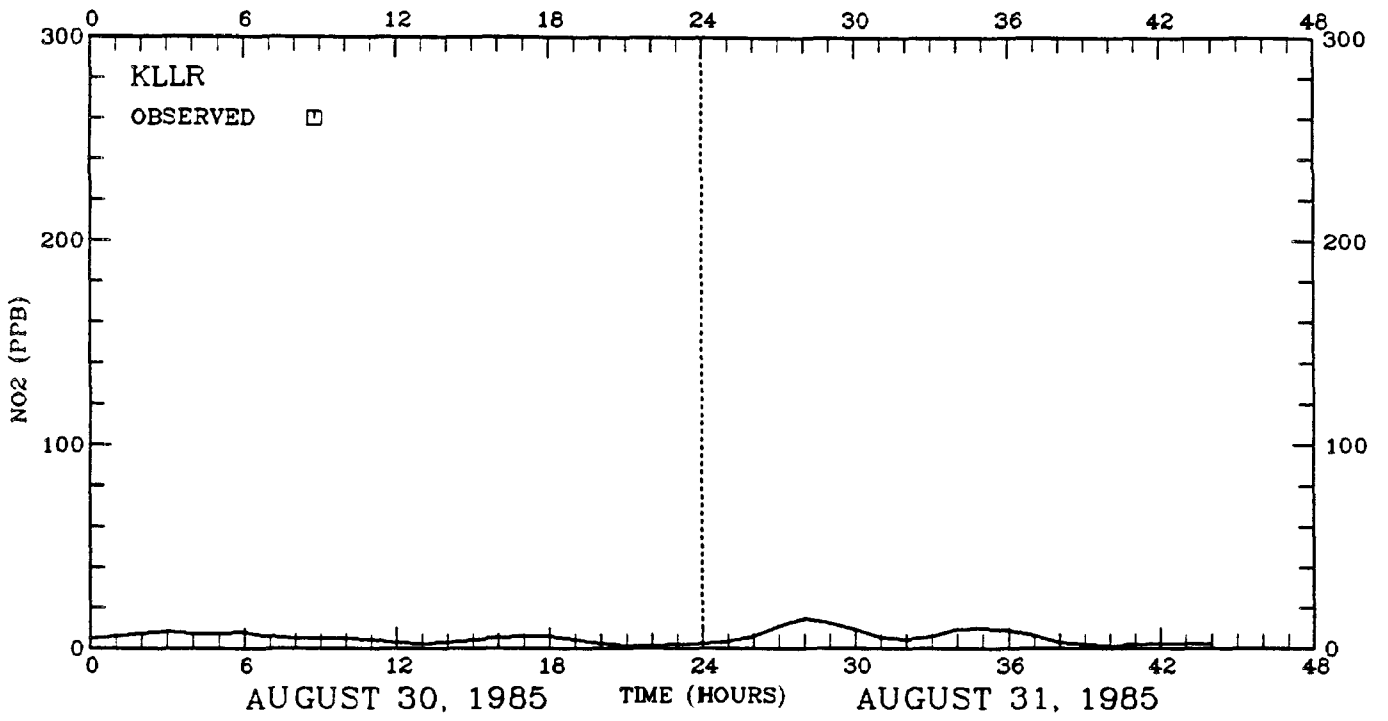

FIGURE 4-12 concluded.

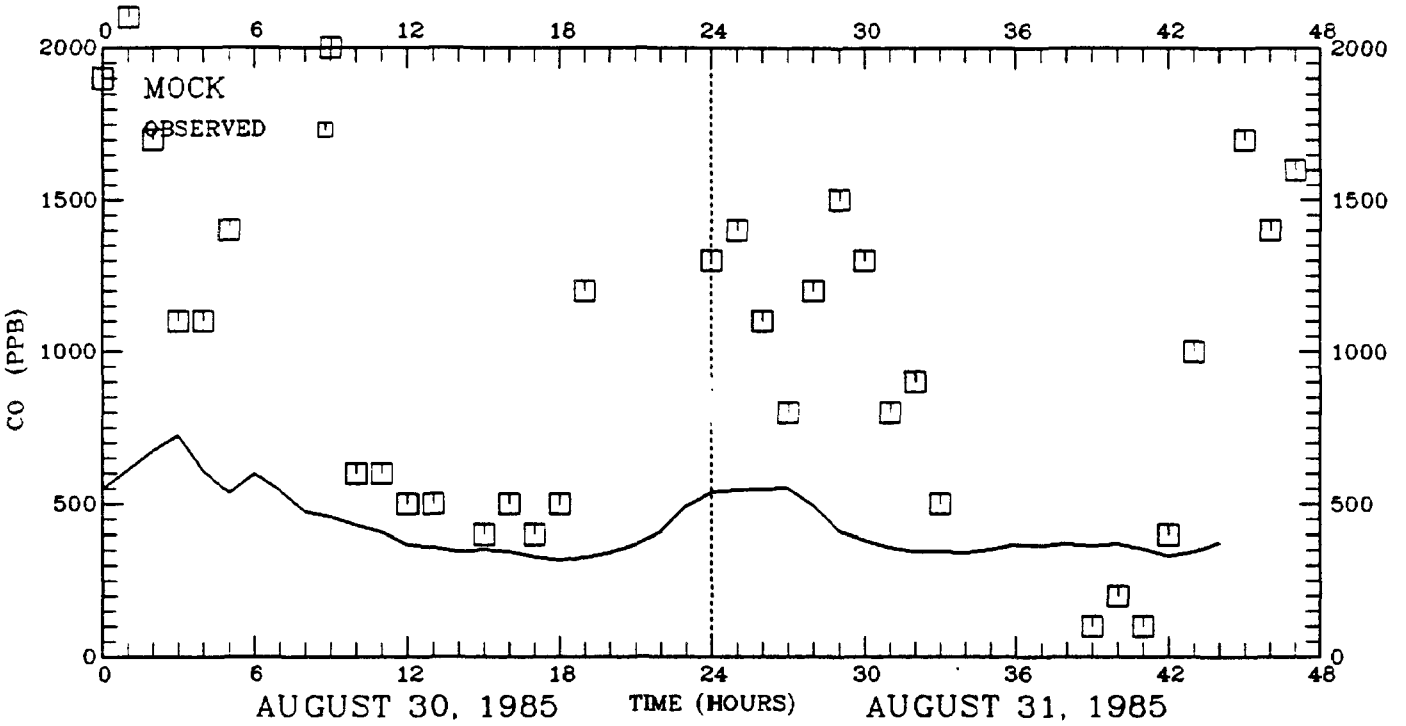

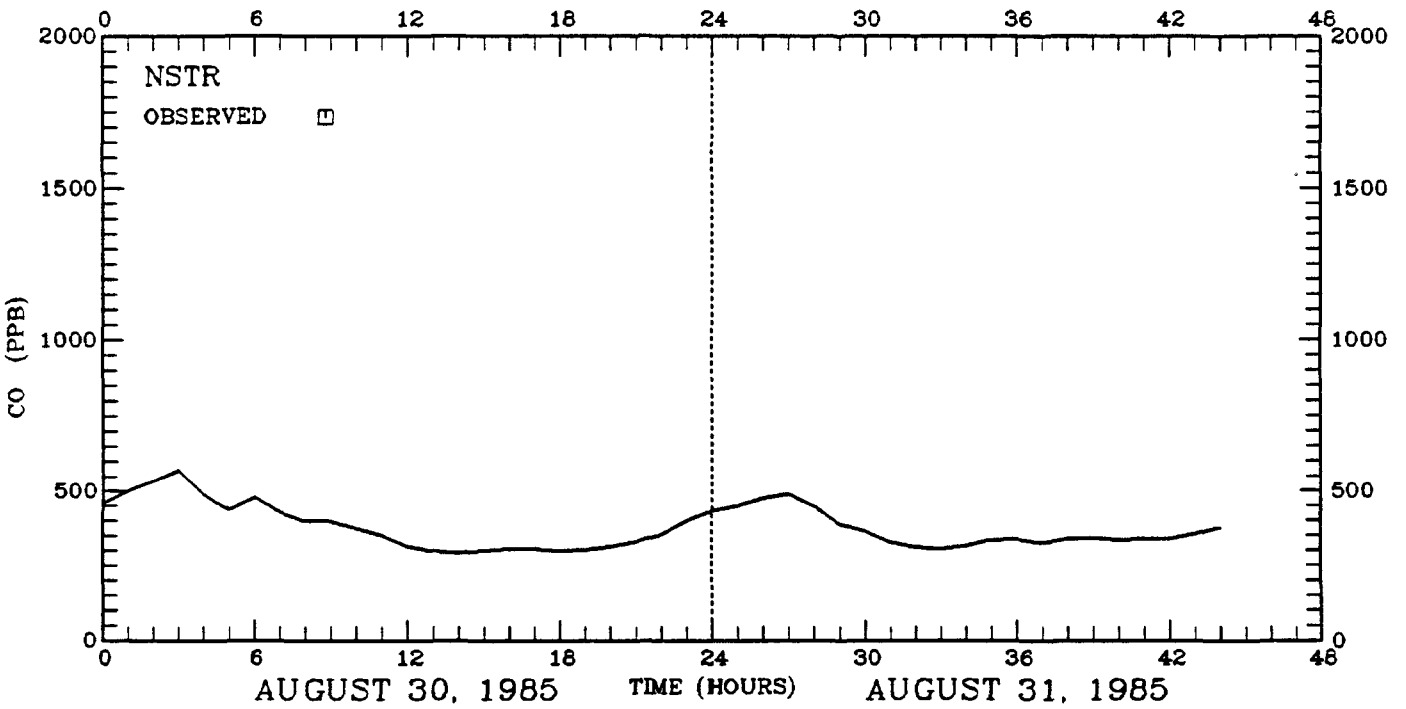

FIGURE 4-13. Time series of predicted and observed hourly CO concentrations (ppb) in Dallas-Fort Worth for diagnostic run 1.

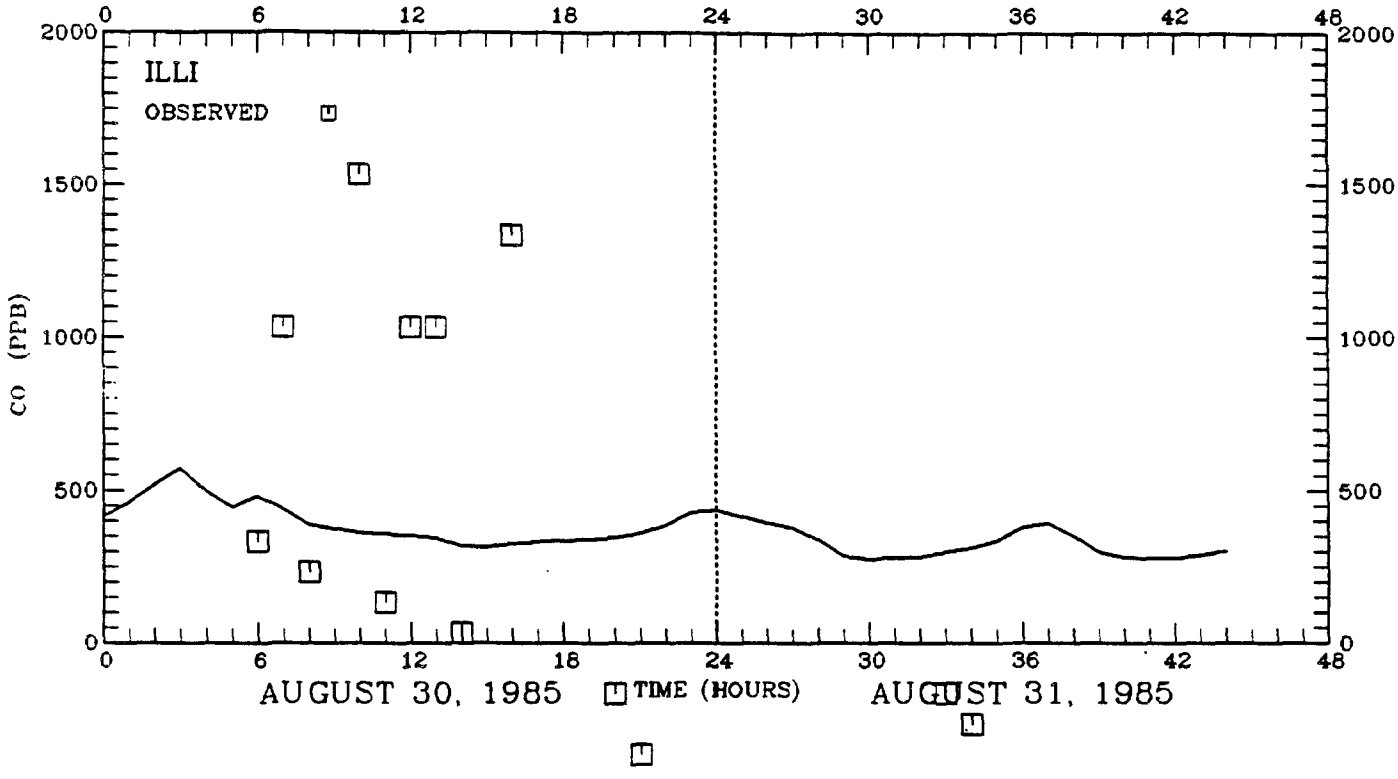

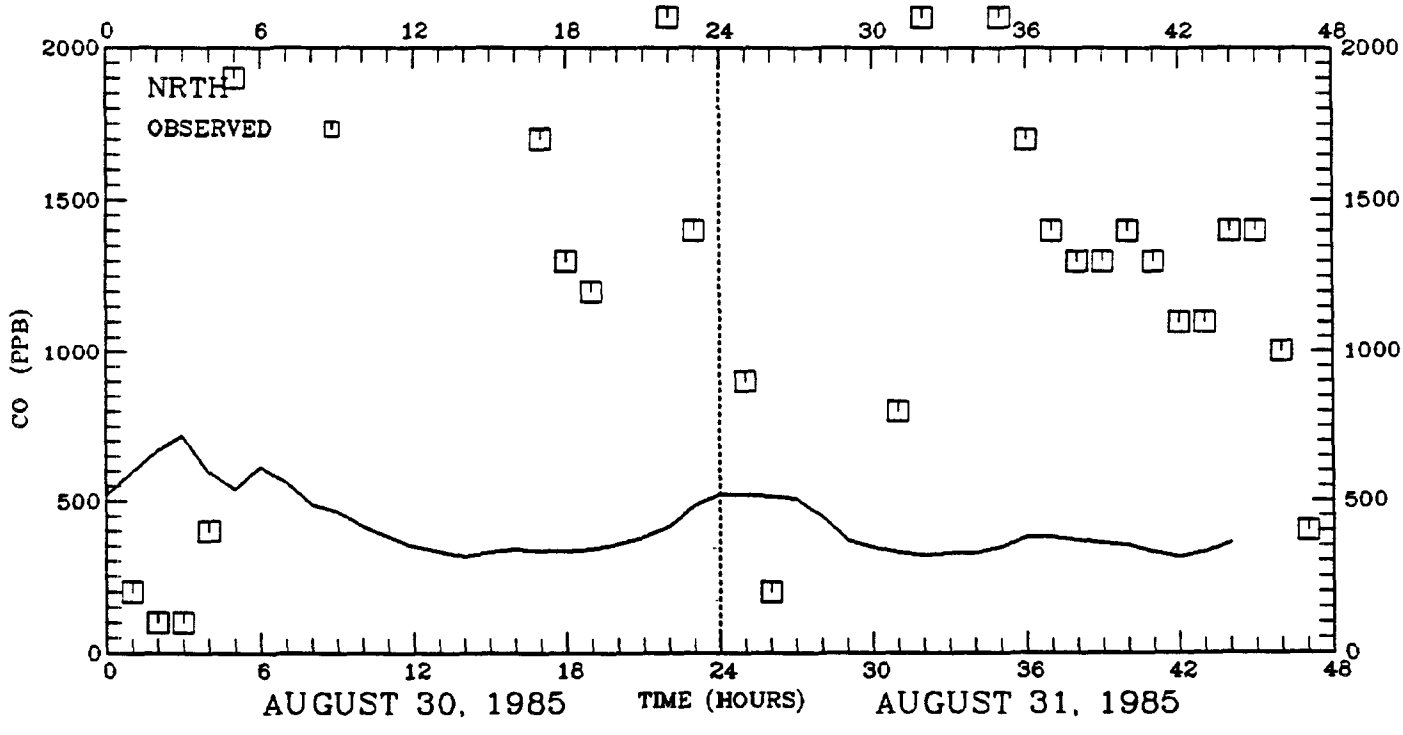

FIGURE 4-13 continued.

SYSTEMS APPLICATIONS, INC.

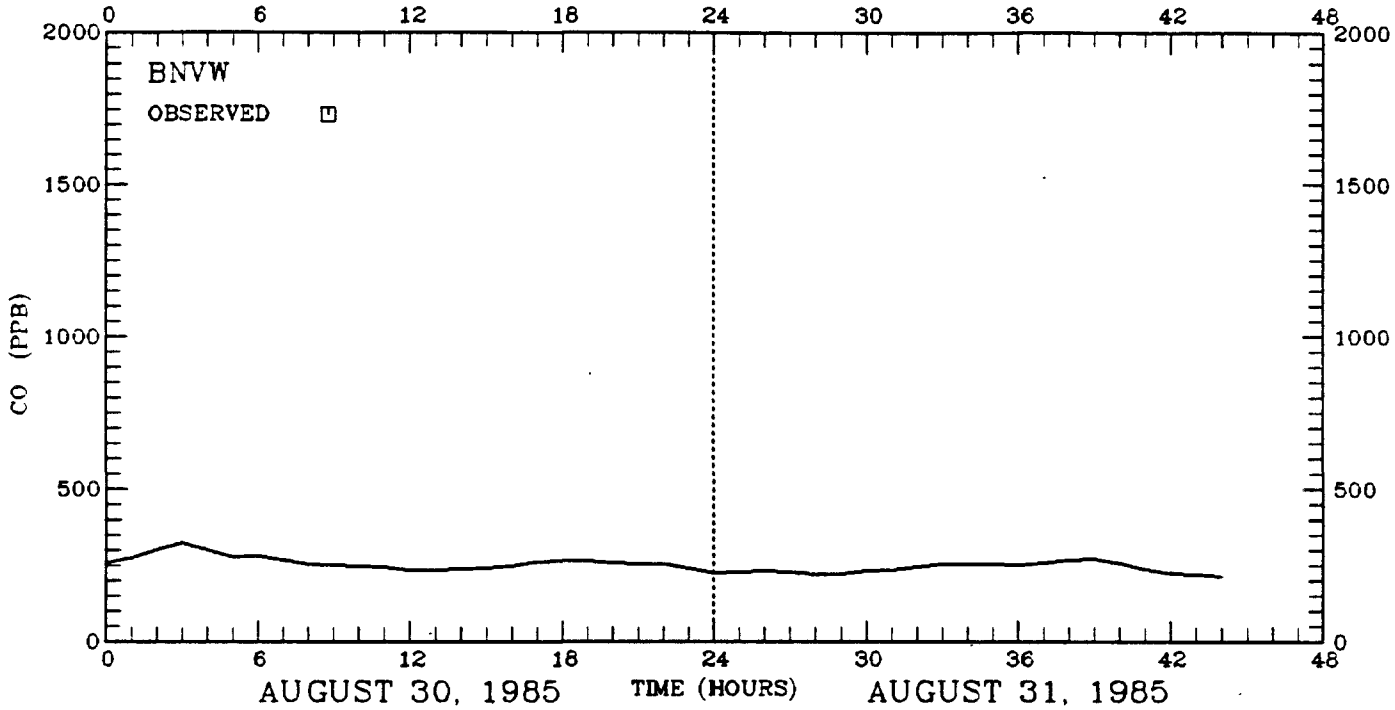

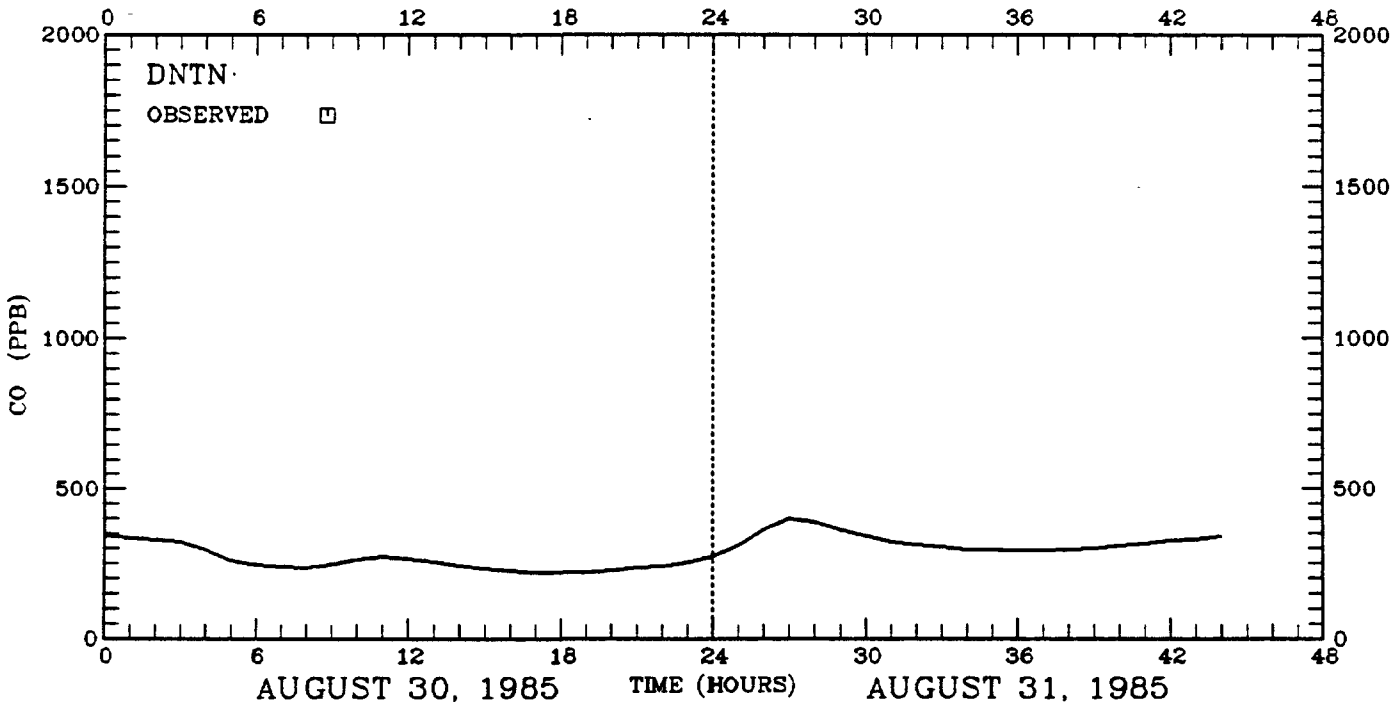

FIGURE 4-13 continued.

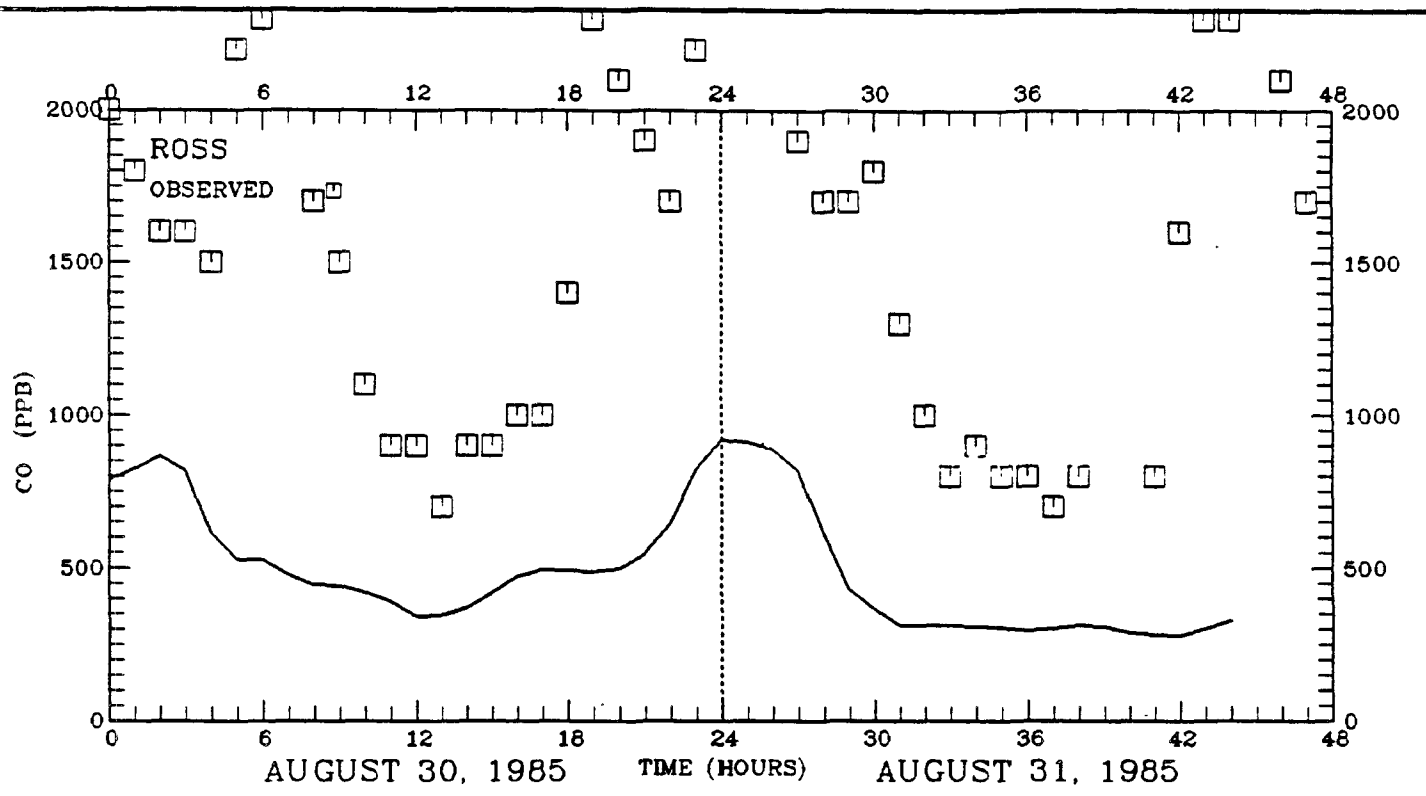

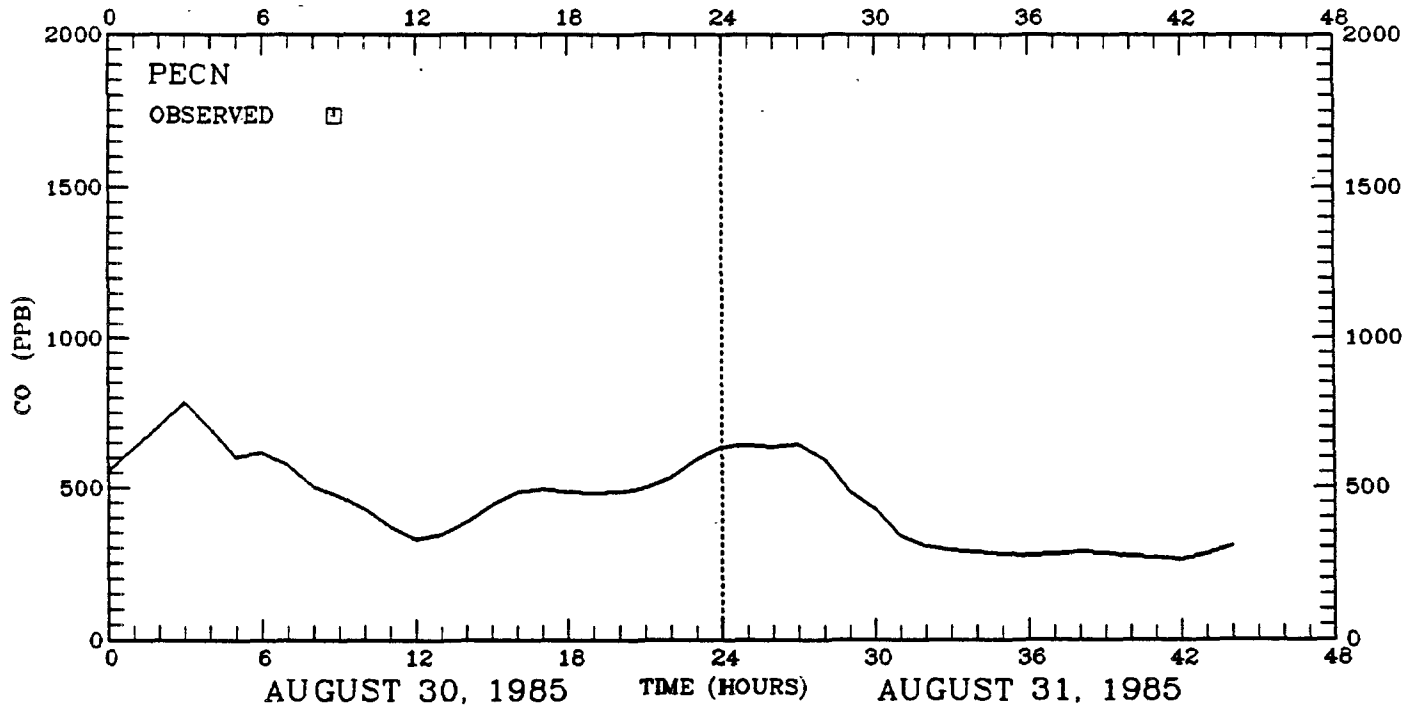

FIGURE 4-13 continued.

SYSTEMS APPLICATIONS, INC.

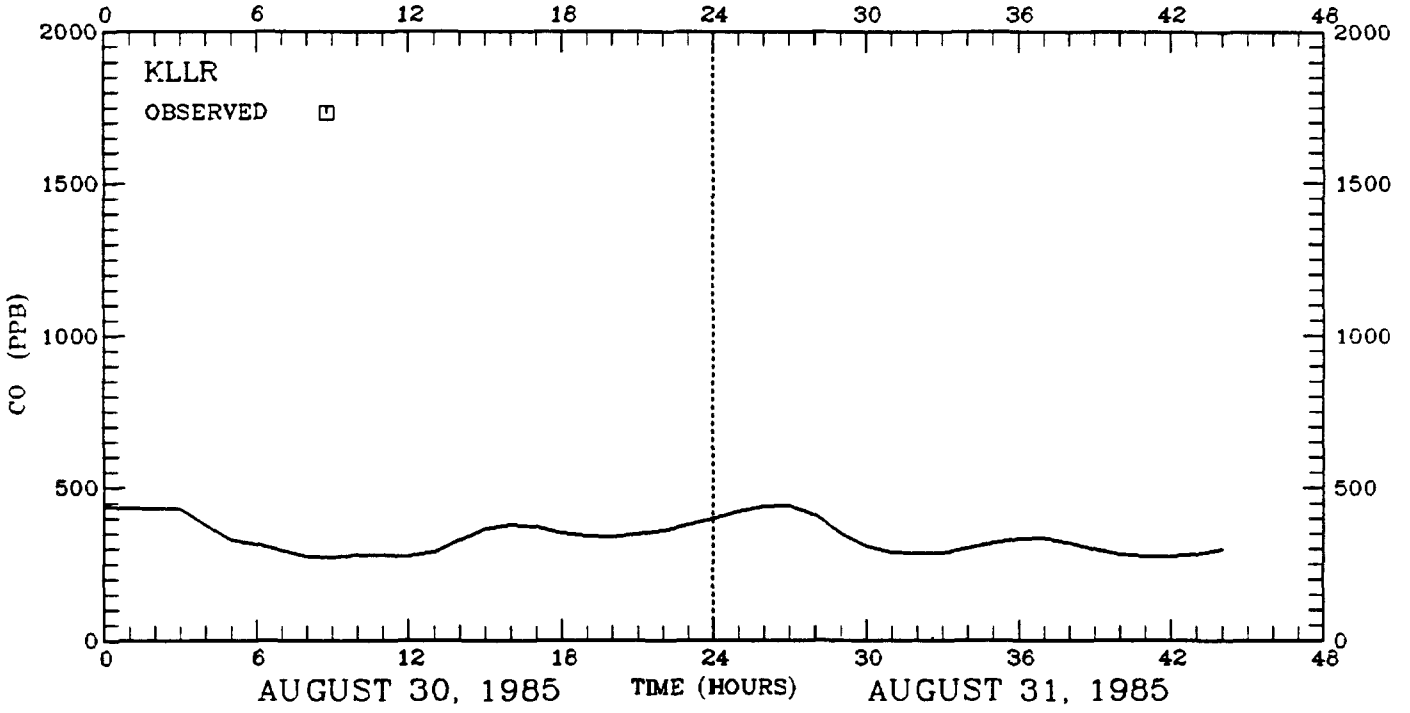

FIGURE 4-13 concluded.

SYSTEMS APPLICATIONS, INC.

underpredicts the peak ozone observations as well as observations of primary pollutants (NO, NO_2, and CO), it appears that the ozone concentrations and precursors may be excessively diluted.

Diagnostic Run 2

As indicated above, it was suspected that diagnostic run 1 underpredicted the peak observations due to excessive dilution. Several modeling inputs can be adjusted to lower the amount of dilution of the ozone and ozone precursors: smaller horizontal grid spacing, lower mixing height, slower wind speeds, elimination of any wind shear, and increases in emission levels. Because of cost and logistical limitations it is not possible to reduce the horizontal grid spacing. In the past there has been some justification for lowering wind speeds when instantaneous FAA wind observations are used (see Appendix D). However, for this application only hourly average surface wind observations were used. The elimination of wind shear in the mixed layer may produce higher ozone concentrations, but would involve alterations to the wind input and wind field preparation procedure that may not be desirable. Although it is suspected that the amount of actual VOC emissions is underestimated in the emission inventory, the inventory is the current best estimate and any modifications would be arbitrary. However, there is quite a bit of justification for lowering the maximum daily mixing height.

Calculated maximum mixing heights at both the Longview and Stephenville upper-air sites on August 31 exceeded 3,000 m AGL. Both of these soundings indicated super-adiabatic conditions near the surface. The use of a mixing height algorithm that uses an hourly surface temperature and a dry adiabatic during super-adiabatic conditions (e.g., Kelley, 1981) may result in an overestimate of the actual mixing height. Ozone episodes are usually associated with hot, dry, stagnant conditions with limited mixing. Due to the presence of a high-pressure system over the area during the episode, it is expected that subsidence may exist over the region, resulting in limited vertical mixing. Thus, for diagnostic run 2 the maximum mixing height was limited to the summer afternoon climatological average of 2,000 m AGL as reported by Holzworth (1976). All other UAM modeling inputs were as in diagnostic run 1.

30 August 1985

On 30 August the predicted region-wide maximum ozone concentration for diagnostic run 2 is 13.2 pphm (Figure 4-14 and Appendix H) which is within 6 percent of the peak observation (14 pphm) for this day. As shown in the comparison of isopleths of predicted daily maximum ozone concentrations with observations (Figure 4-14), the predicted region-wide maximum occurred approximately 40 km east of the location of the peak observation. The predicted maximum concentration at the location of the peak observation (ROSS) is within only 48 percent (6.2 pphm) (Figure 4-15). As in the previous diagnostic simulation, there is considerable spatial variability in the

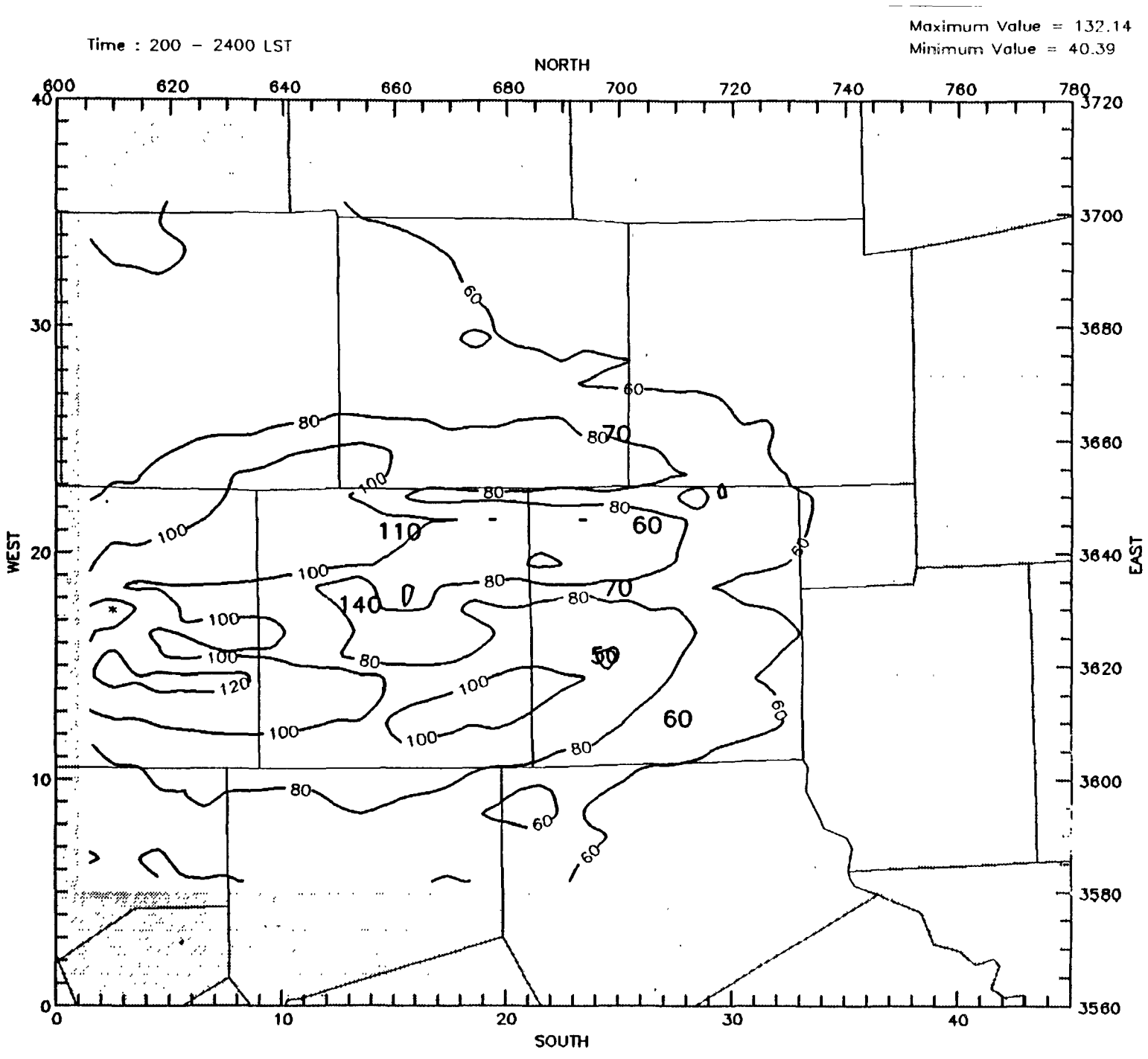

FIGURE 4-14. Isopleths of predicted daily maximum ozone concentrations (ppb) with superimposed observations on 30 August 1985 for the Dallas-Fort Worth diagnostic run 2.

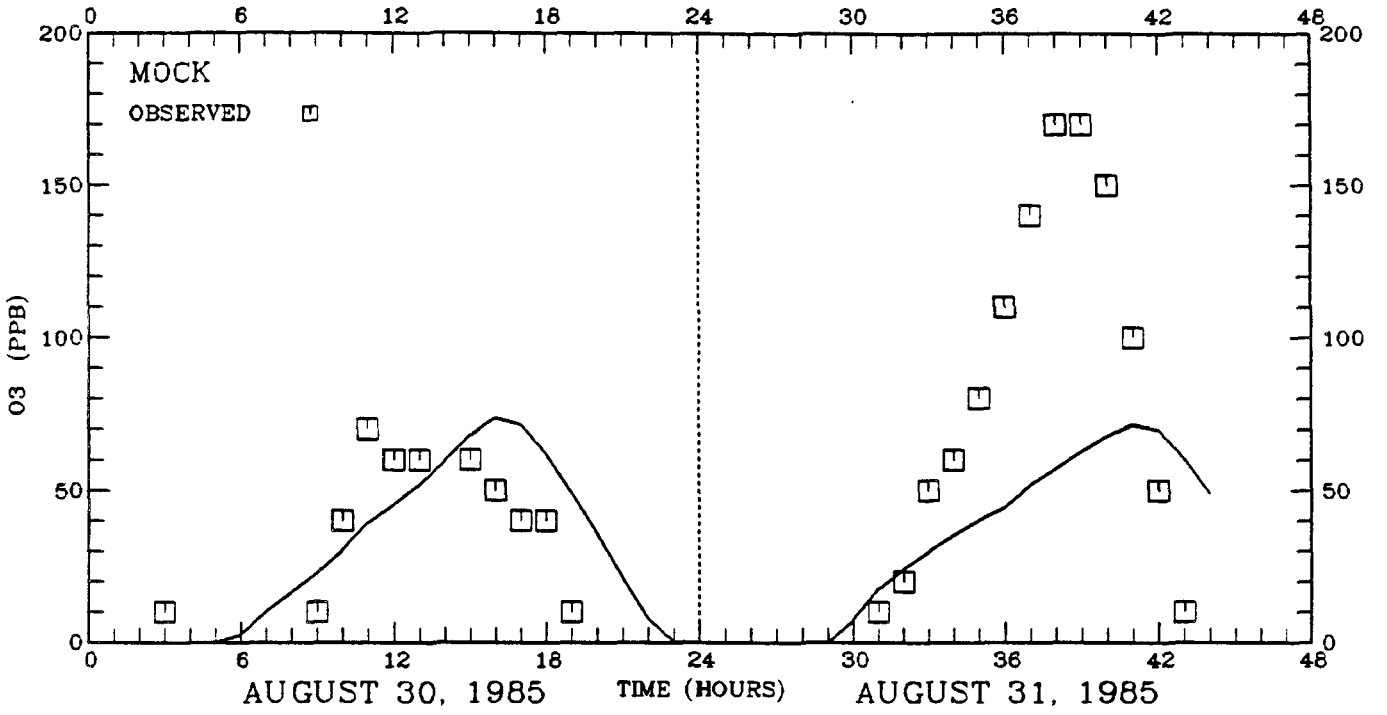

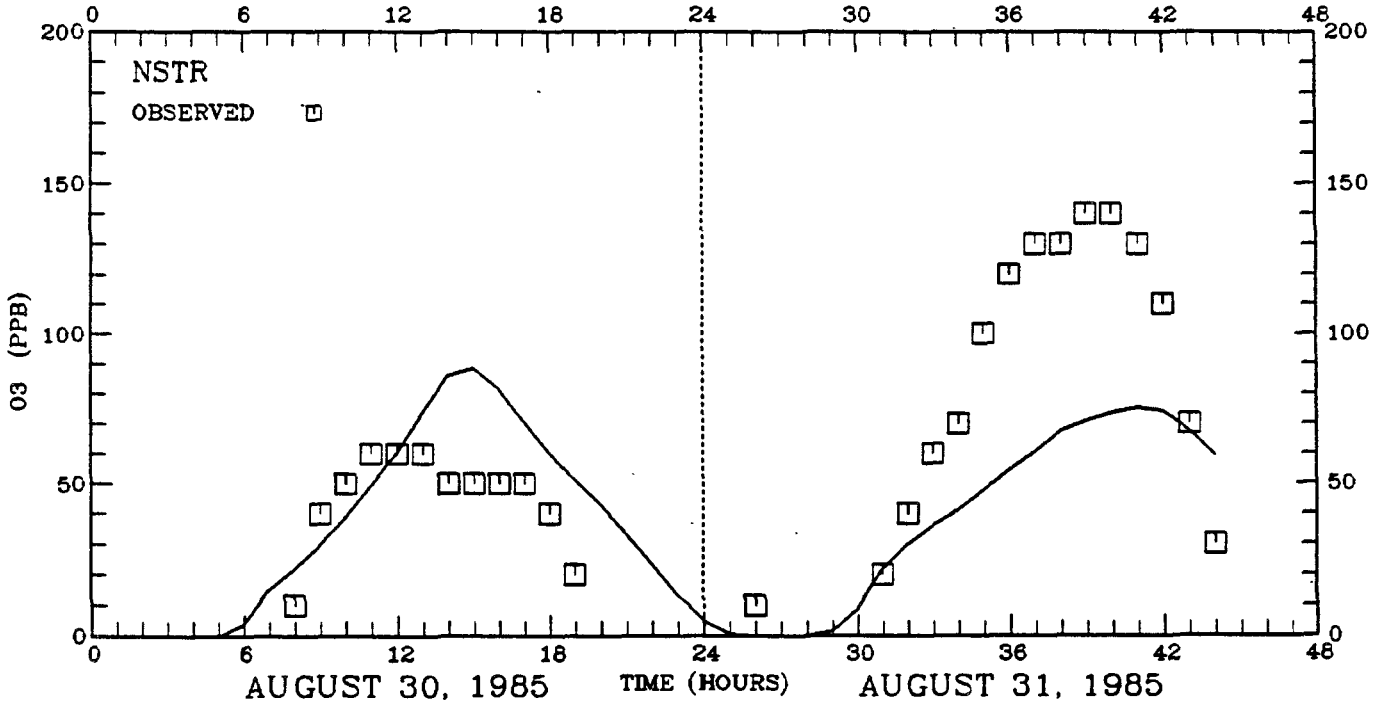

FIGURE 4-15. Time series of predicted and observed hourly ozone concentrations (ppb) for the Dallas-Fort Worth diagnostic run 2.

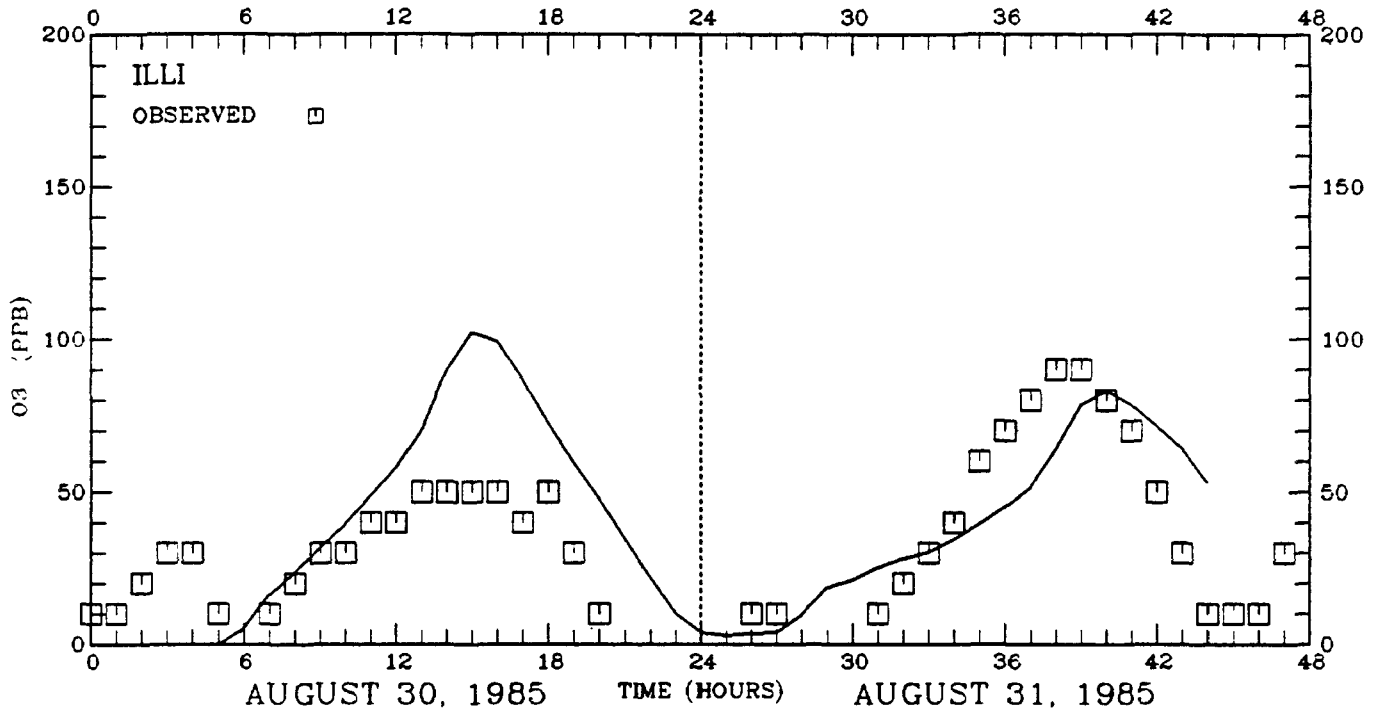

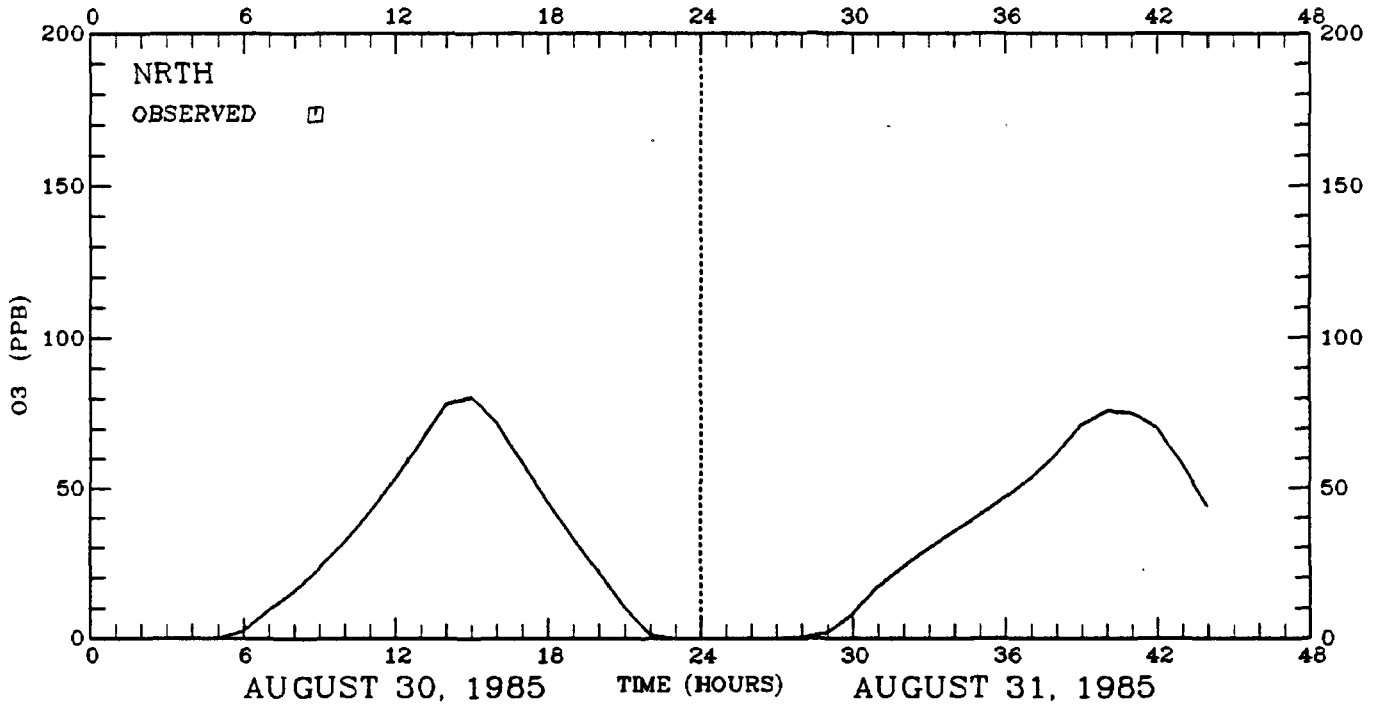

FIGURE 4-15. Continued.

SYSTEMS APPLICATIONS, INC.

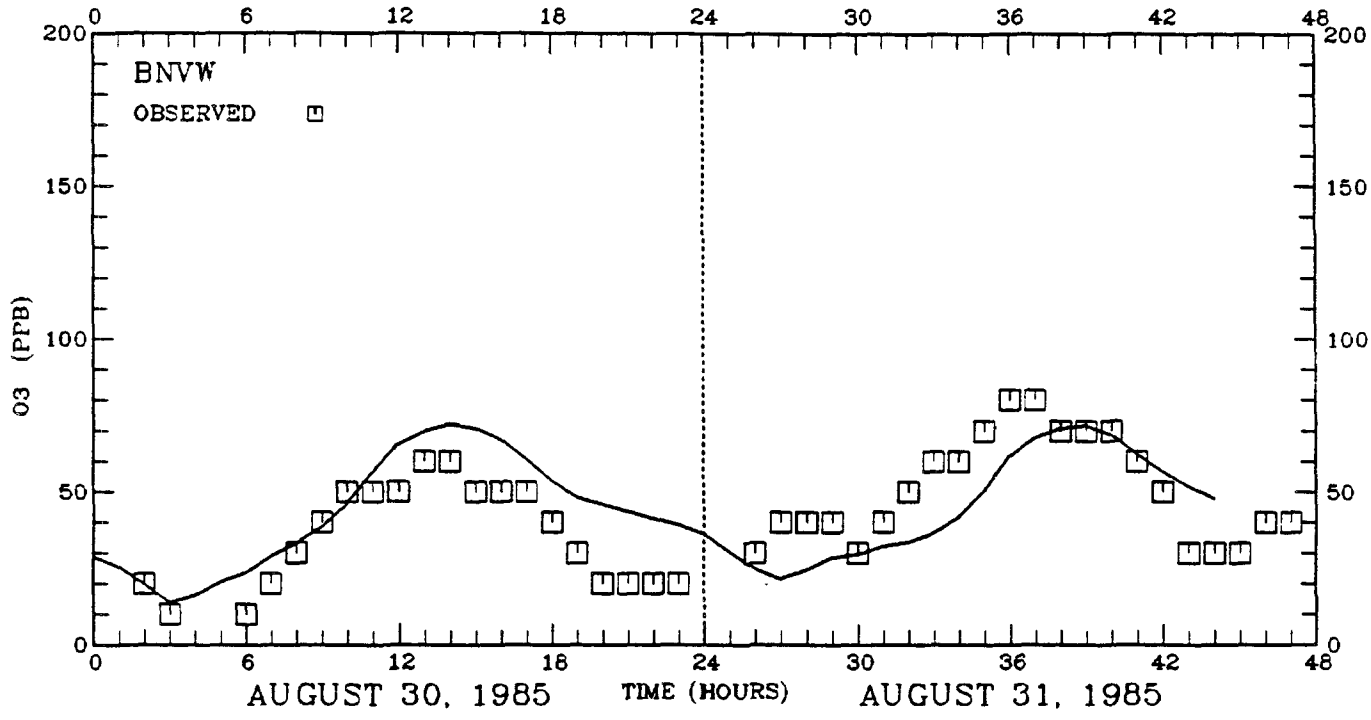

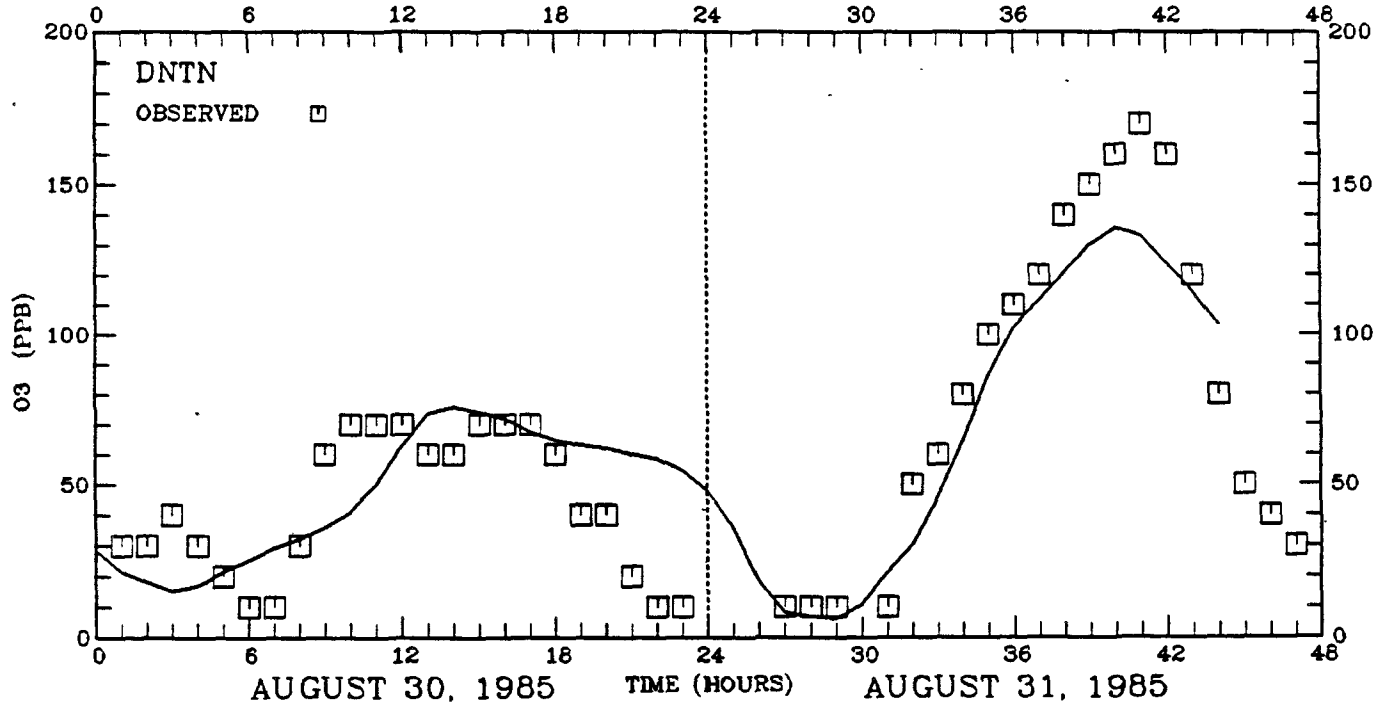

FIGURE 4-15. Continued.

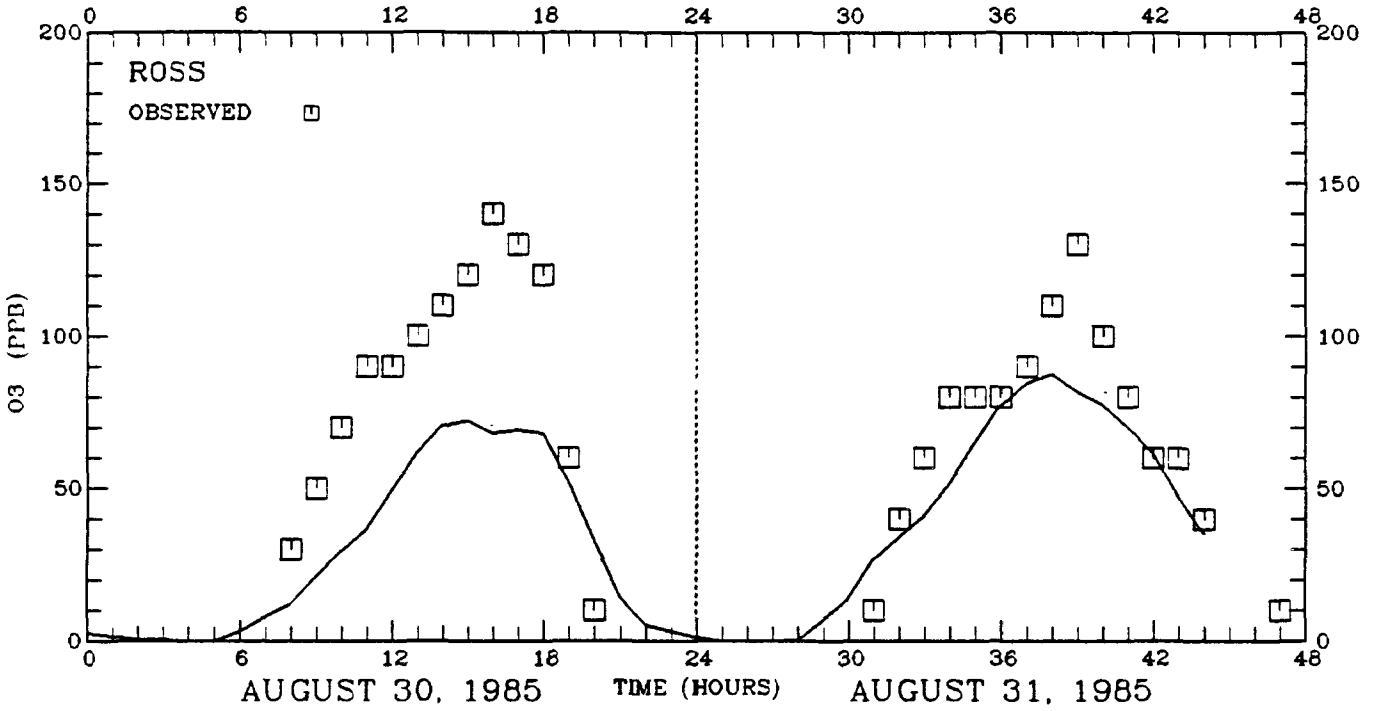

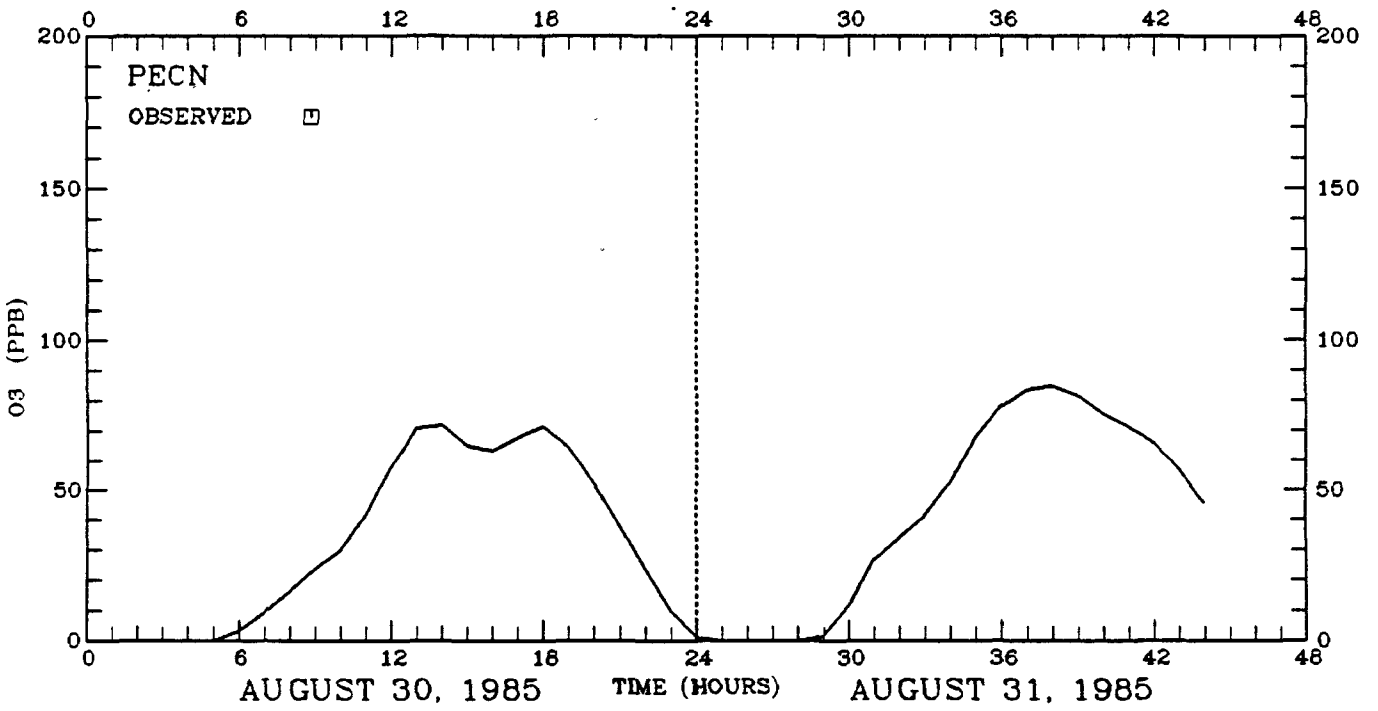

Continued 4-15. Continued.

SYSTEMS APPLICATIONS, INC.

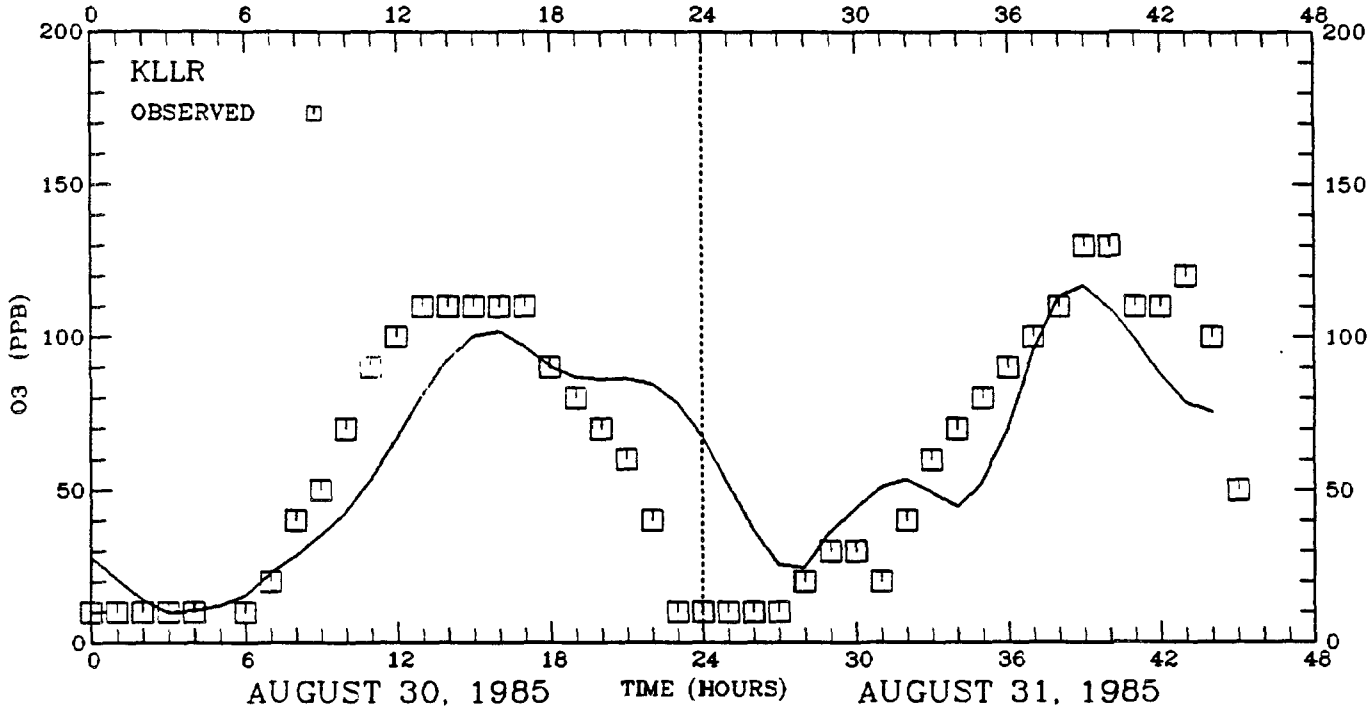

FIGURE 4-15. Concluded.

predicted ozone concentration fields in diagnostic run 2, as shown in the isopleth plots in Appendix H. Around the time of the peak observation at ROSS (1500 - 1600) there is a cloud of predicted ozone concentrations to the north of the ozone monitor in excess of 10 pphm (i.e., within 30 percent). The spatial displacement of the predicted concentration peaks is discussed below. As in diagnostic run 1, the daily maximum ozone concentrations in Dallas predicted in run 2 (7 to 10 pphm) are higher than the observed (5 to 7 pphm).

A scatterplot and statistical model performance measures that indicate how well diagnostic run 2 simulates hourly ozone concentrations on 30 August is given in Figure 4-16. Over all hours and sites the model has a bias toward overprediction of about 6 percent (0.3 pphm) and a gross error of approximately 43 percent (2.0 pphm). Model performance statistics are comparable between diagnostic runs 1 (Figure 4-9) and 2 (Figure 4-16) on 30 August. For 30 August there does not seem to be much improvement in model performance in diagnostic run 2, although the observed peak is reproduced better in diagnostic run 2 (within 6 percent) than in diagnostic run 1 (within 11 percent).

31 August 1985

The predicted region-wide maximum ozone concentration in diagnostic run 2 on 31 August was 16.4 pphm (Figure 4-17 and Appendix H), within 4 percent of the peak observation (17 pphm). The predicted region-wide maximum is located between the two ozone monitors that recorded the highest observed ozone concentration of the episode, approximately 8 km to the southwest of DNTN and 13 km to the northwest of MOCK (Figure 4-17). At the location of the peak observation, the predicted maximum ozone concentration at MOCK is 7.2 pphm (within 58 percent) and at DNTN 13.6 pphm (within 20 percent) (see Figure 4-15). As seen in Figure 4-17 and Appendix H, a very sharp predicted ozone gradient runs through the middle of Dallas; in a distance of only 14 km (3-4 grid cells) the ozone concentrations increase by more than a factor of two from 7 to 16 pphm. Diagnostic run 2 underpredicts the observed peak ozone concentrations at ozone monitors located near the center of Dallas (MOCK and NSTR), but does a fairly good job of replicating the observed peaks and diurnal variation at monitors located south (ILLI and BNVW) and north (DNTN) of the center of the city (Figure 4-15).

The model reproduces the observed peaks in Fort Worth (13 pphm) to within 33 percent at ROSS (8.8 pphm) and 10 percent at KLLR (11.7 pphm). Again there is considerable spatial variation in the predictions, and there are predicted ozone concentrations similar to the observed peaks within a few grid cells of the location of the observed peaks.

Figure 4-18 displays a scatterplot and model performance statistics for diagnostic run 2 predicted and observed hourly ozone concentrations on 31 August. Over all hours and sites the model underpredicts the observed hourly ozone concentrations on

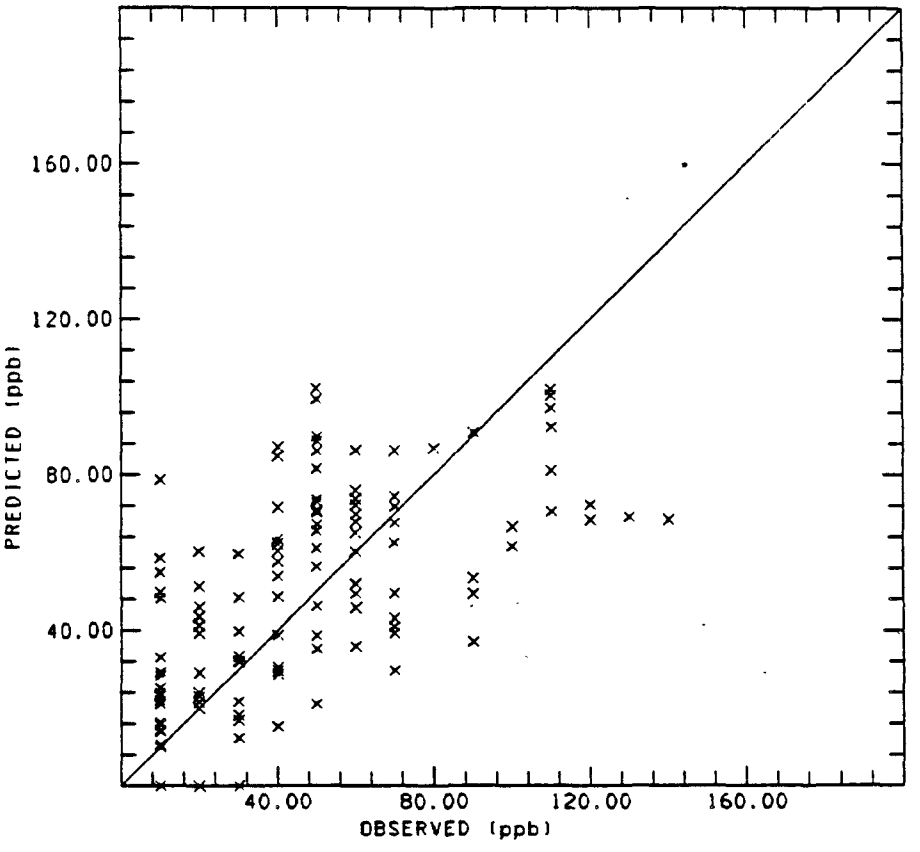

MOMENTS OF THE PROBABILITY DENSITY FUNCTION

	OBSERVED	PREDICTED
AVERAGE	46.96721	49.96617
STANDARD DEVIATION	31.01291	26.66011
SKEWNESS	0.82584	-0.06659
KURTOSIS	0.17512	-0.89927
OTHER MEASURES		
MEDIAN	40.00000	49.79000
UPPER QUARTILE	60.00000	70.14000
LOWER QUARTILE	20.00000	28.68000
MINIMUM VALUE	10.00000	0.01000
MAXIMUM VALUE	140.00000	102.20000

SKILL OF PREDICTION PARAMETERS

CORRELATION COEFFICIENT OF PREDICTED VERSUS OBSERVED 0.617
THE BOUNDS OF THE CORRELATION AT THE CONFIDENCE LEVEL OF 0.050 ARE
LOW BOUND 0.493 HIGH BOUND 0.716
RATIO OF OVER TO UNDER PREDICTIONS 1.490
PERCENT OF OVER PREDICTIONS GREATER THAN 200 PERCENT OF THE OBSERVED 17.213
PERCENT OF UNDER PREDICTIONS LESS THAN 50 PERCENT OF THE OBSERVED 10.656

FIGURE 4-16a. Scatterplot and model performance statistics for predicted and observed hourly ozone concentrations (ppb) on 30 August 1985 in Dallas-Fort Worth for diagnostic run 2 (N=122).

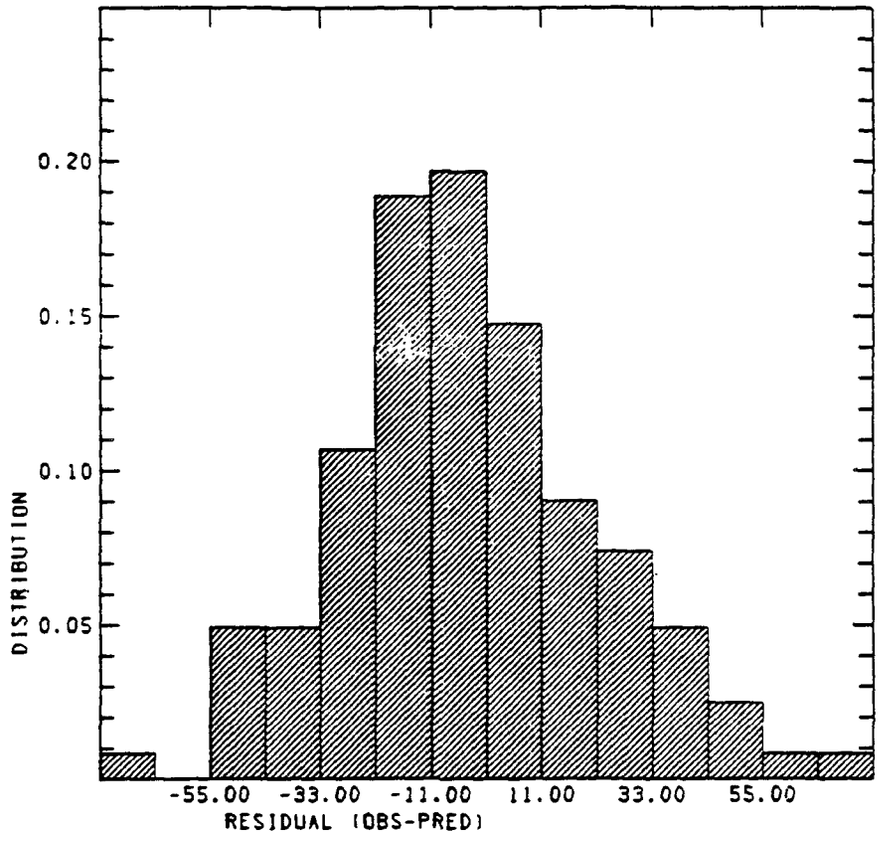

THE BINSIZE EQUALS 11.000

RESIDUAL ANALYSIS

AVERAGE	-2.99921
STANDARD DEVIATION	25.53730
SKEWNESS	0.29124
KURTOSIS	0.06662
OTHER MEASURES	
MEDIAN	-4.48000
UPPER QUARTILE	10.58000
LOWER QUARTILE	-20.48000
MINIMUM VALUE	-68.64000
MAXIMUM VALUE	71.53000

BIAS CONFIDENCE INTERVAL
AT THE 0.0500 LEVEL
LOWER BOUND -9.1375
UPPER BOUND 3.1390

STD RESIDUAL CONFIDENCE INTERVAL
AT THE 0.0500 LEVEL
LOWER BOUND 534.7552
UPPER BOUND 816.1281

THE MEASURES OF GROSS ERROR
THE ROOT MEAN SQUARE ERROR IS 25.61
THE AVERAGE ABSOLUTE ERROR IS 20.36

VARIOUS MEASURES OF RELATIVE VARIABILITY
OBSERVATION COEFFICIENT OF VARIATION
0.6603
RESIDUAL COEFFICIENT OF VARIATION
0.5437
RATIO OF RESIDUAL TO OBSERVED ST. DEV.
0.8234

FIGURE 4-16b. Residual analysis and model performance statistics for predicted and observed hourly ozone concentrations (ppb) on 30 August 1985 in Dallas-Fort Worth for diagnostic run 2 (N=122).

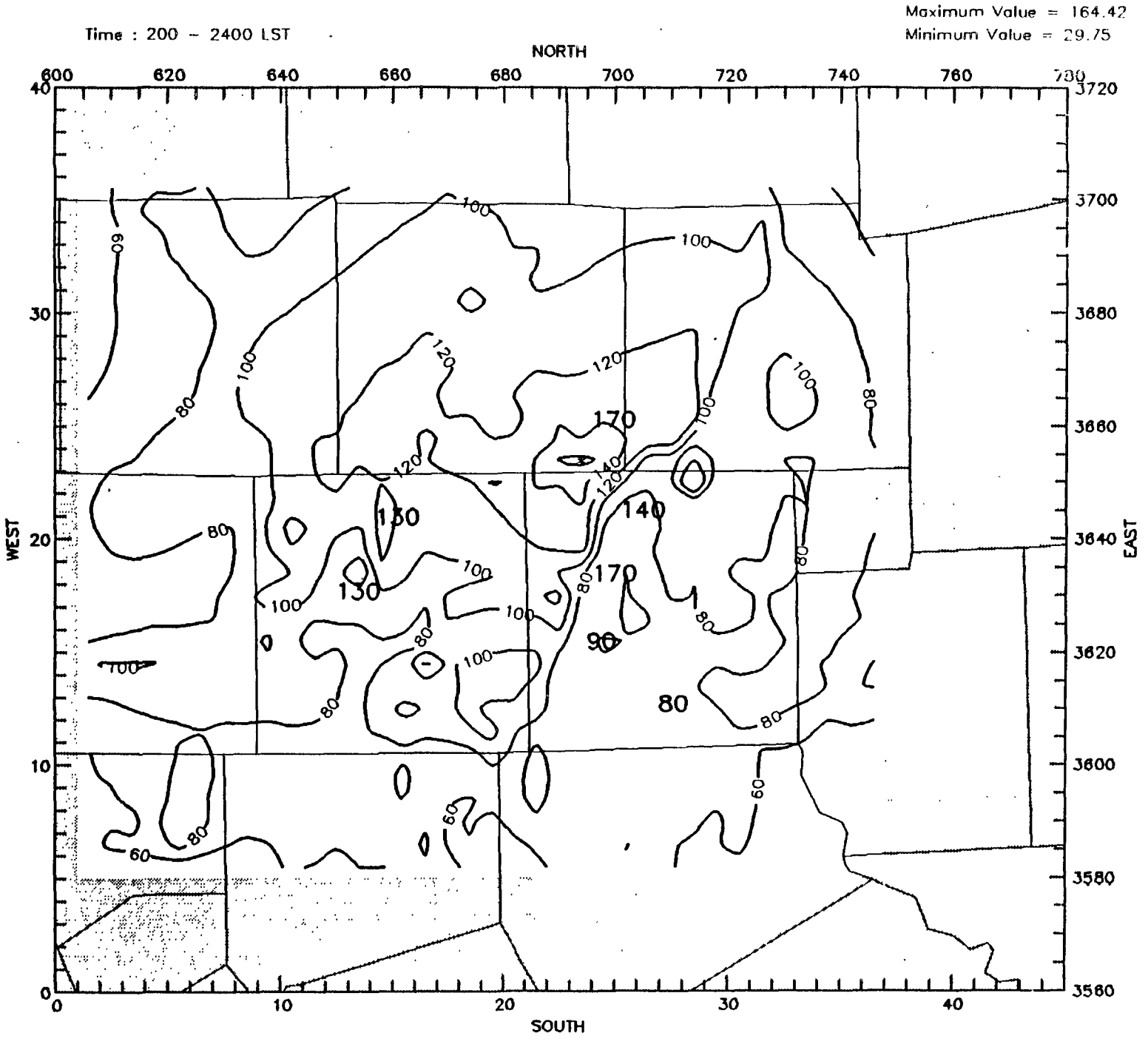

FIGURE 4-17. Isopleths of predicted daily maximum ozone concentrations (ppb) with superimposed observations on 31 August 1985 for the Dallas-Fort Worth diagnostic run 2.

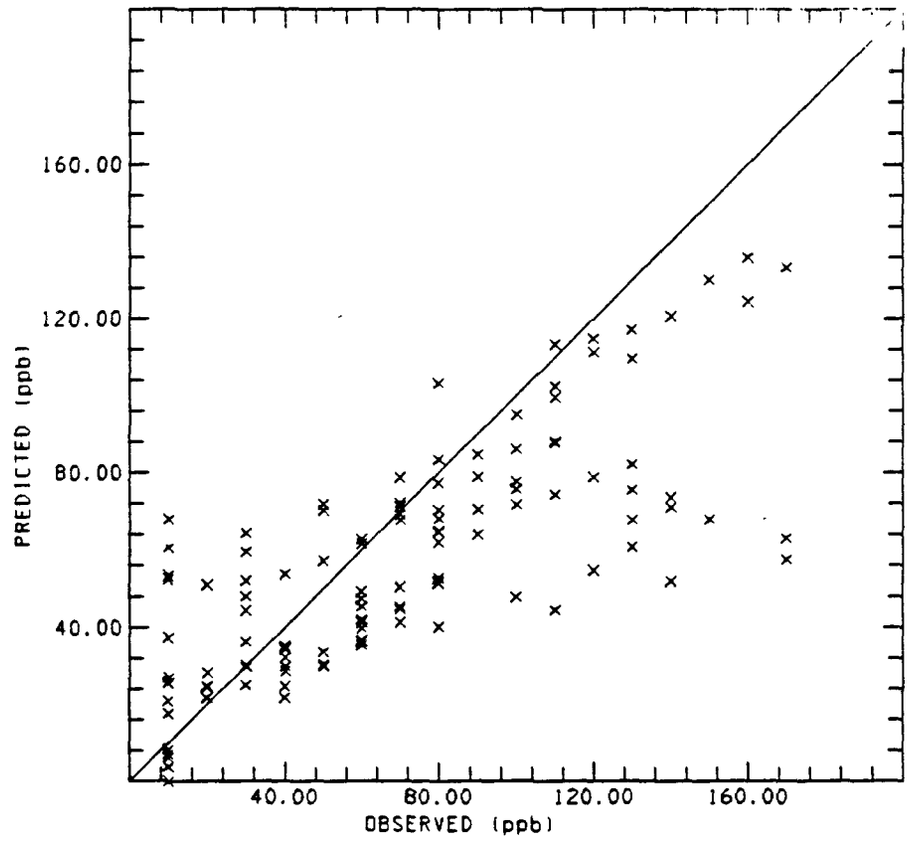

MOMENTS OF THE PROBABILITY DENSITY FUNCTION

	OBSERVED	PREDICTED
AVERAGE	70.60869	57.71497
STANDARD DEVIATION	44.49103	29.85752
SKEWNESS	0.38833	0.51526
KURTOSIS	-0.79089	-0.04070
OTHER MEASURES		
MEDIAN	70.00000	53.30000
UPPER QUARTILE	100.00000	72.10001
LOWER QUARTILE	30.00000	34.67000
MINIMUM VALUE	10.00000	0.01000
MAXIMUM VALUE	170.00000	135.89990

SKILL OF PREDICTION PARAMETERS

CORRELATION COEFFICIENT OF PREDICTED VERSUS OBSERVED 0.763
THE BOUNDS OF THE CORRELATION AT THE CONFIDENCE LEVEL OF 0.050 ARE
LOW BOUND 0.674 HIGH BOUND 0.830
RATIO OF OVER TO UNDER PREDICTIONS 0.420
PERCENT OF OVER PREDICTIONS GREATER THAN 200 PERCENT OF THE OBSERVED 9.565
PERCENT OF UNDER PREDICTIONS LESS THAN 50 PERCENT OF THE OBSERVED 9.565

FIGURE 4-18a. Scatterplot and model performance statistics for predicted and observed hourly ozone concentrations (ppb) on 31 August 1985 in Dallas-Fort Worth for diagnostic run 2 (N=115).

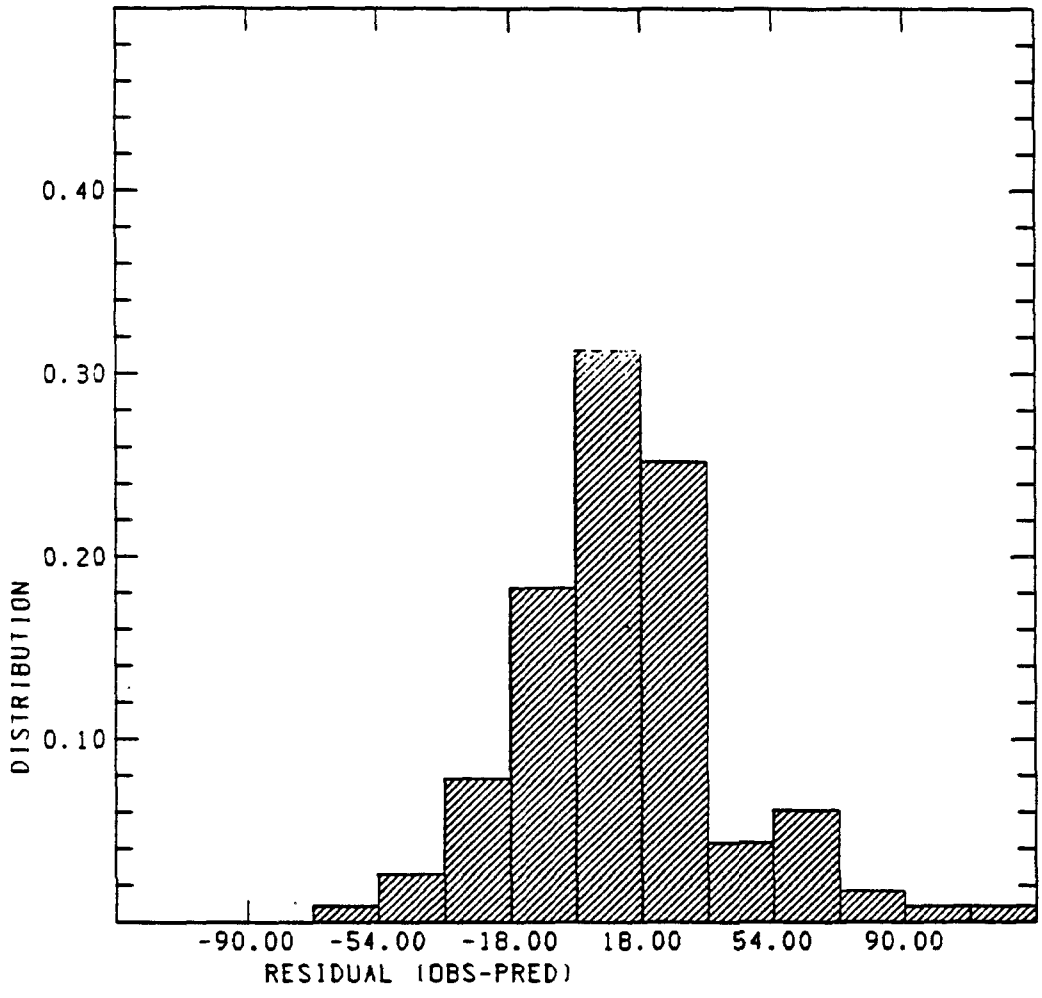

THE BINSIZE EQUALS 18.000

RESIDUAL ANALYSIS

AVERAGE	12.89339
STANDARD DEVIATION	29.04443
SKEWNESS	0.74048
KURTOSIS	1.61677
OTHER MEASURES	
MEDIAN	10.41000
UPPER QUARTILE	23.65000
LOWER QUARTILE	-3.30000
MINIMUM VALUE	-57.83000
MAXIMUM VALUE	112.53990

BIAS CONFIDENCE INTERVAL
AT THE 0.0500 LEVEL
LOWER BOUND 4.6064
UPPER BOUND 21.1804

STD RESIDUAL CONFIDENCE INTERVAL
AT THE 0.0500 LEVEL
LOWER BOUND 687.8611
UPPER BOUND 1063.2840

THE MEASURES OF GROSS ERROR
THE ROOT MEAN SQUARE ERROR IS 31.66
THE AVERAGE ABSOLUTE ERROR IS 22.85

VARIOUS MEASURES OF RELATIVE VARIABILITY
OBSERVATION COEFFICIENT OF VARIATION
0.6301
RESIDUAL COEFFICIENT OF VARIATION
0.4113
RATIO OF RESIDUAL TO OBSERVED ST. DEV.
0.6528

FIGURE 4-18b. Residual analysis and model performance statistics for predicted and observed hourly ozone concentrations (ppb) on 31 August 1985 in Dallas-Fort Worth for diagnostic run 2 (N=115).

average by about 18 percent (1.3 pphm). The gross error is about 32 percent, slightly lower than was seen in diagnostic run 1 (33 percent). In general, model performance statistics for hourly ozone concentrations for diagnostic runs 1 and 2 are comparable. However, diagnostic run 2 does a much better job of replicating the peak observed ozone concentration on 31 August (within 4 percent) than does diagnostic run 1 (within 15 percent).

NO, NO_2, and CO

Time series of predicted and observed hourly NO, NO_2, and CO concentrations for diagnostic run 2 are shown in Figures 4-19, 4-20, and 4-21. In general, the remarks made in the analysis of diagnostic run 1 hold for run 2 also, except diagnostic run 2 does a better job reproducing the peak observations of these species. For example the peak NO observation at ROSS at midnight on 30 August (8 pphm) is reproduced to within 42 percent (4.7 pphm) in diagnostic run 2 (Figure 4-19) as compared to 58 percent (3.4 pphm) in diagnostic run 1. It is also interesting to note that in both diagnostic simulations the model does an excellent job reproducing the observed hourly NO_2 concentrations at ROSS (Figure 4-20)

Nearest-Neighbor Analysis

It appears that the model predictions of peak ozone concentrations are similar to the observed peaks but slightly displaced from the location of the observed peak. This displacement should not affect the usefulness of the UAM in an evaluation of alternative emission control strategies, but does affect model performance. In order to calculate model performance measures that take into account small displacements at the predicted concentrations, it has been suggested that model predictions in adjacent cells of the observation site be compared with the observation in evaluating model performance (Seinfeld, 1988a; Burton, 1988). This is accomplished by examining predicted concentrations in grid cells adjacent to the cell containing the ozone monitoring (one-cell search) and matching up the prediction that is most like the observation for that hour. Similarly, a two-cell search involves examing predicted concentrations within two cells of the ozone monitor. The results of the one-cell and two-cell searches for diagnostic run 2 are presented in, respectively, Figures 4-22 through 4-24 and Figures 4-25 through 4-27.

It appears that the model predictions of ozone, NO, and NO_2 are comparable to the observations within only one or two grid cells almost all of the time. The exceptions are (1) the peak ozone observations at ROSS on 30 August (Figure 4-22 and 4-25); (2) the peak ozone observations at MOCK on 31 August (Figure 4-22 and 4-25); and (3) the high NO observations around midnight 30 August at MOCK and ROSS (Figures 4-23 and 4-26). Other then these three situations, model performance based on nearest-neighbor analysis is quite good.

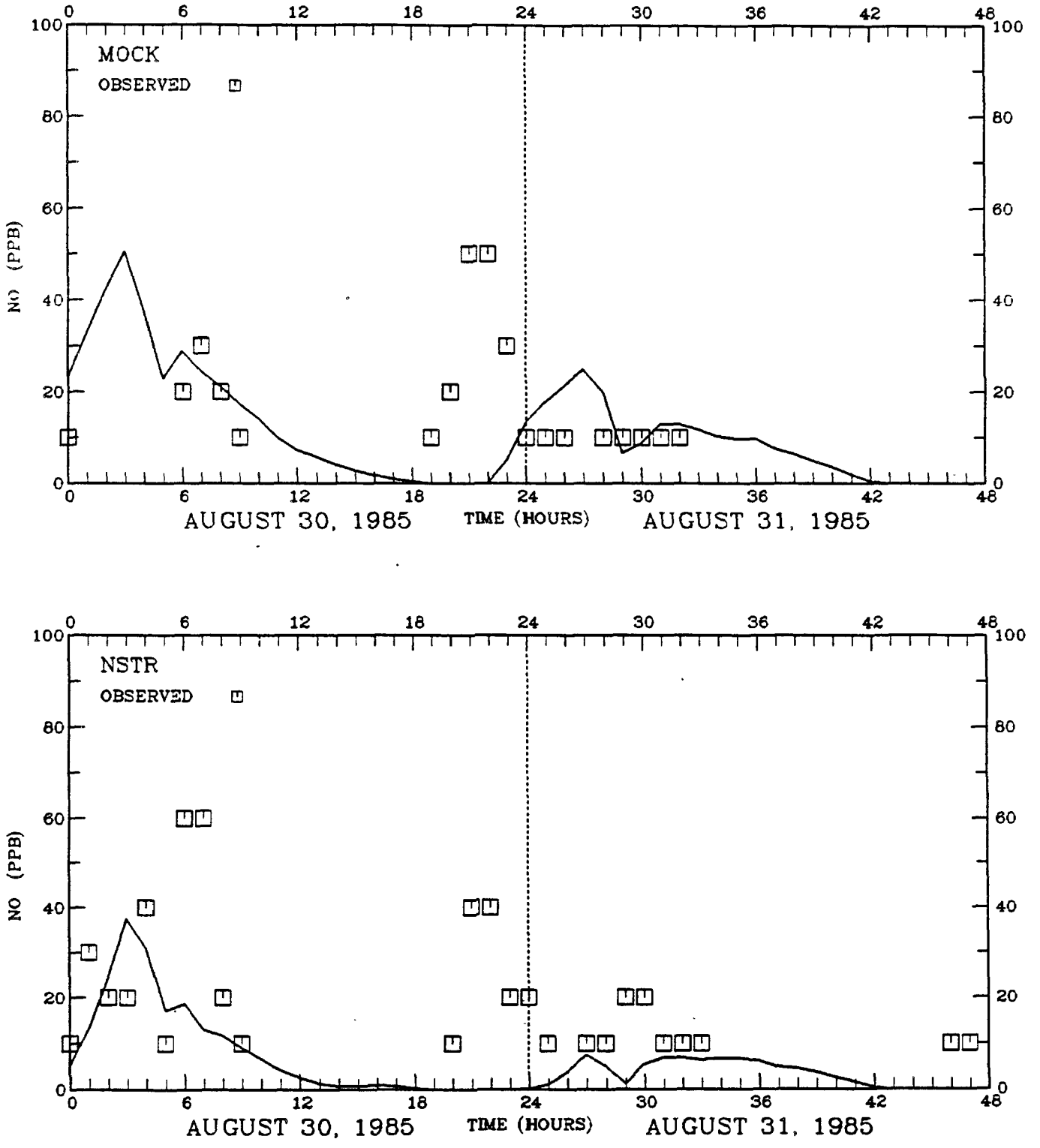

FIGURE 4-19. Time series of predicted and observed hourly NO concentrations (ppb) in Dallas-Fort Worth for diagnostic run 2.

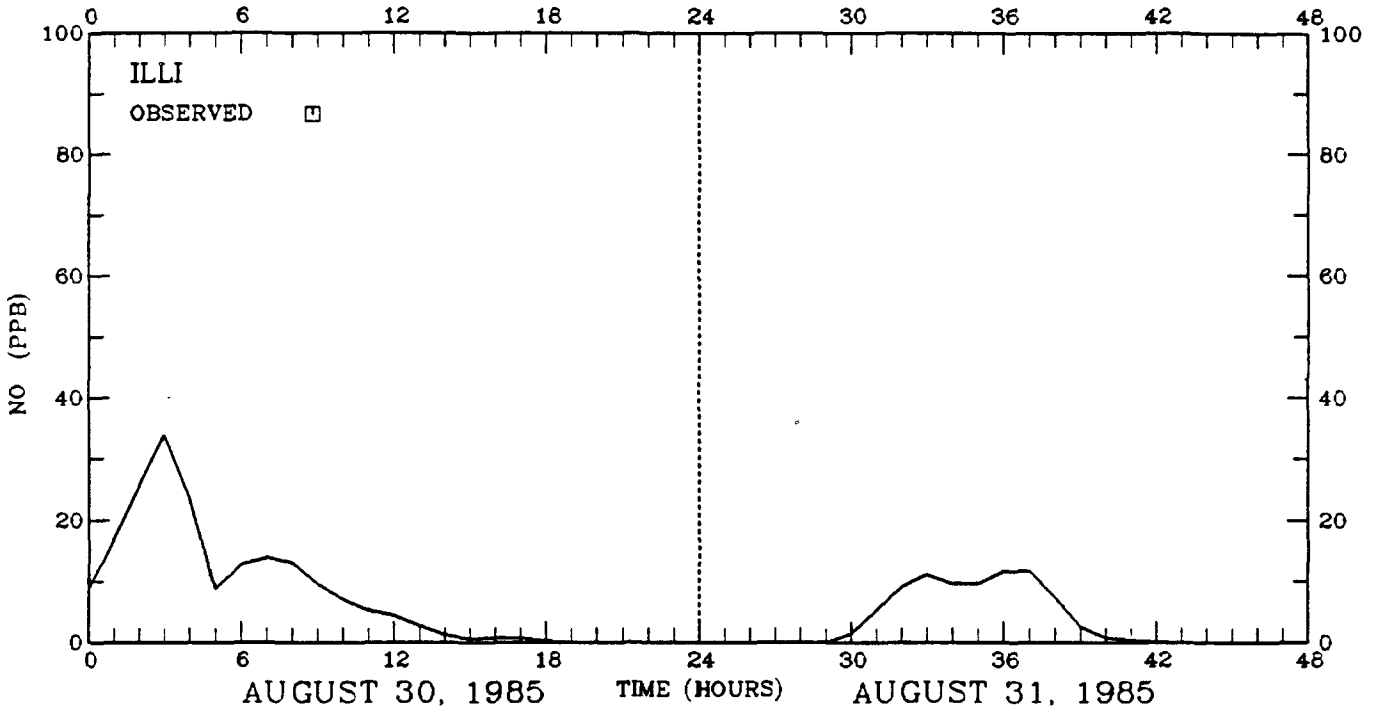

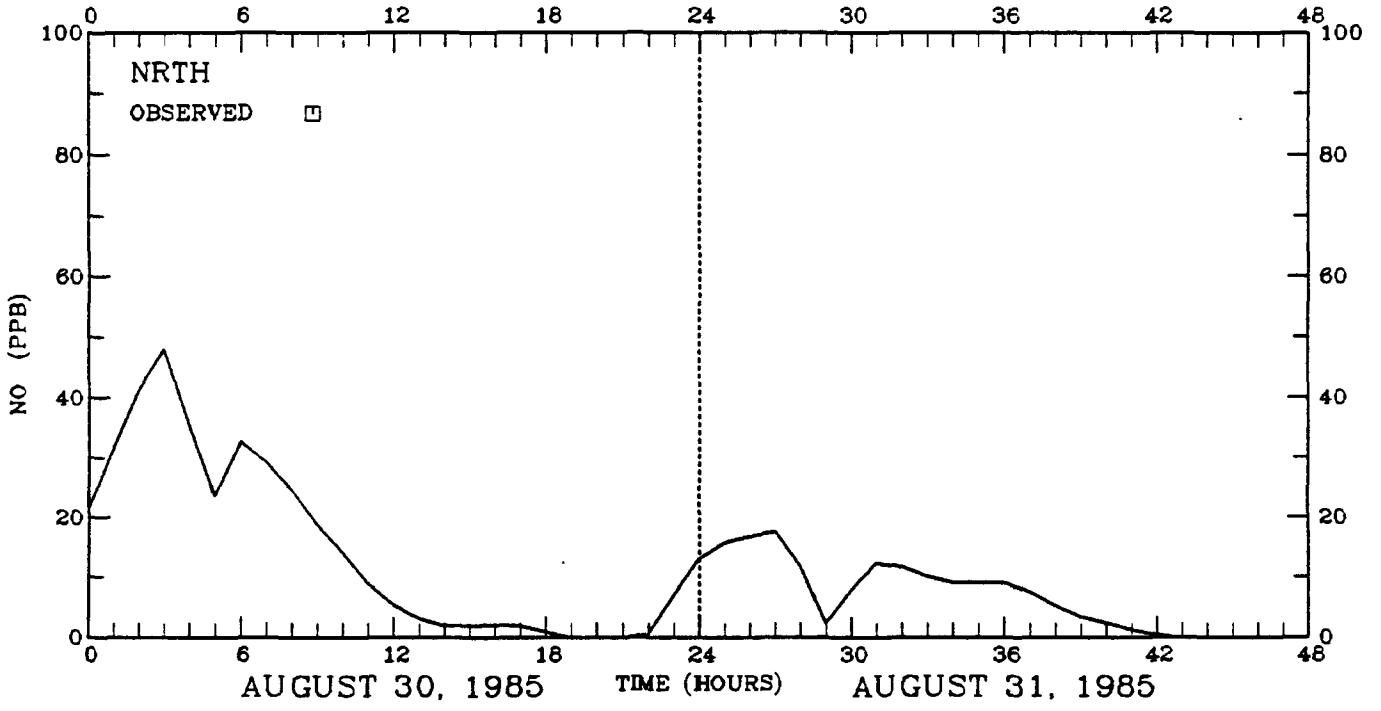

FIGURE 4-19. Continued.

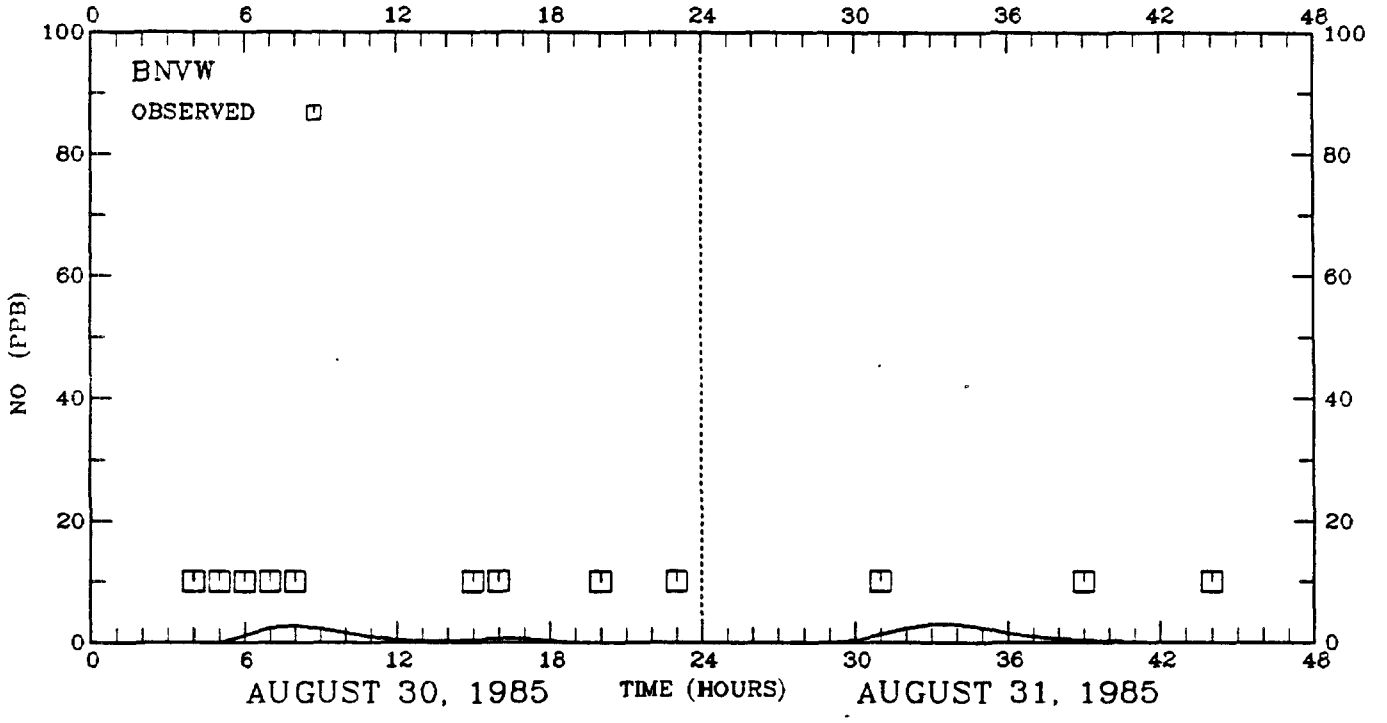

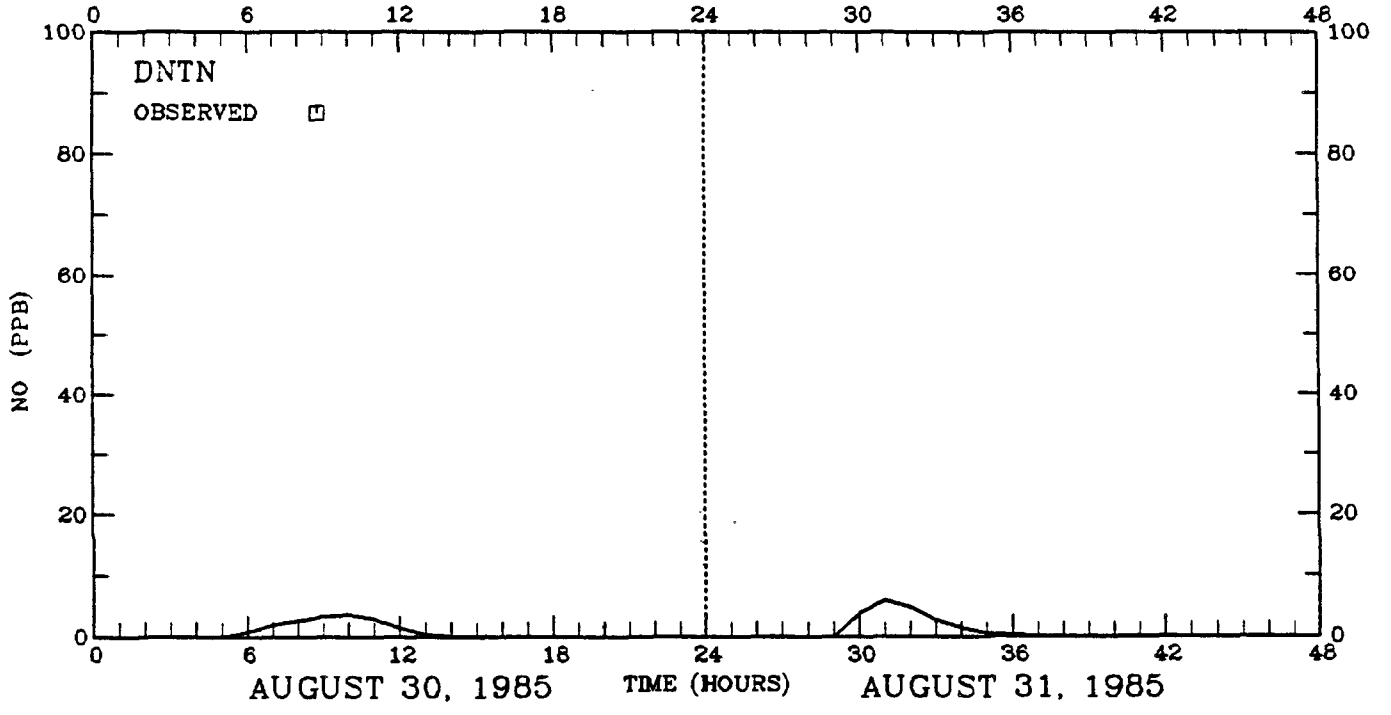

FIGURE 4-19. Continued.

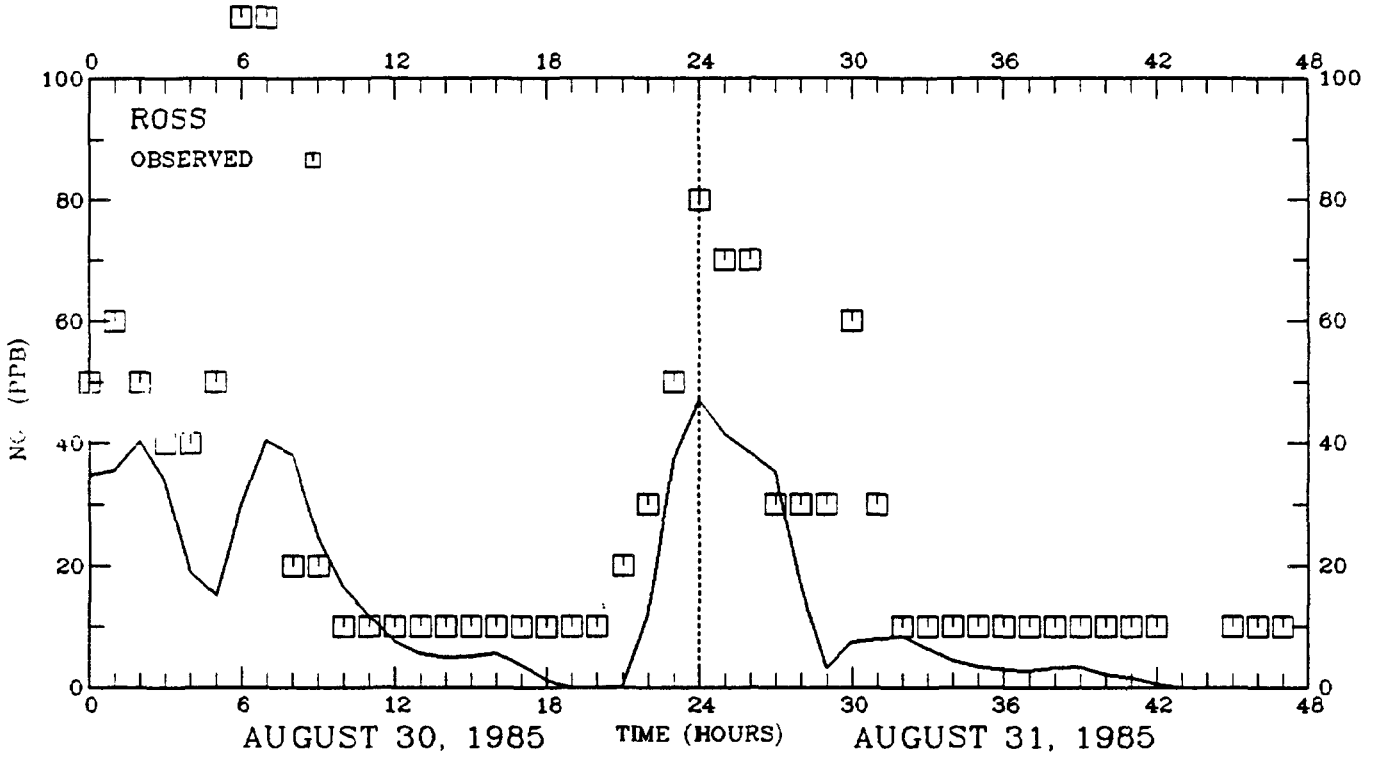

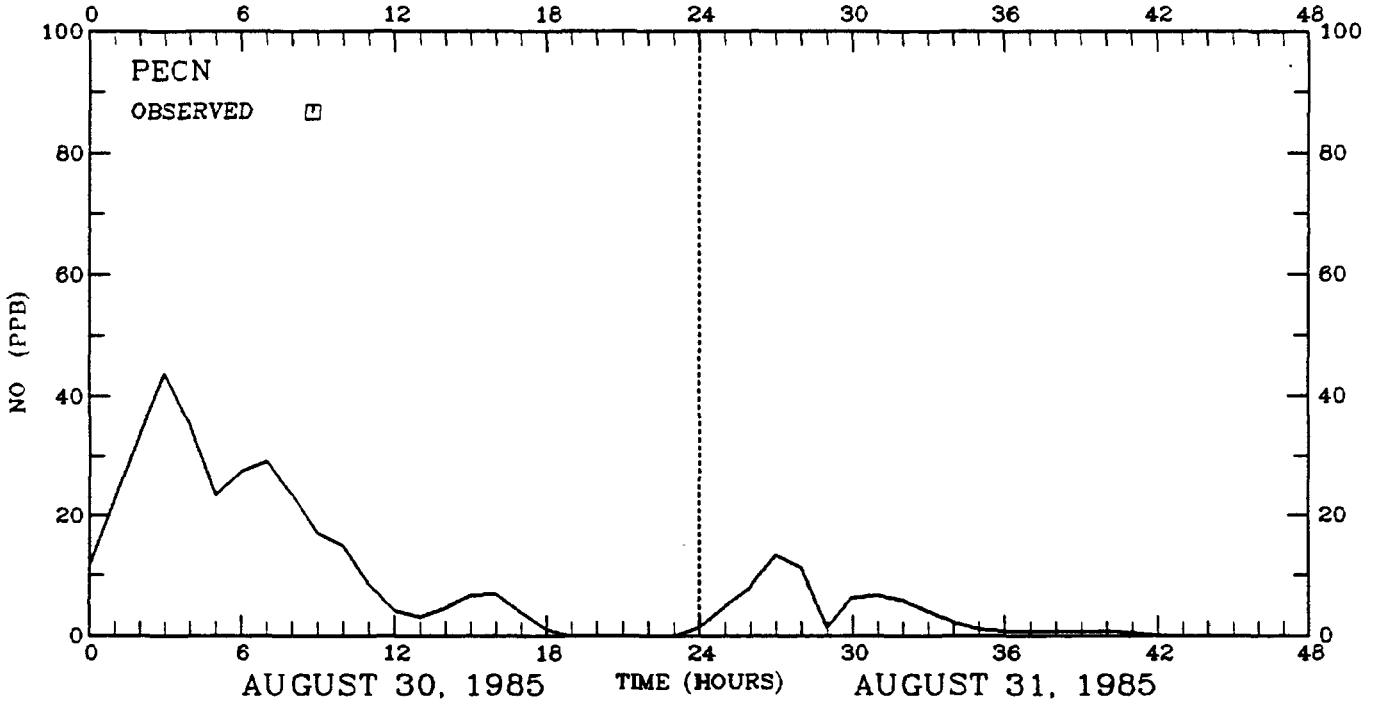

FIGURE 4-19. Continued.

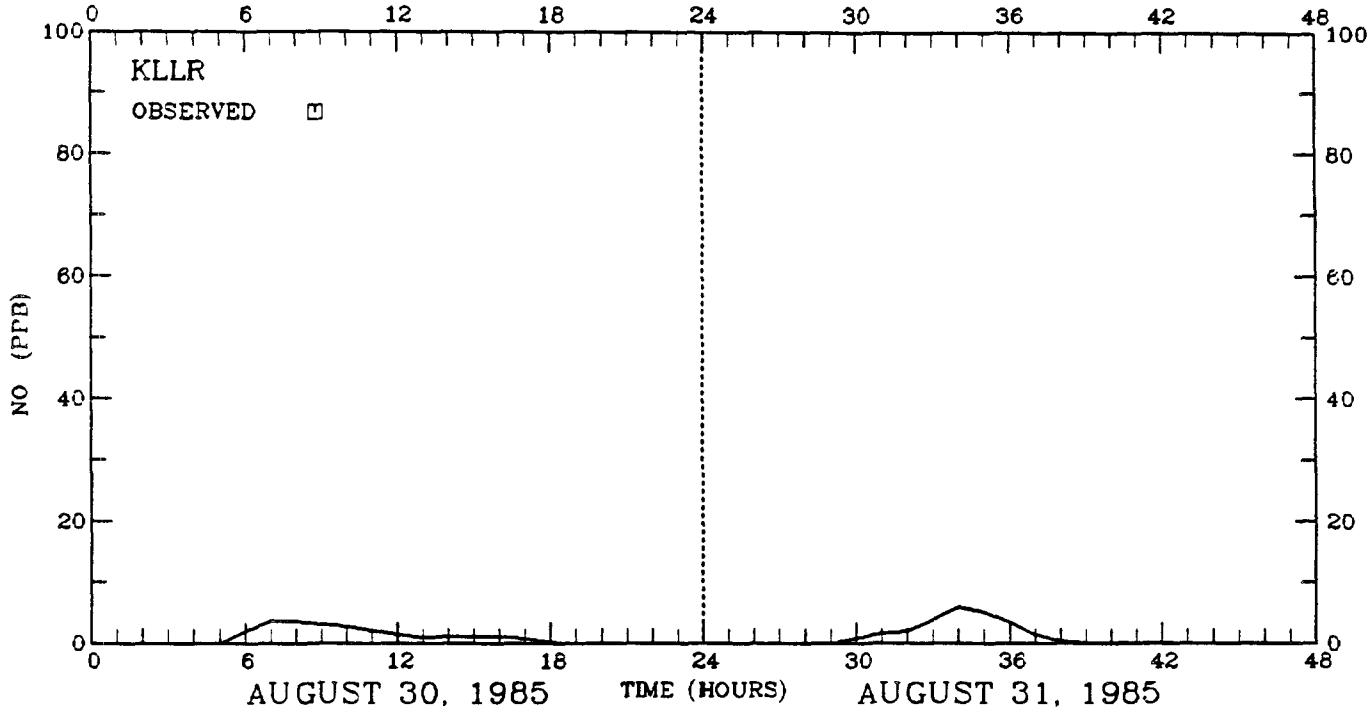

FIGURE 4-19. Concluded.

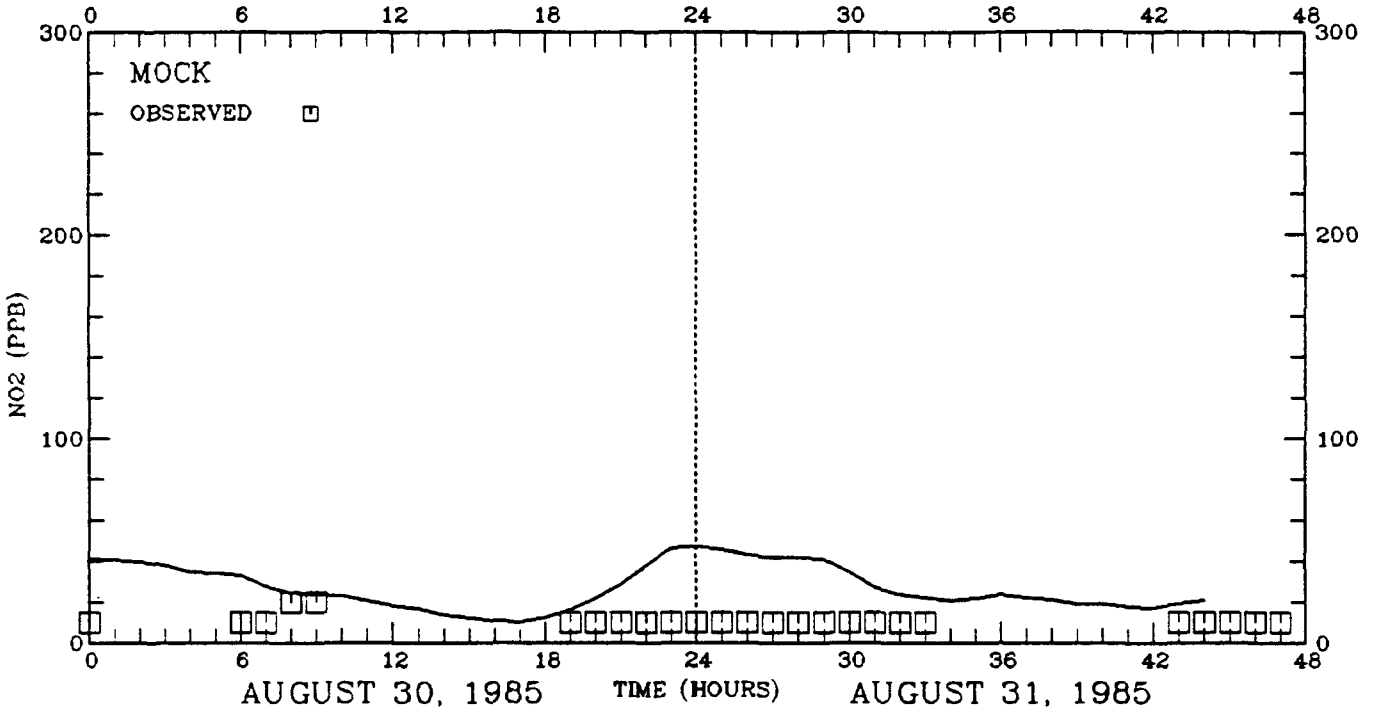

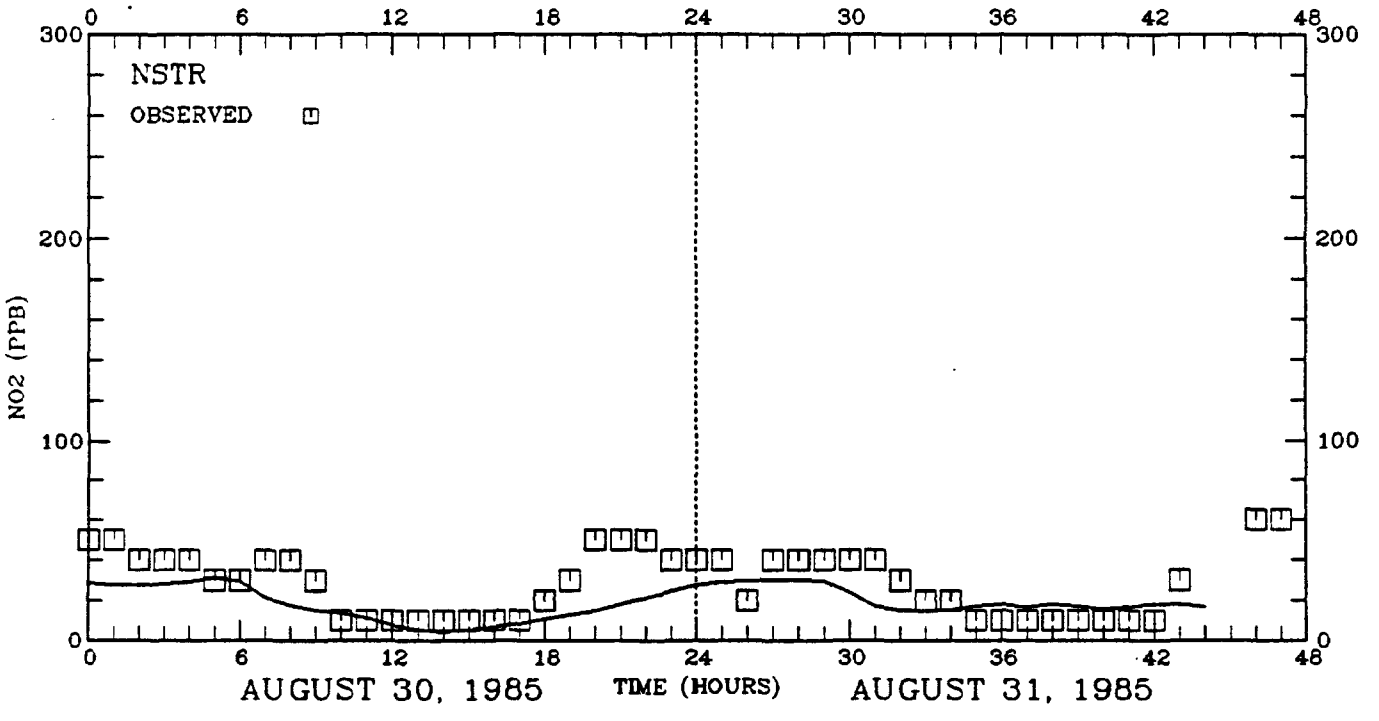

FIGURE 4-20. Time series of predicted and observed hourly NO_2 concentrations (ppb) in Dallas-Fort Worth for diagnostic run 2.

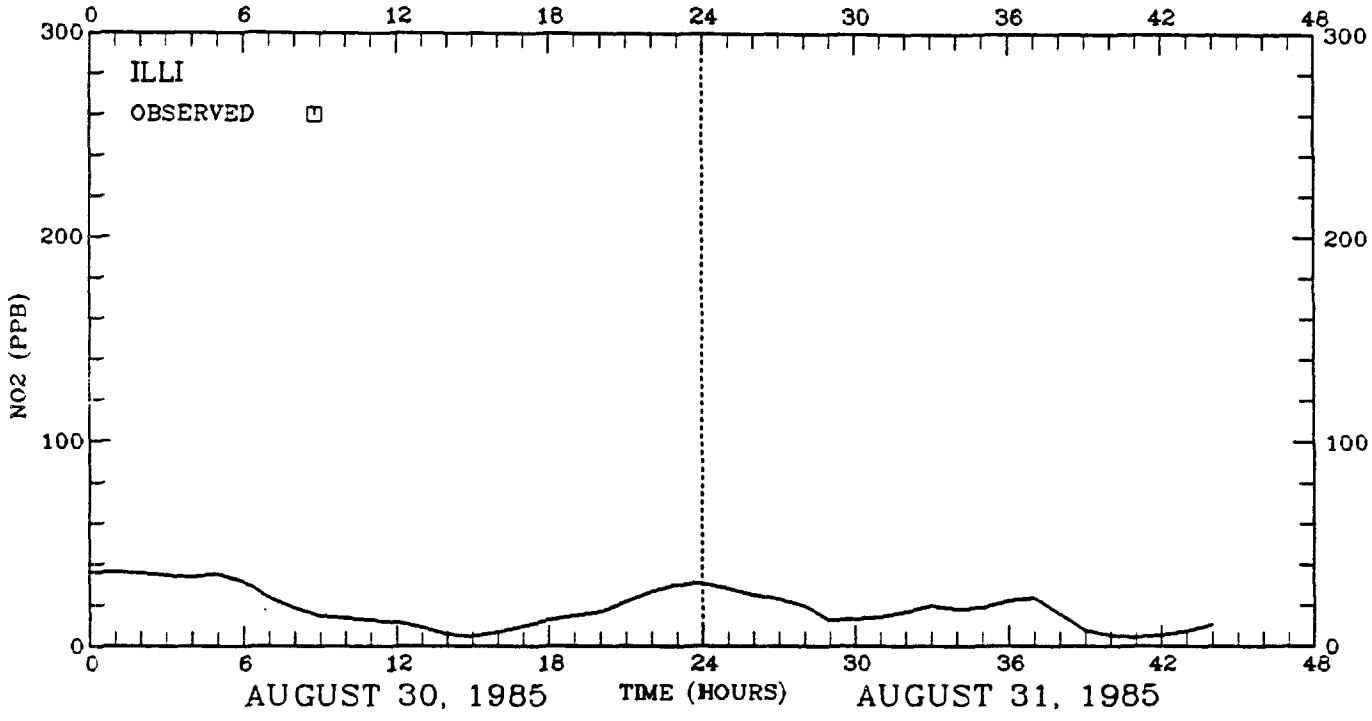

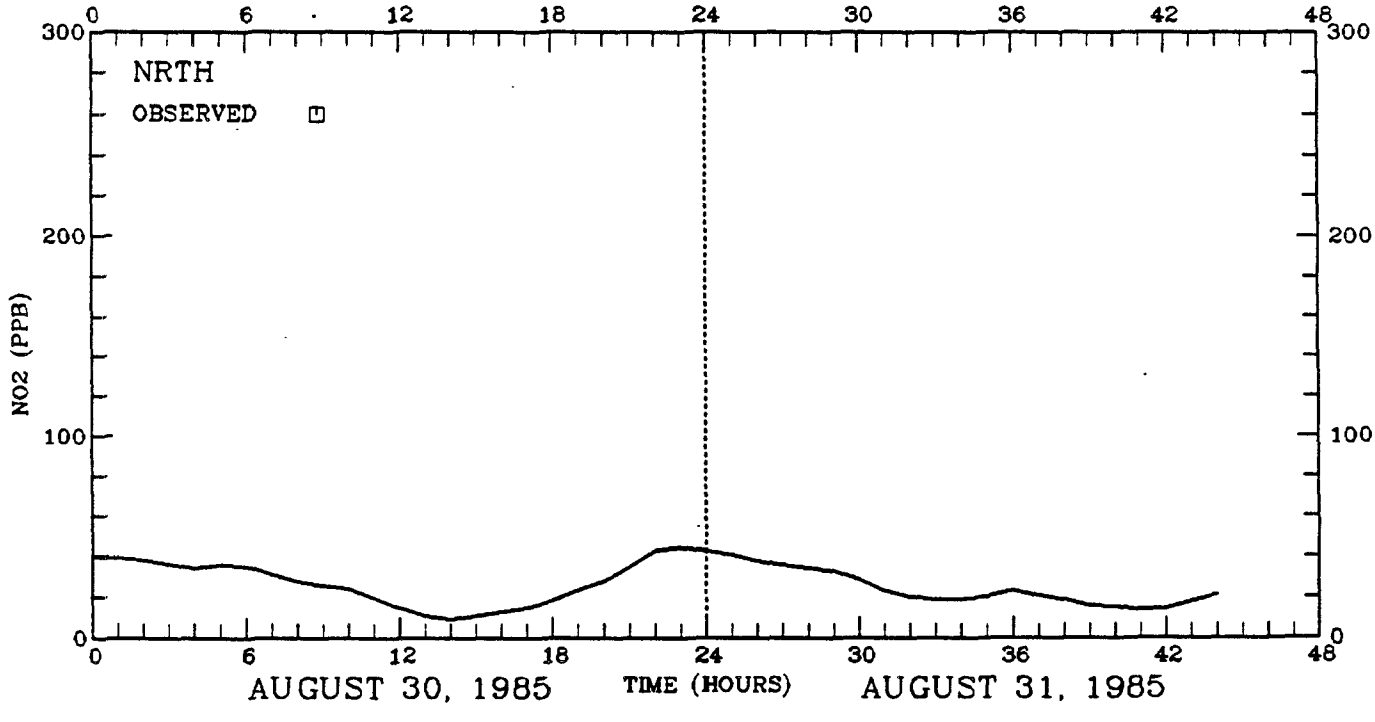

FIGURE 4-20. Continued.

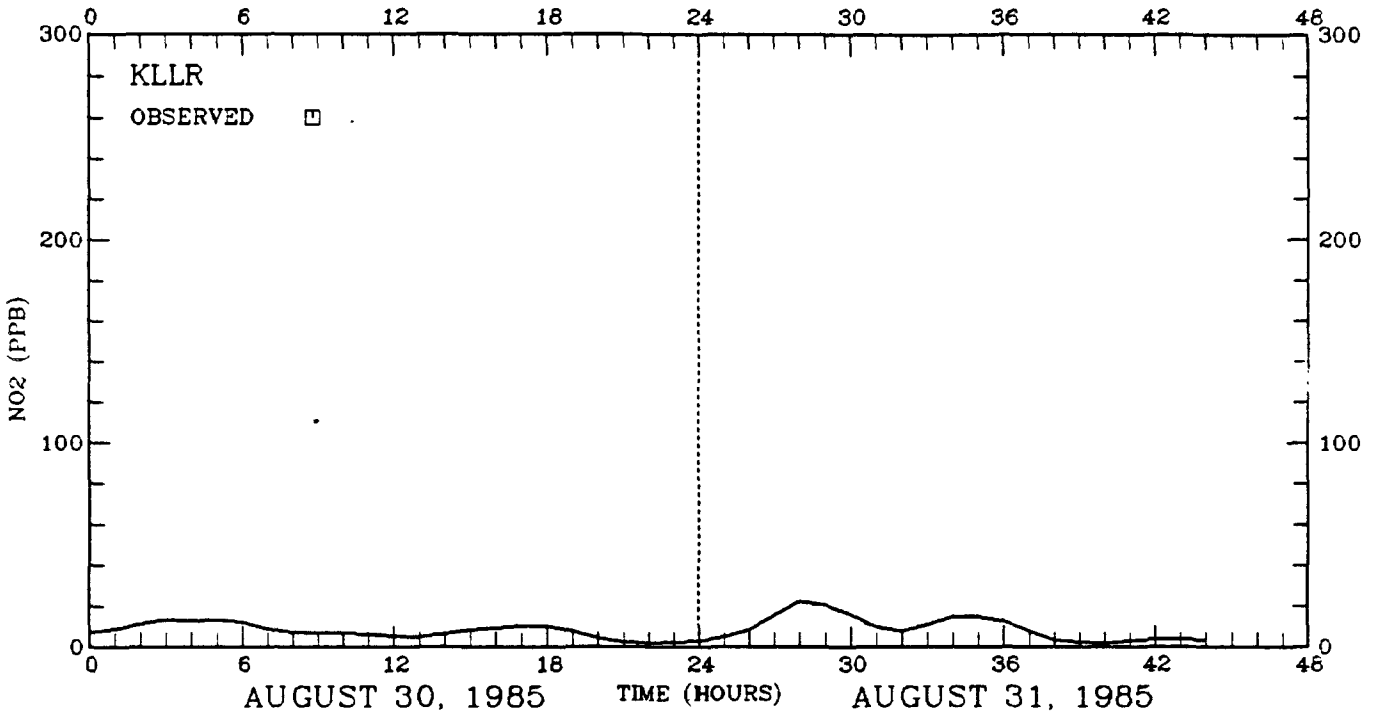

FIGURE 4-20. Continued.

SYSTEMS APPLICATIONS, INC.

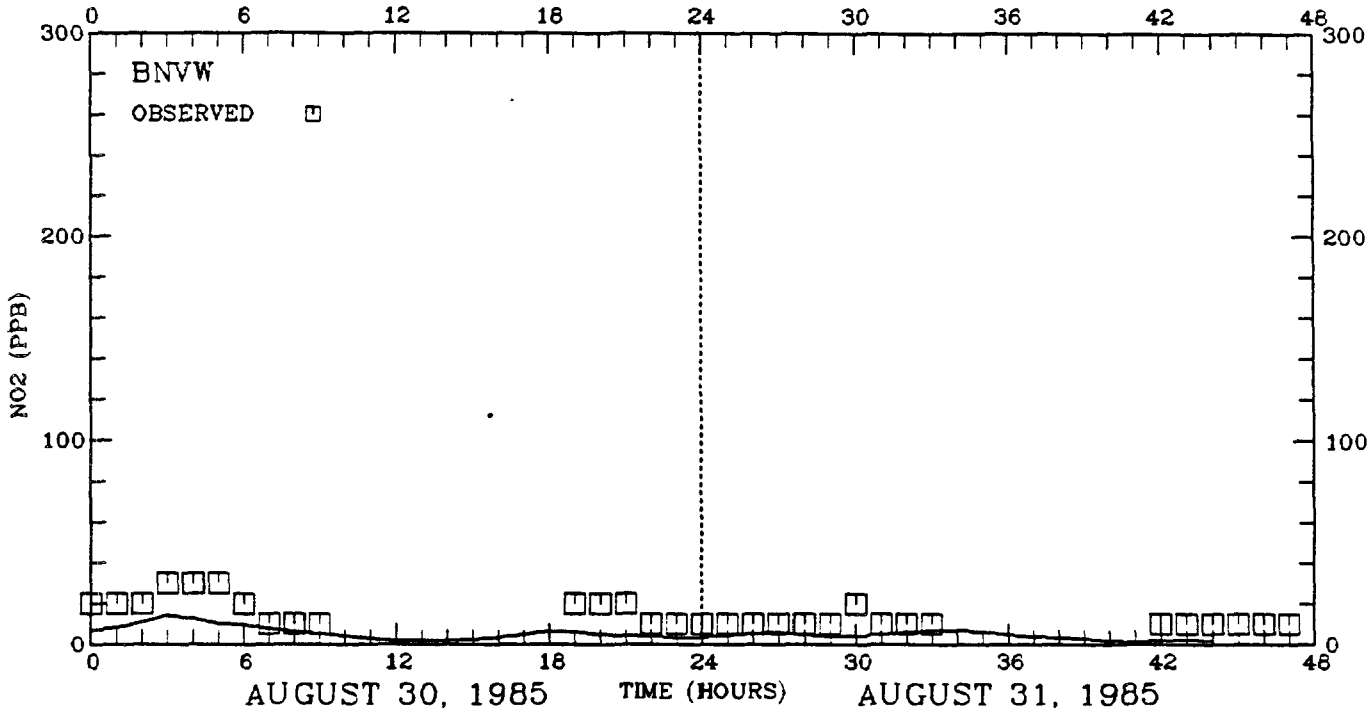

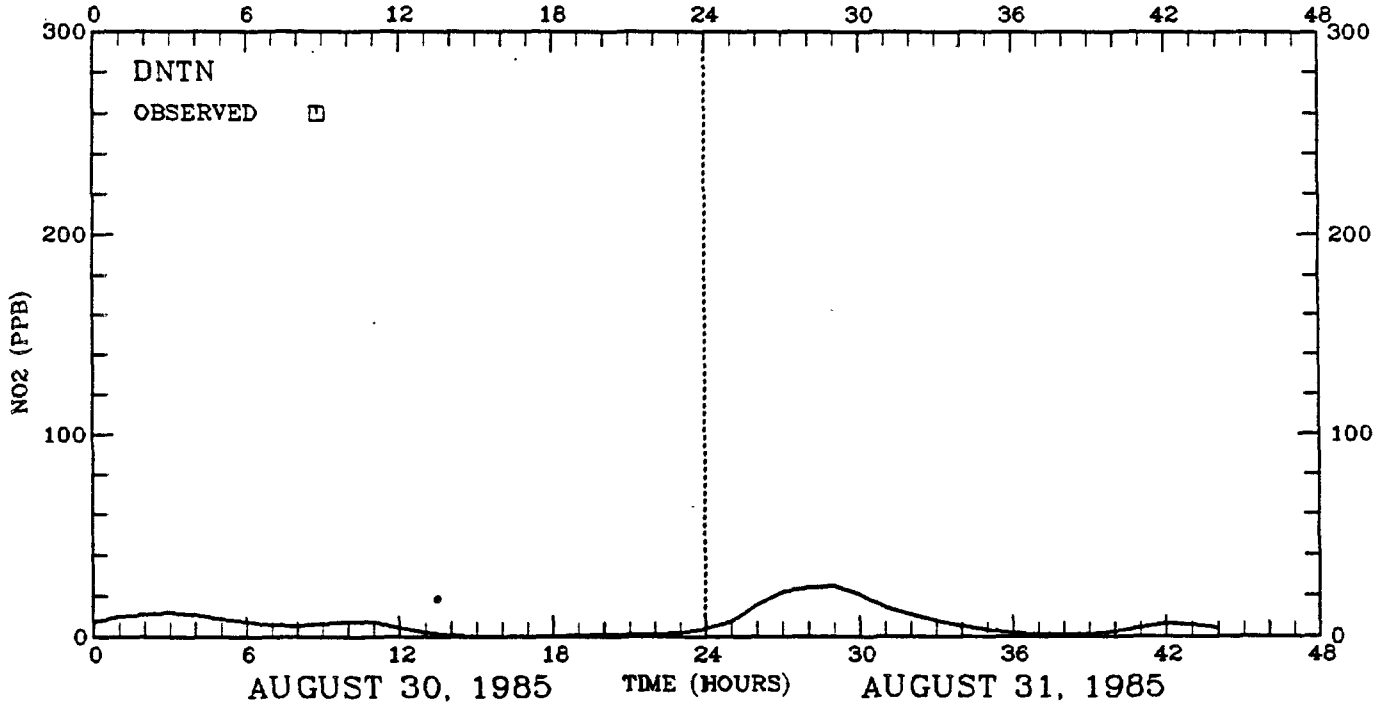

FIGURE 4-20. Continued.

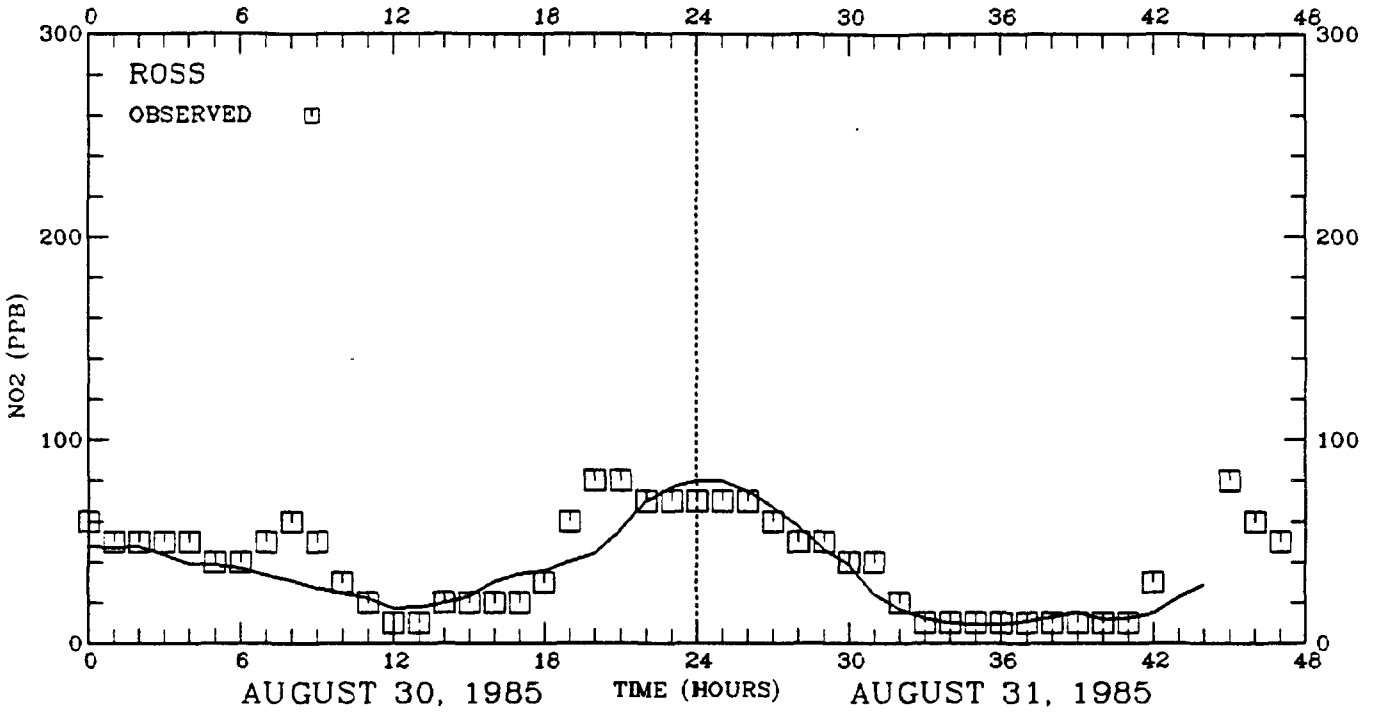

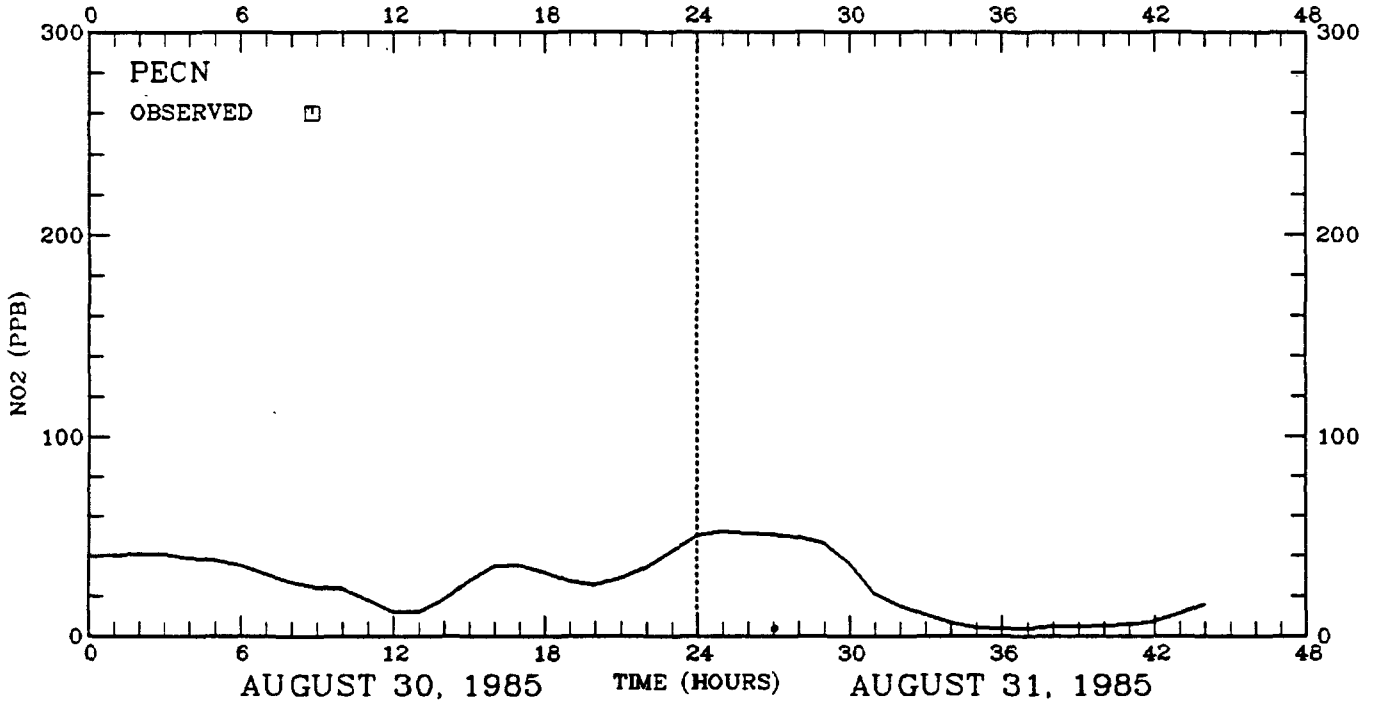

FIGURE 4-20. Continued.

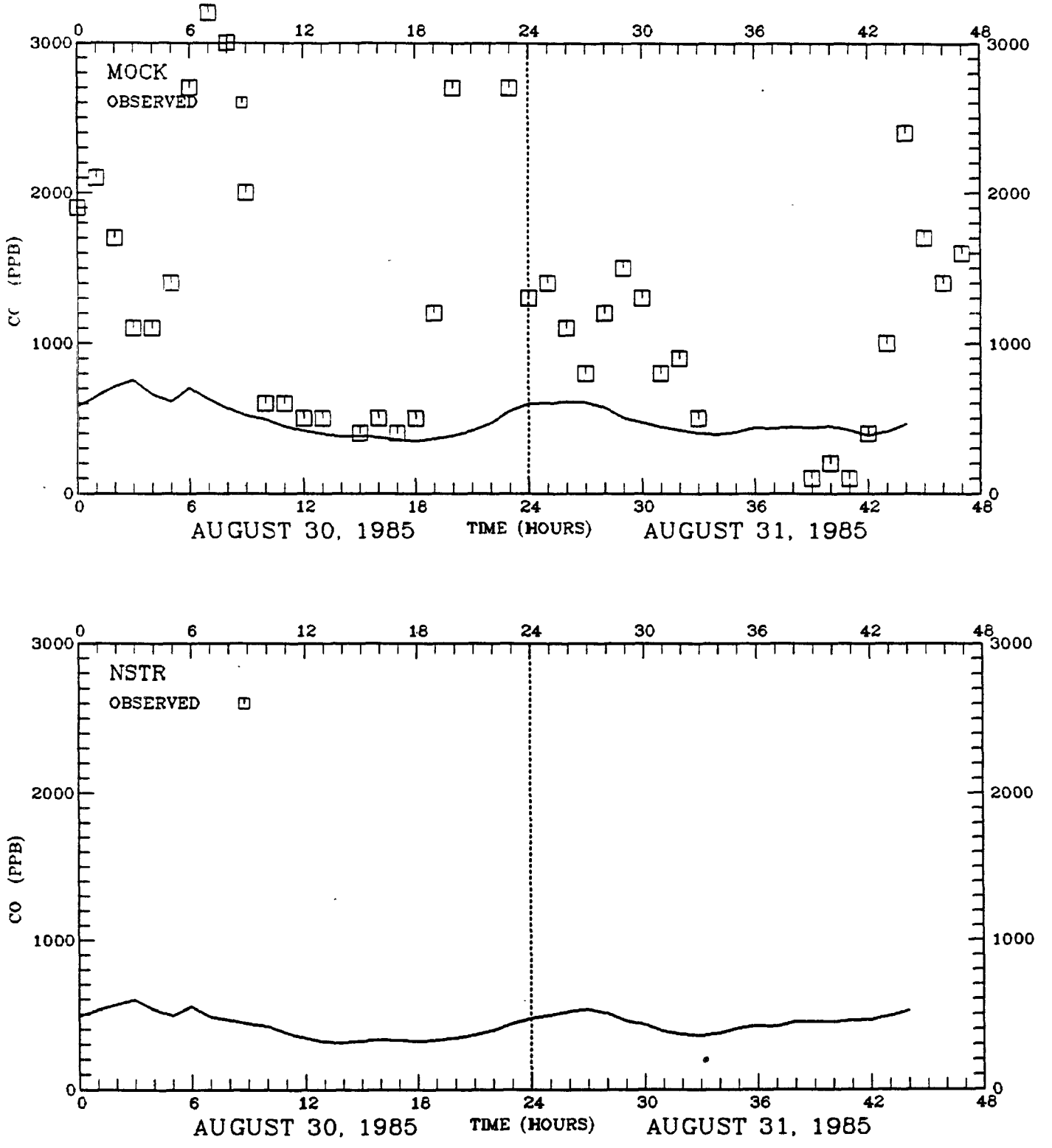

FIGURE 4-21. Time series of predicted and observed hourly CO concentrations (ppb) in Dallas-Fort Worth for diagnostic run 2.

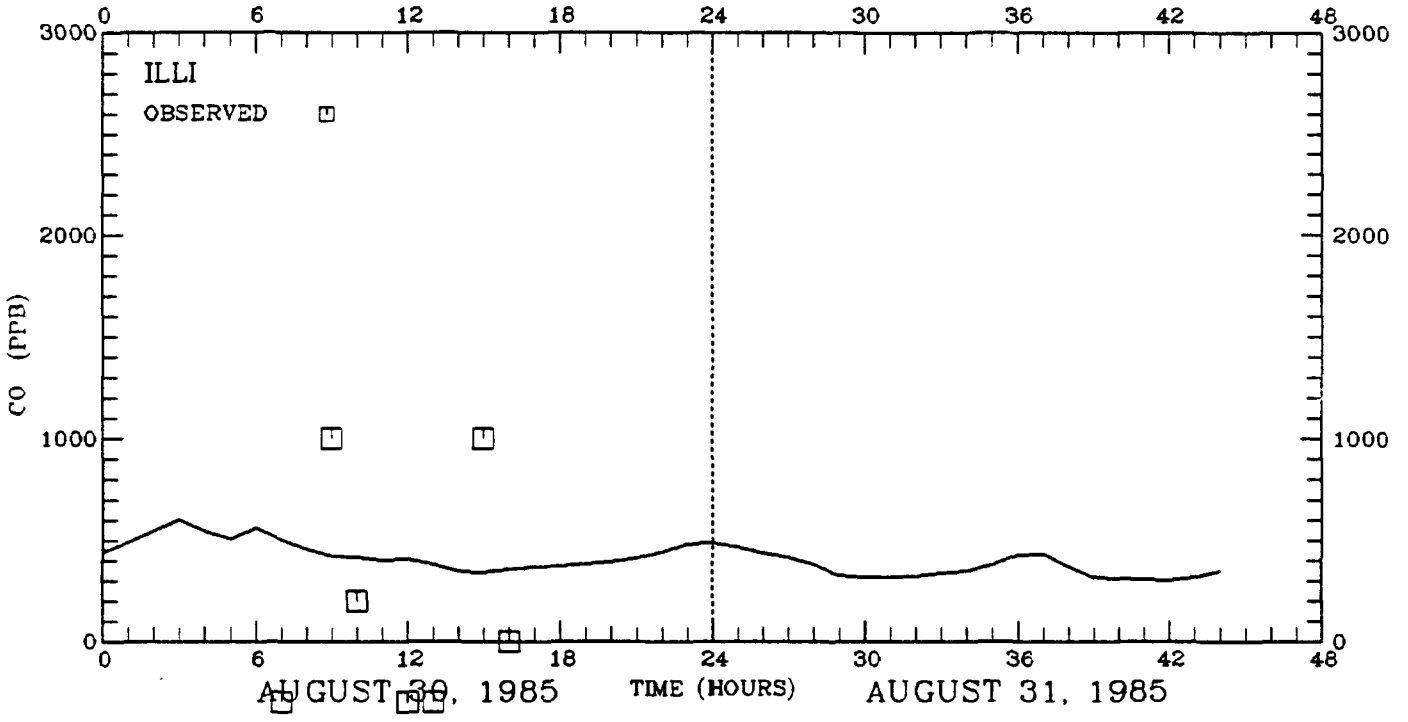

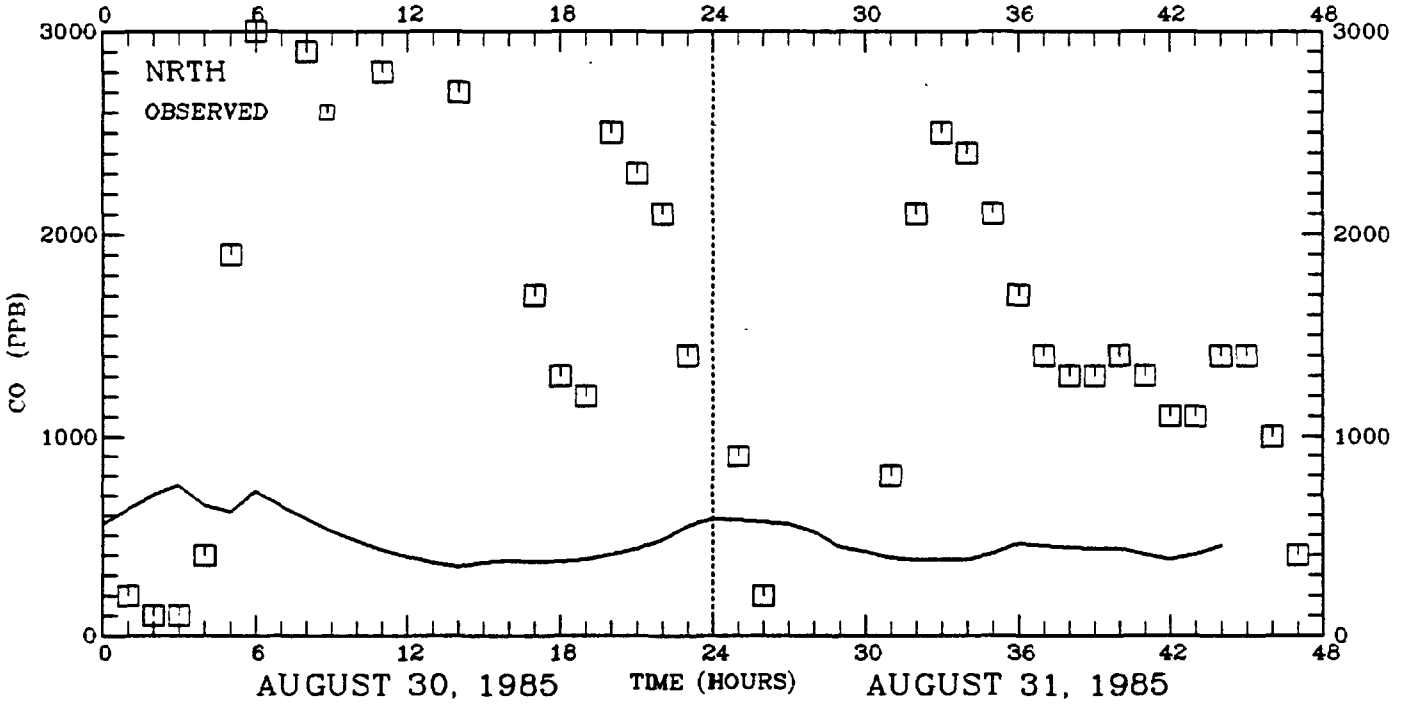

FIGURE 4-21. Continued.

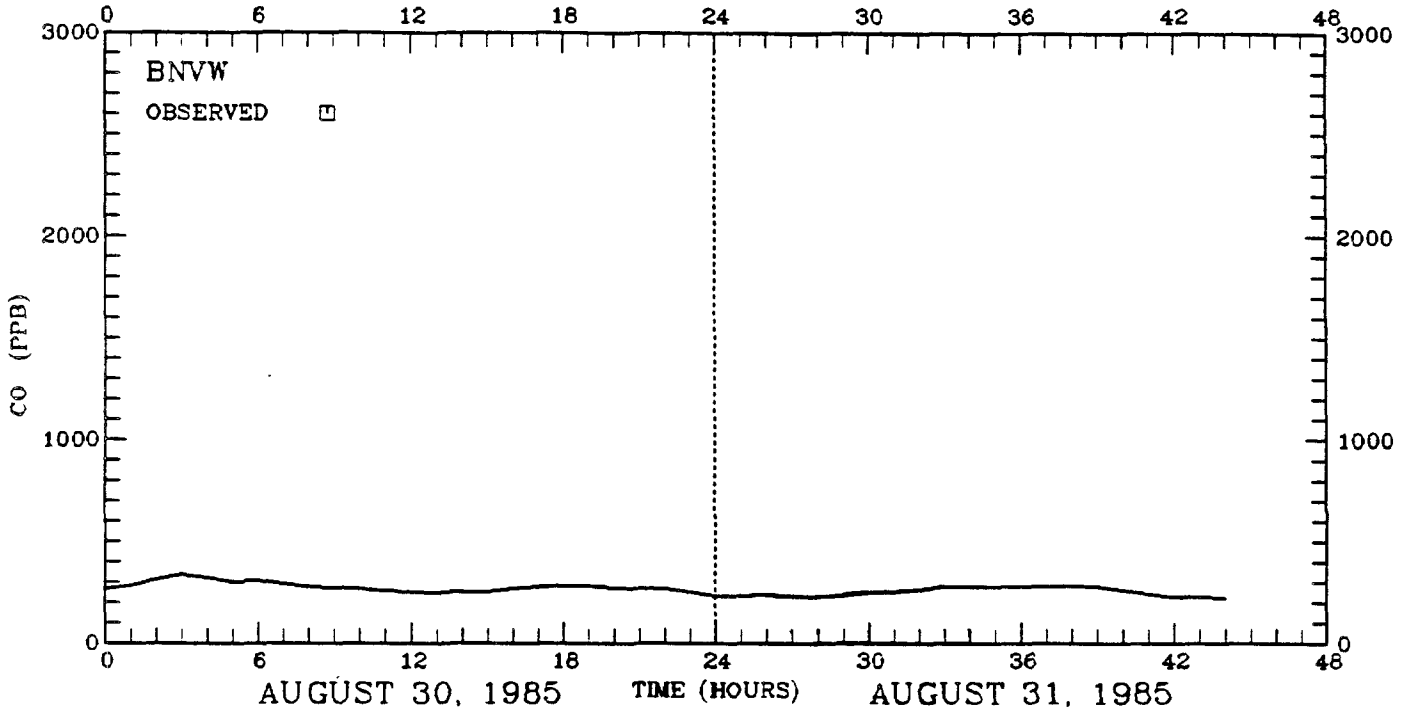

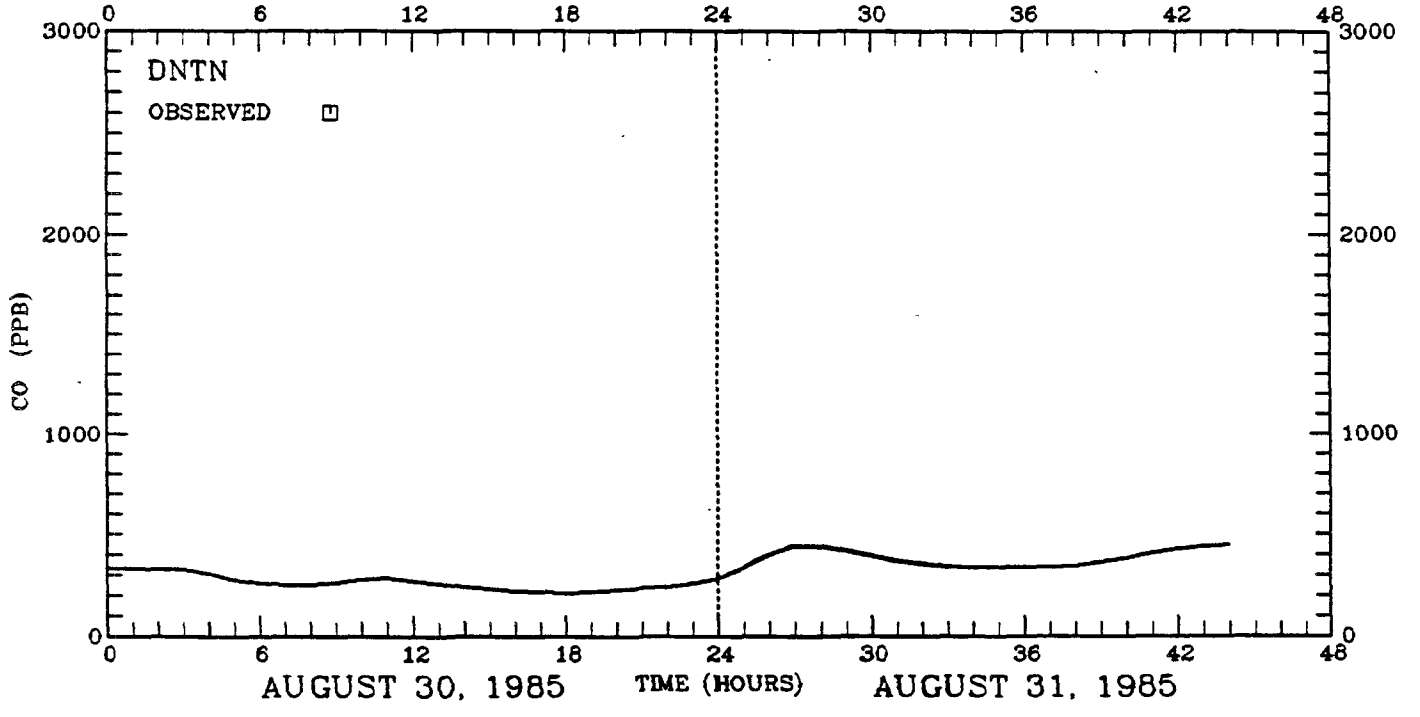

FIGURE 4-21. Continued.

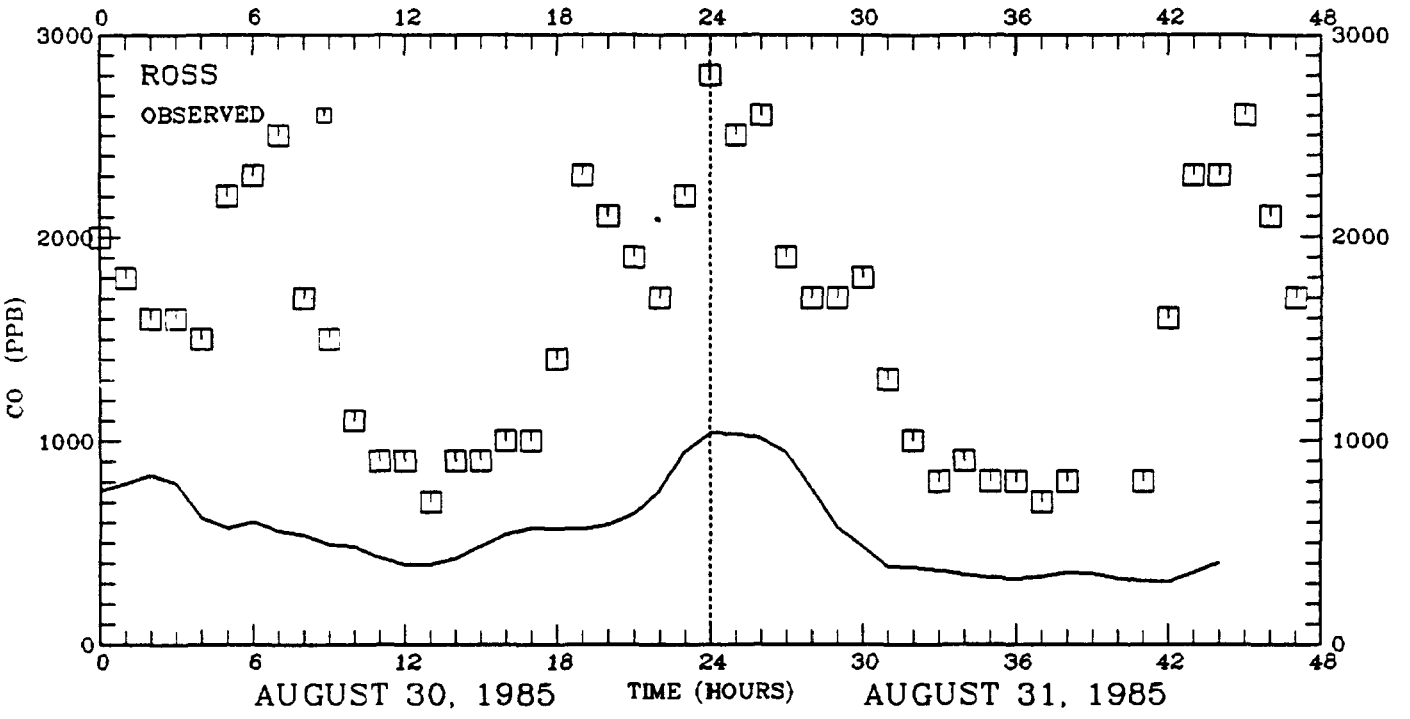

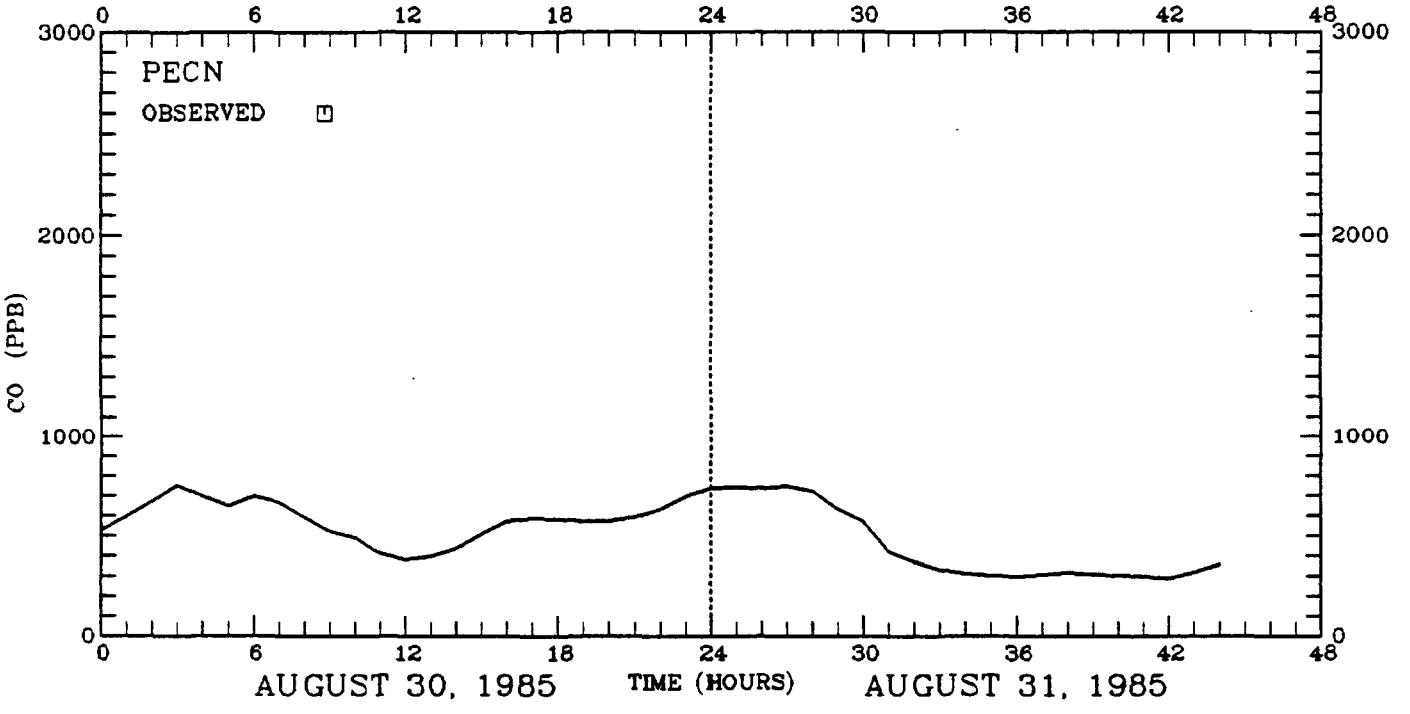

FIGURE 4-21. Continued.

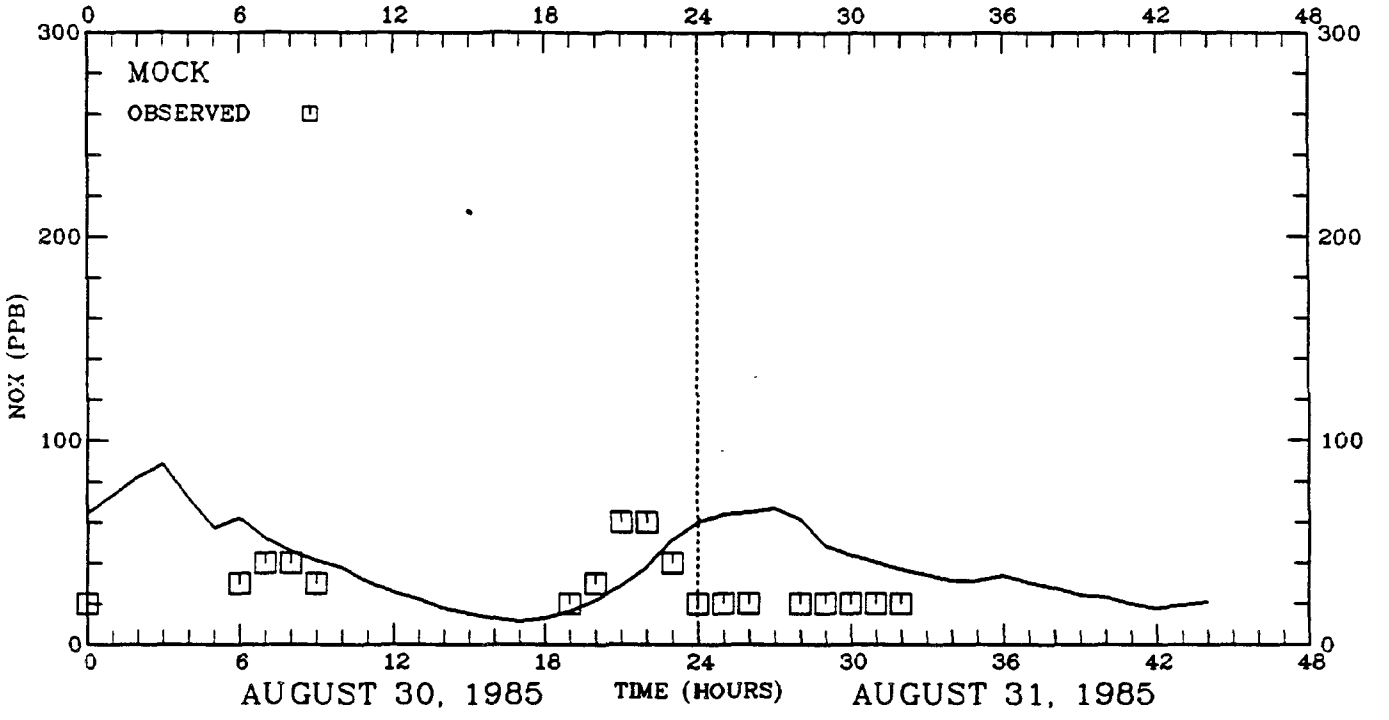

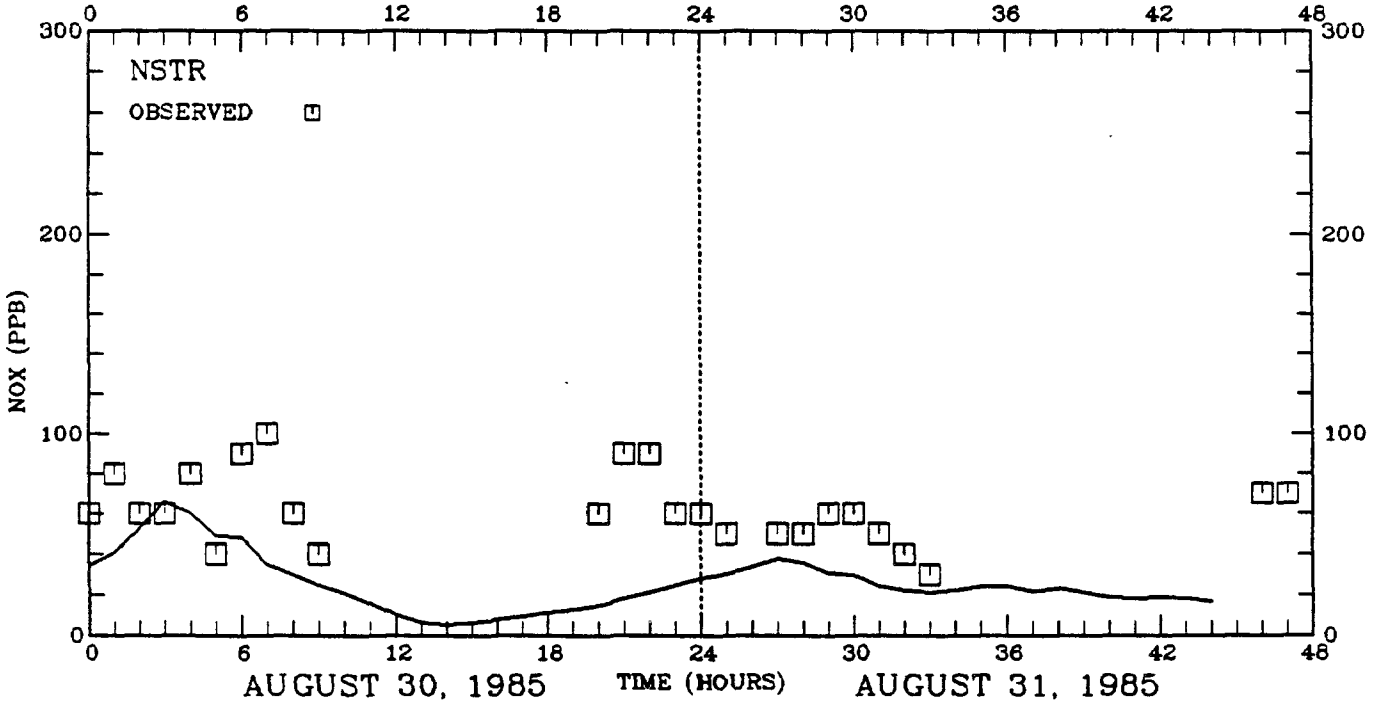

FIGURE 4-21. Continued.

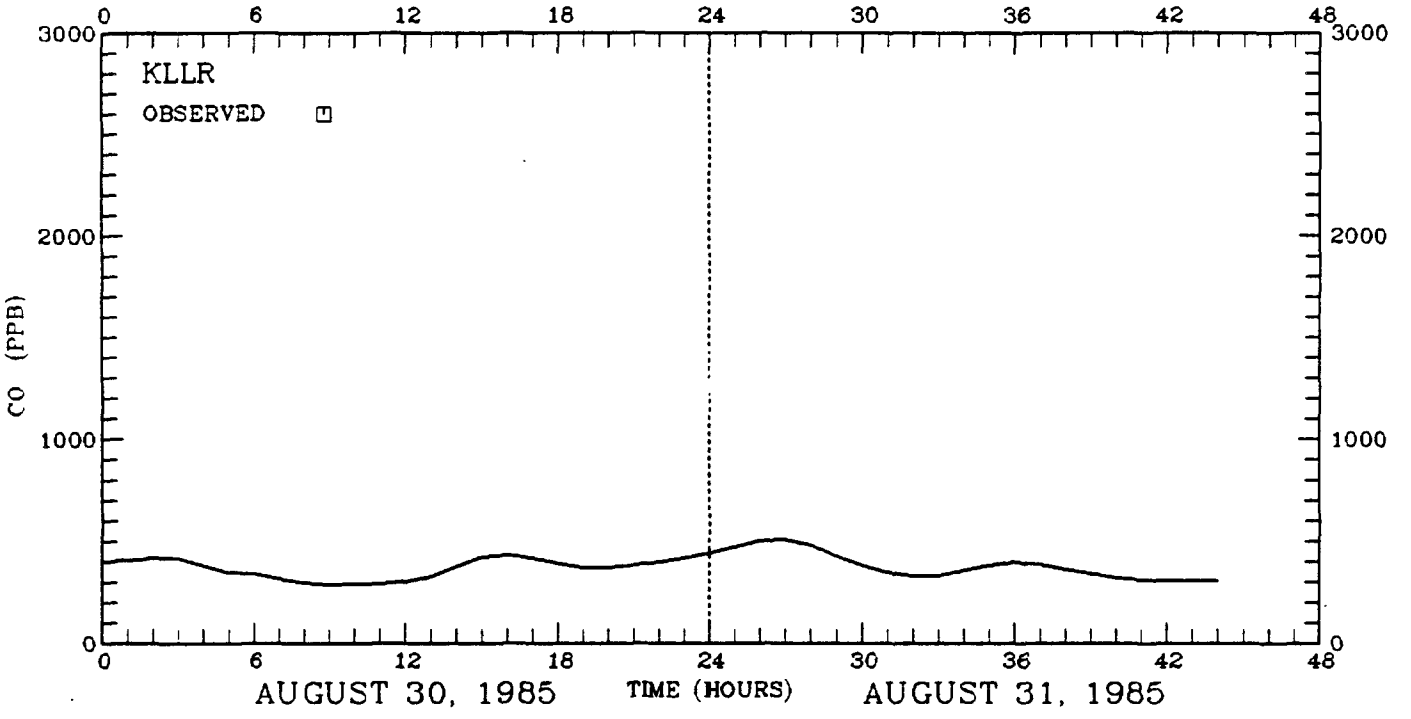

FIGURE 4-21. Concluded.

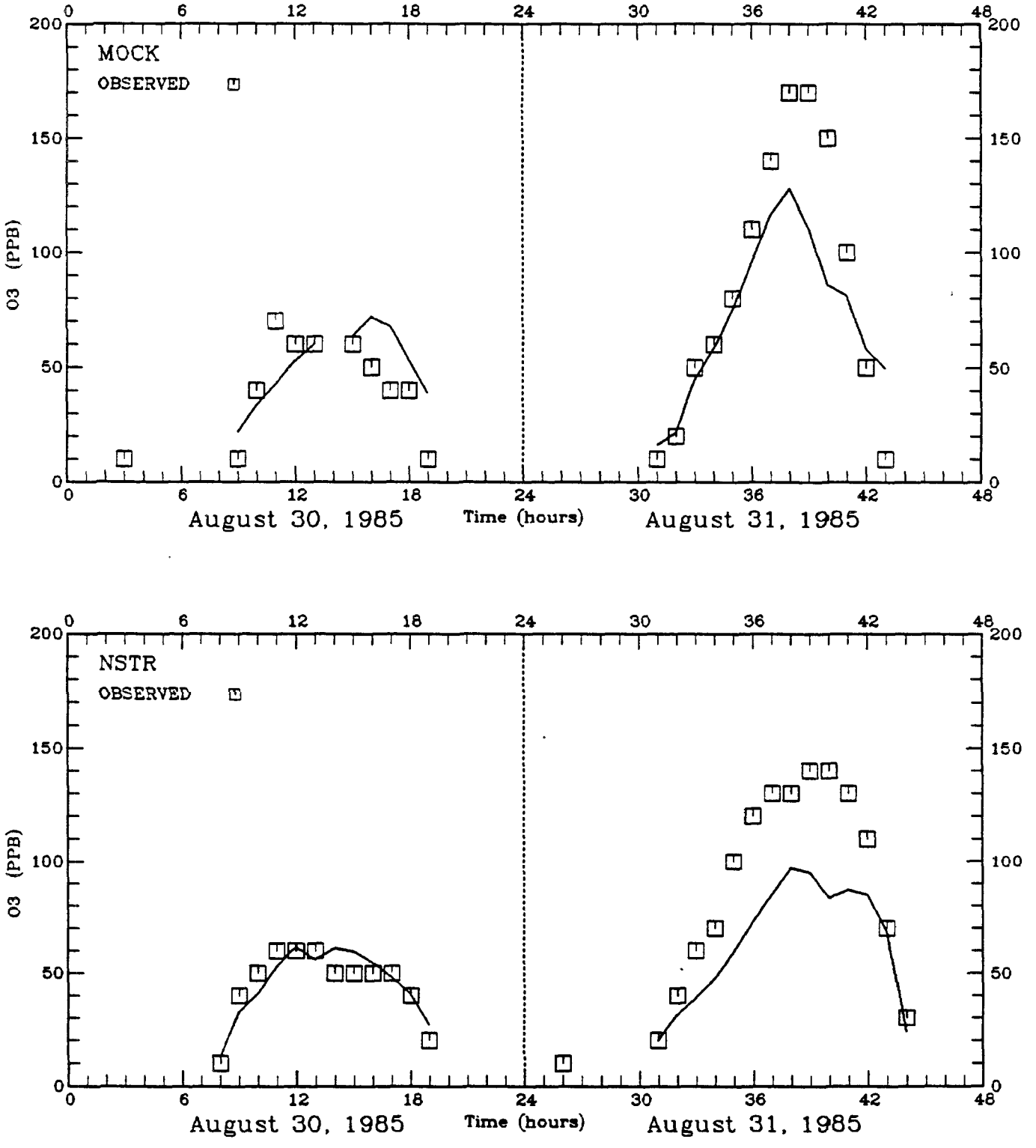

FIGURE 4-22. Time series of predicted and observed hourly ozone concentrations for the Dallas-Fort Worth diagnostic run 2 using a one-cell search nearest neighbor analysis.

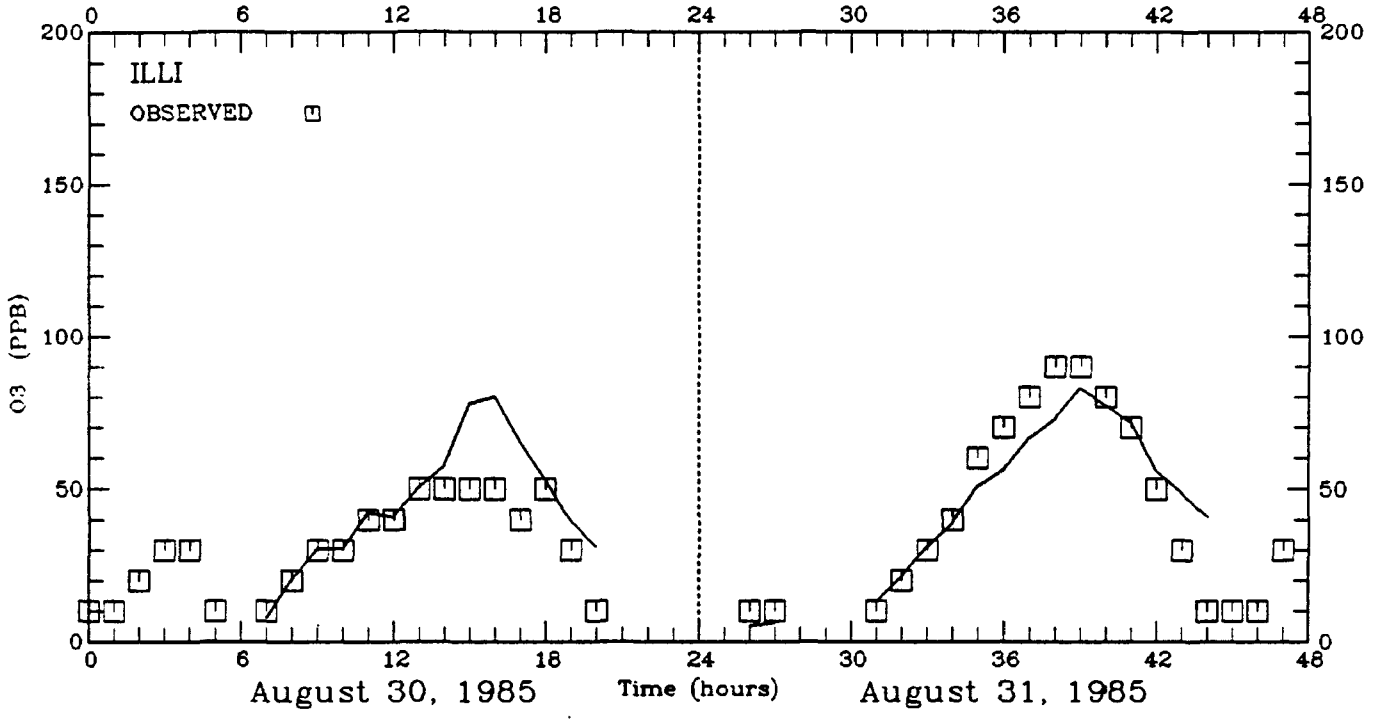

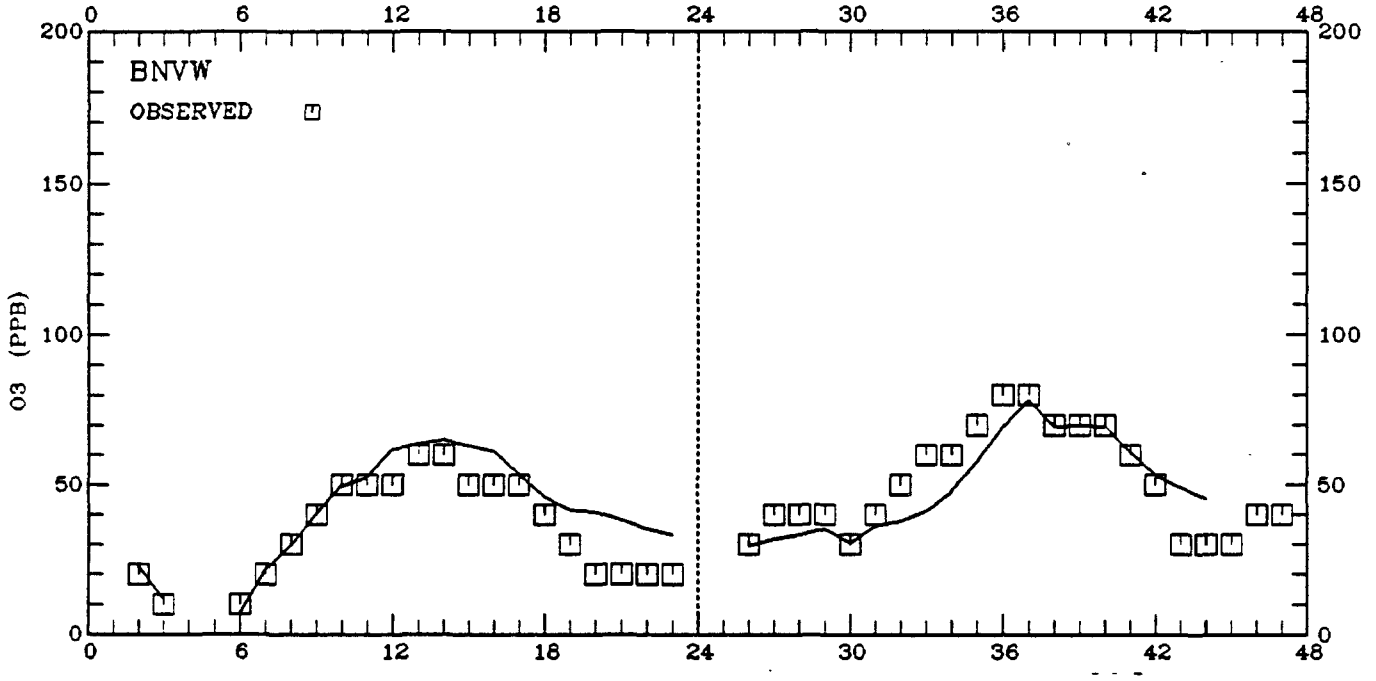

FIGURE 4-22. Continued.

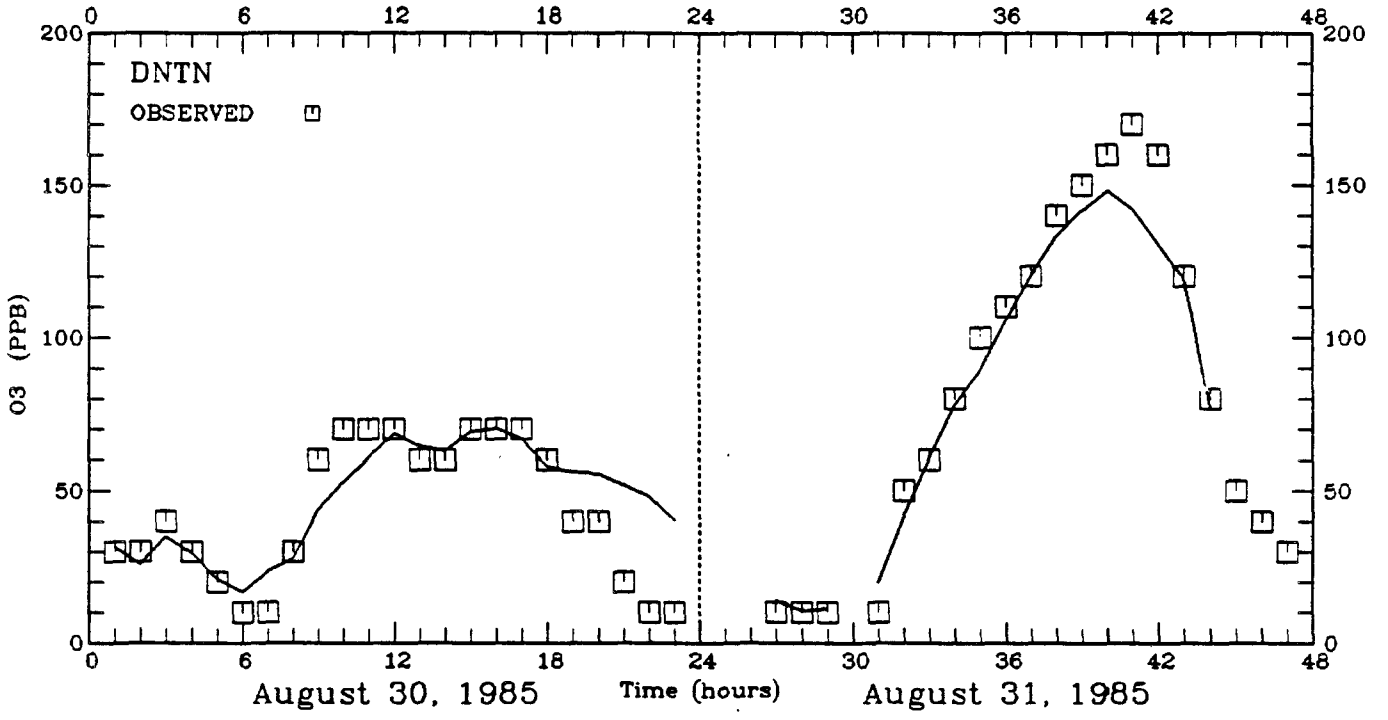

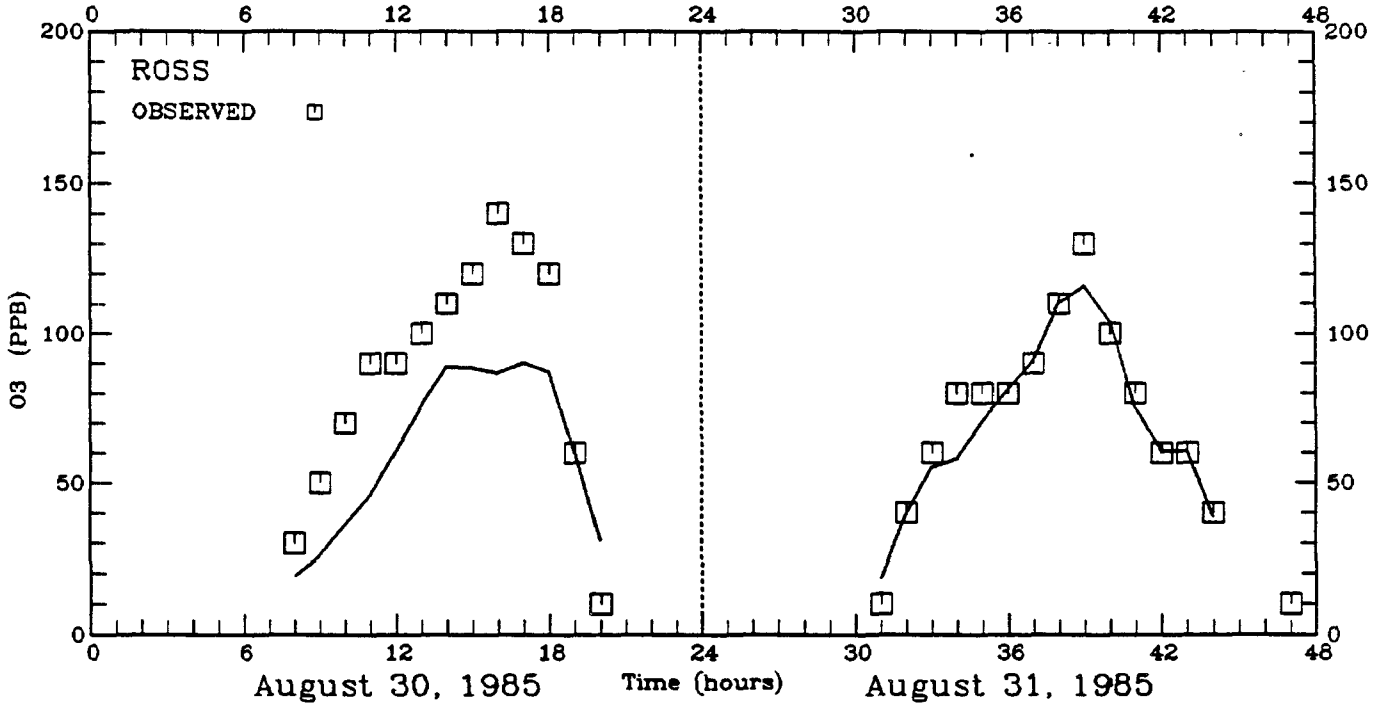

FIGURE 4-22. Continued.

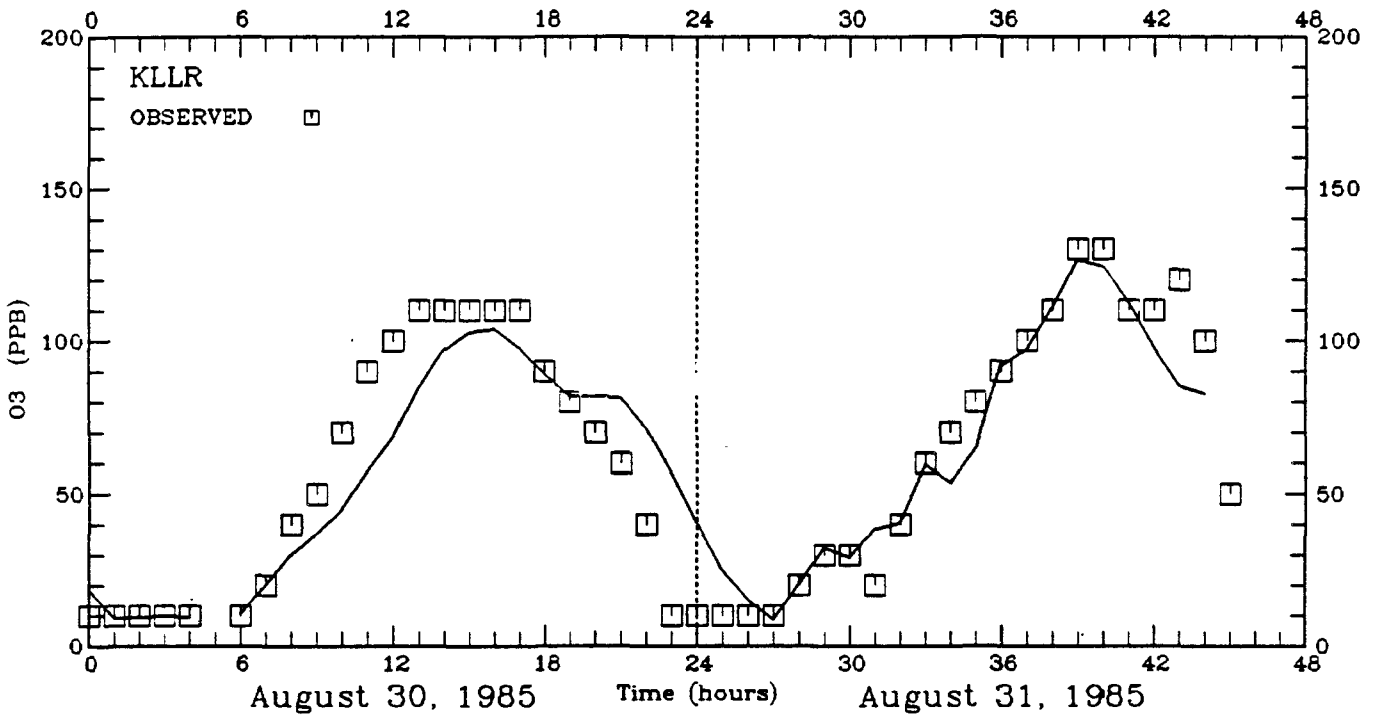

FIGURE 4-22. Concluded.

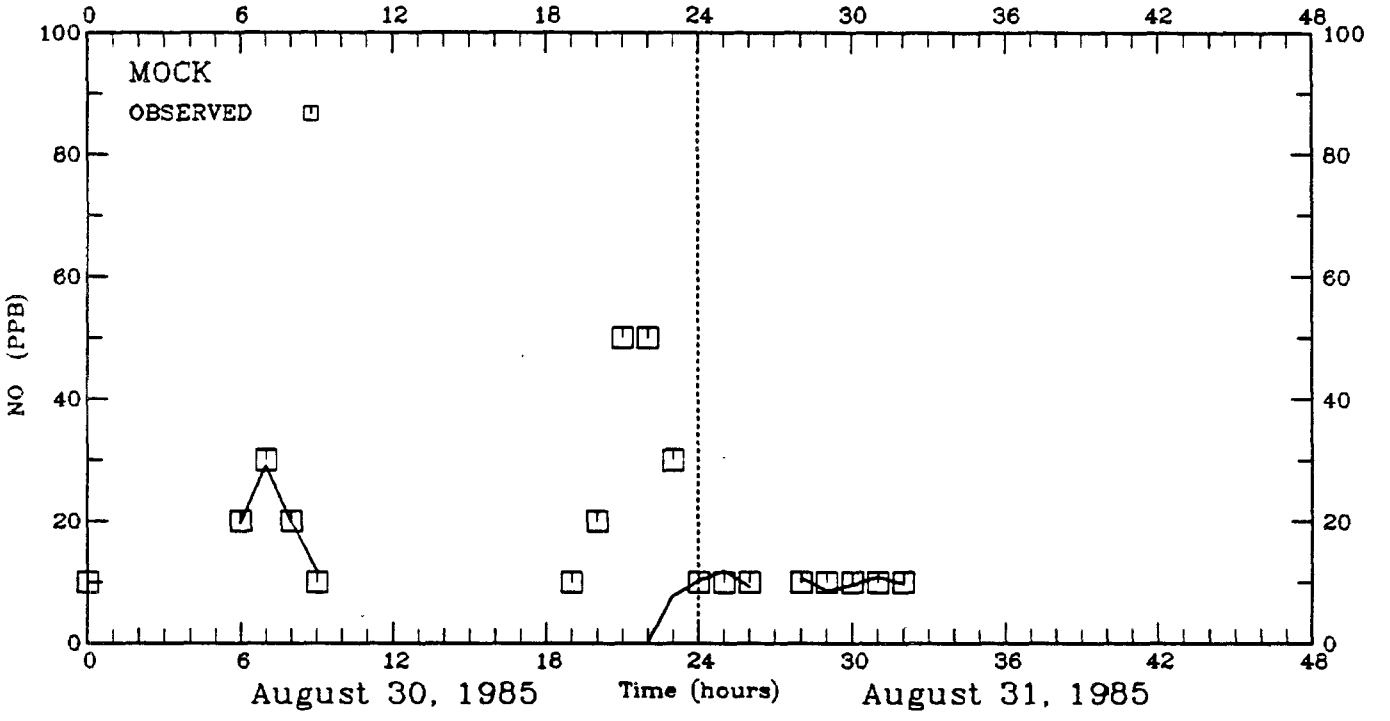

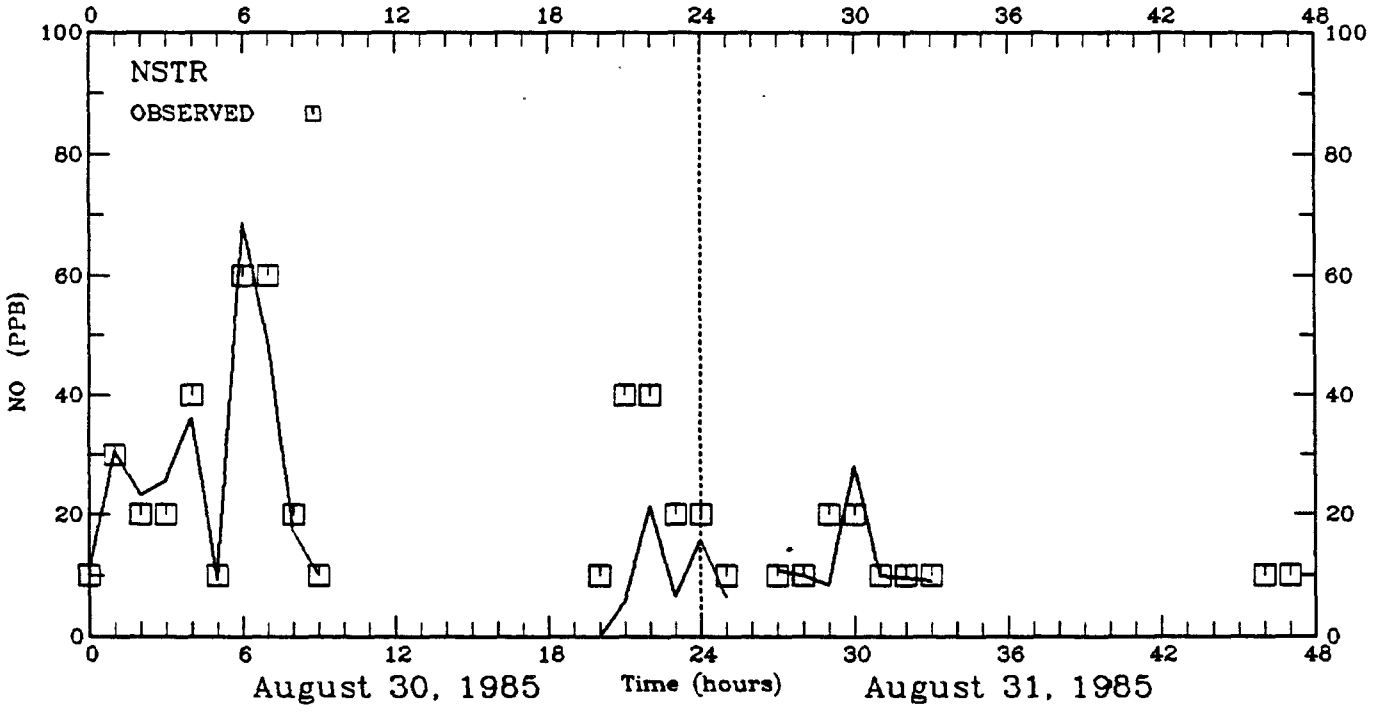

FIGURE 4-23. Time series of predicted and observed hourly NO concentrations (ppb) for the Dallas-Fort Worth diagnostic run 2 using a one-cell search nearest neighbor analysis.

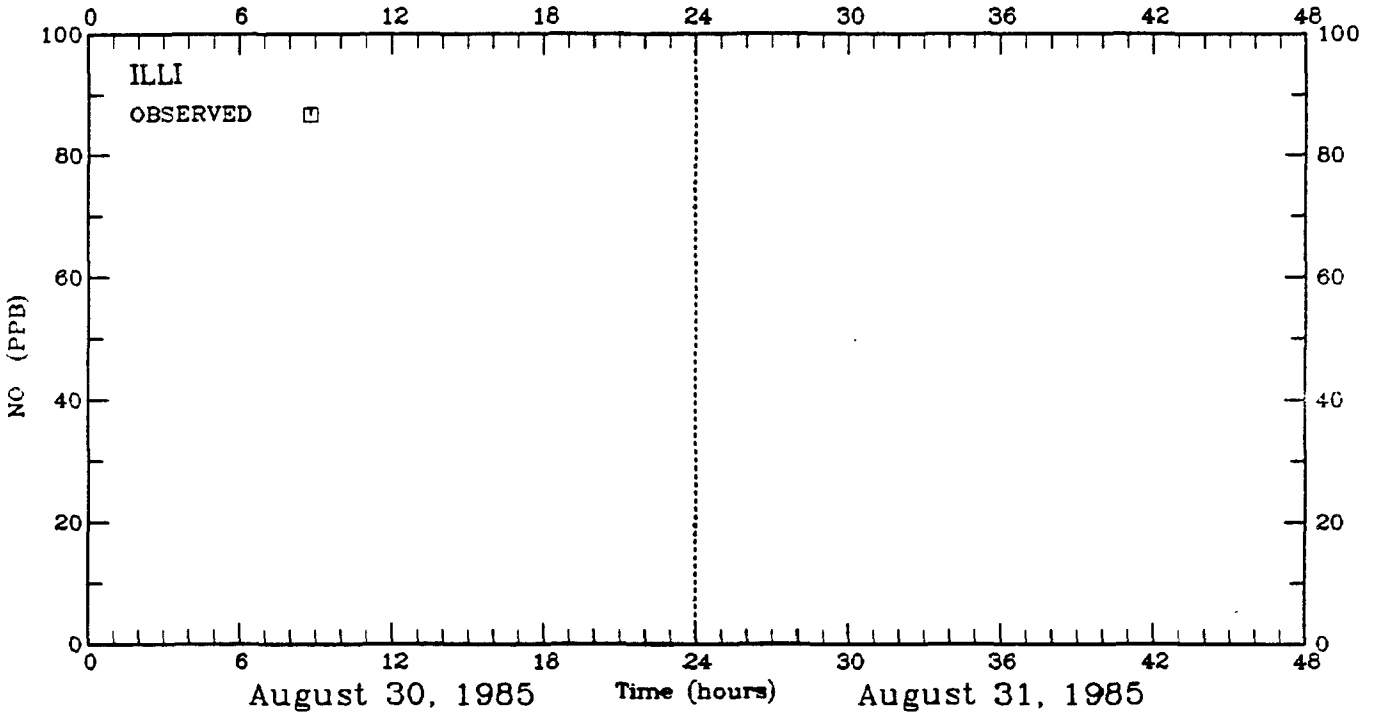

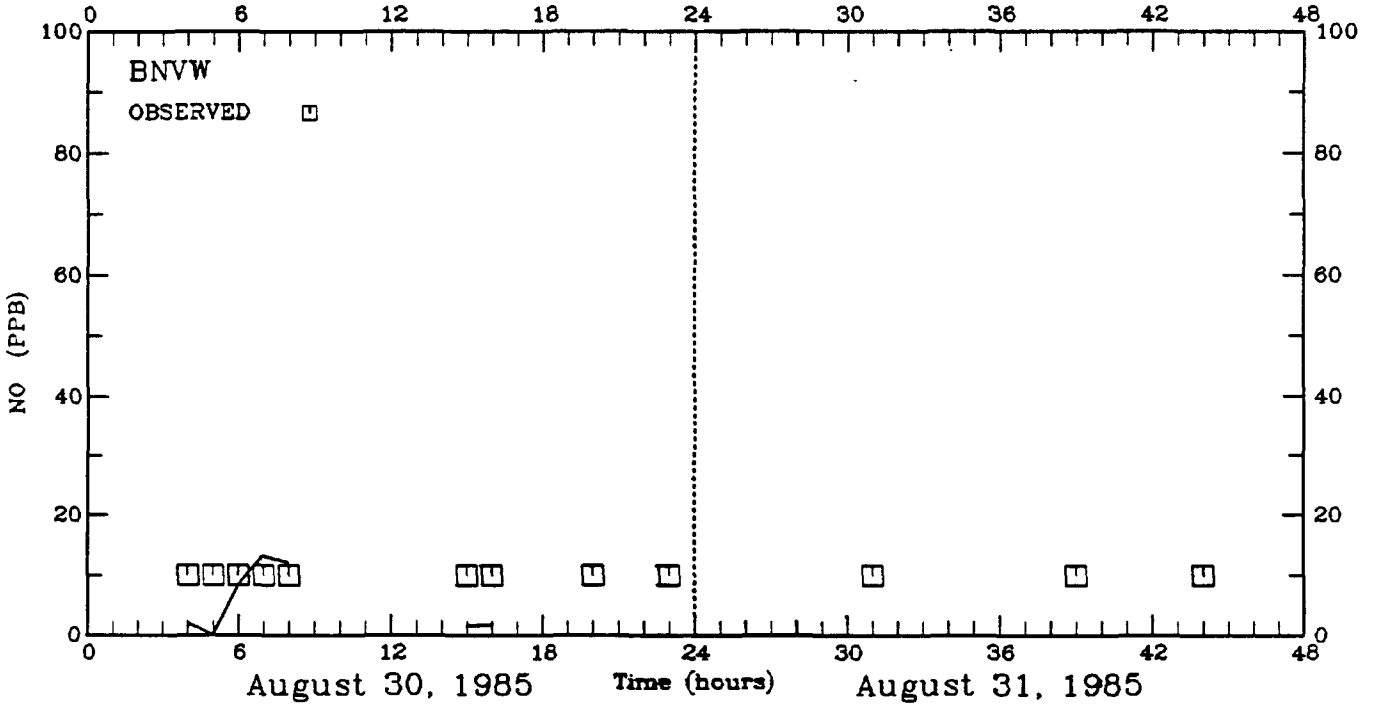

FIGURE 4-23. Continued.

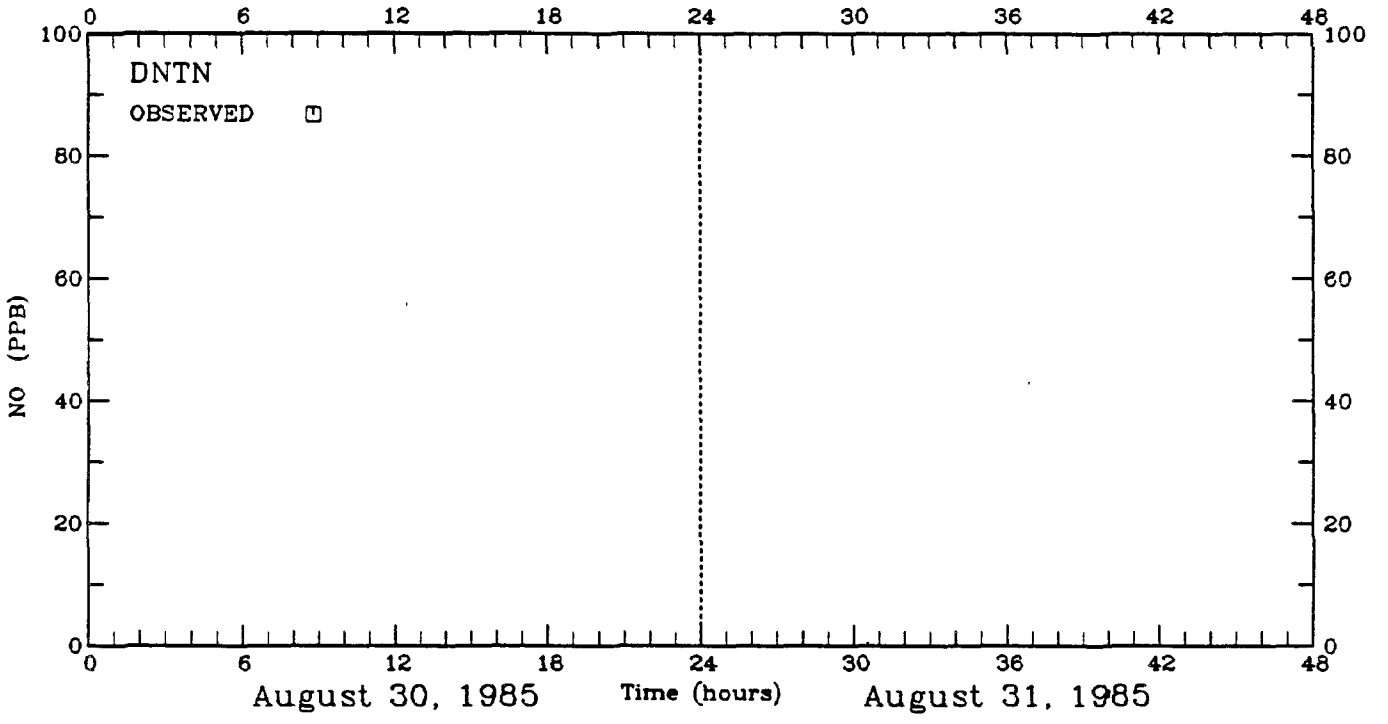

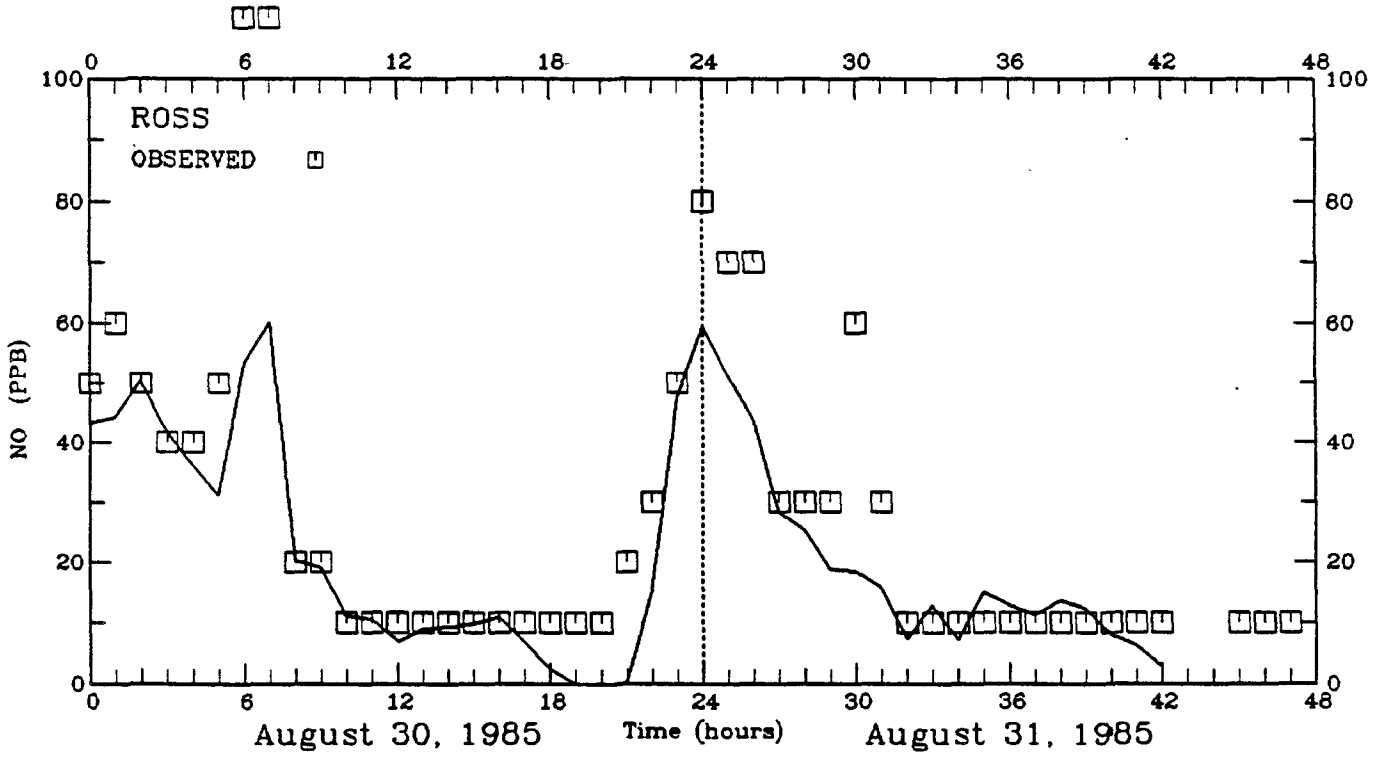

FIGURE 4-23. Concluded.

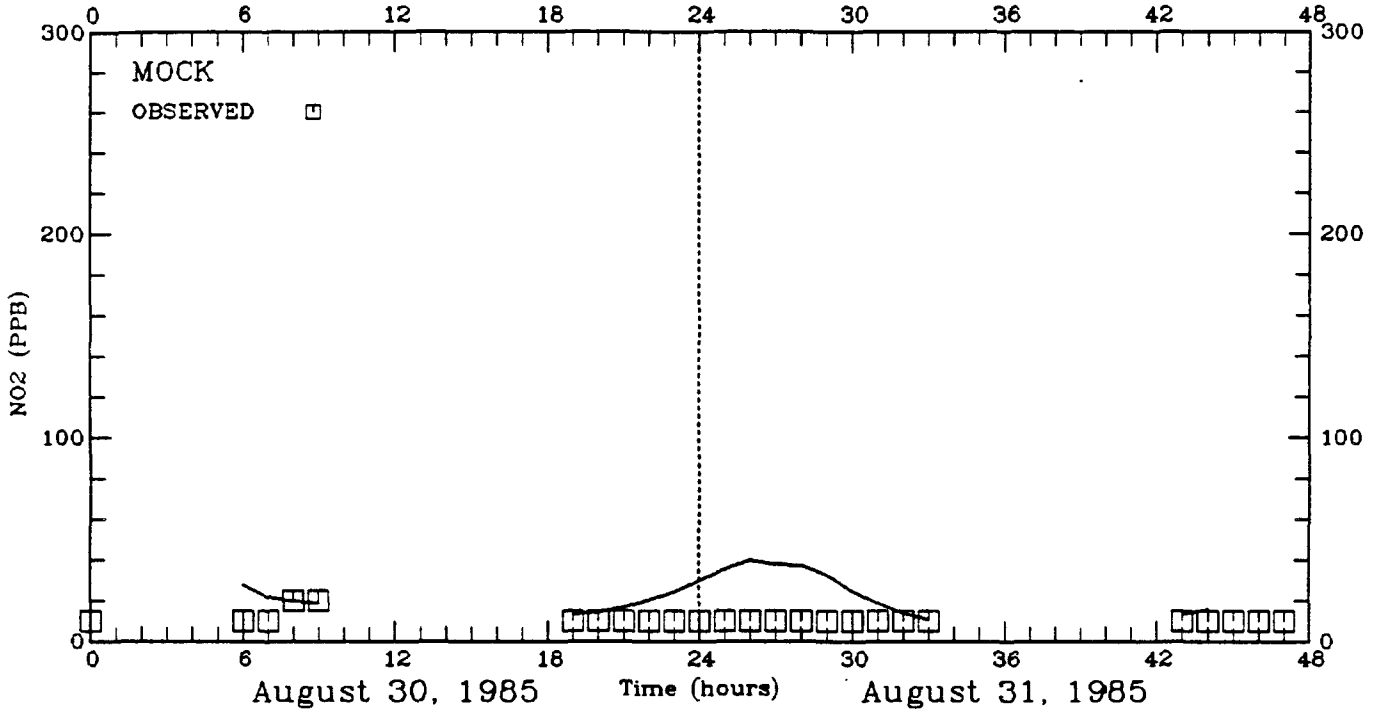

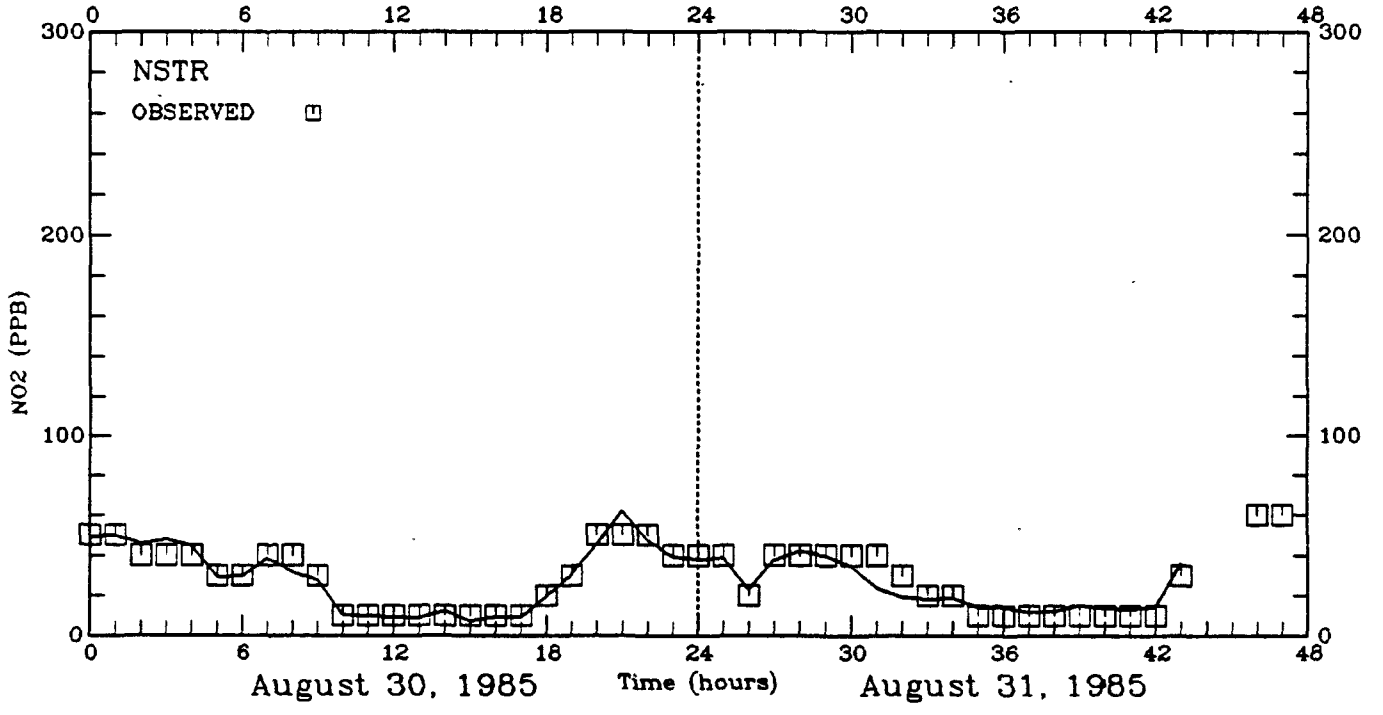

FIGURE 4-24. Time series of predicted and observed hourly NO_2 concentrations (ppb) for the Dallas-Fort Worth diagnostic run 2 using a one-cell search nearest neighbor analysis.

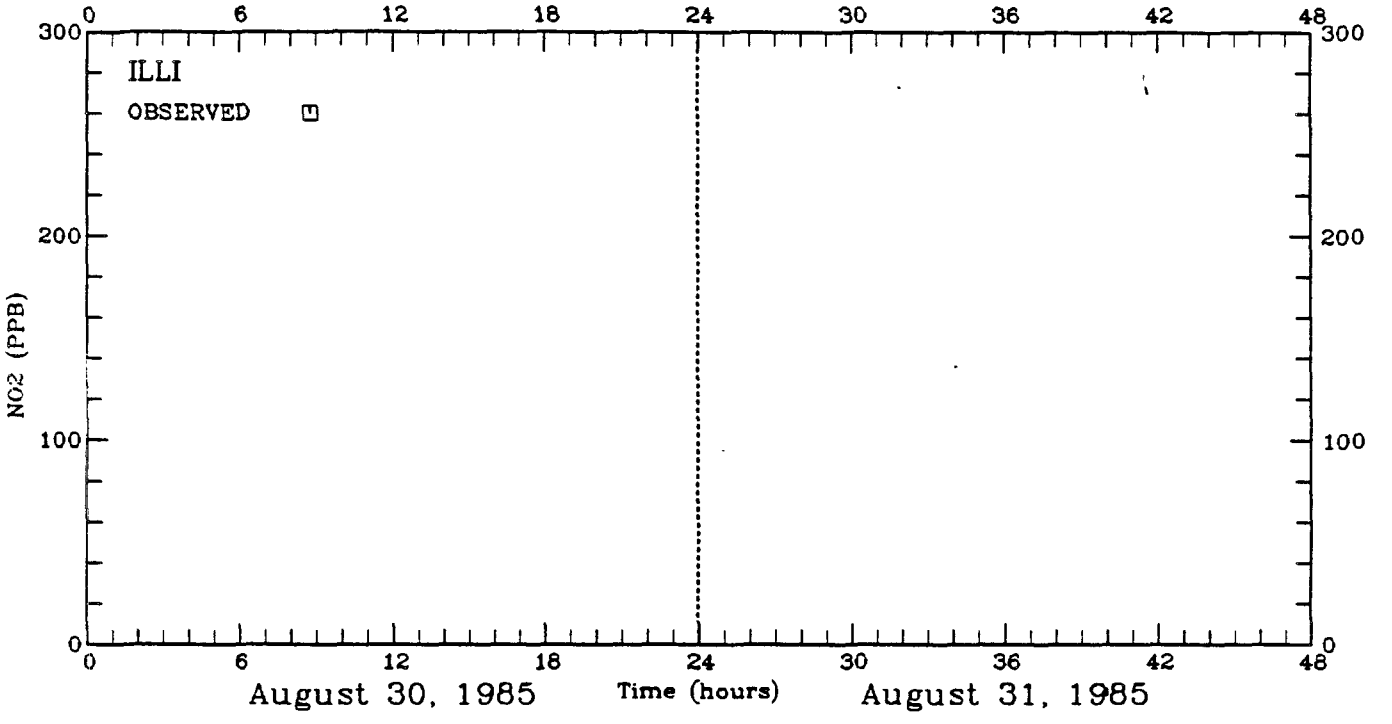

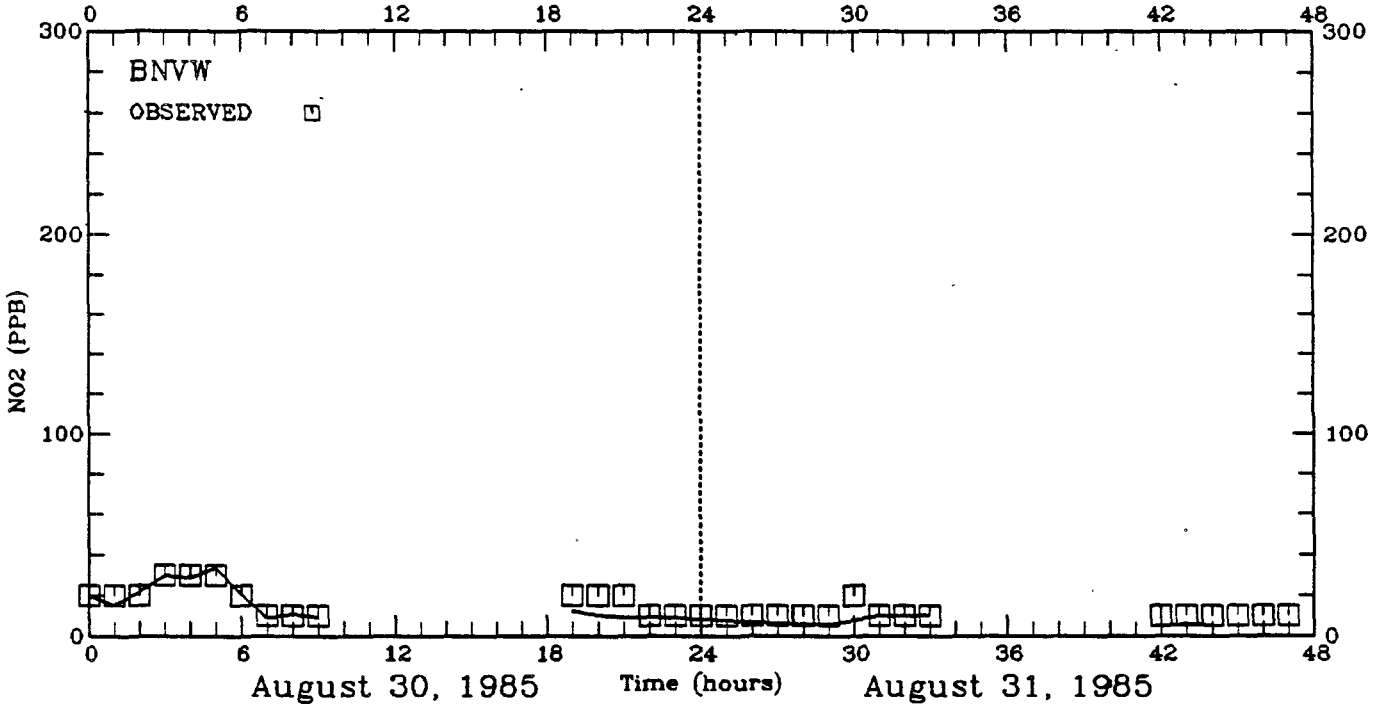

FIGURE 4-24. Continued.

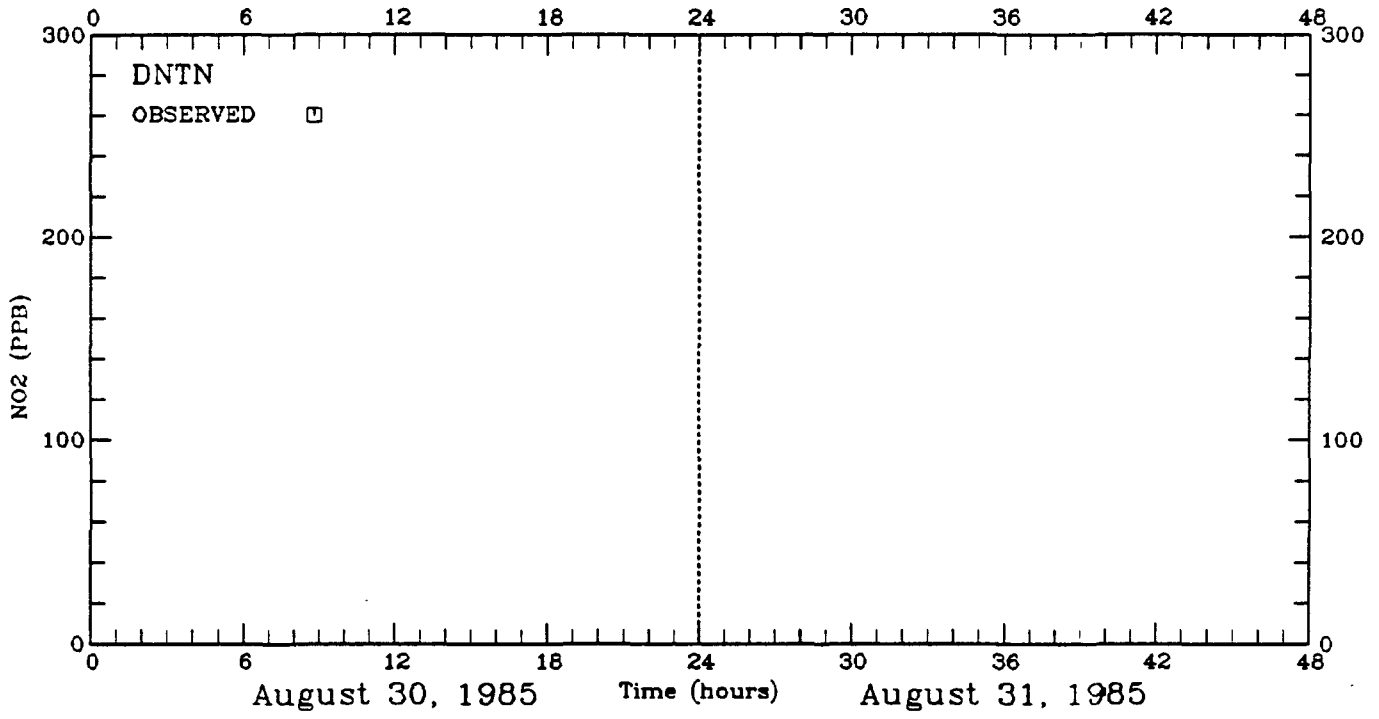

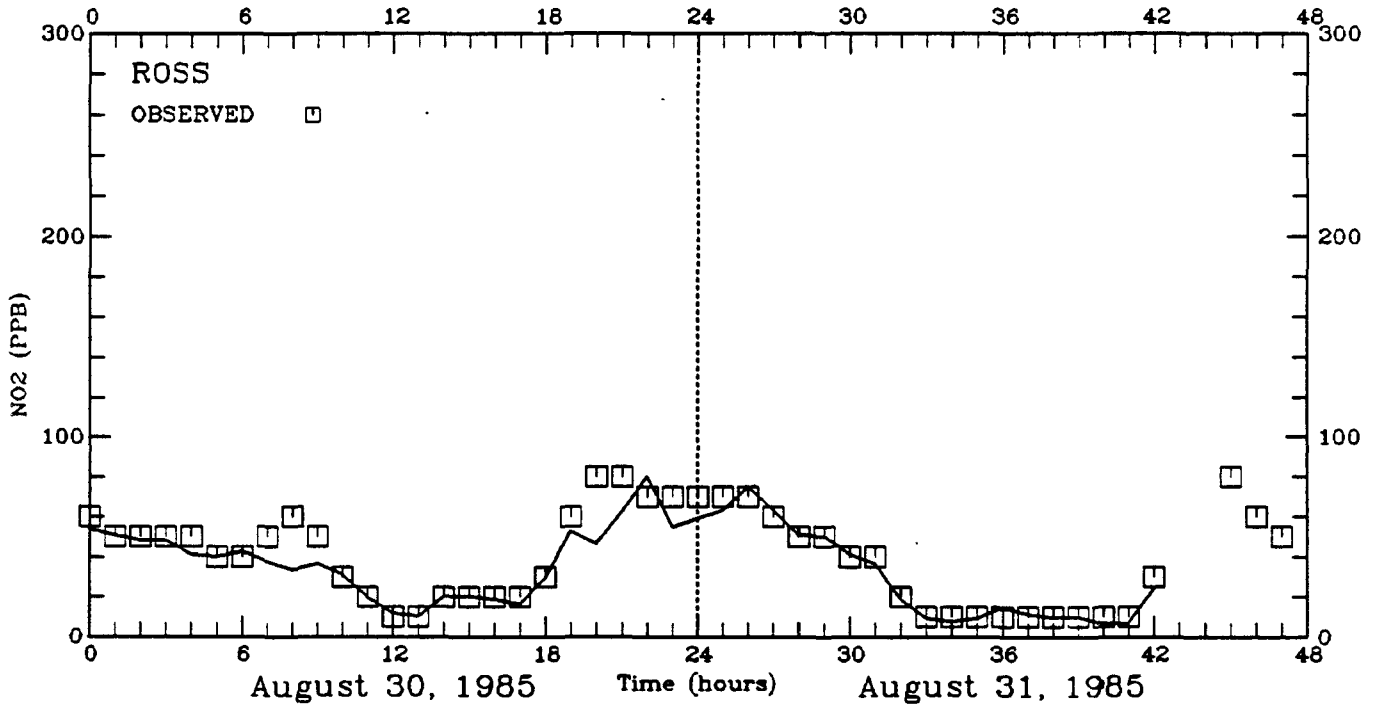

FIGURE 4-24. Concluded.

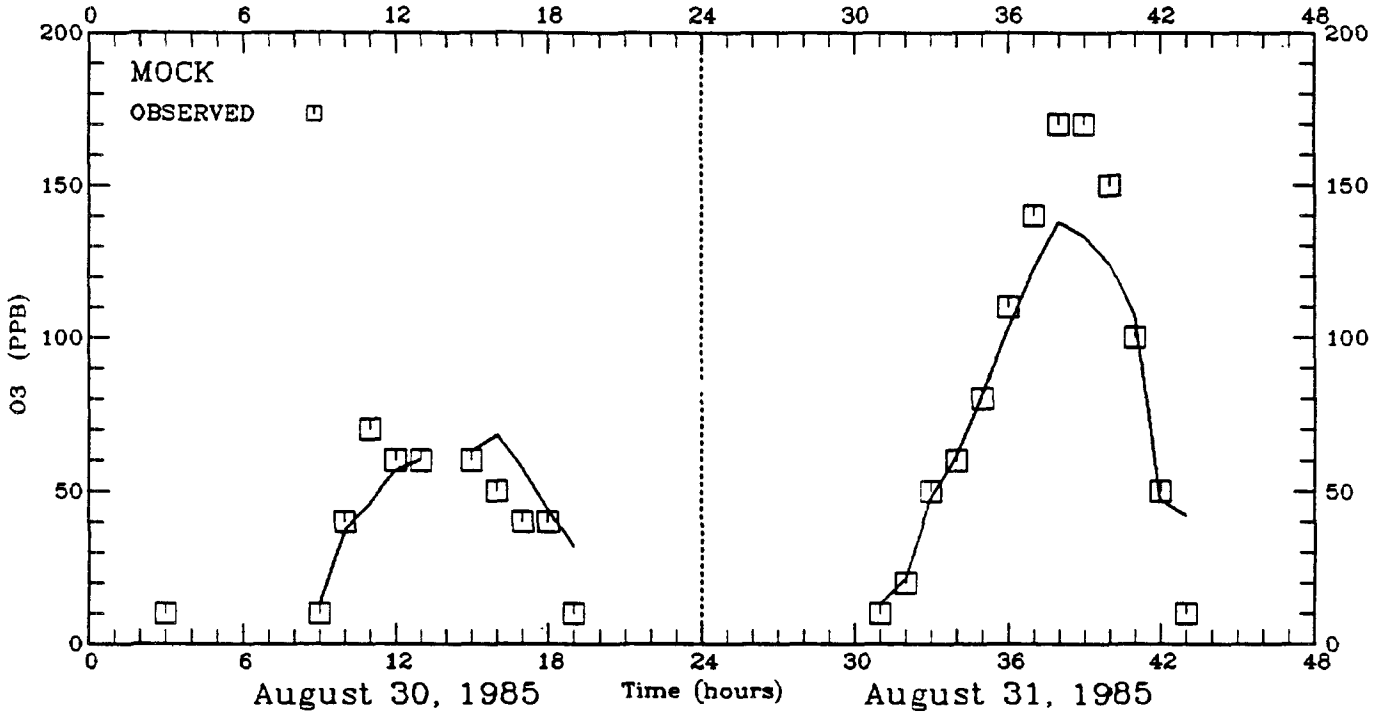

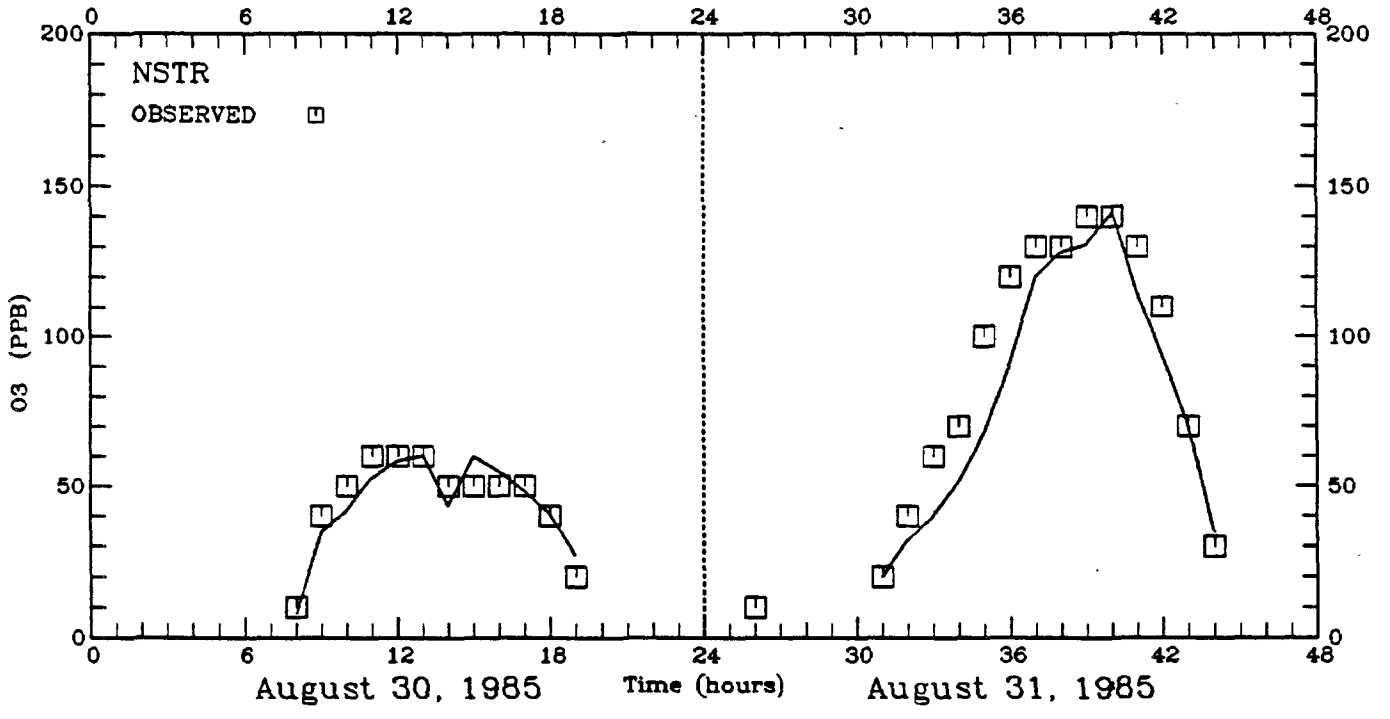

FIGURE 4-25. Time series of predicted and observed hourly ozone concentrations for the Dallas-Fort Worth diagnostic run 2 using a two-cell search nearest neighbor analysis.

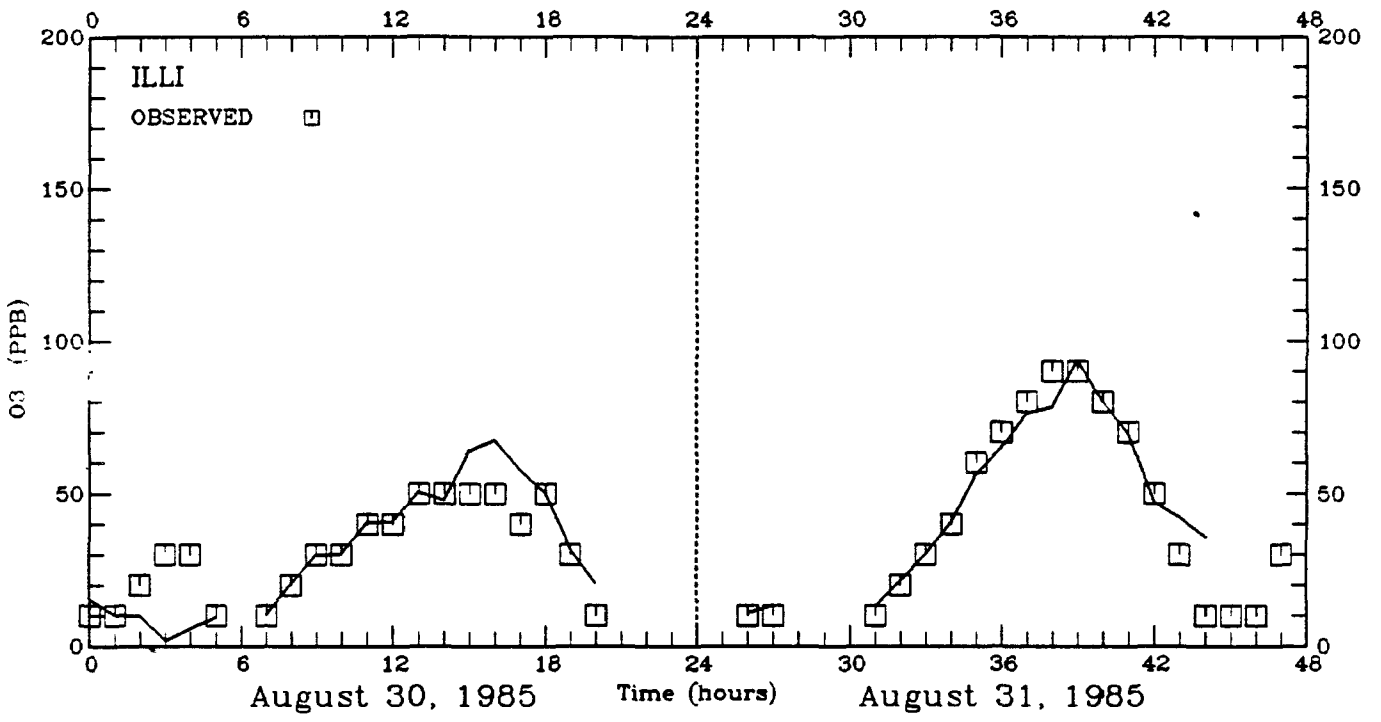

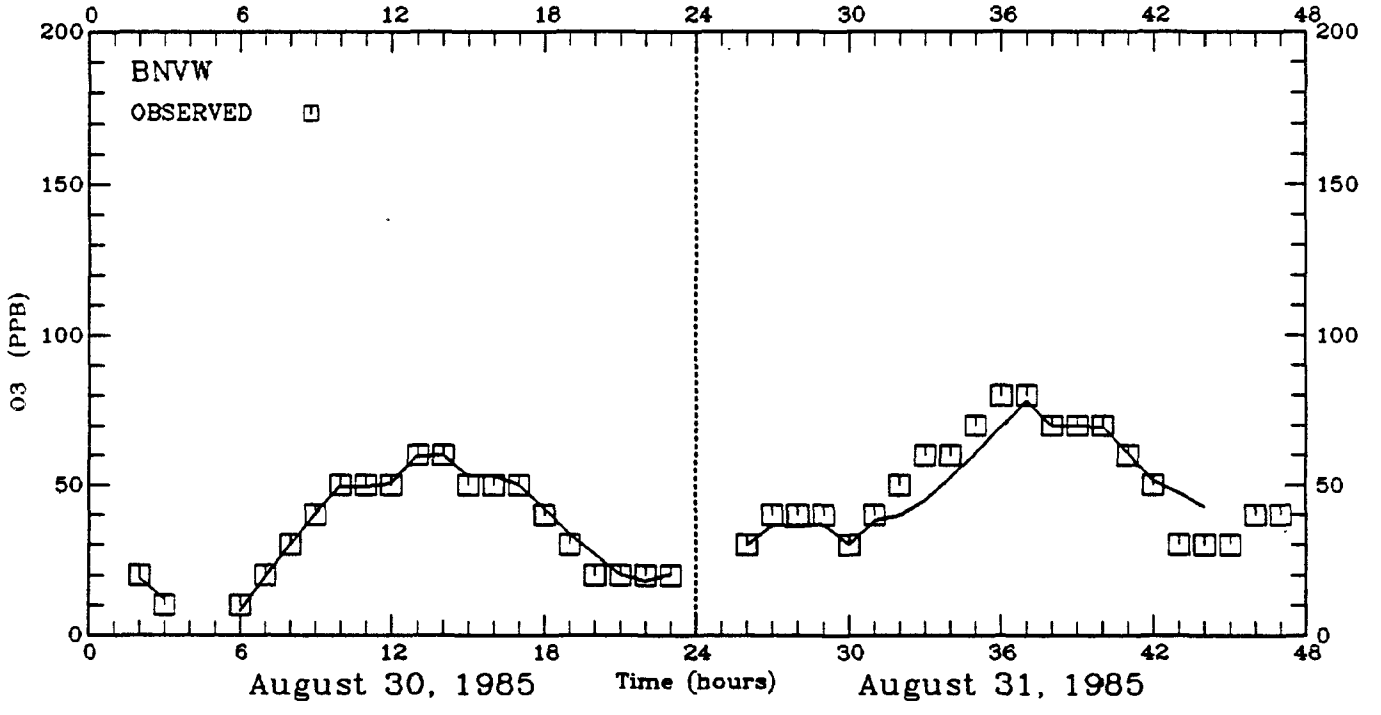

FIGURE 4-25. Continued.

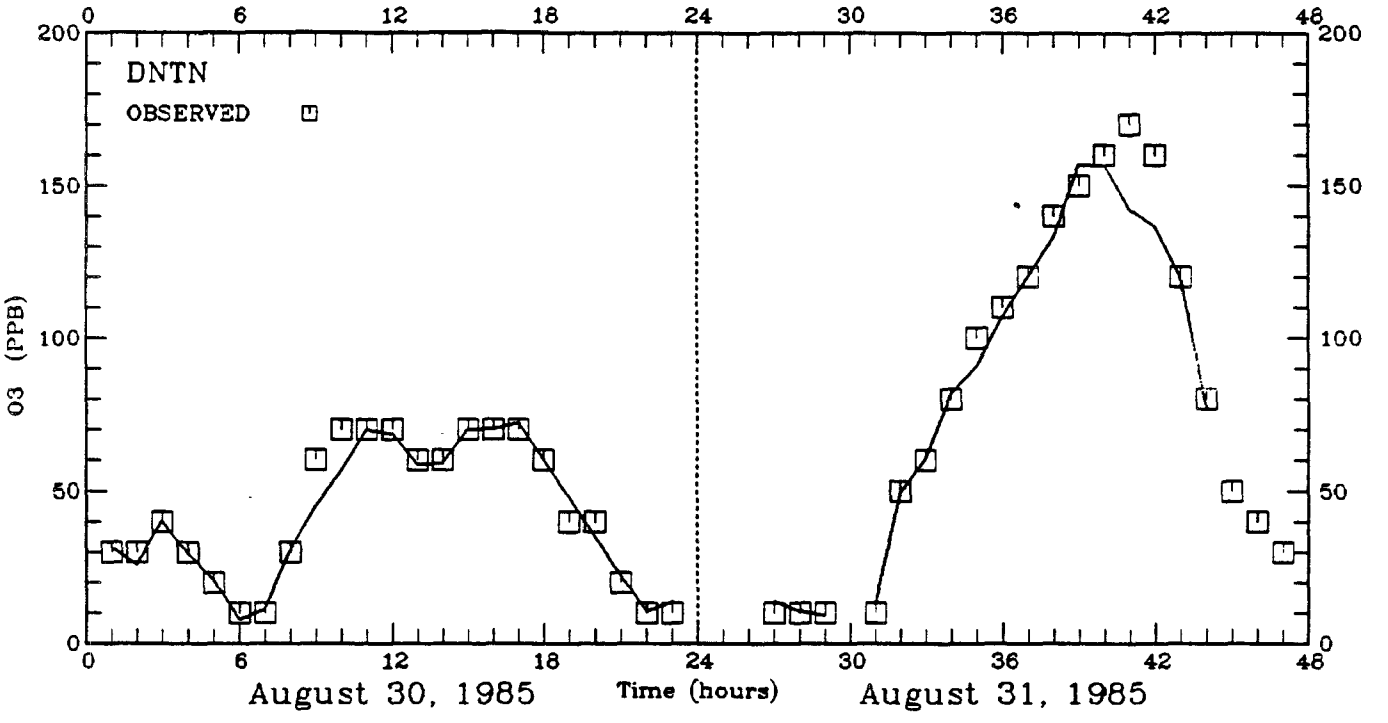

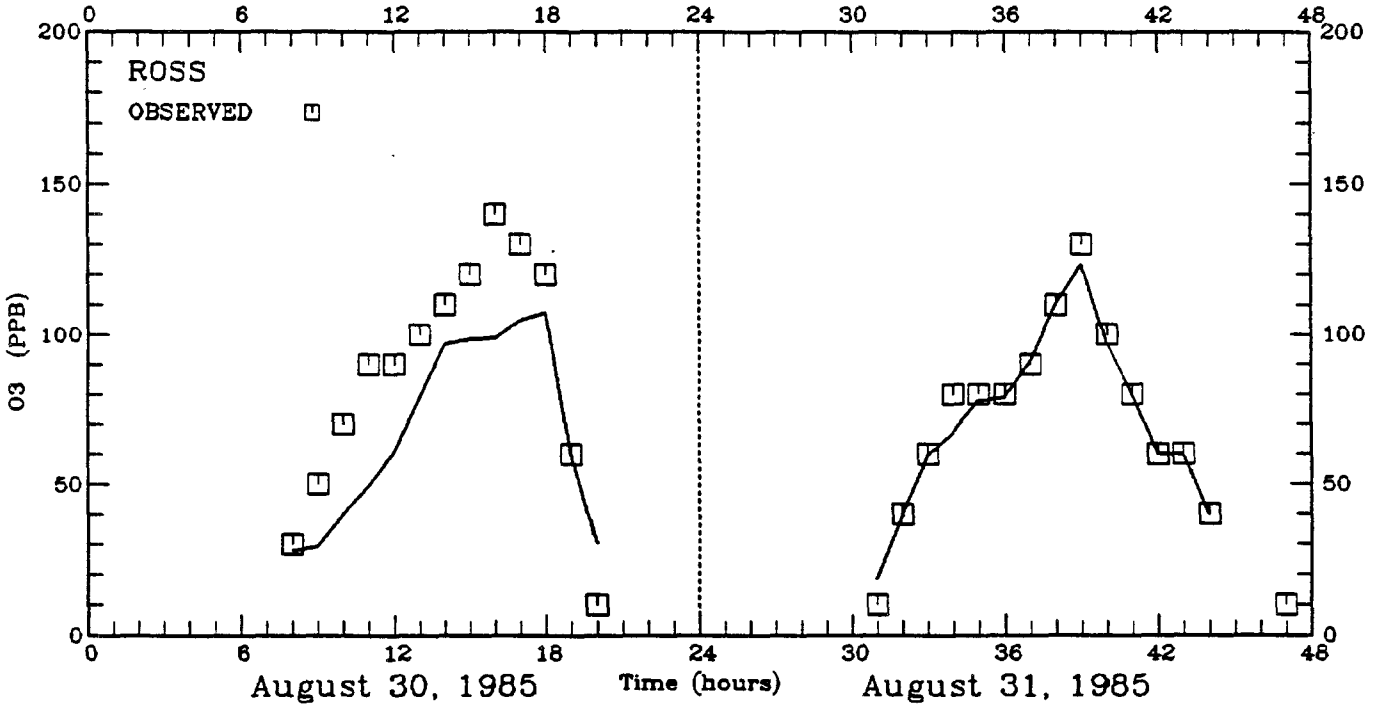

FIGURE 4-25. Continued.

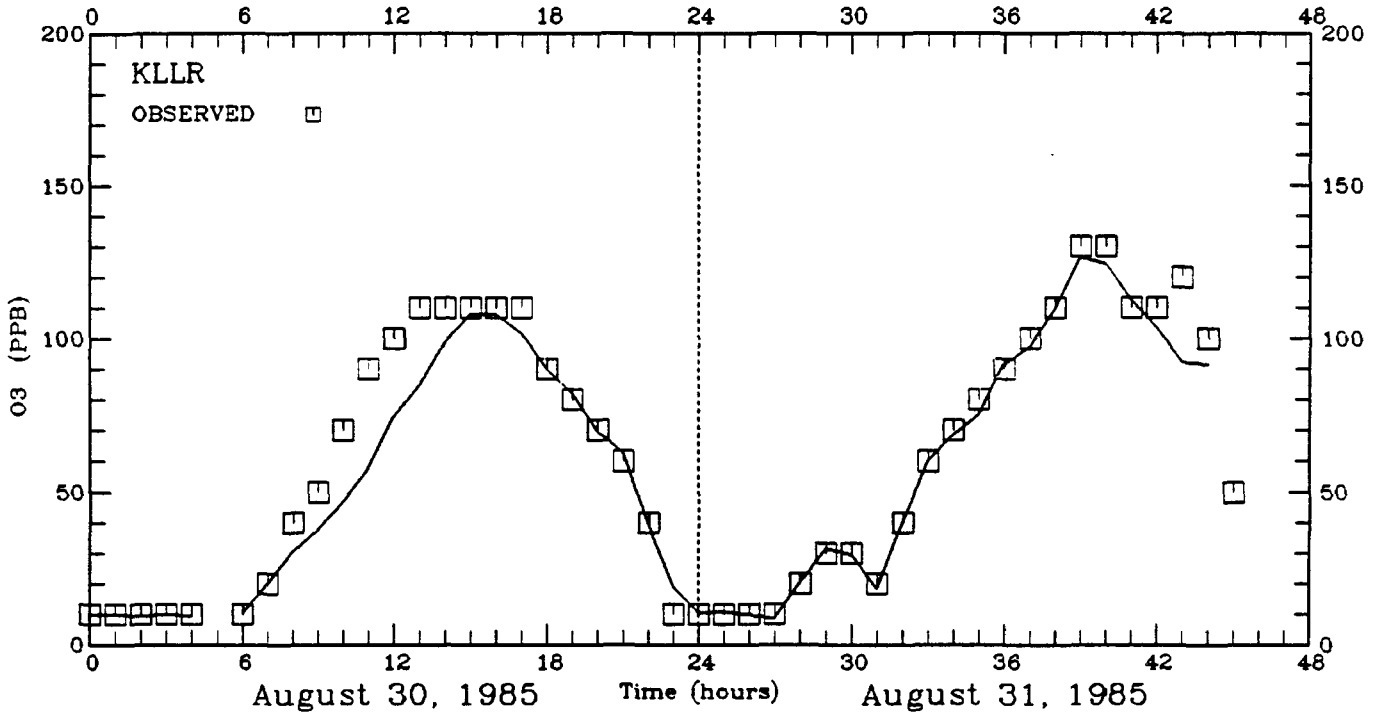

FIGURE 4-25. Concluded.

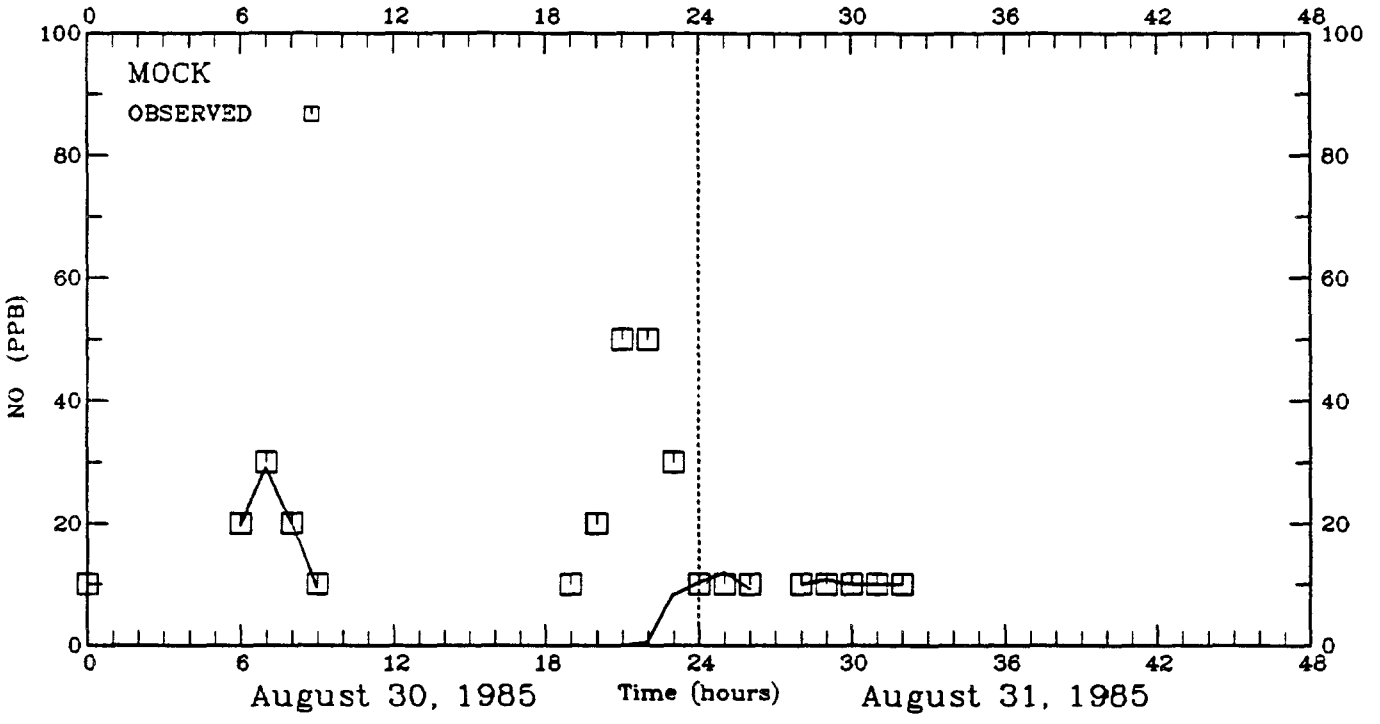

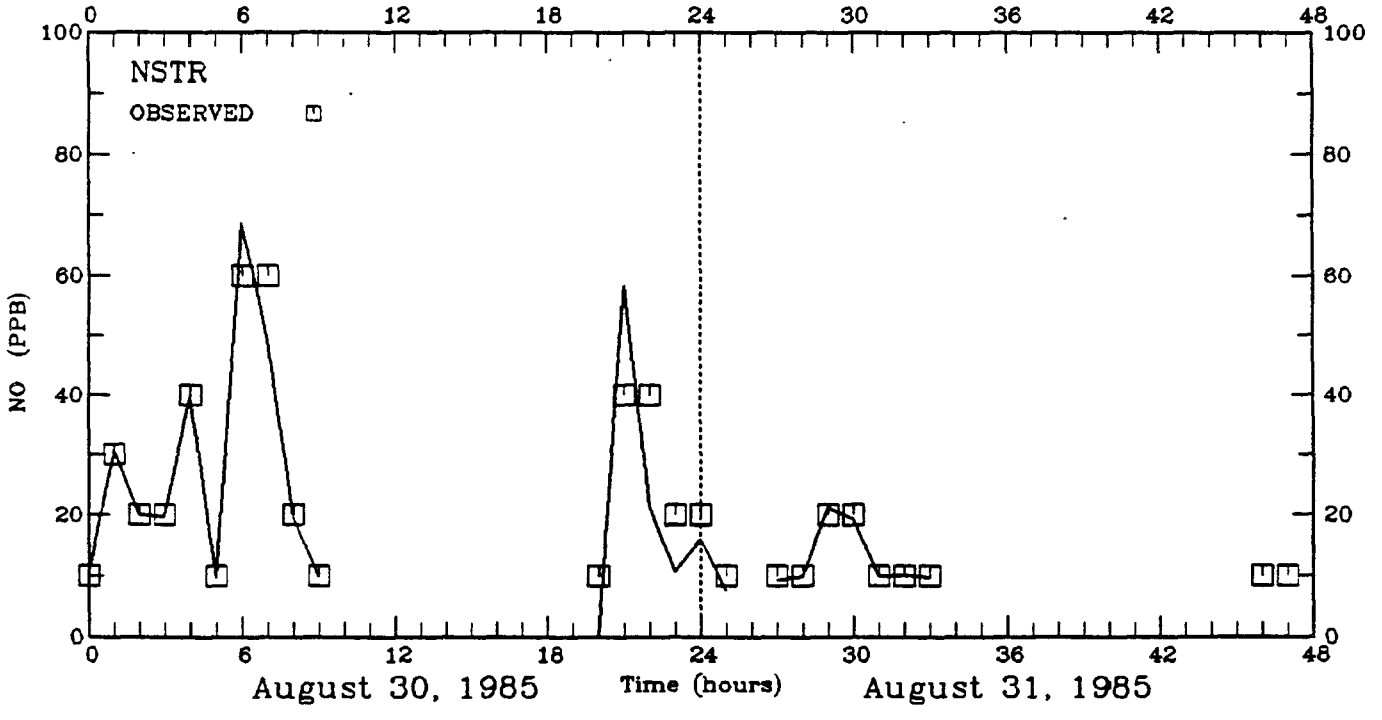

FIGURE 4-26. Time series of predicted and observed hourly NO_2 concentrations (ppb) for the Dallas-Fort Worth diagnostic run 2 using a two-cell search nearest neighbor analysis.

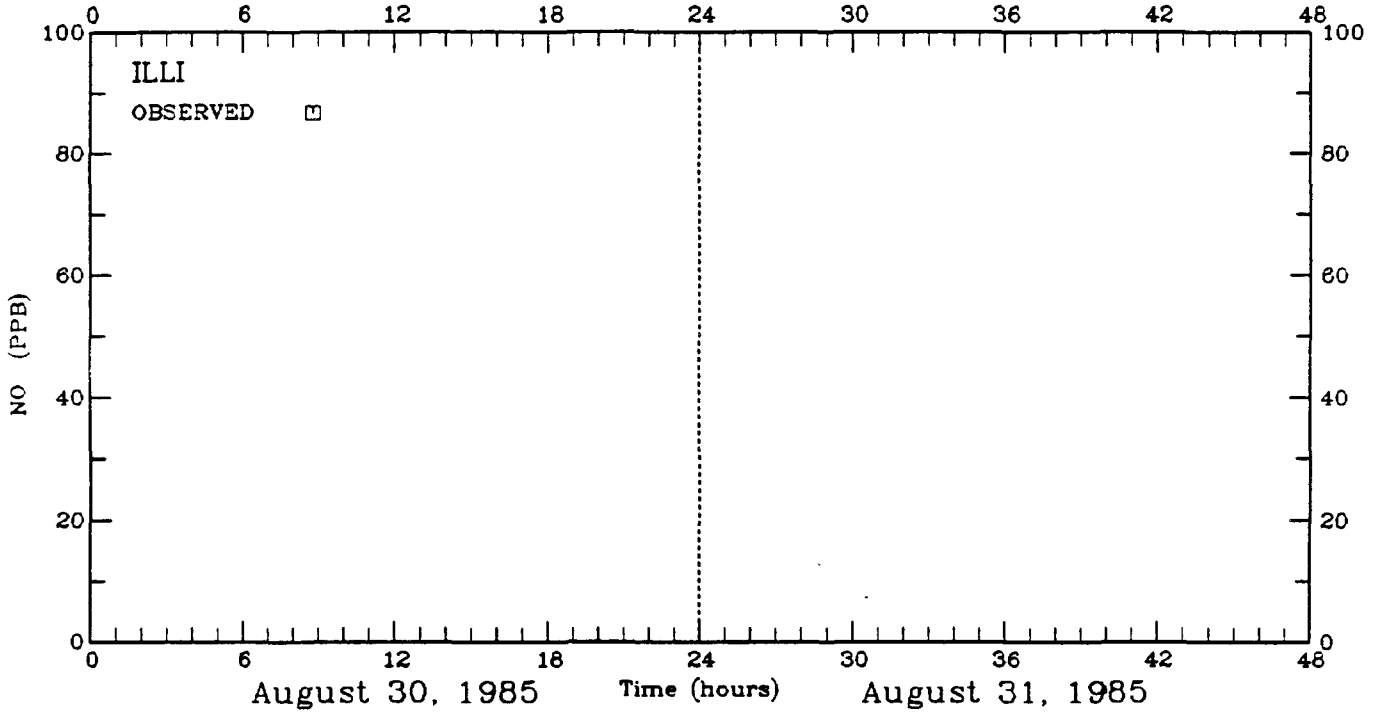

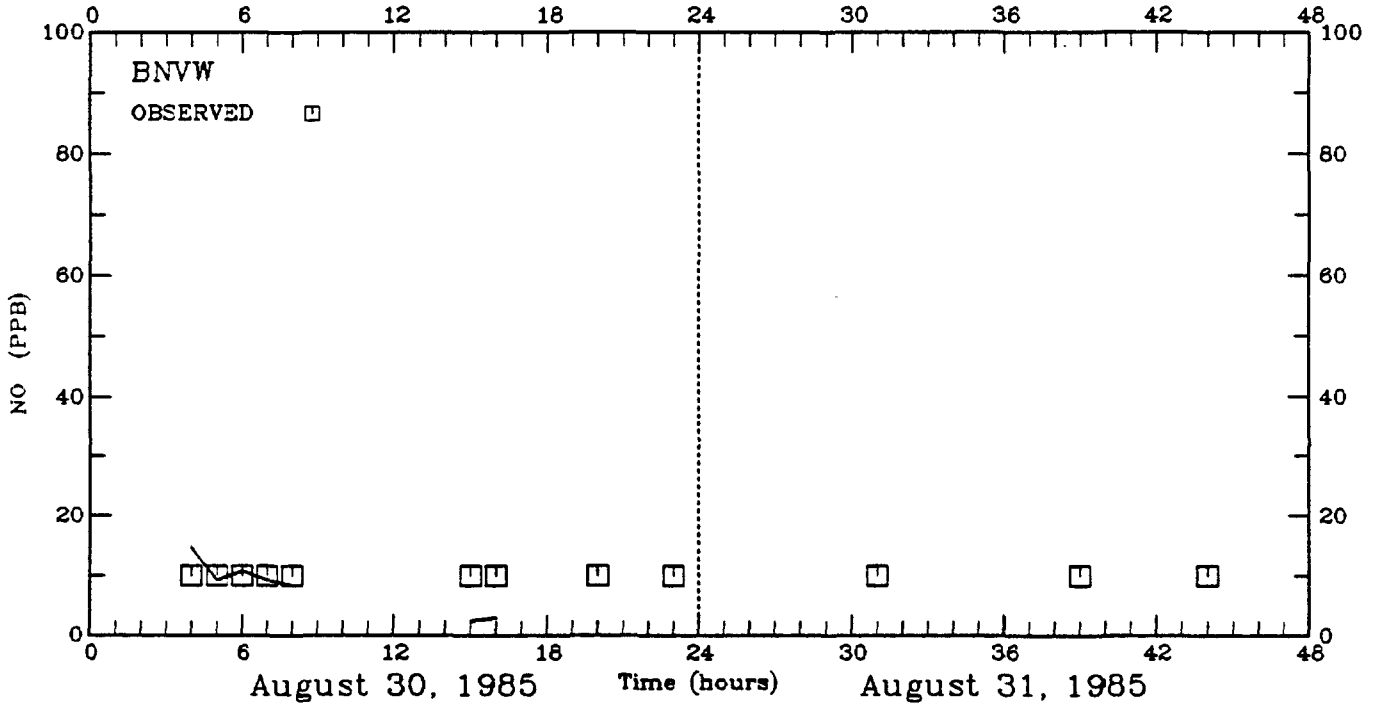

FIGURE 4-26. Continued.

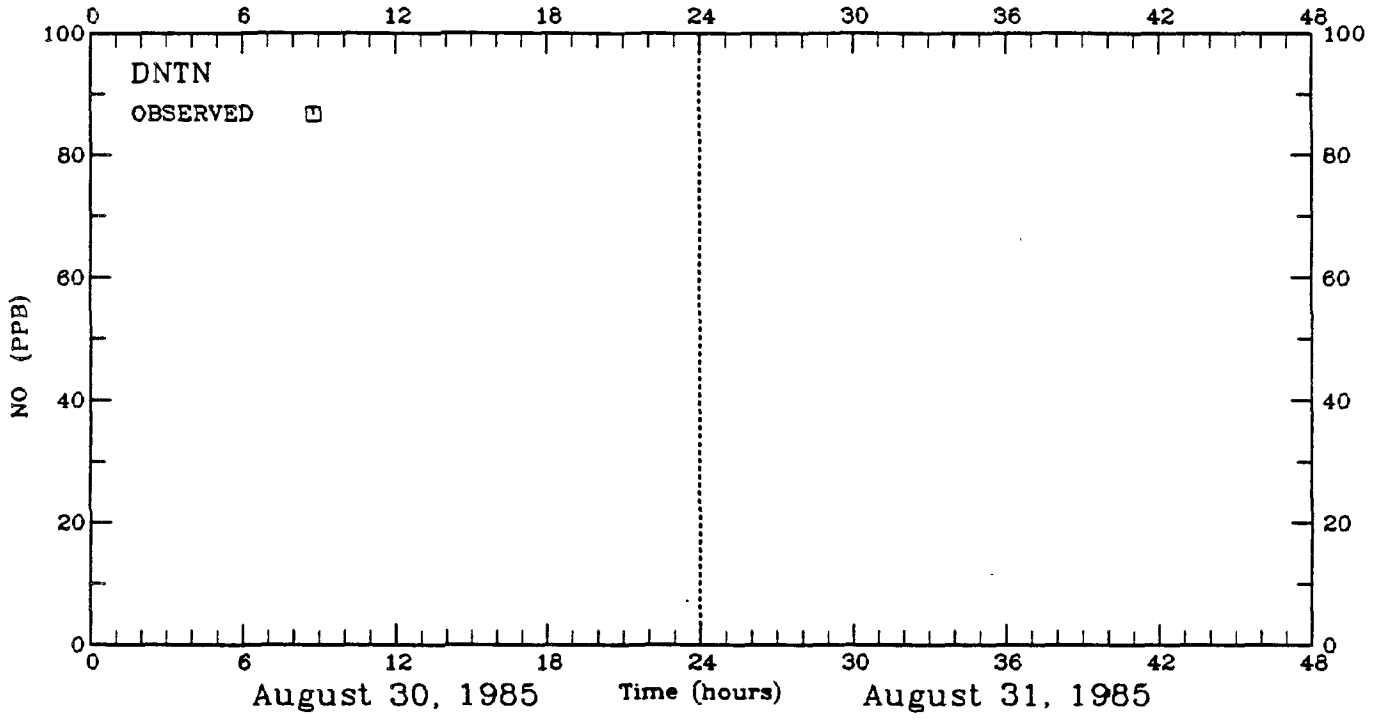

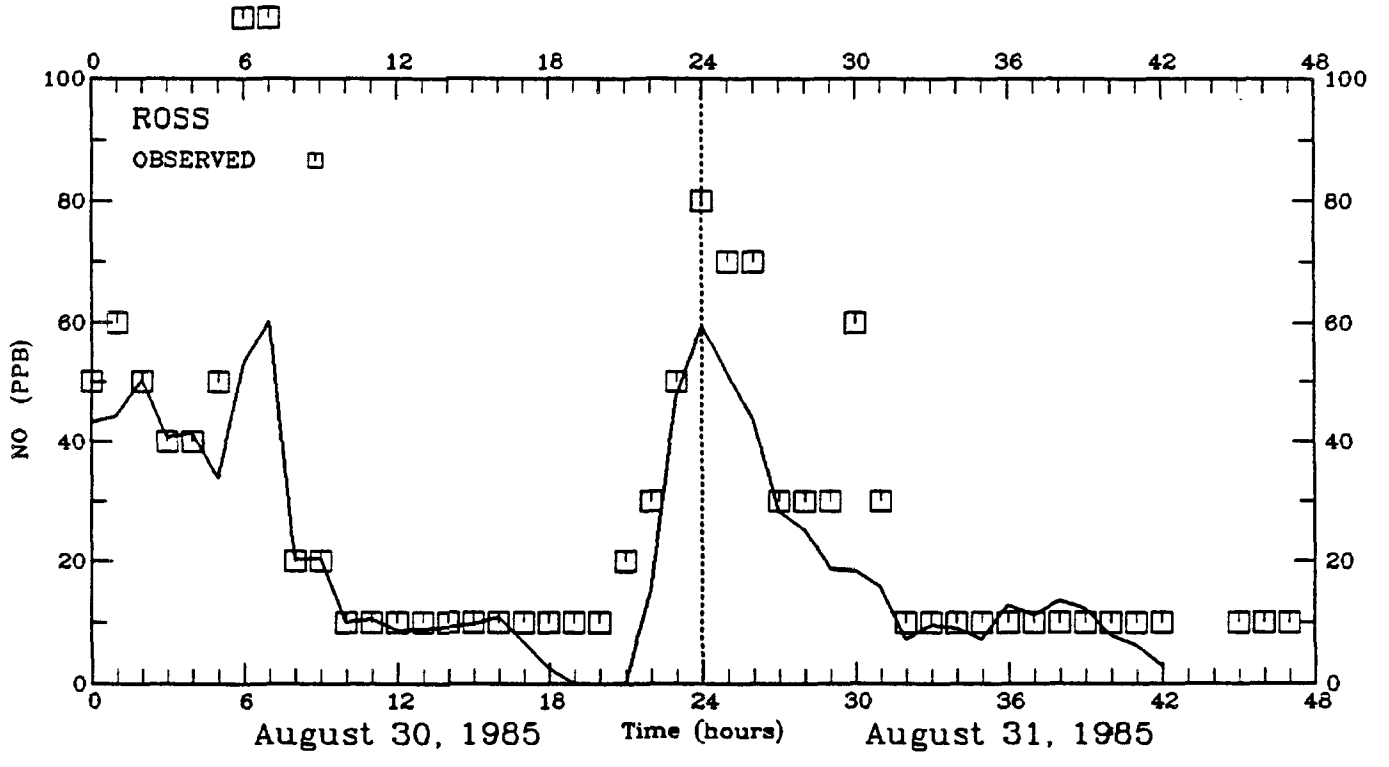

FIGURE 4-26. Concluded.

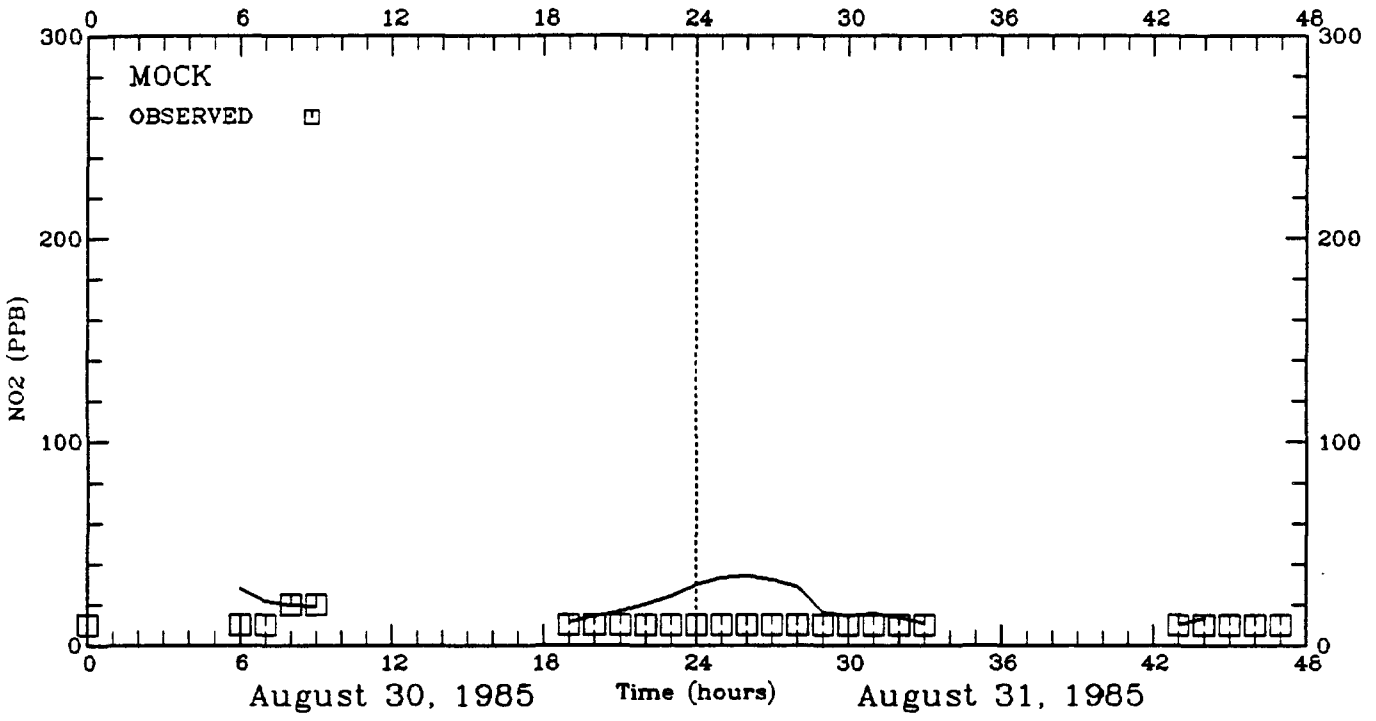

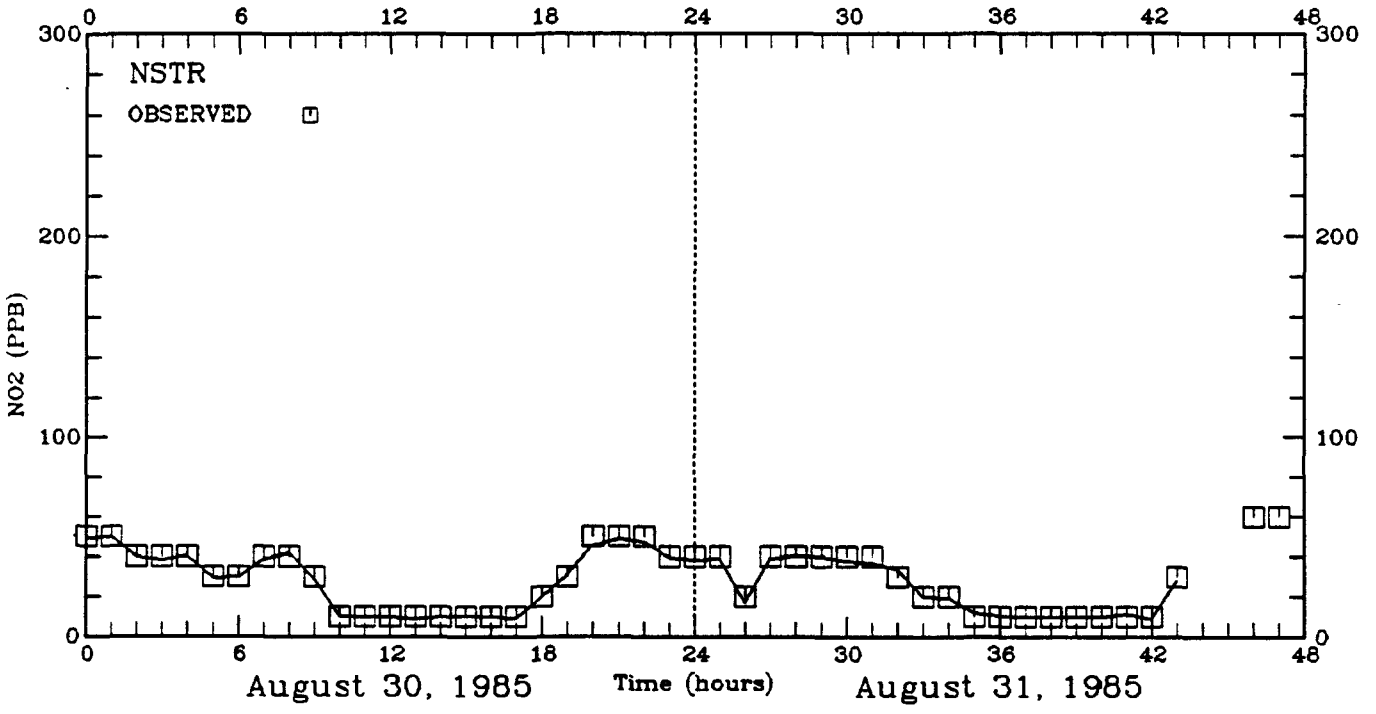

FIGURE 4-27. Time series of predicted and observed hourly ozone concentrations for the Dallas-Fort Worth diagnostic run 2 using a two-cell search nearest neighbor analyis.

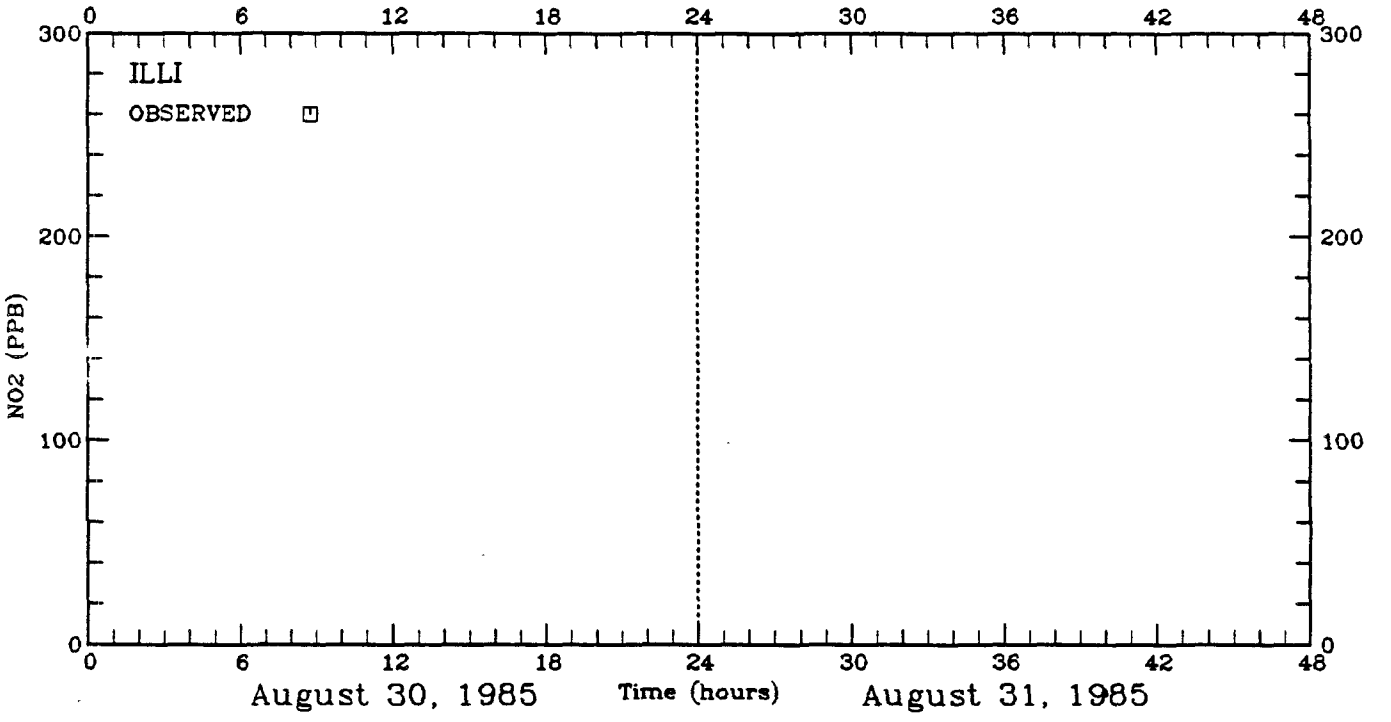

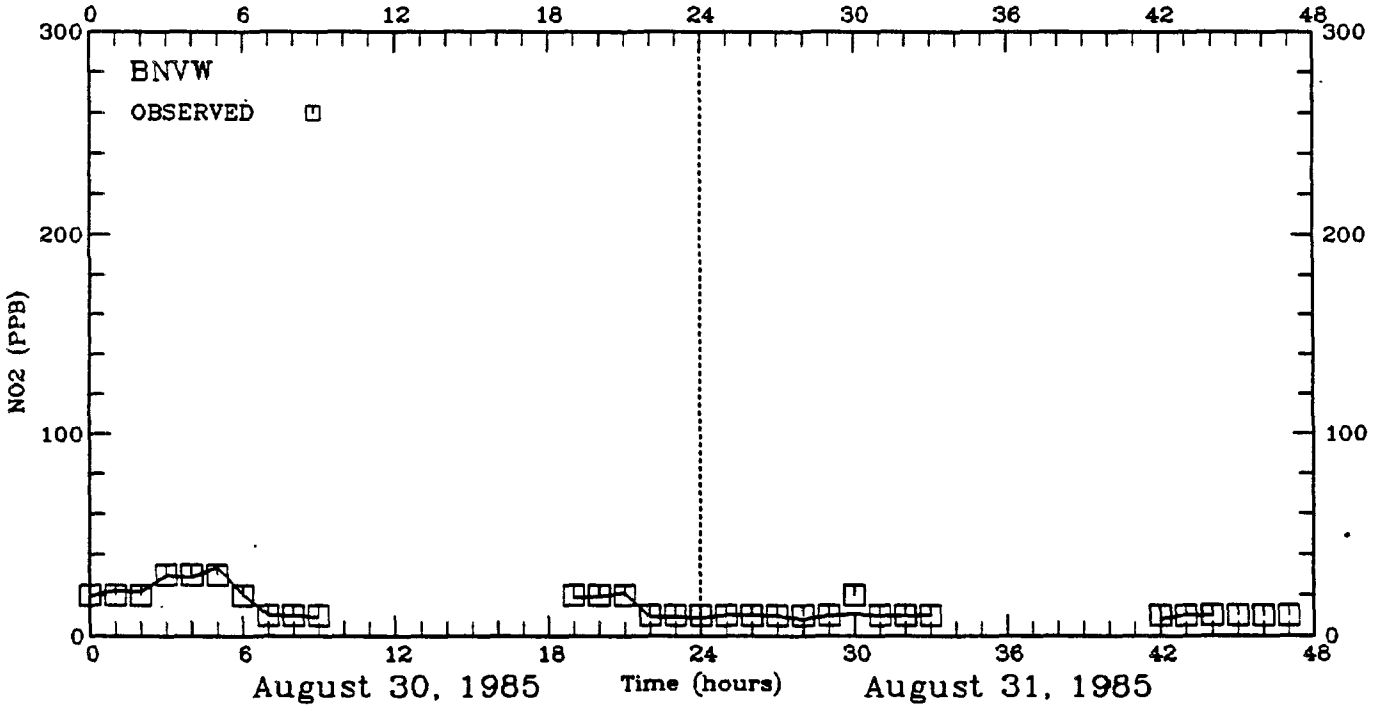

FIGURE 4-27. Continued.

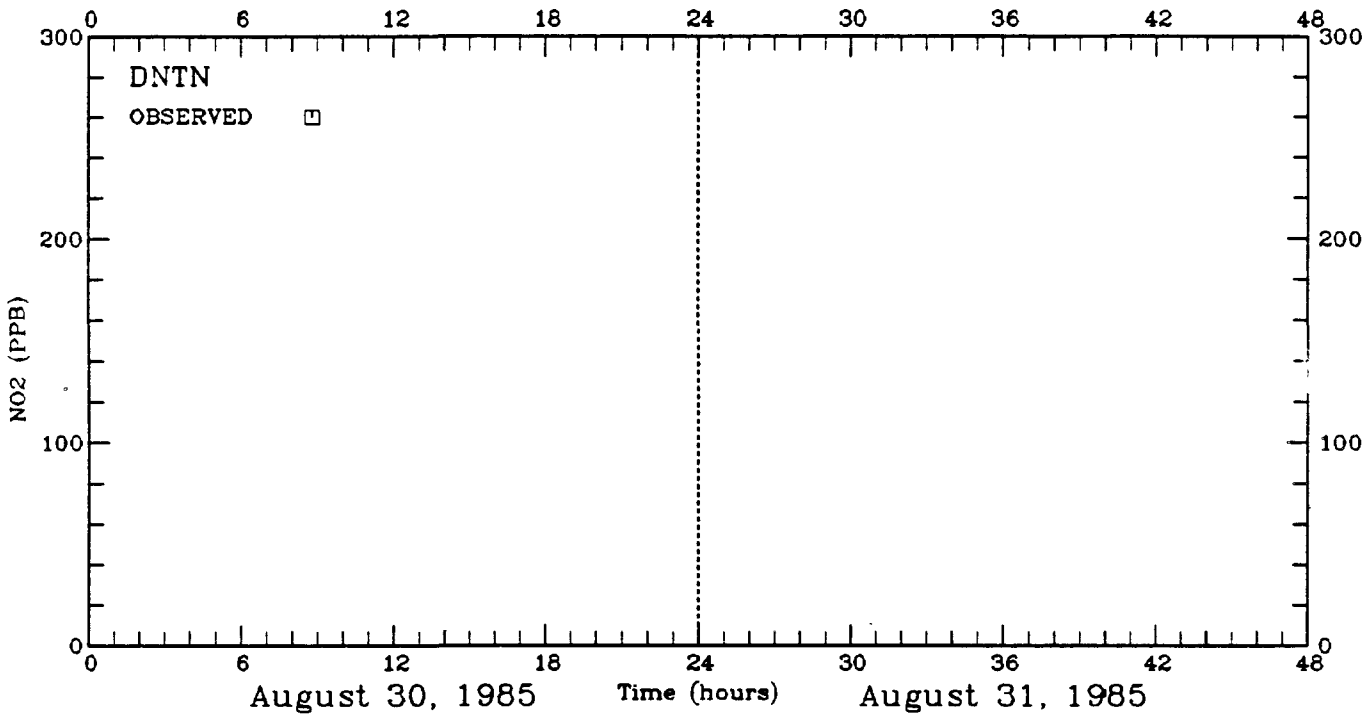

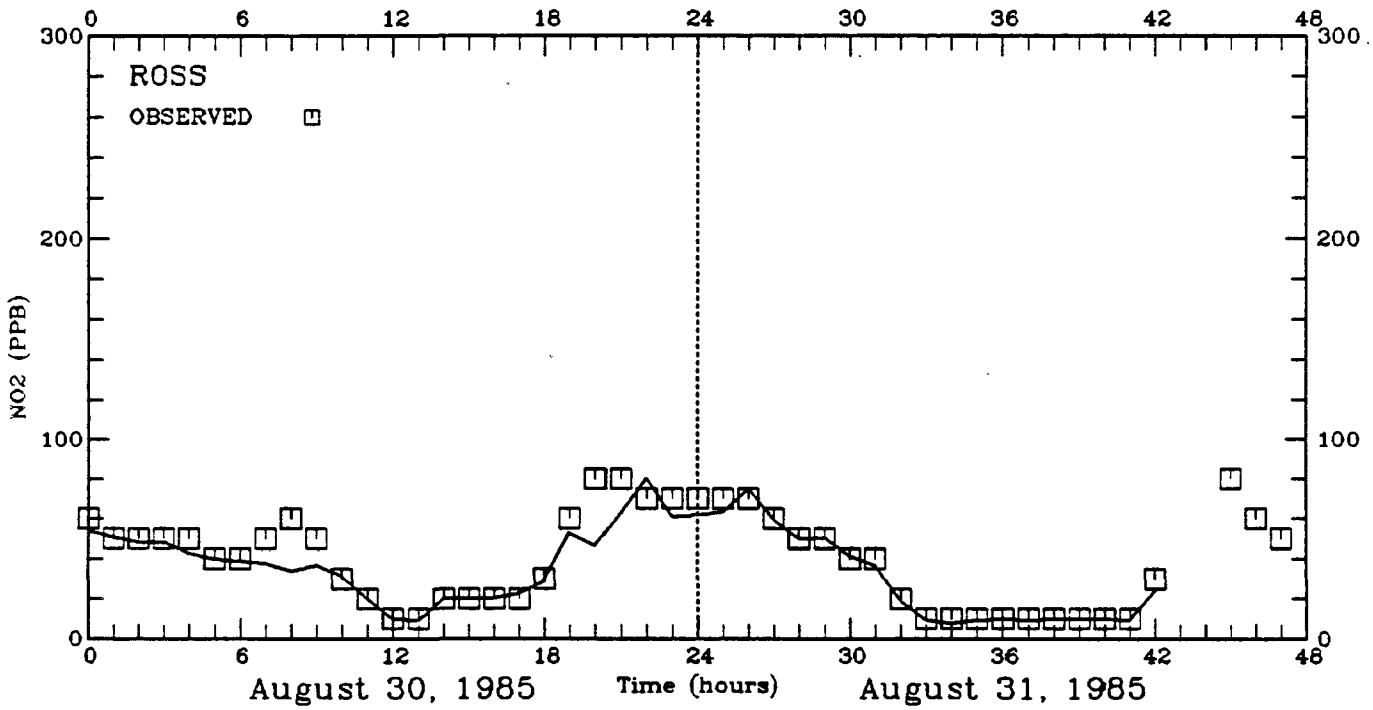

FIGURE 4-27. Concluded.

Summary

The diagnostic run 2 for Dallas-Fort Worth does a quite good job of predicting the observed region-wide peak ozone concentration on August 30 and 31. The predicted region-wide maximums on August 30 and 31 are within 6 and 4 percent of the observed peak respectively. On August 31 at the location of one of the peak observations (DNTN) the model replicates the peak to within 20 percent. However, at the location of the peak observed ozone on 30 August (ROSS) and at the other location of the peak observed ozone on 31 August (MOCK) the model replicates the peak observations to within only 48 and 58 percent, respectively. The nearest-neighbor analysis indicates that there are slight displacements of the elevated ozone cloud in the model predictions and that predicted concentrations of comparable values to the peak observations are within a few grid cells of the locations of the peak observations. Because this slight displacement of predicted ozone concentrations will not affect usefulness of the UAM when evaluating alternative emission control strategies, and the fact that diagnostic run 2 does satisfy the model performance goal (the predicted region-wide maximum is within 4 percent of the observed peak and occurs 8 km to the southwest of the observed peak, and the predicted peak at the location of the observed peak is within 20 percent), then diagnostic run 2 is a suitable base case.

Because of the high degree of spatial variability in the predicted ozone concentrations in diagnostic run 2, model performance could be improved by adjusting the wind fields so that the predicted elevated ozone clouds occur over the ozone monitors where the highest ozone observations occur. However, this may involve several diagnostic simulations with arbitrary adjustments to the wind fields, a process not consistent with the PLANR use of the UAM. Besides, as noted earlier, this displacement of the ozone peaks will not affect the evaluation of emission control strategies.

5 SUMMARY AND CONCLUSIONS

The PLANR use of the UAM was demonstrated for two regions: the city of Atlanta and the Dallas-Fort Worth metroplex. It was shown that UAM performance is adequate (i.e., model performance satisfied the model performance goal) when only routinely available data are used as inputs in a limited number of diagnostic simulations. However, it has also been shown here and elsewhere (Morris, Myers, and Carr, 1989) that use of routine meteorological data (hourly surface measurements and twice-daily upper-air sites) to develop UAM inputs in a "cook book" type fashion (i.e., running data through preprocessors without interpretation of the representativeness of the observations) generally results in less then satisfactory model performance. Thus two of the key elements of the PLANR use of the UAM are (1) characterization of the meteorological conditions that lead to the elevated ozone episode (base on analysis of meteorological data, daily weather maps, and observed air quality data) and (2) adjustment of the meteorological data to represent the conceptual picture of the meteorological conditions. In this adjustment process we have indentified the following as important considerations:

Twice-daily upper-air soundings
Surface wind speeds
Emissions

TWICE-DAILY UPPER-AIR SOUNDINGS

It is particularly difficult to develop hourly wind fields above the surface with just routine twice-daily upper-air observations. The upper-air observations are collected in the morning at 1200 GMT (approximately 0700 LST) and evening at 0000 GMT (approximately 1900 LST). This makes it very difficult to characterize transport of pollutants in the late morning and afternoon, the key period of photochemical activity. For the first diagnostic simulation we used linear vector interpolation between the morning and afternoon soundings; for subsequent diagnostic simulations we used more creative interpolation techniques (e.g., the techniques used to characterize frontal passages as described below) when warranted.

Characterization of Fronts

When a front passes through the modeling region, as occurred in the Atlanta episode reported here and in a St. Louis episode reported elsewhere (Morris, Myers, and Carr, 1989), it is particularly difficult to characterize the upper-level winds using the twice-daily upper-air soundings. The time of passage of the front through a region can be estimated by examining the surface meteorological observations to find an hour with a wind shift, temperature change, or other meteorological phenomena. This information can then be used to develop an interpolation scheme for defining the hourly wind sounding from the twice-daily upper-air soundings for input into the DWM. For example, if surface data indicate that a front passes through at 1300 LST, then use of the morning sounding until 1300 and the afternoon sounding after 1300 will probably result in more representative wind fields than is obtained by linear interpolation of soundings.

Mixing Height Definition

The characterization of the mixing height is also very difficult using just routine twice-daily upper-air observations and the hourly surface temperatures. In the UAM application to Dallas-Fort Worth reported here it was suspected that a subsidence inversion caused by a stationary high-pressure system was responsible for the limited mixing conditions that led to the ozone episode. Since ozone episodes generally occur during hot, stagnant conditions with limited mixing, we used the summer afternoon climatalogical mixing height as the maximum mixing height for the Dallas base case.

Wind Shear

During the middle of the day, when convective activity is greatest and there is a well-defined, well-mixed layer below the temperature inversion, not much wind shear within the mixed-layer is expected. However, interpolating between the morning and evening soundings, periods in which there may be significant amounts of wind shear, may result in incorrect specification of wind shear within the mixed layer in the middle of the day. This wind shear, in turn, would result in excessive dilution of the urban plume and, consequently, underprediction of the peak ozone concentrations. One approach to get around this problem is to use identical wind fields in all UAM layers below the mixing height. For the PLANR use of the UAM this is partially done because the lowest layer of the Diagnostic Wind Model (DWM), which uses the surface wind observations, is used exclusively in layer one of the UAM and weighted 50 percent in the remaining layer of the UAM (layer 2) that lies below the mixing height. It should be pointed out that wind shear may occur in the mixed layer during the day. For example, in the Atlanta episode wind shear occurred due to the passage of a front through the modeling domain in the afternoon.

Recommendations

Specification of upper-level hourly wind fields using routine twice-daily upper-air soundings may involve developing interpolation schemes based on the meteorological characterization of the episode. Guidelines for interpolation procedures need to be developed and tested. The collection of an afternoon upper-air sounding (1800 GMT) would greatly reduce the uncertainty in the upper-level wind fields and mixing heights. It is recommended that consideration be given to collecting one extra sounding at 1800 GMT in the vicinity of cities with severe ozone attainment problems during the ozone season. At little extra cost in monitoring, the uncertainty in the wind fields and mixing heights can be reduced and the preparation of the UAM meteorological inputs can be simplified.

SURFACE WIND SPEEDS

Surface meteorological measurements are usually the only hourly meteorological measurements available for constructing the hourly varying UAM inputs. As noted in Appendix D and in the evaluation of the PLANR use of the UAM for St. Louis (Morris, Myers, and Carr, 1989), the instantaneous wind speeds reported at Federal Aviation Administration or National Weather Service (FAA/NWS) sites may overestimate the wind speeds for the hourly average wind vectors required by the UAM during low wind speed conditions. An analysis of wind speeds from seven "collocated" hourly average and FAA/NWS wind monitoring sites during episodic ozone conditions in the South Coast Air Basin (SOCAB) of California revealed that the continuous hourly average wind speeds are on average only 55 percent of their instantaneous FAA/NWS counterpart. When examining each of the seven station pairs individually, it was found that five of the seven continuous stations measured wind speeds that were 44 to 55 percent of the FAA/NWS values, while the other two continuous sites recorded wind speeds that were 71 and 98 percent of the instantaneous values.

Based on this apparent bias in wind speeds reported at FAA/NWS sites, a sensitivity test for Atlanta was run in which FAA/NWS wind speeds were reduced 50 percent. This sensitivity test resulted in much better model performance. Similar results were reported in the PLANR application of the UAM to St. Louis (Morris, Myers, and Carr, 1989). Note that because of the possibility of this wind speed bias and the fairly good coverage of continuous wind measurements in Dallas-Fort Worth, the FAA/NWS sites were not used in the development of wind fields for the Dallas-Fort Worth application.

Further analysis of the possibility of wind speed bias at FAA/NWS stations during episodic ozone (low wind speed) conditions needs to be performed. The wind speed data from the seven collocated sites from the SOCAB needs to be examined in a more statistically rigorous manner to determine if the bias is statistically significant. Collocated instantaneous and hourly average wind data from other regions

(e.g., the Regional Air Pollution Study and Northeast Corridor studies) also needs to be analyzed. Finally, some guidence needs to be formulated to eliminate this bias from the UAM analysis. For the PLANR UAM sensitivity analysis for Atlanta and the PLANR UAM application to St. Louis the FAA/NWS wind speeds were reduced by 50 percent. This is probably on the high side of reductions, but more research is needed to determine what is an appropriate reduction factor or whether it is appropriate to modify the wind speeds at all. It is recommended that a network of surface wind monitors reporting hourly averages be set up in ozone nonattainment regions.

AIR QUALITY DATA

Air quality data for photochemical modeling is needed for initial concentrations, boundary conditions, and model performance evaluation. The trend in UAM modeling is to simulate multiple days (in order to eliminate the need for defining initial concentrations) and to simulate a large region (in order to reduce the sensitivity of the model calculations to the specification of boundary conditions). Accordingly, for the PLANR application of the UAM, "clean" concentration values have been used for initial and boundary conditions in the first diagnostic simulations. Note that for the PLANR UAM application to Atlanta the presence of biogenic emissions indicated that higher VOC and ISOP concentrations were present, thus the boundary conditions were adjusted accordingly. For the PLANR application of the UAM to Philadelphia, air quality data indicated that there was a large amount of transported ozone and ozone precursors, thus the initial and boundary conditions were adjusted accordingly.

The importance of air quality data for model performance evaluation cannot be understated. The comparison of predicted and observed concentrations is the main indication that the model is working properly for each application. Because of the limited air quality data available for Atlanta (three ozone sites), it was very difficult to determine whether the model was operating correctly, thus a sensitivity test was also performed. For the Dallas-Fort Worth application, despite some descrepancies at a couple of the air quality monitoring sites, the model replicated enough of the features of the observed ozone, NO, NO_2, and CO concentrations that there is more confidence in model predictions. More air quality monitoring data is always desirable for model performance evaluation.

EMISSIONS

There is considerable uncertainty in the anthropogenic and biogenic emissions data. The uncertainity may be biased toward an underprediction in the total emissions which makes it very difficult to evaluate the model since a model's underprediction may be due to insufficient emissions. Attempts to improve model performance by adjusting other inputs (e.g., boundary conditions or meteorology) may result in better model performance, but the model may be getting the right answer for the wrong reason.

Anthropogenic Emissions

Recent photochemical modeling simulations using the UAM(CB-IV) have produced a disturbing trend toward underprediction of the peak ozone observations. This underprediction has occurred in the California South Coast Air Basin (Los Angeles) (Hogo, Mahoney, and Yocke, 1988), Philadelphia (Haney and Burton, 1988), Atlanta, and Dallas-Fort Worth. The old UAM(CB-II), which we know may have considerable problems in the chemistry (e.g., aromatic and carbonyl chemistry), tended to over- and underpredict about equally. However, since the improvements in chemistry were made, it appears that the model tends to underpredict more than overpredict. In light of recent discoveries of previously uninventoried VOC sources (e.g., running losses, solvents) and emission reconcilation studies that have measured higher VOC emissions than estimated in emission inventories (e.g., the SCAQS tunnel study), this tendency toward underprediction indicates that VOCs in current emission inventories may be underestimated.

In all of the PLANR UAM applications performed to date the peak observations are underpredicted. Remedial actions generally are limited to adjustments in the boundary conditions, wind fields, or mixing heights. Although it appears the VOC emissions are underestimated, information on this underprediction is not available; thus the emissions have not been adjusted to improve model performance. However, sensitivity tests that look at the level of VOC emission increase needed to obtain the best model performance may provide insight into the degree of the underestimate of the VOC emissions.

In the PLANR diagnostic simulations to improve UAM performance (i.e., reduce the level of underprediction) we have focused on adjusting wind fields and mixing depths to better reflect the conceptual picture of the meteorological conditions of the ozone episode. This adjustment has consisted mainly of interpolation schemes for the upper-air data, reduction of wind speeds at FAA/NWS sites, and reduction of the maximum mixing height. The reduction in wind speeds and mixing height will have an effect similar to increasing the emissions when analyzing emission control strategies. An increase in boundary conditions, which also would reduce an underprediction, would have a different effect than increasing emissions when analyzing emission control strategies. Until high-quality emission inventories are developed, adjustments to improve model performance should be limited to variables that act in the same direction as increasing emissions when analyzing emission control strategies. Unless there is evidence of transported ozone or ozone precursors into the region of interest, or unless a small modeling domain is specified, there should not be extensive modifications to the boundary conditions to improve model performance.

Biogenic Emissions

Current estimates of biogenic emissions are very uncertain in the amounts, reactivity and composition, spatial distribution, and diurnal variations. More research is needed to reduce the uncertainities in all areas of biogenic emission estimates. In addition, the chemistry of biogenic emissions is not well understood. The use of chemical mechanisms designed mainly to simulate the atmospheric chemistry of anthropogenic emissions may incorrectly characterize the chemistry of rural biogenic emissions. Again, more research is required to better define the chemical kinetics of biogenic emissions. Even with all the uncertainties in the current estimates and chemistry of biogenic emissions, biogenic emissions affect the efficiency of emission control reduction strategies designed to reduce ozone concentrations and should be included, to the extent possible, in all future analyses.

CONCLUSIONS

It has been demonstrated that the UAM can be exercised using only routine data and that it performs in an acceptable way. Given the current uncertainity in estimates and reactivities of anthropogenic and biogenic emissions, it appears that obtaining very good model performance would be fortuitous at best. However, even given the current uncertainty in emissions and meteorological inputs, the use of the UAM by air quality planners for air quality planning, ozone attainment demonstration, and sensitivity analyses will provide a powerful tool for developing air quality management plans.

References

Ames, J., T. C. Myers, L. E. Reid, D. C. Whitney, S. H. Golding, S. R. Hayes, and S. D. Reynolds. 1985a. SAI Airshed Model Operations Manuals. Volume I--User's Manual. U.S. Environmental Protection Agency (EPA-600/8-85-007a).

Ames, J., S. R. Hayes, T. C. Myers, and D. C. Whitney. 1985b. SAI Airshed Model Operations Manuals. Volume II--System's Manual. U.S. Environmental Protection Agency (EPA-600/8-85-007b).

Chameides, W. L., R. W. Lindsay, J. Richardson, and C. S. Kiang. 1988. The role of biogenic hydrocarbons in urban photochemical smog: Atlanta as a case study. Science, 241:1473-1475.

Douglas, S., and R. Kessler. 1988. "User's Guide to the Diagnostic Wind Model. Version 1.0." Systems Applications, Inc., San Rafael, California.

Gery, M. W., G. Z. Whitten, and J. P. Killus. 1988. "Development and Testing of the CBM-IV for Urban and Regional Modeling." Systems Applications, Inc., San Rafael, California (SYSAPP-88/002).

Haney, J. L., and C. S. Burton. 1988. "UAM-CBM-IV-Calculated Effects of Emission Reductions on Ozone Levels in the Philadelphia Metropolitan Area." Systems Applications, Inc., San Rafael, California (SYSAPP-88/117)

Haney, J. L., D. R. Souten, T. W. Tesche, L. R. Chinkin, H. Hogo, and M. C. Dudik. 1986. "Evaluation and Application of the PARIS Photochemical Model in the South Central Coast Air Basin. Volume I." Systems Applications, Inc., San Rafael, California (SYSAPP-85/065).

Hogo, H., M. W. Gery. 1988. "Guidelines for Using OZIPM-4 With CBM-IV or Optional Mechanisms. Volume 1. Description of the Ozone Isopleth Plotting Package Version 4." Systems Applications, Inc., San Rafael, California (SYSAPP-88/001).

Hogo, H., L. A. Mahoney, and M. A. Yocke. 1988. "Draft Air Quality Management Plan 1988 Revision. Draft Appendix V-R. Urban Airshed Model Performance Evaluation for 5-7 June 1985." Systems Applications, Inc., San Rafael, California (SYSAPP-88/138).

Holzworth, G. C. 1972. Mixing Heights, Wind Speeds, and Potential for Urban Air Pollution Throughout the Continuous United States. U.S. Environmental Protection Agency.

Kelley, R. F. 1981. User's Manual for Mixing Height Computer Program. U.S. Environmental Protection Agency (EPA-450/4-81-022).

Killus, J. P., and P. D. Gutfreund. 1984. "The Development and Use of Protocols in the Urban Airshed Model in Regulatory and Research Applications." Systems Applications, Inc., San Rafael, California (SYSAPP-84/133).

Lamb, B., A. Guenther, D. Gay, and H. Westberg. 1987. A national inventory of biogenic hydrocarbon emissions. Atmos. Environ., 21(8):1695-1706.

Lamb, B., H. Westberg, and G. Allwine. 1986. Isoprene emission fluxes determined by an atmospheric tracer technique. Atmos. Environ., 20(1):1-8.

Morris, R. E., T. C. Myers, and E. L. Carr. 1989. "Urban Airshed Model Study of Five Cities: Evaluation of Base Case Model Performance for the City of St. Louis Using Rich and Sparse Meteorological Inputs." Systems Applications, Inc., San Rafael, California.

Morris, R. E., M. W. Gery, M. K. Liu, G. E. Moore, C. Daly, and S. M. Greenfield. 1989c. "Sensitivity of a Regional Oxidant Model to Variations in Climate Parameters. Volume I: Results." Systems Applications, Inc., San Rafael, California (SYSAPP-89/014a).

Morris, R. E., R. C. Kessler, S. G. Douglas, K. R. Styles, and G. E. Moore. 1988. "Rocky Mountain Acid Deposition Model Assessment Acid Rain Mountain Mesoscale Model (ARM3)." Systems Applications, Inc., San Rafael, California (SYSAPP-88/152).

Morris, R. E., T. C. Myers, M. C. Causley, L. Gardner, and E. L. Carr. 1989b. "Urban Airshed Model Study of Five Cities. Low-Cost Application of the Model to Atlanta and Evaluation of the Effects of Biogenic Emissions on Emission Control Strategies." Systems Applications, Inc., San Rafael, California (SYSAPP-89/117).

Morris, R. E., T. C. Myers, H. Hogo, L. R. Chinkin, L. A. Gardner, and R. G. Johnson. 1989a. "A Low-Cost Application of the Urban Airshed Model to the New York Metropolitan Area and the City of St. Louis." Systems Applications, Inc., San Rafael, California (SYSAPP-89/038).

Reynolds, S. D., T. W. Tesche, and L. E. Reid. 1979. "An Introduction to the SAI Airshed Model and Its Usage." Systems Applications, Inc., San Rafael, California (SYSAPP-79/031).

Smolarkiewicz, P. K. 1983. A simple positive definite advection scheme with small implicit diffusion. Monthly Weather Review, 111:479-486.

SAI. 1989. "User's Manual for Preparing Emission Files for Use in the Urban Airshed Model." Systems Applications, Inc., San Rafael, California (SYSAPP-89/114).

Tingey, D. T., et al. 1978a. Isoprene Emissions Rates from Live Oak. U.S. Environmental Protection Agency (EPA-904/9-78-004).

Tingey, D. T., et al. 1978b. Monoterpene Emission Rates from Slash Pine. U.S. Environmental Protection Agency (EPA-904/9-78-013).

Zimmerman, D., W. Tax, M. Smith, J. Demmy, and R. Battye. 1983. "Anthropogenic Emissions Data for the 1985 NAPAP Inventory." Alliance Technologies Corporation, Chapel Hill, North Carolina (EPA-600/7-88-022).

Appendix A

PERCENT CONTRIBUTION OF INITIAL CONCENTRATIONS, BOUNDARY CONDITIONS (FOUR LATERAL FACES PLUS TOP BOUNDARY) ANTHROPOGENIC AREA SOURCE EMISSIONS, POINT SOURCE EMISSIONS, AND BIOGENIC EMISSIONS TO HOURLY TRACER, NO_x, AND VOC CONCENTRATIONS FOR ATLANTA ON 4 JUNE 1984

A-1a: 0800 Initial NO_x tracer contibution
A-1b: 0800 Boundary NO_x tracer contribution
A-1c: 0800 Area source NO_x tracer contribution
A-1d: 0800 Point source NO_x tracer contribution

A-2a: 0800 Initial VOC tracer contribution
A-2b: 0800 Boundary VOC tracer contribution
A-2c: 0800 Anthropogenic VOC tracer contribution
A-2d: 0800 Biogenic VOC tracer contribution

A-3a: 1200 Initial NO_x tracer contribution
A-3b: 1200 Boundary NO_x tracer contribution
A-3c: 1200 Area source NO_x tracer contribution
A-3d: 1200 Point source NO_x tracer contribution

A-4a: 1200 Initial VOC tracer contribution
A-4b: 1200 Boundary VOC tracer contribution
A-4c: 1200 Anthropogenic VOC tracer contribution
A-4d: 1200 Biogenic VOC tracer contribution

A-5a: 1600 Initial NO_x tracer contibution
A-5b: 1600 Boundary NO_x tracer contribution
A-5c: 1600 Area source NO_x tracer contribution
A-5d: 1600 Point source NO_x tracer contribution

A-6a: 1600 Initial VOC tracer contribution
A-6b: 1600 Boundary VOC tracer contribution
A-6c: 1600 Anthropogenic VOC tracer contribution
A-6d: 1600 Biogenic VOC tracer contribution

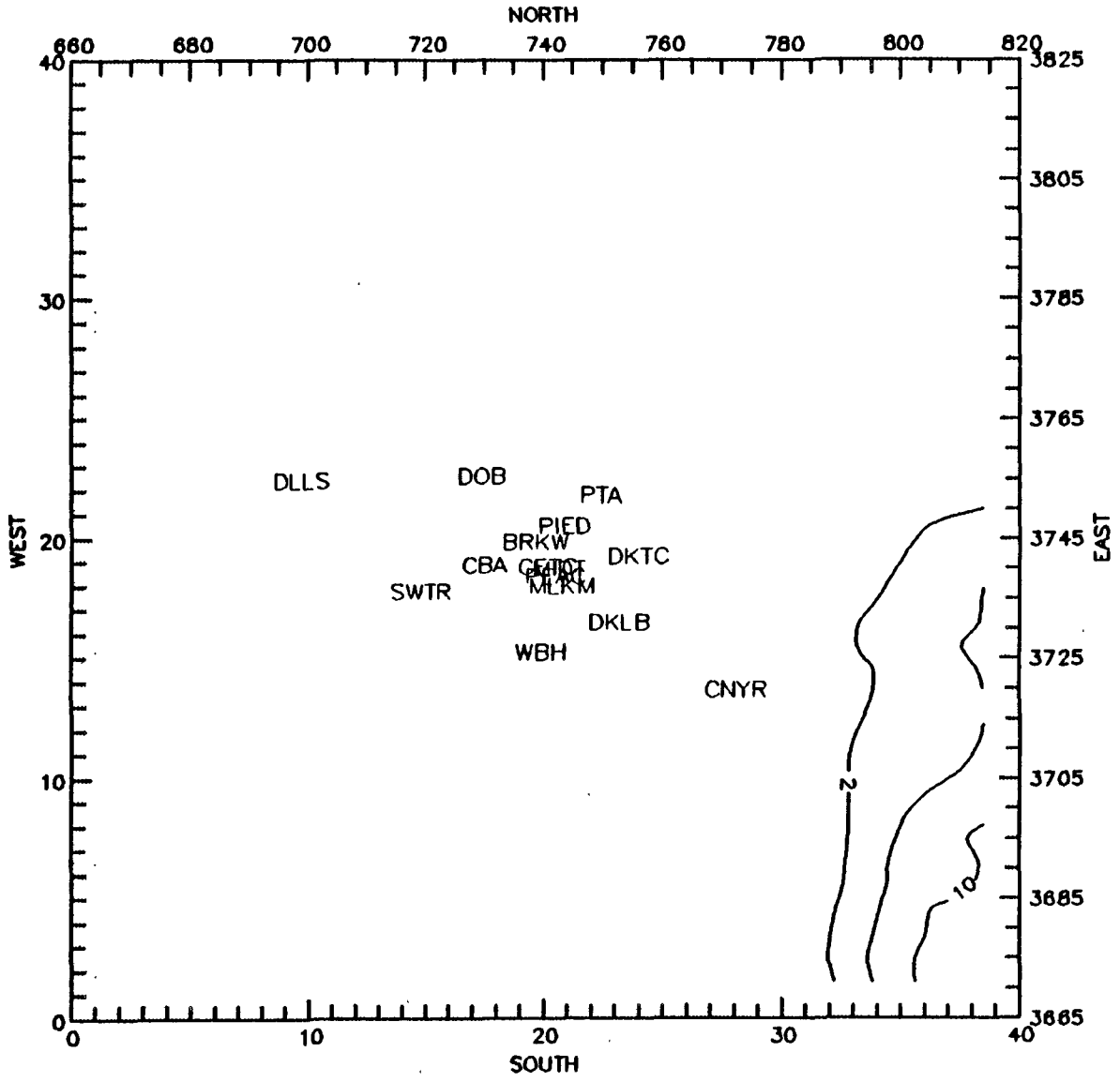

FIGURE A- 1a. Percent contribution of initial NOx tracer at 800 EST, 4 June 1984.

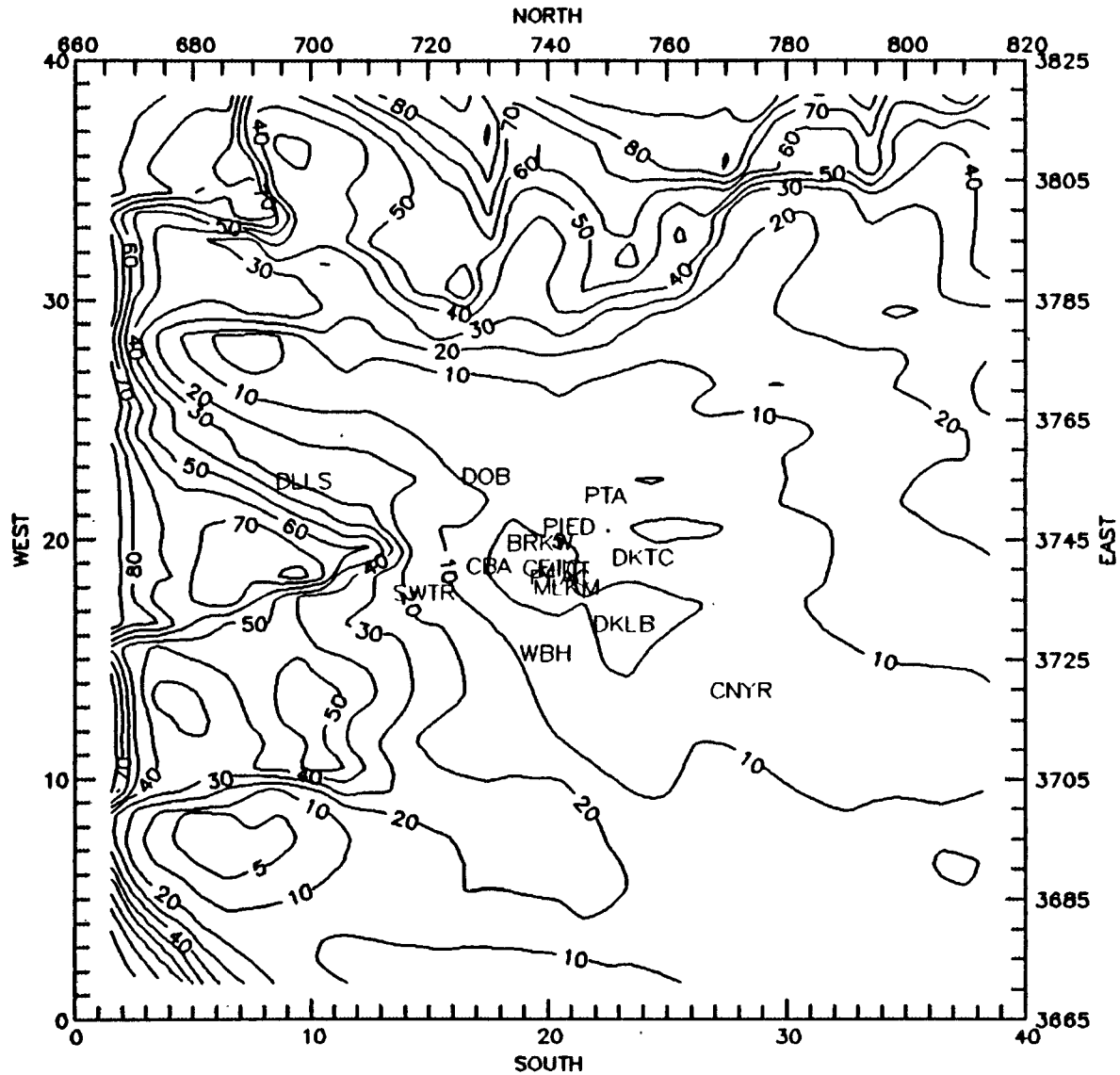

FIGURE A-1b. Percent contribution of boundary NOx tracer at 800 EST, 4 June 1984.

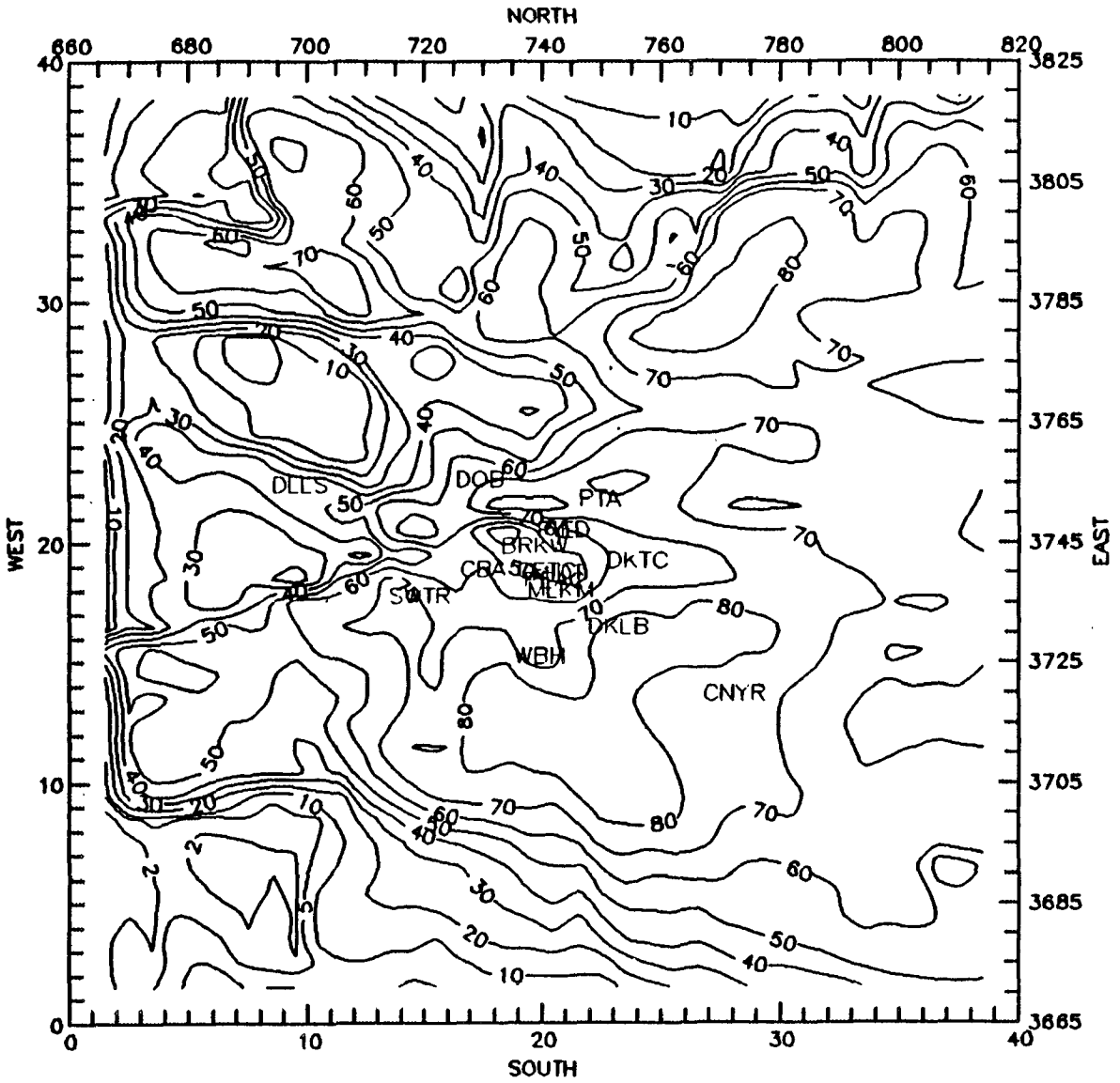

FIGURE A-1c . Percent contribution of area source NOx tracer at 800 EST, 4 June 1984.

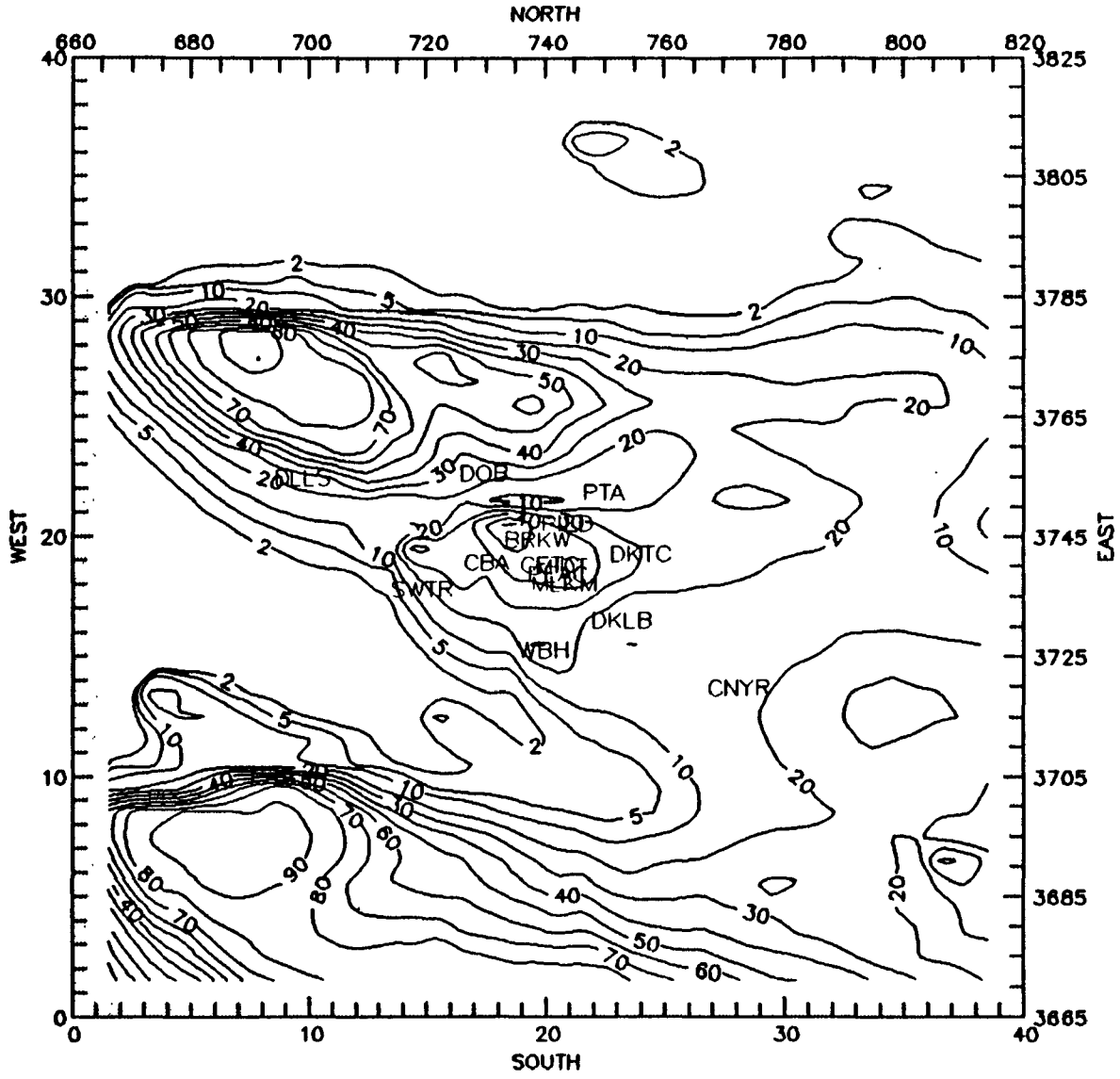

FIGURE A-1d . Percent contribution of point source NOx tracer at 800 EST, 4 June 1984.

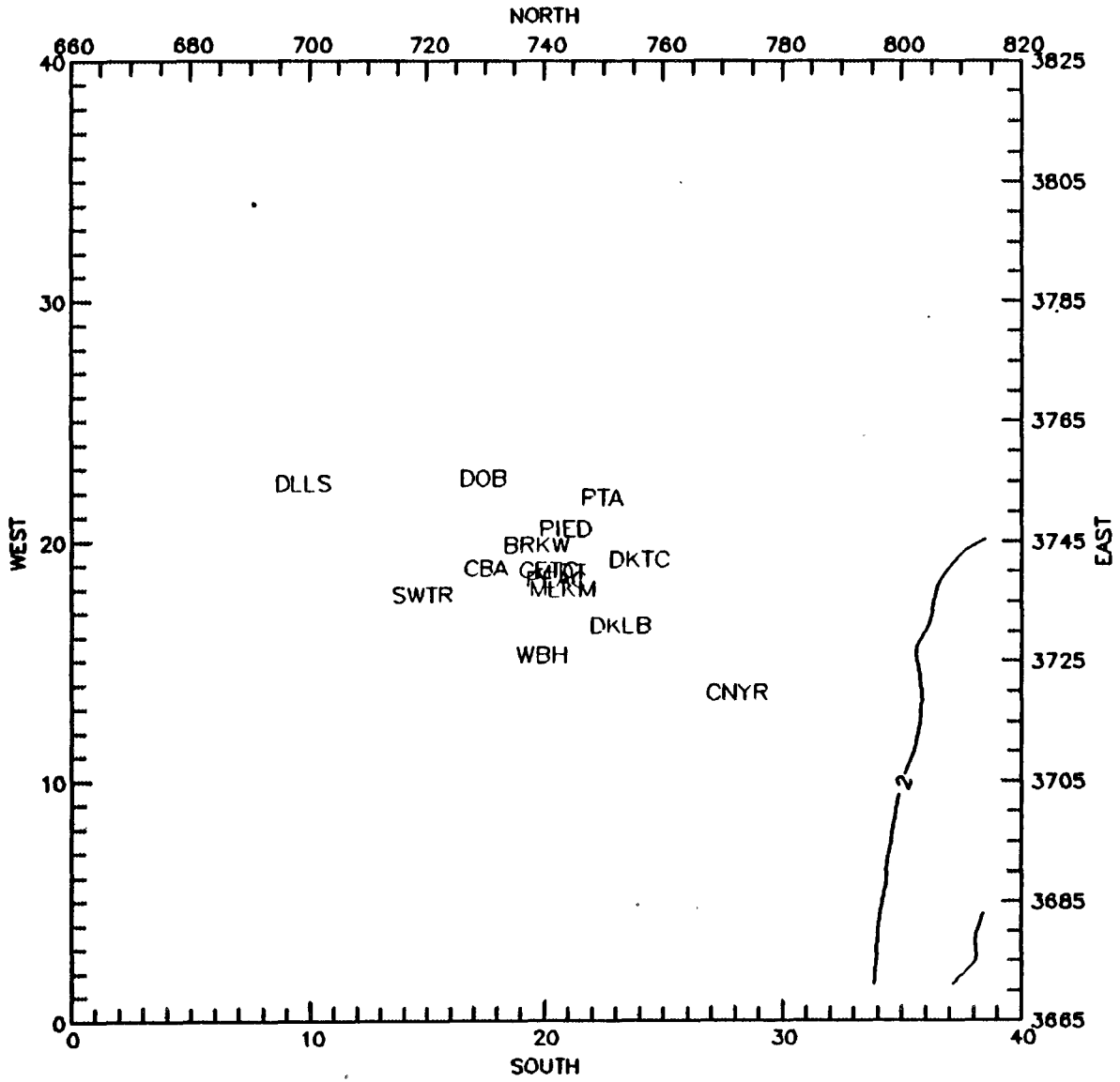

FIGURE A-2a . Percent contribution of initial VOC tracer at 800 EST, 4 June 1984.

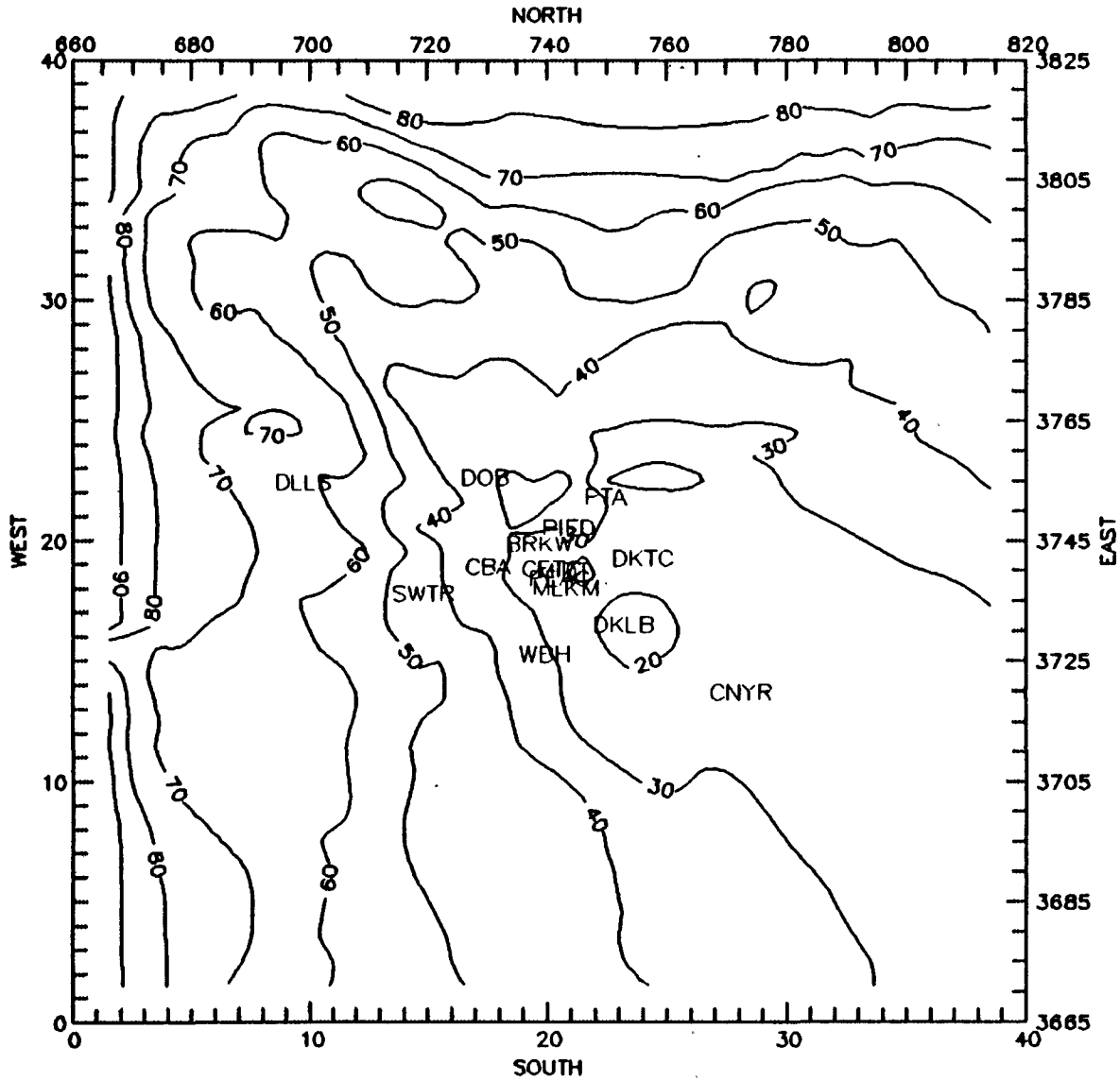

FIGURE A-2b . Percent contribution of boundary VOC tracer at 800 EST, 4 June 1984.

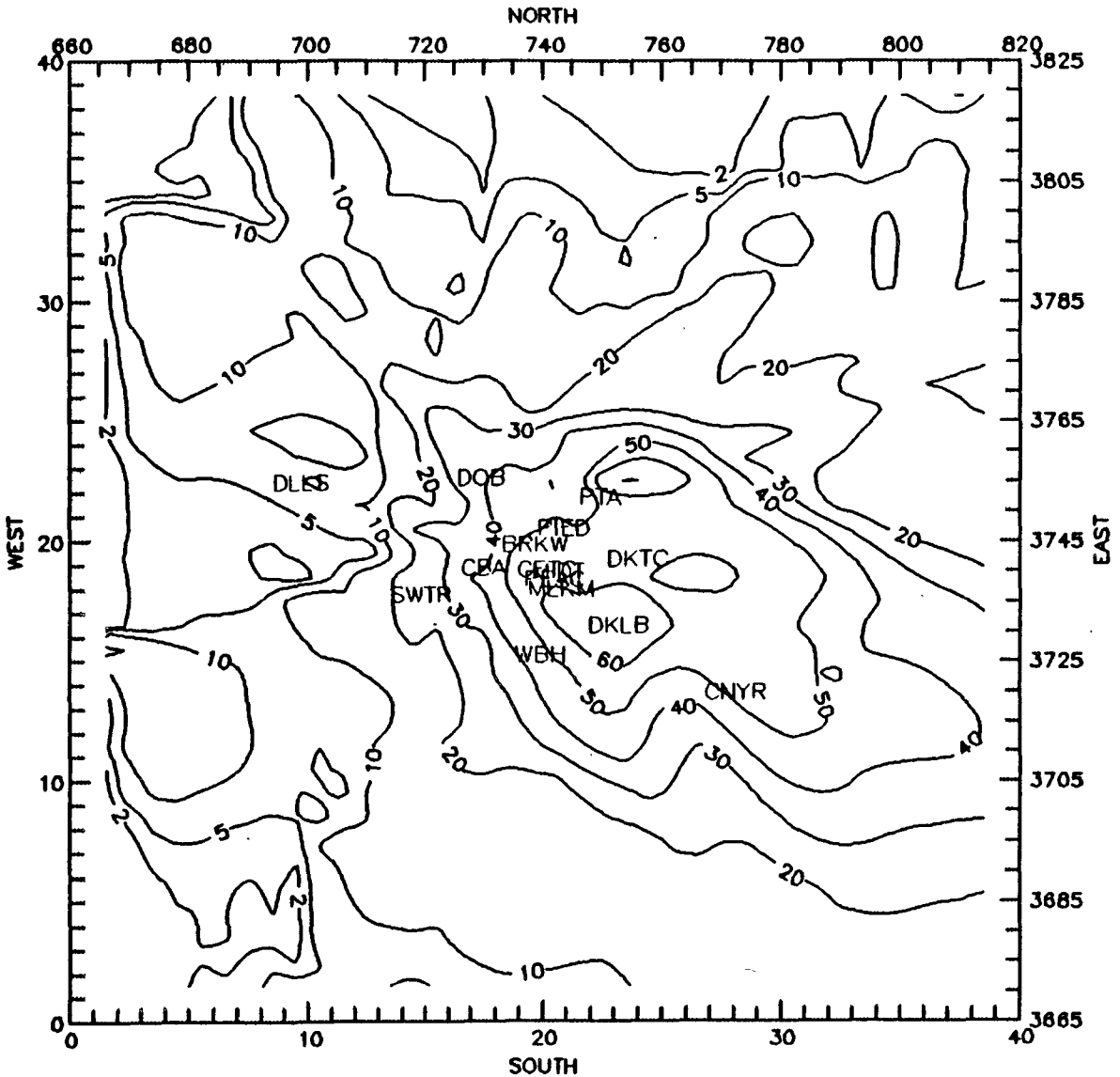

FIGURE A-2c. Percent contribution of anthropogenic VOC tracer at 800 EST, 4 June 1984.

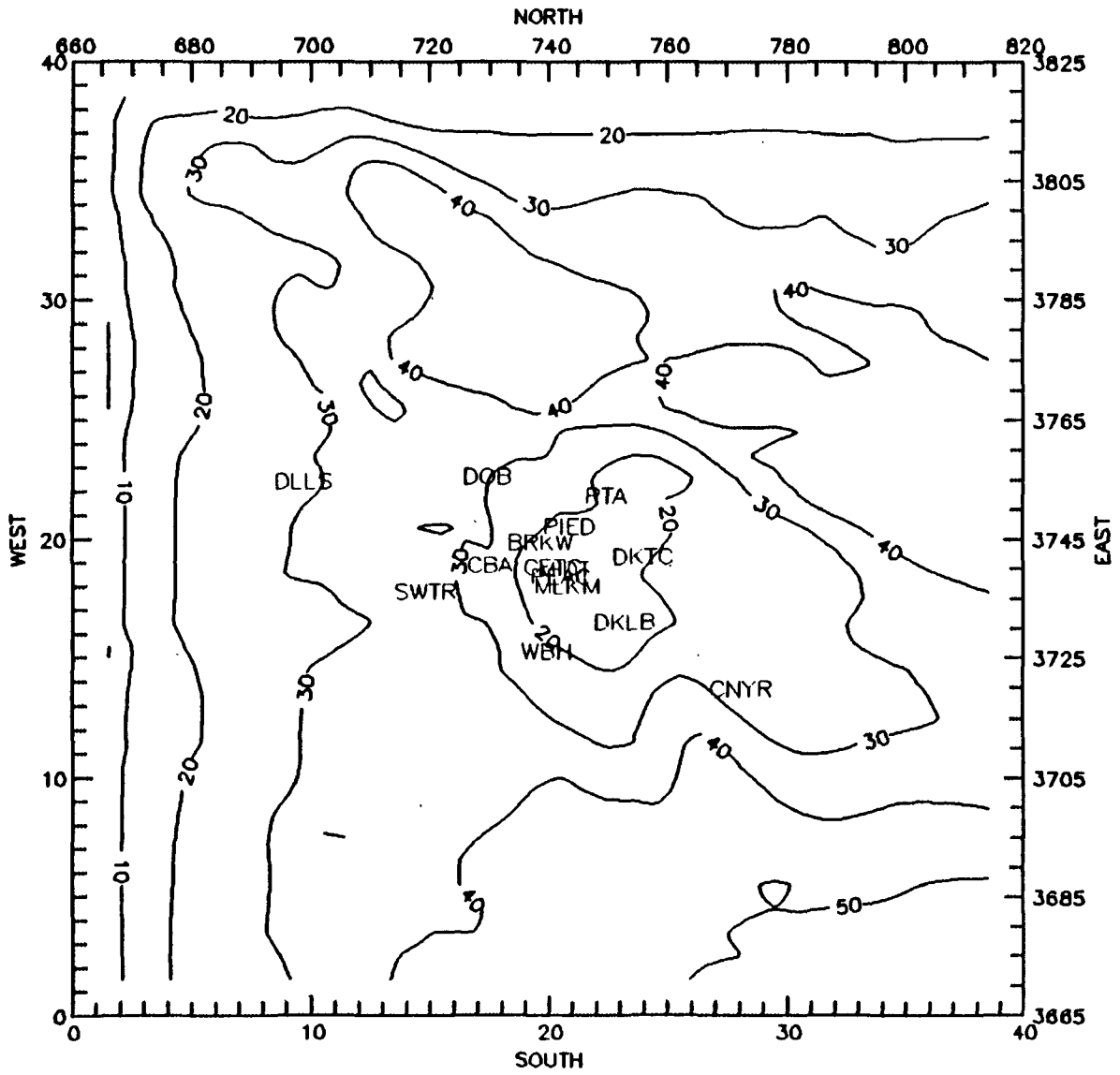

FIGURE A-2d . Percent contribution of biogenic VOC tracer at 800 EST, 4 June 1984.

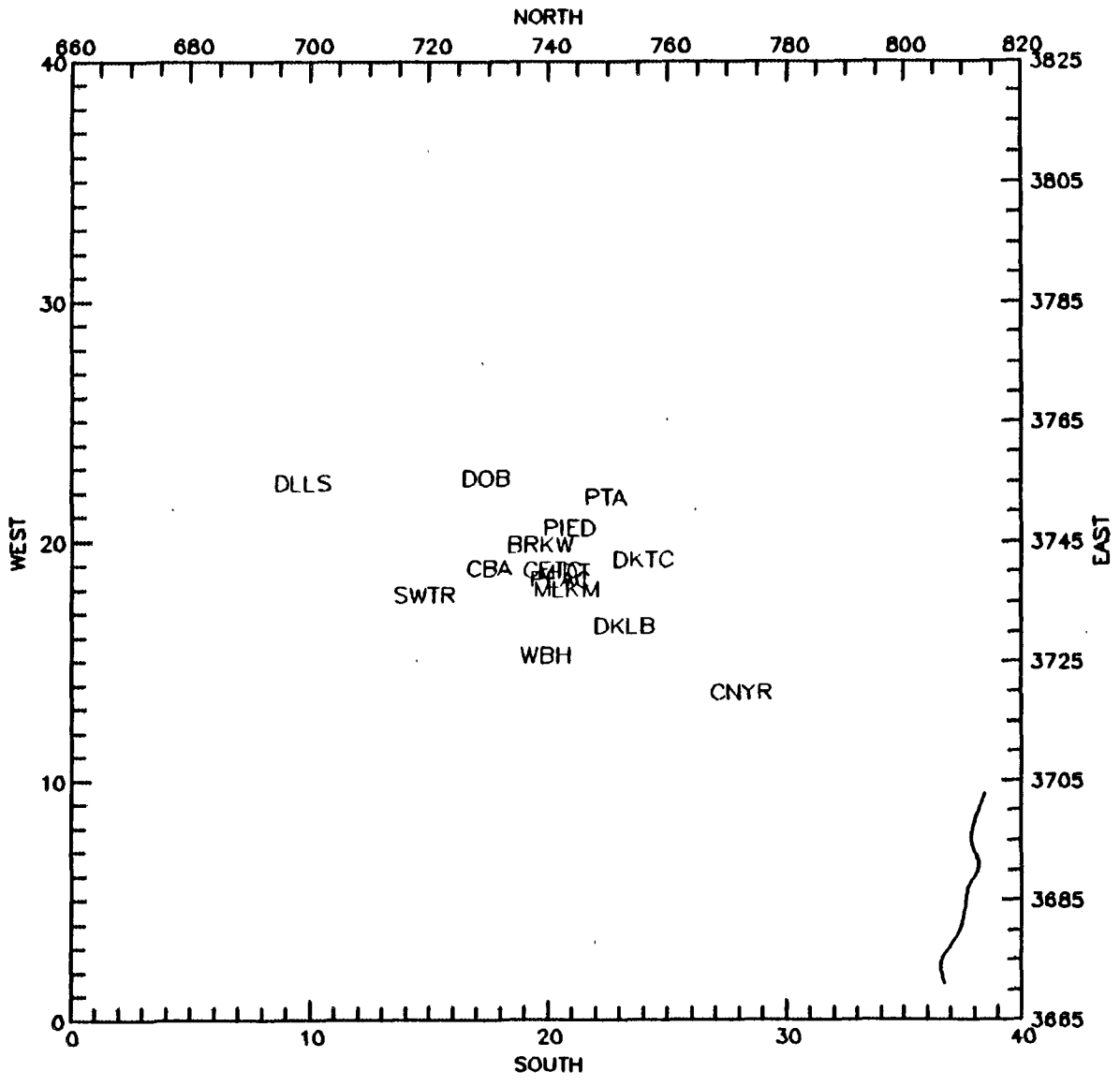

FIGURE A-3a. Percent contribution of initial NOx tracer at 1200 EST, 4 June 1984.

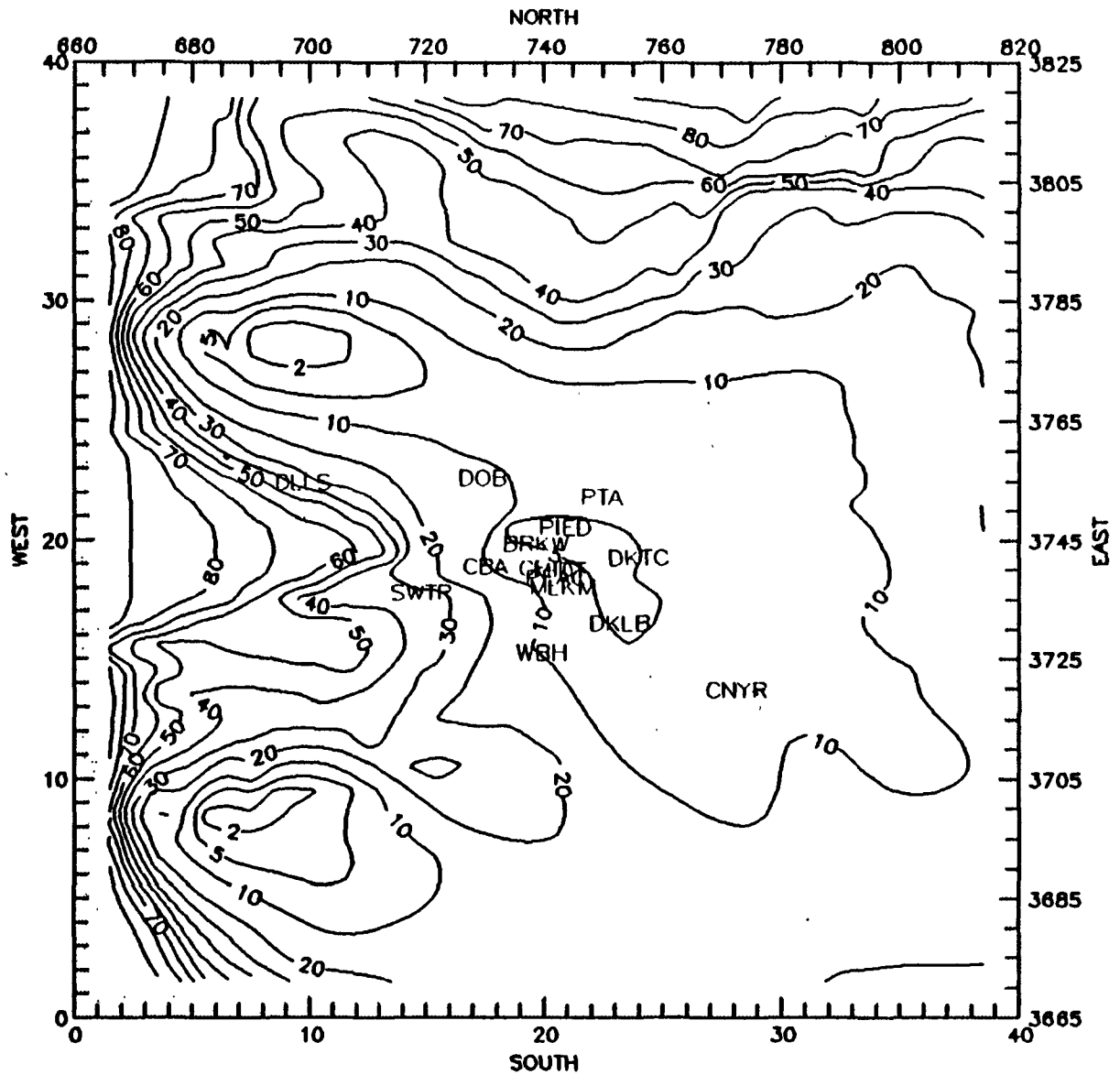

FIGURE A-3b. Percent contribution of boundary NOx tracer at 1200 EST, 4 June 1984.

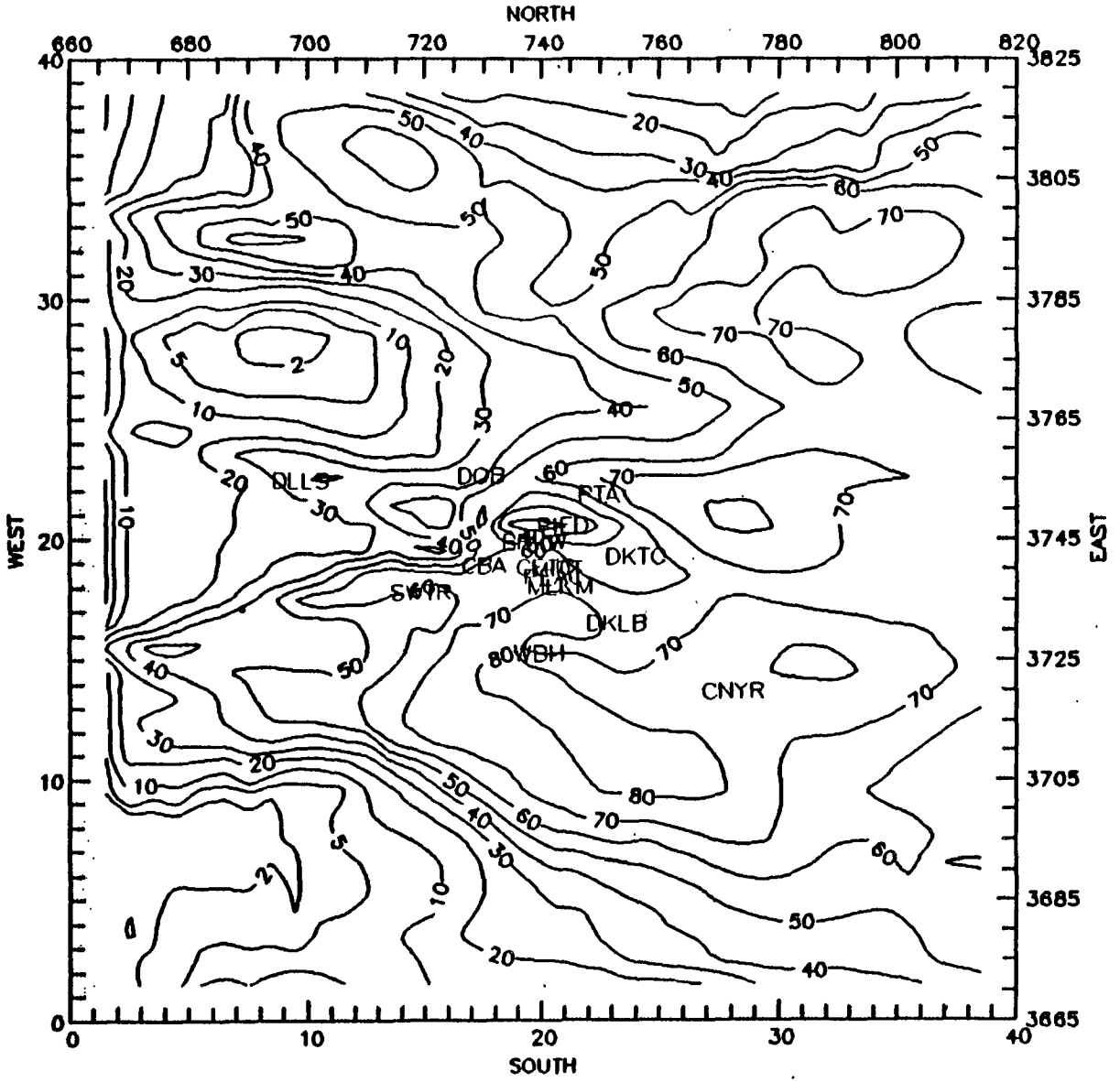

FIGURE A-3c . Percent contribution of area source NOx tracer at 1200 EST, 4 June 1984.

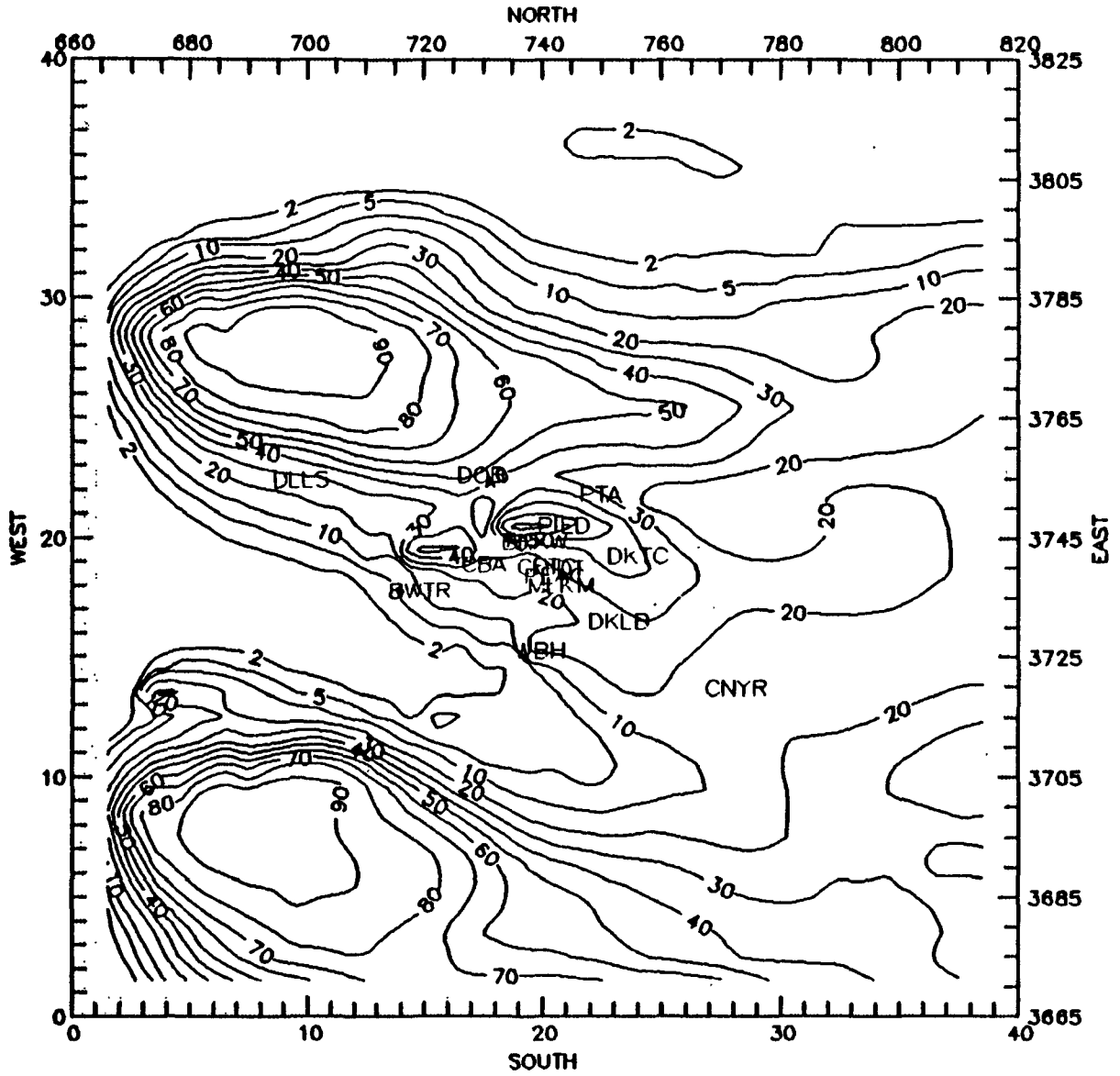

FIGURE A-3d. Percent contribution of point source NOx tracer at 1200 EST. 4 June 1984.

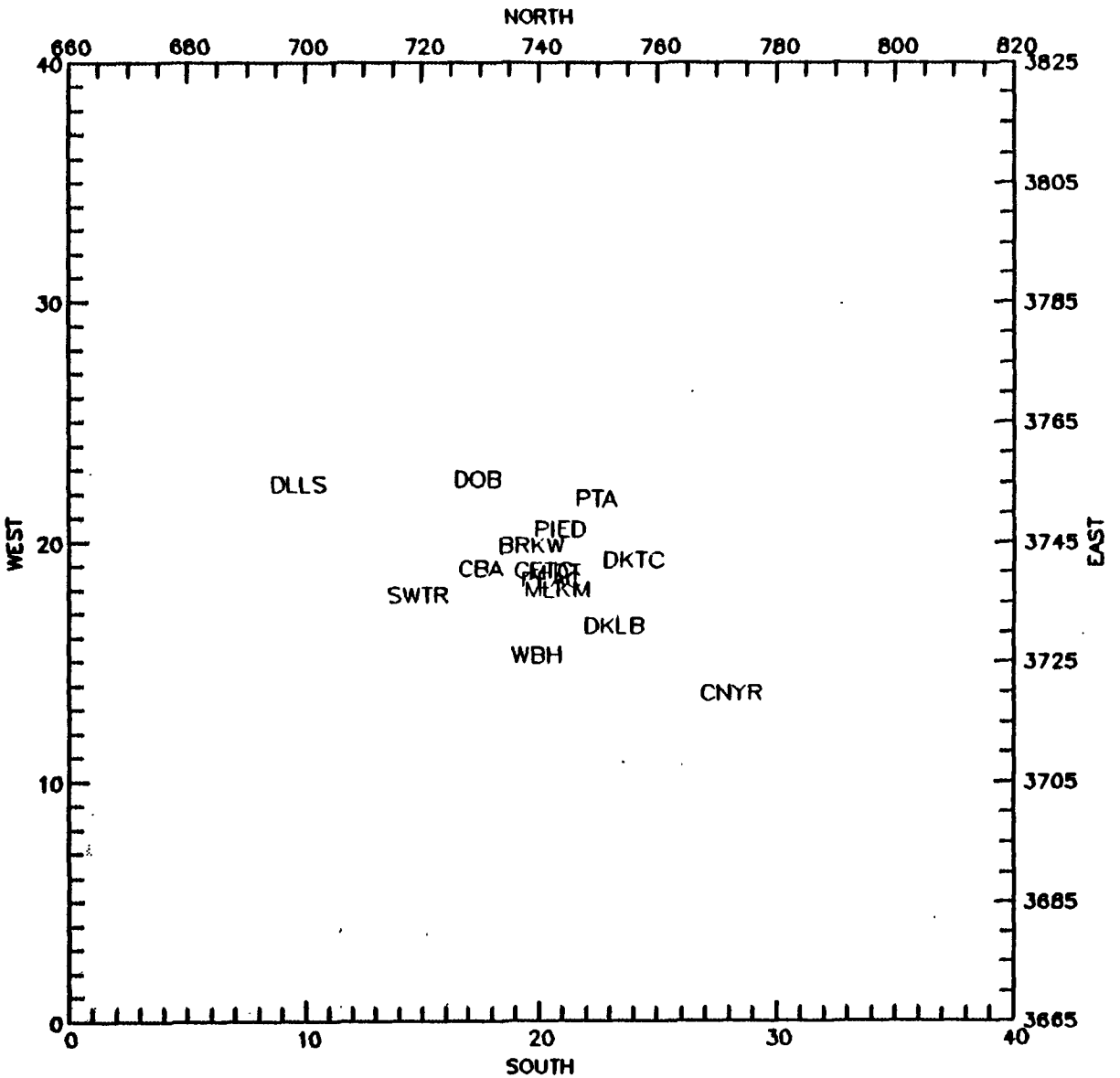

FIGURE A-4a. Percent contribution of initial VOC tracer at 1200 EST, 4 June 1984.

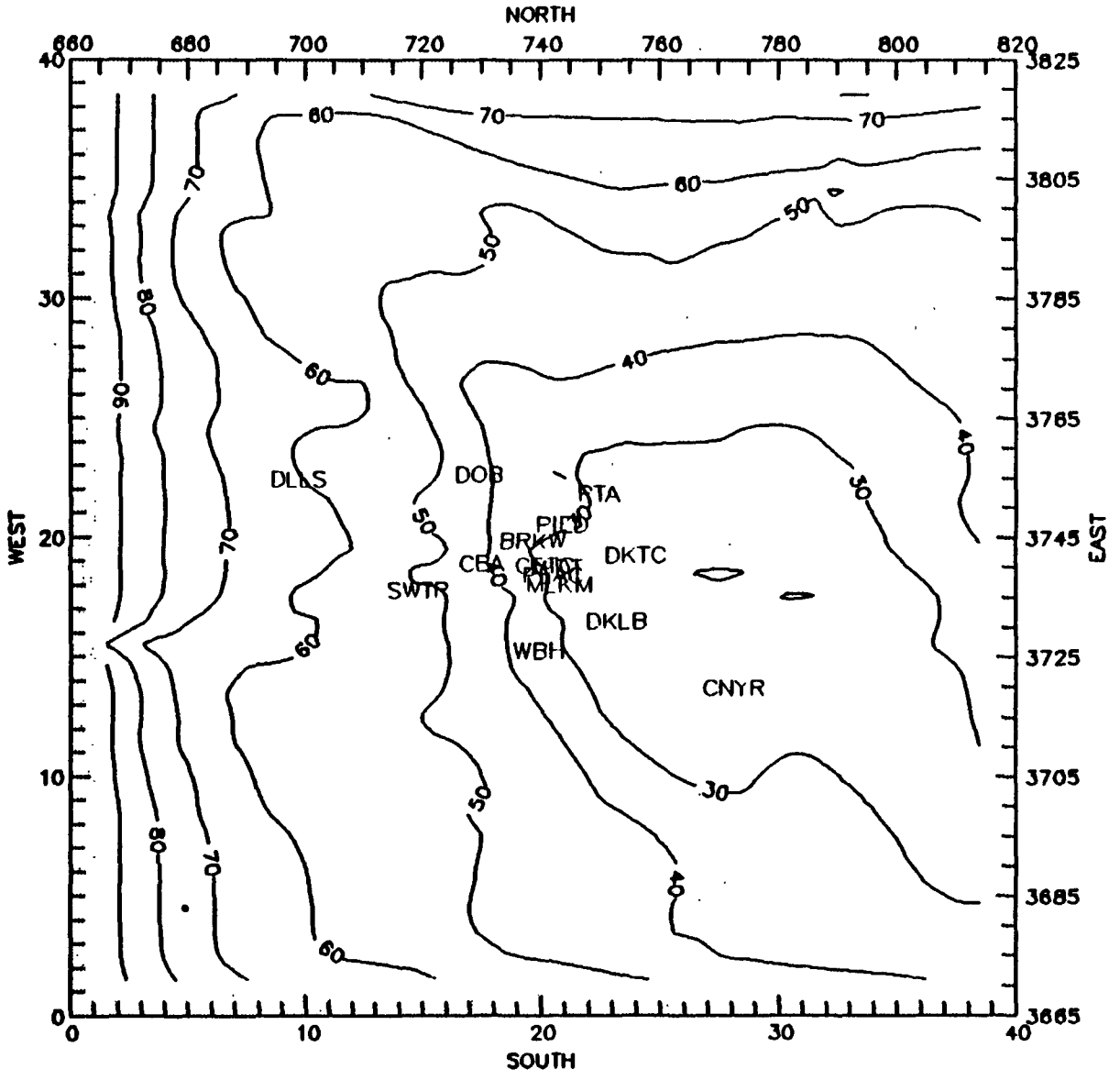

FIGURE A-4b . Percent contribution of boundary VOC tracer at 1200 EST, 4 June 1984.

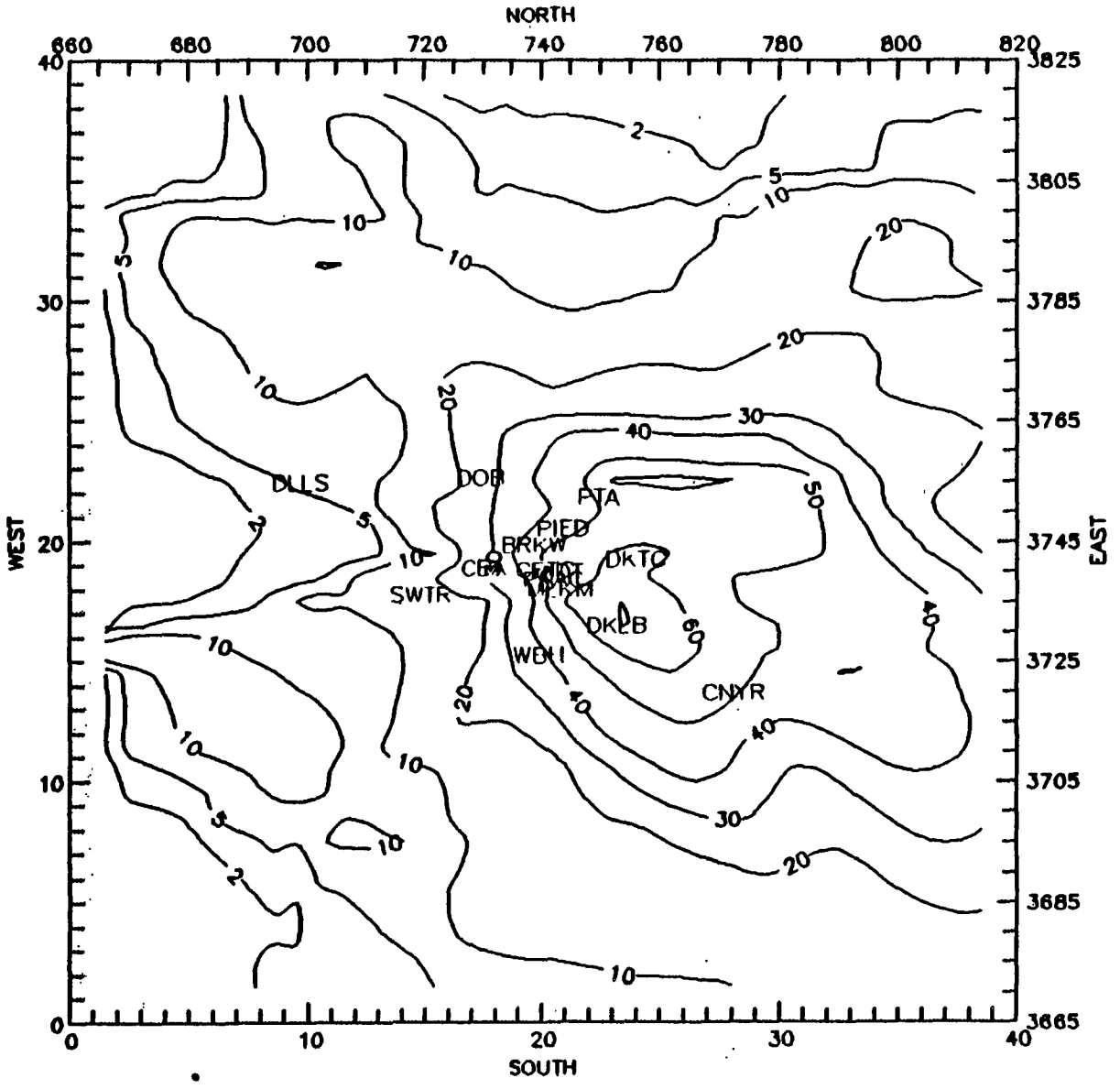

FIGURE A-4c. Percent contribution of anthropogenic VOC tracer at 1200 EST, 4 June 1984.

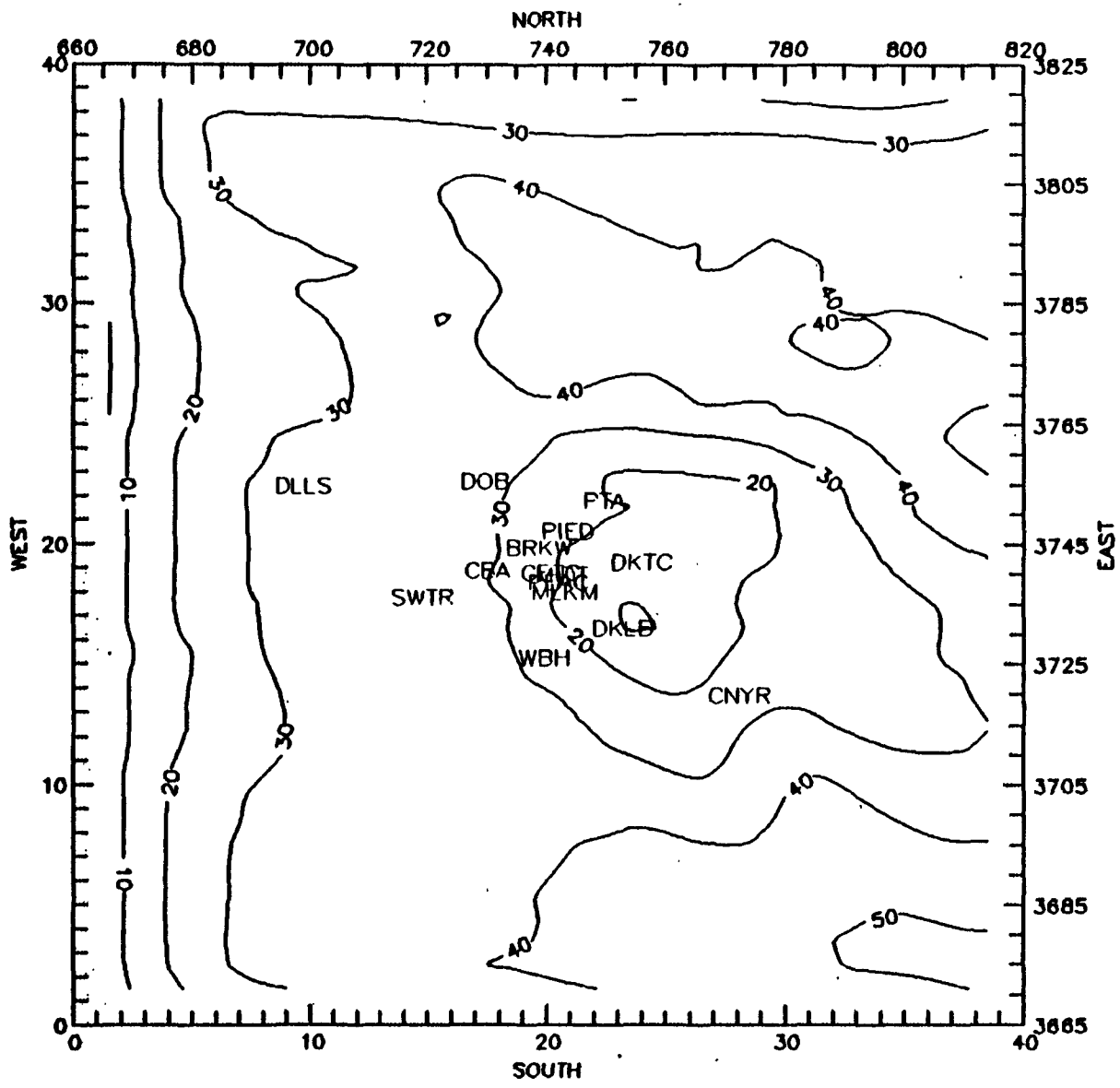

FIGURE A-4d. Percent contribution of biogenic VOC tracer at 1200 EST, 4 June 1984

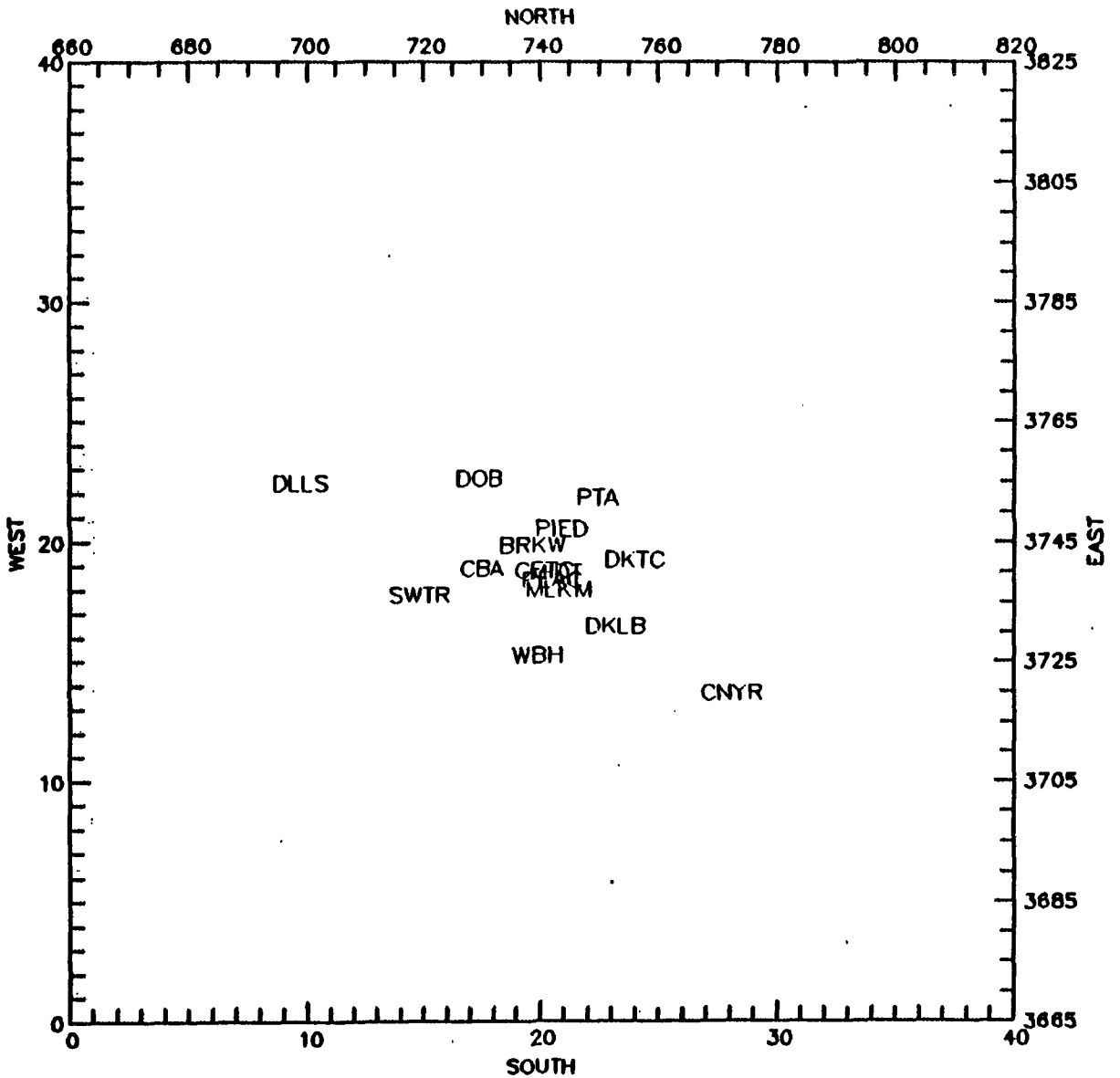

FIGURE A-5a. Percent contribution of initial NOx tracer at 1600 EST, 4 June 1984.

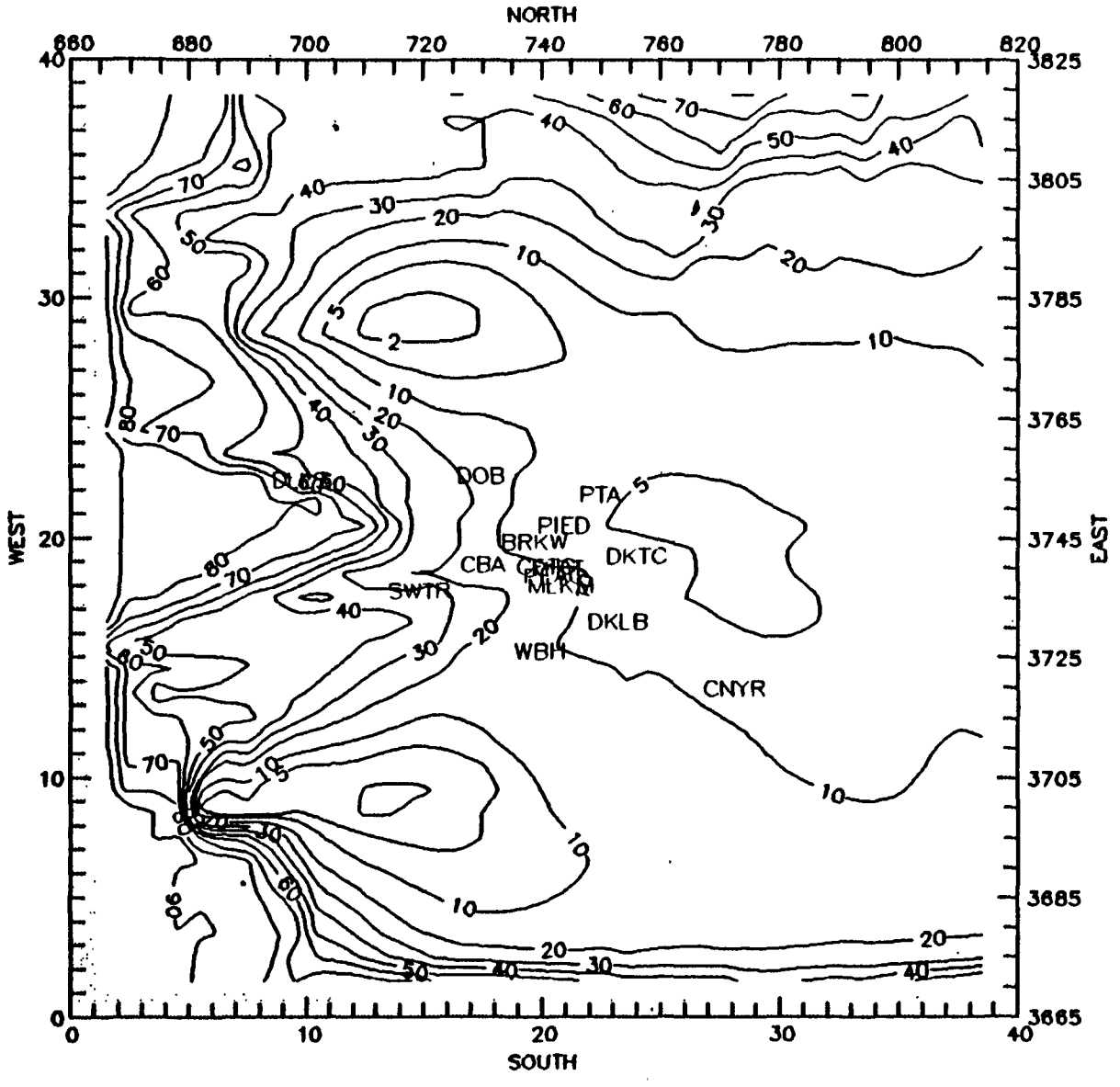

FIGURE A-5b . Percent contribution of boundary NOx tracer at 1600 EST, 4 June 1984.

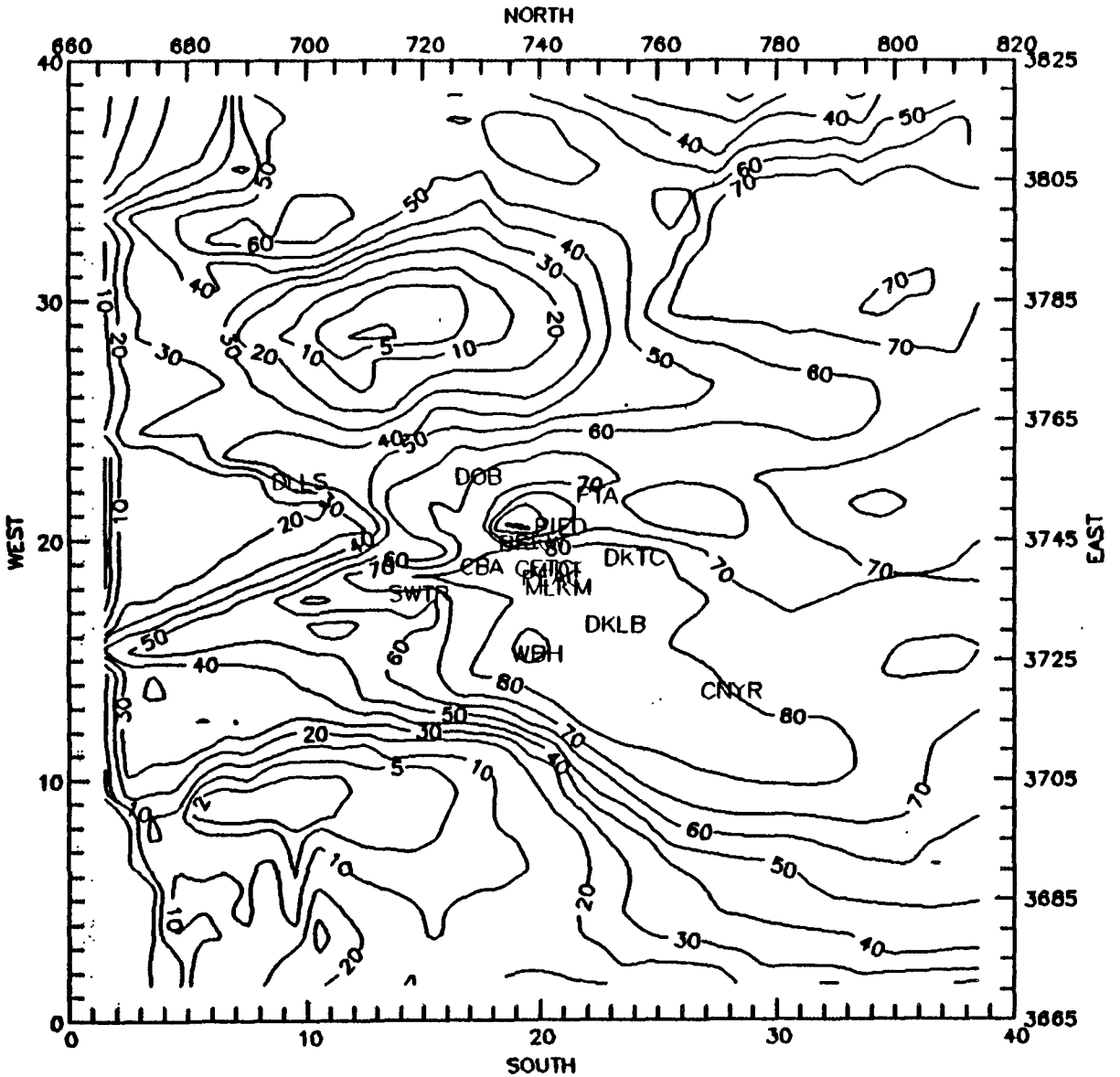

FIGURE A-5c . Percent contribution of area source NOx tracer at 1600 EST, 4 June 1984.

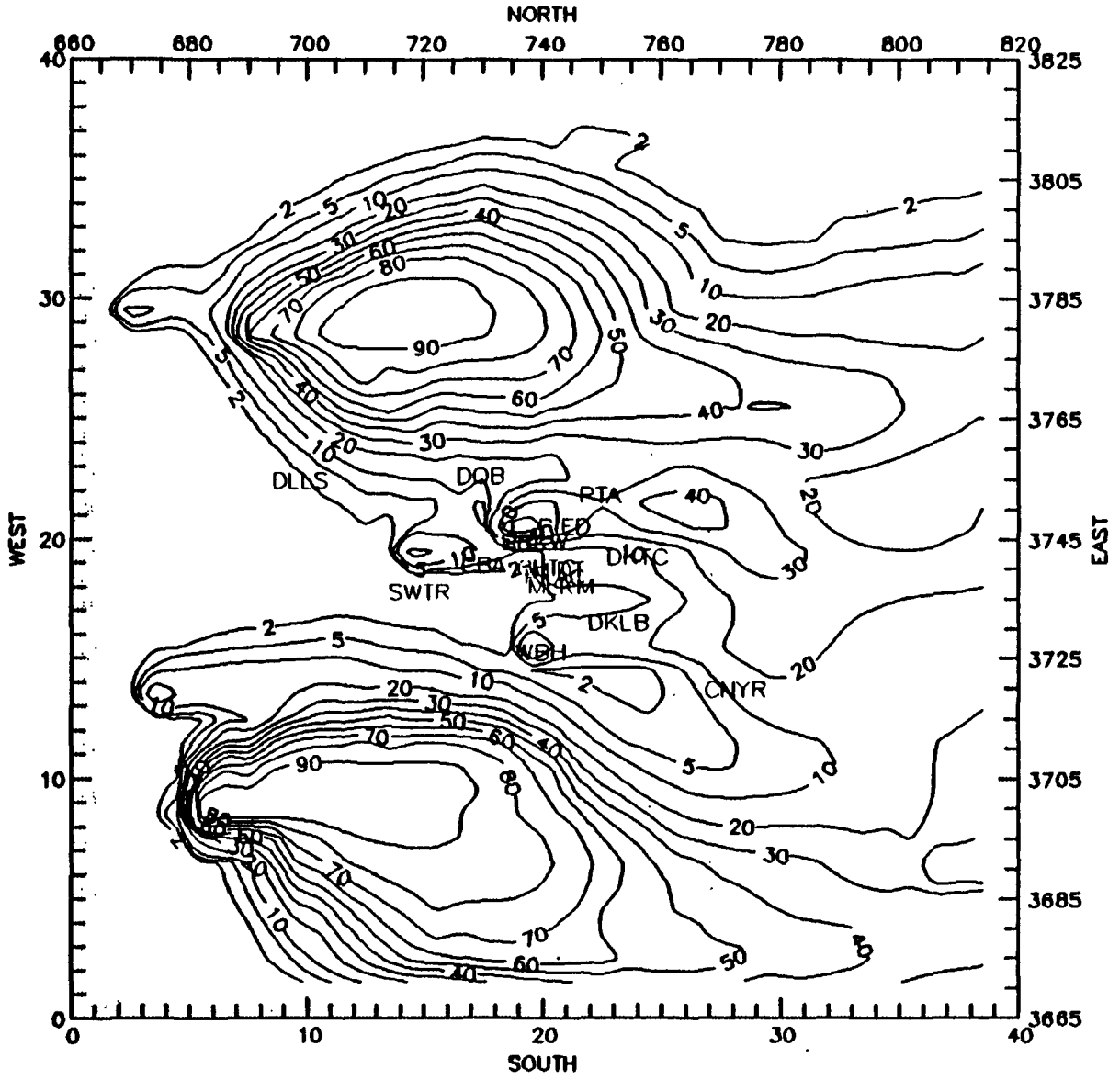

FIGURE A-5d . Percent contribution of point source NOx tracer at 1600 EST, 4 June 1984.

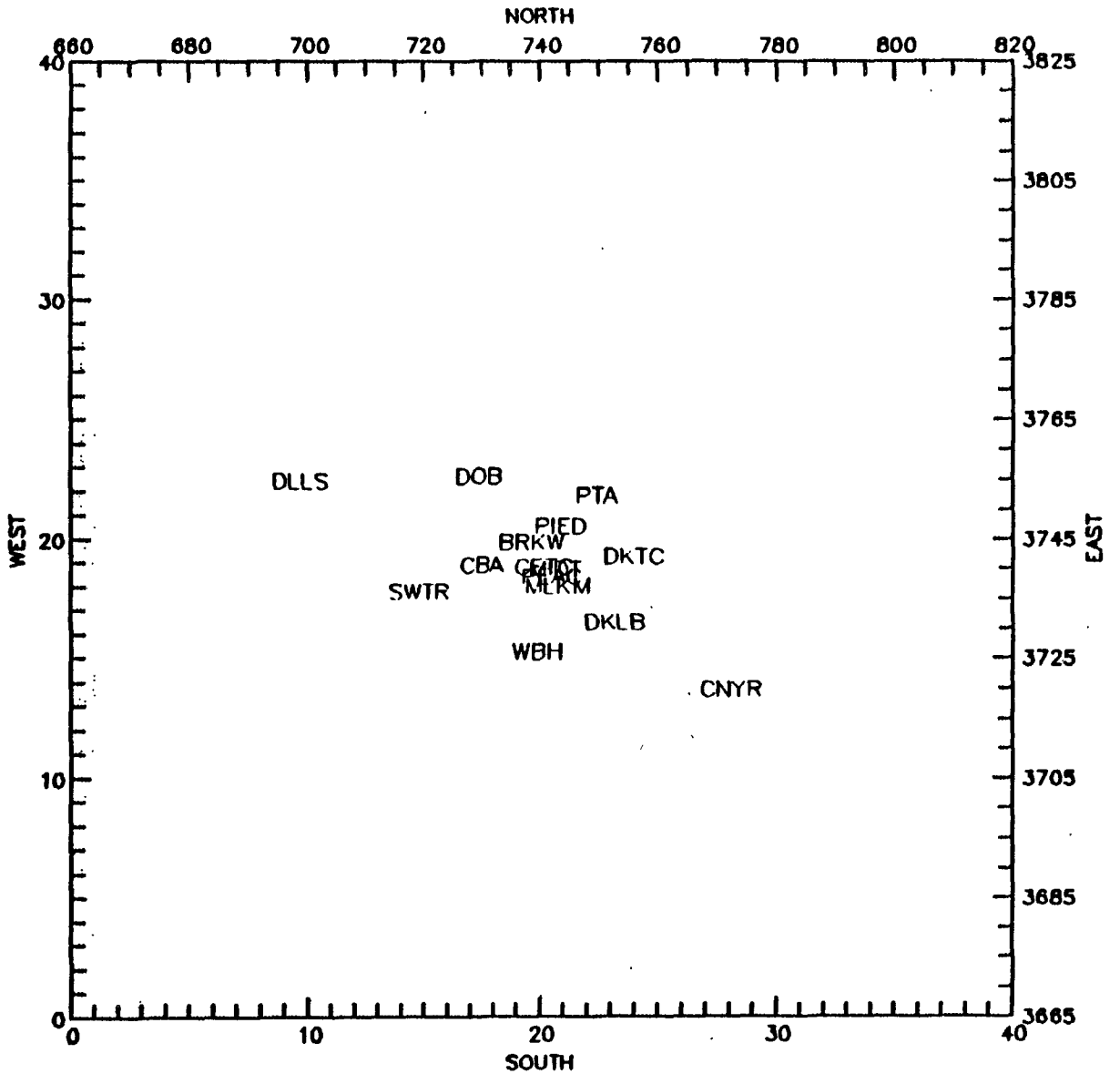

FIGURE A-6a . Percent contribution of initial VOC tracer at 1600 EST, 4 June 1984.

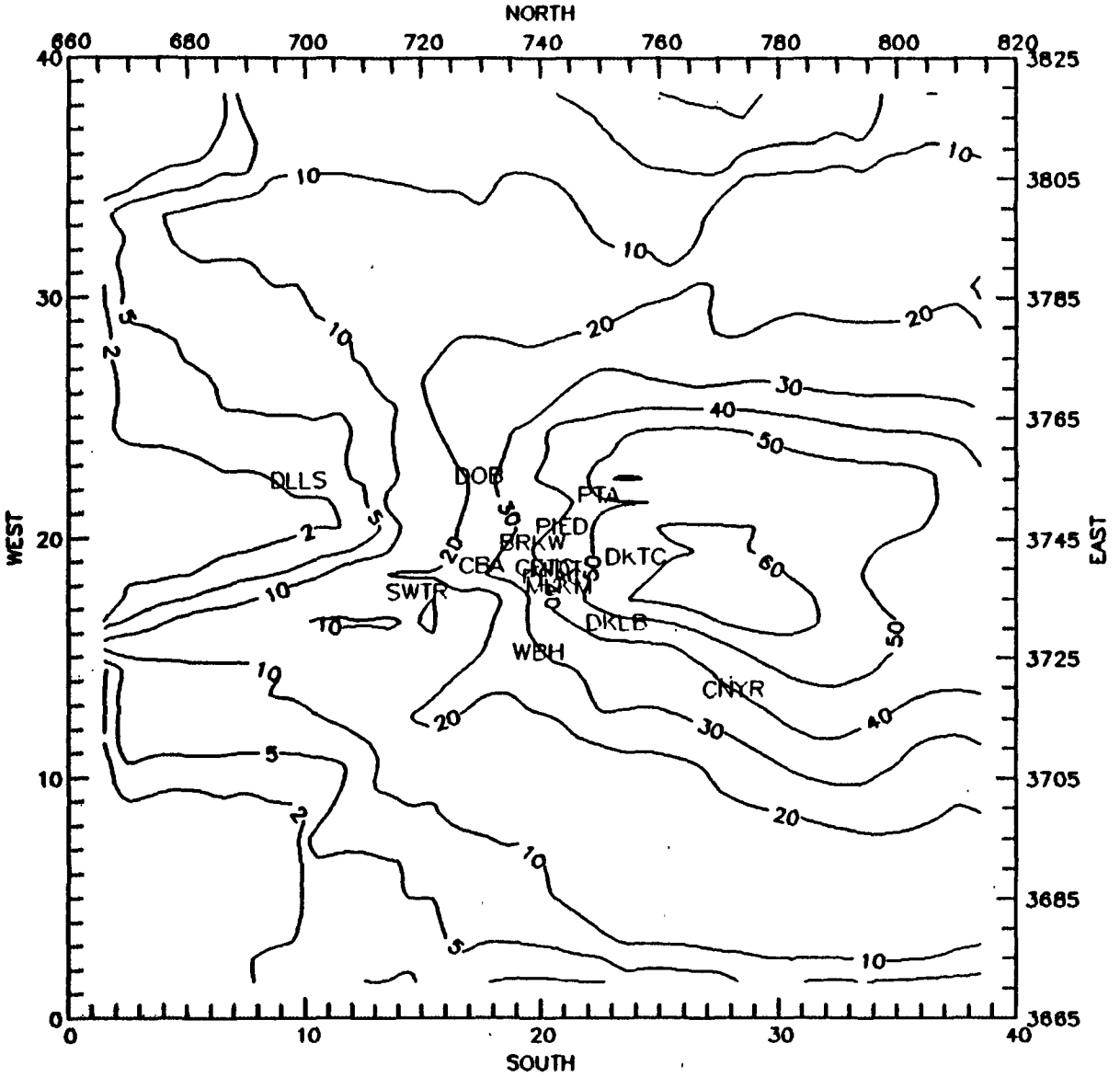

FIGURE A-6b. Percent contribution of anthropogenic VOC tracer at 1600 EST, 4 June 1984.

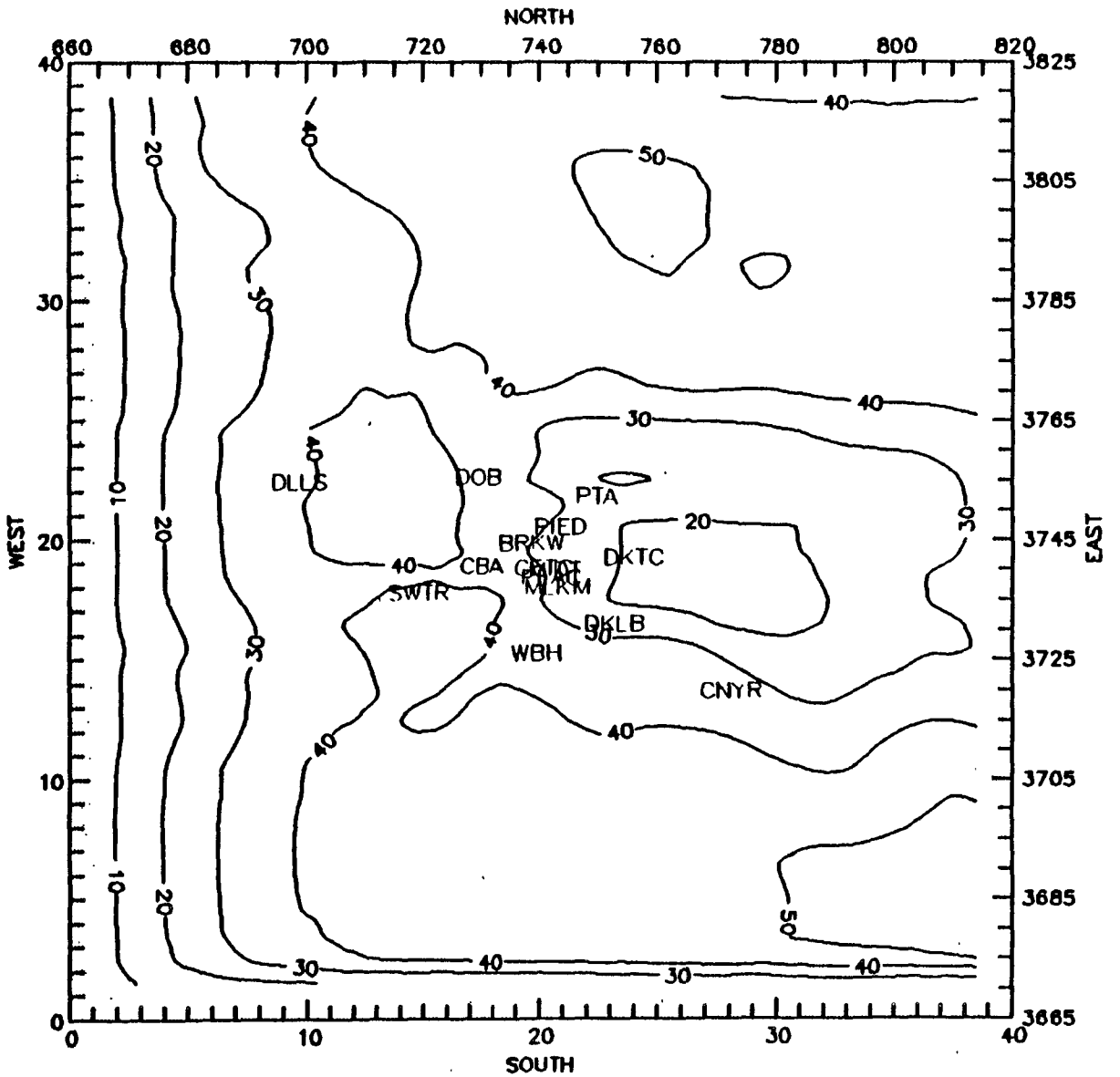

FIGURE A-6c. Percent contribution of biogenic VOC tracer at 1600 EST, 4 June 1984.

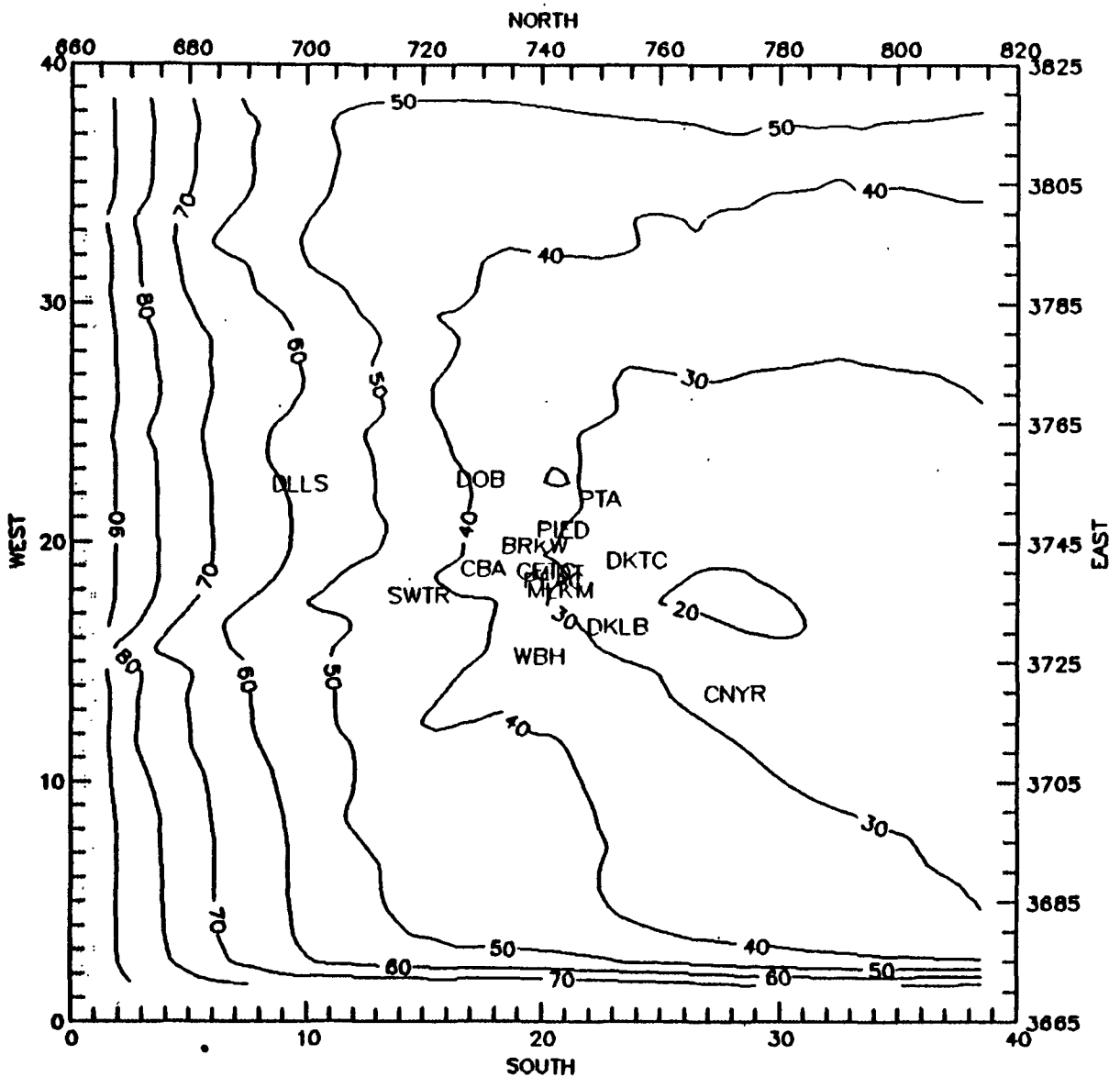

FIGURE A-6d. Percent contribution of boundary VOC tracer at 1600 EST, 4 June 1984.

Appendix B

HOURLY PREDICTED OZONE CONCENTRATIONS (pphm) FOR ATLANTA DIAGNOSTIC RUN 1

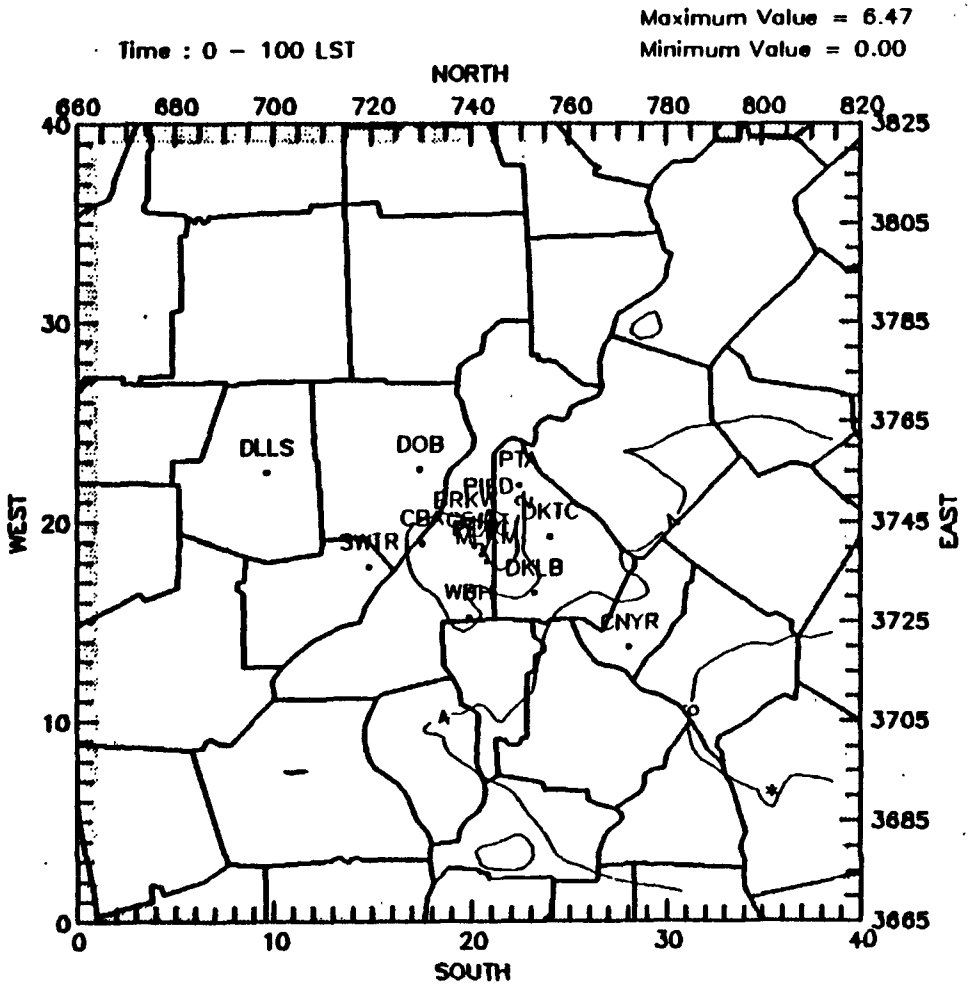

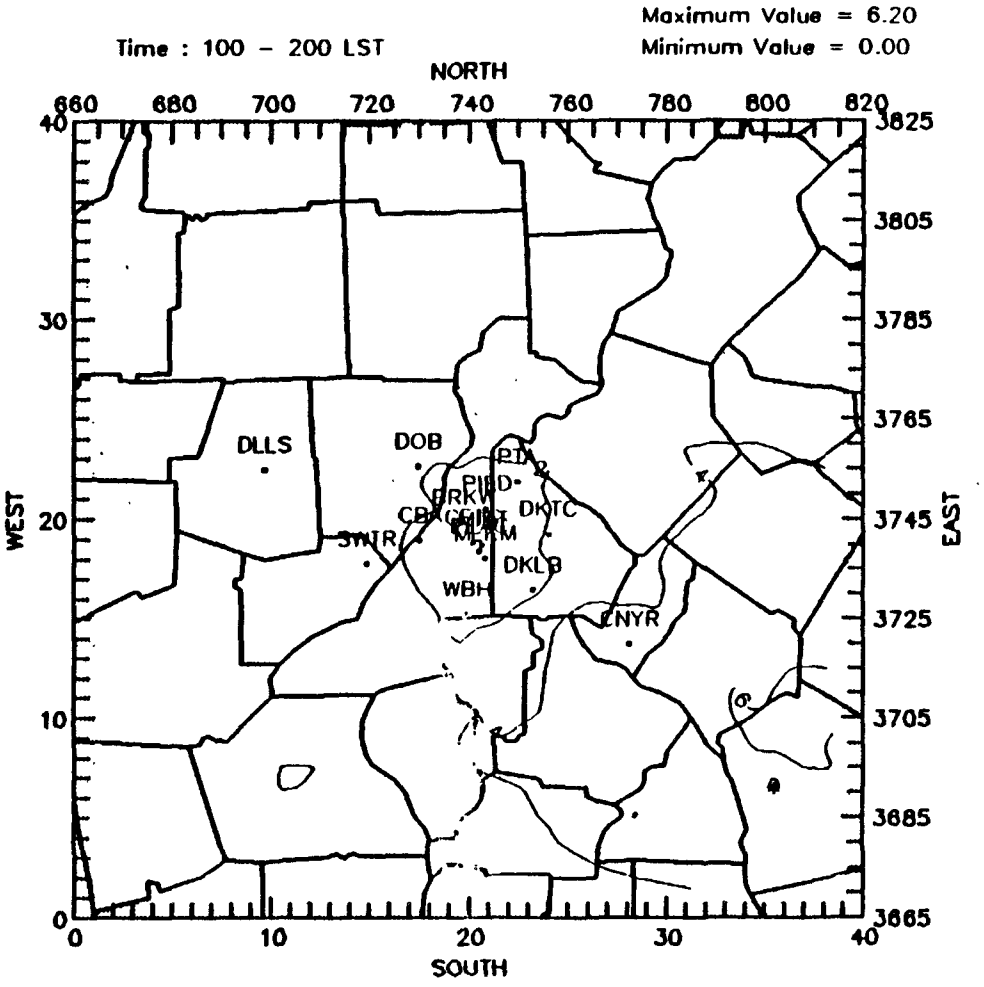

Ozone Concentration Evaluation run #1, June 4, 1984 (pphm)

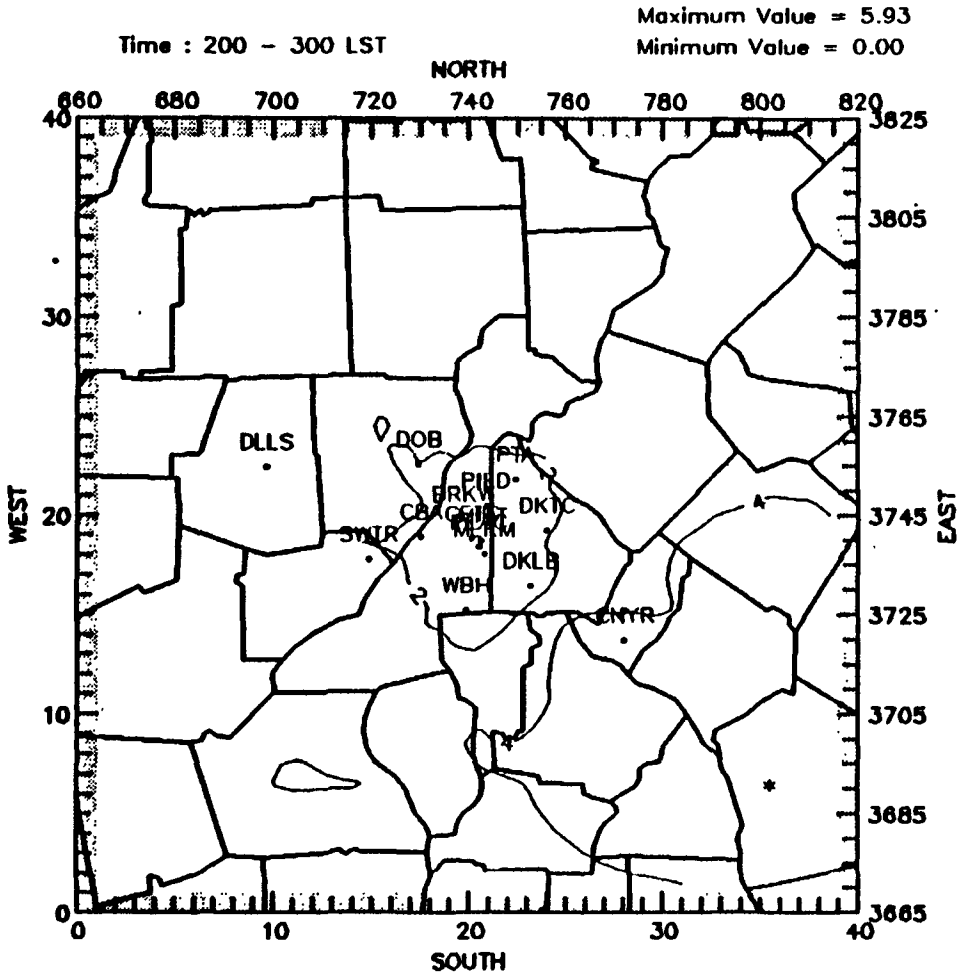

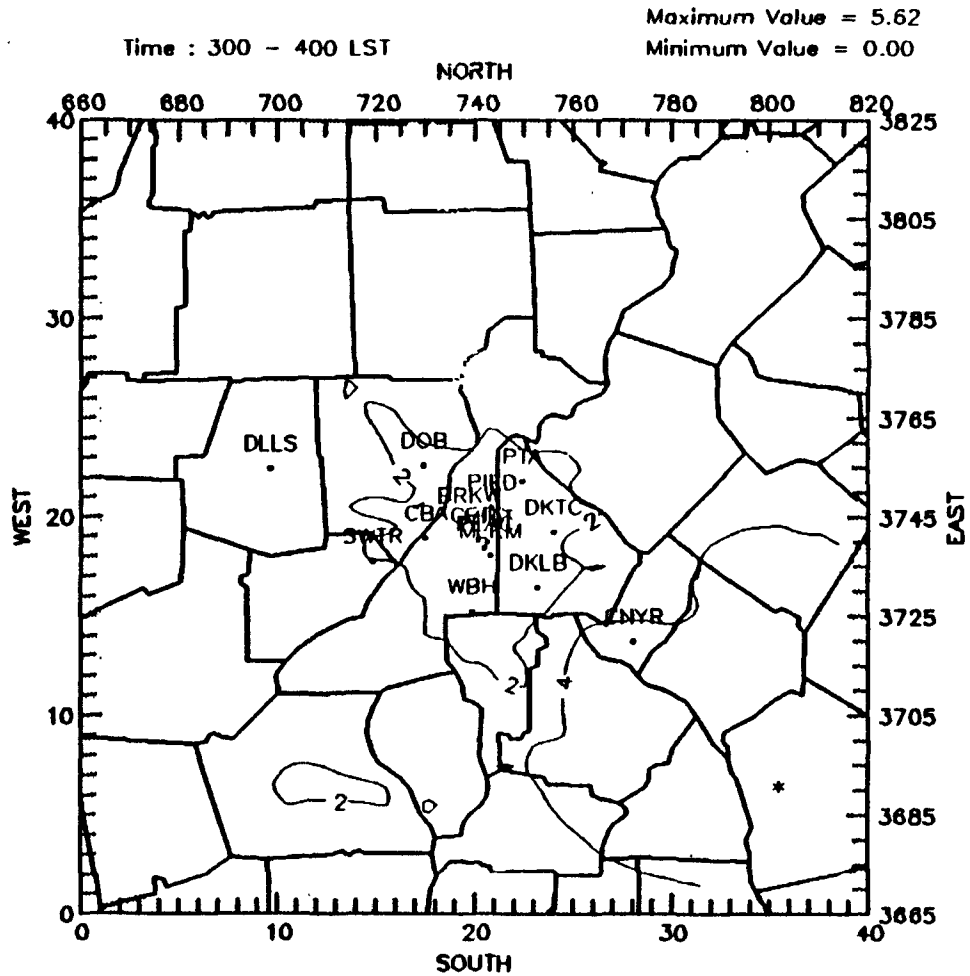

Ozone Concentration Evaluation run #1, June 4, 1984 (pphm)

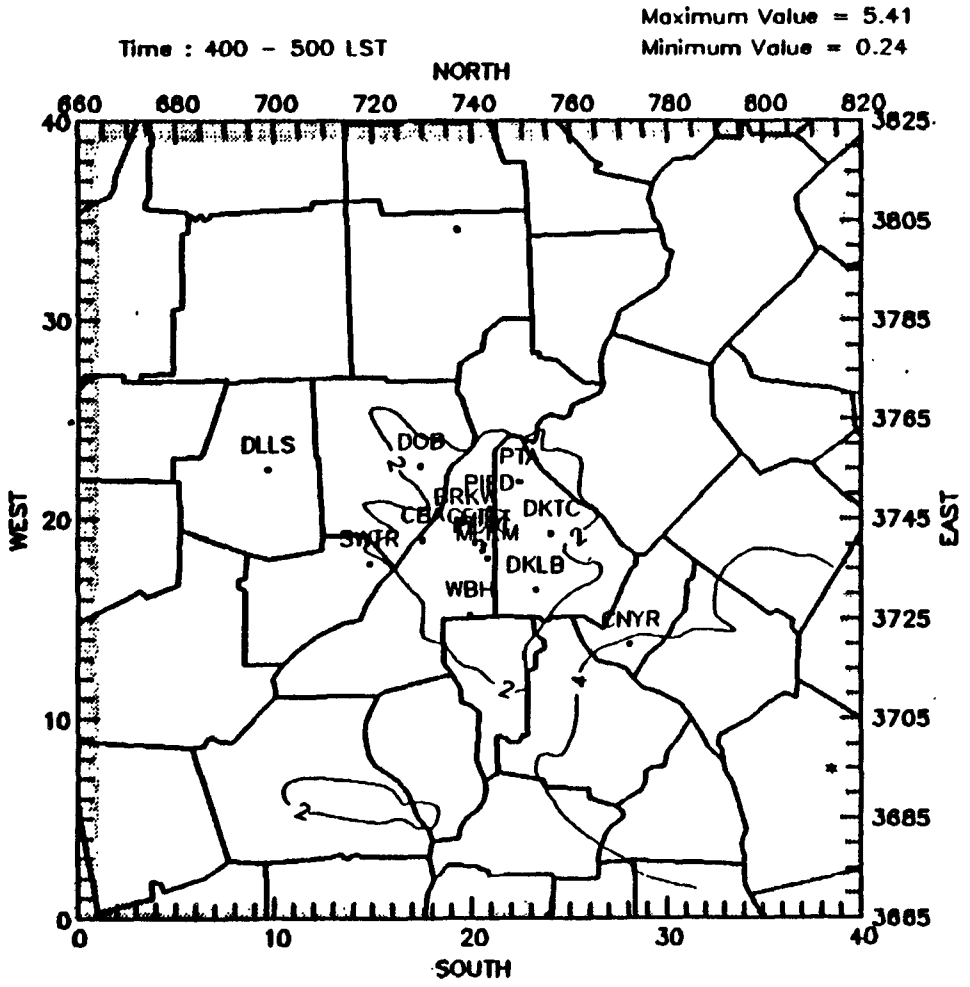

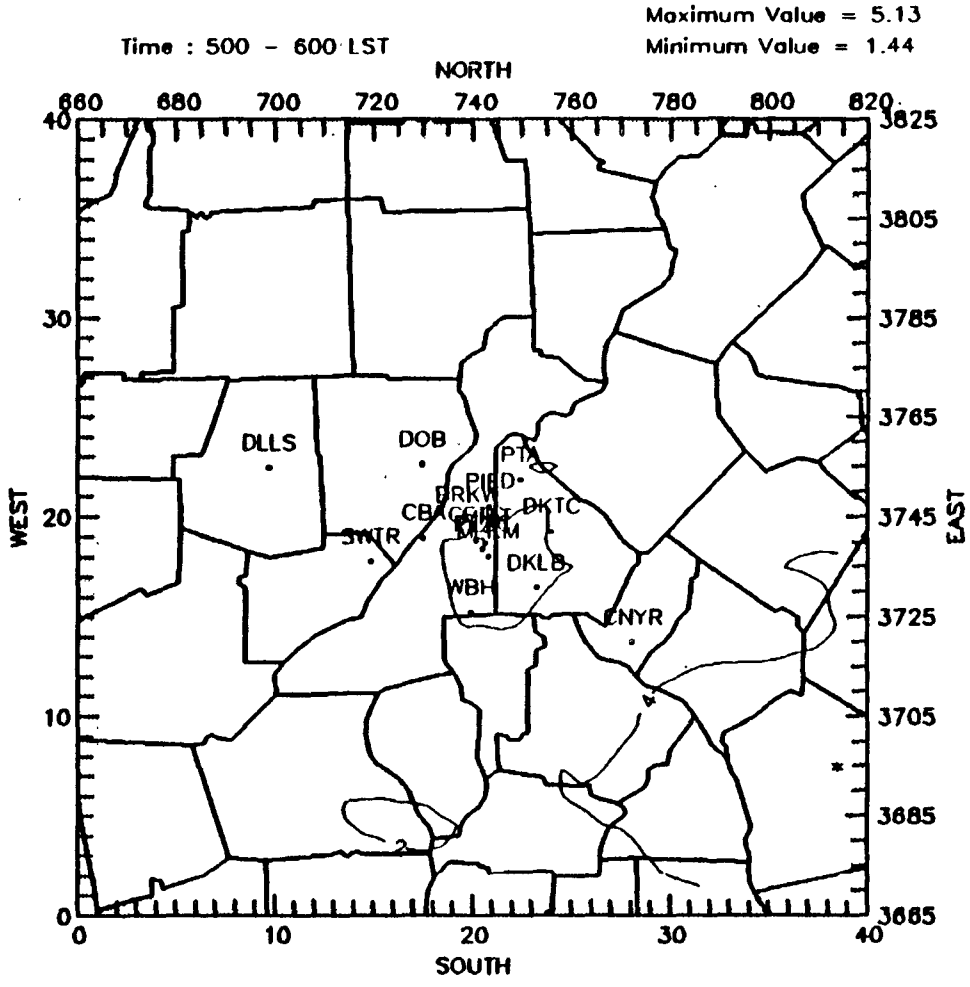

Ozone Concentration Evaluation run #1, June 4, 1984 (pphm)

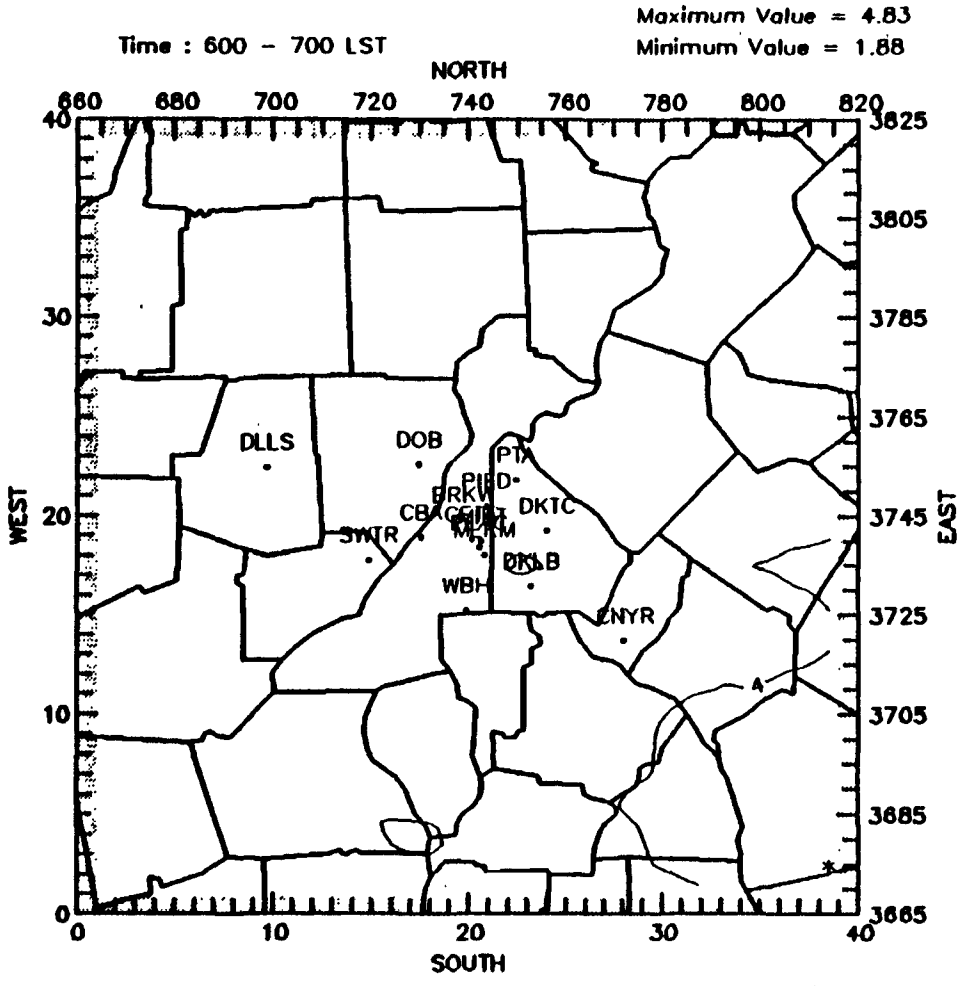

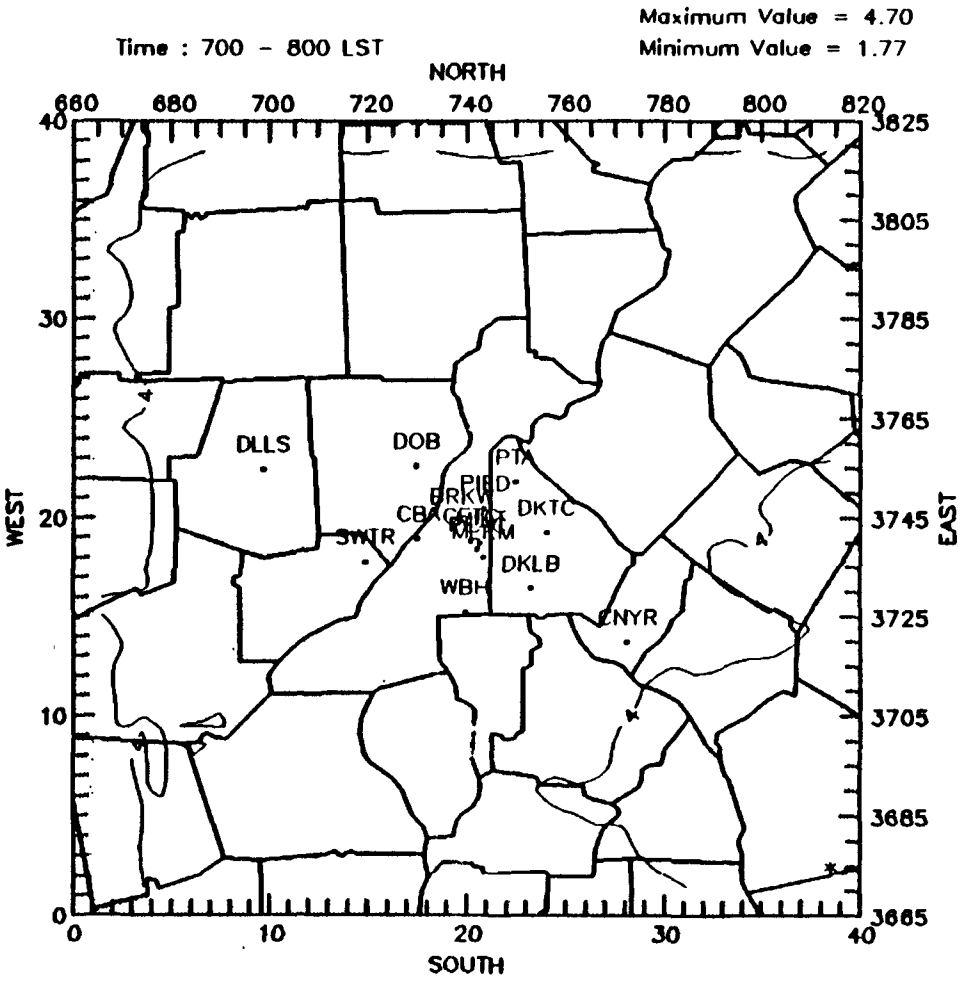

Ozone Concentration Evaluation run #1, June 4, 1984 (pphm)

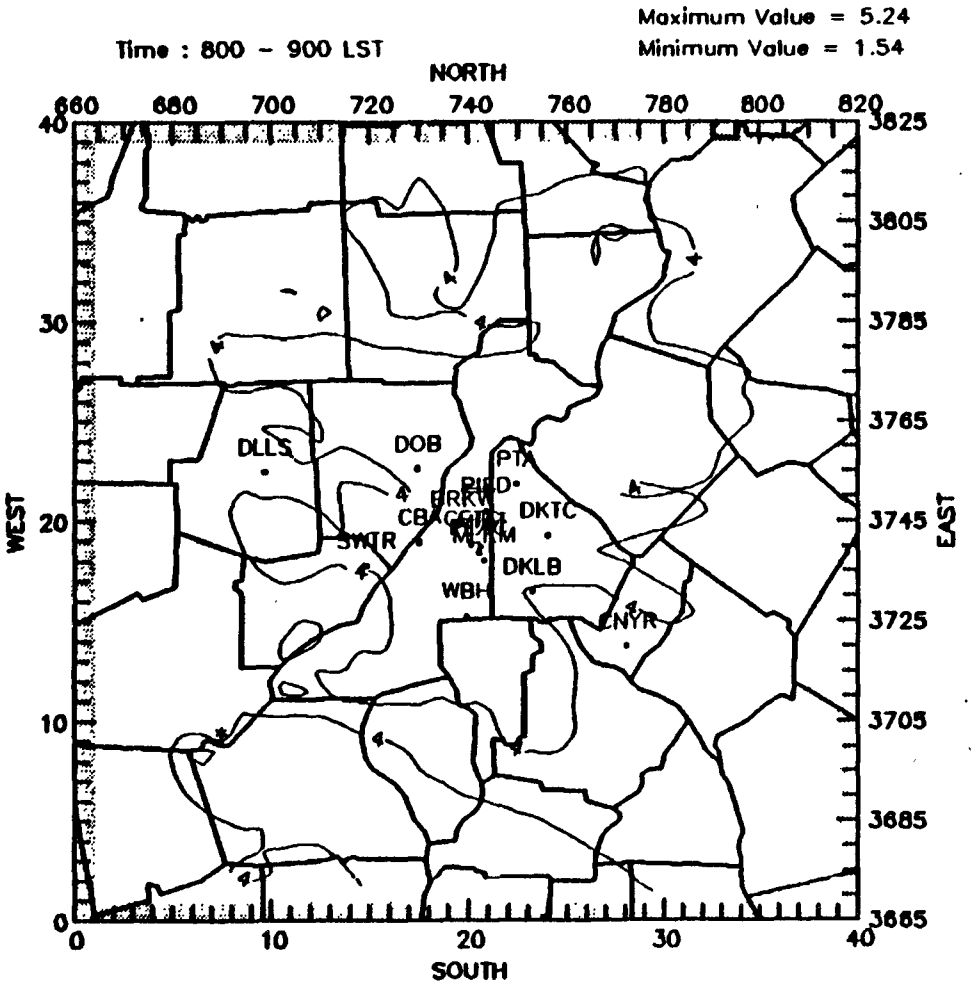

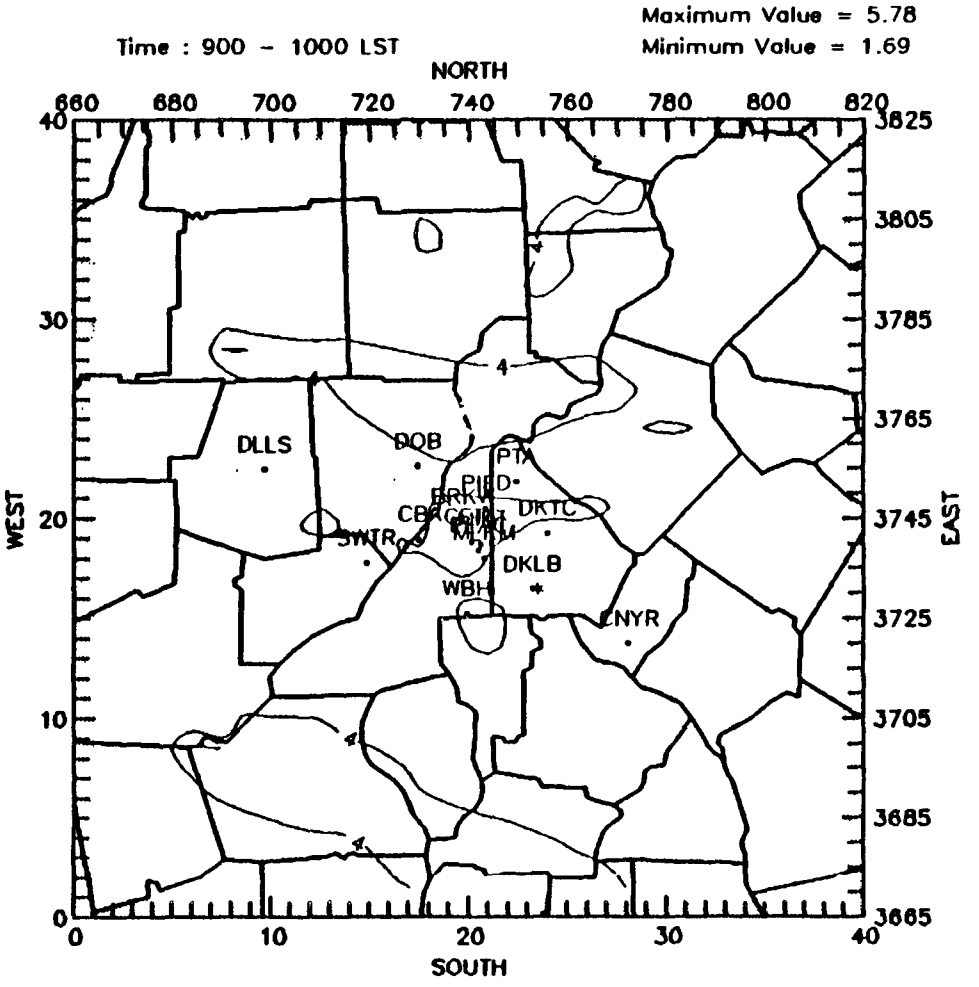

Ozone Concentration Evaluation run #1, June 4, 1984 (pphm)

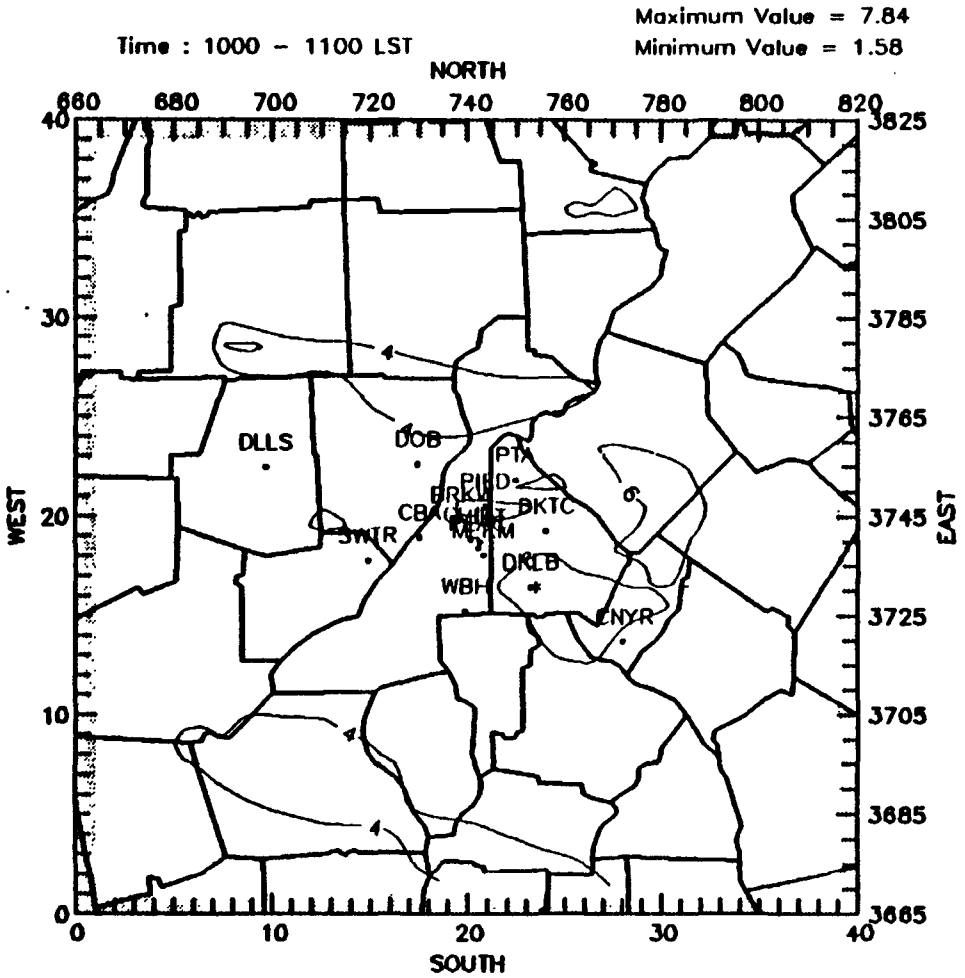

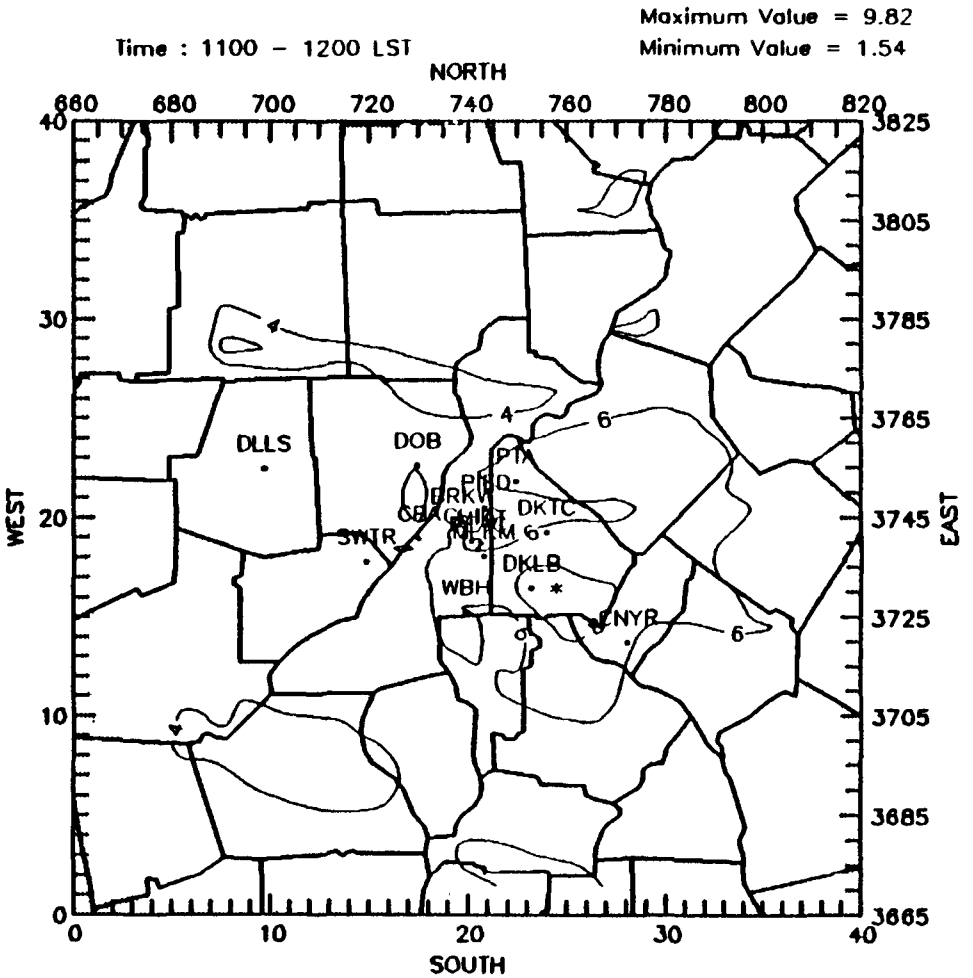

Ozone Concentration Evaluation run #1, June 4, 1984 (pphm)

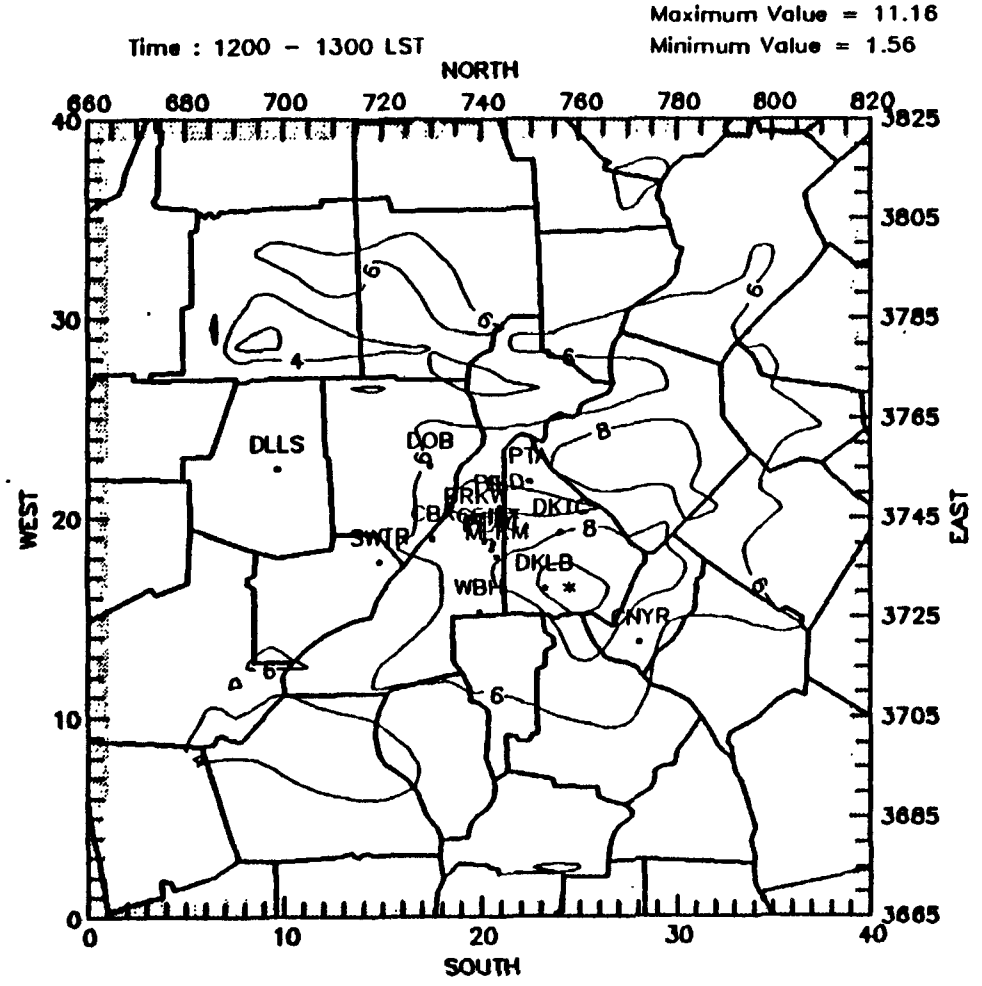

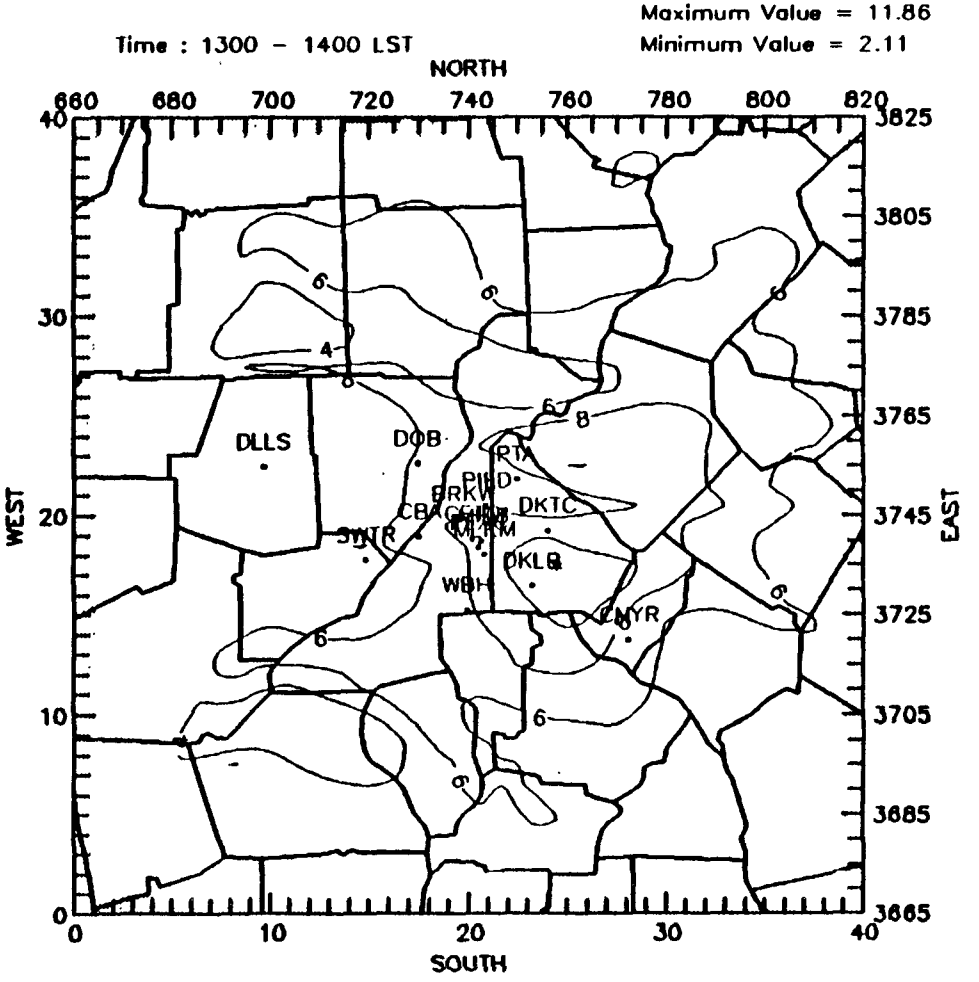

Ozone Concentration Evaluation run #1, June 4, 1984 (pphm)

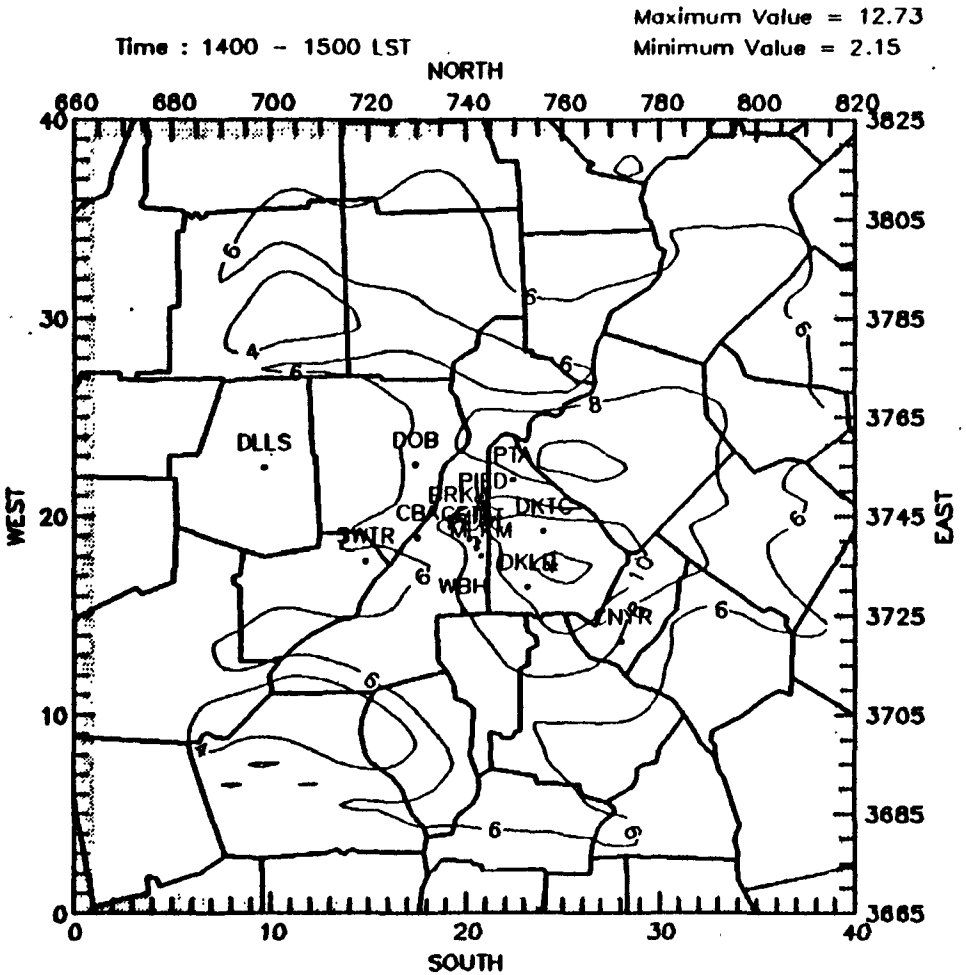

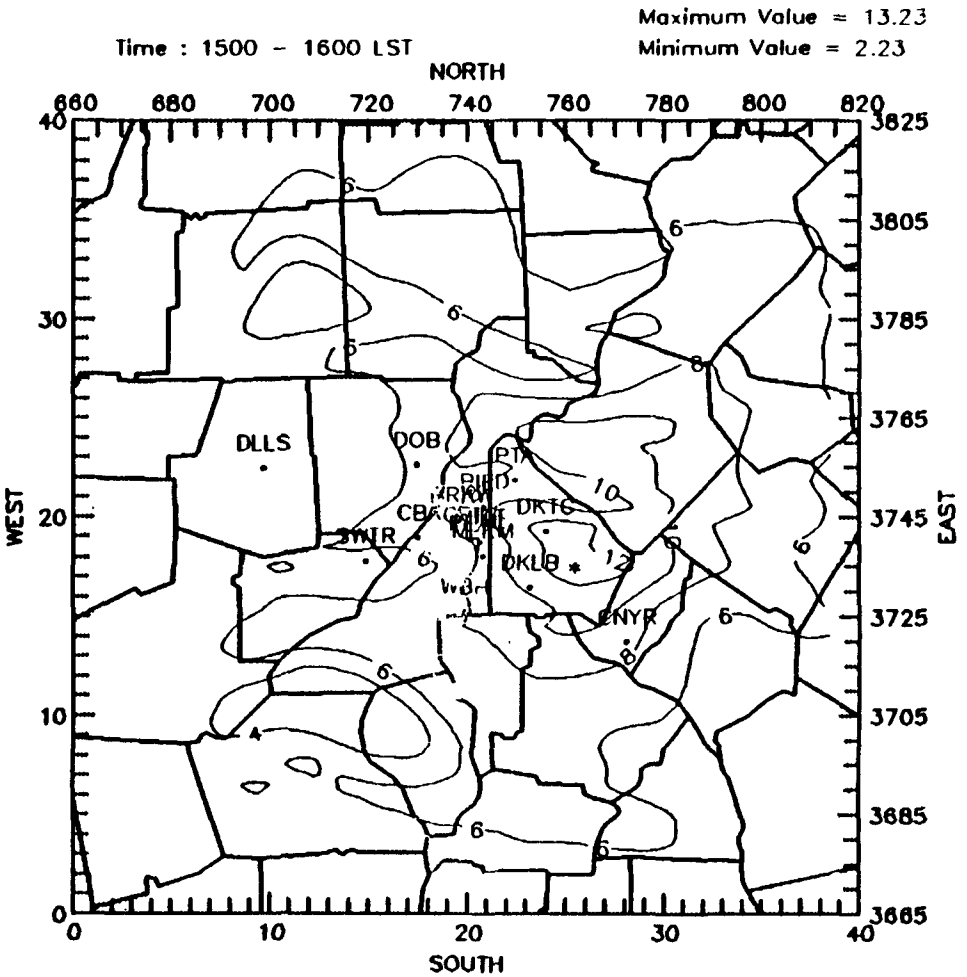

Ozone Concentration Evaluation run #1, June 4, 1984 (pphm)

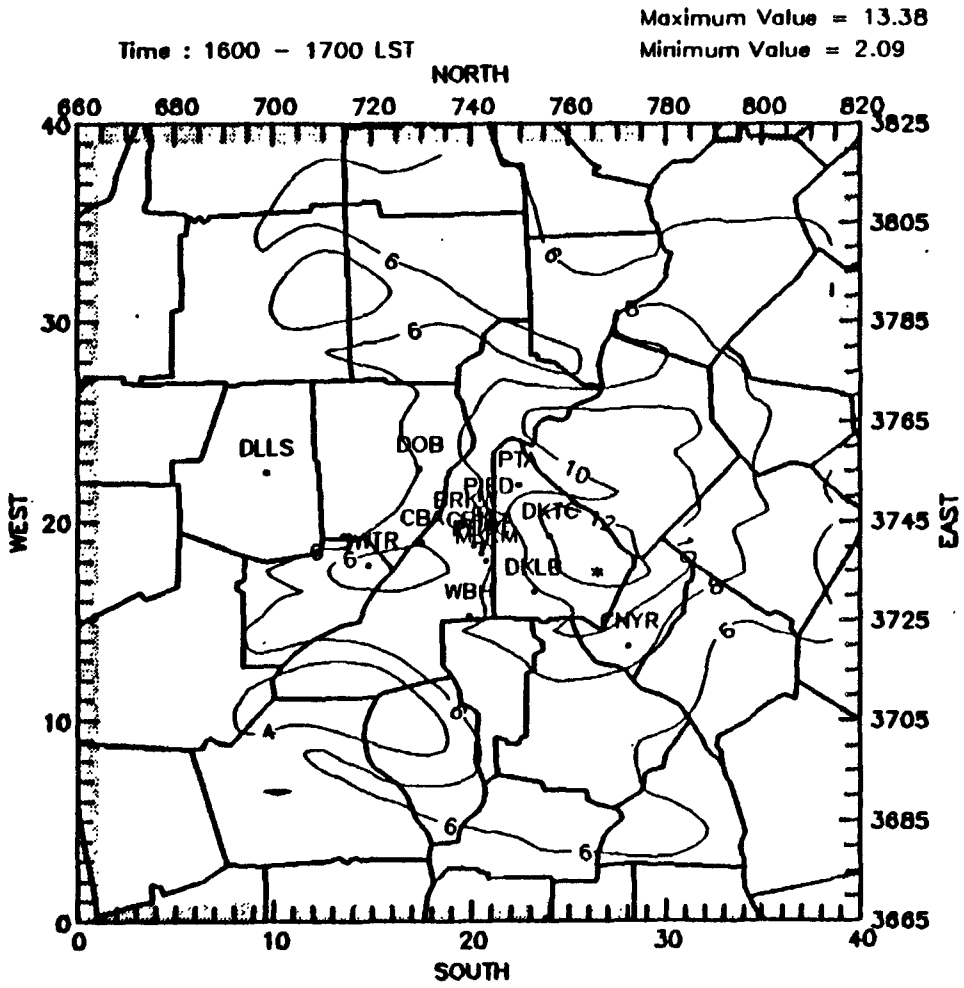

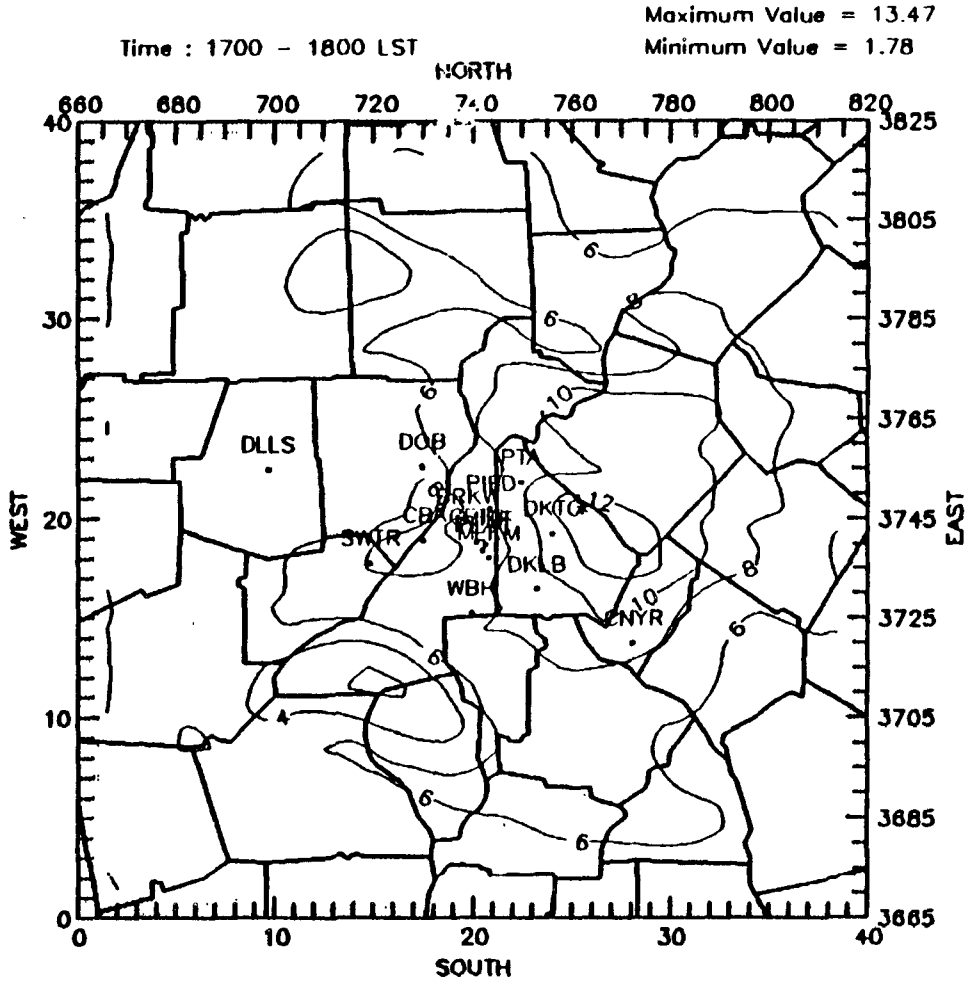

Ozone Concentration Evaluation run #1, June 4, 1984 (pphm)

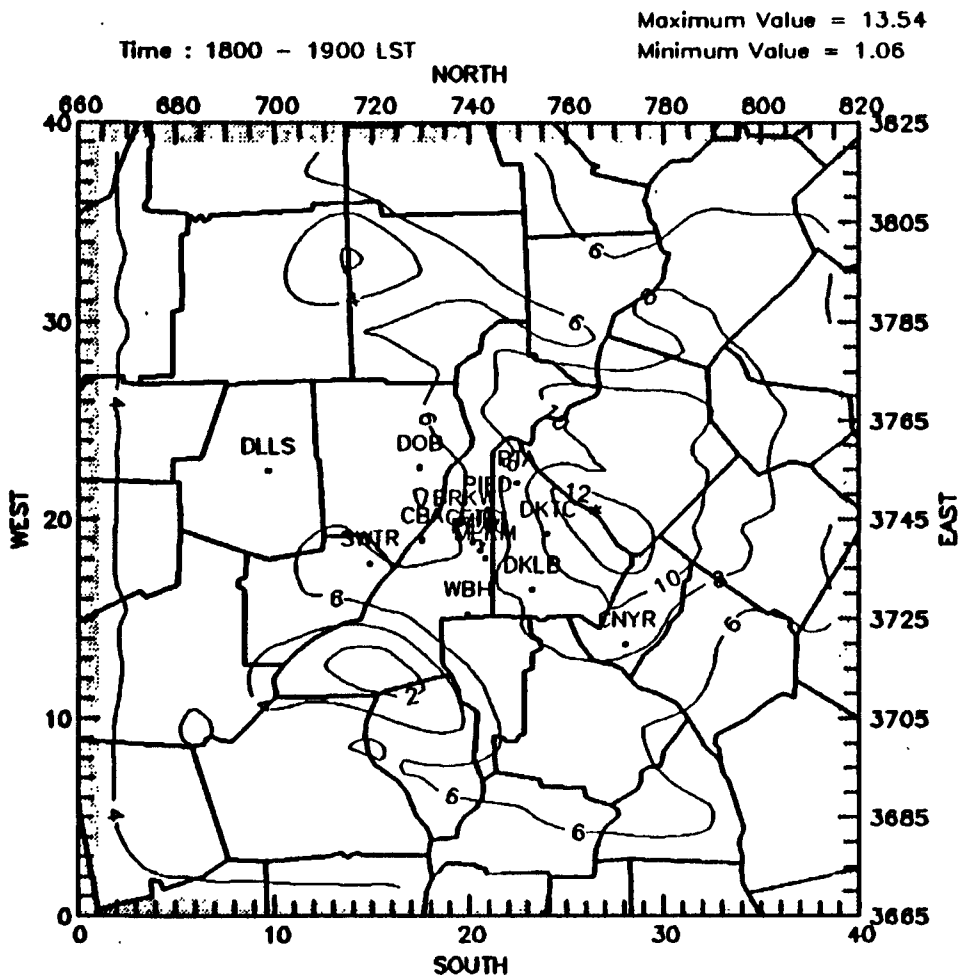

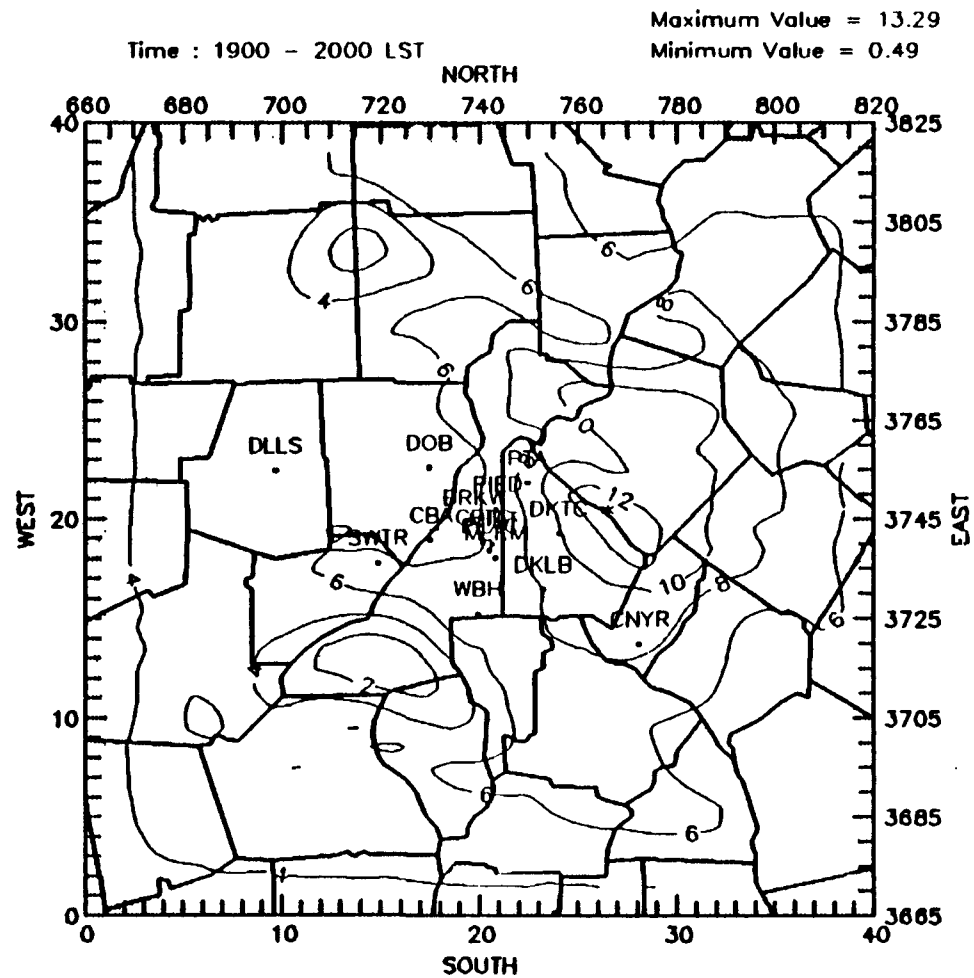

Ozone Concentration Evaluation run #1, June 4, 1984 (pphm)

Appendix C

HOURLY PREDICTED OZONE CONCENTRATIONS (pphm) FOR ATLANTA DIAGNOSTIC RUN 2

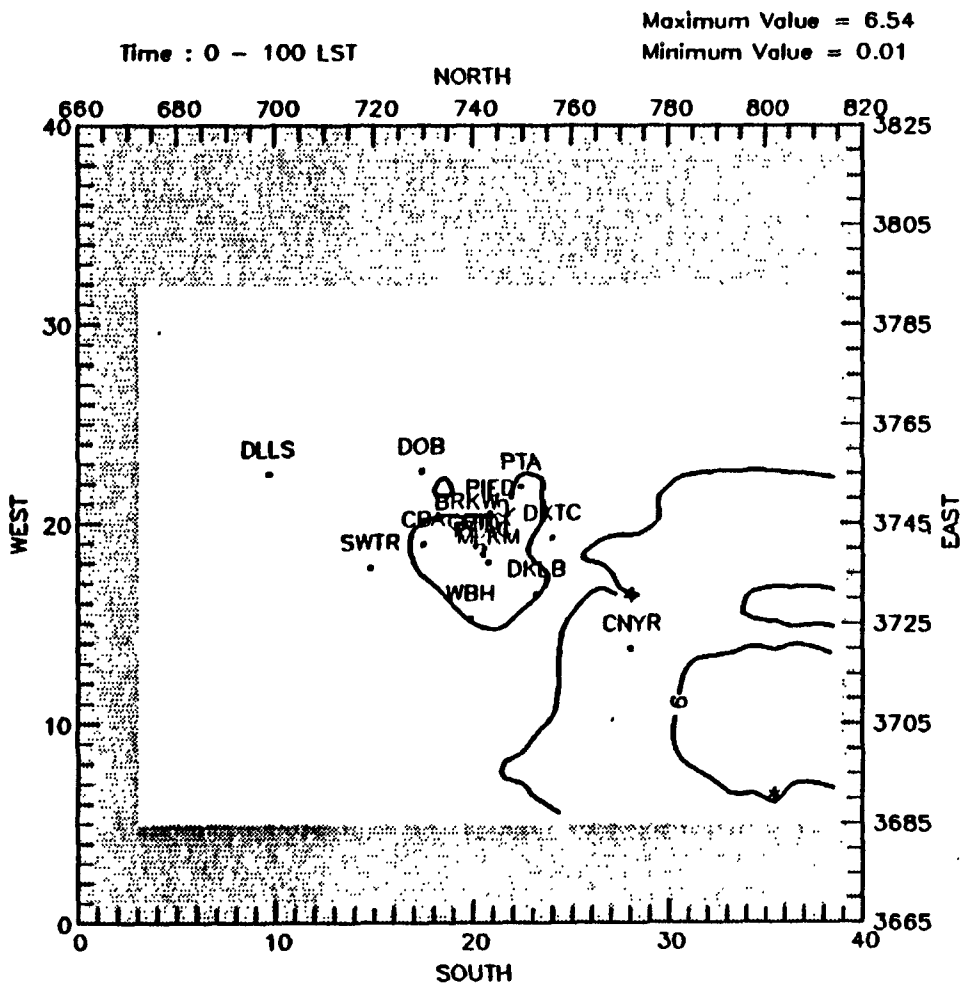

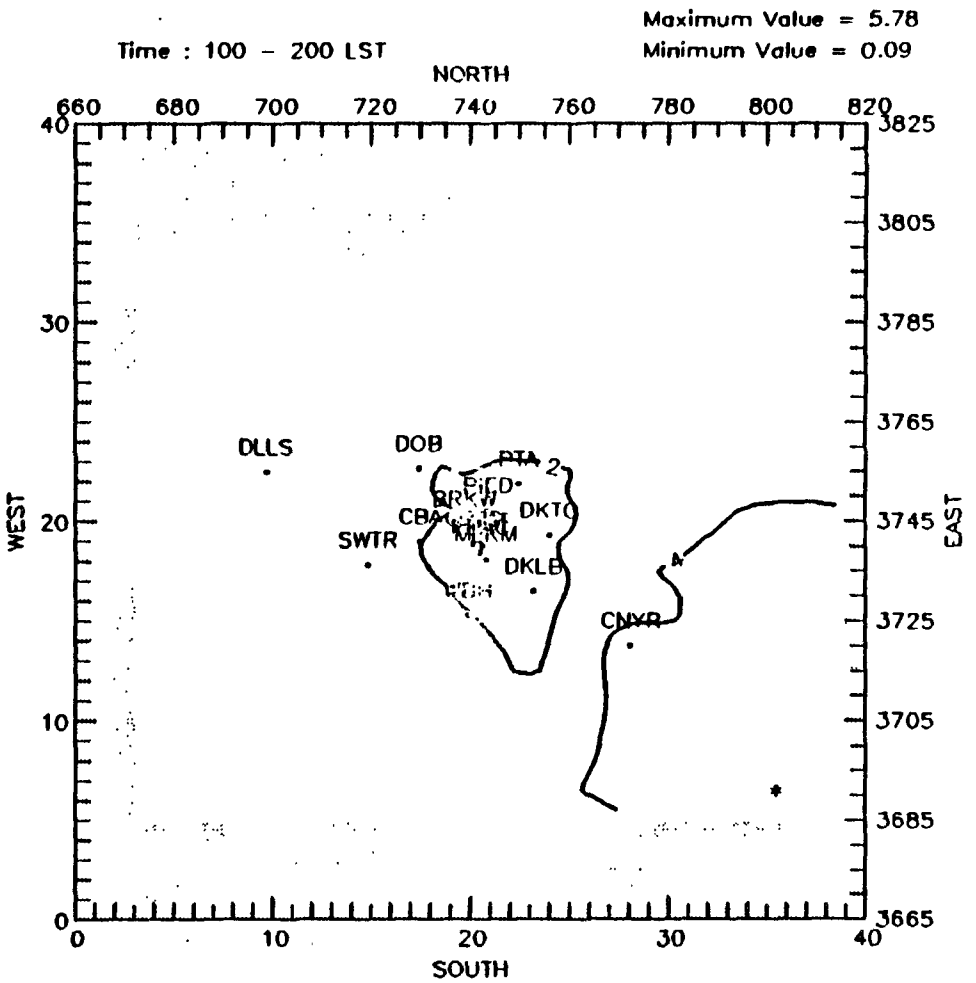

Ozone (pphm) 1985 base emissions, June 4, 1984 (pphm)

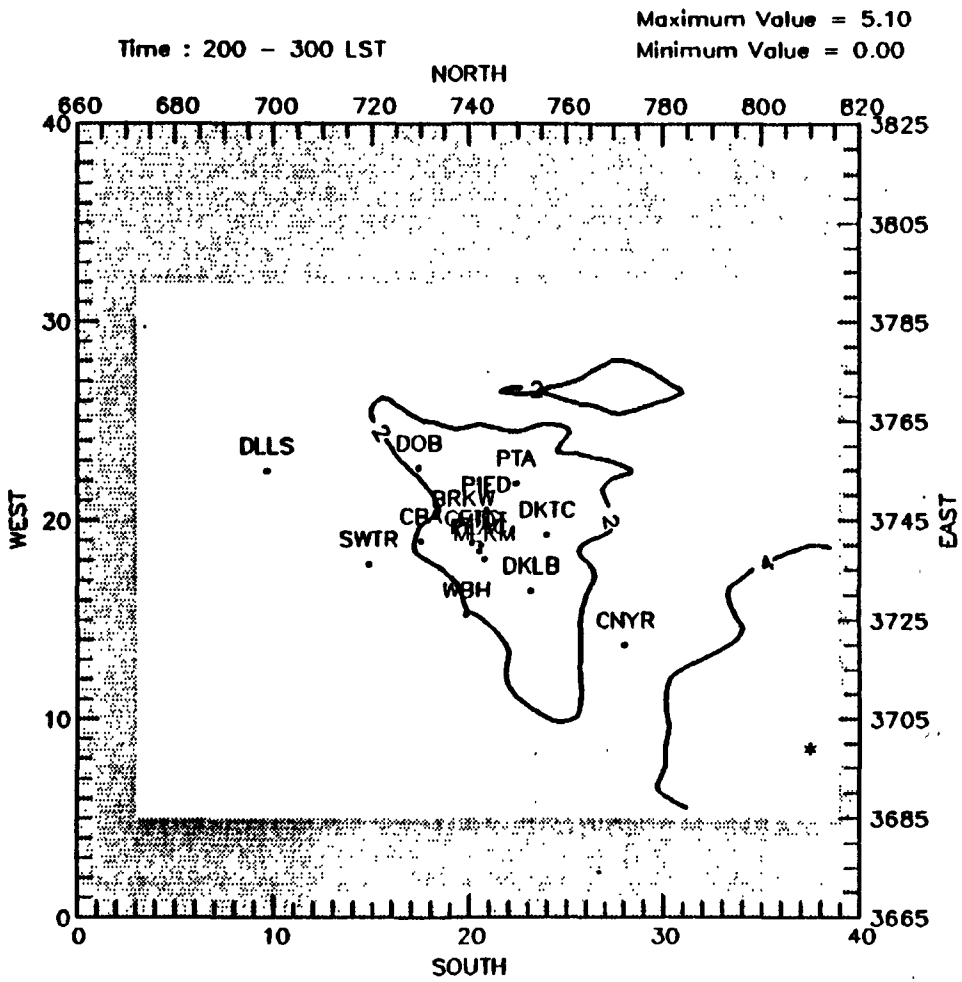

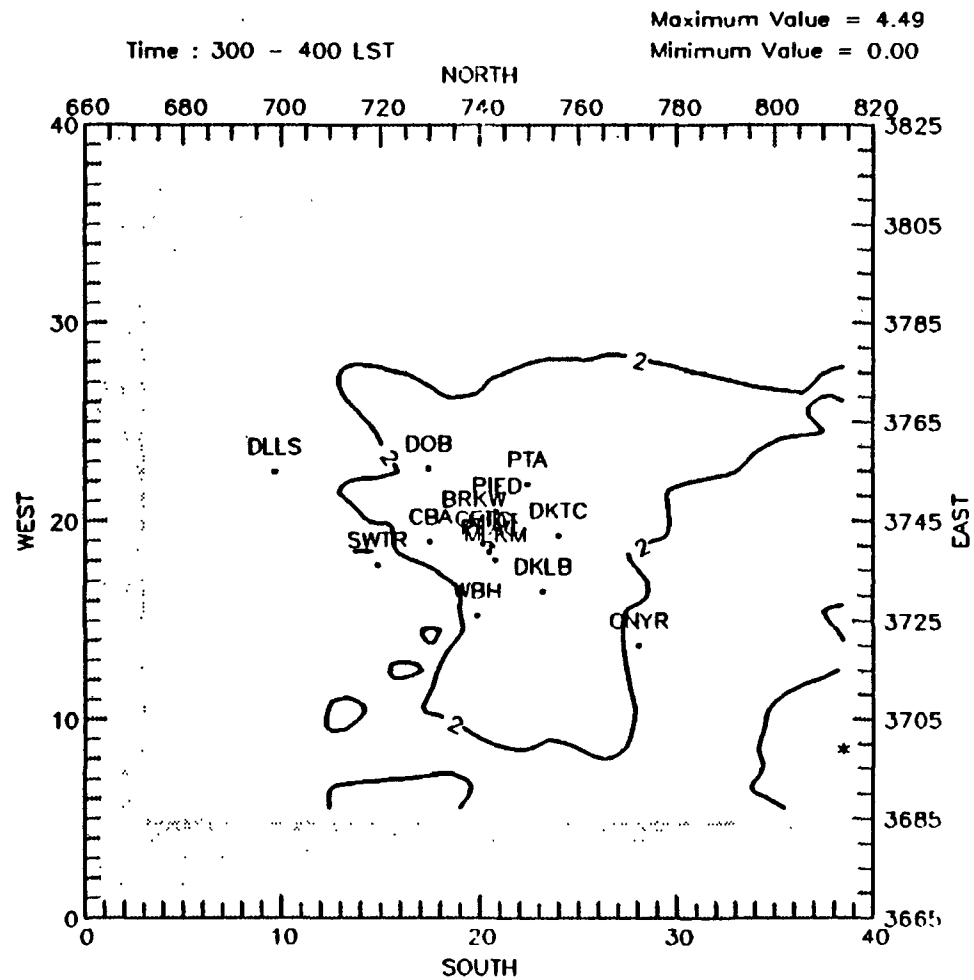

Ozone (pphm) 1985 base emissions, June 4, 1984 (pphm)

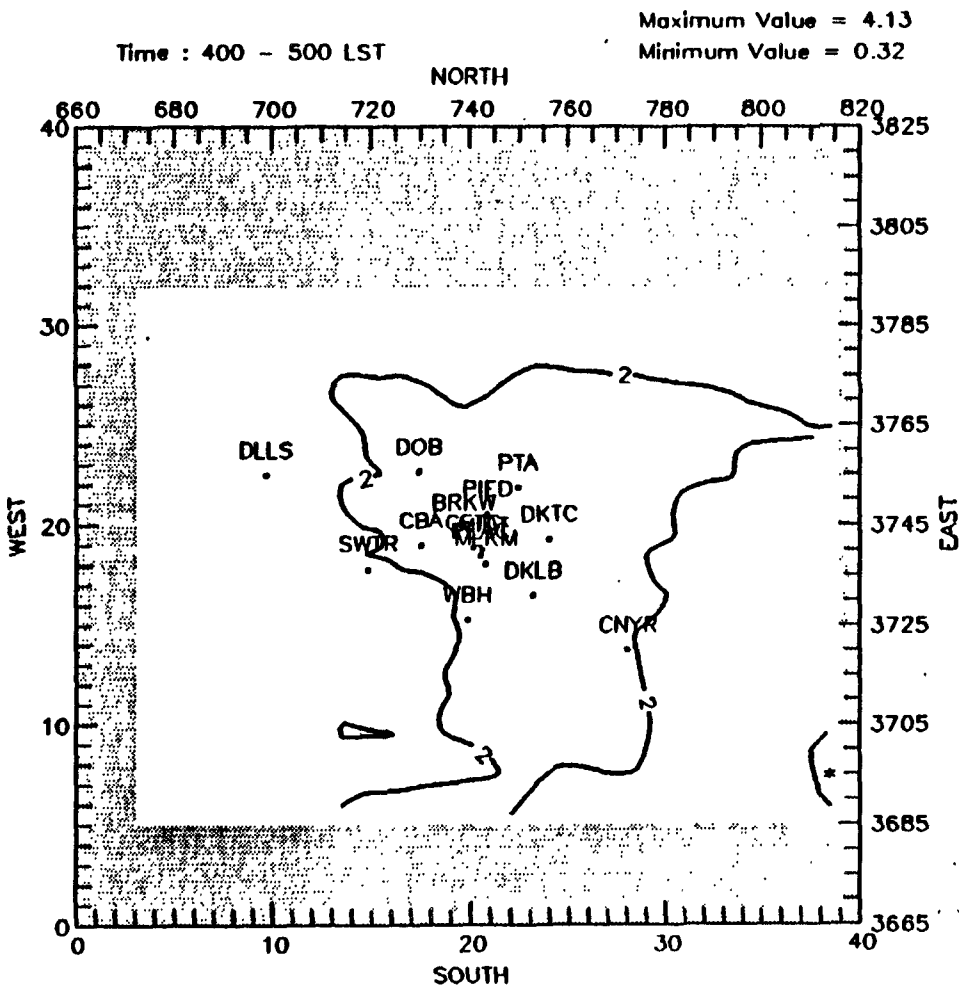

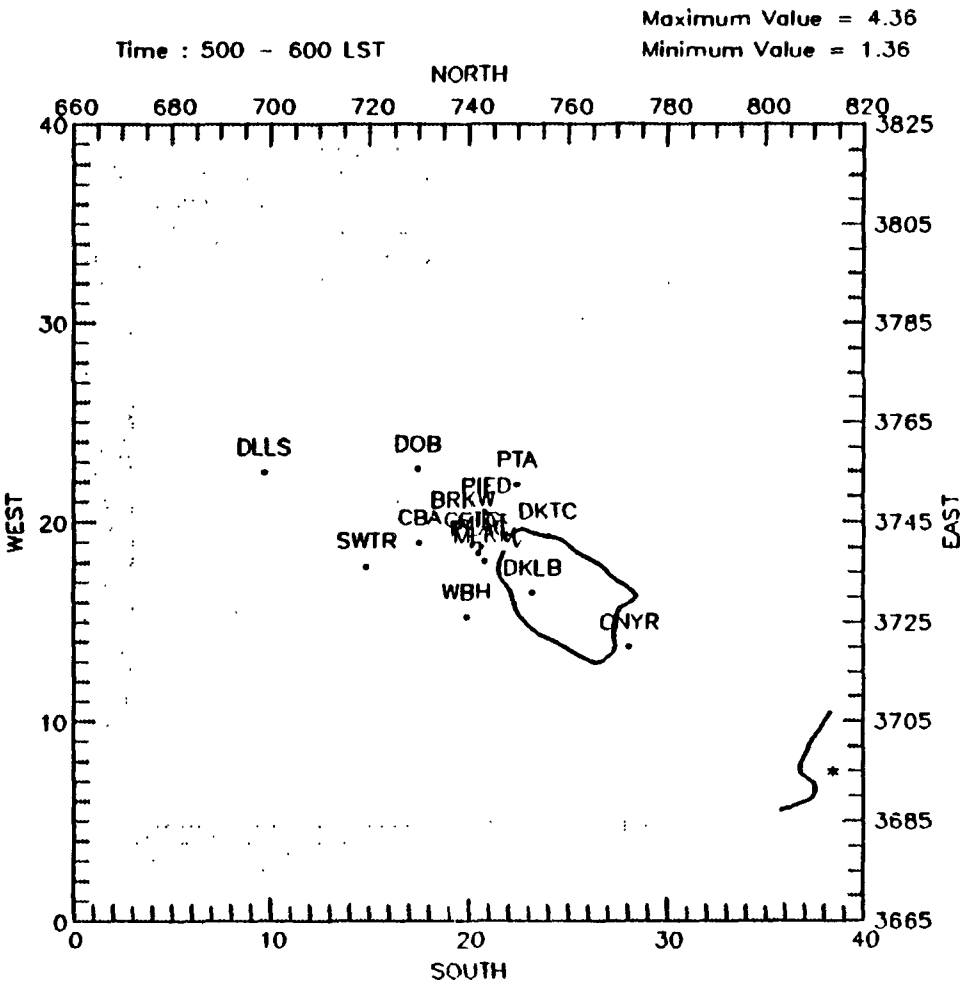

Ozone (pphm) 1985 base emissions, June 4, 1984 (pphm)

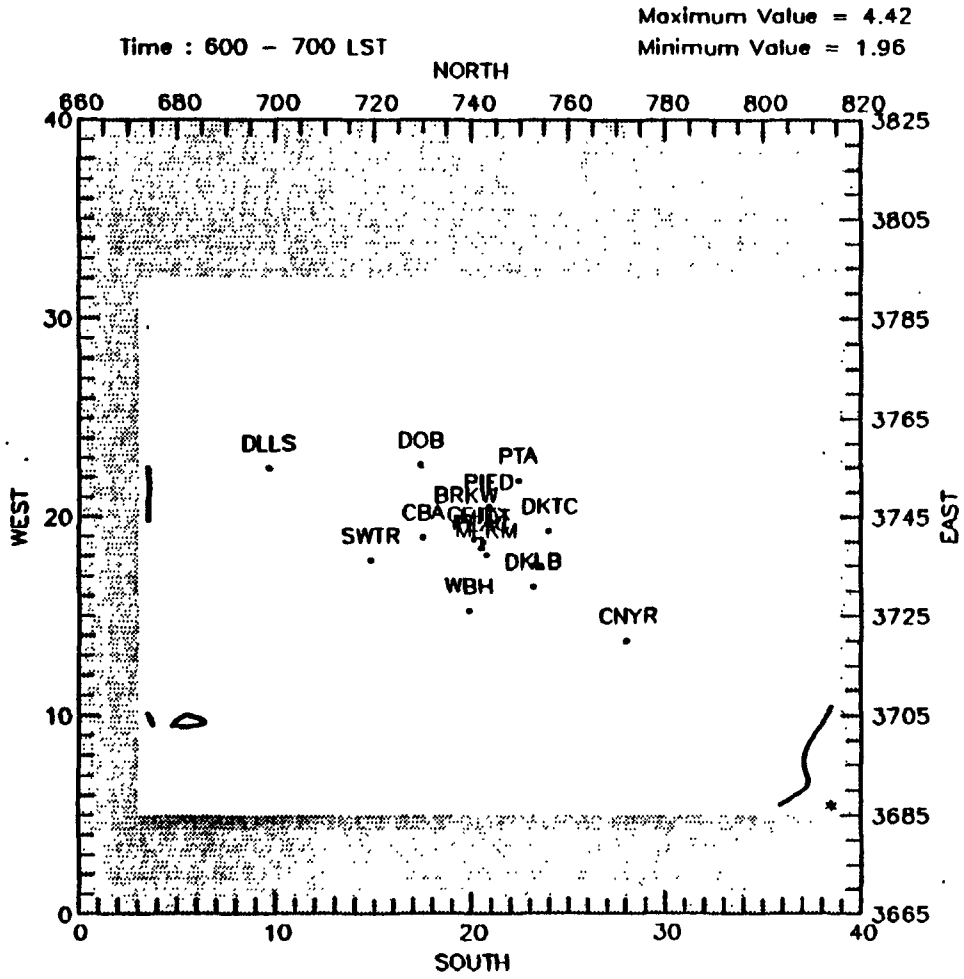

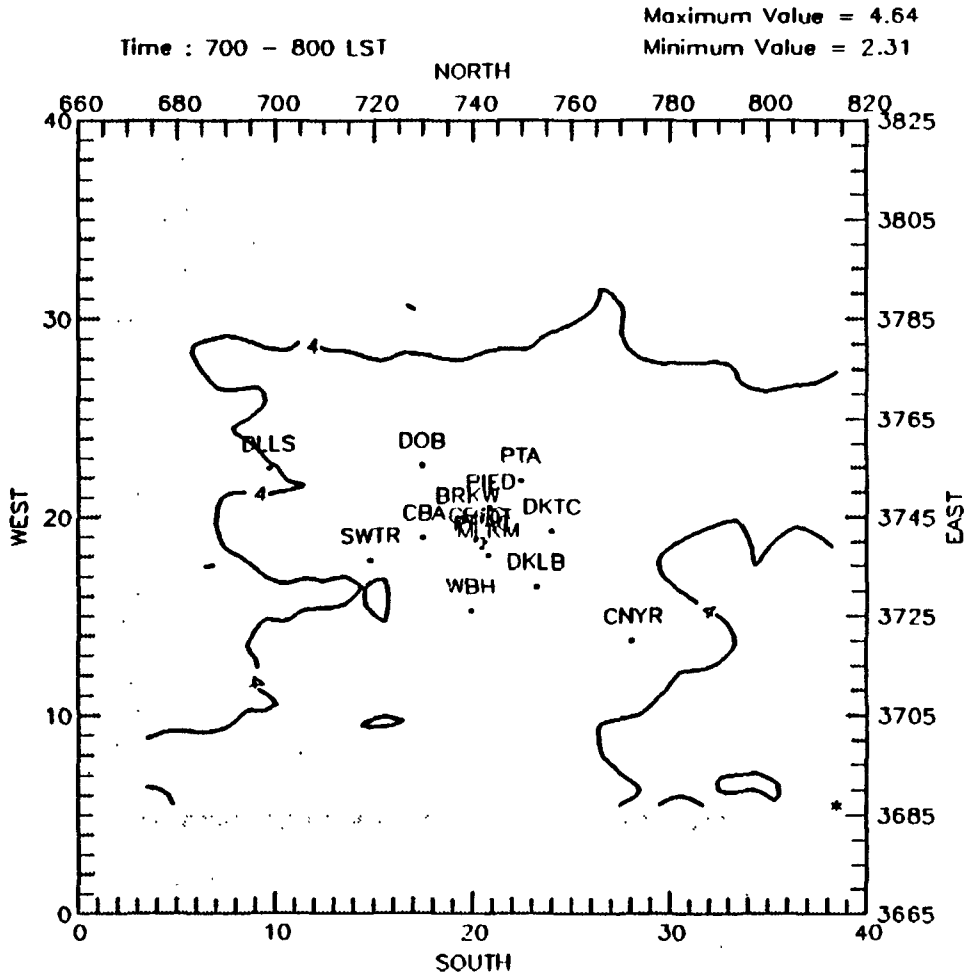

Ozone (pphm) 1985 base emissions, June 4, 1984 (pphm)

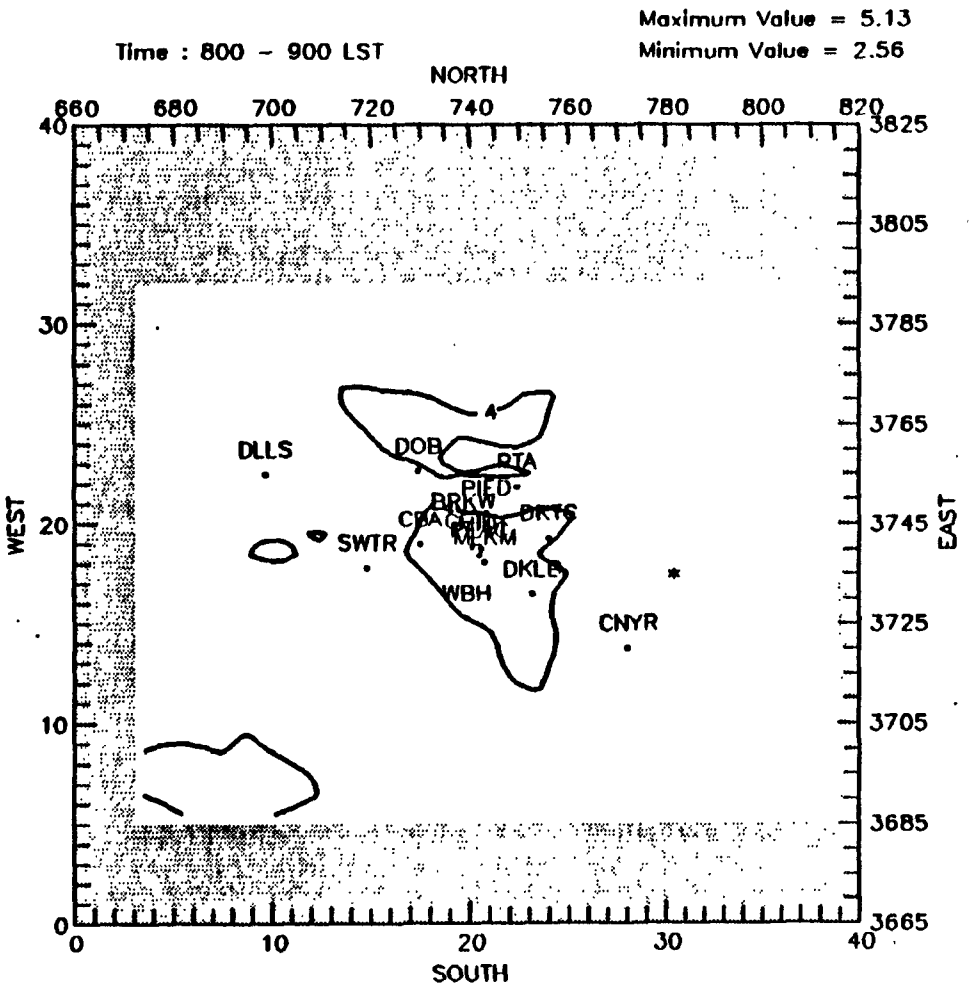

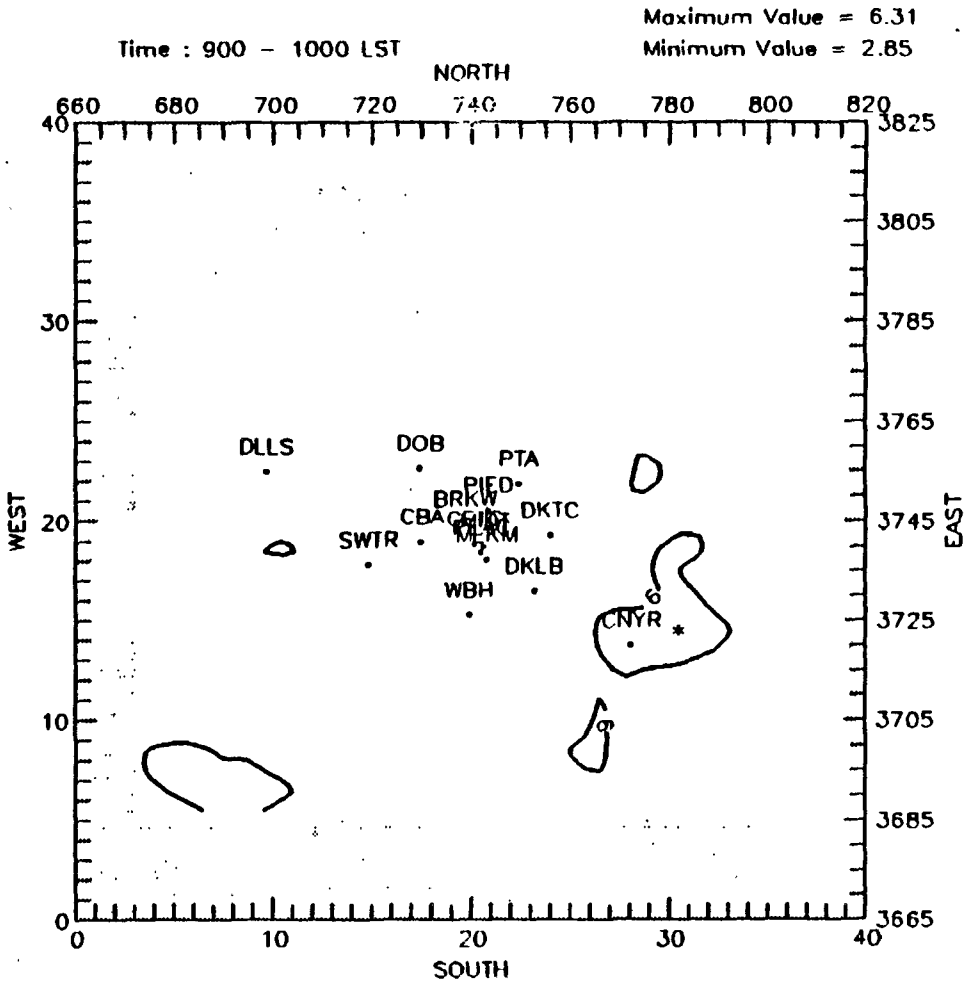

Ozone (pphm) 1985 base emissions, June 4, 1984 (pphm)

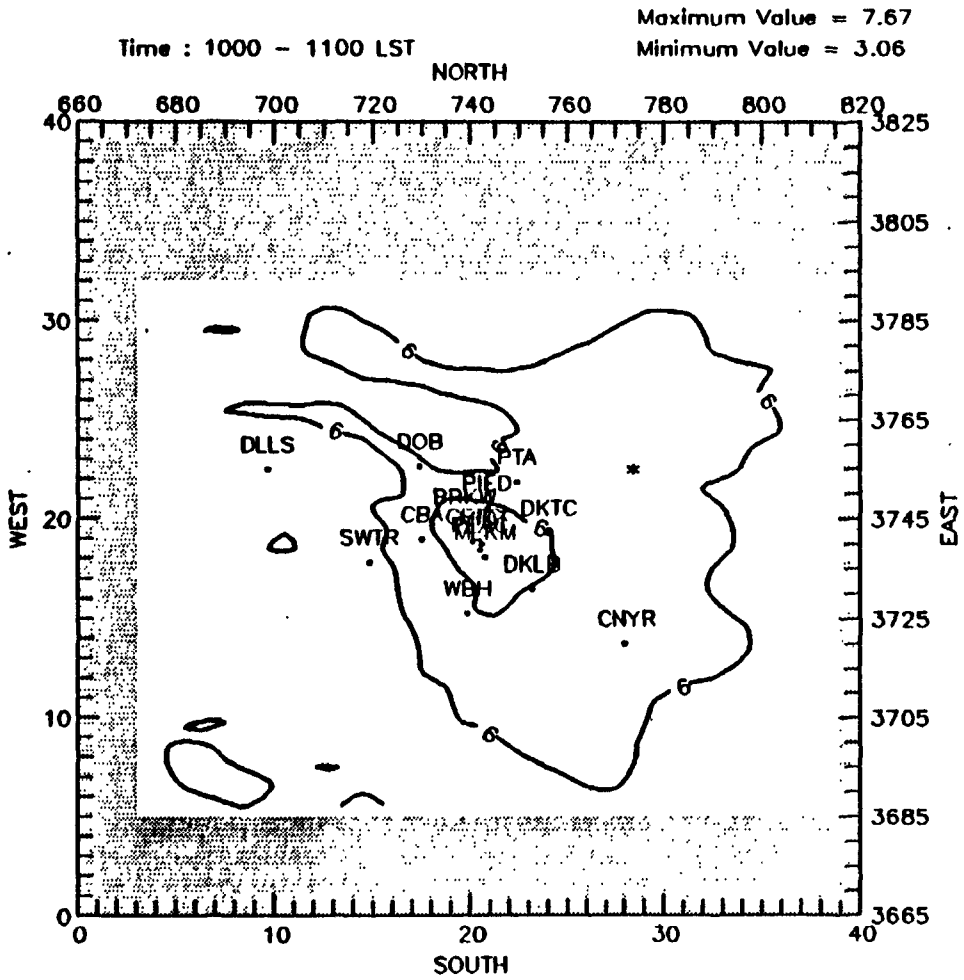

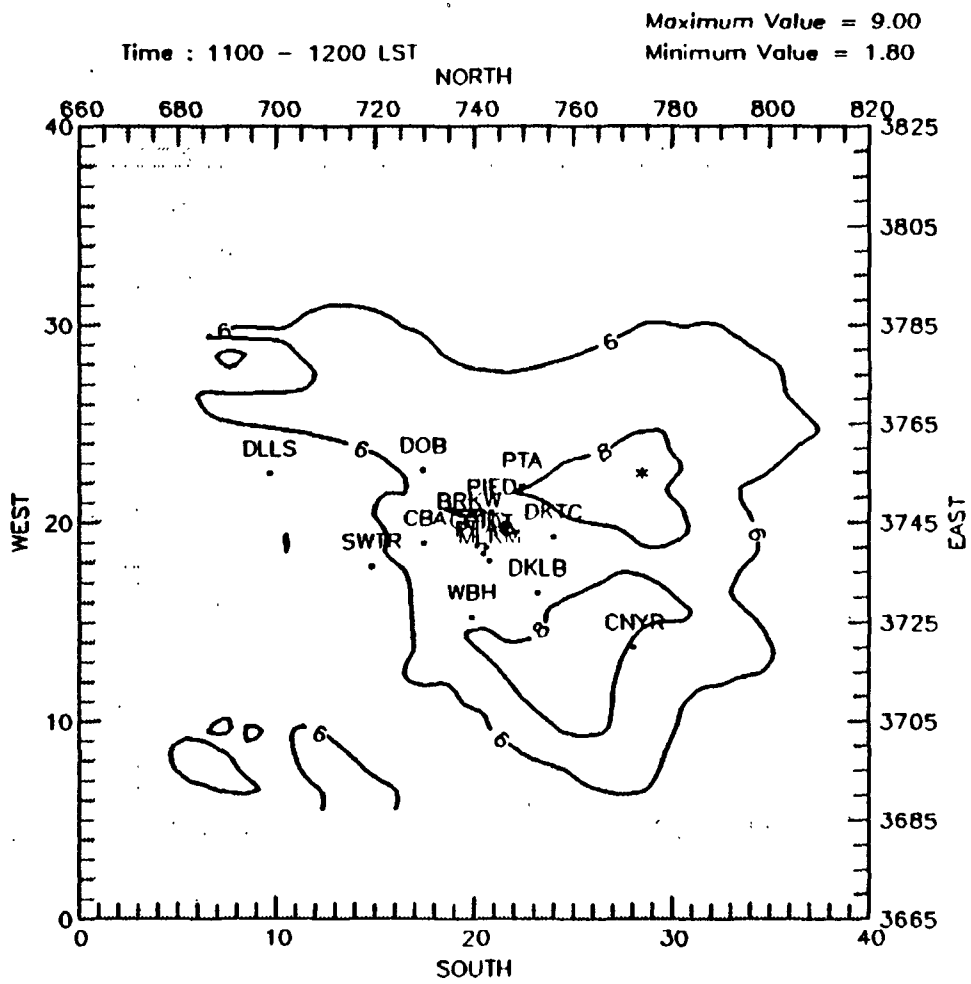

Ozone (pphm) 1985 base emissions, June 4, 1984 (pphm)

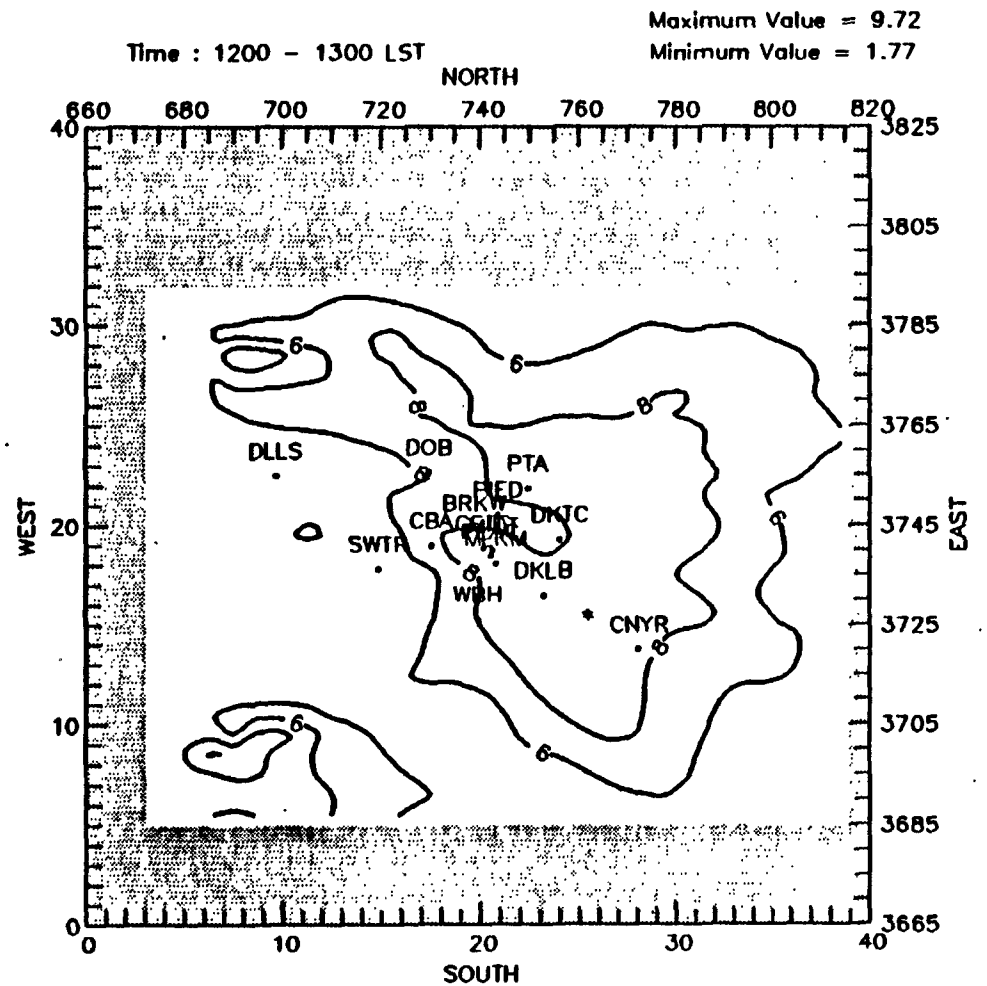

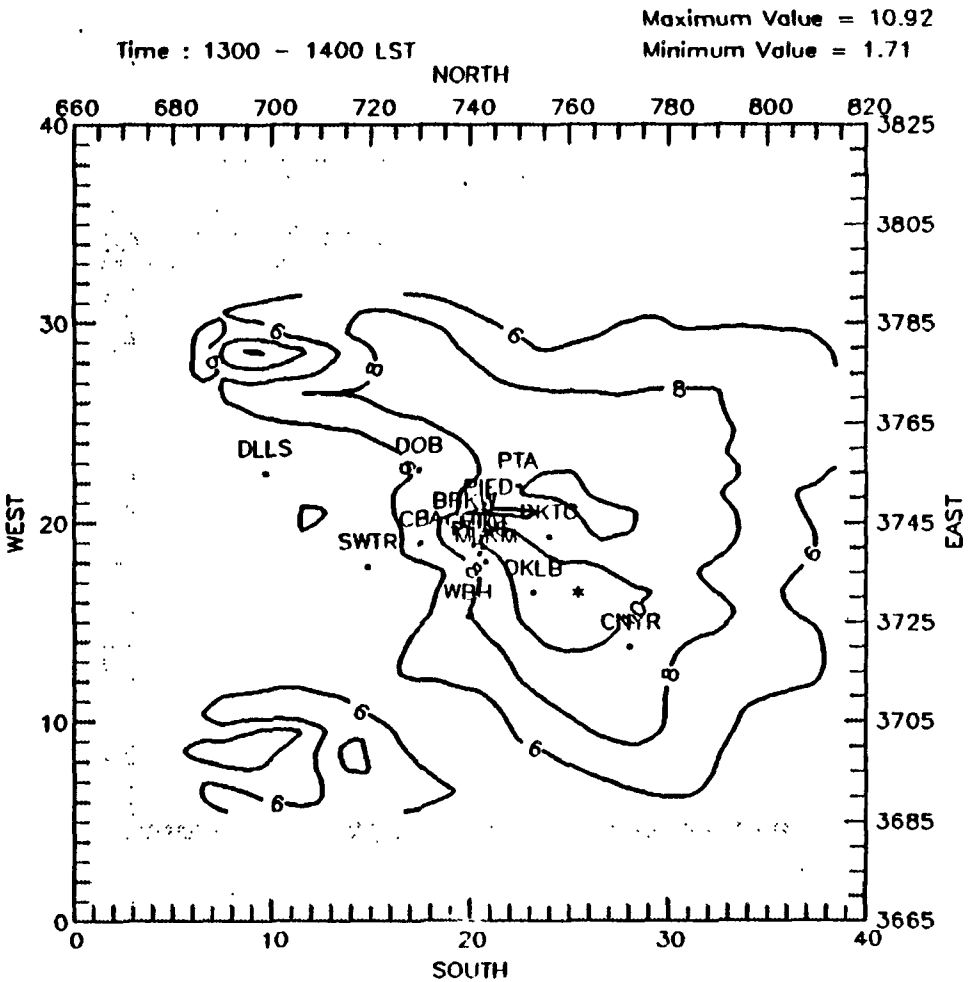

Ozone (pphm) 1985 base emissions, June 4, 1984 (pphm)

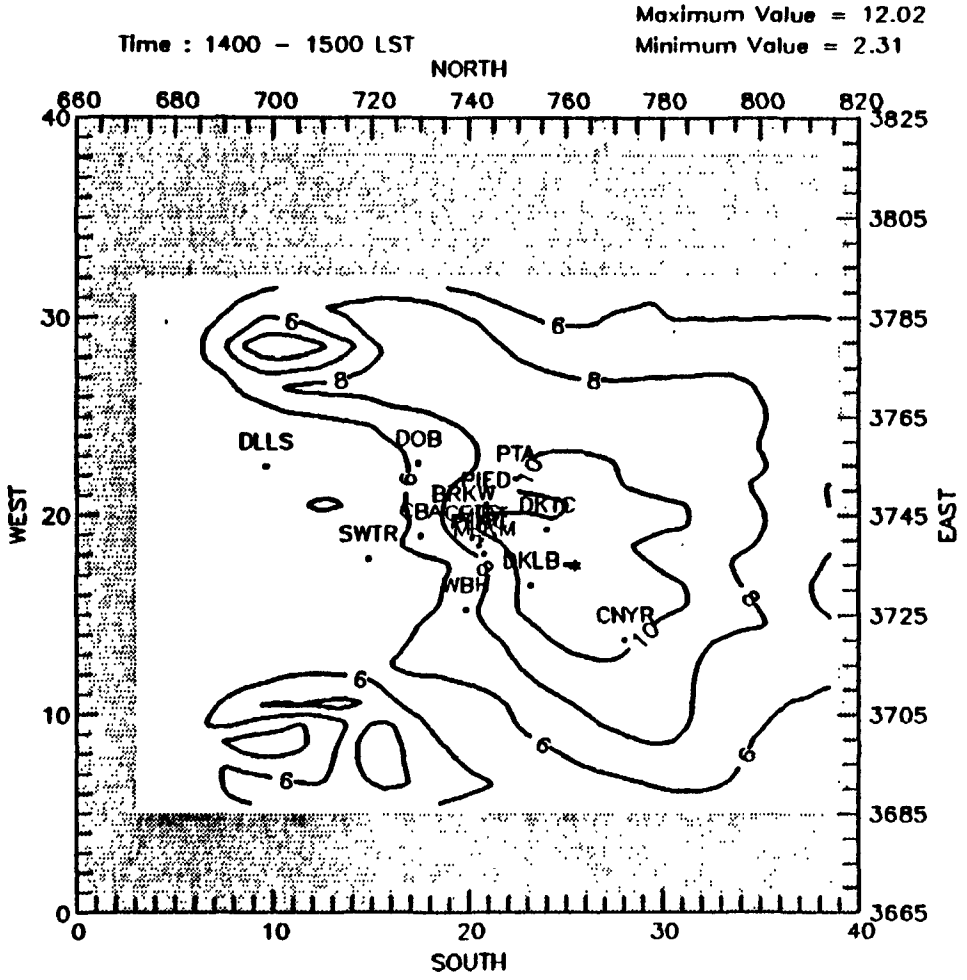

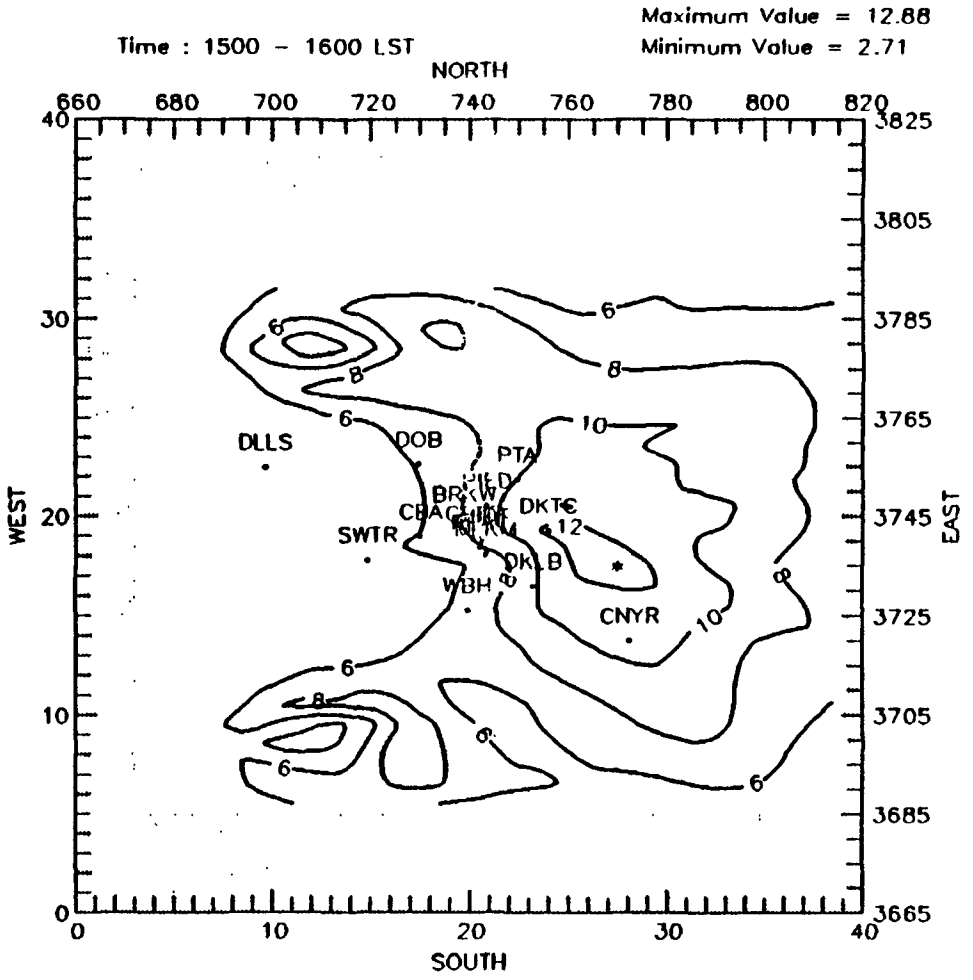

Ozone (pphm) 1985 base emissions, June 4, 1984 (pphm)

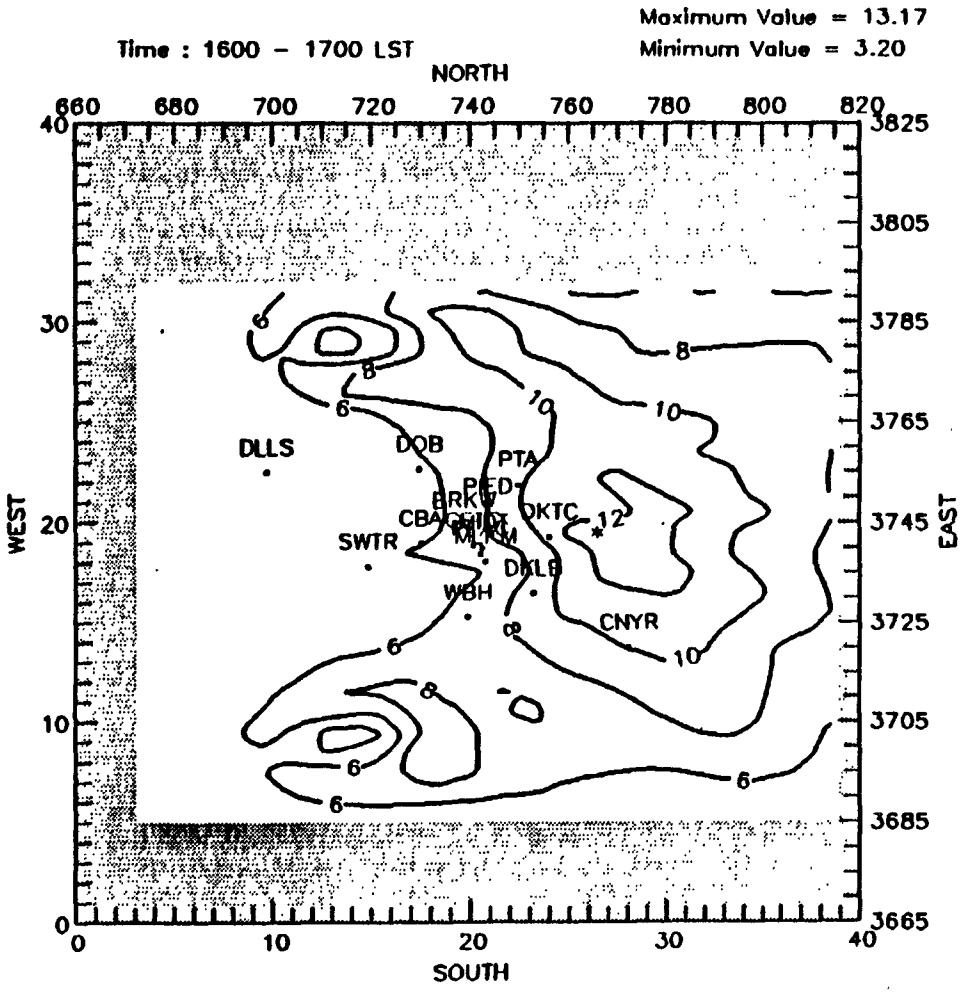

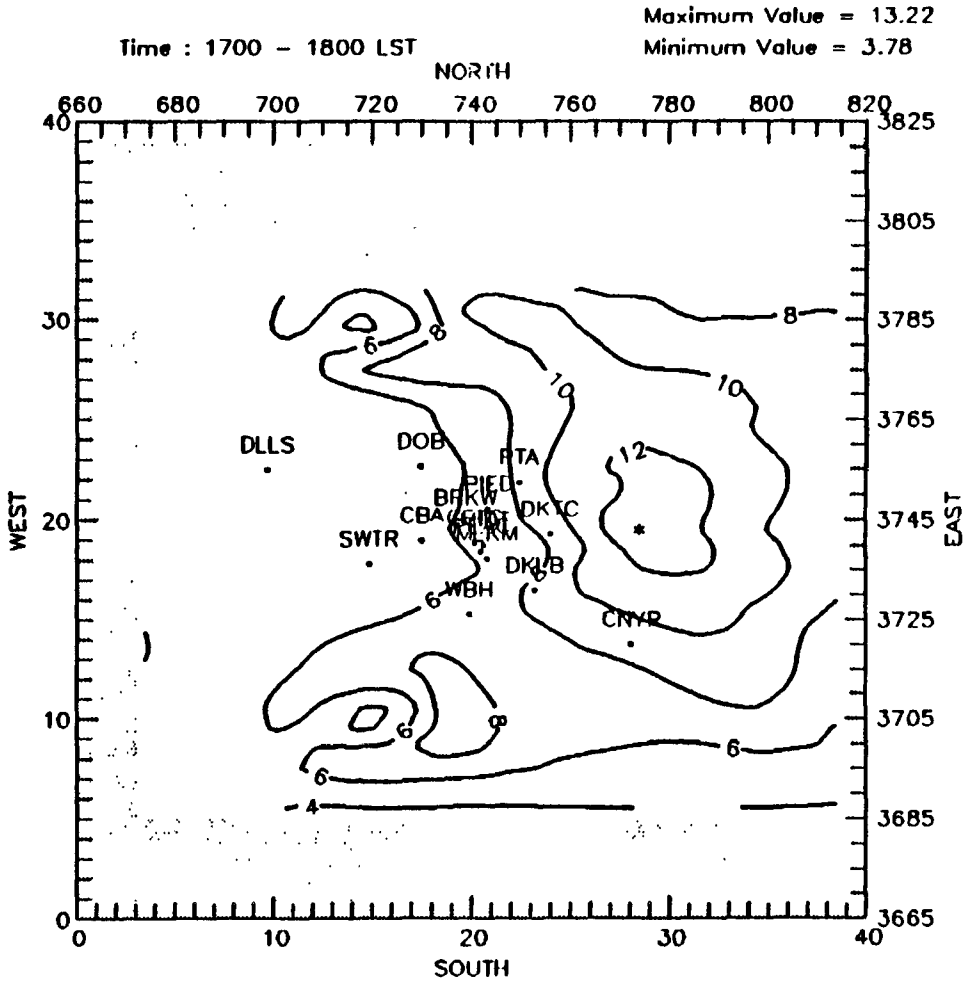

Ozone (pphm) 1985 base emissions, June 4, 1984 (pphm)

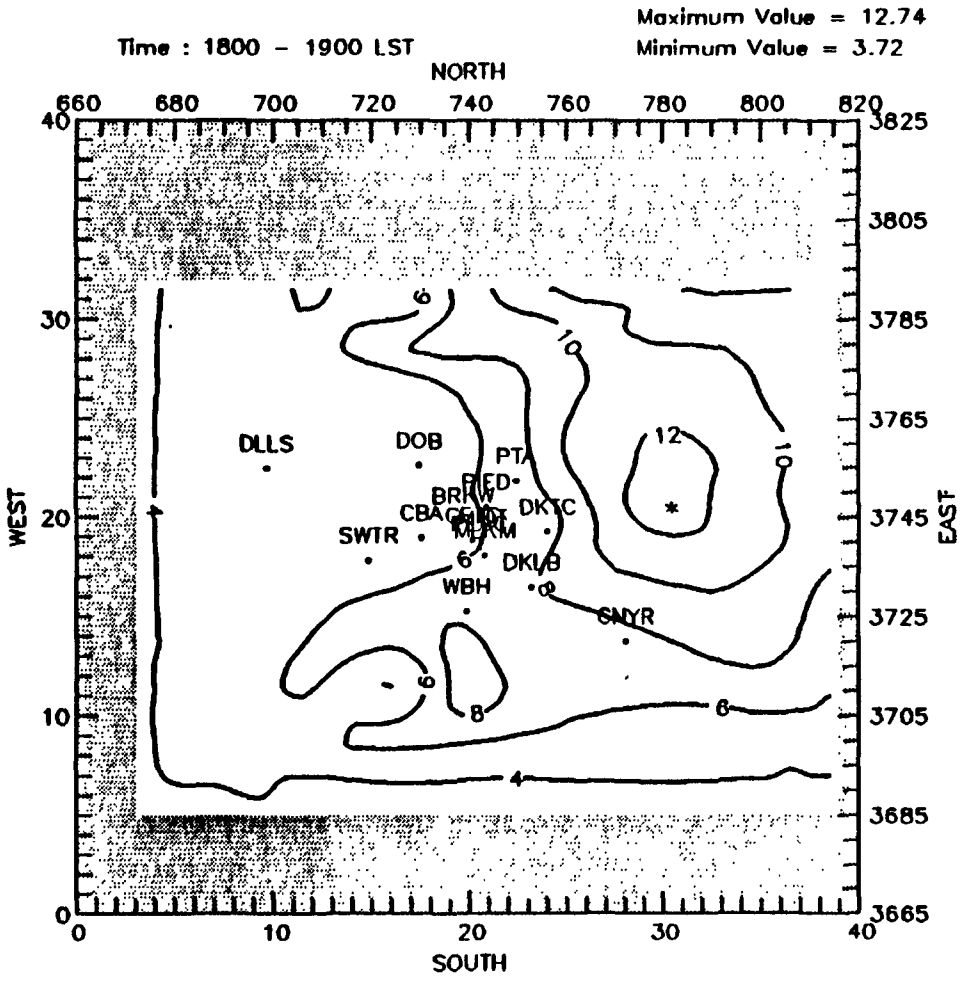

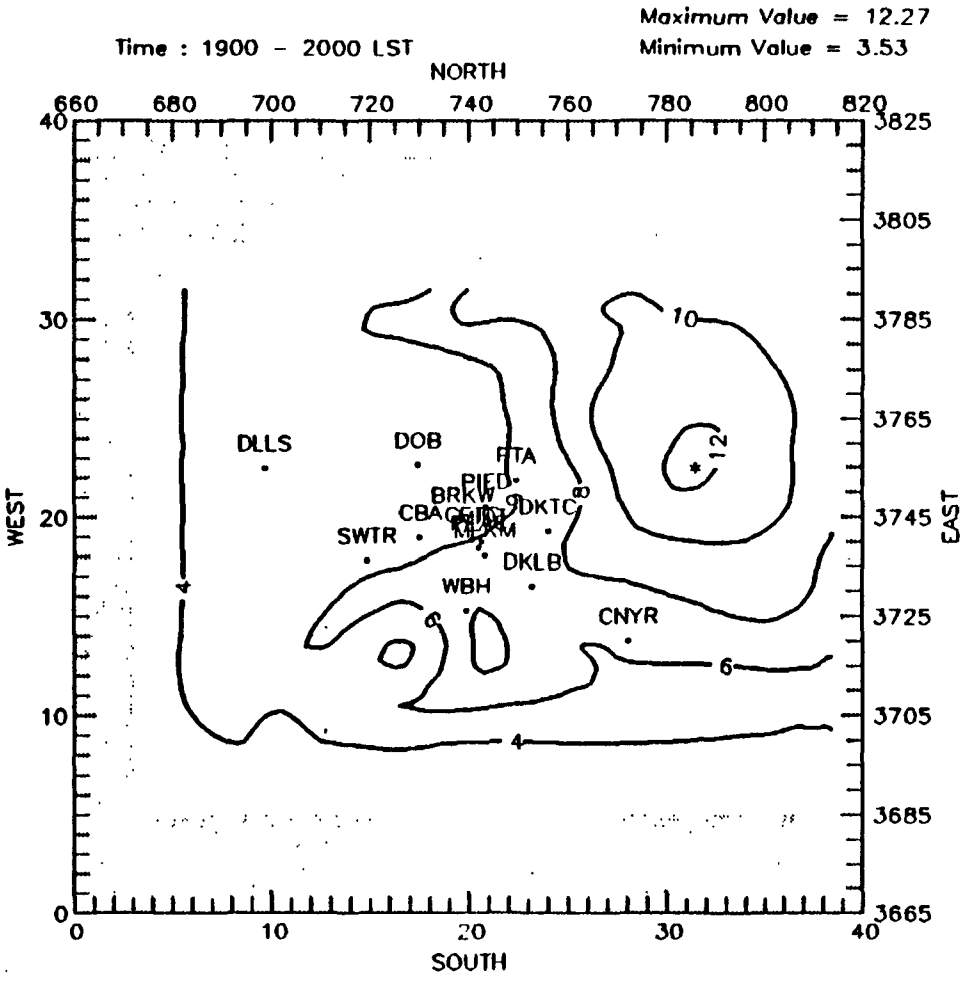

Ozone (pphm) 1985 base emissions, June 4, 1984 (pphm)

Appendix D

SENSITIVITY ANALYSIS OF THE CALCULATIONS OF OZONE CONCENTRATIONS TO WIND SPEED SPECIFICATION

Appendix D

SENSITIVITY ANALYSIS OF THE CALCULATIONS OF OZONE CONCENTRATIONS TO WIND SPEED SPECIFICATION

Because of the limited air quality and meteorological monitoring data in the vicinity of Atlanta, there is some question whether the base case UAM simulation is simulating all of the pertinent physical, meteorological, and chemical processes that led to the ozone episode of June 4, 1984. The only indication of whether the model is correctly simulating such an episode is its ability to predict the hourly ozone concentrations at the three ozone monitoring sites. The base case modeling inputs from diagnostic run 2 produced model performance that barely passed the performance goal. There were several explanations given for the descrepancies between the predicted and observed ozone concentrations, including underestimation of the anthropogenic emissions inventory, use of too low boundary conditions; excessive wind shear that tended to dilute the urban plume, and excessive wind speads that also tended to dilute the urban plume. Thus it was decided to do a sensitivity test that would result in less dilution of the urban plume. This was accomplished by reducing the wind speeds at all FAA wind observations sites by 50 percent.

The justification of this wind speed reduction is based on the instantaneous nature of the observed FAA wind speeds versus the hourly integrated wind speeds required by the UAM and the bias in the human FAA observations versus the mechanical wind averaging techniques. When there is wind variation throughout the hour, the vector-averaging of the hourly average wind speeds will result in a lower value than reported at an FAA site, which is essentially an instantaneous value taken at the end of an hour. In addition, the human element and uses of the FAA wind speeds are different from the wind information required by the UAM. An important use of the FAA wind observations is to advise pilots of adverse wind conditions at the airport for take-offs and landings. During slow wind conditions, which are typical of ozone episodes, the FAA observer may report higher wind gusts that will affect an aircraft

operation. The fact that the hourly average wind speed is calm is of no use to the pilot. This bias of FAA wind speeds was noted while developing UAM inputs for the California South Coast Air Basin where there were several hourly integrated and FAA wind observation sites located in the proximity to each other. A brief analysis of these sites is reported next.

COMPARISON OF HOURLY AVERAGED AND FAA WIND SPEED OBSERVATIONS

During the development of the California South Coast Air Basin (SCAB) Air Quality Management Plan (AQMP), in which four 3-day episodes of high ozone days were extensively studied, a systematic bias was seen between the 1-hour vector-averaged observations from SCAQMD (South Coast Air Quality Management District) surface wind speed monitors and nearby one-minute averaged NWS/FAA (National Weather Service/ Federal Aviation Administration) observations of surface wind speed. To estimate the extent of the bias, seven "collocated" station pairs of NWS/FAA stations with SCAQMD wind monitors were studied. Table D-1 shows the station pairs and the distance between the collocated pairs.

The study periods were the ozone episodes of 5-7 June, 12-14 August, 21-23 August, and 26-28 August 1985. A total of 1920 collocated data points were collected. This set was reduced by 801 data points because of either a missing station pair or a station pair that was below the speed of 1 knot. The speed of 1 knot represents the lowest value that FAA/NWS wind monitoring stations can measure. Thus, comparison between SCAQMD stations reporting wind speeds as low as 0.1 mph might introduce a bias toward the higher values being reported for FAA/NWS stations.

The mean value for the remaining 1119 data points for the FAA/NWS stations was 3.49 m/s, while the mean for the SCAQMD stations was 1.93 m/s, suggesting that the FAA/NWS stations were biased by approximately 45 percent (i.e., the observed hourly average wind speeds were a little over half of the FAA wind observations). The median values were very similar, with values of 3.10 m/s for FAA/NWS stations and 1.80 m/s for SCAQMD stations. Each day was examined to see if any particular

day showed an extreme bias; the bias ranged from 36 percent on 13 August to 51 percent on 26 August.

Similarly, all seven stations were examined to see if any particular station may have been the cause of the bias. Five of the seven stations showed similar bias, ranging from 45 to 56 percent. However, two pairs showed a significantly smaller bias; the Upland and Ontario airport showed a bias of only 28.8 percent and the San Bernadino and Norton Air Force Base pair showed a bias of only 2.4 percent In an attempt to see if the agreement was caused by low wind speeds at Norton Air Force Base at night, the wind observations were stratified into a daytime period only; we still found that almost no bias occurred for the San Bernadino-Norton Air Force pair. The possibility exists that the data may have been incorrectly processed or reported; if the data was incorrectly converted from knots to m/s, this may account for the small bias.

We believe that the wind speeds reported for 1-minute averages from FAA/NWS stations are correct; however, what is needed for the UAM is the 1-hour vector-averaged wind speed. As a result of the SCAQMD study, which should be true for all locations in the United States, it was concluded that FAA/NWS surface wind observations have a positive bias of about a factor of 2 and should be reduced by approximately 50 to 75 percent when hourly average wind speeds are desired.

This preliminary analysis is by no means complete or statistically roboust, however it does have important implications in the development of wind fields for air quality simulations models, such as the UAM. It also helps explain some underprediction tendency of the UAM at some locations in the past (e.g., St. Louis and Philadelphia). Further analysis of the SCAQMD wind data base and data from other locations is necessary to determine the extent and frequency of this bias. For example, hourly average wind speeds are calculated by vector-averaging of a series of lower-frequency wind observations. A comparison of the final one-minute wind speed for each hour with the hourly average may give some indication of the extent of the bias.

MODEL PERFORMANCE EVALUATION

The UAM(CB-IV) was exercised with the exact same inputs as in diagnostic run 2, except that in the wind fields the observed wind speeds from FAA observations were reduced by 50 percent. The resultant predicted ozone concentrations at each of the ozone monitoring sites are shown in Figure D-1. Similar time series plots of predicted and observed ozone concentrations using a one-cell and two-cell search are given in Figure D-2 and D-3. Scatterplots, residual analysis plots, and model performance statistics for predicted and observed hourly ozone concentrations and the sensitivity test (reduced wind speed) are shown in Figure D-4. The isopleths of hourly ozone concentrations for sensitivity test are given in Figure D-5. Note that these five figures correspond to Figures 3-4 through 3-7 in the main body of the report and Appendix C for diagnostic run 2.

The predicted region-wide maximum ozone concentration in the reduced wind speed sensitivity test matches the observed peak ozone concentration exactly (14.7 pphm). At the location of the observed peak ozone the model prediction (11.4) is within 22 percent. At other ozone monitors the model predicts the peak within 2 (DKLB) and 33 (DLLS) percent. The sensitivity test produces superior model performance over diagnostic run 2 as exhibited in the scatterplots of hourly predicted and observed ozone concentrations (Figure D-4, and Figure 3-7 in the main body of the report).

TABLE D-1. Surface meteorological observation sites and distance between collocated observations pairs.

NWS/FAA Site Name	Location UTM (Zone10) UTM_x	UTM_y	SCAQMD Site Name	Location UTM (Zone 10) UTM_x	UTM_y	Distance between Collocated Stations
Burbank Airport	356.48	3768.00	Burbank	359.60	3766.40	3.52 km
Los Angeles International Airport	352.48	3744.40	Lennox	354.40	3744.00	1.96 km
Long Beach Airport	370.88	3733.76	Long Beach	368.00	3734.40	2.95 km
El Toro Airport	401.60	3720.16	El Toro	404.8	3716.72	4.70 km
Ontario Airport	411.68	3754.16	Upland	408.00	3758.48	5.67 km
Norton Air Force Base	438.80	3756.96	San Bernardino	434.40	3759.20	4.94 km
Compton Airport	364.40	3740.24	Lynwood	366.40	3743.20	3.57 km

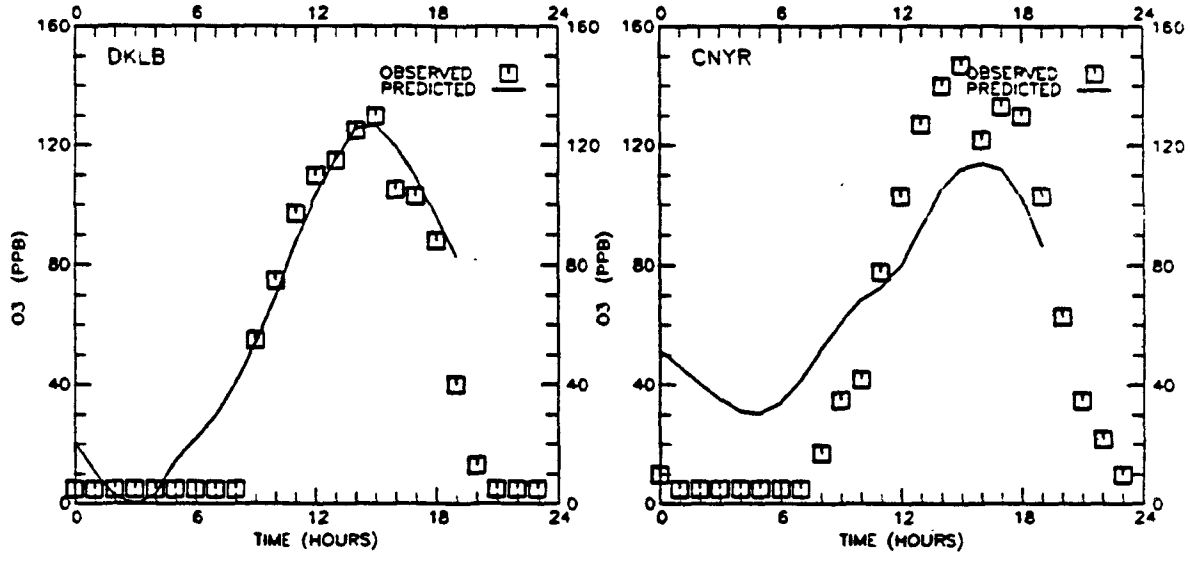

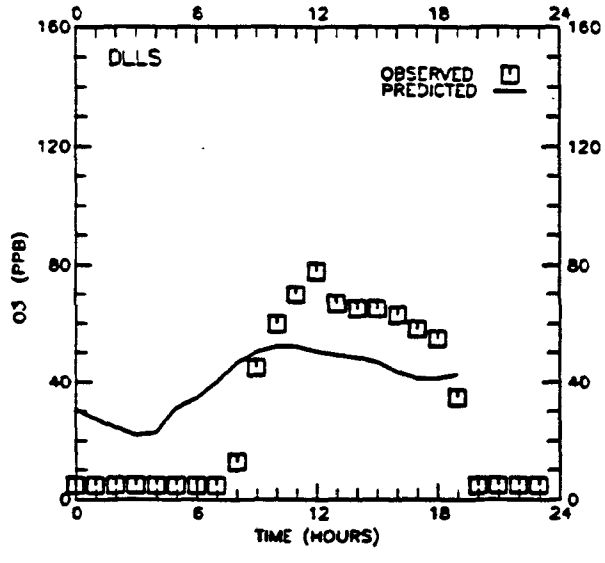

SYSTEMS APPLICATIONS, INC.

FIGURE D-1. Observed and predicted ozone concentrations (ppb) for Atlanta reduced wind speed sensitivity test.

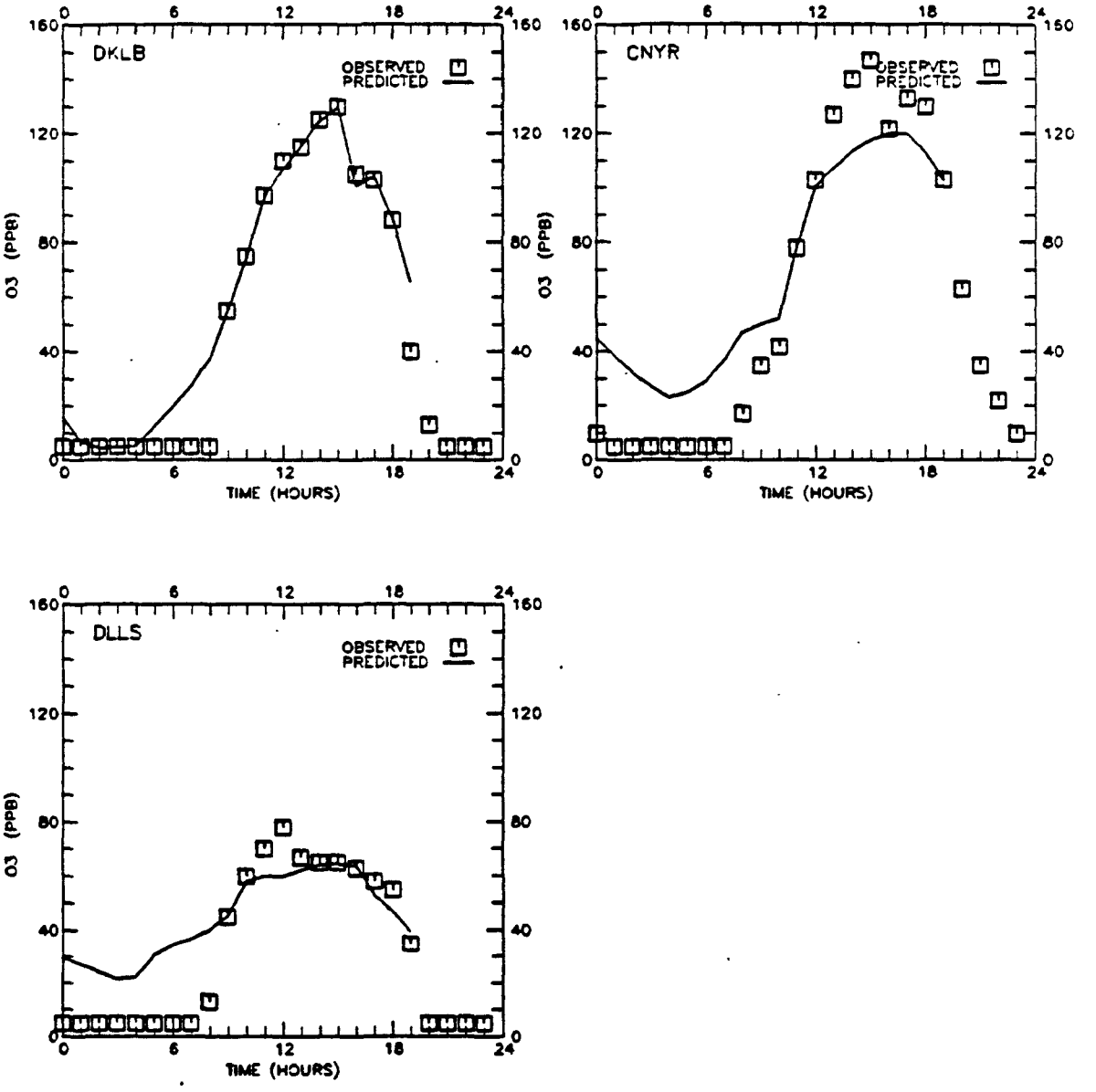

SYSTEMS APPLICATIONS, INC.

FIGURE D-3. Observed and nearest-neighbor predicted (two-cell search) ozone concentration (ppb) for the Atlanta reduced wind speed sensitivity test.

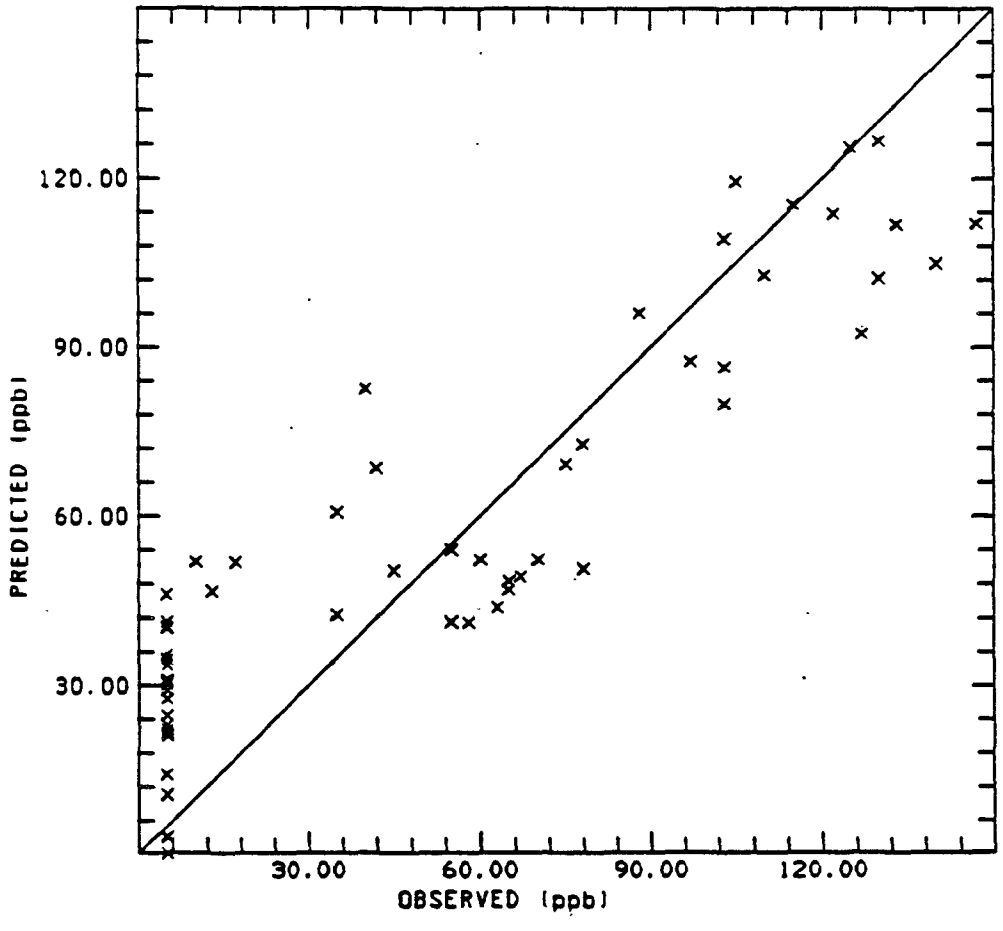

MOMENTS OF THE PROBABILITY DENSITY FUNCTION

	OBSERVED	PREDICTED
AVERAGE	50.39999	56.68703
STANDARD DEVIATION	47.63355	34.20863
SKEWNESS	0.51320	0.52057
KURTOSIS	-1.22432	-0.84048
OTHER MEASURES		
MEDIAN	40.00000	46.90000
UPPER QUARTILE	88.00000	82.56000
LOWER QUARTILE	5.00000	31.13000
MINIMUM VALUE	5.00000	0.02000
MAXIMUM VALUE	147.00000	126.60000

SKILL OF PREDICTION PARAMETERS

CORRELATION COEFFICIENT OF PREDICTED VERSUS OBSERVED 0.904
THE BOUNDS OF THE CORRELATION AT THE CONFIDENCE LEVEL OF 0.050 ARE
LOW BOUND 0.844 HIGH BOUND 0.942
RATIO OF OVER TO UNDER PREDICTIONS 1.308
PERCENT OF OVER PREDICTIONS GREATER THAN 200 PERCENT OF THE OBSERVED 41.667
PERCENT OF UNDER PREDICTIONS LESS THAN 50 PERCENT OF THE OBSERVED 1.667

FIGURE D-4a. Scatterplot and model performance statistics for hourly ozone concentrations and Atlanta reduced wind speeds sensitivity test (N = 60).

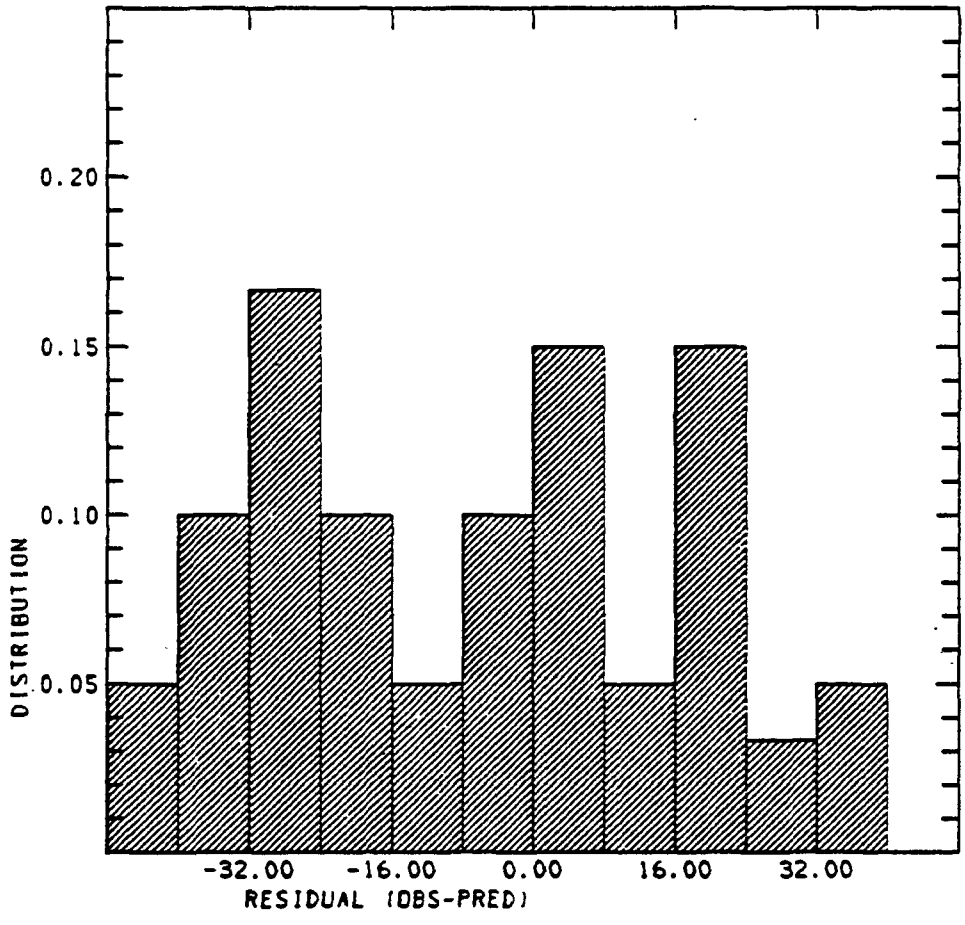

THE BINSIZE EQUALS 8.000

RESIDUAL ANALYSIS

AVERAGE	-6.28719
STANDARD DEVIATION	22.19390
SKEWNESS	0.10702
KURTOSIS	-1.19285
OTHER MEASURES	
MEDIAN	-6.30000
UPPER QUARTILE	9.57001
LOWER QUARTILE	-26.13000
MINIMUM VALUE	-42.56000
MAXIMUM VALUE	35.00000

BIAS CONFIDENCE INTERVAL
AT THE 0.0500 LEVEL
LOWER BOUND -18.9385
UPPER BOUND 6.3641

STD RESIDUAL CONFIDENCE INTERVAL
AT THE 0.0500 LEVEL
LOWER BOUND 373.7107
UPPER BOUND 684.3732

THE MEASURES OF GROSS ERROR
THE ROOT MEAN SQUARE ERROR IS 22.89
THE AVERAGE ABSOLUTE ERROR IS 19.52

VARIOUS MEASURES OF RELATIVE VARIABILITY
OBSERVATION COEFFICIENT OF VARIATION
0.9451
RESIDUAL COEFFICIENT OF VARIATION
0.4404
RATIO OF RESIDUAL TO OBSERVED ST. DEV.
0.4659

FIGURE D-4b. Residual analysis plot and model performance statistics for hourly ozone concentrations and Atlanta reduced wind speeds sensitivity test.

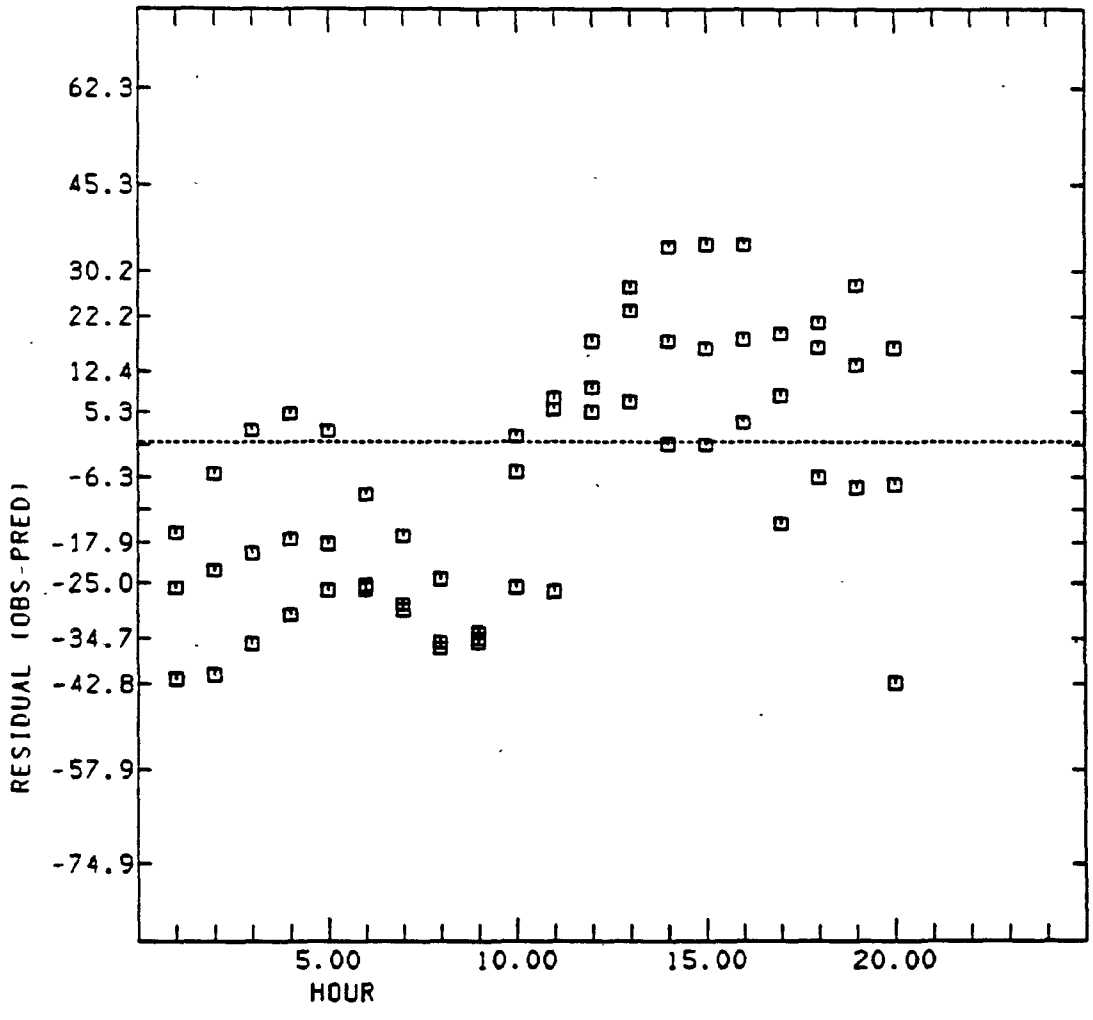

THE LINEAR MODEL PARAMETERS
THE CORRELATION IS 0.5829
THE LOWER BOUND IS 0.3861
THE UPPER BOUND IS 0.7290
AT THE 0.0500 PERCENT LEVEL
THE Y-X LINEAR MODEL INTERCEPT IS 11.460
THE Y-X LINEAR MODEL SLOPE IS 0.153
THE X-Y LINEAR MODEL INTERCEPT IS -29.647
THE X-Y LINEAR MODEL SLOPE IS 2.225

FIGURE D-4c. Plot of residuals versus time of day for hourly ozone concentrations and Atlanta reduced wind speeds sensitivity test.

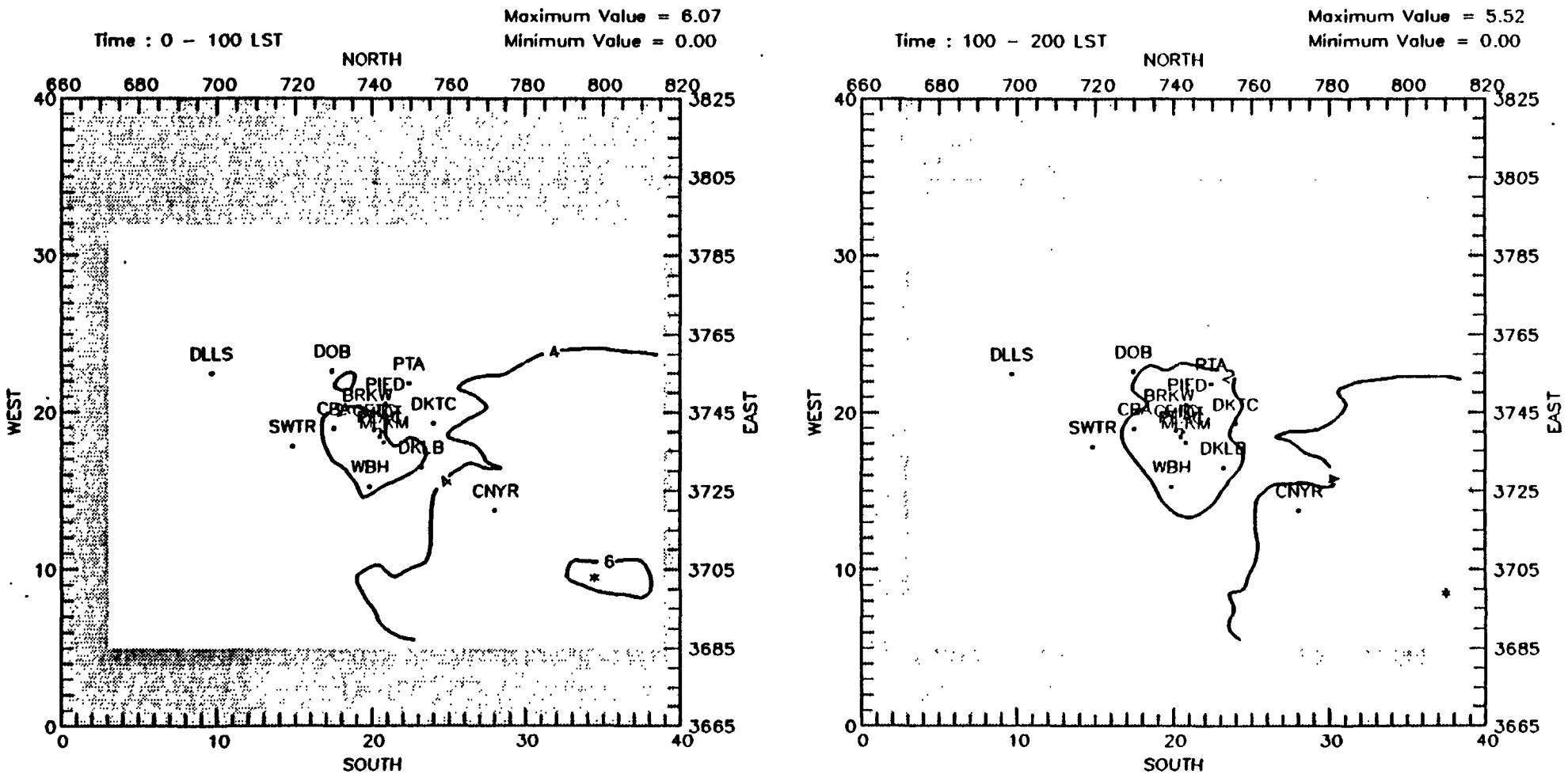

FIGURE D-5. Ozone (pphm) 1985 base emissions, June 4, 1984 (pphm).

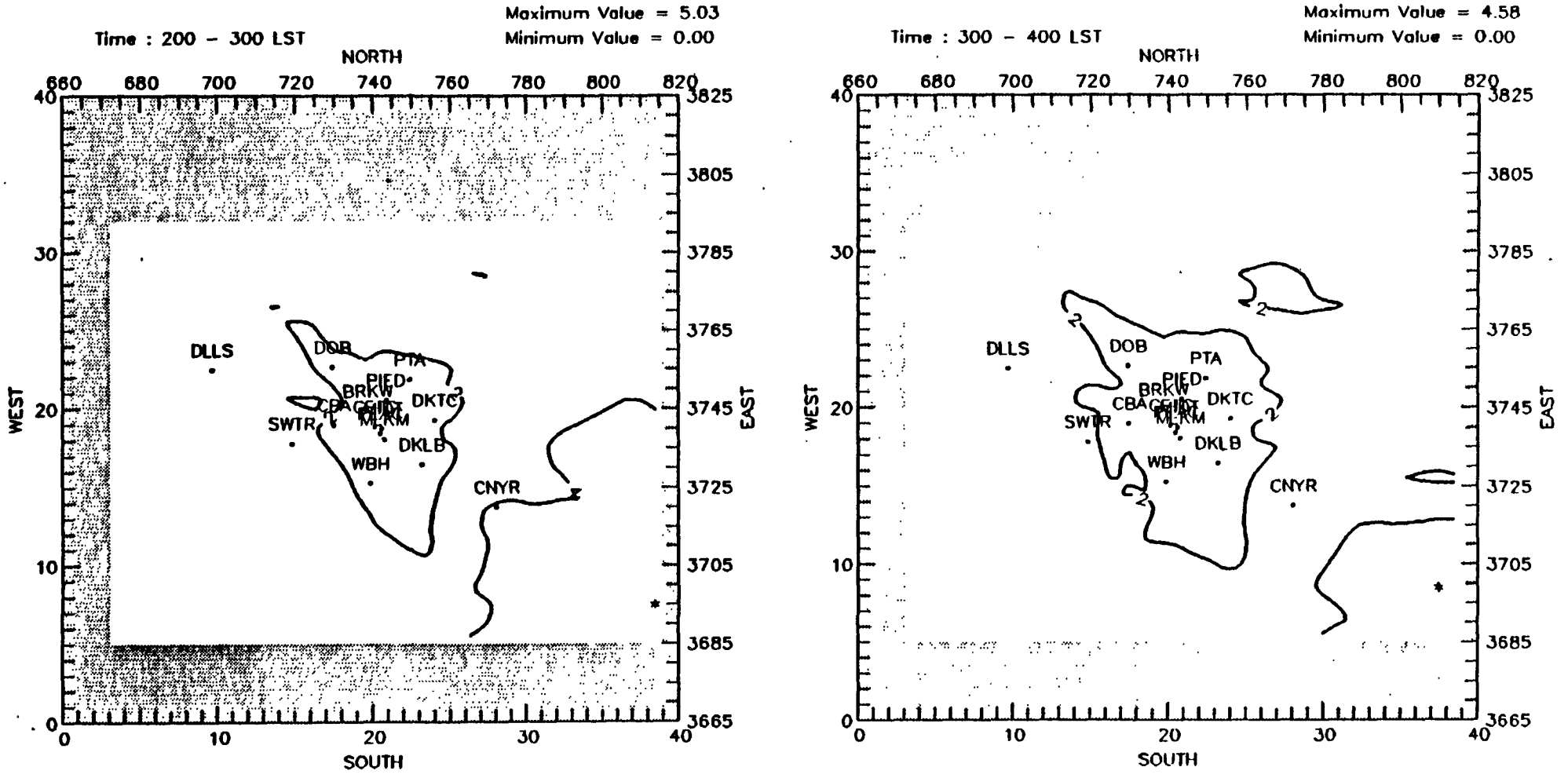

Ozone (pphm) 1985 base emissions, June 4, 1984 (pphm)

FIGURE D-5. Continued.

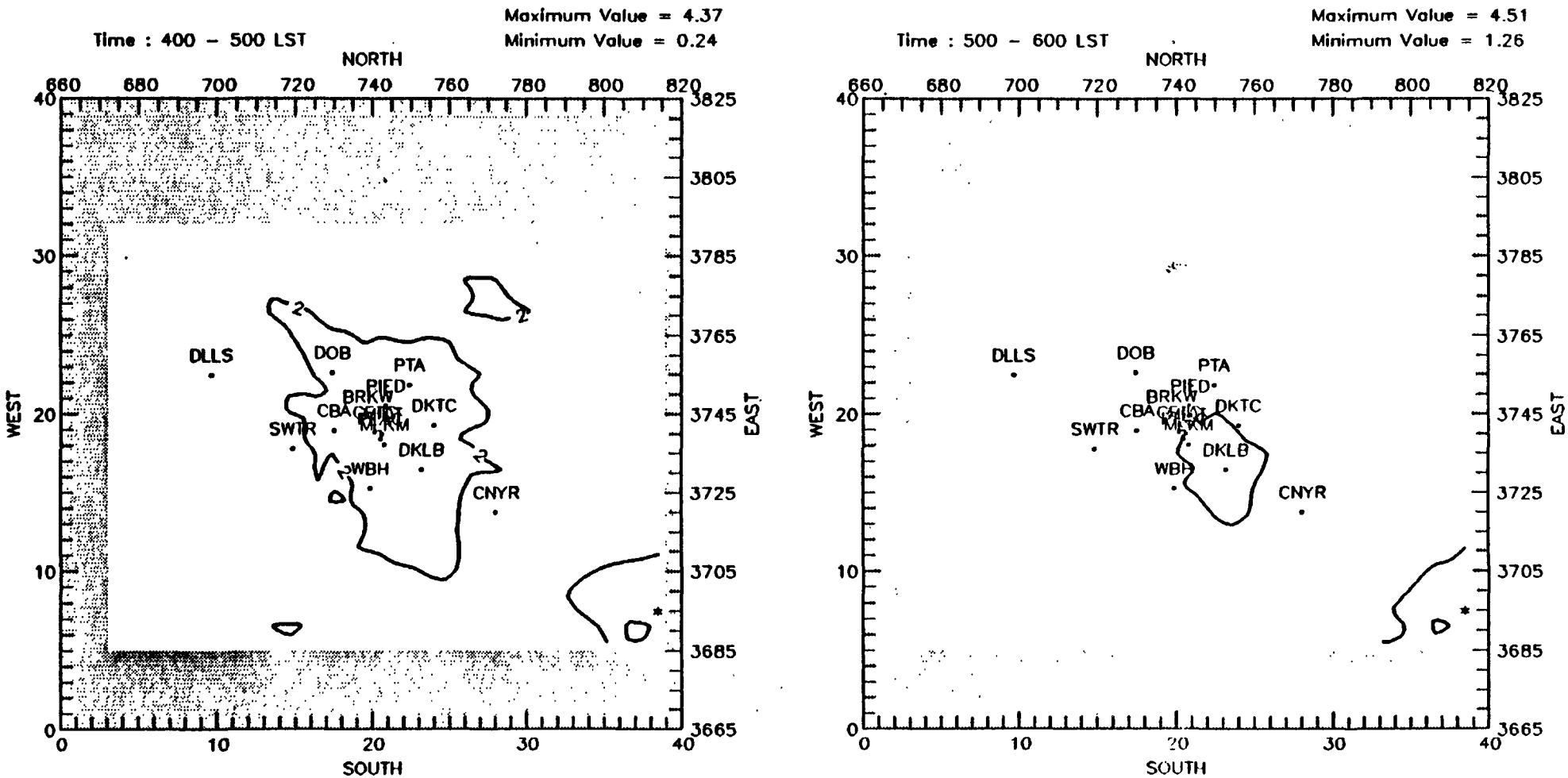

Ozone (pphm) 1985 base emissions, June 4, 1984 (pphm)

FIGURE D-5. Continued.

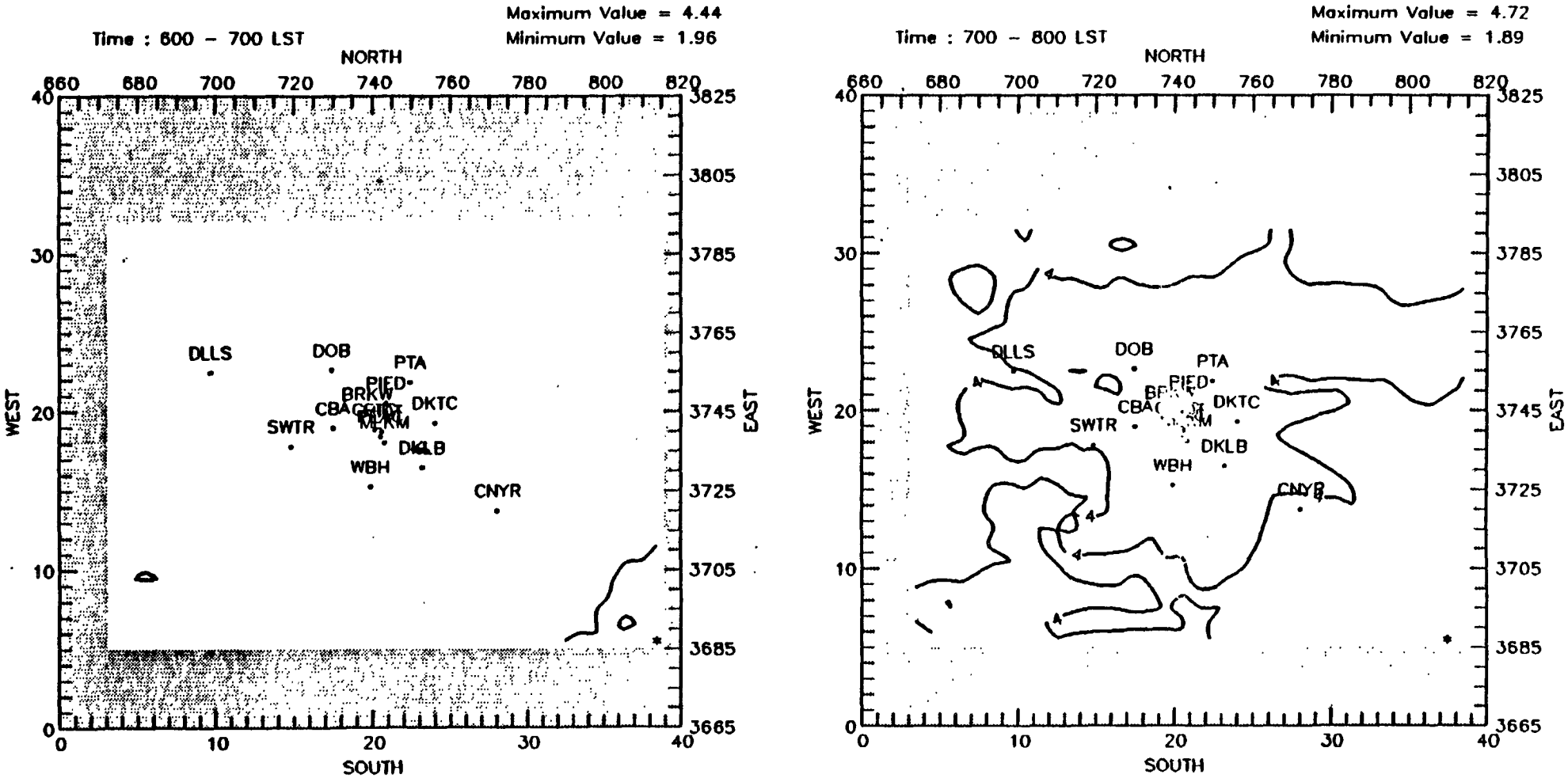

Ozone (pphm) 1985 base emissions, June 4, 1984 (pphm)

FIGURE D-5. Continued.

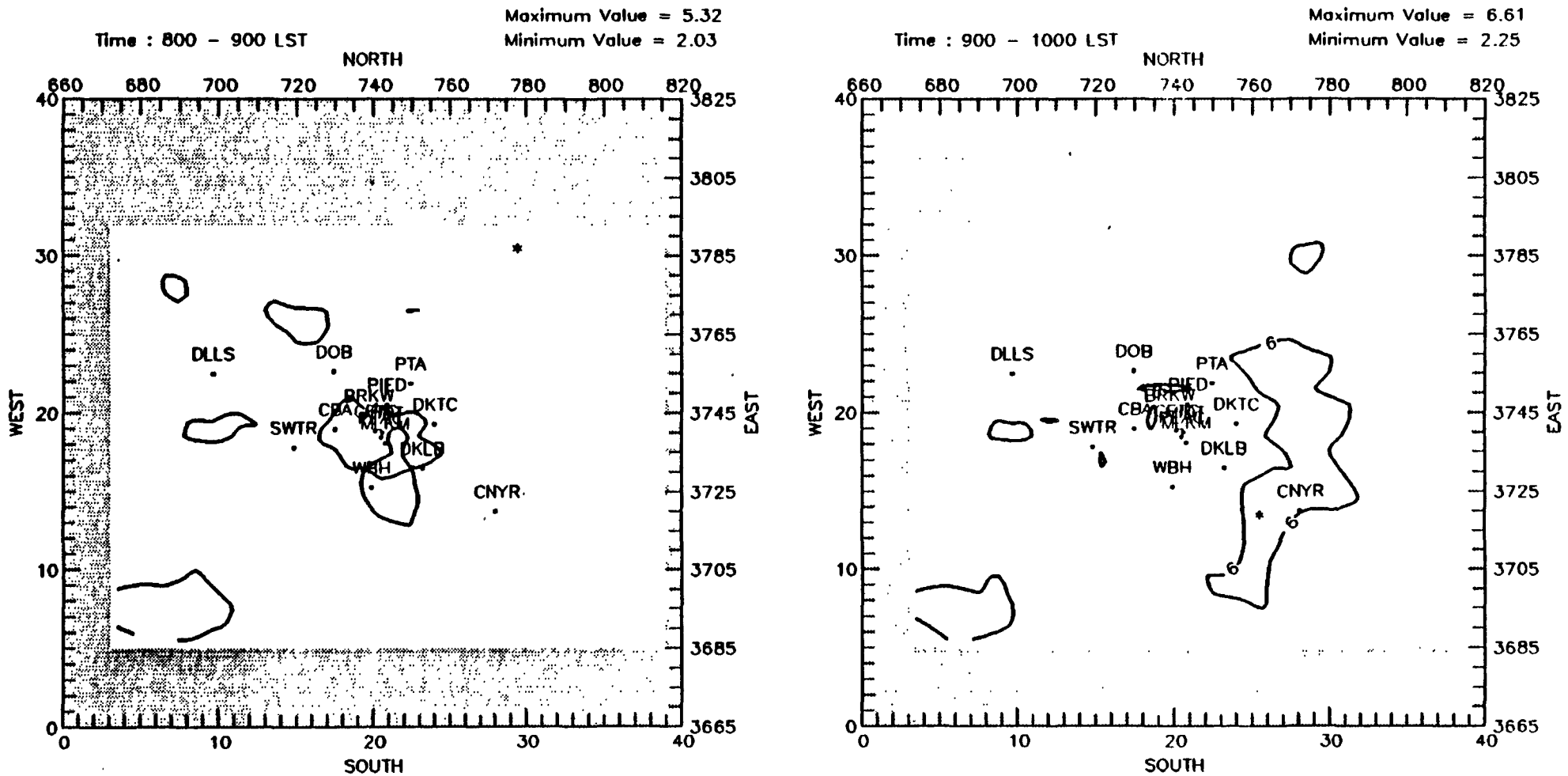

Ozone (pphm) 1985 base emissions, June 4, 1984 (pphm)

FIGURE D-5. Continued.

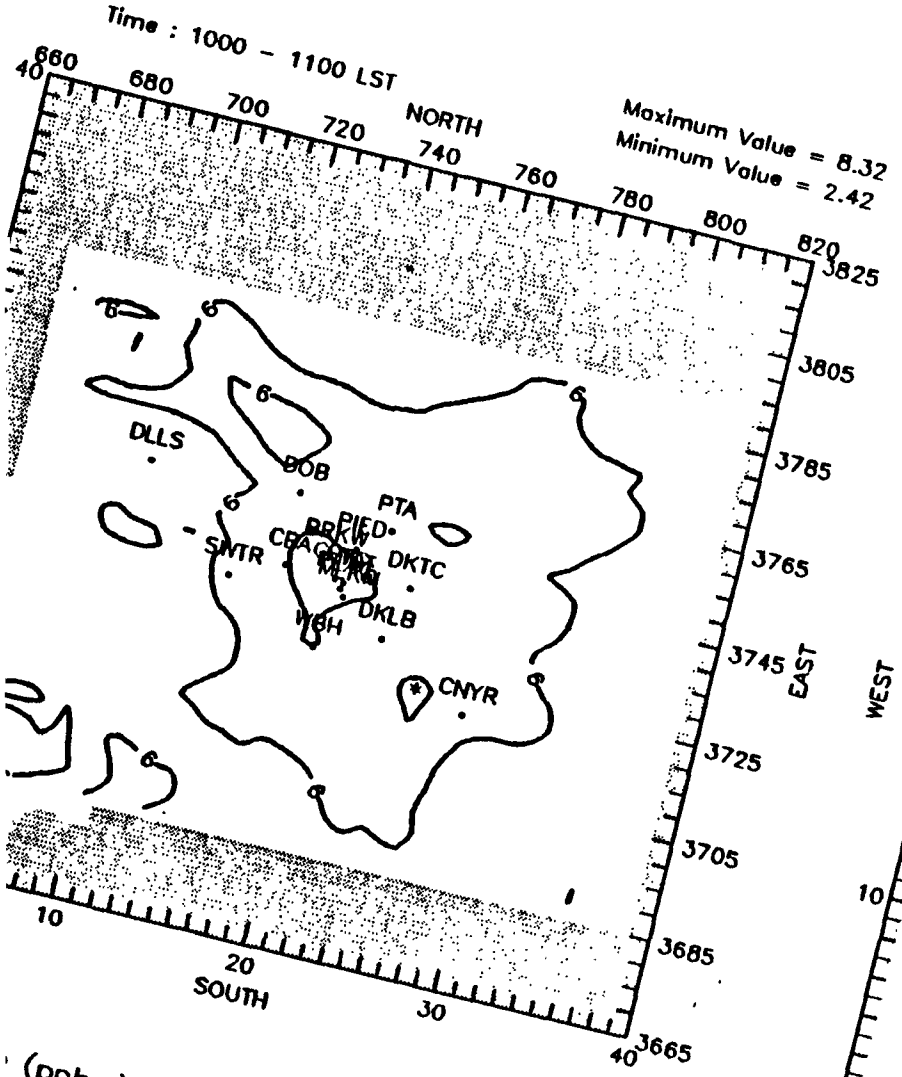

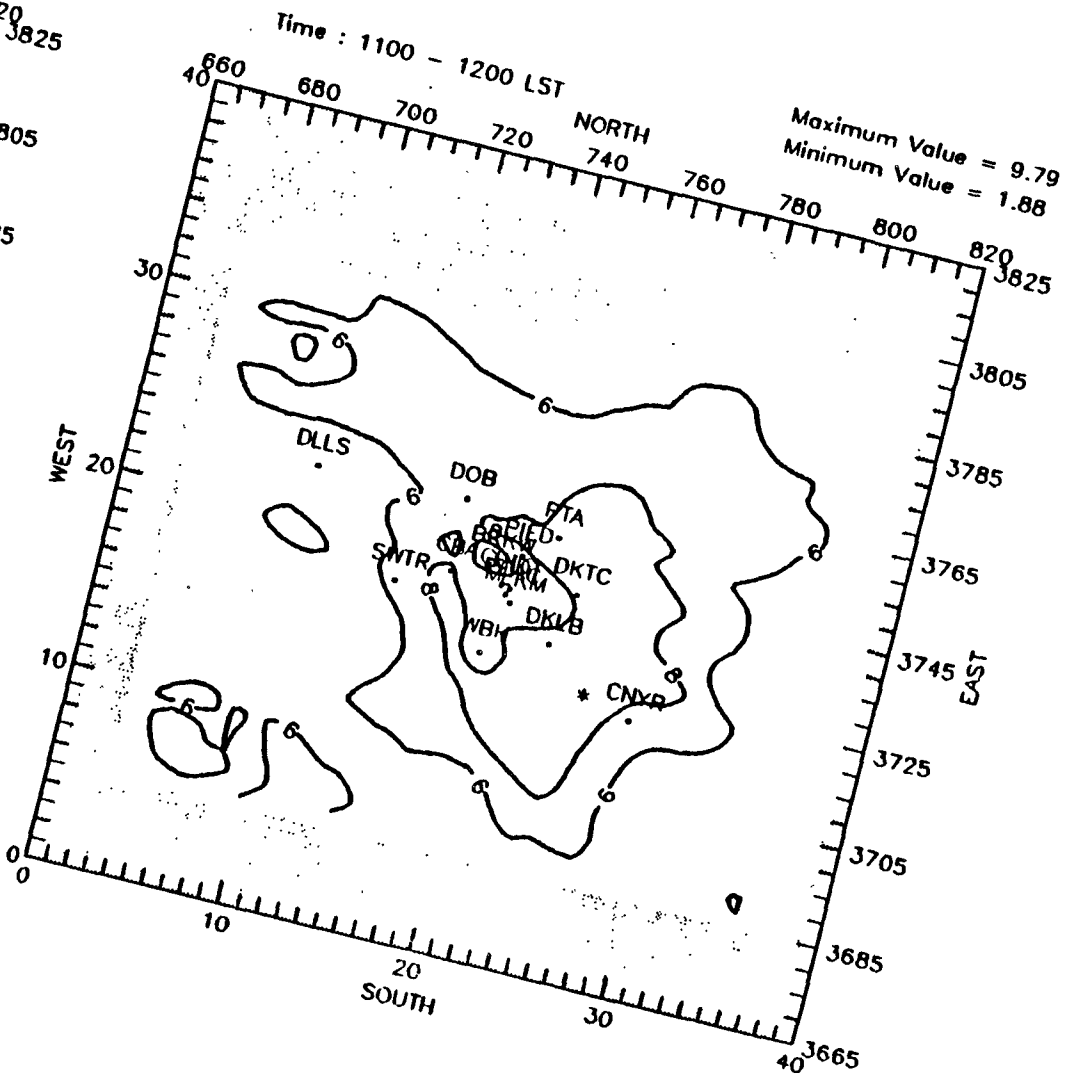

(pphm) 1985 base emissions, June 4, 1984 (pphm)

Continued.

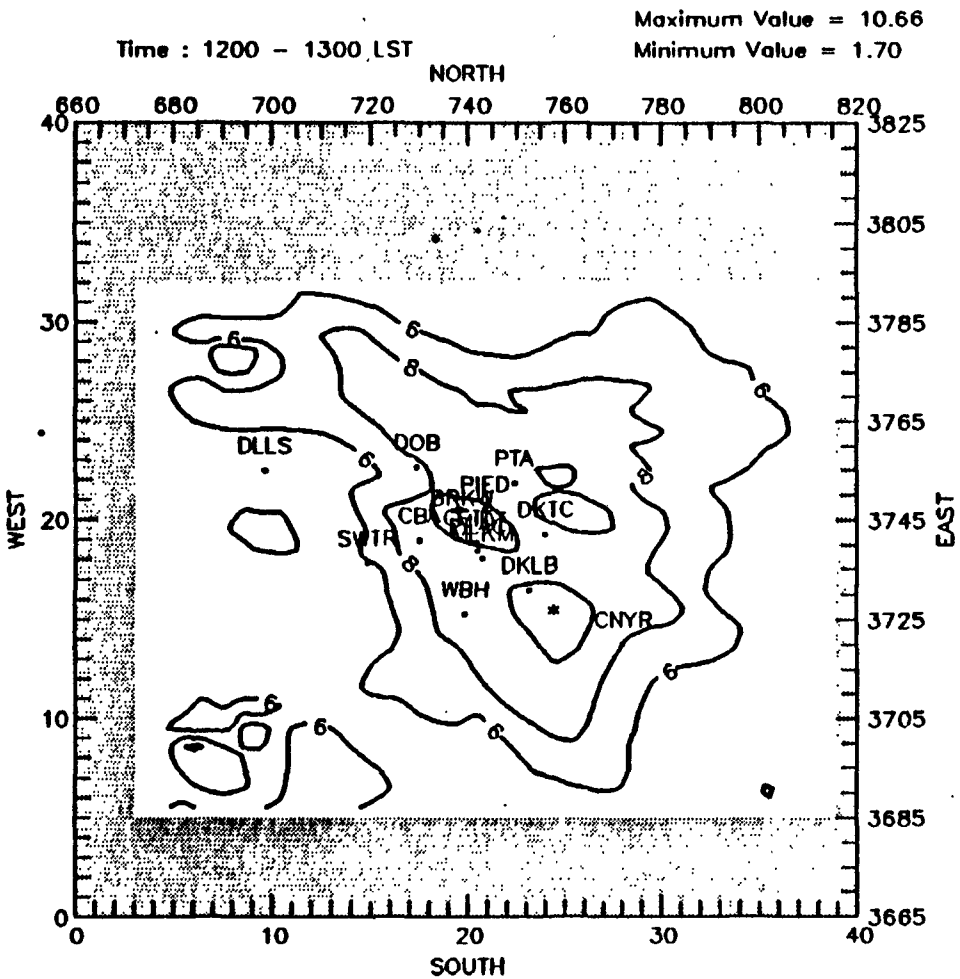

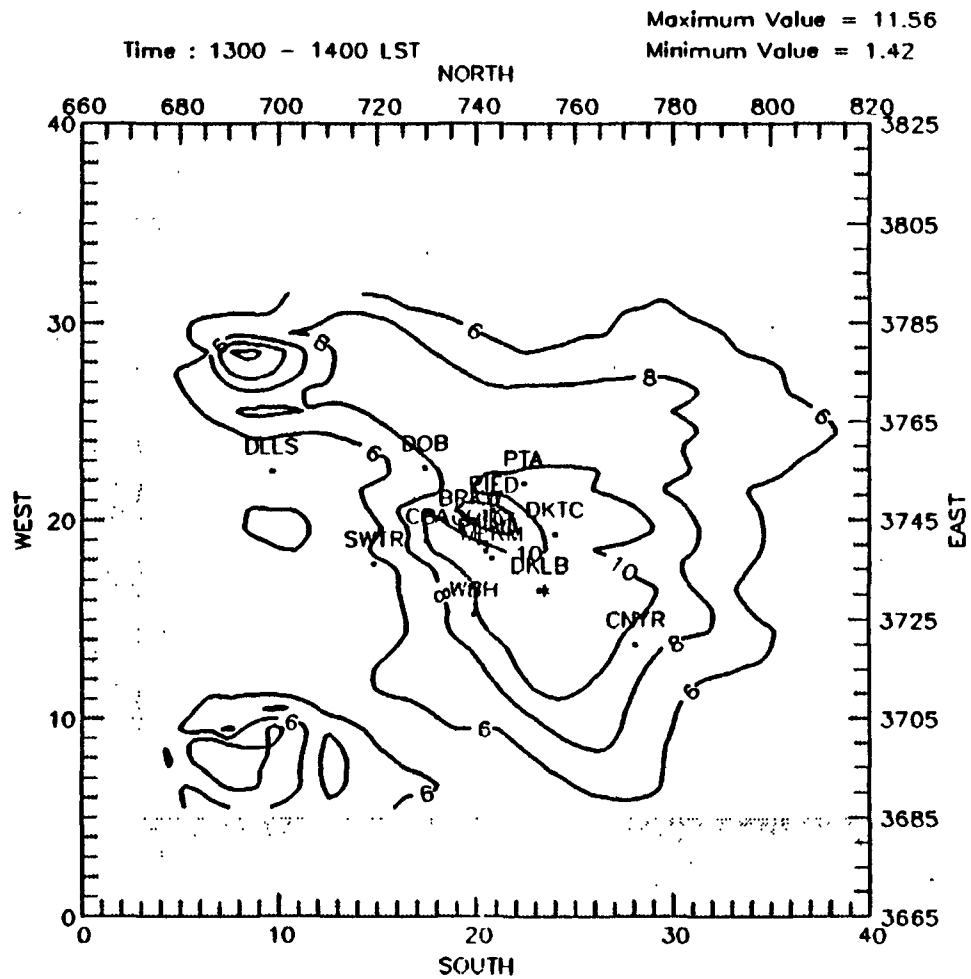

Ozone (pphm) 1985 base emissions, June 4, 1984 (pphm)

FIGURE D-5. Continued.

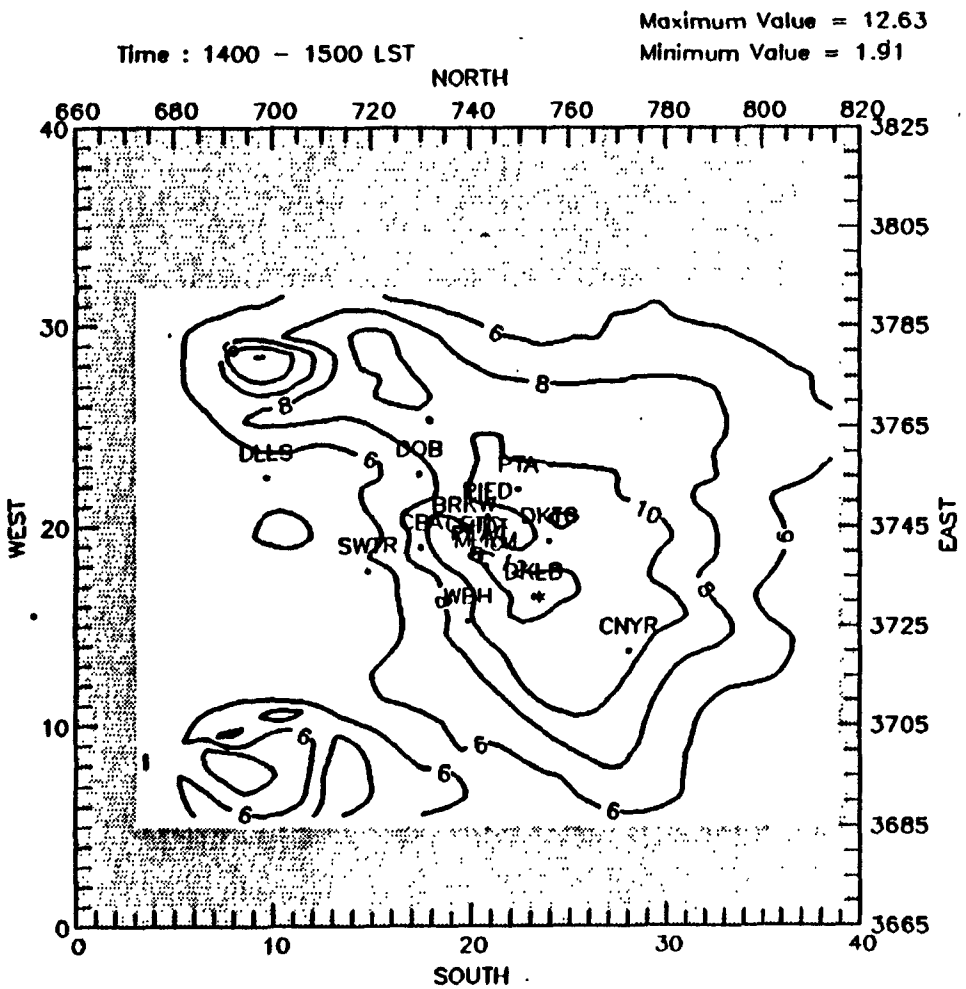

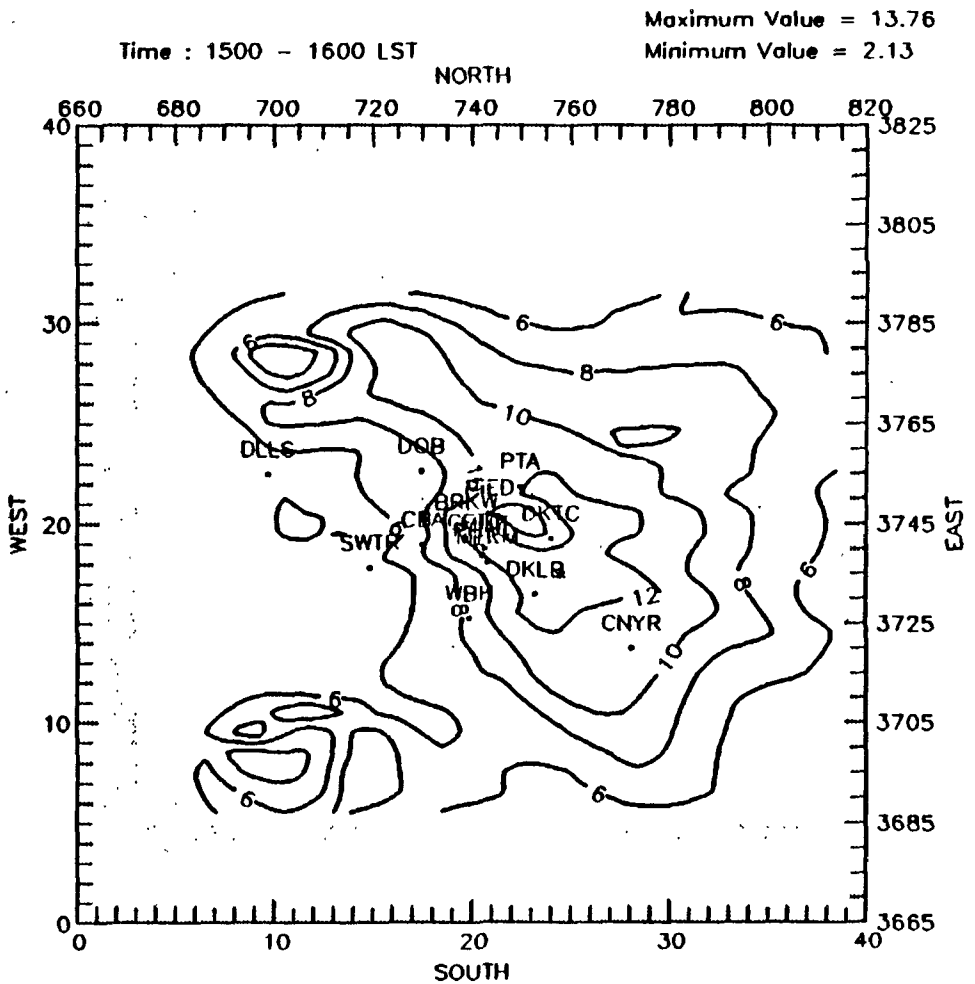

Ozone (pphm) 1985 base emissions, June 4, 1984 (pphm)

FIGURE D-5. Continued.

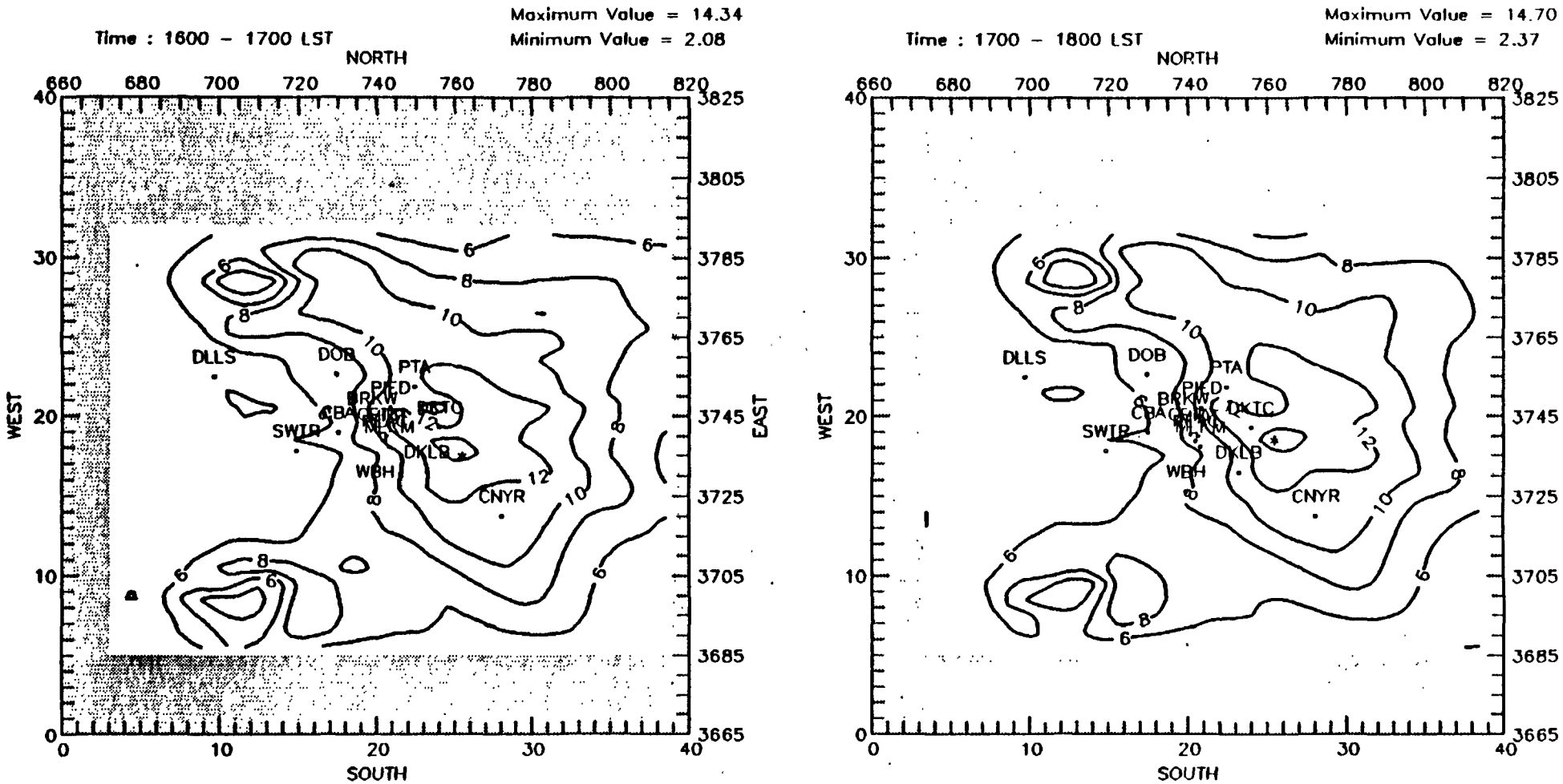

Ozone (pphm) 1985 base emissions, June 4, 1984 (pphm)

FIGURE D-5. Continued.

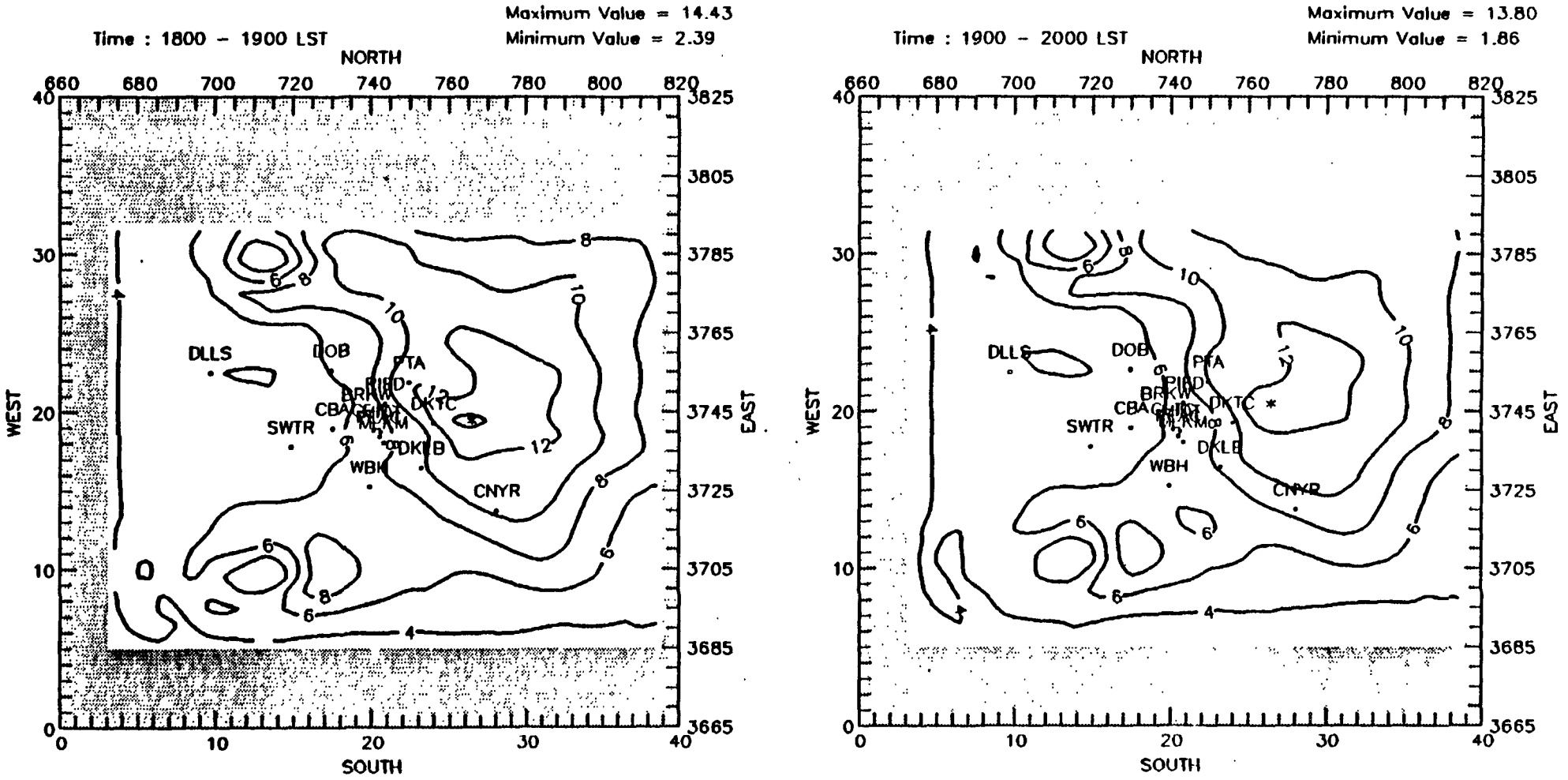

Ozone (pphm) 1985 base emissions, June 4, 1984 (pphm)

FIGURE D-5. Concluded.

Appendix E

MEMORANDUM OF 10 MAY 1989 ON THE SELECTION OF A UAM MODELING EPISODE FOR THE DALLAS-FORT WORTH METROPLEX AREA

MEMORANDUM

TO: Richard Scheffe, EPA/OAQPS
Les Montgomery, TACB
Jim Yarborough, EPA Region VI

FROM: Ralph Morris, Tom Myers, and Ed Carr, Systems Applications, Inc.

DATE: 10 May 1989

SUBJECT: EPA Five Cities UAM Study - Selection of a UAM modeling episode and modeling domain for Dallas-Fort Worth, Texas.

This memorandum provides information for the selection of a UAM modeling episode and domain for the Dallas-Fort Worth metroplex area. At this point, we would like to solicit input from TACB, EPA/OAQPS, and EPA Region VI concerning the definition of the final episode and modeling domain.

SELECTION OF A UAM MODELING EPISODE

A multiday ozone episode will be chosen for the Dallas-Fort Worth area based on observed air quality and meteorological conditions from the years 1984 through 1987. The modeling episode will be selected on the basis of the following criteria:

High and widespread ozone concentrations;

No atypical meteorological conditions; and

Completeness of routine data.

The selection process consists of the following activities:

Analysis of observed elevated ozone days (ozone concentrations greater than the ozone National Ambient Air Quality Standard (NAAQS) of 120 ppb) in the Dallas-Fort Worth area for the years 1984 to 1987;

Definition of possible UAM modeling episodes from grouping of highest observed ozone days;

Examination of the number of station-hours within each possible modeling episode exceeding the ozone NAAQS, and elimination of candidate episodes with low number of station-hours of elevated ozone concentrations;

Analysis of meteorological conditions for the candidate ozone episodes. Perform meteorological classification to determine most typical conditions that lead to elevated ozone episodes in the Dallas-Fort Worth area;

Determination of routine data availability (meteorological and air quality) for candidate modeling episodes; and

Recommendations of possible UAM modeling episodes.

Starting with 106 days of ozone exceedences from the years 1984 to 1987 (and parts of 1988) we have identified three modeling episodes as candidates for the UAM modeling episode. The following paragraphs describe this selection process.

Elevated Ozone Observations

Ozone monitors in the Dallas-Fort Worth area that were in operation during the period of 1984 to 1988 are listed in Table 1. The locations of these monitors are given in Figure 1. Also given in Table 1 is the period of operation for the 14 ozone monitors. Many of these sites were in operation for only a few months in 1986 (FRNK, ERWN, and COIT), 1987 (DAIR), or 1988 (WTHR and FATE). However, there were 6 monitors in continuous operation during the years 1984 to 1987 (NSTR, ILLI, BNVW, DNTN, ROSS, KLLR, and the combined record of MOCK and HNTN which were located close together).

For the period of record that we obtained from the AIRS data base, which includes 1984 to 1987 and parts of 1988 for some monitors, there were 106 days of exceedences of the ozone NAAQS. The rankings of these exceedence days, the monitor where the highest ozone was observed, and the maximum daily ozone concentrations at the other monitors are given in Table 2. By analyzing the top 15 percent of days with ozone exceedences (i.e. the top 16 days) we have identified 12 possible UAM modeling episodes that are listed in Table 3. Table 3 also contains the number of station hours for each day in which the observed ozone concentration exceeds the NAAQS. Since we wish to pick a modeling episode with wide spread occurrence of elevated ozone concentrations (i.e. we do not want to model an ozone exceedence day that just occurs at one monitor and may be due to local effects) we eliminated the days from Table 3 which have less than 15 station-hours of ozone concentrations in excess of the ozone NAAQS. This results in the six candidate UAM modeling episodes that are listed in Table 4.

Meteorological Characterization of Candidate Modeling Days

The meteorology for the high ozone days from Table 4 have been reviewed. The following is a brief discussion of the meteorology on each of those days and recommendations as to it's suitability as a modeling day.

31 July - 3 August, 1984

The dominant feature during this 4-day period (Tuesday-Friday) was the persistent upper-level low pressure system centered along the Oklahoma-Texas border. This persistent upper-level low suggests that elevated levels of ozone and precursors may have been the result of transport from upwind areas. Between the upper levels (at 700 mb approximately 3000m) and the surface, a wind shear in direction of 180 degrees is present throughout the 4-day period. The surface winds are generally light, with the direction predominately from the southeast. Recommendation: The transport of ozone and precursors is probably significant on this day. The multiday nature of the ozone episode would require modeling many days and a larger region, resulting in a need for more computer resources than required for other episodes. Therefore, this episode is probably not appropriate for demonstrating the low-cost application of the UAM.

31 August, 1985

On Friday the 30th of August an upper-level high pressure ridge was located approximately 800 km to the west. The upper level high pressure continued to dominate the region on the 31st and on into the 1st of September. The surface pattern showed light and variable winds throughout the 3 days. At 7 a.m. on 31 August, surface winds were light and from the northwest, while southerly winds were measured aloft. By 7 p.m., the surface and winds aloft were light and from the south. The maximum temperature climbs during this three day period from 96 to 100 to 103. No frontal passages or troughs were present seen throughout the period. It is speculated that the 30th served as a buildup period for the high ozone values seen on the 31st. No significant break in the meteorology occurred during this period. The most likely reason the maximum ozone concentration was lower on the 1st was that the precursor emissions were probably much lower on Sunday the 1st of September resulting in much lower observed ozone values. Recommendation: This is a possible modeling day, however, the only reservation is that the emissions for Saturday may be more difficult to characterize than normal weekday emissions. In addition, the Saturday emissions may be atypical and not representative of conditions that occur during weekday periods.

25 June, 1984

Surface high pressure dominated the region on the 24th - 25th. Upper level winds were light and variable from the east to northeast with speeds less than 9 knots throughout the planetary boundary layer. These nearly stagnant conditions at the surface and aloft allowed the high levels of ozone to develop on the Monday the 25th. Recommendation: This is a possible modeling day, no unusual meteorology occurs during this time period and ozone is locally produced. Again the only reservations are that the emissions on Sunday the 24th (the initialization day) may be more difficult to estimate than normal weekday emissions.

3 September, 1985

The transition of tropical Storm "Elena" to an extratropical cyclone created the conditions necessary for the high ozone episode. The upper air flow near Dallas on Monday the 2nd showed winds from the northeast. These winds became stronger and more southerly on the 3rd when the extratropical cyclone regressed towards the Texas-Louisiana border. Recommendation: This should not be used as a model day, it does not appear to be a typical high ozone episode case because of the influence of the tropical storm "Elena".

9 September, 1987

A fairly complex surface pattern existed on Wednesday morning the 9th of September with a low pressure trough located to the NW near Amarillo, Texas. The low deepened during the day which resulted in areas of widely spread precipitation just north of Dallas the following day. Surface winds were generally light and from the northwest while upper air winds were more westerly. Ozone generated on this day was most likely locally produced. Recommendation: This would not be the best choice for a modeling day, because of the previous day precipitation and the complex flow that developed on the 9th.

1 August, 1986

The three day period (30 July to 1 August, 1986) from a Wednesday - Friday was characterized by a surface high pressure and an upper-level high pressure system. This resulted in three consecutive days in which the temperature reached a maximum of 106 F. Upper-level air flow during this three day period was generally weak with most winds under 10 knots below 700mb. Surface flow was from the southwest to

southeast. Passage of a very weak cold front on the afternoon of the 1st and the migration of the upper level high eastward resulted in a large increase in the ventilation with wind speeds of 12 knots or more throughout the layer from the surface to 1500 meters ending the stagnation episode. Recommendation: This looks like a possible choice for an ozone modeling day because the meteorology appears to be typical of a high ozone day and the conditions show that transport of ozone and precursors are of minimal importance. However, the frontal passage that occurs on 1 August may be difficult to characterize the transition of the upper-level winds with only the routine twice daily upper air observations.

Data Availability and Discussion

Routine meteorological data was available for each of the six candidate UAM modeling episodes listed in Table 4. Figure 2 displays time series of ozone concentrations at each of the 14 ozone monitors for the days from the six candidate modeling episodes. The spatial distribution of the observed maximum daily ozone concentrations for each of the candidate modeling days are given in Figure 3. All of the candidate episodes had at least 7 ozone monitors in operation for some of the time with the August 1, 1986 episode having up to nine ozone monitors in operation. The meteorological analysis has identified three modeling days as most suitable: June 25, 1984; August 31 1985; and August 1, 1986.

June 25, 1984

As seen in Figure 2f, some observed hourly ozone concentrations were missing from the seven ozone monitors in operation on June 25, 1984. The stagnant conditions on this day resulted in the occurrence of high observed ozone concentrations (150 ppb) in both Dallas and Fort Worth (see Figure 3f). The 150 ppb observation in Fort Worth occurred at noon, which indicates it may be partially due to the previous days ozone cloud that is entrained into the mixed-layer as the mixing height rises. The maximum daily ozone concentration (150 ppb) for Dallas occurred in the late afternoon, thus it was most likely locally produced. The twice daily upper-air soundings for June 25, 1984 show upper-level winds that are fairly persistent from the east to northeast at all levels. The upwind ozone monitor (DNT2) measured a maximum daily ozone concentration of 90 ppb which persisted throughout the day from 9 in the morning to 6 in the afternoon. Thus, sources upwind of the Dallas-Fort Worth metroplex area, or recirculation of emissions, may be contributing 90 ppb to the peak observed ozone concentrations.

August 31, 1985

As noted previously, August 31, 1985 is a Saturday at the end of a three-day ozone episode. There are most likely differences in emissions levels and distribution on this day due to differences in weekend industrial activity and traffic patterns. As seen in the time series (Figure 2e), the seven ozone monitors in operation have a complete data record and the maximum daily observed ozone concentrations occur in the afternoon. This indicates the possibility that the ozone was most likely formed from emitted precursors on this day rather through the entrainment of concentrations aloft that may have been formed earlier. Winds are predominantly from the south, and the upwind ozone monitor (BNVW) observes relatively low ozone concentrations with a peak of 80 ppb (see Figure 3e). The August 31, 1985 is mainly a Dallas ozone episode with high maximum daily ozone concentrations (170 ppb) occurring at two monitors (MCK3 and DNTN). Although ozone concentrations are lower in Fort Worth, ozone exceedences are observed at both ozone monitors there (130 ppb).

August 1, 1986

During the August 1, 1986 ozone episode there are more ozone monitors in operation than the other candidate episodes (see Figure 2i), however two of the monitors upwind or in Dallas (HNT2 and BNVW) are missing afternoon ozone observations. The frontal passage that occurs on this day results in a turning of the winds from the southwest at 7 a.m. to the southeast by 7 p.m.. The westerly component in the morning wind may result in the transport of ozone precursors from Fort Worth to Dallas. There is an orderly buildup of maximum daily ozone concentrations going from south to north through Dallas. Fort Worth does not observed and exceedence of the ozone standard on this day.

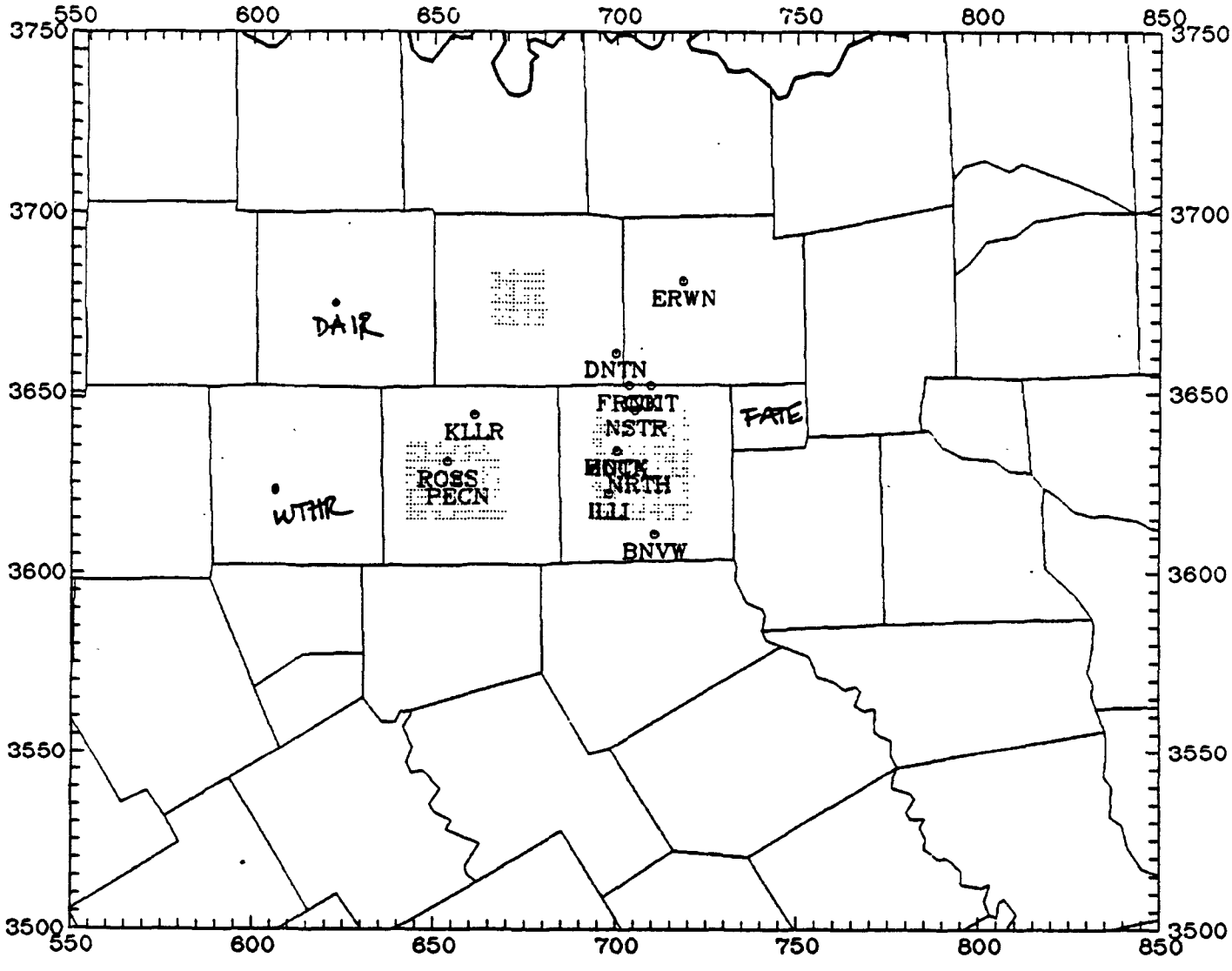

FIGURE 1. Location of ozone monitors in the Dallas-Fort Worth region.

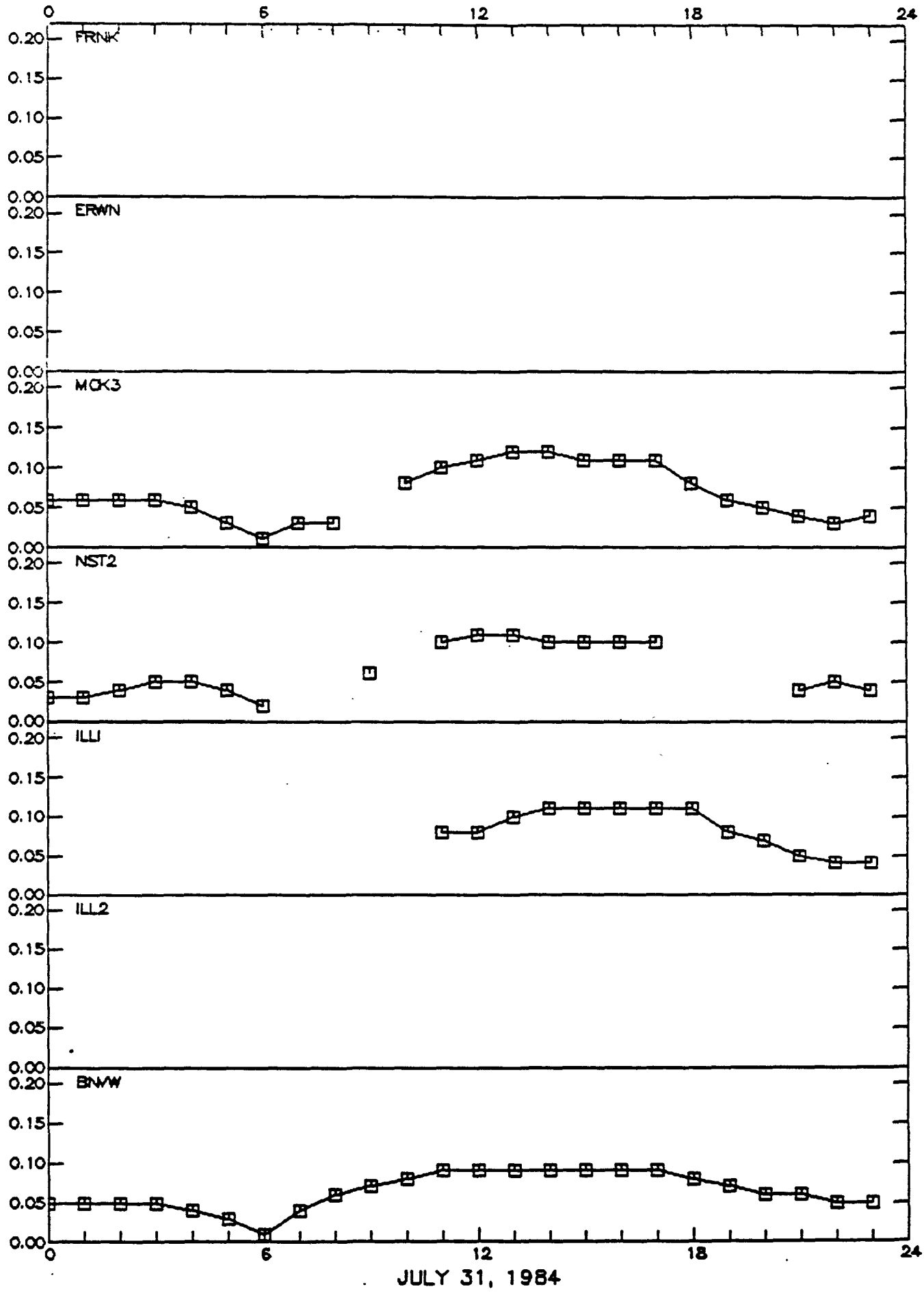

Figure 2a. Observed ozone concentrations (ppm) for Dallas – Fort Worth Area

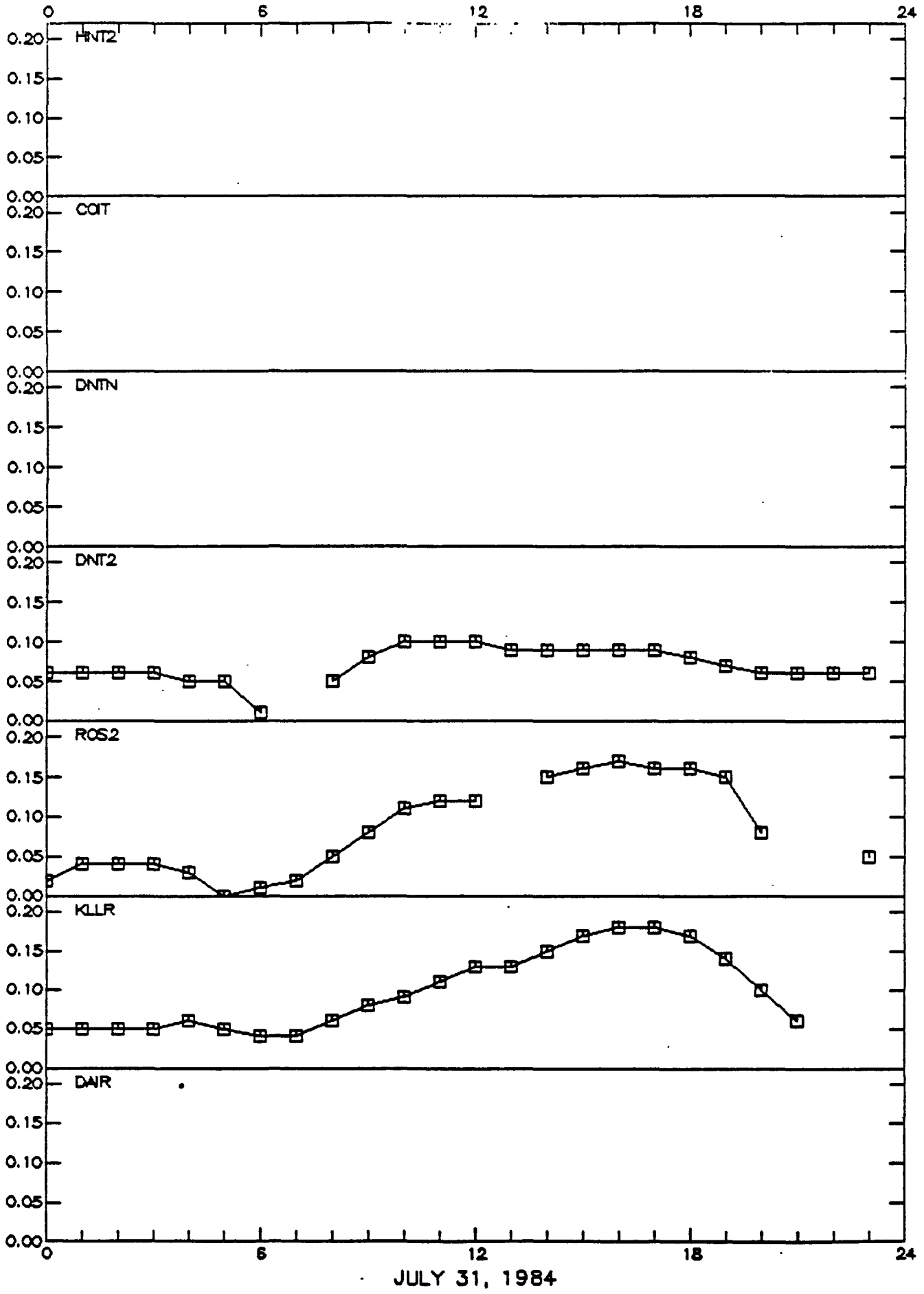

Figure 2a. Observed ozone concentrations (ppm) for Dallas – Fort Worth Area

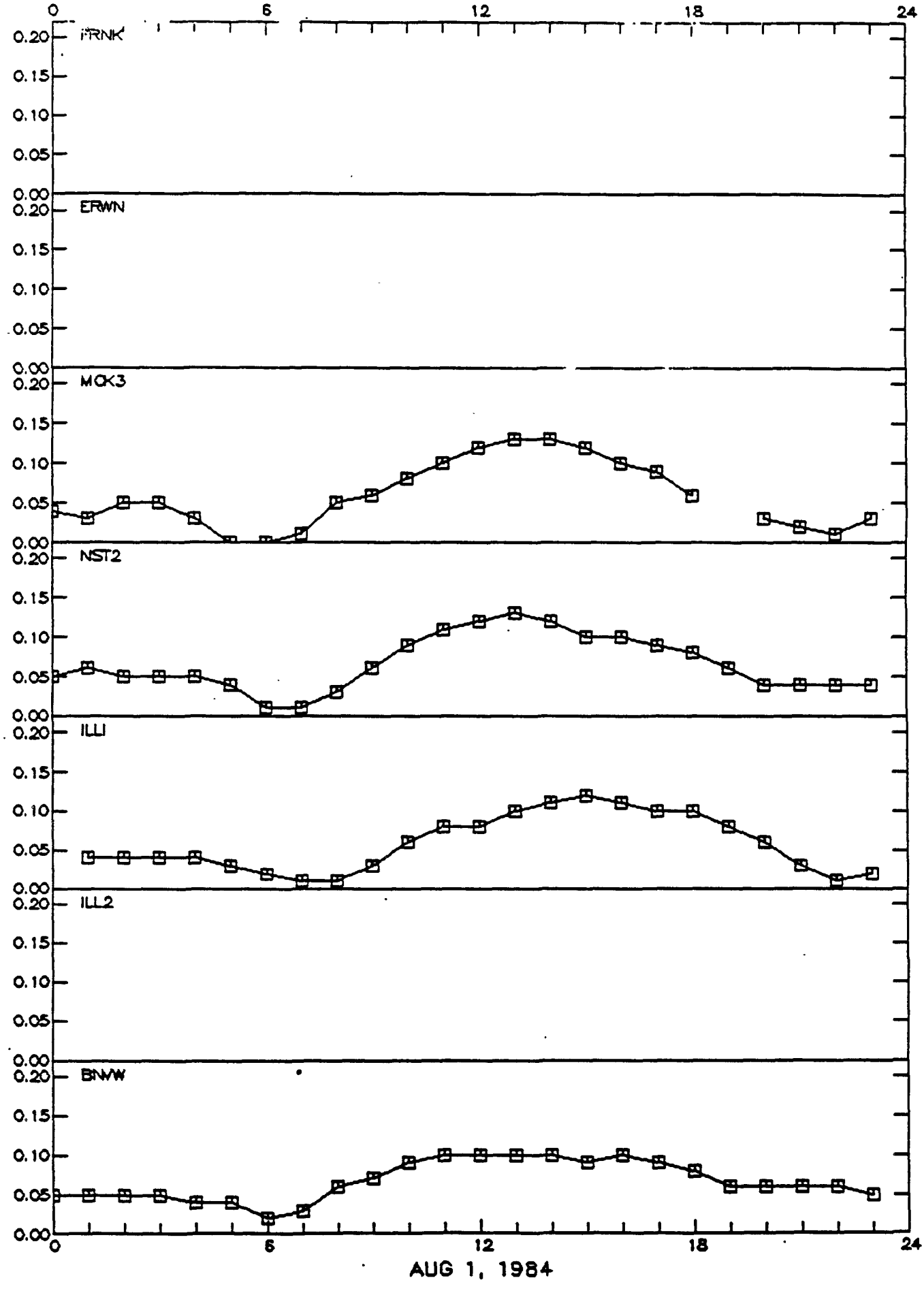

Figure 2b. Observed ozone concentrations (ppm) for Dallas – Fort Worth Area

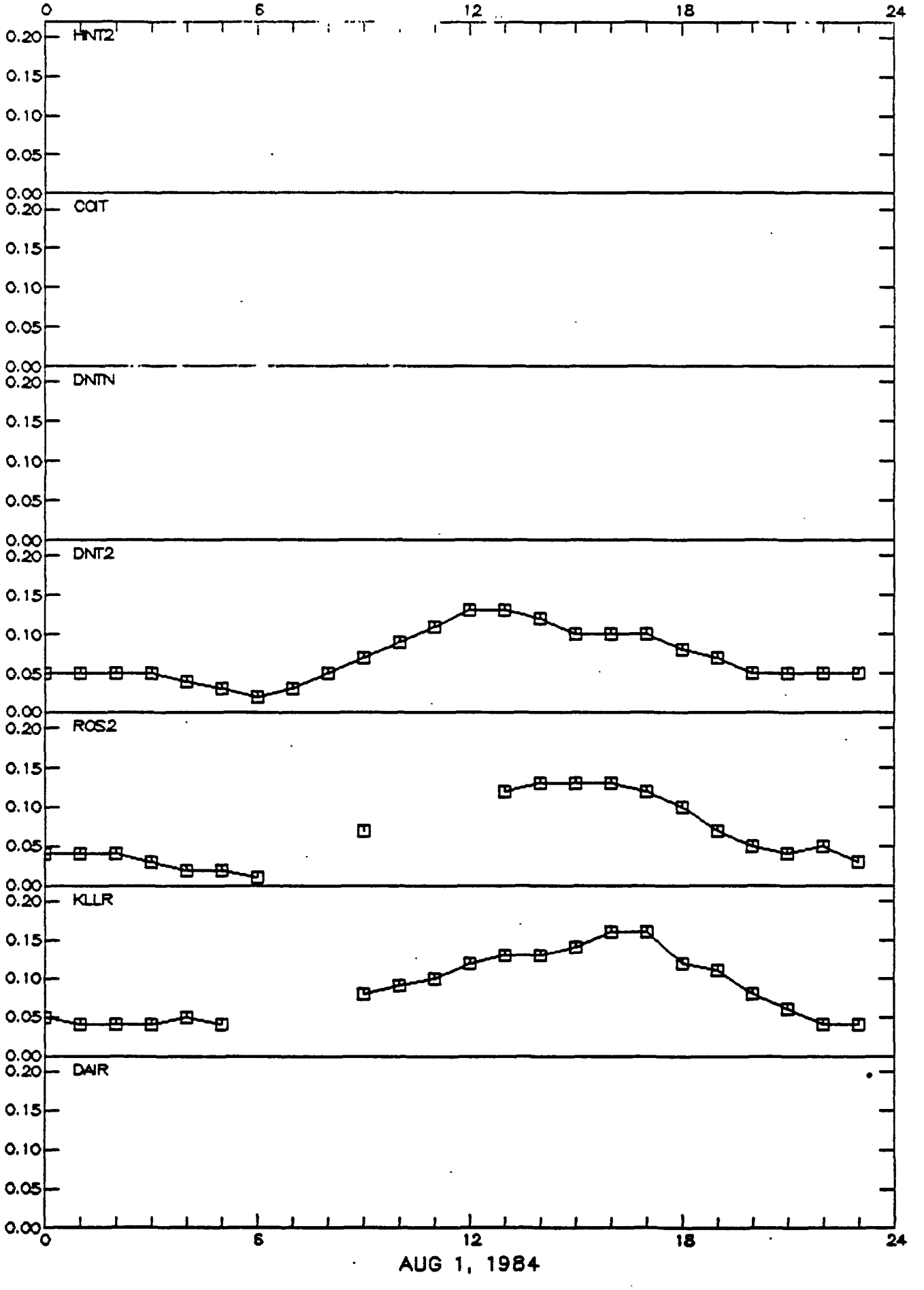

Figure 2b. Observed ozone concentrations (ppm) for Dallas – Fort Worth Area

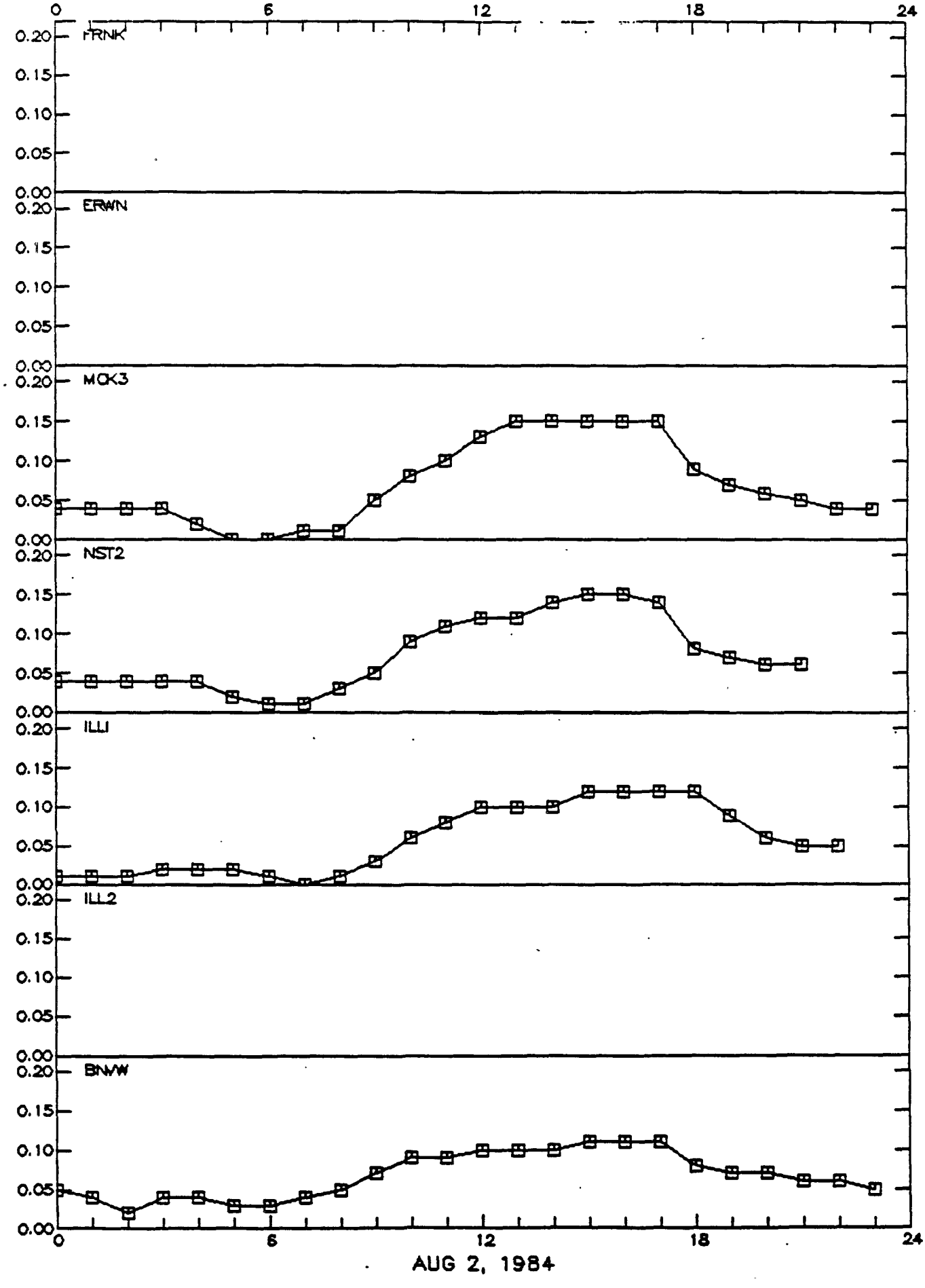

Figure 2c. Observed ozone concentrations (ppm) for Dallas – Fort Worth Area

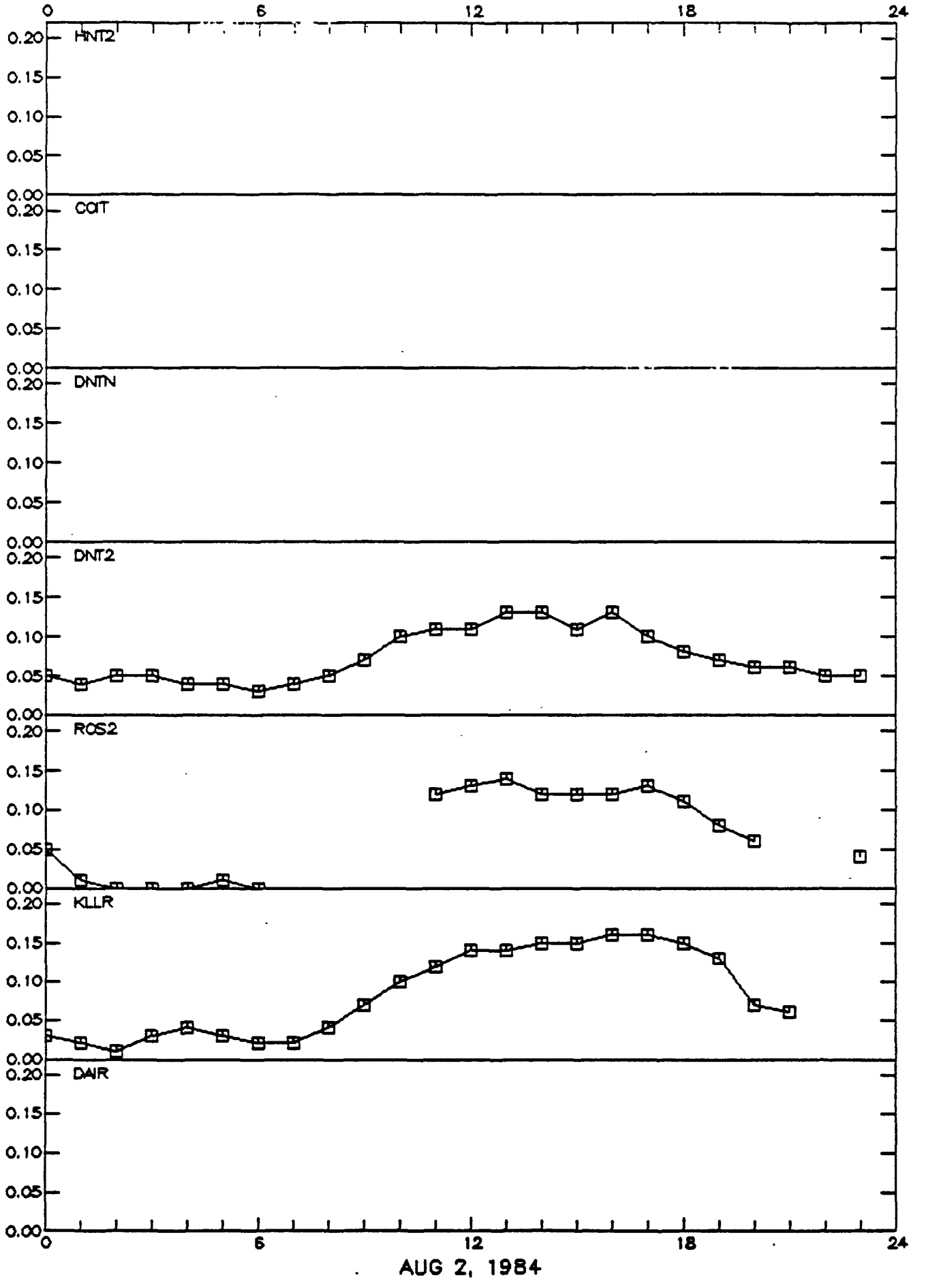

Figure 2c. Observed ozone concentrations (ppm) for Dallas – Fort Worth Area

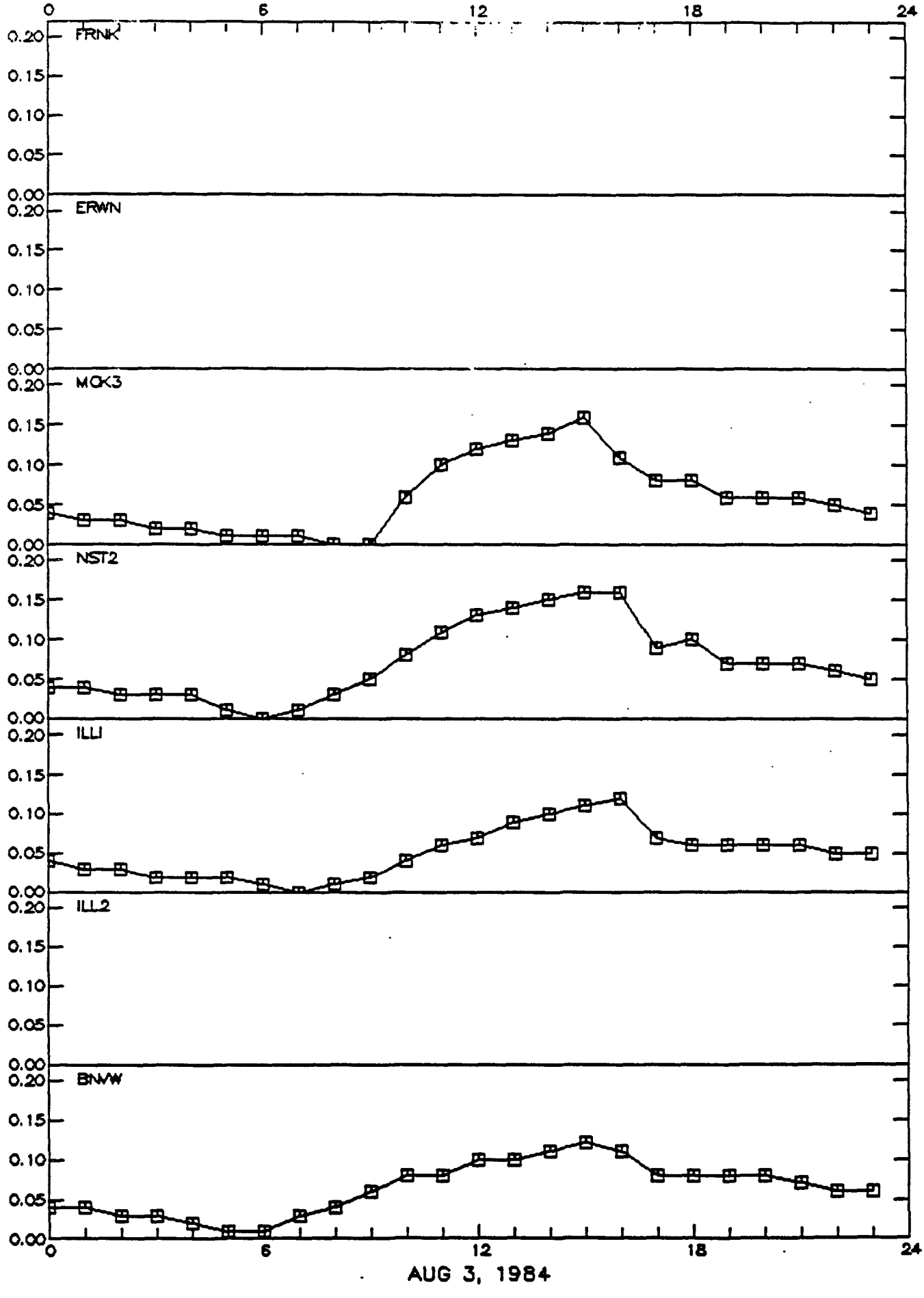

Figure 2d. Observed ozone concentrations (ppm) for Dallas – Fort Worth Area

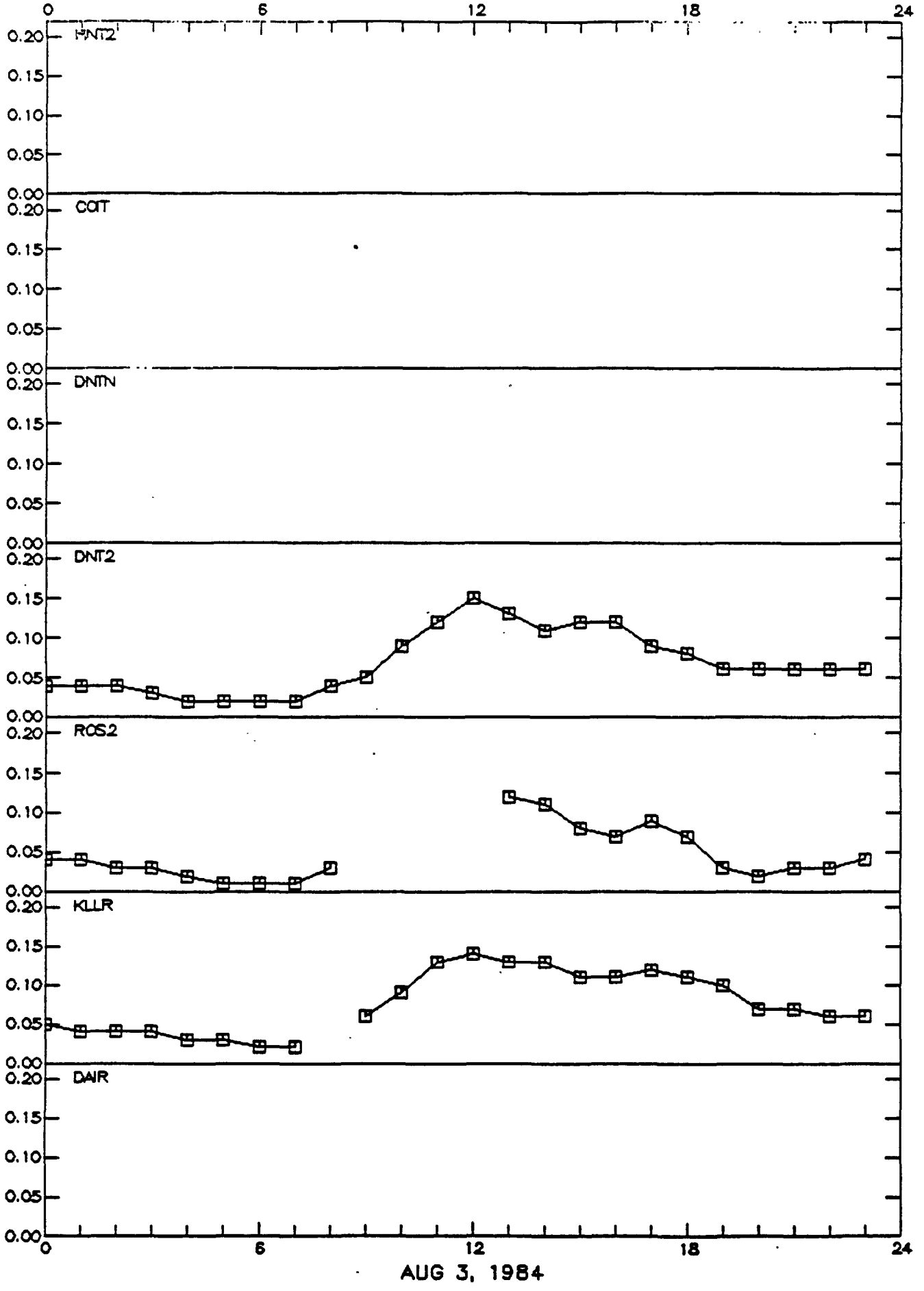

Figure 2d. Observed ozone concentrations (ppm) for Dallas – Fort Worth Area

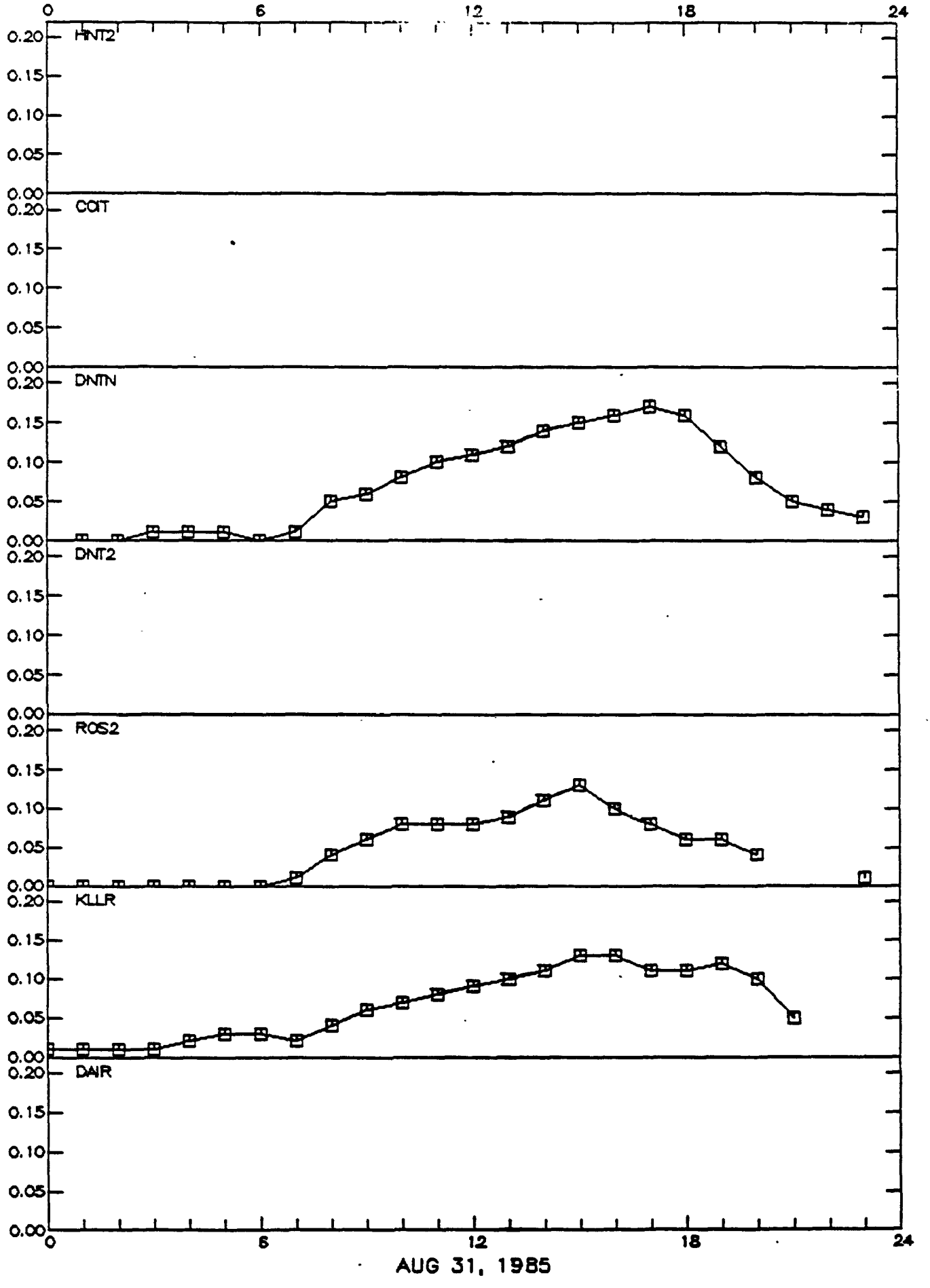

Figure 2e. Observed ozone concentrations (ppm) for Dallas – Fort Worth Area

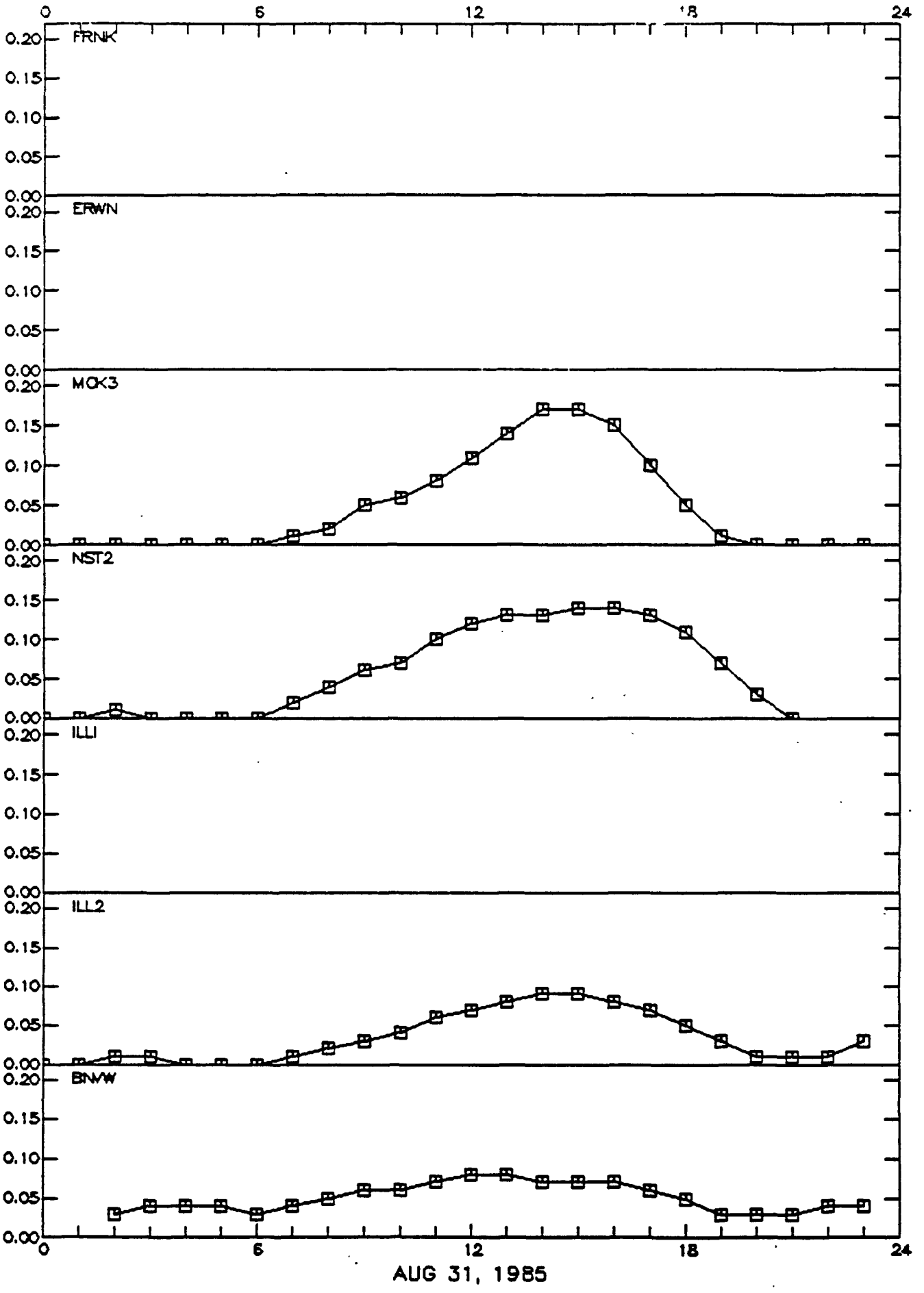

Figure 2e. Observed ozone concentrations (ppm) for Dallas – Fort Worth Area

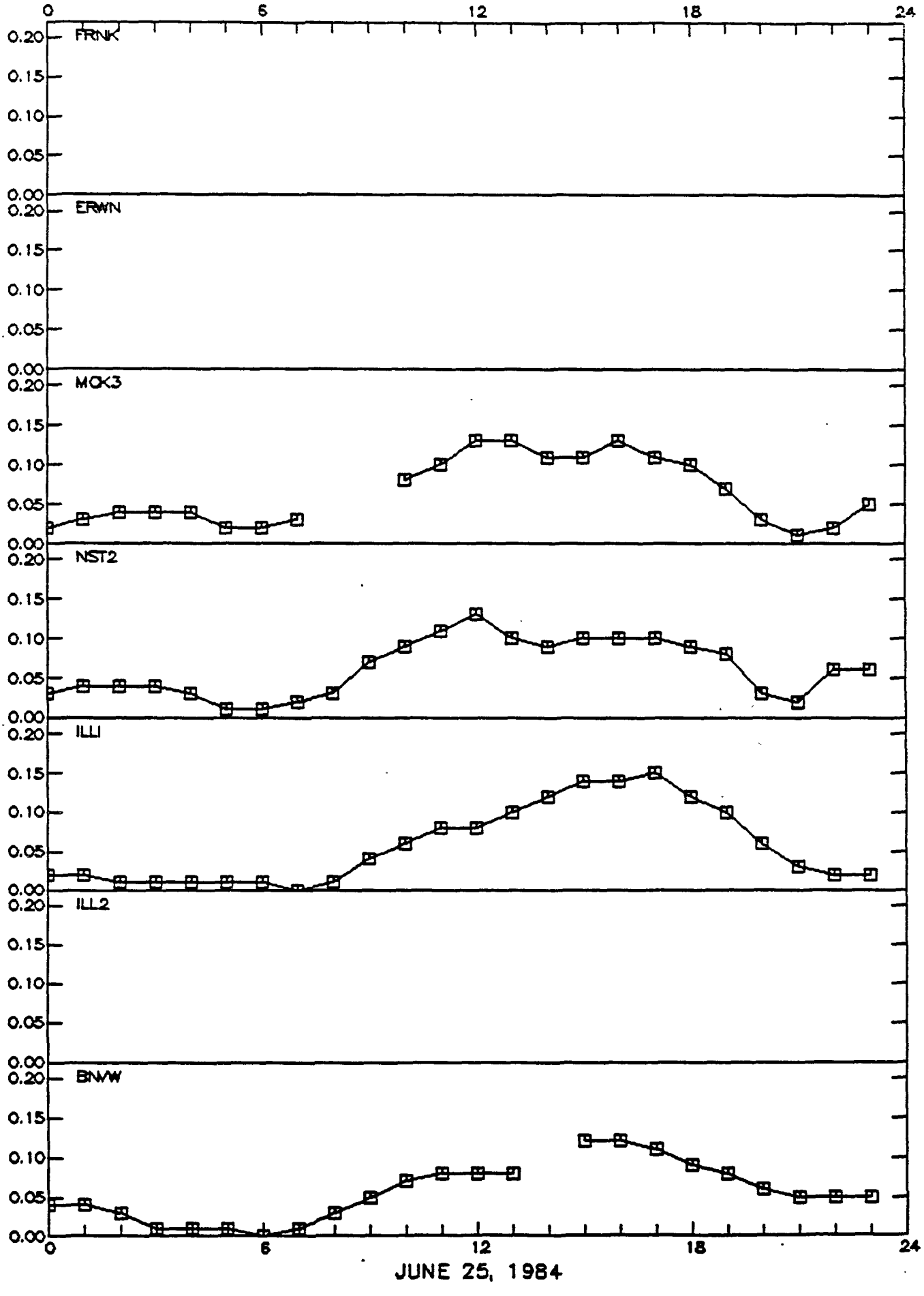

Figure 2f. Observed ozone concentrations (ppm) for Dallas – Fort Worth Area

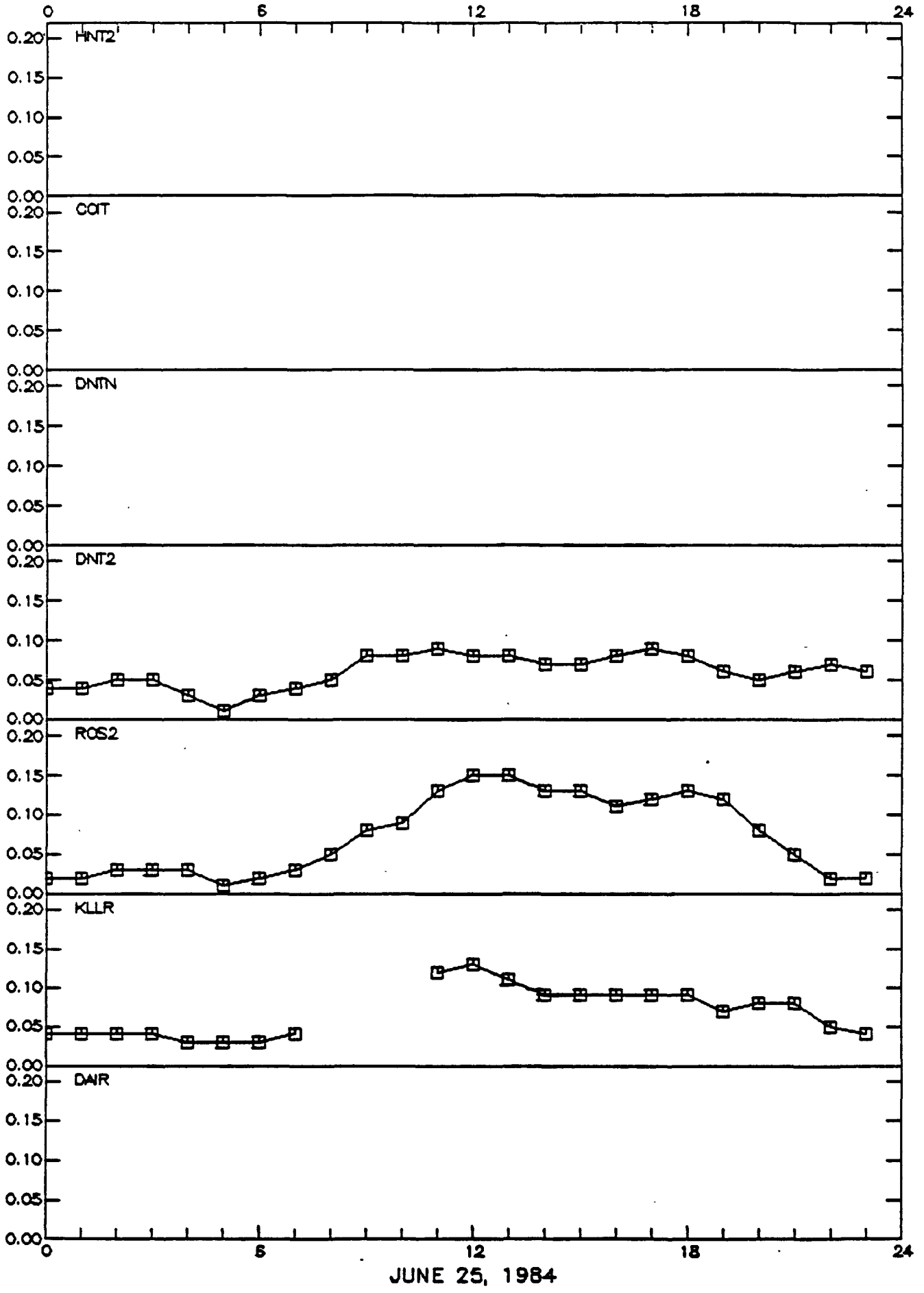

Figure 2f. Observed ozone concentrations (ppm) for Dallas – Fort Worth Area

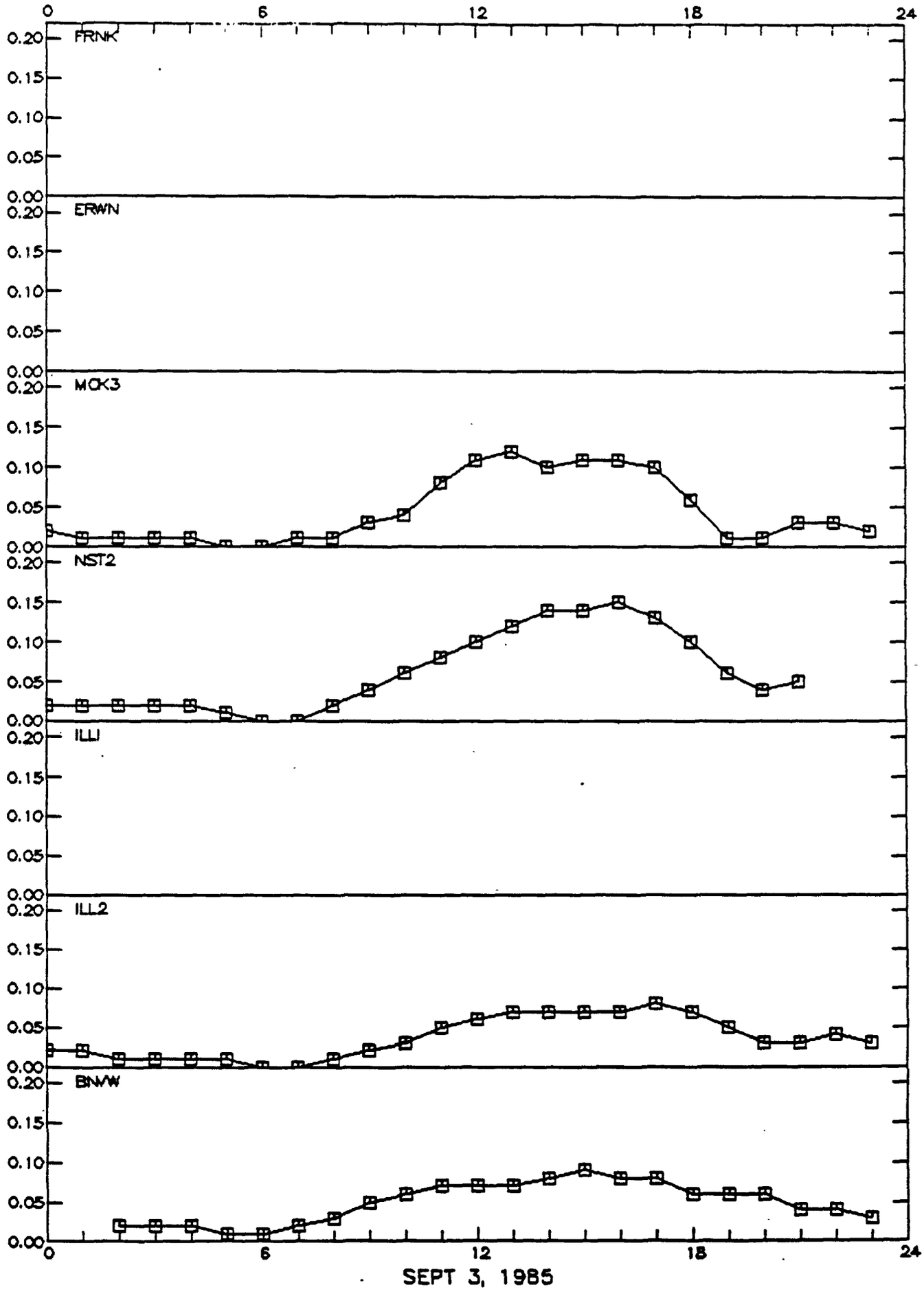

Figure 2g. Observed ozone concentrations (ppm) for Dallas – Fort Worth Area

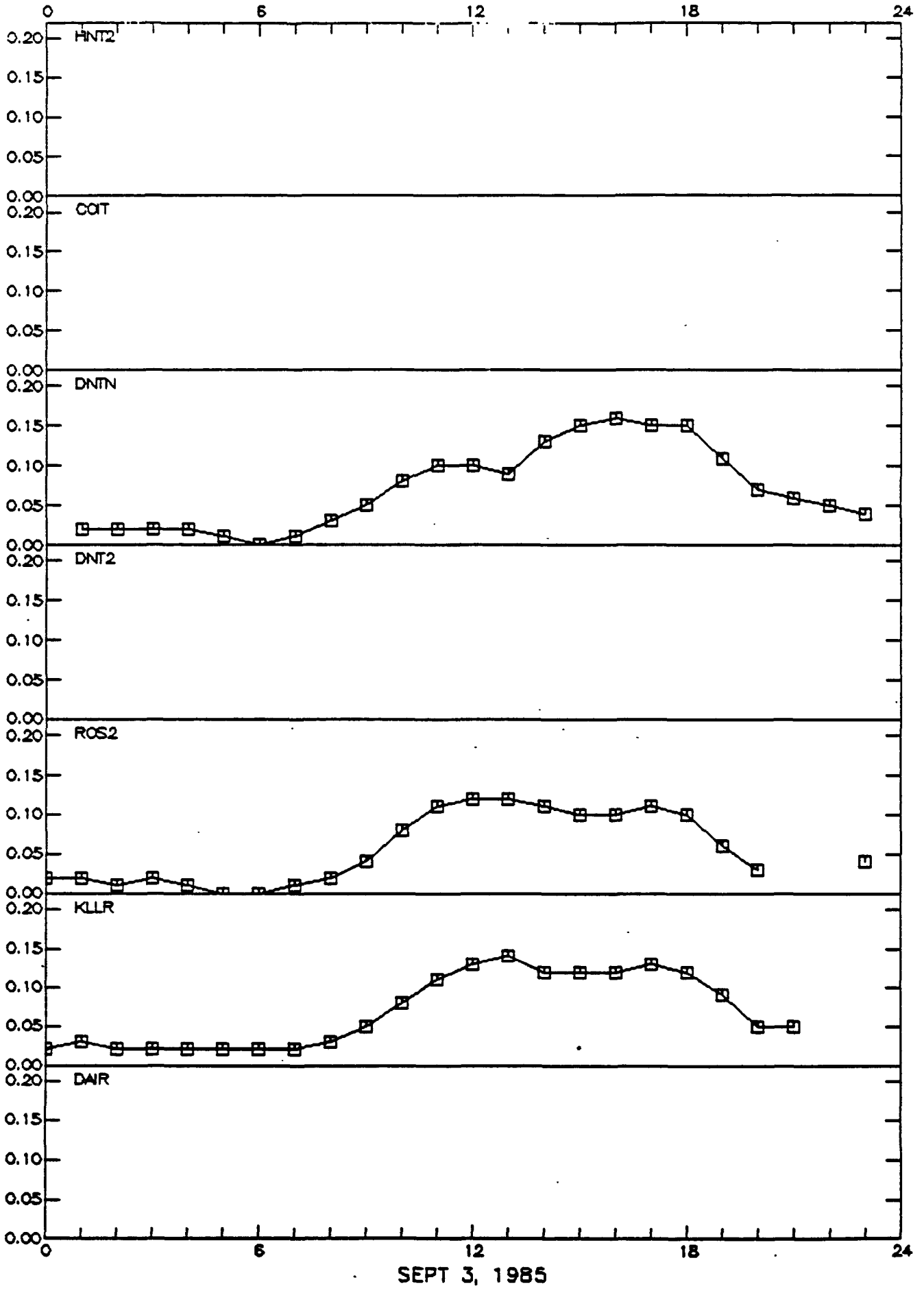

Figure 2g. Observed ozone concentrations (ppm) for Dallas – Fort Worth Area

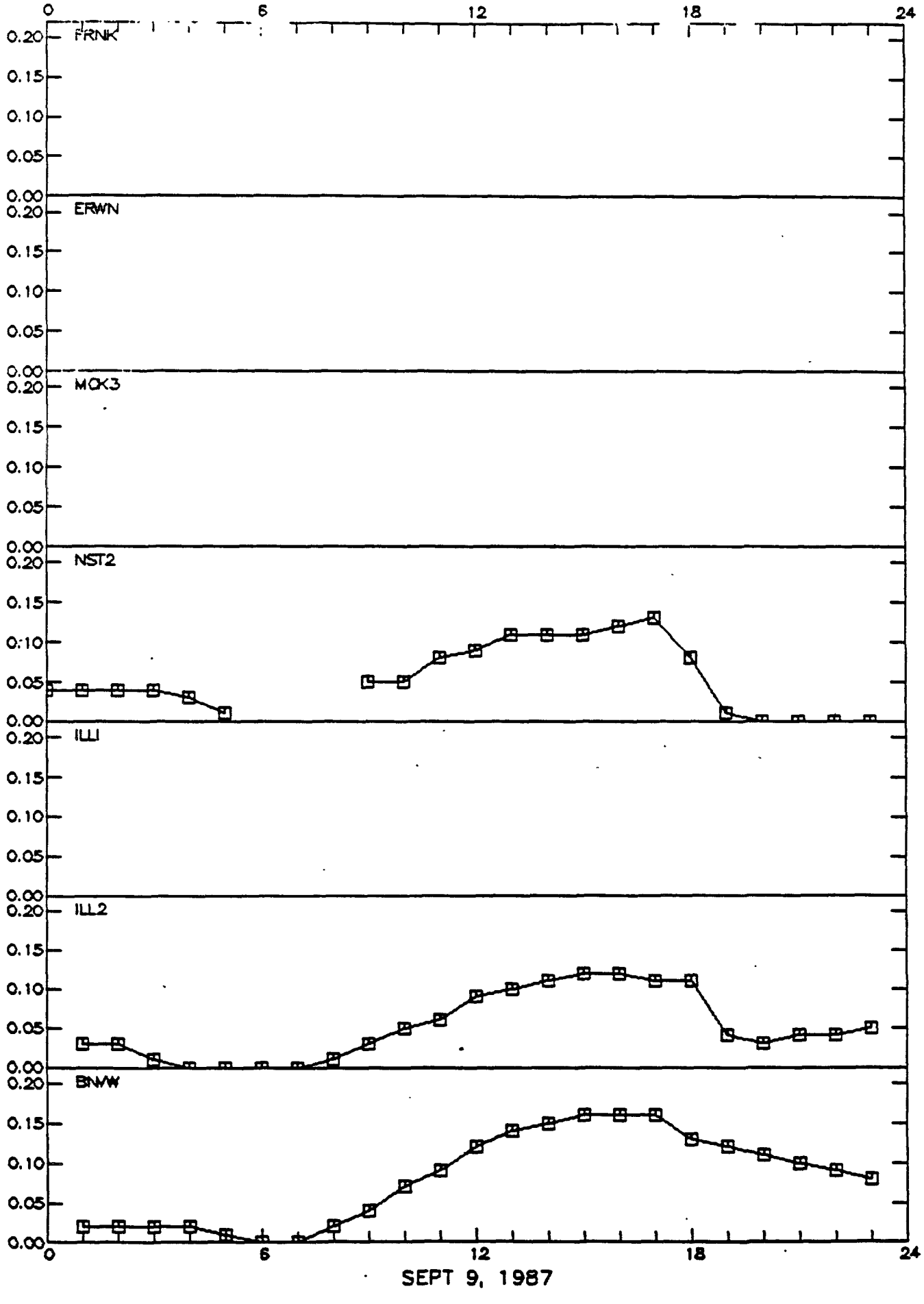

Figure 2h. Observed ozone concentrations (ppm) for Dallas – Fort Worth Area

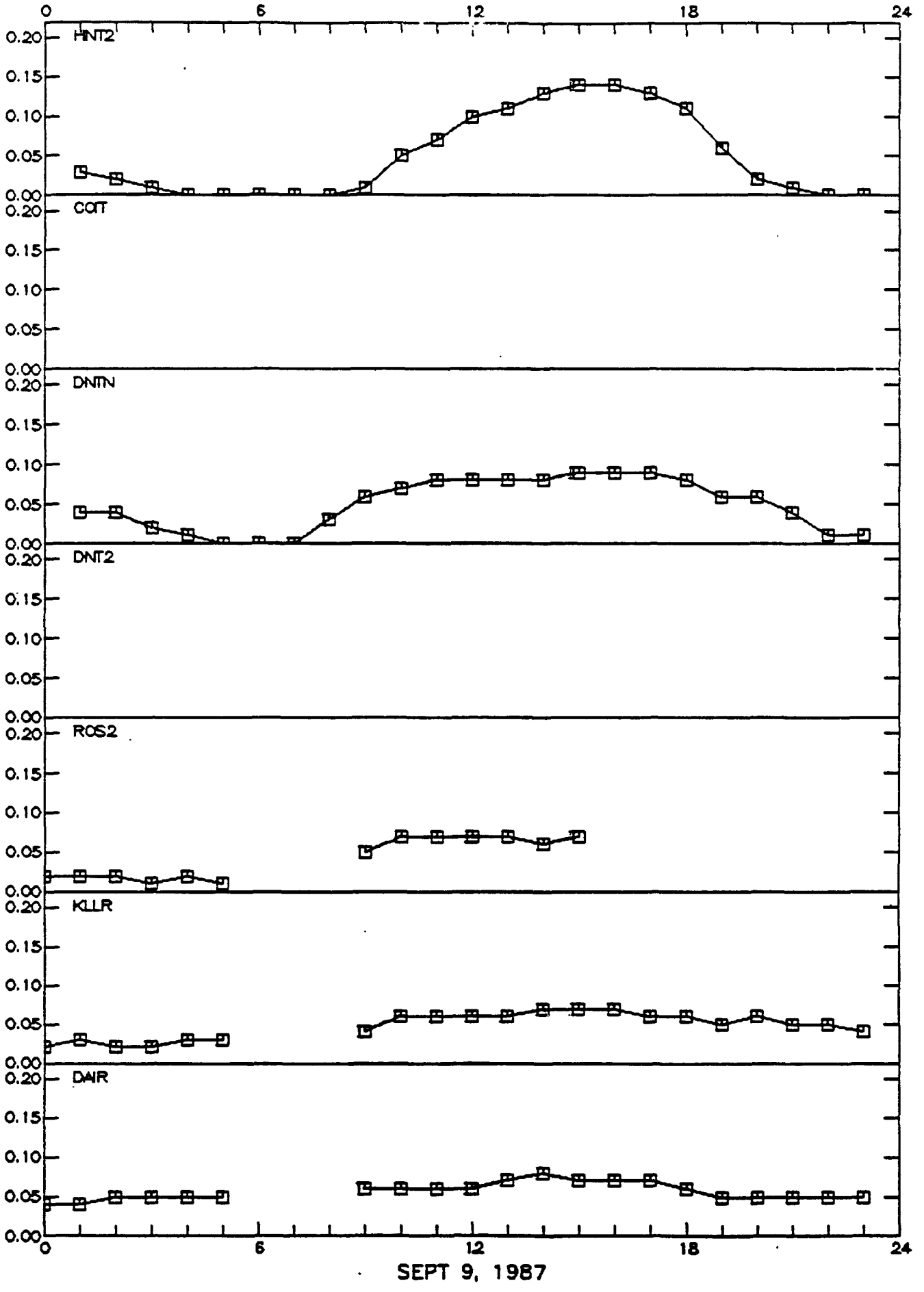

Figure 2h. Observed ozone concentrations (ppm) for Dallas – Fort Worth Area

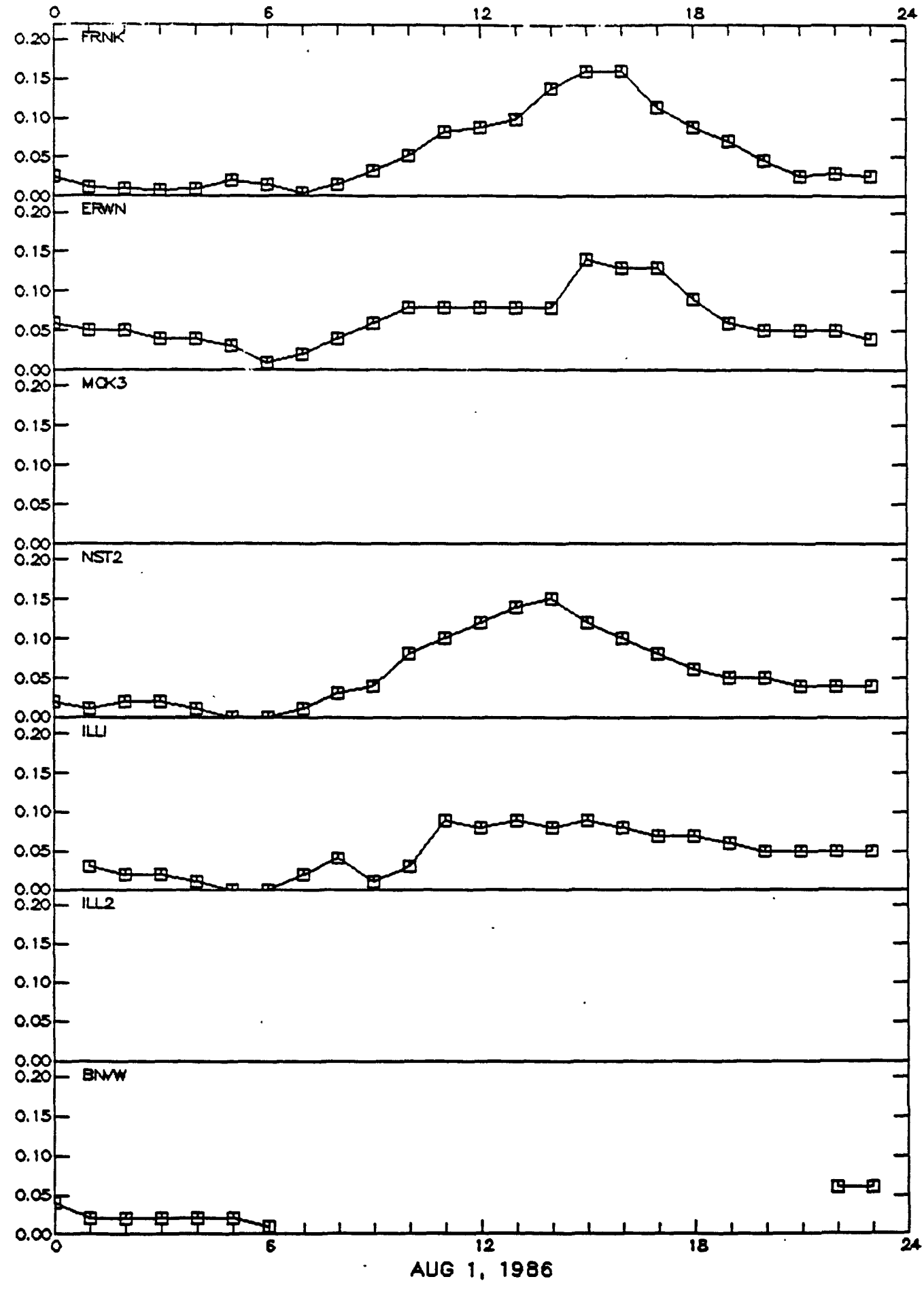

Figure 2i. Observed ozone concentrations (ppm) for Dallas – Fort Worth Area

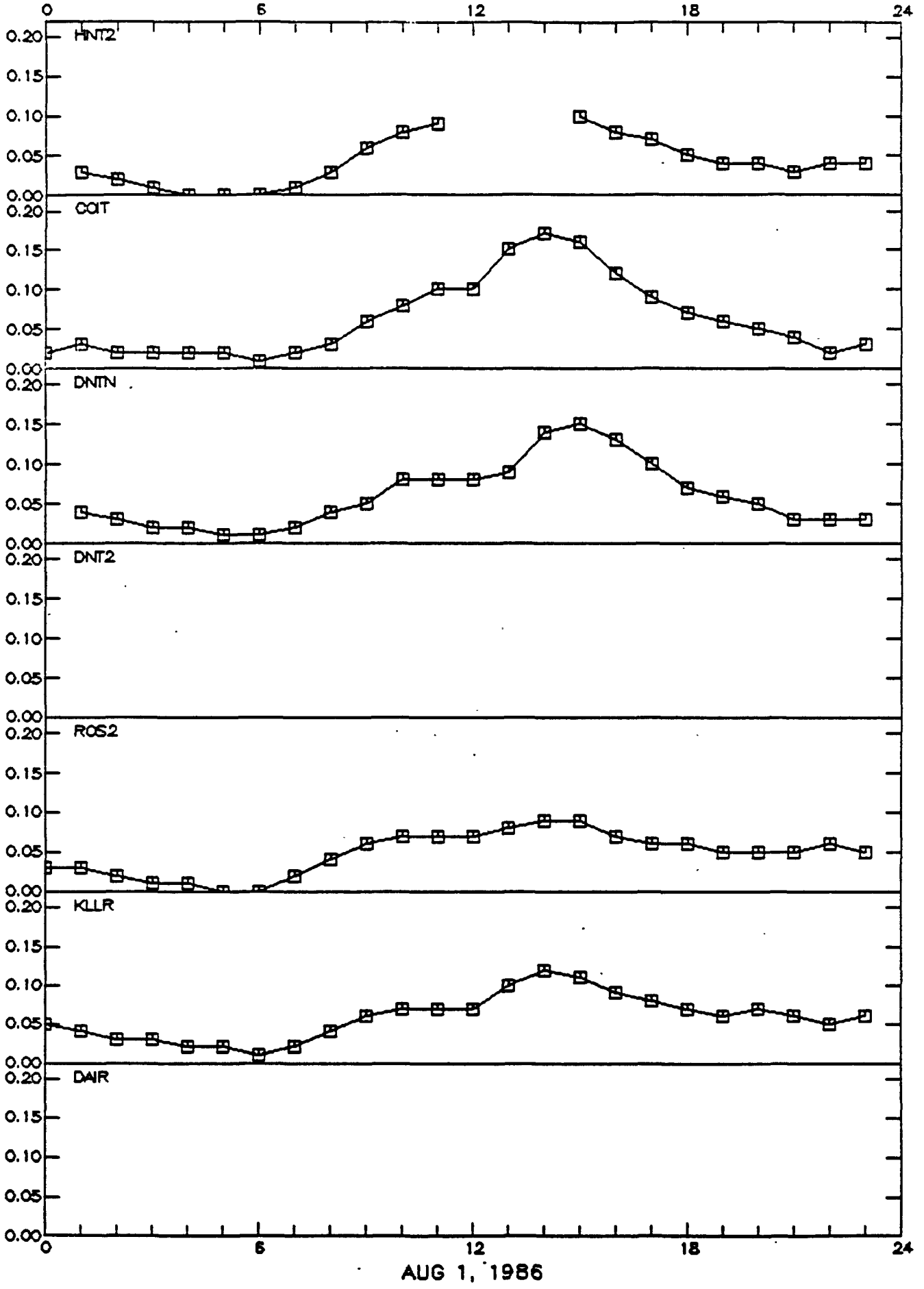

Figure 2i. Observed ozone concentrations (ppm) for Dallas – Fort Worth Area

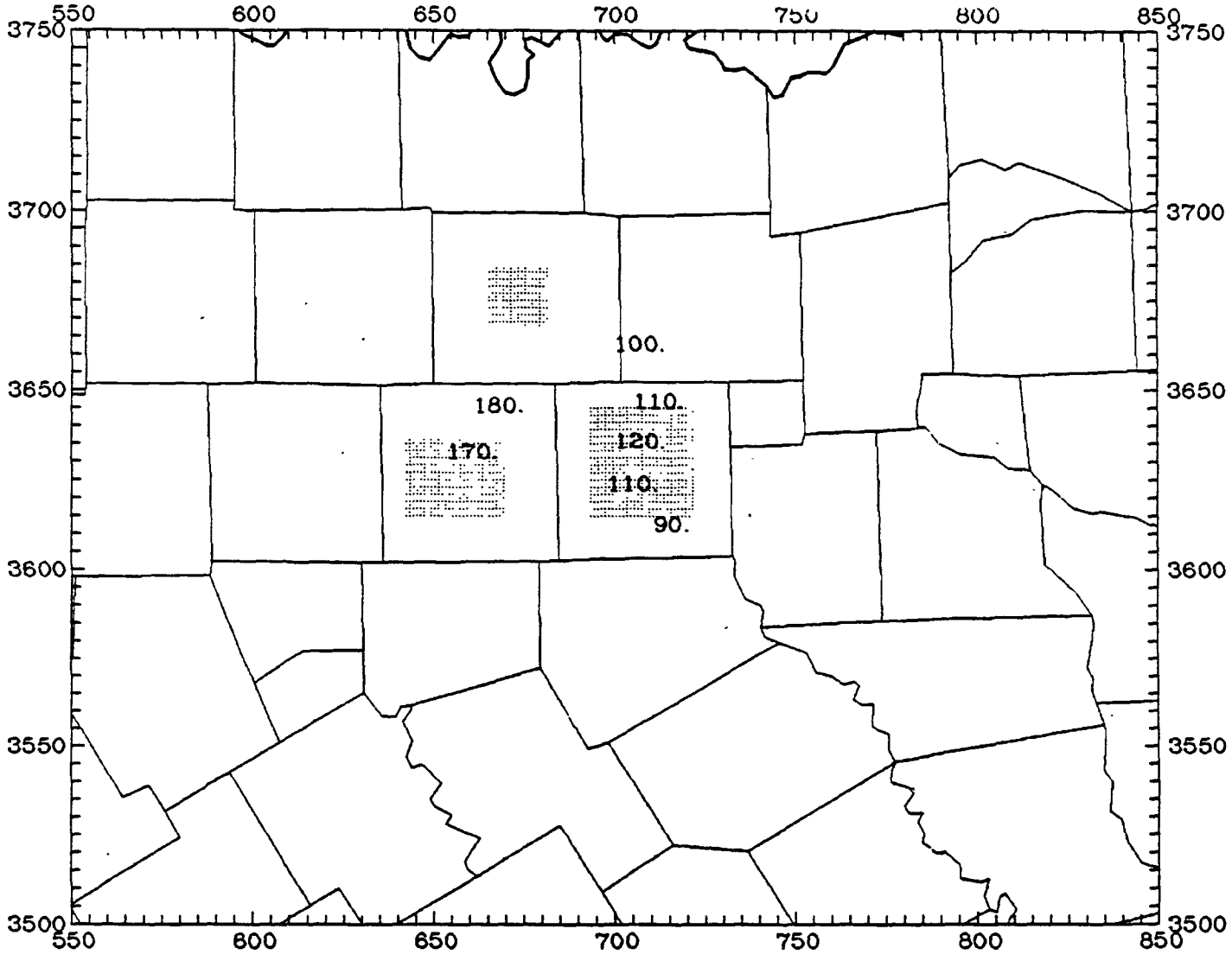

Figure 3a. Observed Peak Ozone Concentrations (ppb) for Dallas – Fort Worth Area 7/31/84

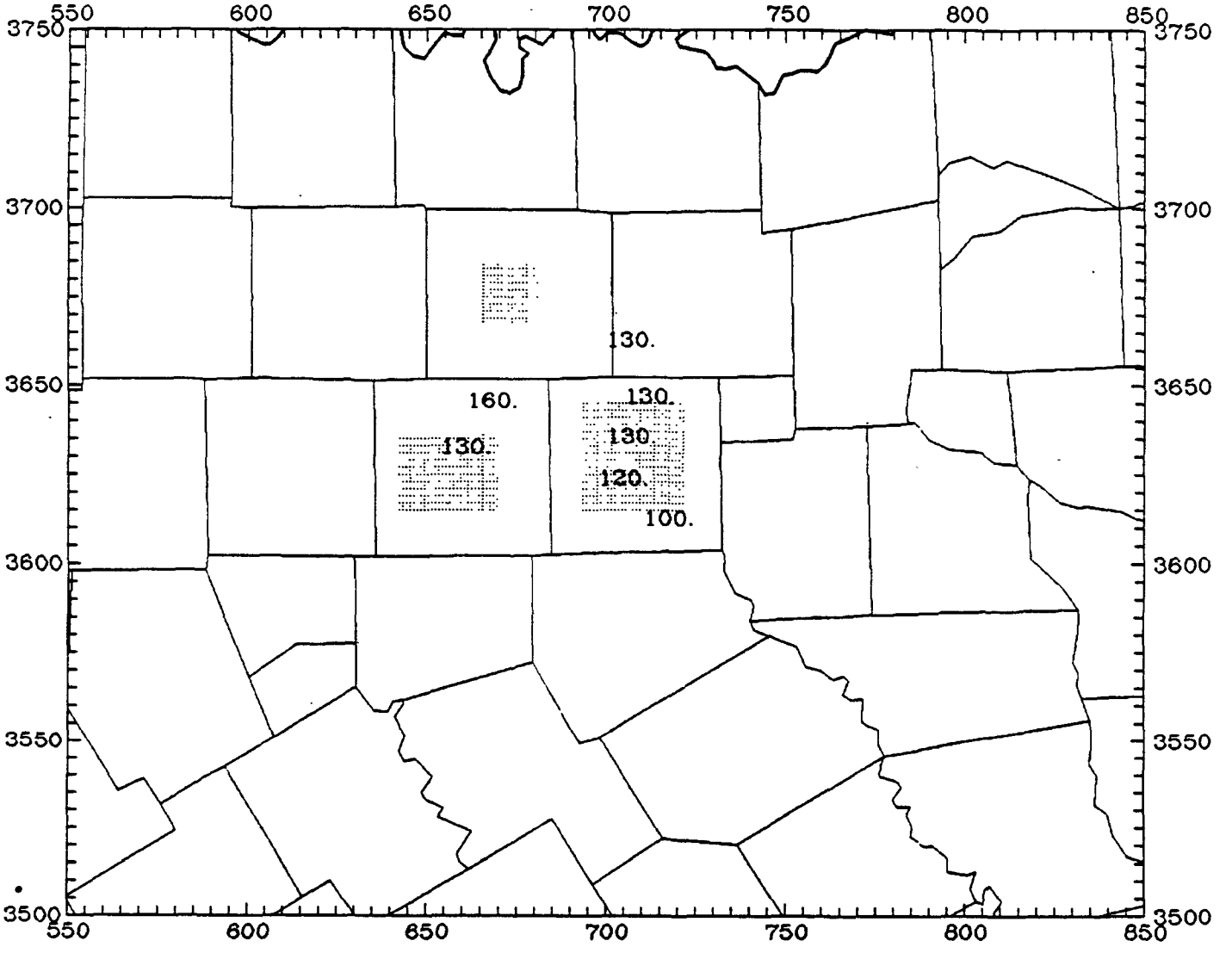

Figure 3b. Observed Peak Ozone Concentrations (ppb) for Dallas - Fort Worth Area 8/ 1/84

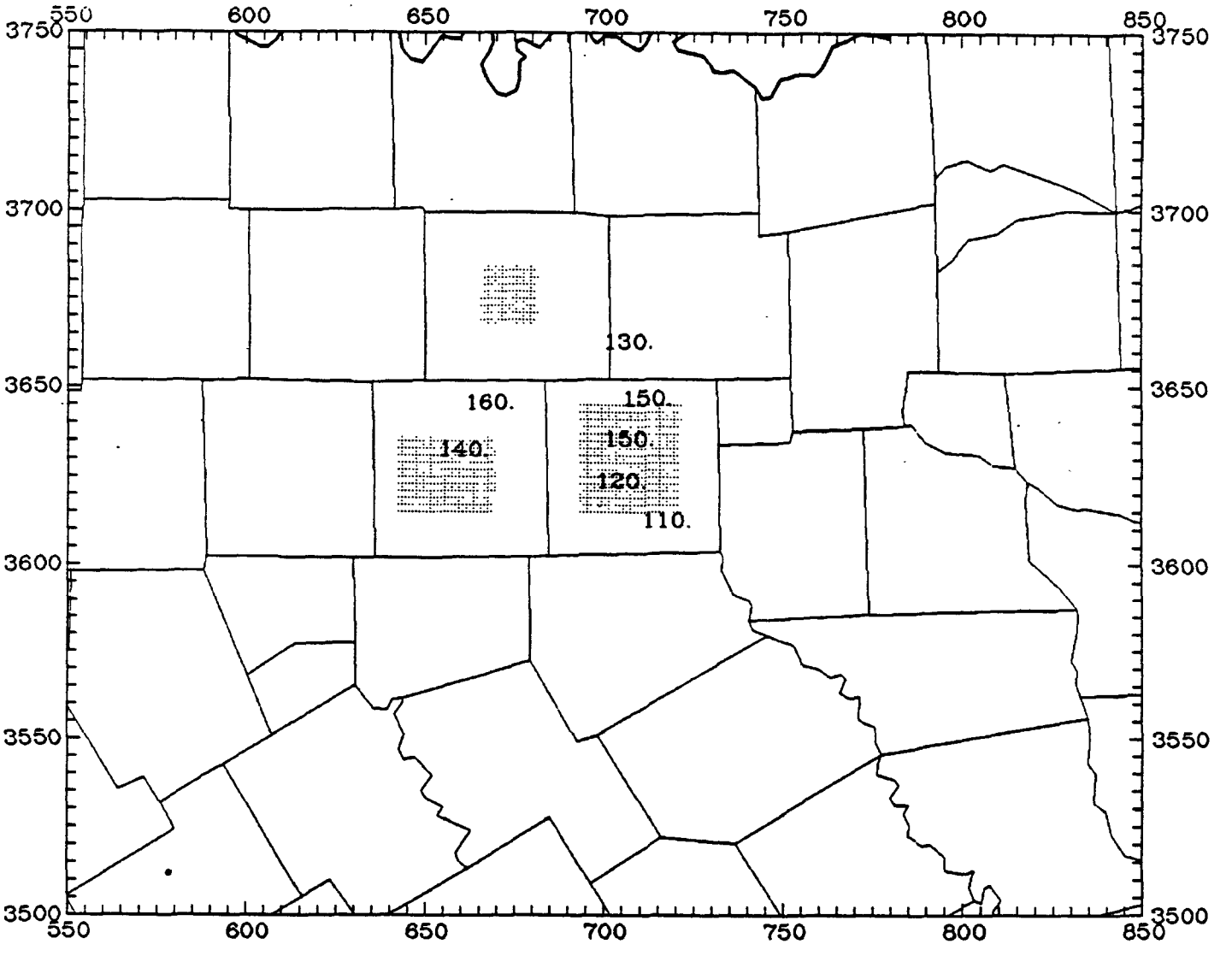

Figure 3c. Observed Peak Ozone Concentrations (ppb) for
Dallas - Fort Worth Area
8/ 2/84

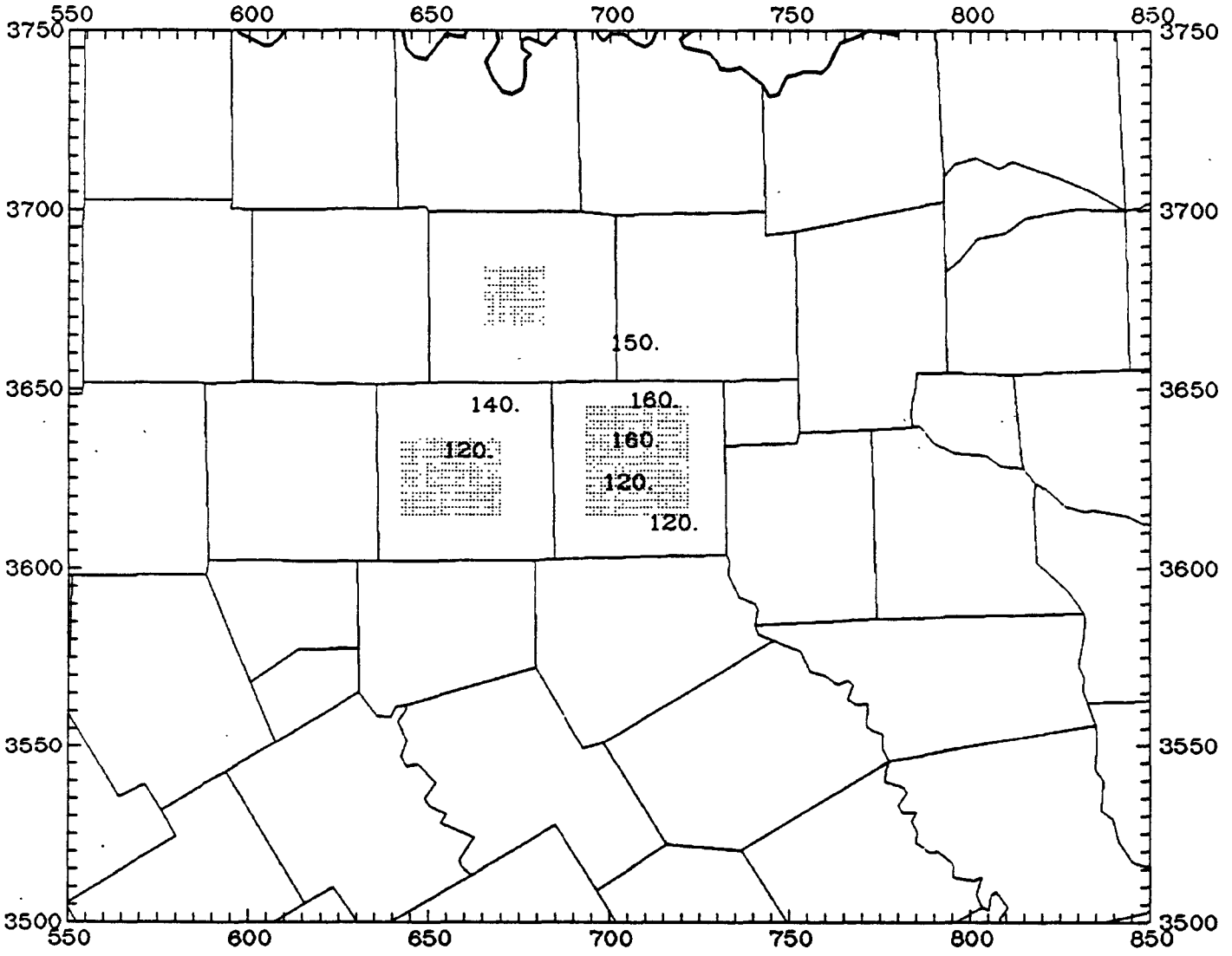

Figure 3d. Observed Peak Ozone Concentrations (ppb) for
Dallas – Fort Worth Area
8/ 3/84

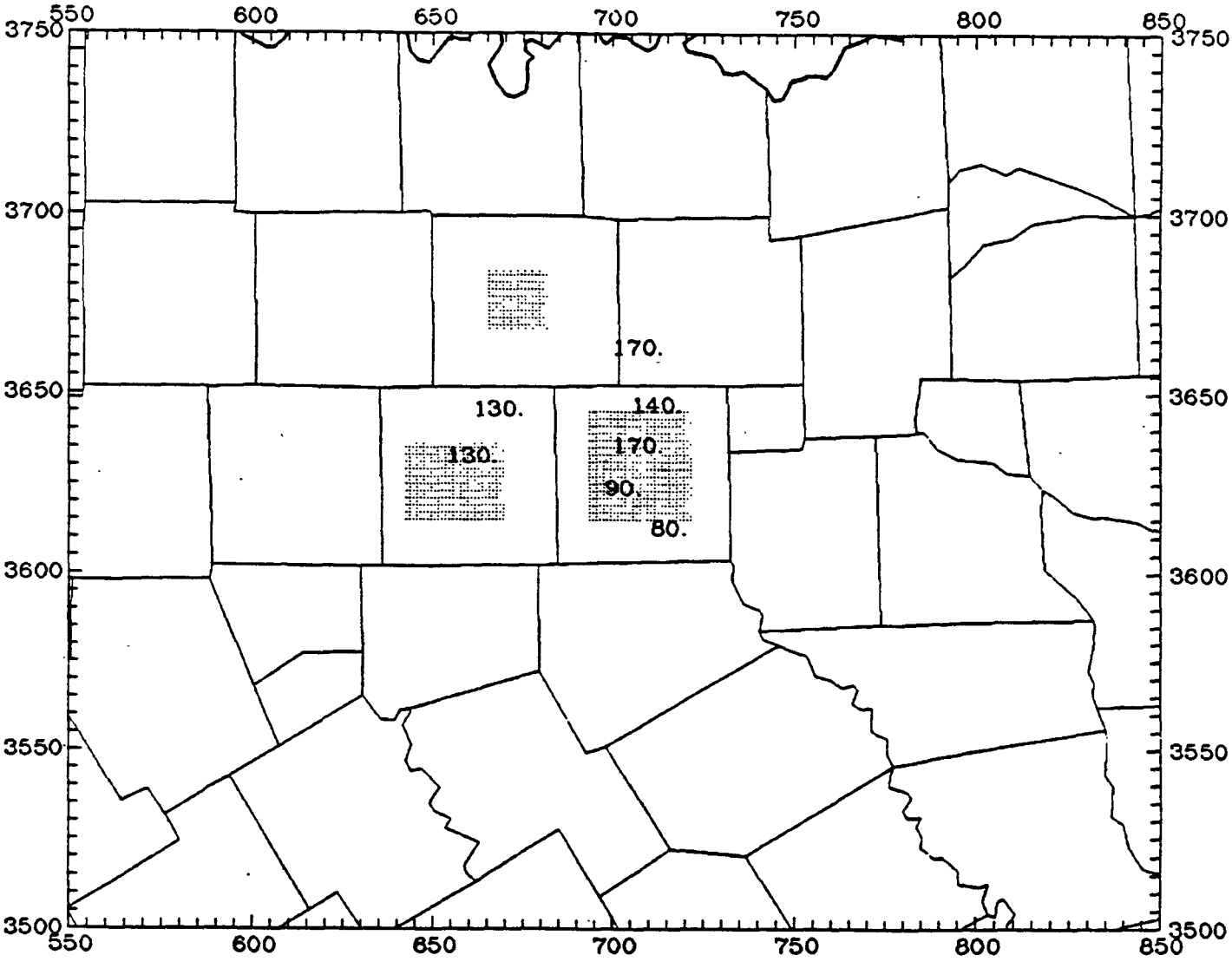

Figure 3e. Observed Peak Ozone Concentrations (ppb) for Dallas - Fort Worth Area 8/31/85

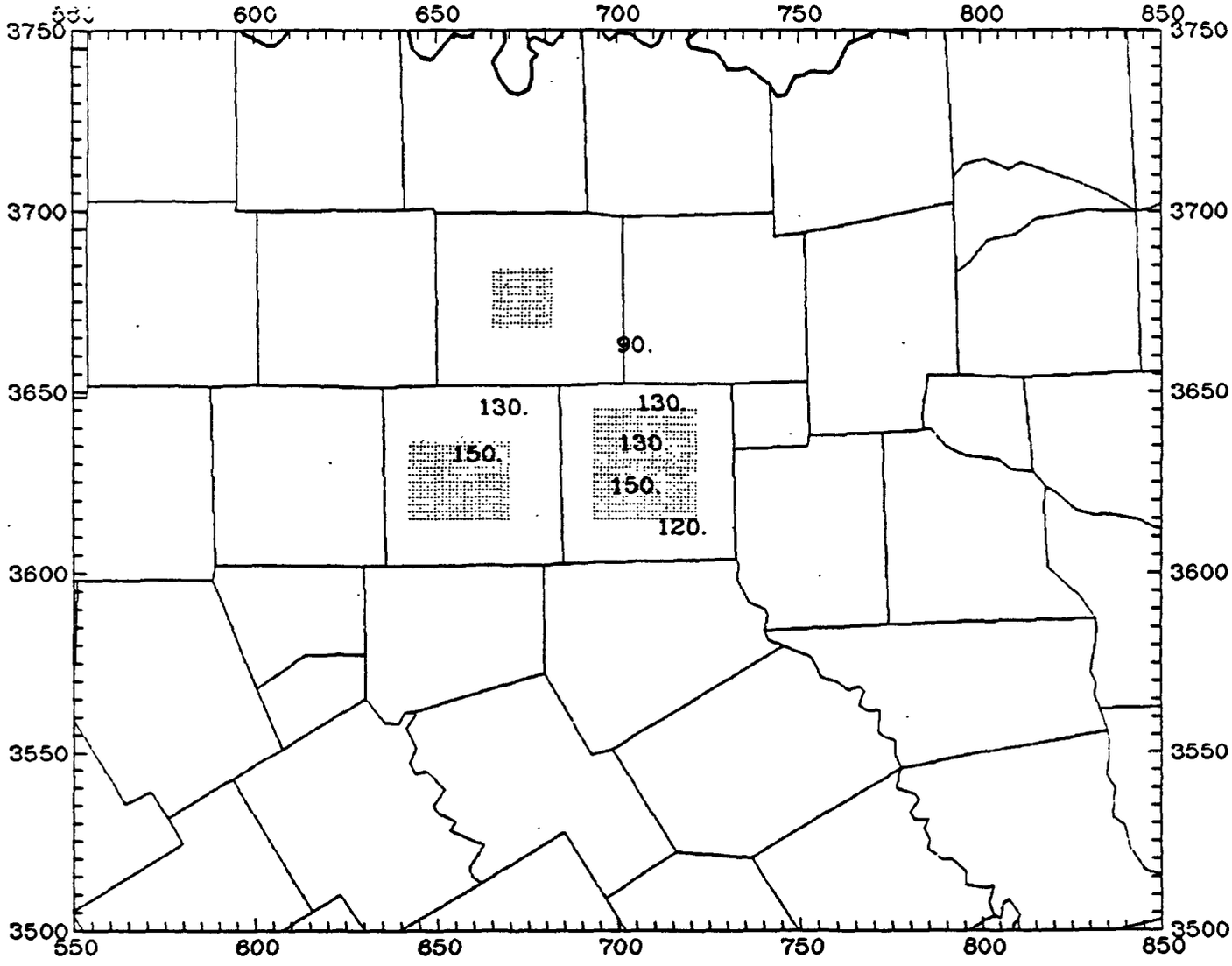

Figure 3f. Observed Peak Ozone Concentrations (ppb) for
Dallas - Fort Worth Area
6/25/84

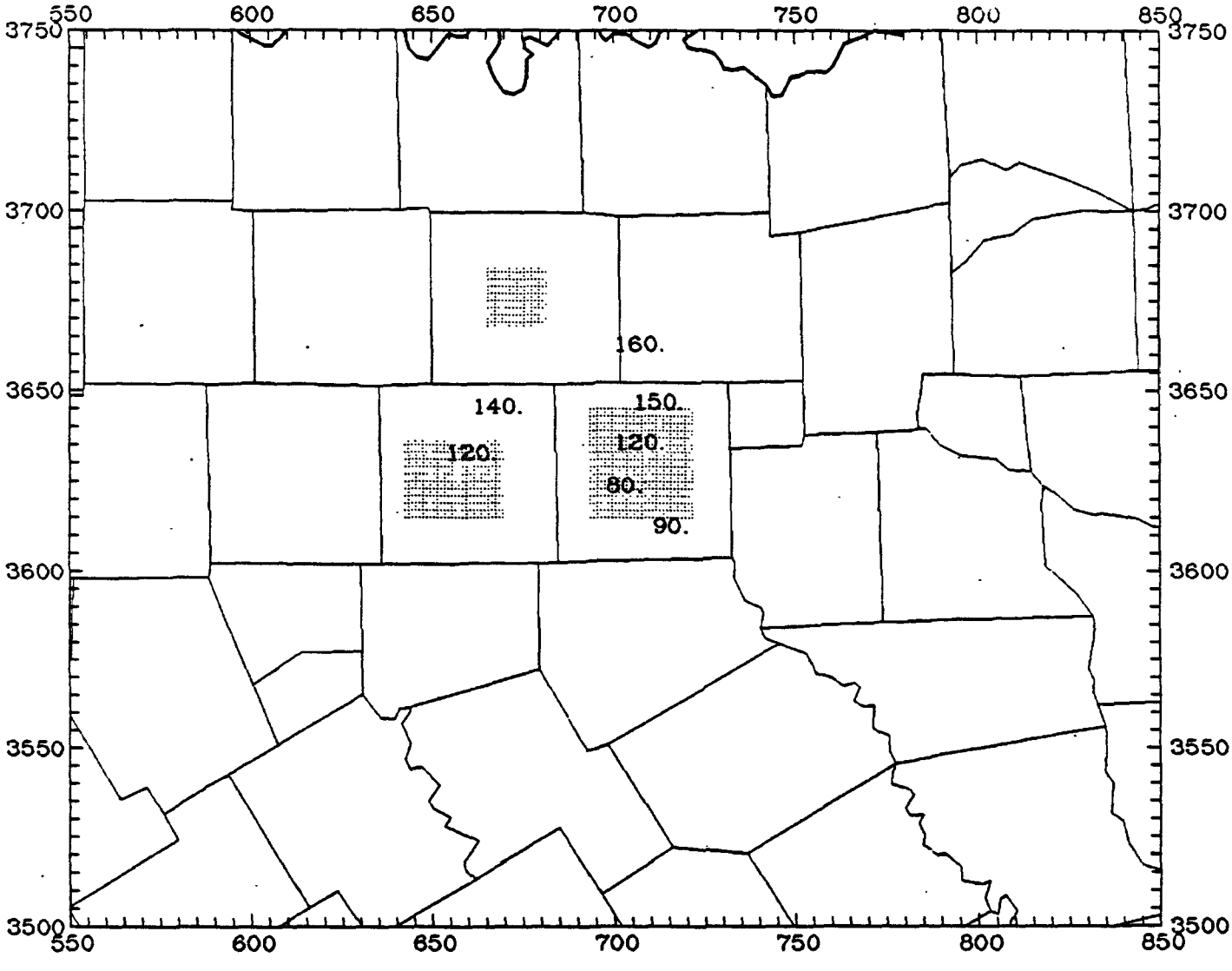

Figure 3g. Observed Peak Ozone Concentrations (ppb) for
Dallas - Fort Worth Area
9/ 3/85

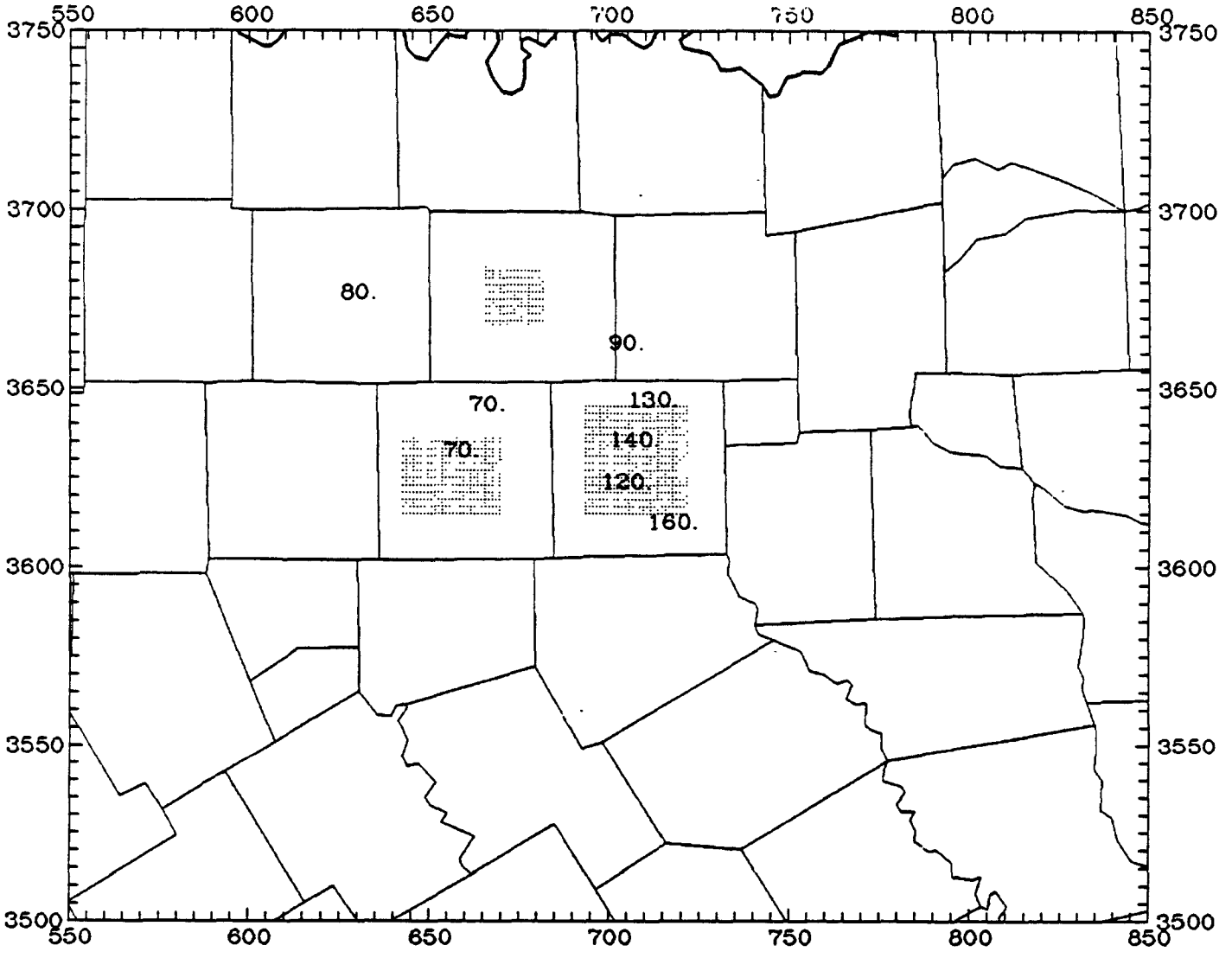

Figure 3h. Observed Peak Ozone Concentrations (ppb) for Dallas - Fort Worth Area 9/ 9/87

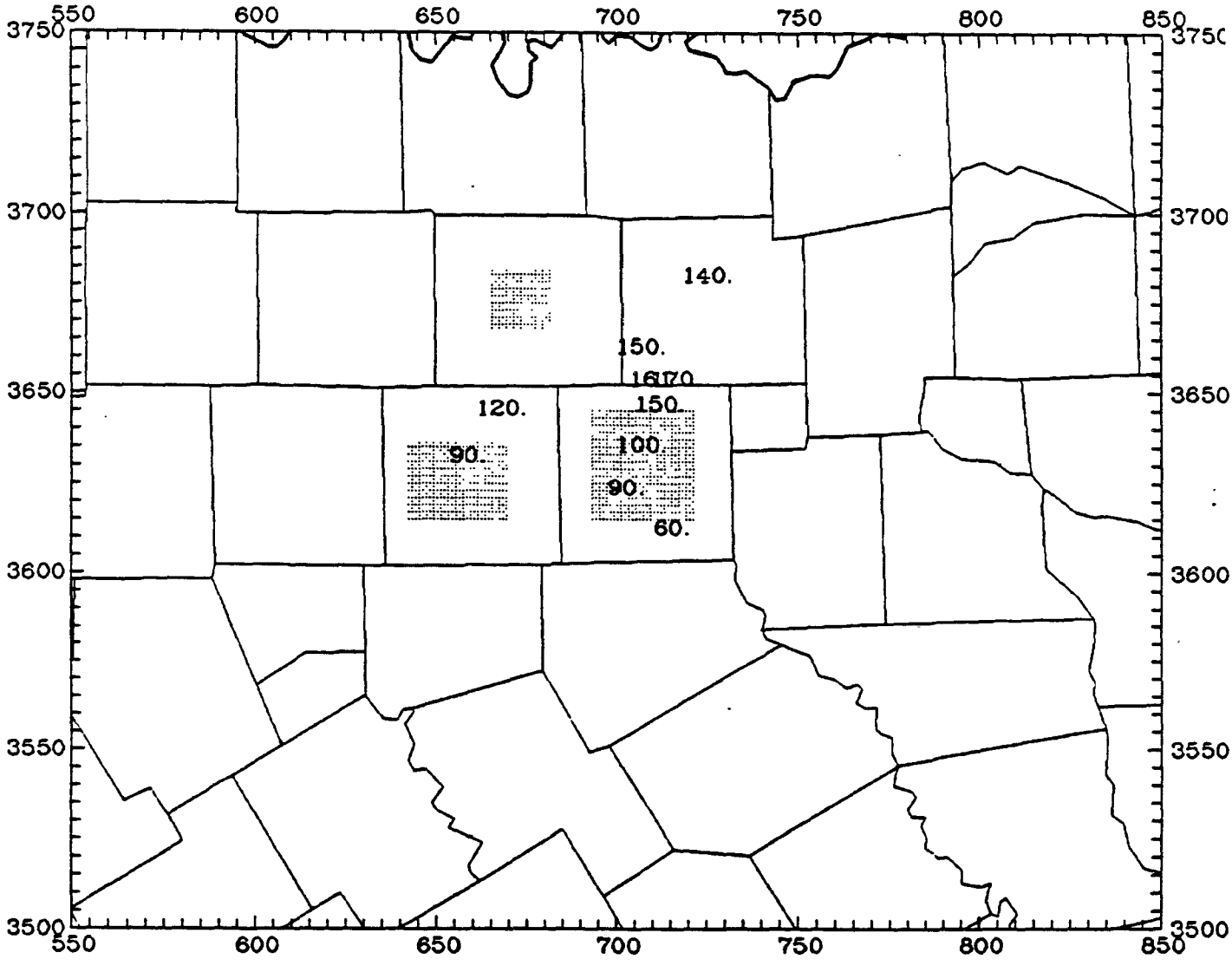

Figure 3i. Observed Peak Ozone Concentrations (ppb) for Dallas - Fort Worth Area 8/ 1/86

TABLE 1. Ozone monitors in operation in the Dallas-Fort Worth area for the years 1984 through 1987 plus part of 1988.

Indentifier	Alias	Site Name	County	UTM Coordinates (Zone 14) UTMX	UTMY	Period of Record Months/Years
FRNK	---	Old Frankford Cemetary	Collin	703.463	3651.969	7/86 - 10/86
ERWN	---	Erwin Central Park	Collin	718.322	3680.889	4/86 - 9/86
Mock	MCK2, MCK3	1500 West Mocking Bird	Dallas	699.961	3633.841	1/84 - 4/86
NSTR	NSTI	12532 Nuestra Drive	Dallas	704.983	3645.068	1/84 - 6/88
ILLI	ILL2	4230 W. Illinois @ Cockrell Hill	Dallas	697.673	3621.962	1/84 - 12/87
BNVW	BNV2	10501 Bonnie View	Dallas	710.465	3610.823	1/84 - 3/88
HNTN	HNT2	1415 Hinton Street	Dallas	699.960	3633.840	7/86 - 3/88
COIT	---	17360 Coit Road	Dallas	709.411	3651.907	4/86 - 9/86
CNTN	DNT2	Quiter Mill Rf. off Hwy 121	Denton	699.641	3661.105	1/84 - 12/8[illegible]
WTHR	---	Weatherford Agricultural College	Parker	n/a	n/a	6/88
FATE	---	130 East Fate Man Place	Rockwell	n/a	n/a	6/88
ROSS	ROS2	Ross Ave between Long & 34th St.	Tarrant	653.810	3630.705	1/84 - 6/88
KLLR	---	FAA Site off of Alta Vista Road	Tarrant	660.907	3643.787	1/84 - 6/88
DAIR	---	Decatur Air Field	Wise	631.968	3680.075	7/87 - 9/87

rem9984

Table 2. Highest Ozone Days for Dallas-Fort Worth 1984 - 1988

Rank	Peak O3	Monitor	Date	Maximum Daily Ozone 480850004 FRNK	480850085 ERWN	481130044 MOCK	481130044 MCK2	481130044 MCK3	481130045 NSTR	481130045 NST2	481130052 ILLI
1	180.	KLLR	7/31/84	-99.	-99.	-99.	-99.	120.	-99.	110.	110.
2	170.	DNT2	9/ 5/84	-99.	-99.	-99.	-99.	110.	-99.	110.	100.
3	170.	BNVW	6/ 7/85	-99.	-99.	-99.	-99.	120.	-99.	80.	120.
4	170.	MCK3	8/31/85	-99.	-99.	-99.	-99.	170.	-99.	140.	-99.
5	170.	COIT	8/ 1/86	161.	140.	-99.	-99.	-99.	-99.	150.	90.
6	160.	NST2	6/27/84	-99.	-99.	-99.	-99.	110.	-99.	160.	100.
7	160.	ROS2	7/23/84	-99.	-99.	-99.	-99.	120.	-99.	110.	-99.
8	160.	KLLR	8/ 1/84	-99.	-99.	-99.	-99.	130.	-99.	130.	120.
9	160.	KLLR	8/ 2/84	-99.	-99.	-99.	-99.	150.	-99.	150.	120.
10	160.	MCK3	8/ 3/84	-99.	-99.	-99.	-99.	160.	-99.	160.	120.
11	160.	DNT2	7/10/85	-99.	-99.	-99.	-99.	90.	-99.	-99.	110.
12	160.	DNTN	9/ 3/85	-99.	-99.	-99.	-99.	120.	-99.	150.	-99.
13	160.	COIT	7/30/86	142.	150.	-99.	-99.	-99.	-99.	140.	80.
14	160.	ILLI	6/18/87	-99.	-99.	-99.	-99.	-99.	-99.	90.	160.
15	160.	DNTN	7/22/87	-99.	-99.	-99.	-99.	-99.	-99.	110.	-99.
16	160.	BNVW	9/ 9/87	-99.	-99.	-99.	-99.	-99.	-99.	130.	-99.
17	150.	ILLI	6/25/84	-99.	-99.	-99.	-99.	130.	-99.	130.	150.
18	150.	ROS2	8/24/84	-99.	-99.	-99.	-99.	100.	-99.	90.	70.
19	150.	MCK3	8/30/84	-99.	-99.	-99.	-99.	150.	-99.	130.	120.
20	150.	MCK3	5/24/85	-99.	-99.	-99.	-99.	150.	-99.	100.	150.
21	150.	ROS2	6/29/85	-99.	-99.	-99.	-99.	110.	-99.	-99.	130.
22	150.	DNT2	7/ 5/85	-99.	-99.	-99.	-99.	100.	-99.	-99.	90.
23	150.	BNVW	7/26/85	-99.	-99.	-99.	-99.	90.	-99.	70.	110.
24	150.	BNVW	7/27/85	-99.	-99.	-99.	-99.	110.	-99.	90.	120.
25	150.	ROS2	8/ 2/85	-99.	-99.	-99.	-99.	110.	-99.	130.	110.
26	150.	KLLR	8/26/85	-99.	-99.	-99.	-99.	110.	-99.	80.	-99.
27	150.	ERWN	7/31/86	136.	150.	-99.	-99.	-99.	-99.	140.	90.
28	150.	KLLR	8/19/86	91.	90.	-99.	-99.	-99.	-99.	90.	80.
29	150.	BNVW	6/24/87	-99.	-99.	-99.	-99.	-99.	-99.	70.	80.
30	140.	ROS2	7/28/84	-99.	-99.	-99.	-99.	90.	-99.	90.	-99.
31	140.	MCK3	9/14/84	-99.	-99.	-99.	-99.	140.	-99.	120.	80.
32	140.	DNT2	6/14/85	-99.	-99.	-99.	-99.	110.	-99.	110.	110.
33	140.	DNT2	7/ 1/85	-99.	-99.	-99.	-99.	80.	-99.	80.	90.
34	140.	ROS2	8/30/85	-99.	-99.	-99.	-99.	70.	-99.	60.	-99.
35	140.	ILLI	6/24/86	-99.	80.	-99.	-99.	-99.	-99.	110.	140.
36	140.	KLLR	6/25/86	-99.	100.	-99.	-99.	-99.	-99.	110.	110.
37	140.	KLLR	7/22/86	-99.	90.	-99.	-99.	-99.	-99.	-99.	110.
38	140.	ERWN	7/29/86	116.	140.	-99.	-99.	-99.	-99.	100.	70.
39	140.	ROS2	6/ 6/87	-99.	-99.	-99.	-99.	-99.	-99.	80.	80.
40	140.	DNTN	7/30/87	-99.	-99.	-99.	-99.	-99.	-99.	120.	-99.
41	140.	ROS2	9/ 2/87	-99.	-99.	-99.	-99.	-99.	-99.	80.	-99.
42	130.	NST2	6/28/84	-99.	-99.	-99.	-99.	90.	-99.	130.	80.
43	130.	KLLR	7/ 2/84	-99.	-99.	-99.	-99.	90.	-99.	110.	60.
44	130.	NST2	7/16/84	-99.	-99.	-99.	-99.	90.	-99.	130.	-99.
45	130.	KLLR	7/20/84	-99.	-99.	-99.	-99.	100.	-99.	110.	-99.
46	130.	MCK3	7/25/84	-99.	-99.	-99.	-99.	130.	-99.	120.	-99.

Table 2. Highest Ozone Days for Dallas-Fort Worth 1984 - 1988

Rank	Peak O3	Monitor	Date	Maximum Daily Ozone 481130052 ILL2	481130055 BNVW	481130055 BNV2	481130069 HNTN	481130069 HNT2	481130086 COIT	481210054 DNTN	481210054 DNT2
1	180.	KLLR	7/31/84	-99.	90.	-99.	-99.	-99.	-99.	-99.	100.
2	170.	DNT2	9/ 5/84	-99.	70.	-99.	-99.	-99.	-99.	-99.	170.
3	170.	BNVW	6/ 7/85	-99.	170.	-99.	-99.	-99.	-99.	-99.	90.
4	170.	MCK3	8/31/85	90.	80.	-99.	-99.	-99.	-99.	170.	-99.
5	170.	COIT	8/ 1/86	-99.	60.	-99.	-99.	100.	170.	150.	-99.
6	160.	NST2	6/27/84	-99.	60.	-99.	-99.	-99.	-99.	-99.	160.
7	160.	ROS2	7/23/84	-99.	100.	-99.	-99.	-99.	-99.	-99.	100.
8	160.	KLLR	8/ 1/84	-99.	100.	-99.	-99.	-99.	-99.	-99.	130.
9	160.	KLLR	8/ 2/84	-99.	110.	-99.	-99.	-99.	-99.	-99.	130.
10	160.	MCK3	8/ 3/84	-99.	120.	-99.	-99.	-99.	-99.	-99.	150.
11	160.	DNT2	7/10/85	-99.	80.	-99.	-99.	-99.	-99.	-99.	160.
12	160.	DNTN	9/ 3/85	80.	90.	-99.	-99.	-99.	-99.	160.	-99.
13	160.	COIT	7/30/86	-99.	80.	-99.	-99.	120.	160.	130.	-99.
14	160.	ILLI	6/18/87	-99.	140.	-99.	-99.	150.	-99.	70.	-99.
15	160.	DNTN	7/22/87	60.	70.	-99.	-99.	70.	-99.	160.	-99.
16	160.	BNVW	9/ 9/87	120.	160.	-99.	-99.	140.	-99.	90.	-99.
17	150.	ILLI	6/25/84	-99.	120.	-99.	-99.	-99.	-99.	-99.	90.
18	150.	ROS2	8/24/84	-99.	70.	-99.	-99.	-99.	-99.	-99.	90.
19	150.	MCK3	8/30/84	-99.	110.	-99.	-99.	-99.	-99.	-99.	130.
20	150.	MCK3	5/24/85	-99.	110.	-99.	-99.	-99.	-99.	-99.	130.
21	150.	ROS2	6/29/85	-99.	90.	-99.	-99.	-99.	-99.	-99.	130.
22	150.	DNT2	7/ 5/85	-99.	60.	-99.	-99.	-99.	-99.	-99.	150.
23	150.	BNVW	7/26/85	-99.	150.	-99.	-99.	-99.	-99.	-99.	-99.
24	150.	BNVW	7/27/85	-99.	150.	-99.	-99.	-99.	-99.	-99.	-99.
25	150.	ROS2	8/ 2/85	-99.	70.	-99.	-99.	-99.	-99.	-99.	-99.
26	150.	KLLR	8/26/85	80.	90.	-99.	-99.	-99.	-99.	0.	-99.
27	150.	ERWN	7/31/86	-99.	80.	-99.	-99.	130.	150.	100.	-99.
28	150.	KLLR	8/19/86	-99.	80.	-99.	-99.	100.	90.	80.	-99.
29	150.	BNVW	6/24/87	-99.	150.	-99.	-99.	70.	-99.	70.	-99.
30	140.	ROS2	7/28/84	-99.	90.	-99.	-99.	-99.	-99.	-99.	100.
31	140.	MCK3	9/14/84	-99.	-99.	80.	-99.	-99.	-99.	-99.	110.
32	140.	DNT2	6/14/85	-99.	100.	-99.	-99.	-99.	-99.	-99.	140.
33	140.	DNT2	7/ 1/85	-99.	90.	-99.	-99.	-99.	-99.	-99.	140.
34	140.	ROS2	8/30/85	50.	60.	-99.	-99.	-99.	-99.	70.	-99.
35	140.	ILLI	6/24/86	-99.	90.	-99.	-99.	-99.	-99.	90.	-99.
36	140.	KLLR	6/25/86	-99.	90.	-99.	-99.	-99.	70.	100.	-99.
37	140.	KLLR	7/22/86	-99.	110.	-99.	-99.	130.	90.	100.	-99.
38	140.	ERWN	7/29/86	-99.	60.	-99.	-99.	70.	120.	110.	-99.
39	140.	ROS2	6/ 6/87	-99.	100.	-99.	-99.	100.	-99.	100.	-99.
40	140.	DNTN	7/30/87	80.	90.	-99.	-99.	90.	-99.	140.	-99.
41	140.	ROS2	9/ 2/87	80.	80.	-99.	-99.	90.	-99.	80.	-99.
42	130.	NST2	6/28/84	-99.	60.	-99.	-99.	-99.	-99.	-99.	100.
43	130.	KLLR	7/ 2/84	-99.	90.	-99.	-99.	-99.	-99.	-99.	120.
44	130.	NST2	7/16/84	-99.	60.	-99.	-99.	-99.	-99.	-99.	120.
45	130.	KLLR	7/20/84	-99.	80.	-99.	-99.	-99.	-99.	-99.	110.
46	130.	MCK3	7/25/84	-99.	110.	-99.	-99.	-99.	-99.	-99.	90.

Table 2. Highest Ozone Days for Dallas-Fort Worth 1984 - 1988

ank	Peak O3	Monitor	Date	Maximum Daily Ozone 483670080 WTHR	483970081 FATE	484391002 ROSS	484391002 ROS2	484392003 KLLR	484970087 DAIR		
1	180.	KLLR	7/31/84	-99.	-99.	-99.	170.	180.	-99.		
2	170.	DNT2	9/ 5/84	-99.	-99.	-99.	110.	120.	-99.		
3	170.	BNVW	6/ 7/85	-99.	-99.	-99.	90.	80.	-99.		
4	170.	MCK3	8/31/85	-99.	-99.	-99.	130.	130.	-99.		
5	170.	COIT	8/ 1/86	-99.	-99.	-99.	90.	120.	-99.		
6	160.	NST2	6/27/84	-99.	-99.	-99.	160.	50.	-99.		
7	160.	ROS2	7/23/84	-99.	-99.	-99.	160.	120.	-99.		
8	160.	KLLR	8/ 1/84	-99.	-99.	-99.	130.	160.	-99.		
9	160.	KLLR	8/ 2/84	-99.	-99.	-99.	140.	160.	-99.		
10	160.	MCK3	8/ 3/84	-99.	-99.	-99.	120.	140.	-99.		
11	160.	DNT2	7/10/85	-99.	-99.	-99.	100.	120.	-99.		
12	160.	DNTN	9/ 3/85	-99.	-99.	-99.	120.	140.	-99.		
13	160.	COIT	7/30/86	-99.	-99.	-99.	70.	100.	-99.		
14	160.	ILLI	6/18/87	-99.	-99.	-99.	100.	80.	-99.		
5	160.	DNTN	7/22/87	-99.	-99.	-99.	70.	30.	90.		
6	160.	BNVW	9/ 9/87	-99.	-99.	-99.	70.	70.	80.		
7	150.	ILLI	6/25/84	-99.	-99.	-99.	150.	130.	-99.		
8	150.	ROS2	8/24/84	-99.	-99.	-99.	150.	130.	-99.		
9	150.	MCK3	8/30/84	-99.	-99.	-99.	120.	110.	-99.		
20	150.	MCK3	5/24/85	-99.	-99.	-99.	80.	80.	-99.		
21	150.	ROS2	6/29/85	-99.	-99.	-99.	150.	110.	-99.		
22	150.	DNT2	7/ 5/85	-99.	-99.	-99.	70.	90.	-99.		
23	150.	BNVW	7/26/85	-99.	-99.	-99.	-99.	60.	-99.		
24	150.	BNVW	7/27/85	-99.	-99.	-99.	-99.	80.	-99.		
25	150.	ROS2	8/ 2/85	-99.	-99.	-99.	150.	150.	-99.		
26	150.	KLLR	8/26/85	-99.	-99.	-99.	140.	150.	-99.		
27	150.	ERWN	7/31/86	-99.	-99.	-99.	100.	100.	-99.		
28	150.	KLLR	8/19/86	-99.	-99.	-99.	140.	150.	-99.		
29	150.	BNVW	6/24/87	-99.	-99.	-99.	70.	70.	-99.		
30	140.	ROS2	7/28/84	-99.	-99.	-99.	140.	110.	-99.		
31	140.	MCK3	9/14/84	-99.	-99.	-99.	120.	110.	-99.		
32	140.	DNT2	6/14/85	-99.	-99.	-99.	80.	90.	-99.		
33	140.	DNT2	7/ 1/85	-99.	-99.	-99.	80.	80.	-99.		
4	140.	ROS2	8/30/85	-99.	-99.	-99.	140.	110.	-99.		
5	140.	ILLI	6/24/86	-99.	-99.	-99.	130.	120.	-99.		
6	140.	KLLR	6/25/86	-99.	-99.	-99.	120.	140.	-99.		
7	140.	KLLR	7/22/86	-99.	-99.	-99.	120.	140.	-99.		
8	140.	ERWN	7/29/86	-99.	-99.	-99.	80.	100.	-99.		
9	140.	ROS2	6/ 6/87	-99.	-99.	-99.	140.	120.	-99.		
0	140.	DNTN	7/30/87	-99.	-99.	-99.	80.	80.	80.		
1	140.	ROS2	9/ 2/87	-99.	-99.	-99.	140.	130.	100.		
2	130.	NST2	6/28/84	-99.	-99.	-99.	100.	-99.	-99.		
3	130.	KLLR	7/ 2/84	-99.	-99.	-99.	110.	130.	-99.		
4	130.	NST2	7/16/84	-99.	-99.	-99.	70.	100.	-99.		
5	130.	KLLR	7/20/84	-99.	-99.	-99.	110.	130.	-99.		
6	130.	MCK3	7/25/84	-99.	-99.	-99.	130.	130.	-99.		

Table 2. Highest Ozone Days for Dallas-Fort Worth 1984 - 1988

Rank	Peak O3	Monitor	Date	Maximum Daily Ozone 480850004 FRNK	480850085 ERWN	481130044 MOCK	481130044 MCK2	481130044 MCK3	481130045 NSTR	481130045 NST2	481130052 ILLI
47	130.	BNVW	8/14/84	-99.	-99.	-99.	-99.	120.	-99.	100.	30.
48	130.	DNT2	8/26/84	-99.	-99.	-99.	-99.	110.	-99.	120.	80.
49	130.	DNT2	5/ 4/85	-99.	-99.	-99.	-99.	100.	-99.	100.	90.
50	130.	KLLR	7/17/85	-99.	-99.	-99.	-99.	80.	-99.	90.	90.
51	130.	DNT2	7/19/85	-99.	-99.	-99.	-99.	80.	-99.	80.	80.
52	130.	KLLR	9/ 1/85	-99.	-99.	-99.	-99.	120.	-99.	100.	-99.
53	130.	NST2	6/ 7/86	-99.	80.	-99.	-99.	-99.	-99.	130.	-99.
54	130.	NST2	7/19/86	119.	110.	-99.	-99.	-99.	-99.	130.	80.
55	130.	KLLR	7/20/86	91.	80.	-99.	-99.	-99.	-99.	120.	90.
56	130.	DNTN	7/31/87	-99.	-99.	-99.	-99.	-99.	-99.	100.	-99.
57	130.	HNT2	8/ 5/87	-99.	-99.	-99.	-99.	-99.	-99.	90.	-99.
58	130.	DNTN	8/11/87	-99.	-99.	-99.	-99.	-99.	-99.	120.	-99.
59	130.	DNTN	9/17/87	-99.	-99.	-99.	-99.	-99.	-99.	80.	-99.
60	120.	DNT2	6/16/84	-99.	-99.	-99.	-99.	-99.	-99.	110.	100.
61	120.	ROS2	6/30/84	-99.	-99.	-99.	-99.	90.	-99.	90.	80.
62	120.	DNT2	7/ 7/84	-99.	-99.	-99.	-99.	70.	-99.	90.	70.
63	120.	ROS2	7/19/84	-99.	-99.	-99.	-99.	100.	-99.	80.	-99.
64	120.	MCK3	7/26/84	-99.	-99.	-99.	-99.	120.	-99.	100.	-99.
65	120.	KLLR	8/15/84	-99.	-99.	-99.	-99.	100.	-99.	90.	-99.
66	120.	DNT2	8/16/84	-99.	-99.	-99.	-99.	80.	-99.	110.	70.
67	120.	ILLI	8/20/84	-99.	-99.	-99.	-99.	110.	-99.	80.	120.
68	120.	KLLR	4/24/85	-99.	-99.	-99.	-99.	70.	-99.	70.	80.
69	120.	DNT2	5/25/85	-99.	-99.	-99.	-99.	100.	-99.	100.	90.
70	120.	DNT2	6/ 8/85	-99.	-99.	-99.	-99.	90.	-99.	100.	80.
71	120.	DNT2	6/16/85	-99.	-99.	-99.	-99.	90.	-99.	100.	90.
72	120.	KLLR	6/19/85	-99.	-99.	-99.	-99.	100.	-99.	80.	100.
73	120.	DNT2	7/ 2/85	-99.	-99.	-99.	-99.	80.	-99.	90.	80.
74	120.	DNT2	7/ 3/85	-99.	-99.	-99.	-99.	80.	-99.	40.	70.
75	120.	ILLI	7/ 7/85	-99.	-99.	-99.	-99.	110.	-99.	-99.	120.
76	120.	DNT2	7/ 8/85	-99.	-99.	-99.	-99.	70.	-99.	-99.	70.
77	120.	DNT2	7/11/85	-99.	-99.	-99.	-99.	70.	-99.	-99.	70.
78	120.	DNT2	7/12/85	-99.	-99.	-99.	-99.	70.	-99.	50.	80.
79	120.	ILLI	7/16/85	-99.	-99.	-99.	-99.	90.	-99.	90.	120.
80	120.	DNT2	7/18/85	-99.	-99.	-99.	-99.	90.	-99.	90.	80.
81	120.	NST2	8/ 1/85	-99.	-99.	-99.	-99.	90.	-99.	120.	80.
82	120.	NST2	8/ 7/85	-99.	-99.	-99.	-99.	100.	-99.	120.	100.
83	120.	ILLI	8/15/85	-99.	-99.	-99.	-99.	80.	-99.	60.	120.
84	120.	MCK3	8/16/85	-99.	-99.	-99.	-99.	120.	-99.	120.	110.
85	120.	ROS2	9/10/85	-99.	-99.	-99.	-99.	70.	-99.	70.	-99.
86	120.	ERWN	5/12/86	-99.	120.	-99.	-99.	-99.	-99.	90.	80.
87	120.	ERWN	5/29/86	-99.	120.	-99.	-99.	-99.	-99.	110.	-99.
88	120.	BNVW	5/30/86	-99.	90.	-99.	-99.	-99.	-99.	110.	-99.
89	120.	ILLI	6/12/86	-99.	80.	-99.	-99.	-99.	-99.	110.	120.
90	120.	NST2	6/23/86	-99.	100.	-99.	-99.	-99.	-99.	120.	90.
91	120.	COIT	7/26/86	97.	100.	-99.	-99.	-99.	-99.	100.	60.
92	120.	ROS2	8/22/86	84.	80.	-99.	-99.	-99.	-99.	90.	90.

Table 2. Highest Ozone Days for Dallas-Fort Worth 1984 - 1988

k	Peak O3	Monitor	Date	Maximum Daily Ozone 481130052 ILL2	481130055 BNVW	481130055 BNV2	481130069 HNTN	481130069 HNT2	481130086 COIT	481210054 DNTN	481210054 DNT2
	130.	BNVW	8/14/84	-99.	130.	-99.	-99.	-99.	-99.	-99.	90.
	130.	DNT2	8/26/84	-99.	70.	-99.	-99.	-99.	-99.	-99.	130.
	130.	DNT2	5/ 4/85	-99.	70.	-99.	-99.	-99.	-99.	-99.	130.
	130.	KLLR	7/17/85	-99.	90.	-99.	-99.	-99.	-99.	-99.	100.
	130.	DNT2	7/19/85	-99.	80.	-99.	-99.	-99.	-99.	-99.	130.
	130.	KLLR	9/ 1/85	80.	90.	-99.	-99.	-99.	-99.	100.	-99.
	130.	NST2	6/ 7/86	-99.	120.	-99.	-99.	-99.	110.	120.	-99.
	130.	NST2	7/19/86	-99.	60.	-99.	-99.	110.	130.	120.	-99.
	130.	KLLR	7/20/86	-99.	70.	-99.	-99.	120.	90.	90.	-99.
	130.	DNTN	7/31/87	-99.	80.	-99.	-99.	80.	-99.	130.	-99.
	130.	HNT2	8/ 5/87	-99.	-99.	-99.	-99.	130.	-99.	80.	-99.
	130.	DNTN	8/11/87	-99.	70.	-99.	-99.	110.	-99.	130.	-99.
	130.	DNTN	9/17/87	50.	50.	-99.	-99.	60.	-99.	130.	-99.
	120.	DNT2	6/16/84	-99.	100.	-99.	-99.	-99.	-99.	-99.	120.
	120.	ROS2	6/30/84	-99.	50.	-99.	-99.	-99.	-99.	-99.	90.
	120.	DNT2	7/ 7/84	-99.	70.	-99.	-99.	-99.	-99.	-99.	120.
	120.	ROS2	7/19/84	-99.	100.	-99.	-99.	-99.	-99.	-99.	80.
	120.	MCK3	7/26/84	-99.	110.	-99.	-99.	-99.	-99.	-99.	120.
	120.	KLLR	8/15/84	-99.	80.	-99.	-99.	-99.	-99.	-99.	90.
	120.	DNT2	8/16/84	-99.	60.	-99.	-99.	-99.	-99.	-99.	120.
	120.	ILLI	8/20/84	-99.	120.	-99.	-99.	-99.	-99.	-99.	100.
	120.	KLLR	4/24/85	-99.	-99.	-99.	-99.	-99.	-99.	-99.	80.
	120.	DNT2	5/25/85	-99.	70.	-99.	-99.	-99.	-99.	-99.	120.
	120.	DNT2	6/ 8/85	-99.	90.	-99.	-99.	-99.	-99.	-99.	120.
	120.	DNT2	6/16/85	-99.	80.	-99.	-99.	-99.	-99.	-99.	120.
	120.	KLLR	6/19/85	-99.	70.	-99.	-99.	-99.	-99.	-99.	100.
	120.	DNT2	7/ 2/85	-99.	80.	-99.	-99.	-99.	-99.	-99.	120.
	120.	DNT2	7/ 3/85	-99.	50.	-99.	-99.	-99.	-99.	-99.	120.
	120.	ILLI	7/ 7/85	-99.	50.	-99.	-99.	-99.	-99.	-99.	120.
	120.	DNT2	7/ 8/85	-99.	70.	-99.	-99.	-99.	-99.	-99.	120.
	120.	DNT2	7/11/85	-99.	70.	-99.	-99.	-99.	-99.	-99.	120.
	120.	DNT2	7/12/85	-99.	70.	-99.	-99.	-99.	-99.	-99.	120.
	120.	ILLI	7/16/85	-99.	90.	-99.	-99.	-99.	-99.	-99.	80.
	120.	DNT2	7/18/85	-99.	90.	-99.	-99.	-99.	-99.	-99.	120.
	120.	NST2	8/ 1/85	-99.	60.	-99.	-99.	-99.	-99.	-99.	30.
	120.	NST2	8/ 7/85	-99.	90.	-99.	-99.	-99.	-99.	-99.	40.
	120.	ILLI	8/15/85	-99.	20.	-99.	-99.	-99.	-99.	-99.	-99.
	120.	MCK3	8/16/85	-99.	90.	-99.	-99.	-99.	-99.	-99.	40.
	120.	ROS2	9/10/85	40.	60.	-99.	-99.	-99.	-99.	80.	-99.
	120.	ERWN	5/12/86	-99.	-99.	-99.	-99.	-99.	-99.	70.	-99.
	120.	ERWN	5/29/86	-99.	110.	-99.	-99.	-99.	110.	120.	-99.
	120.	BNVW	5/30/86	-99.	120.	-99.	-99.	-99.	80.	100.	-99.
	120.	ILLI	6/12/86	-99.	110.	-99.	-99.	-99.	90.	-99.	-99.
	120.	NST2	6/23/86	-99.	90.	-99.	-99.	-99.	-99.	120.	-99.
	120.	COIT	7/26/86	-99.	70.	-99.	-99.	70.	120.	100.	-99.
	120.	ROS2	8/22/86	-99.	90.	-99.	-99.	90.	-99.	70.	-99.

Table 2. Highest Ozone Days for Dallas-Fort Worth 1984 - 1988

ank	Peak O3	Monitor	Date	Maximum Daily Ozone 483670080 WTHR	483970081 FATE	484391002 ROSS	484391002 ROS2	484392003 KLLR	484970087 DAIR		
47	130.	BNVW	8/14/84	-99.	-99.	-99.	110.	100.	-99.		
48	130.	DNT2	8/26/84	-99.	-99.	-99.	120.	120.	-99.		
49	130.	DNT2	5/ 4/85	-99.	-99.	-99.	90.	90.	-99.		
50	130.	KLLR	7/17/85	-99.	-99.	-99.	110.	130.	-99.		
51	130.	DNT2	7/19/85	-99.	-99.	-99.	80.	100.	-99.		
52	130.	KLLR	9/ 1/85	-99.	-99.	-99.	110.	130.	-99.		
53	130.	NST2	6/ 7/86	-99.	-99.	-99.	90.	90.	-99.		
54	130.	NST2	7/19/86	-99.	-99.	-99.	80.	120.	-99.		
55	130.	KLLR	7/20/86	-99.	-99.	-99.	100.	130.	-99.		
56	130.	DNTN	7/31/87	-99.	-99.	-99.	80.	90.	80.		
57	130.	HNT2	8/ 5/87	-99.	-99.	-99.	80.	80.	70.		
58	130.	DNTN	8/11/87	-99.	-99.	-99.	100.	100.	80.		
59	130.	DNTN	9/17/87	-99.	-99.	-99.	-99.	90.	80.		
60	120.	DNT2	6/16/84	-99.	-99.	-99.	100.	120.	-99.		
61	120.	ROS2	6/30/84	-99.	-99.	-99.	120.	-99.	-99.		
62	120.	DNT2	7/ 7/84	-99.	-99.	-99.	70.	90.	-99.		
63	120.	ROS2	7/19/84	-99.	-99.	-99.	120.	100.	-99.		
64	120.	MCK3	7/26/84	-99.	-99.	-99.	100.	100.	-99.		
65	120.	KLLR	8/15/84	-99.	-99.	-99.	110.	120.	-99.		
66	120.	DNT2	8/16/84	-99.	-99.	-99.	80.	100.	-99.		
67	120.	ILLI	8/20/84	-99.	-99.	-99.	100.	90.	-99.		
68	120.	KLLR	4/24/85	-99.	-99.	-99.	90.	120.	-99.		
69	120.	DNT2	5/25/85	-99.	-99.	-99.	70.	80.	-99.		
70	120.	DNT2	6/ 8/85	-99.	-99.	-99.	70.	90.	-99.		
71	120.	DNT2	6/16/85	-99.	-99.	-99.	70.	80.	-99.		
72	120.	KLLR	6/19/85	-99.	-99.	-99.	100.	120.	-99.		
73	120.	DNT2	7/ 2/85	-99.	-99.	-99.	70.	80.	-99.		
74	120.	DNT2	7/ 3/85	-99.	-99.	-99.	70.	90.	-99.		
75	120.	ILLI	7/ 7/85	-99.	-99.	-99.	110.	110.	-99.		
76	120.	DNT2	7/ 8/85	-99.	-99.	-99.	70.	80.	-99.		
77	120.	DNT2	7/11/85	-99.	-99.	-99.	70.	90.	-99.		
78	120.	DNT2	7/12/85	-99.	-99.	-99.	70.	-99.	-99.		
79	120.	ILLI	7/16/85	-99.	-99.	-99.	70.	60.	-99.		
80	120.	DNT2	7/18/85	-99.	-99.	-99.	70.	90.	-99.		
81	120.	NST2	8/ 1/85	-99.	-99.	-99.	90.	70.	-99.		
82	120.	NST2	8/ 7/85	-99.	-99.	-99.	80.	100.	-99.		
83	120.	ILLI	8/15/85	-99.	-99.	-99.	70.	70.	-99.		
84	120.	MCK3	8/16/85	-99.	-99.	-99.	100.	110.	-99.		
85	120.	ROS2	9/10/85	-99.	-99.	-99.	120.	110.	-99.		
86	120.	ERWN	5/12/86	-99.	-99.	-99.	70.	-99.	-99.		
87	120.	ERWN	5/29/86	-99.	-99.	-99.	90.	100.	-99.		
88	120.	BNVW	5/30/86	-99.	-99.	-99.	120.	110.	-99.		
89	120.	ILLI	6/12/86	-99.	-99.	-99.	70.	80.	-99.		
90	120.	NST2	6/23/86	-99.	-99.	-99.	80.	90.	-99.		
91	120.	COIT	7/26/86	-99.	-99.	-99.	70.	80.	-99.		
92	120.	ROS2	8/22/86	-99.	-99.	-99.	120.	120.	-99.		

Table 2. Highest Ozone Days for Dallas-Fort Worth 1984 - 1988

nk	Peak O3	Monitor	Date	Maximum Daily Ozone 480850004 FRNK	480850085 ERWN	481130044 MOCK	481130044 MCK2	481130044 MCK3	481130045 NSTR	481130045 NST2	481130052 ILLI
3	120.	KLLR	9/ 8/86	88.	60.	-99.	-99.	-99.	-99.	90.	70.
4	120.	BNVW	4/27/87	-99.	-99.	-99.	-99.	-99.	-99.	80.	90.
5	120.	DNTN	7/15/87	-99.	-99.	-99.	-99.	-99.	-99.	100.	-99.
5	120.	ROS2	7/20/87	-99.	-99.	-99.	-99.	-99.	-99.	80.	-99.
7	120.	DA1R	7/21/87	-99.	-99.	-99.	-99.	-99.	-99.	70.	-99.
8	120.	DNTN	7/29/87	-99.	-99.	-99.	-99.	-99.	-99.	90.	-99.
9	120.	DNTN	8/24/87	-99.	-99.	-99.	-99.	-99.	-99.	90.	-99.
0	120.	DNTN	9/ 3/87	-99.	-99.	-99.	-99.	-99.	-99.	90.	-99.
	120.	ROS2	9/20/87	-99.	-99.	-99.	-99.	-99.	-99.	80.	-99.
2	120.	ROS2	5/16/88	-99.	-99.	-99.	-99.	-99.	-99.	70.	-99.
3	120.	KLLR	5/26/88	-99.	-99.	-99.	-99.	-99.	-99.	90.	-99.
.	120.	NST2	6/11/88	-99.	-99.	-99.	-99.	-99.	-99.	120.	-99.
5	120.	KLLR	6/27/88	-99.	-99.	-99.	-99.	-99.	-99.	100.	-99.
5	120.	NST2	6/28/88	-99.	-99.	-99.	-99.	-99.	-99.	120.	-99.

Table 2. Highest Ozone Days for Dallas-Fort Worth 1984 - 1988

ank	Peak O3	Monitor	Date	Maximum Daily Ozone 483670080 WTHR	483970081 FATE	484391002 ROSS	484391002 ROS2	484392003 KLLR	484970087 DAIR		
93	120.	KLLR	9/ 8/86	-99.	-99.	-99.	100.	120.	-99.		
94	120.	BNVW	4/27/87	-99.	-99.	-99.	80.	80.	-99.		
95	120.	DNTN	7/15/87	-99.	-99.	-99.	80.	80.	80.		
96	120.	ROS2	7/20/87	-99.	-99.	-99.	120.	120.	100.		
97	120.	DAIR	7/21/87	-99.	-99.	-99.	100.	110.	120.		
98	120.	DNTN	7/29/87	-99.	-99.	-99.	60.	80.	70.		
99	120.	DNTN	8/24/87	-99.	-99.	-99.	80.	80.	70.		
00	120.	DNTN	9/ 3/87	-99.	-99.	-99.	80.	80.	80.		
01	120.	ROS2	9/20/87	-99.	-99.	-99.	120.	120.	-99.		
02	120.	ROS2	5/16/88	-99.	-99.	-99.	120.	100.	-99.		
03	120.	KLLR	5/26/88	-99.	-99.	-99.	110.	120.	-99.		
04	120.	NST2	6/11/88	-99.	90.	-99.	100.	120.	-99.		
05	120.	KLLR	6/27/88	90.	80.	-99.	100.	120.	-99.		
06	120.	NST2	6/28/88	40.	80.	-99.	70.	90.	-99.		

TABLE 3. Possible UAM modeling days for Dallas-Fort Worth Area.

Date	Rank	O3	Peak Monitor	# station-hrs >= 120 ppb
07/31/84	1	180	KLLR	18
08/01/84	8	160	KLLR	23
08/02/84	9	160	KLLR	35
08/03/84	10	160	MCK2	22
09/05/84	2	170	DNT2	8
06/07/85	3	170	BNVW	10
08/31/85	4	170	MCK2	21
06/25/84	17	150	ILLI	21
06/26/84	?	?	?	?
06/27/84	6	160	NST2	10
07/23/84	7	160	ROS2	11
09/03/85	12	160	DNTN	20
07/10/85	11	160	DNT2	6
06/18/87	14	160	ILLI	13
07/22/87	15	160	DNTN	6
09/09/87	16	160	BNVW	16
07/30/86	13	160	COIT	13
07/31/86	27	150	ERWN	12
08/01/86	5	170	COIT	18

rem9985

TABLE 4. Candidate UAM modeling days for the Dallas-Fort Worth Area

Date	Rank	O3	Peak Monitor	# station-hrs >= 120 ppb
07/31/84	1	180	KLLR	18
08/01/84	8	160	KLLR	23
08/02/84	9	160	KLLR	35
08/03/84	10	160	MCK2	22
08/31/85	4	170	MCK2	21
06/25/84	17	150	ILLI	21
09/03/85	11	160	DNTN	20
09/09/87	16	160	BNVW	16
08/01/86	5	170	COIT	18

rem9985

Table 2. Highest Ozone Days for Dallas-Fort Worth 1984 - 1988

ank	Peak O3	Monitor	Date	Maximum Daily Ozone 481130052 ILL2	481130055 BNVW	481130055 BNV2	481130069 HNTN	481130069 HNT2	481130086 COIT	481210054 DNTN	481210054 DNT2
93	120.	KLLR	9/ 8/86	-99.	70.	-99.	-99.	80.	80.	80.	-99.
94	120.	BNVW	4/27/87	-99.	120.	-99.	90.	-99.	-99.	80.	-99.
95	120.	DNTN	7/15/87	30.	80.	-99.	-99.	80.	-99.	120.	-99.
96	120.	ROS2	7/20/87	70.	70.	-99.	-99.	90.	-99.	80.	-99.
97	120.	DAIR	7/21/87	60.	60.	-99.	-99.	80.	-99.	80.	-99.
98	120.	DNTN	7/29/87	70.	70.	-99.	-99.	70.	-99.	120.	-99.
99	120.	DNTN	8/24/87	70.	80.	-99.	-99.	80.	-99.	120.	-99.
)0	120.	DNTN	9/ 3/87	80.	90.	-99.	-99.	80.	-99.	120.	-99.
)1	120.	ROS2	9/20/87	90.	80.	-99.	-99.	90.	-99.	60.	-99.
)2	120.	ROS2	5/16/88	-99.	-99.	-99.	-99.	-99.	-99.	-99.	-99.
)3	120.	KLLR	5/26/88	-99.	-99.	-99.	-99.	-99.	-99.	-99.	-99.
)4	120.	NST2	6/11/88	-99.	-99.	-99.	-99.	-99.	-99.	-99.	-99.
)5	120.	KLLR	6/27/88	-99.	-99.	-99.	-99.	-99.	-99.	-99.	-99.
)6	120.	NST2	6/28/88	-99.	-99.	-99.	-99.	-99.	-99.	-99.	-99.

Appendix F

INITIAL CONDITION TRACER SIMULATION (INITIATED 1200 ON 24 AUGUST) FOR DALLAS-FORT WORTH

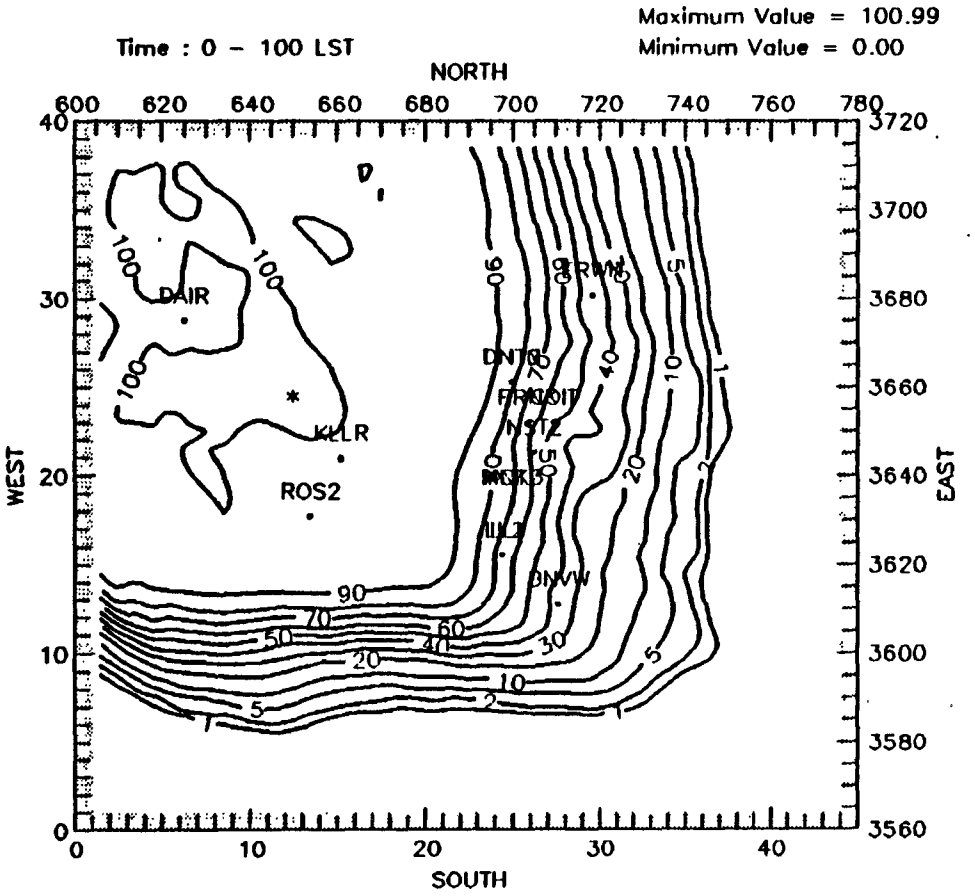

Initial conditions tracer, August 30, 1985 (pphm)

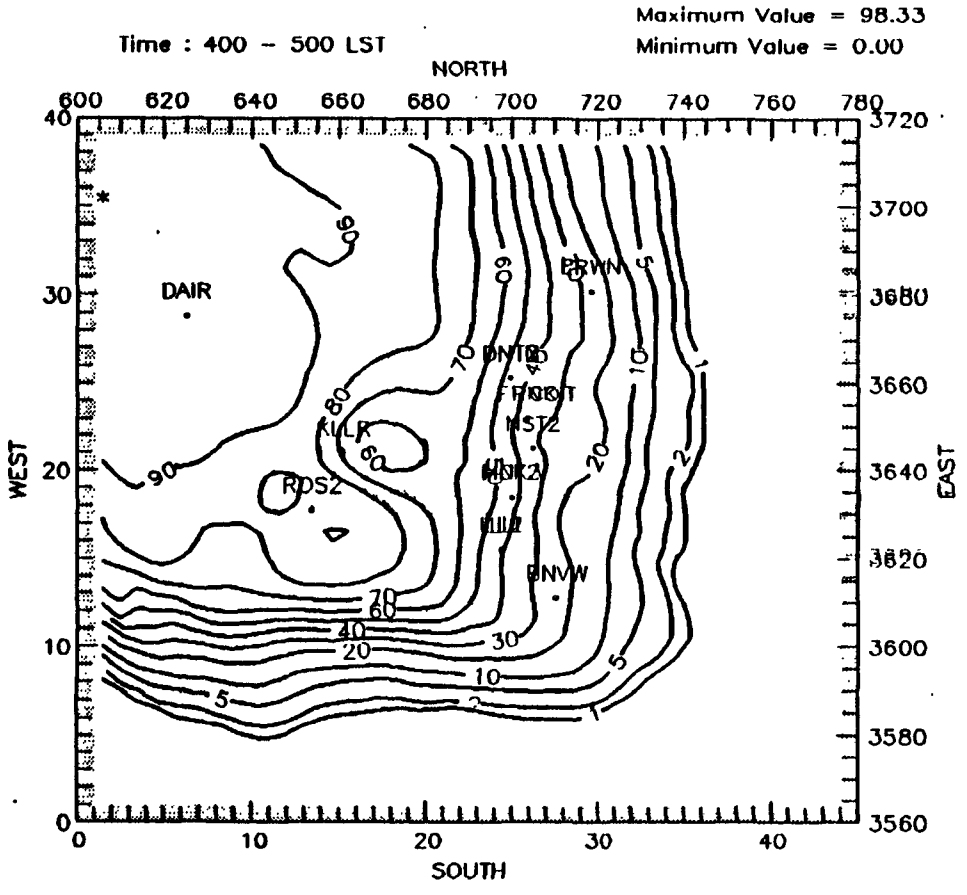

Initial conditions tracer, August 30, 1985 (pphm)

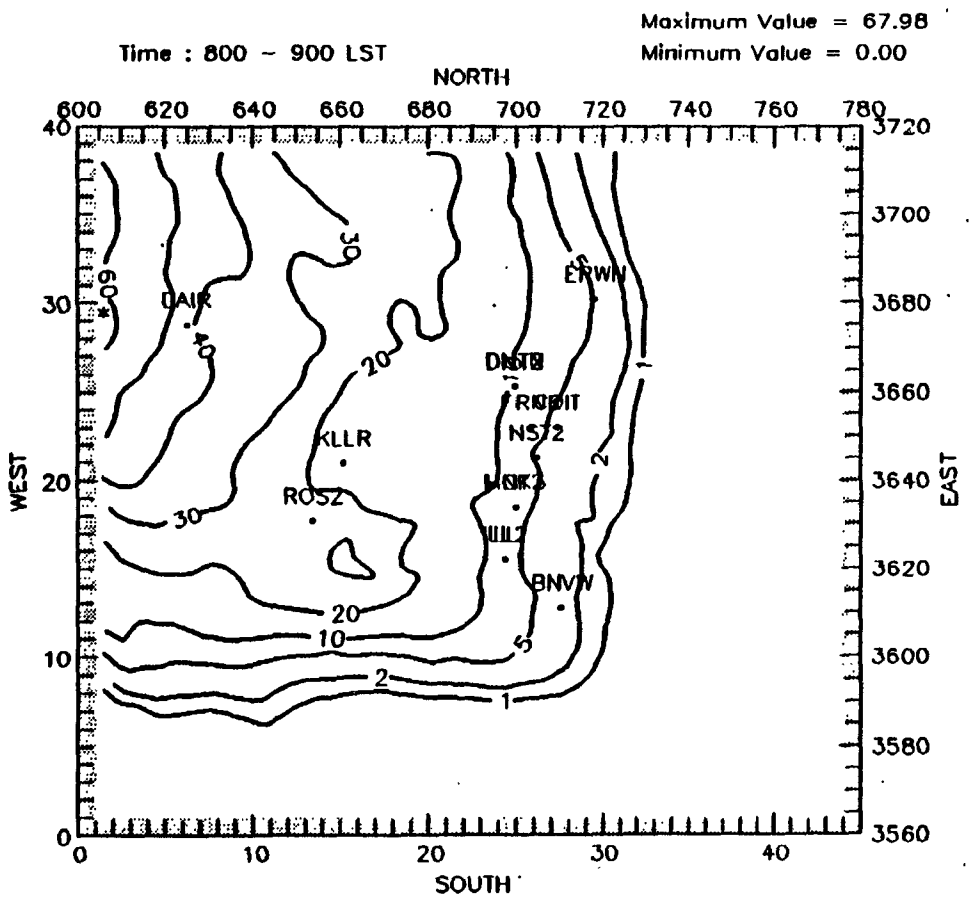

Initial conditions tracer, August 30, 1985 (pphm)

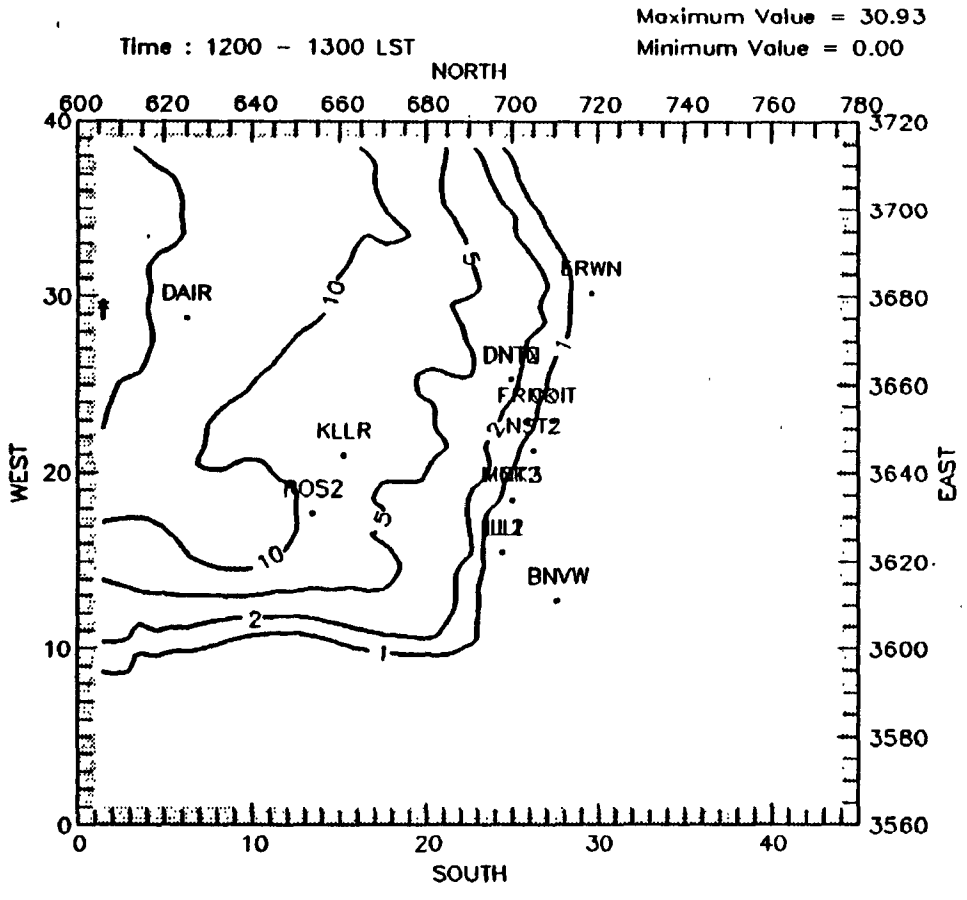

Initial conditions tracer, August 30, 1985 (pphm)

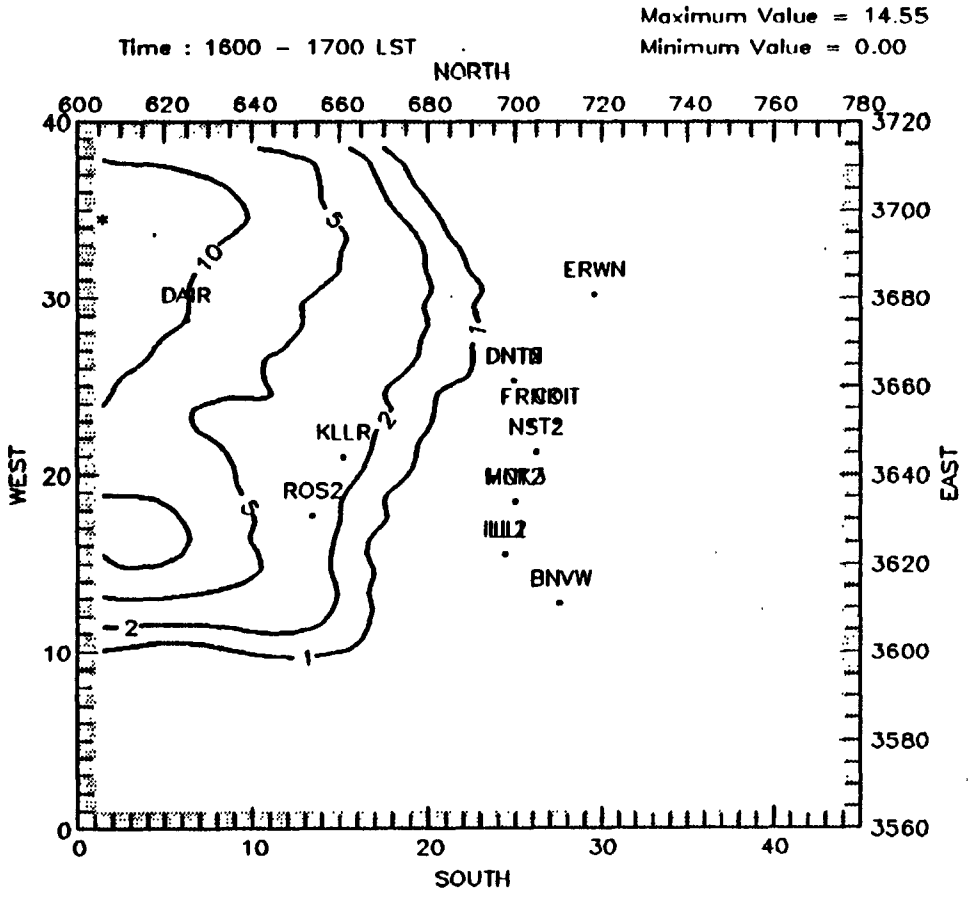

Initial conditions tracer, August 30, 1985 (pphm)

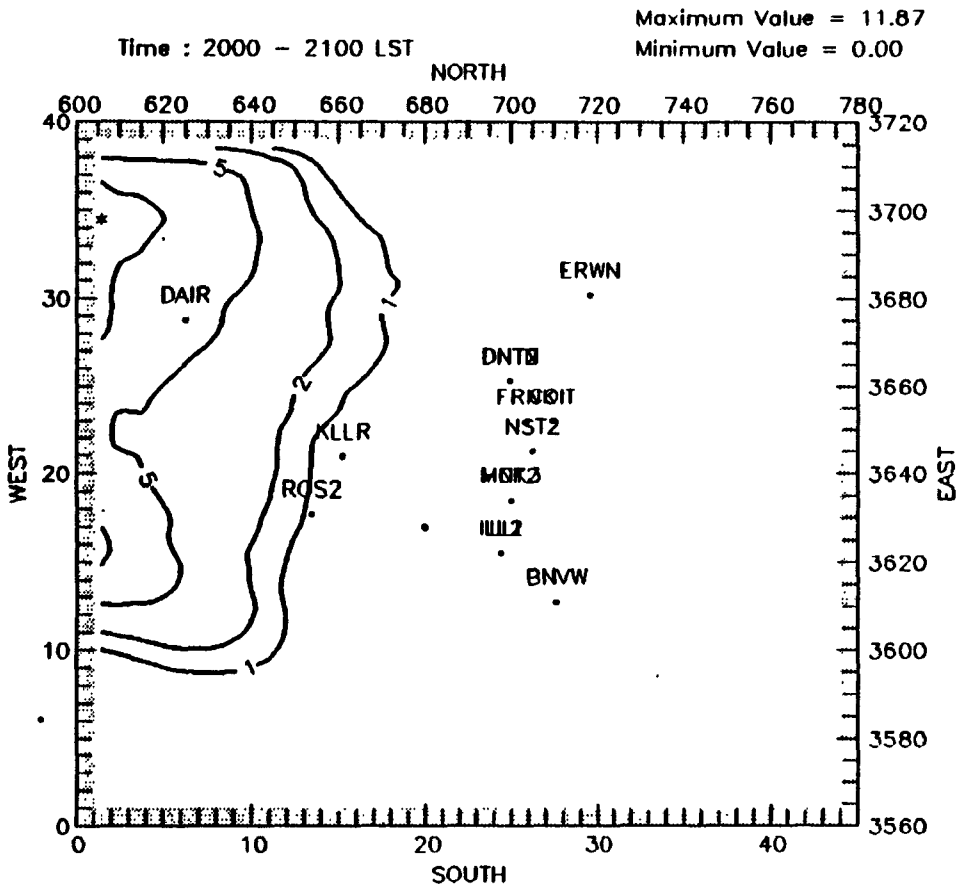

Initial conditions tracer, August 30, 1985 (pphm)

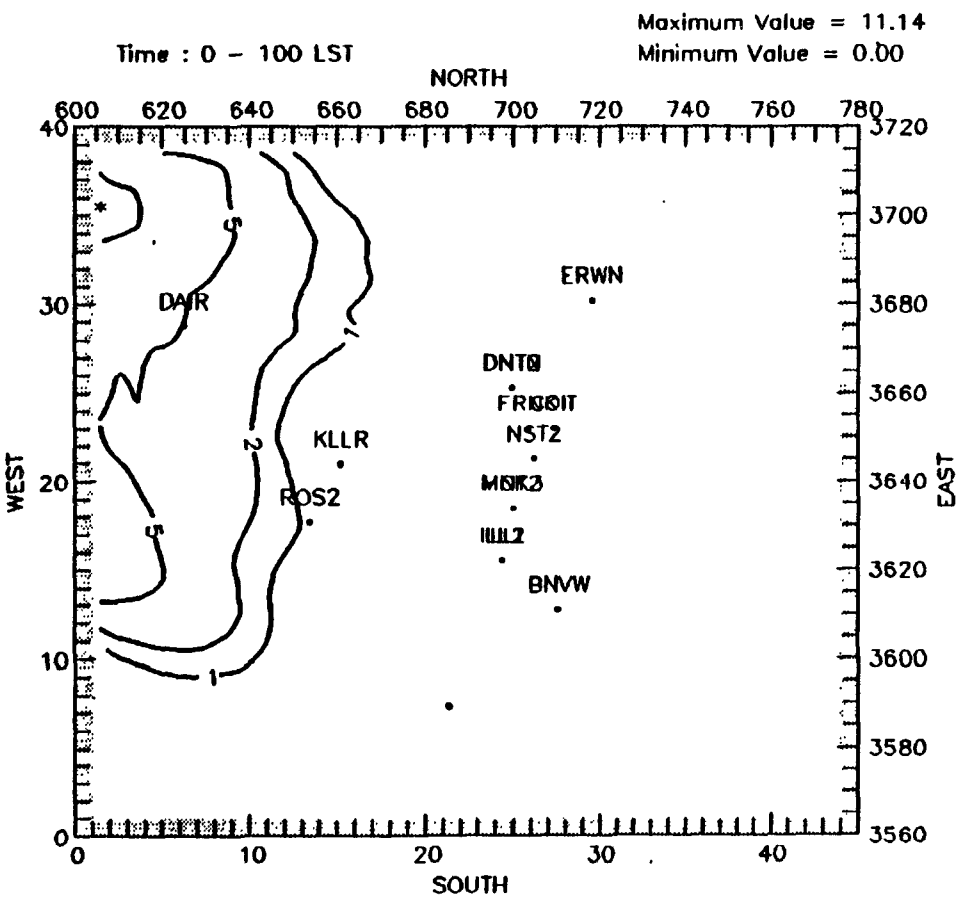

Initial conditions tracer, August 31, 1985 (pphm)

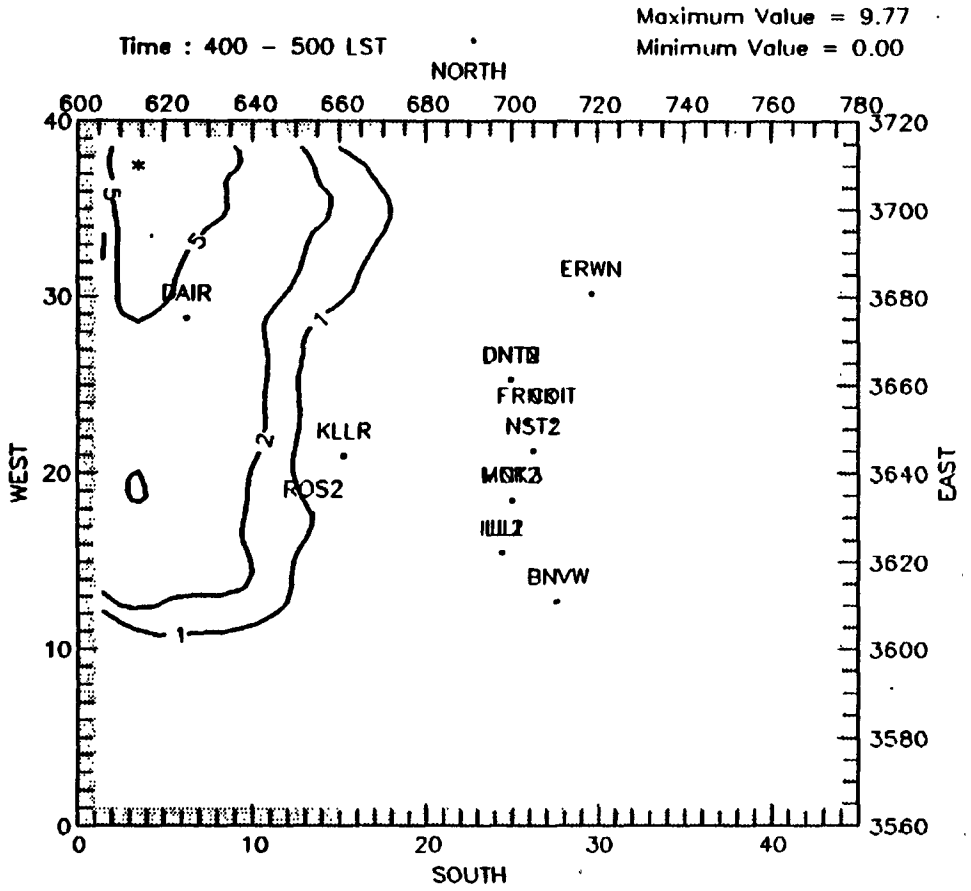

Initial conditions tracer, August 31, 1985 (pphm)

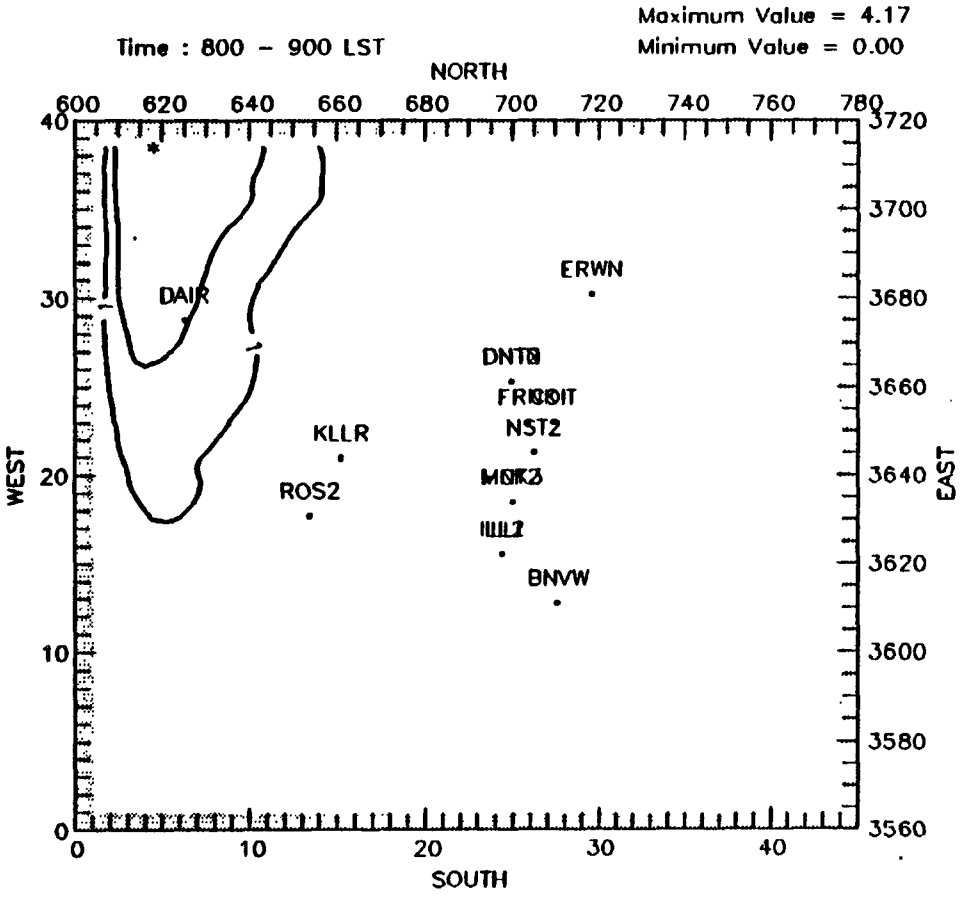

Initial conditions tracer, August 31, 1985 (pphm)

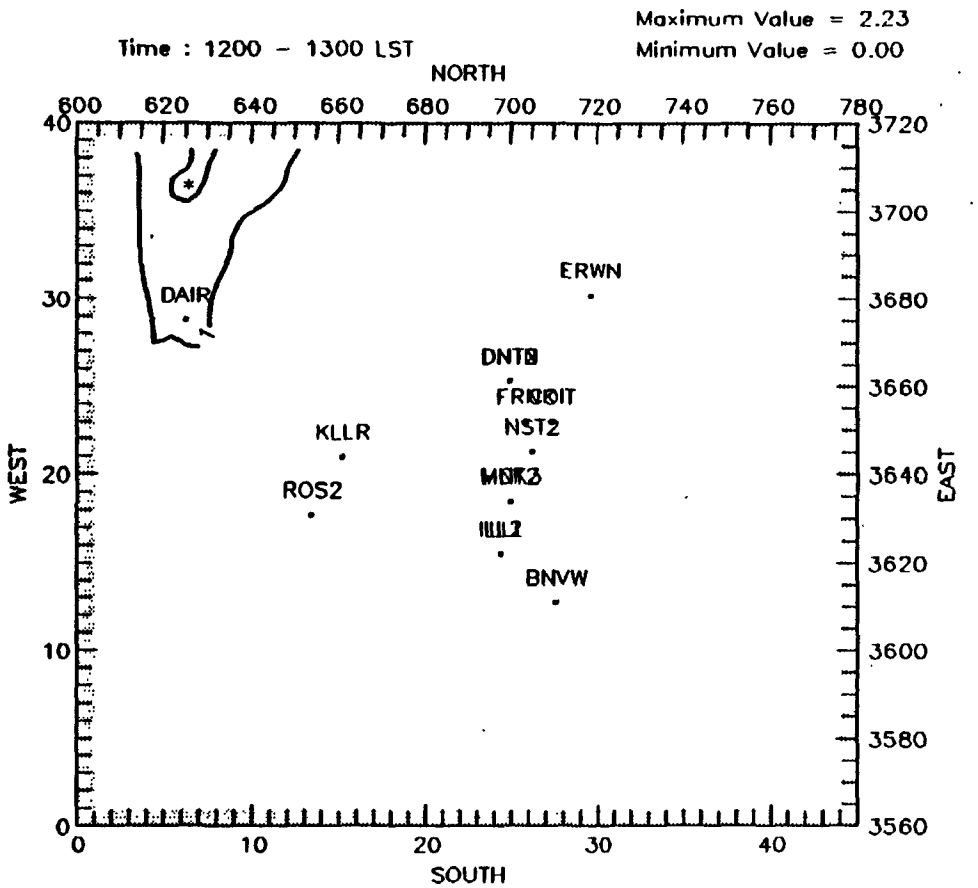

Initial conditions tracer, August 31, 1985 (pphm)

Appendix G

PREDICTED HOURLY OZONE CONCENTRATIONS (pphm) FOR DALLAS-FORT WORTH DIAGNOSTIC RUN 1

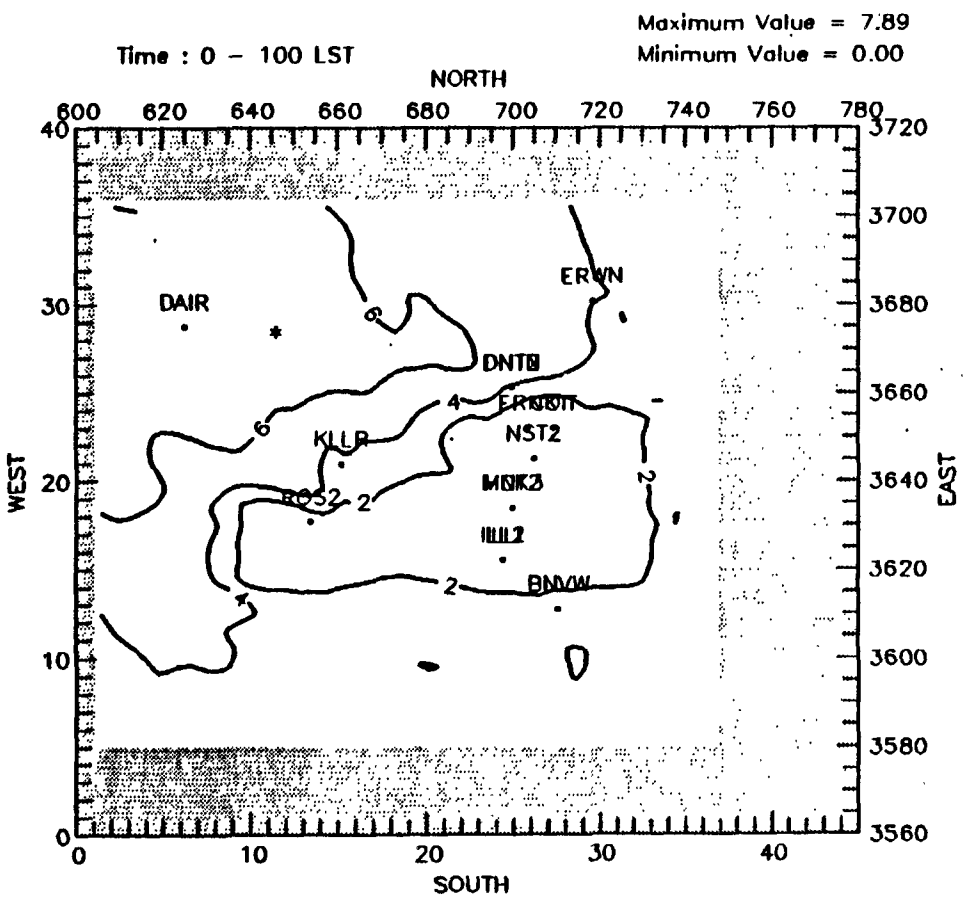

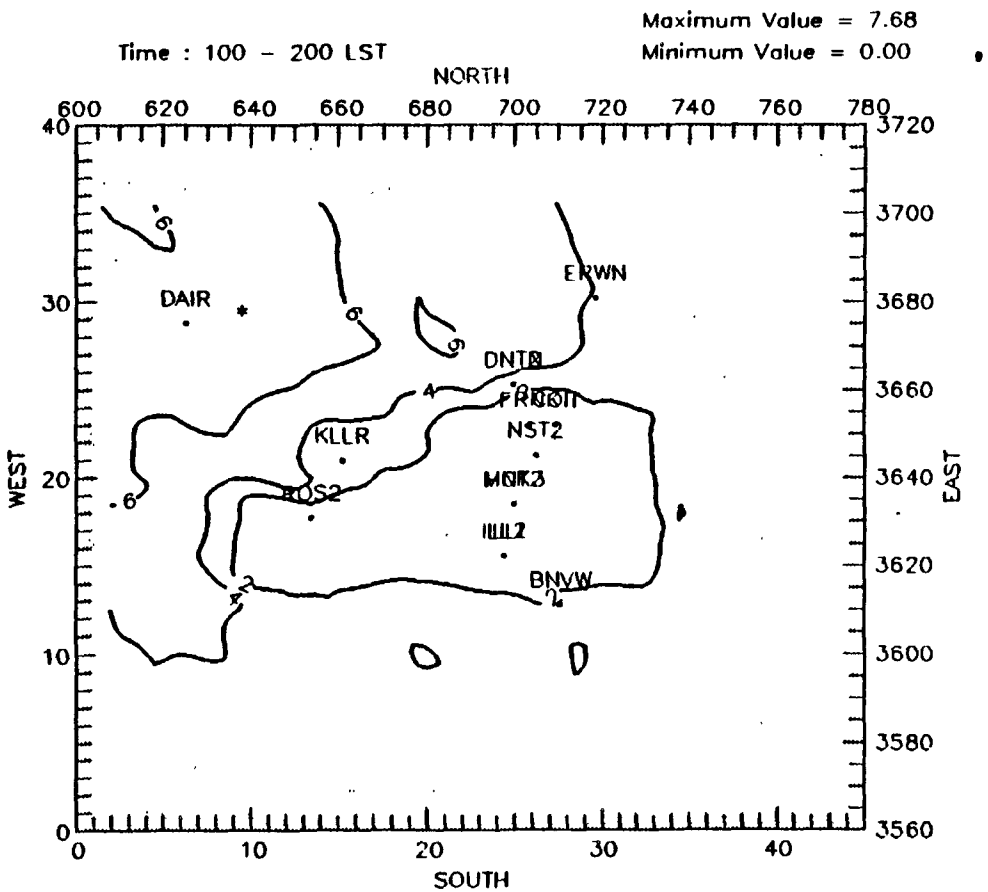

Ozone (pphm), 85 base emissions, August 30, 1985

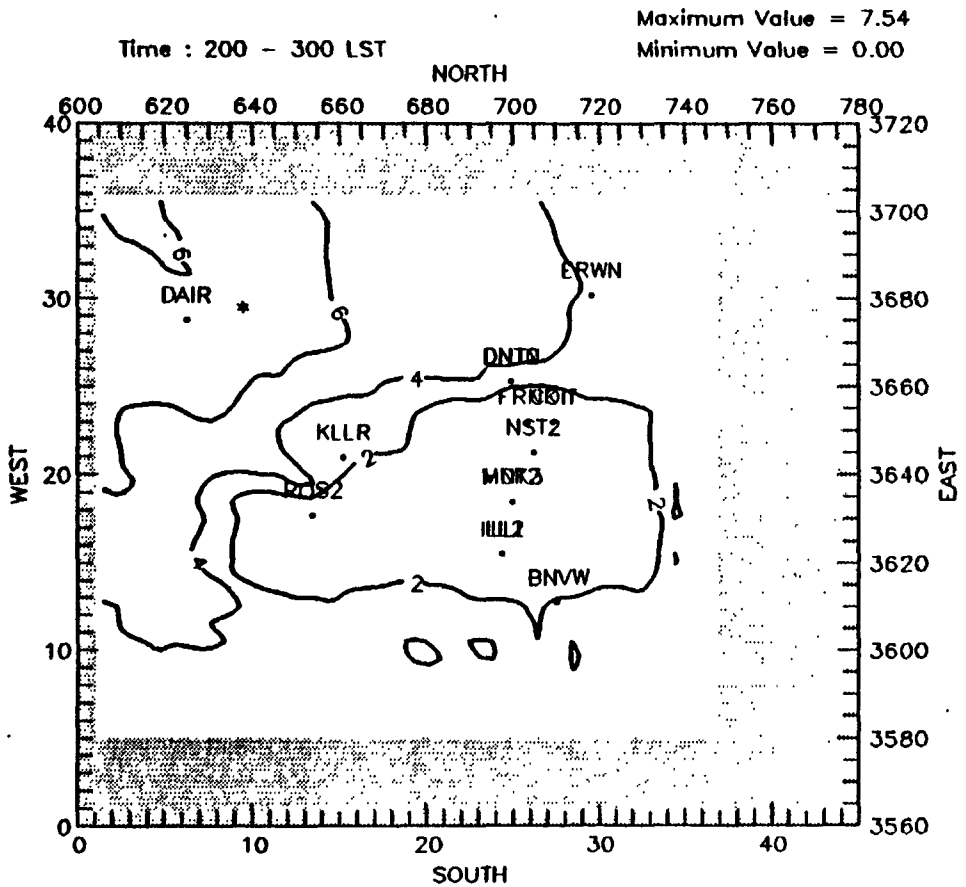

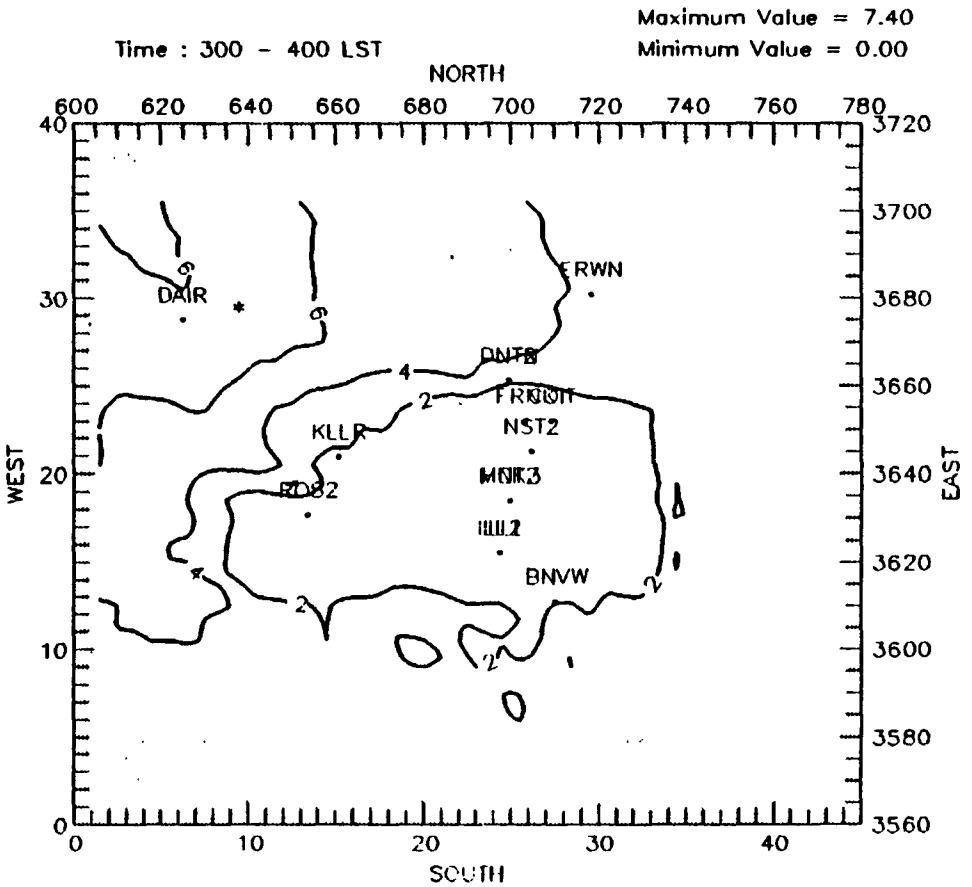

Ozone (pphm), 85 base emissions, August 30, 1985

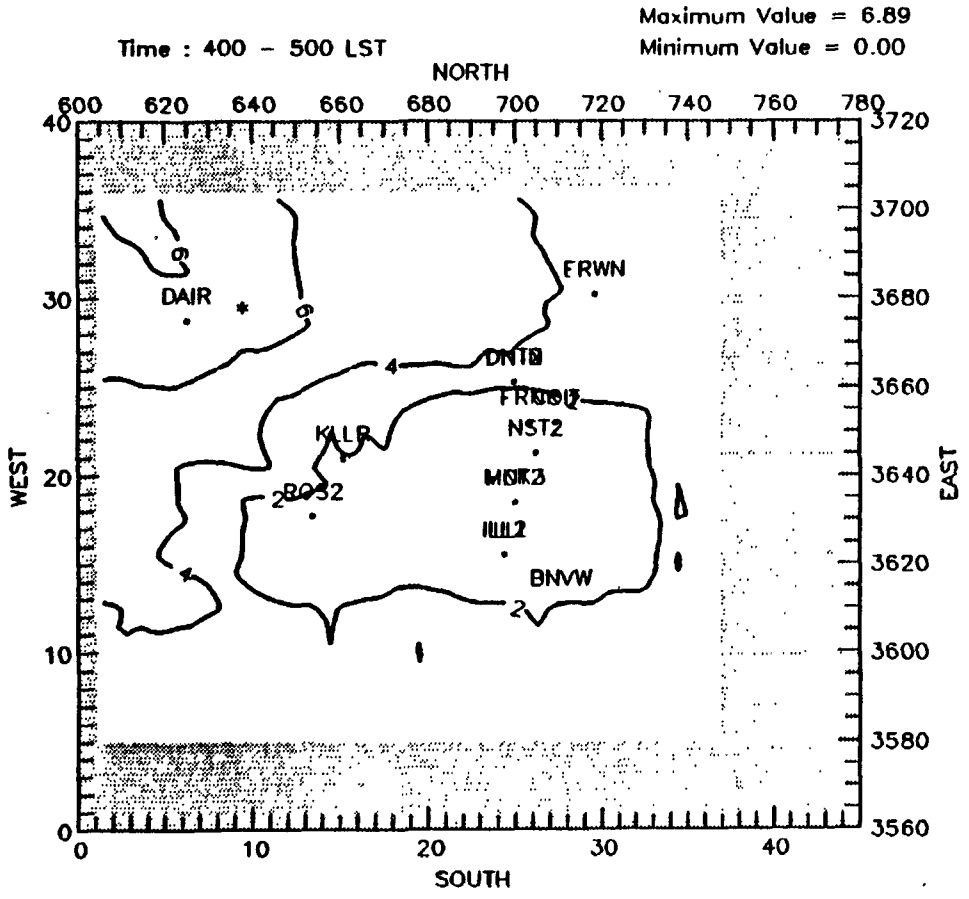

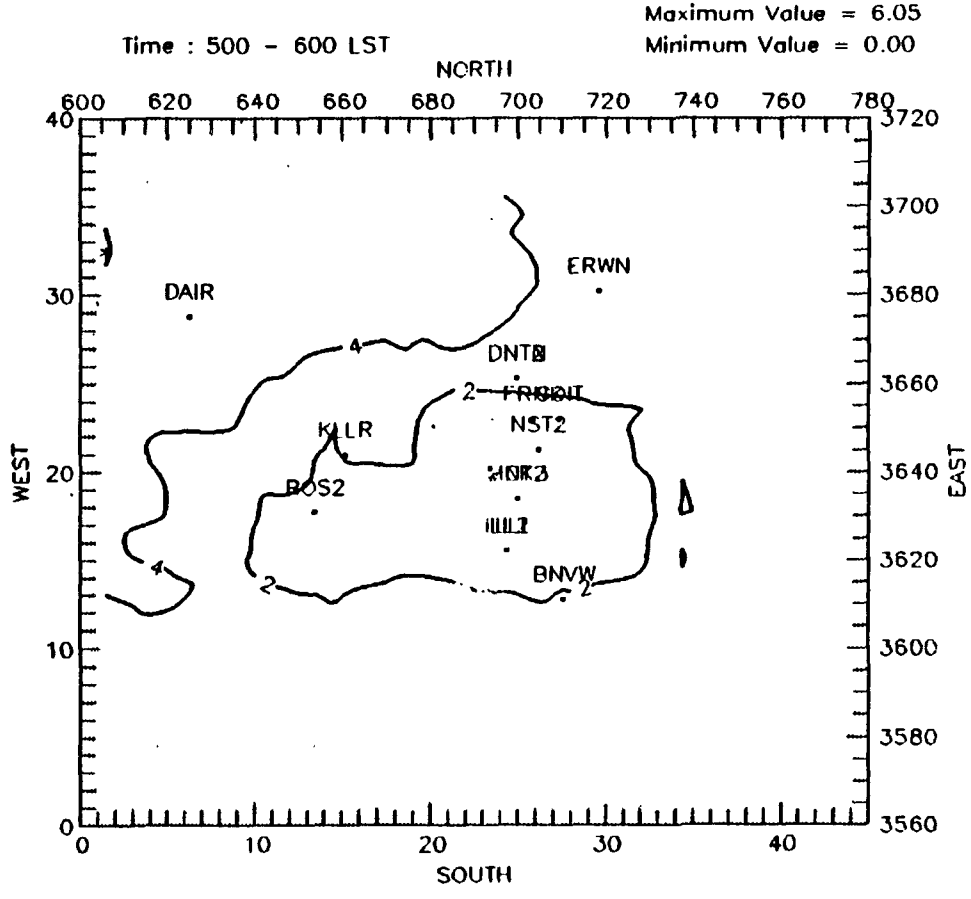

Ozone (pphm), 85 base emissions, August 30, 1985

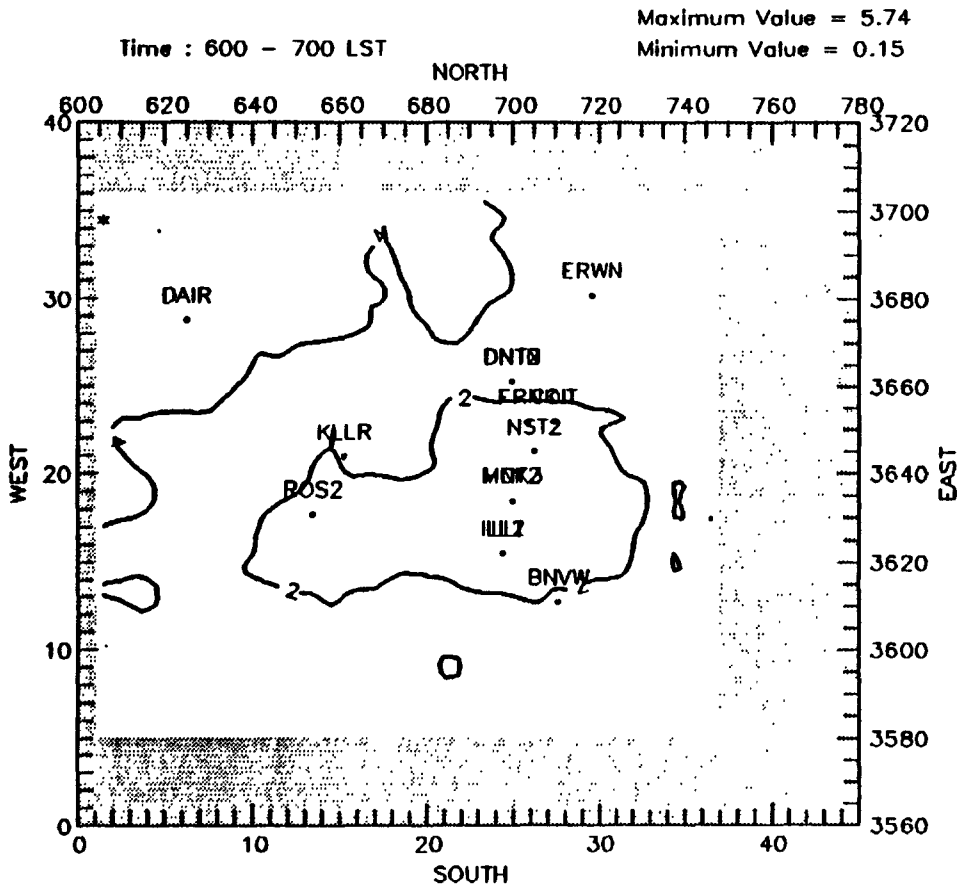

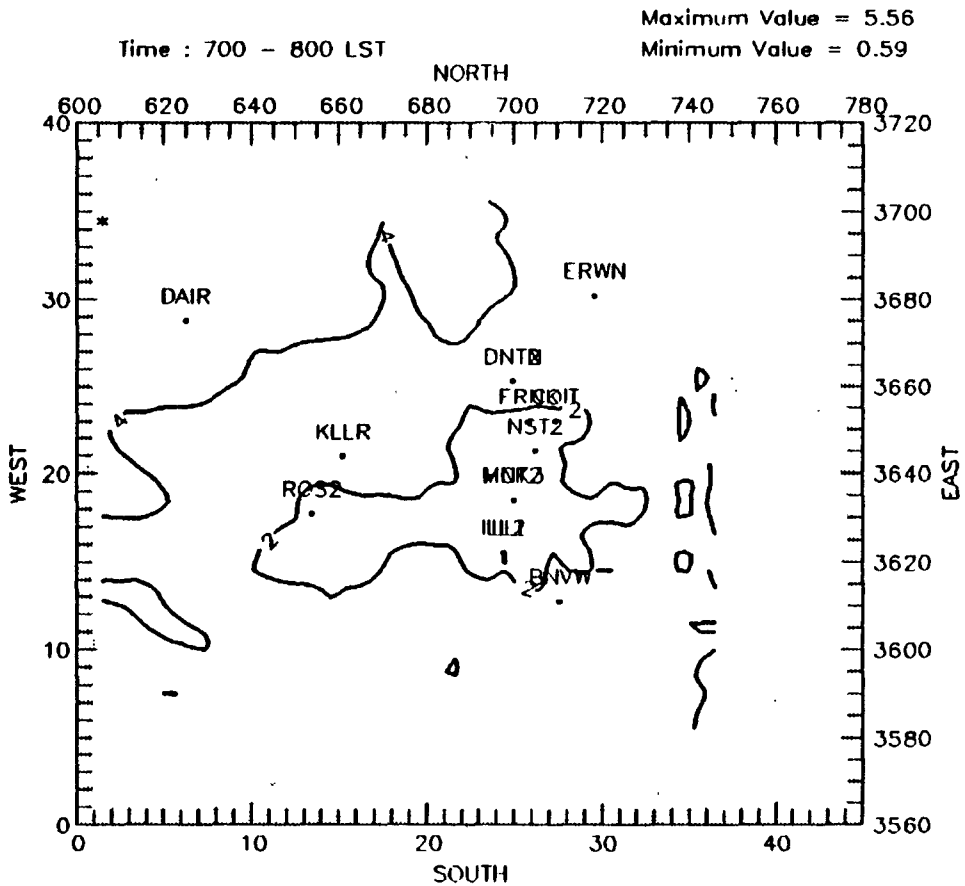

Ozone (pphm), 85 base emissions, August 30, 1985

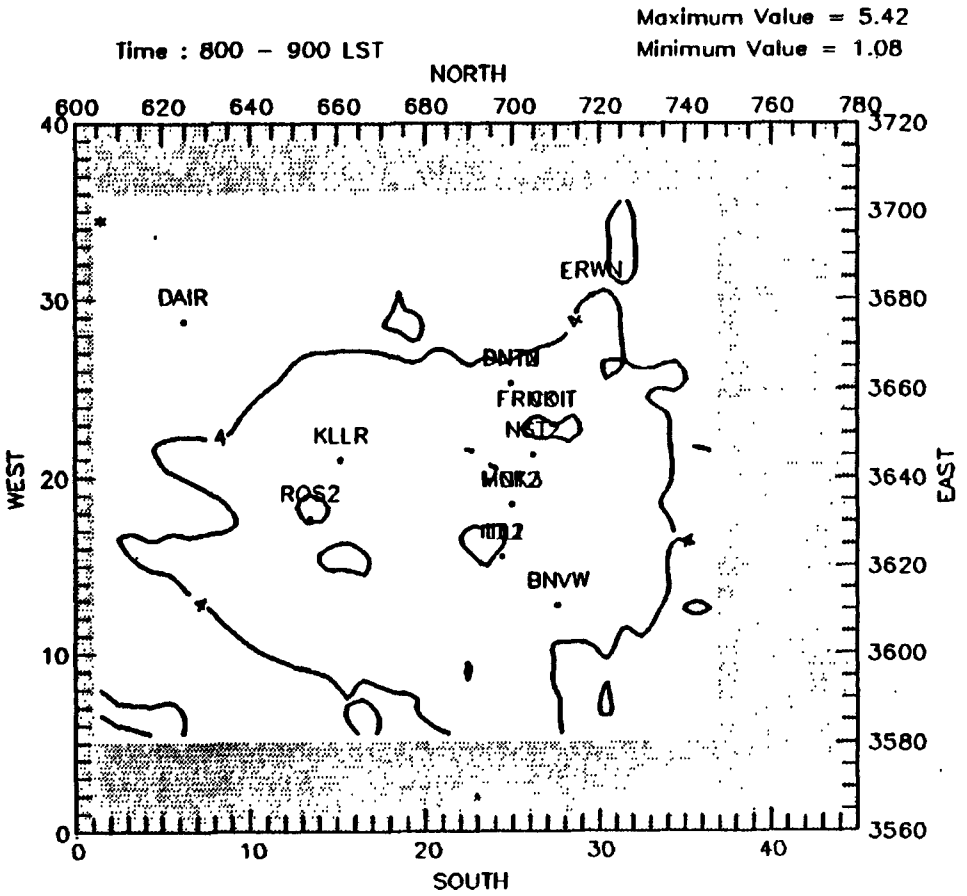

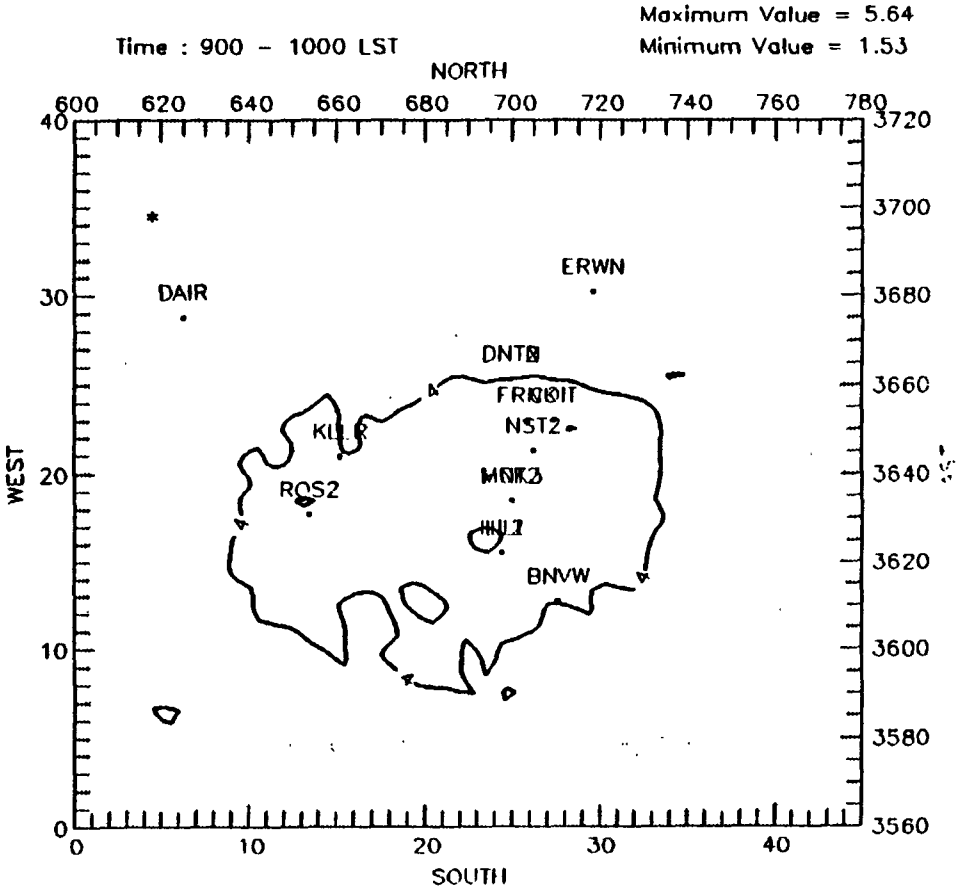

Ozone (pphm), 85 base emissions, August 30, 1985

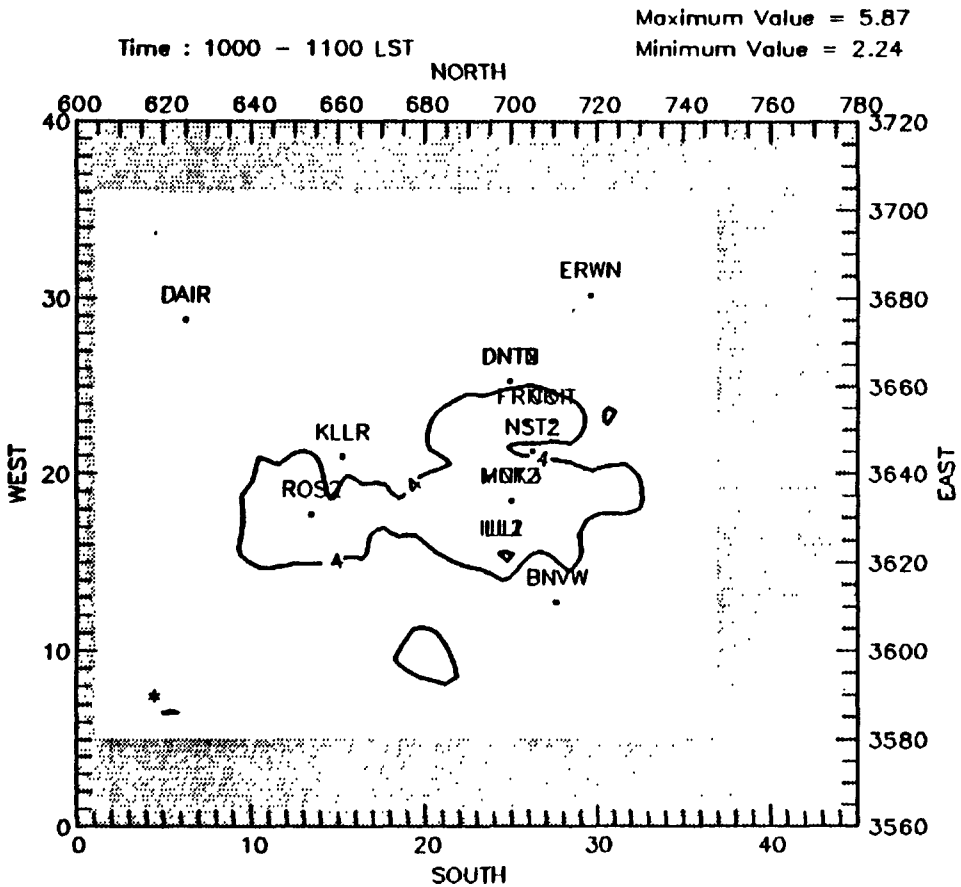

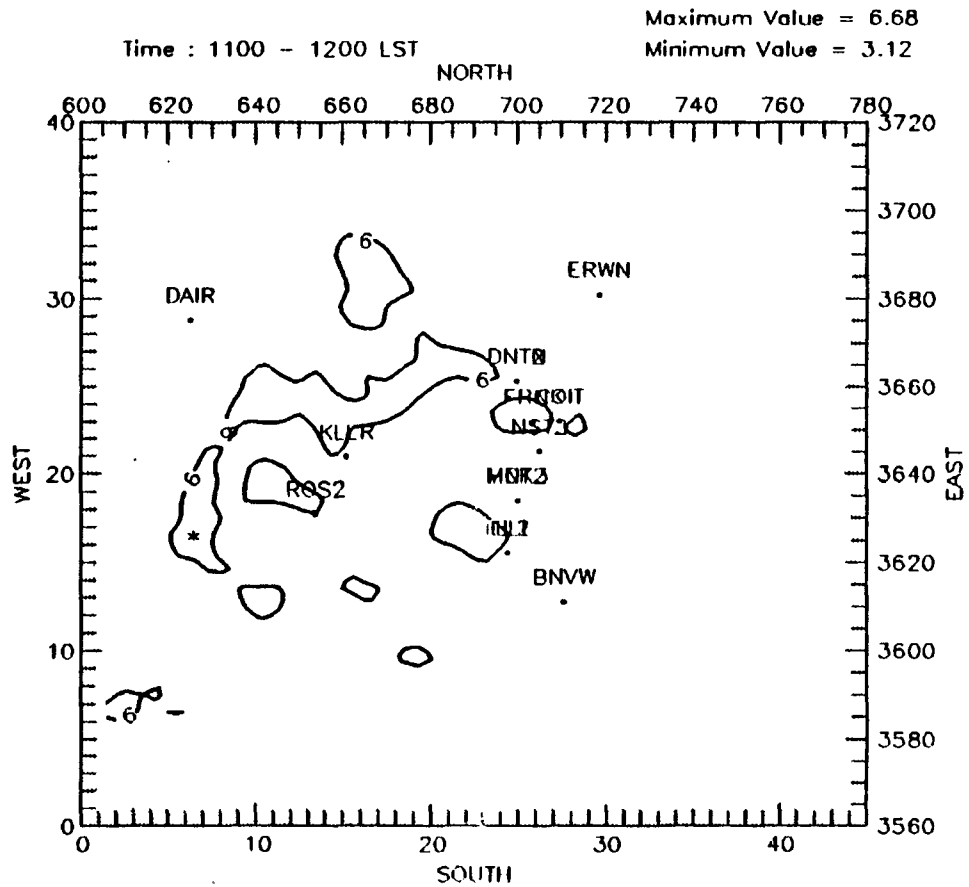

Ozone (pphm), 85 base emissions, August 30, 1985

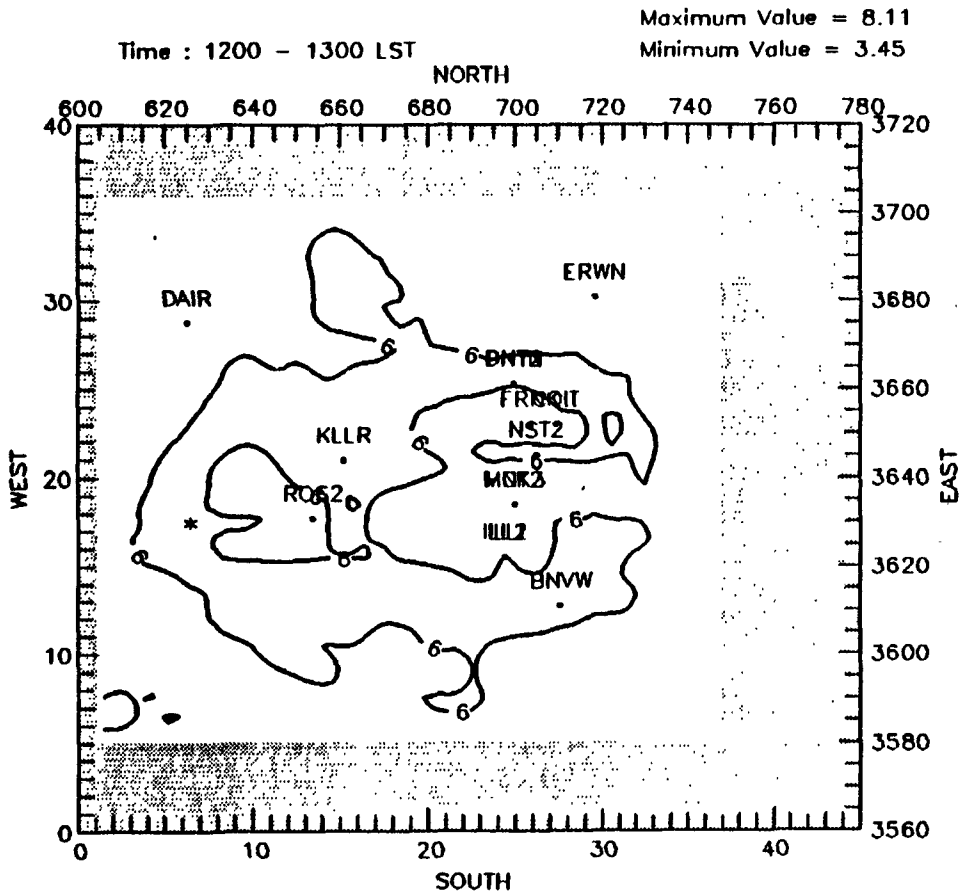

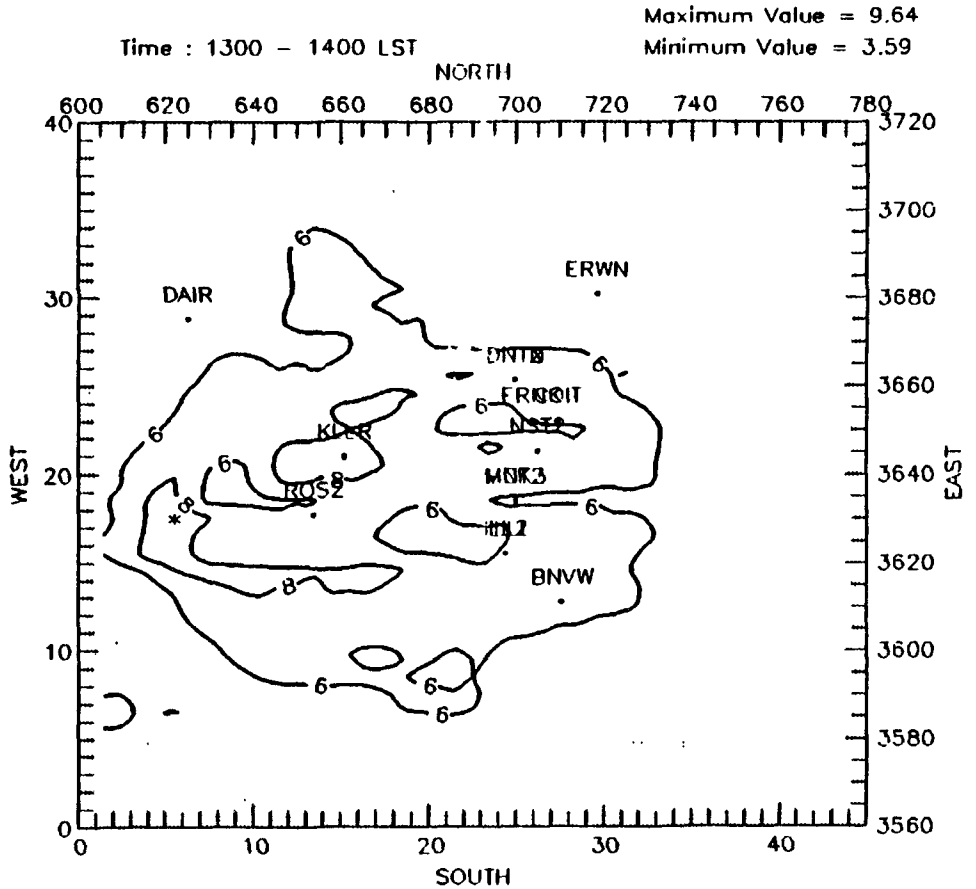

Ozone (pphm), 85 base emissions, August 30, 1985

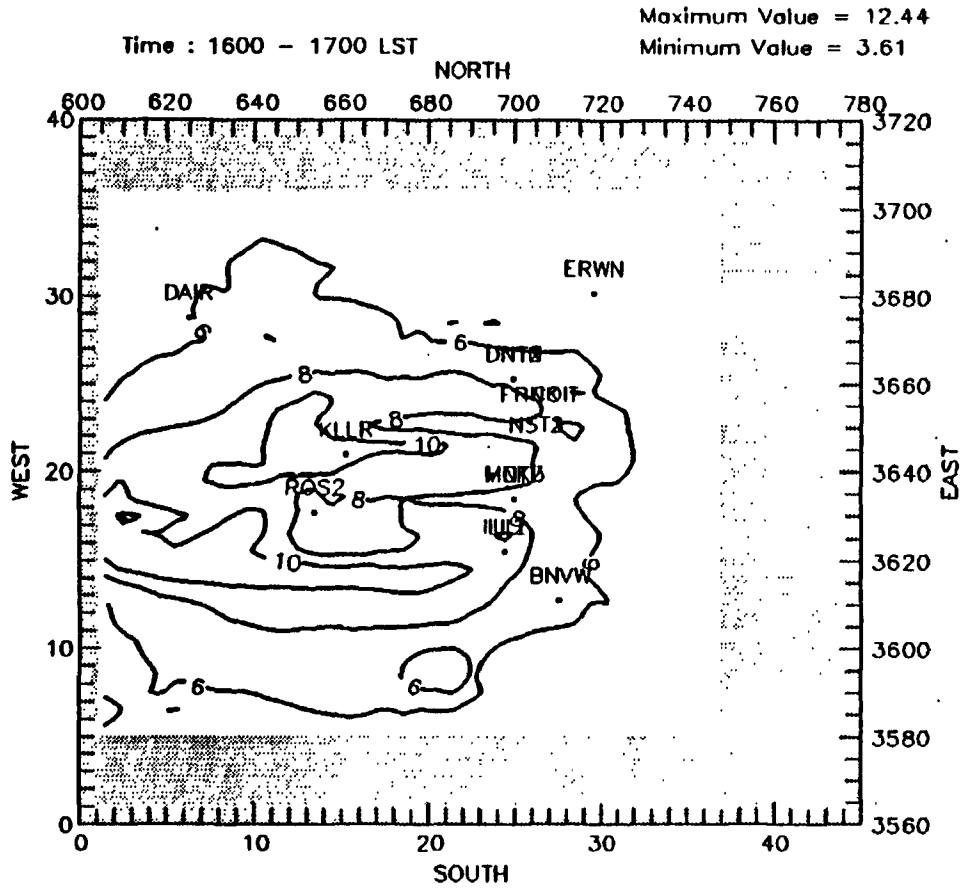

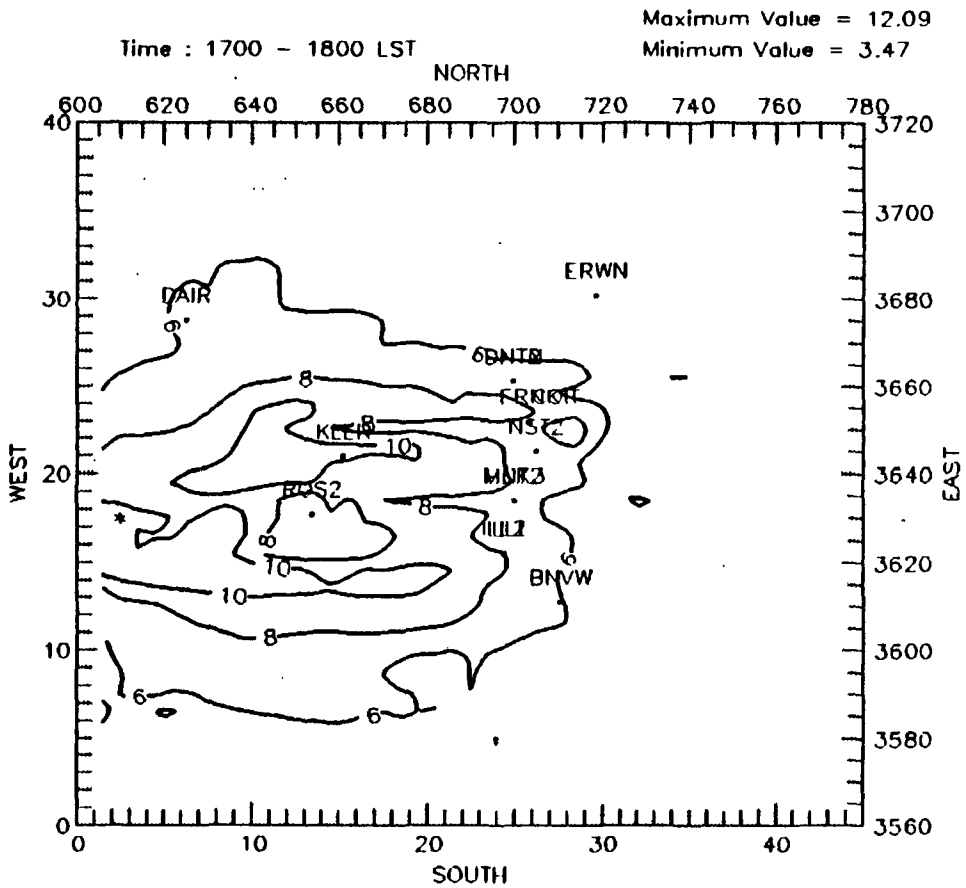

Ozone (pphm), 85 base emissions, August 30, 1985

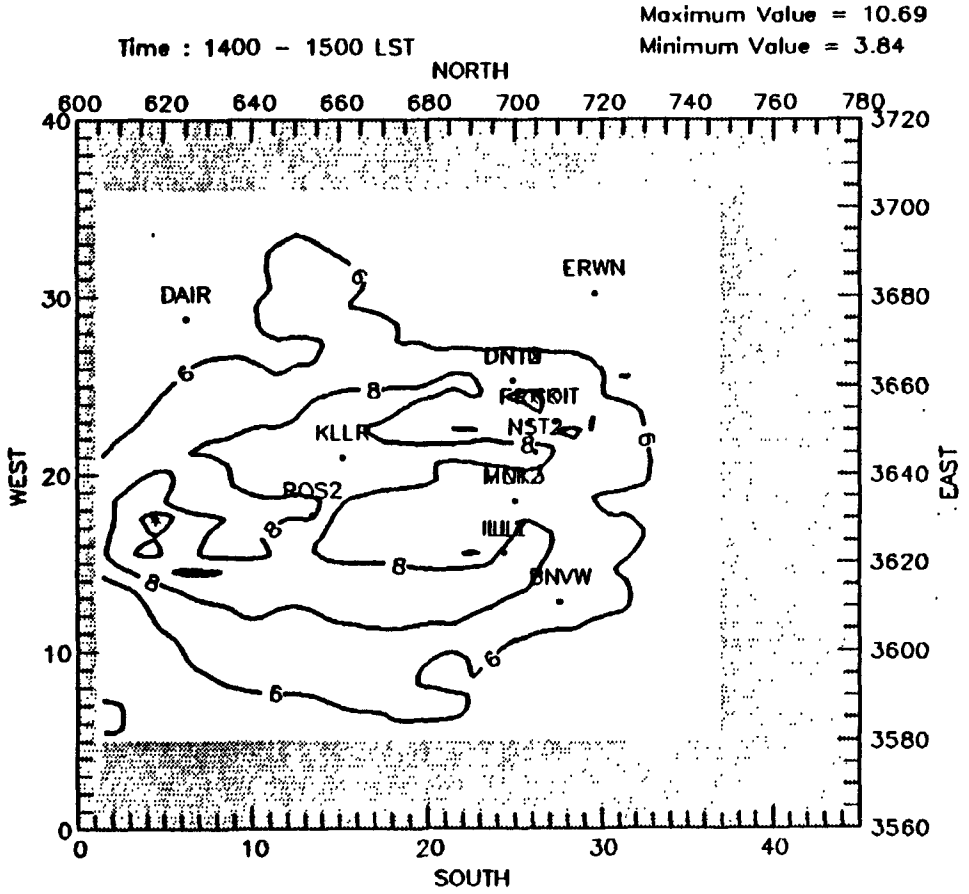

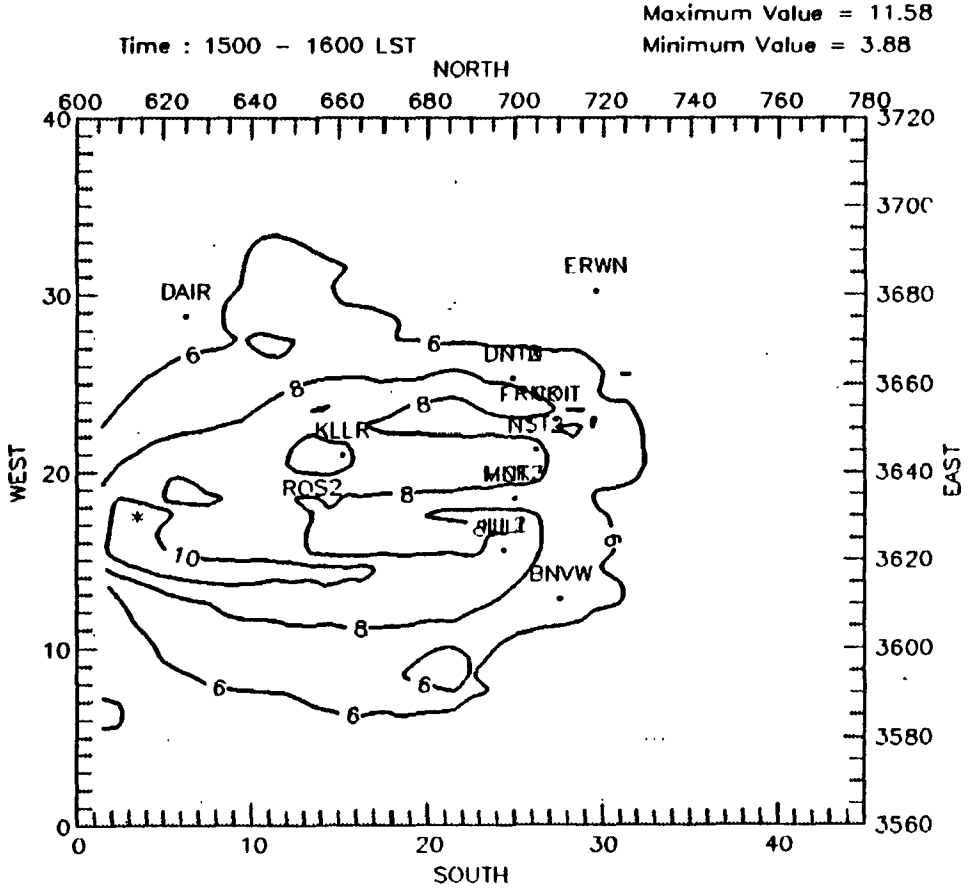

Ozone (pphm), 85 base emissions, August 30, 1985

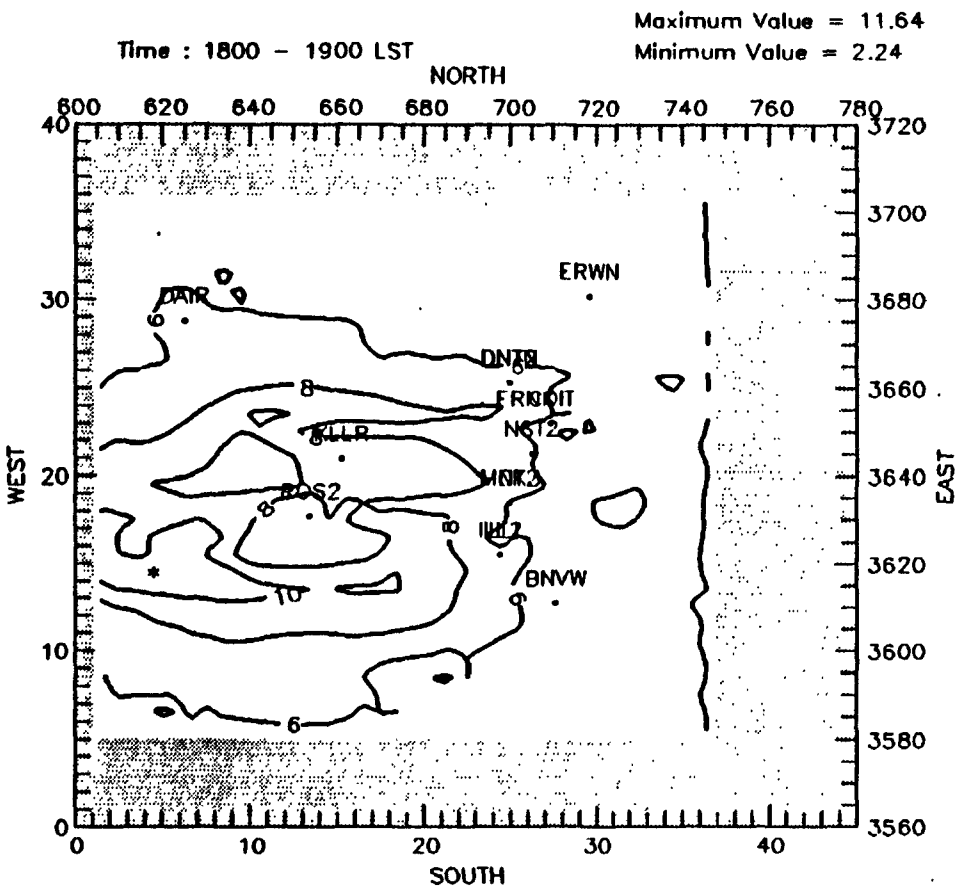

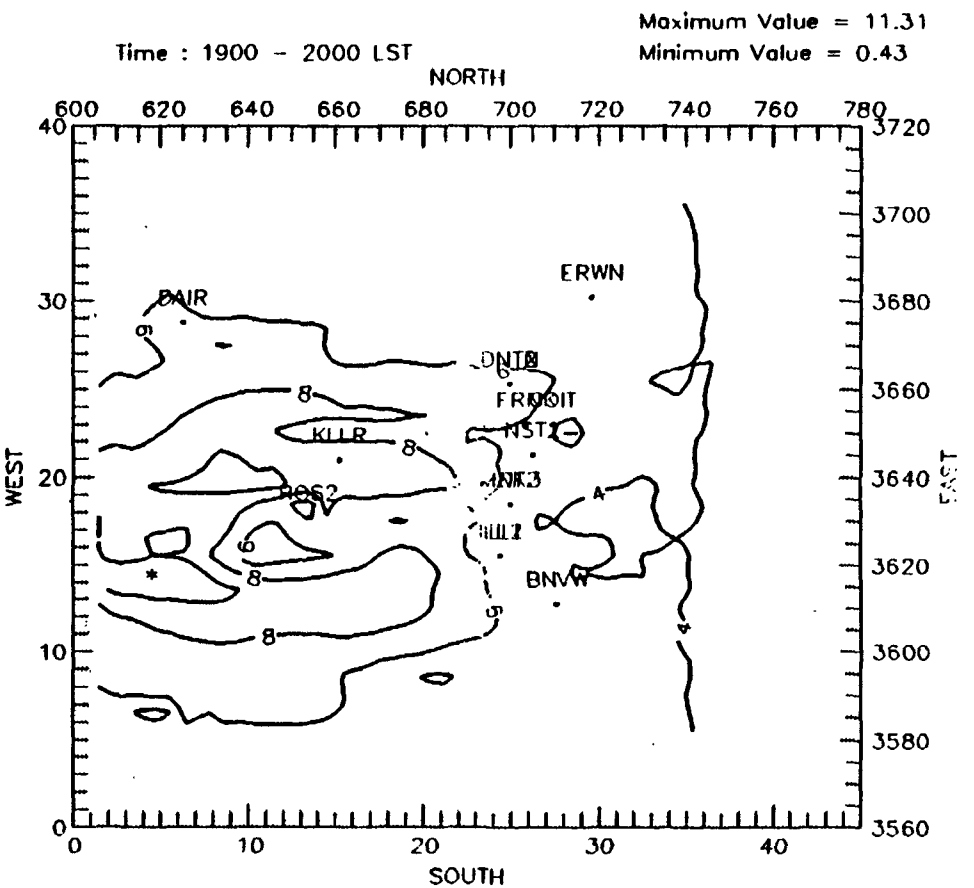

Ozone (pphm), 85 base emissions, August 30, 1985

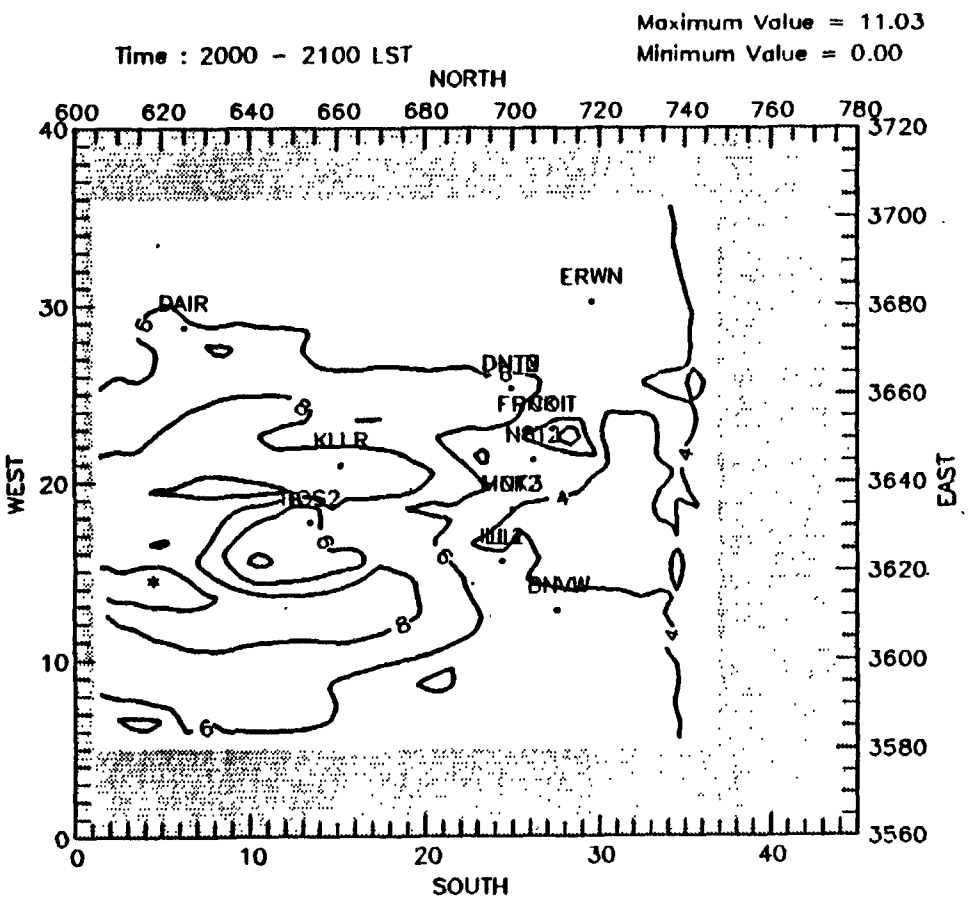

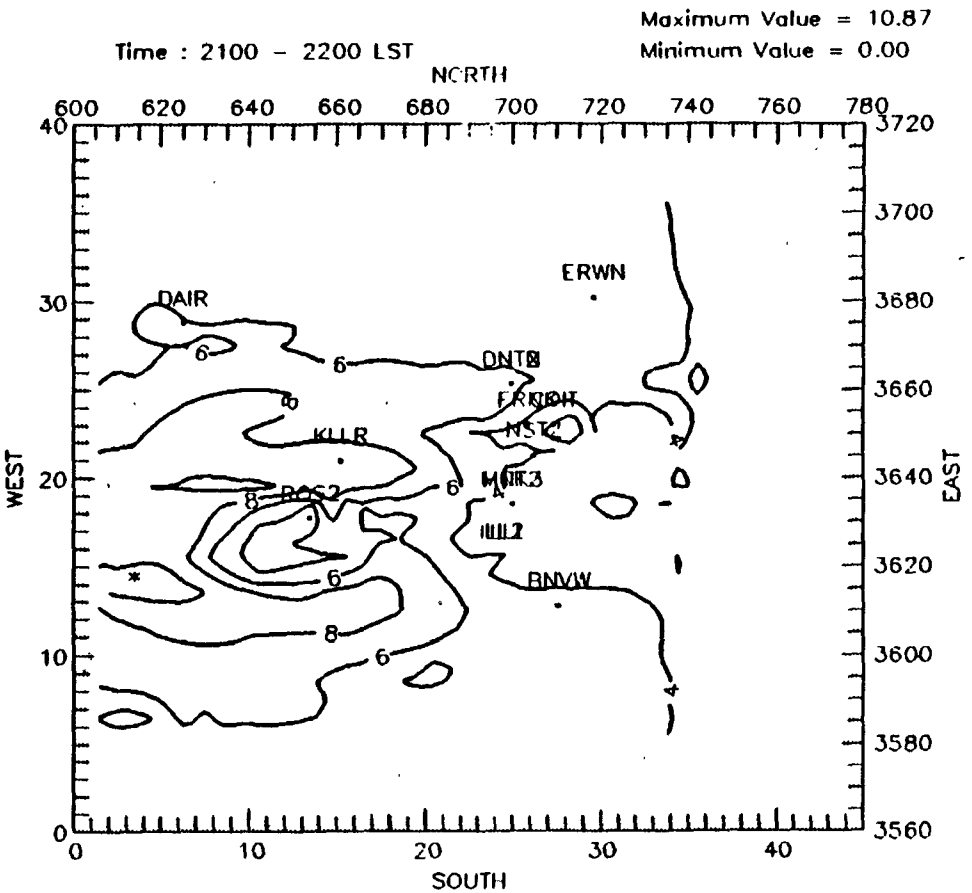

Ozone (pphm), 85 base emissions, August 30, 1985

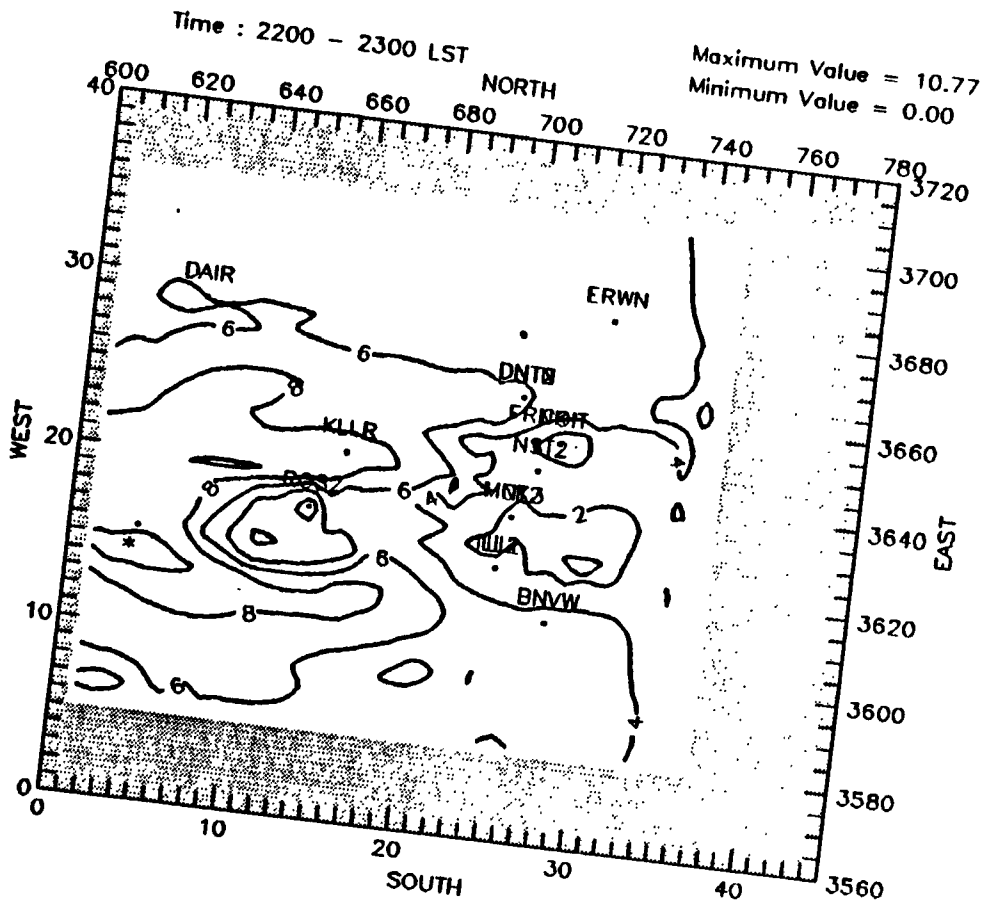

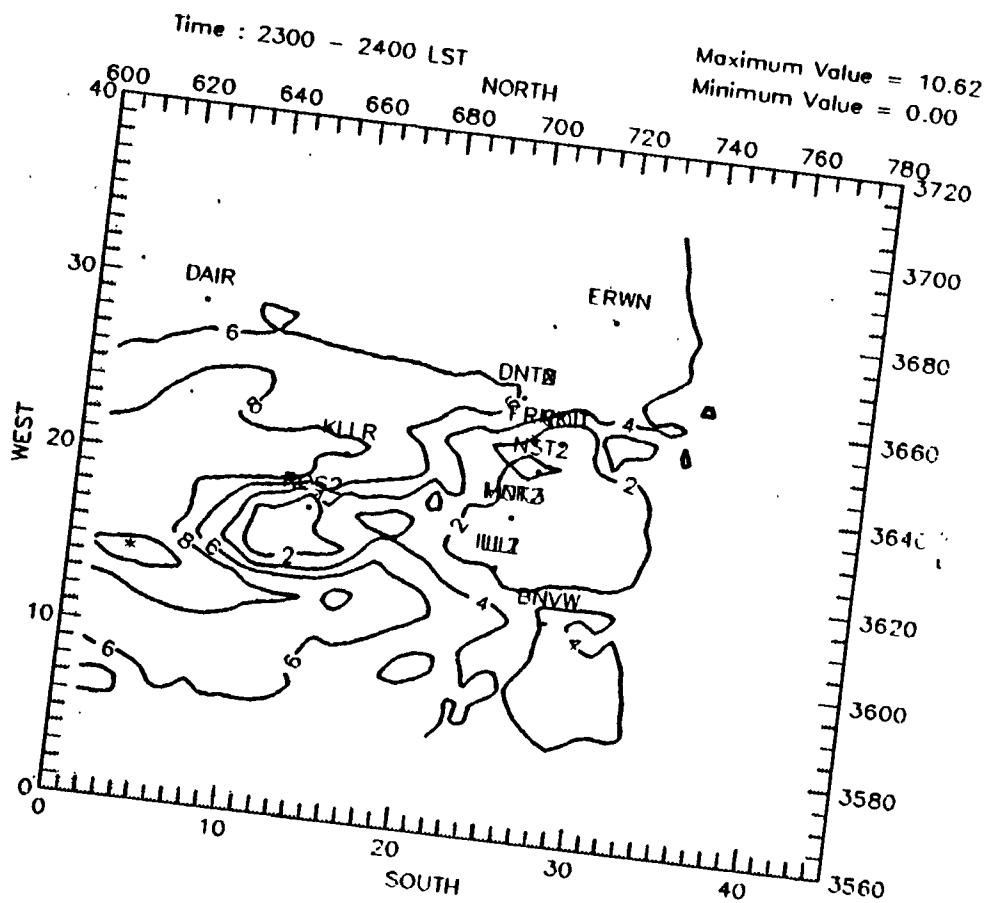

Ozone (pphm), 85 base emissions, August 30, 1985

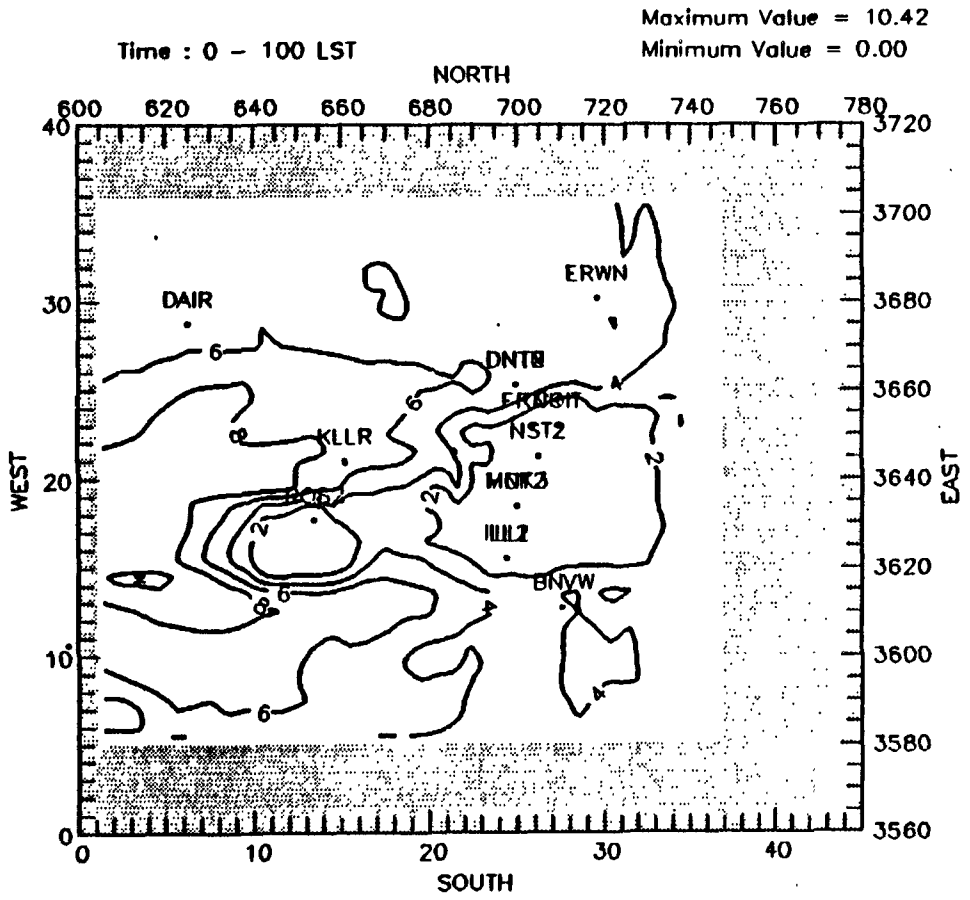

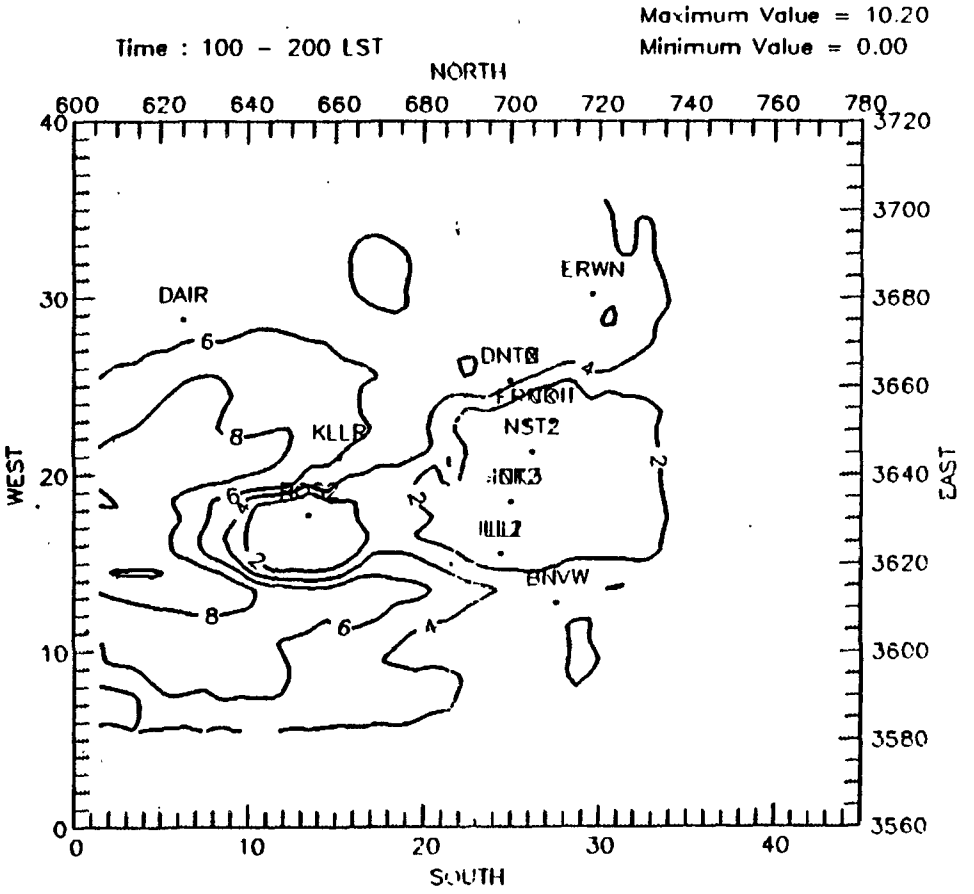

Ozone (pphm), 85 base emissions, August 31, 1985

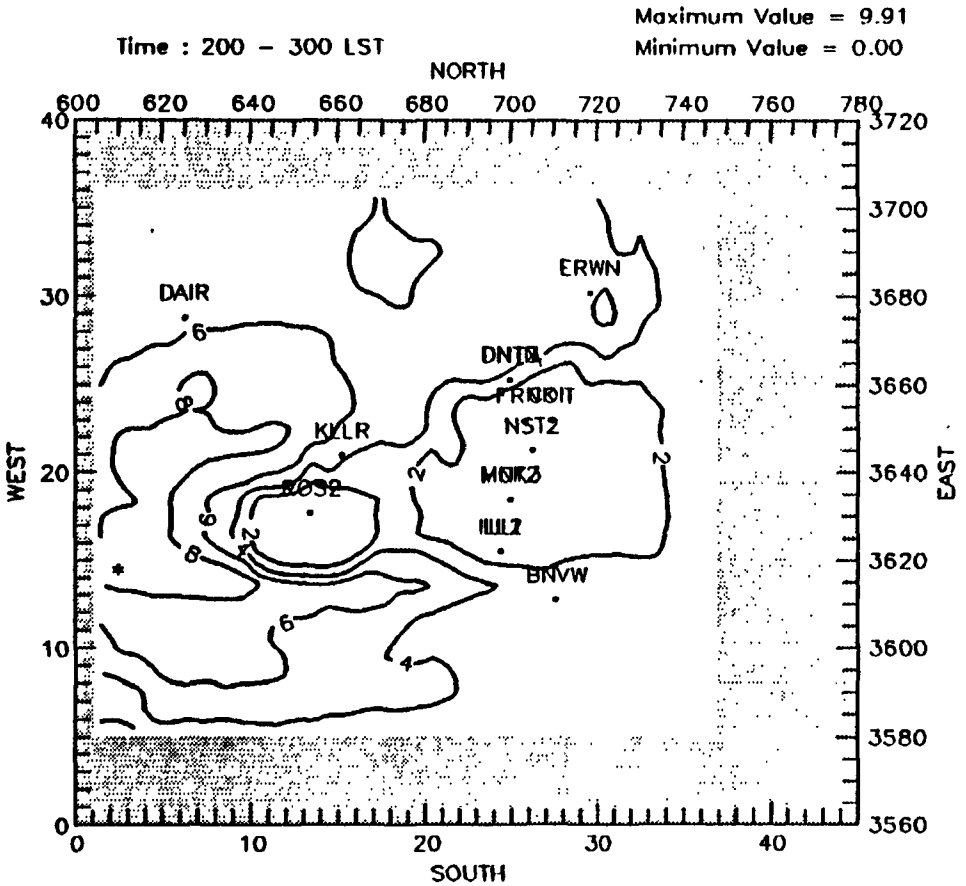

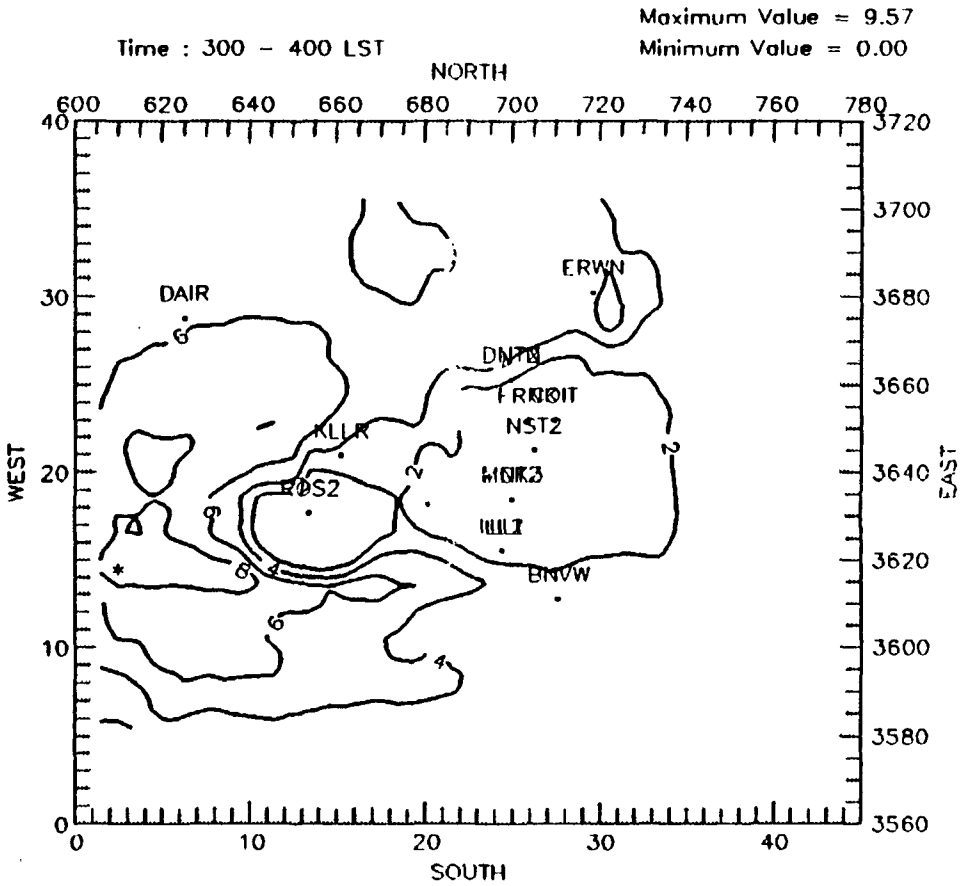

Ozone (pphm), 85 base emissions, August 31, 1985

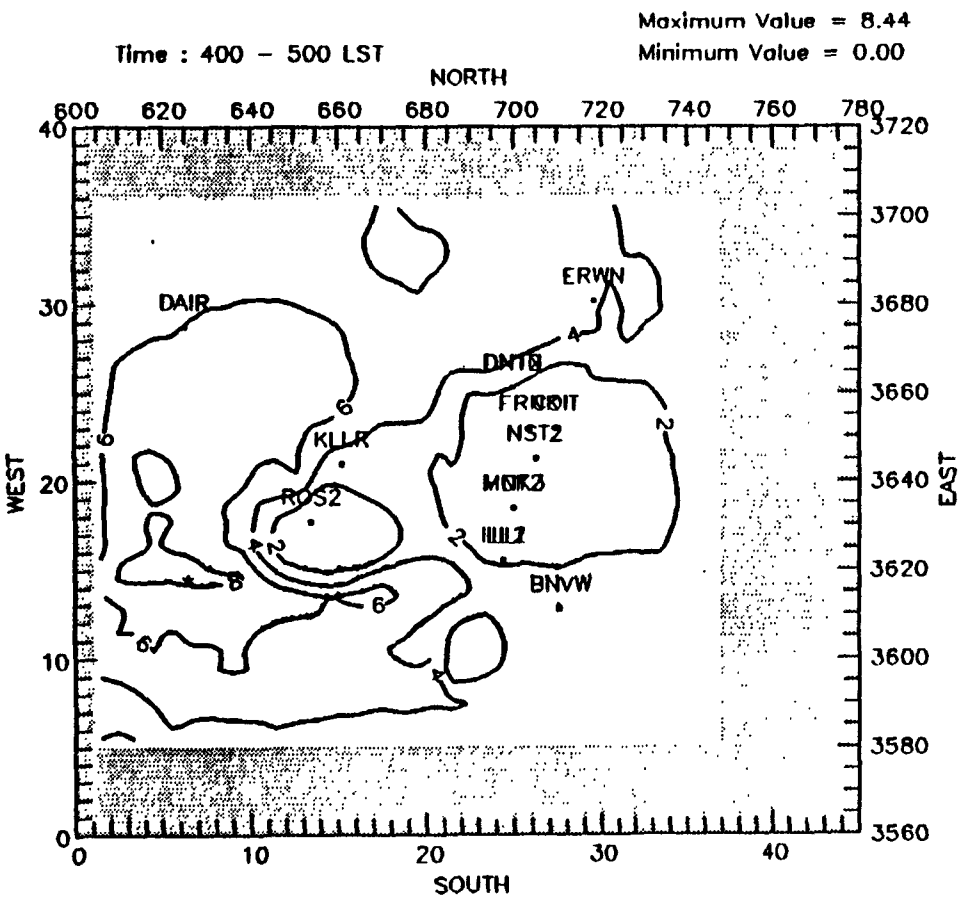

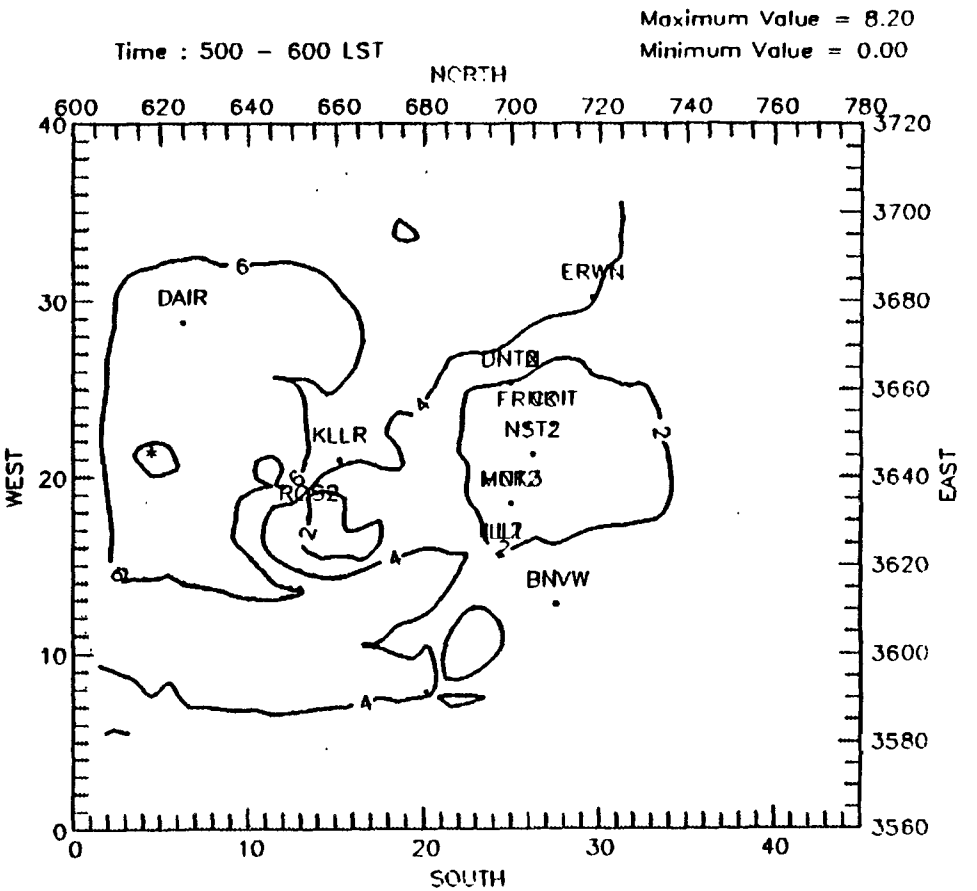

Ozone (pphm), 85 base emissions, August 31, 1985

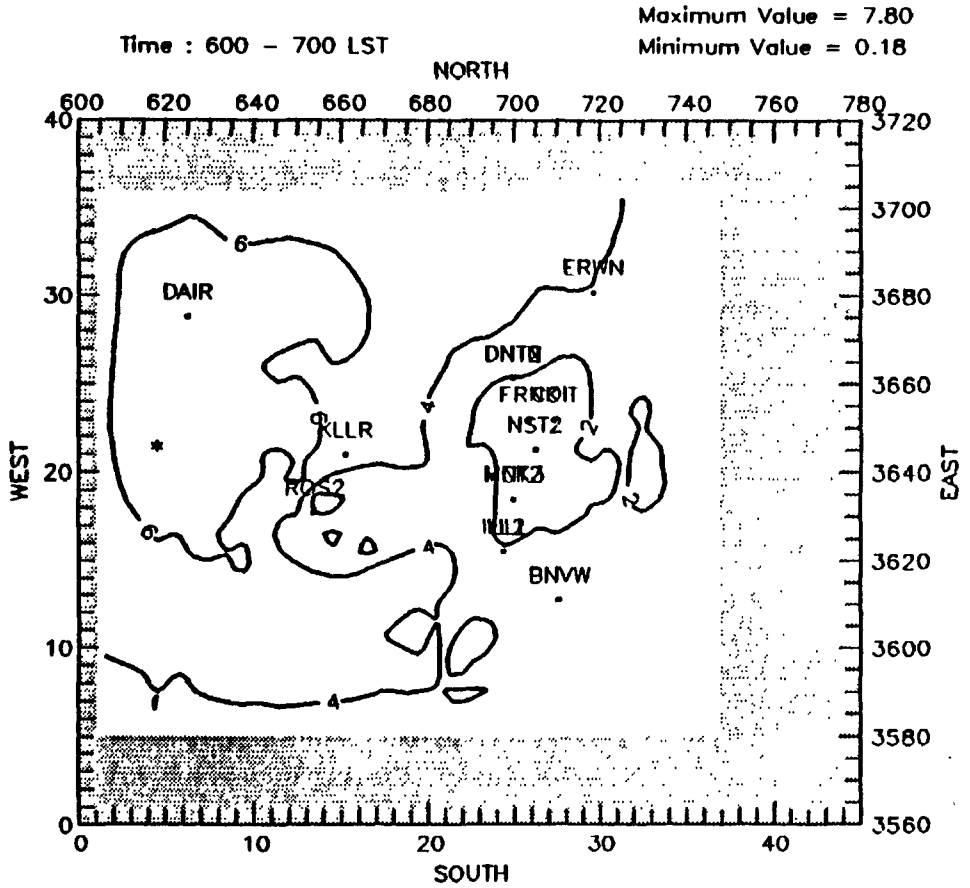

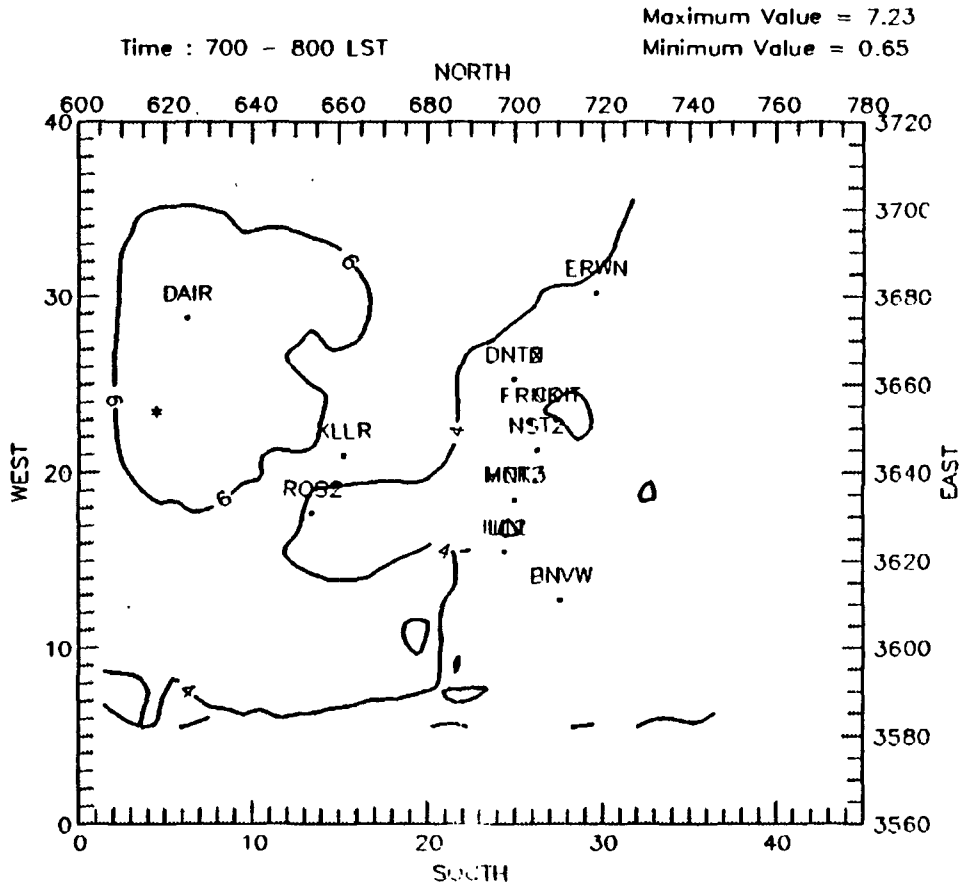

Ozone (pphm), 85 base emissions, August 31, 1985

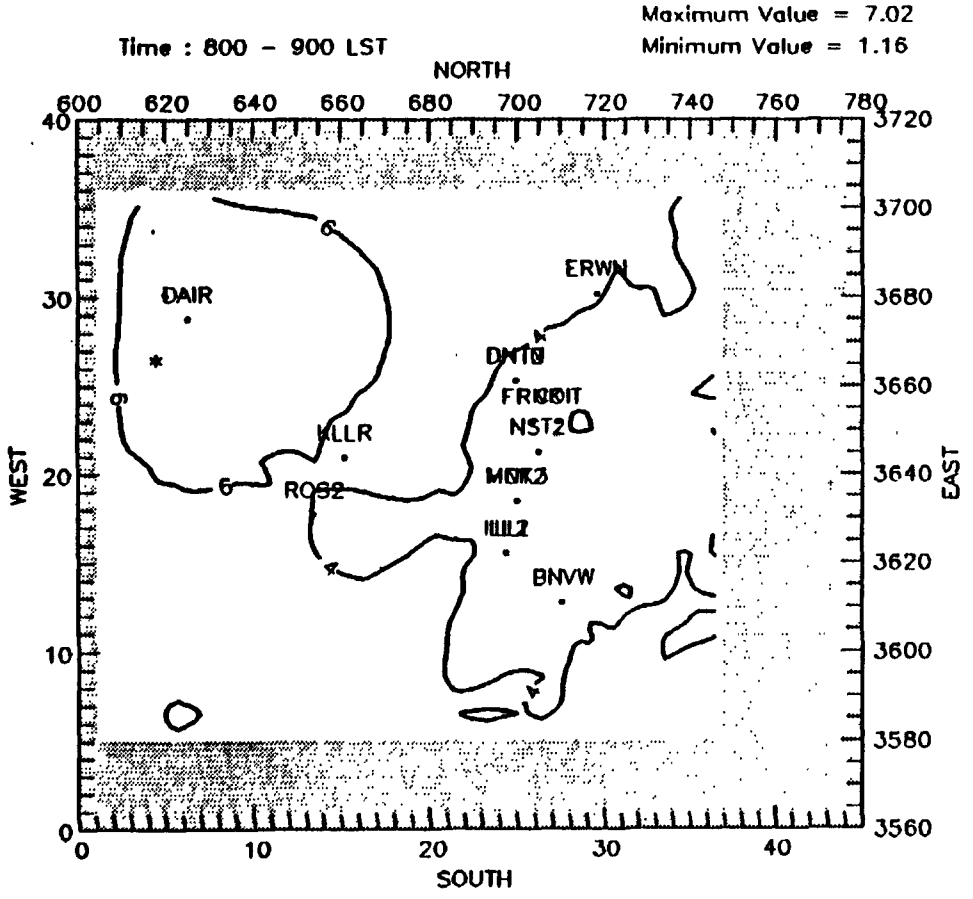

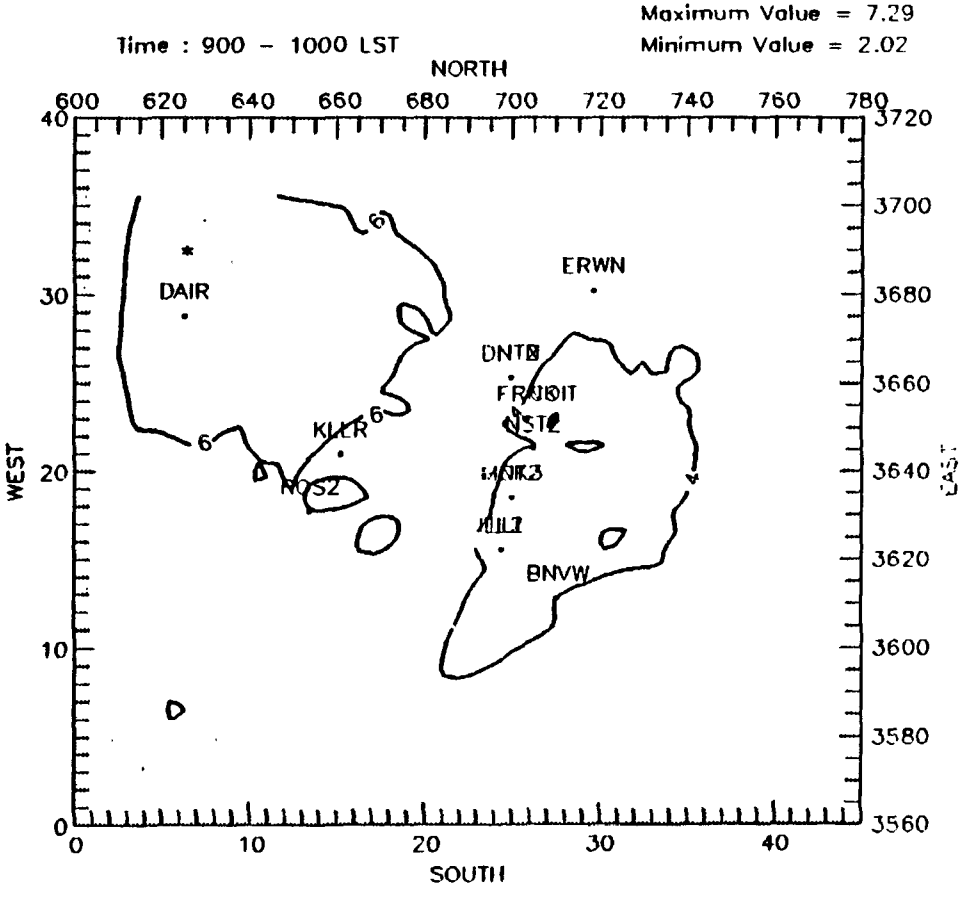

Ozone (pphm), 85 base emissions, August 31, 1985

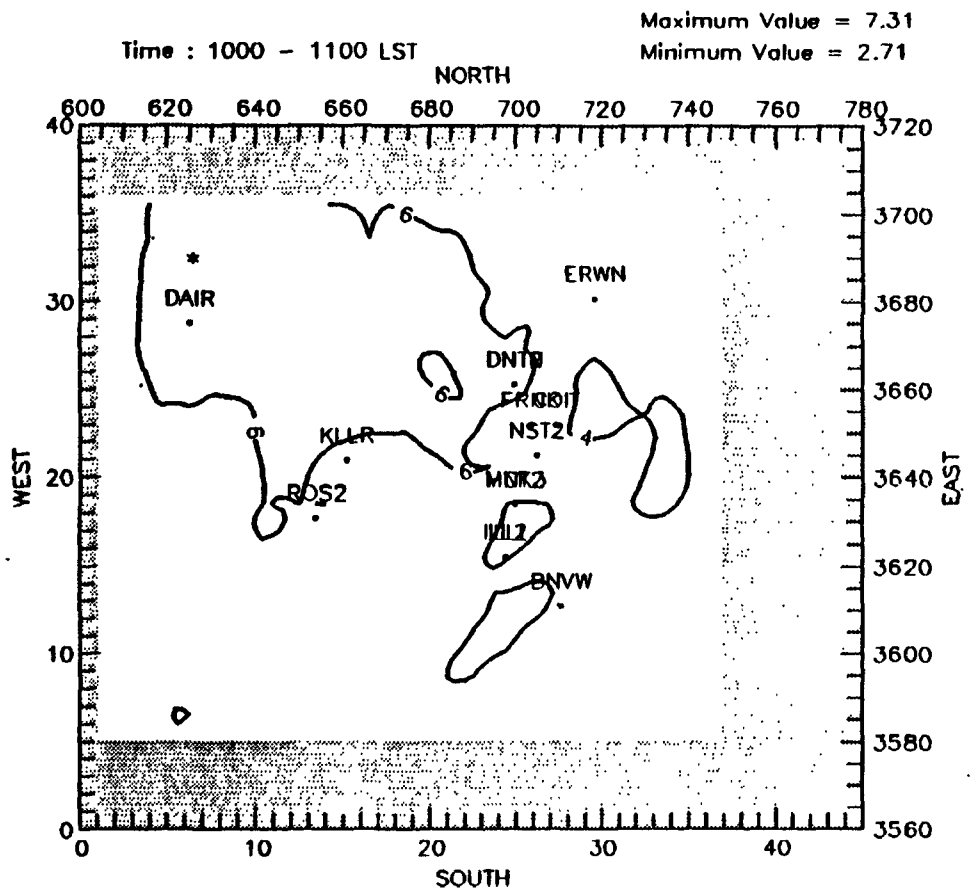

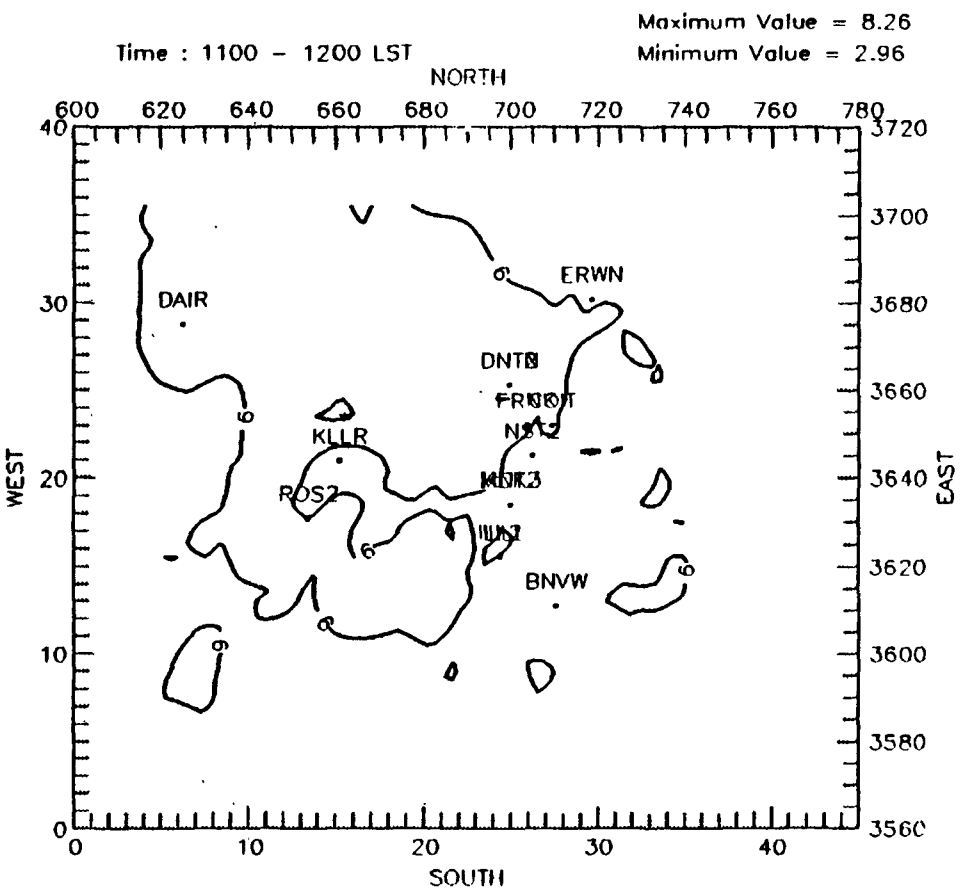

Ozone (pphm), 85 base emissions, August 31, 1985

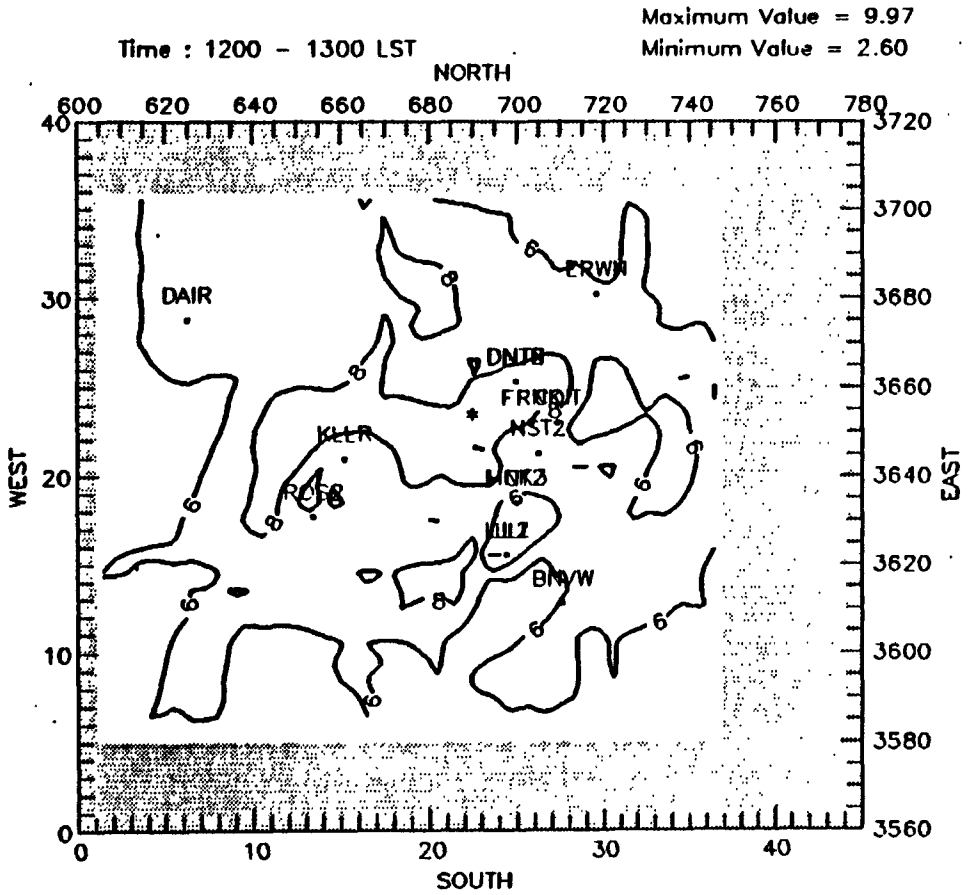

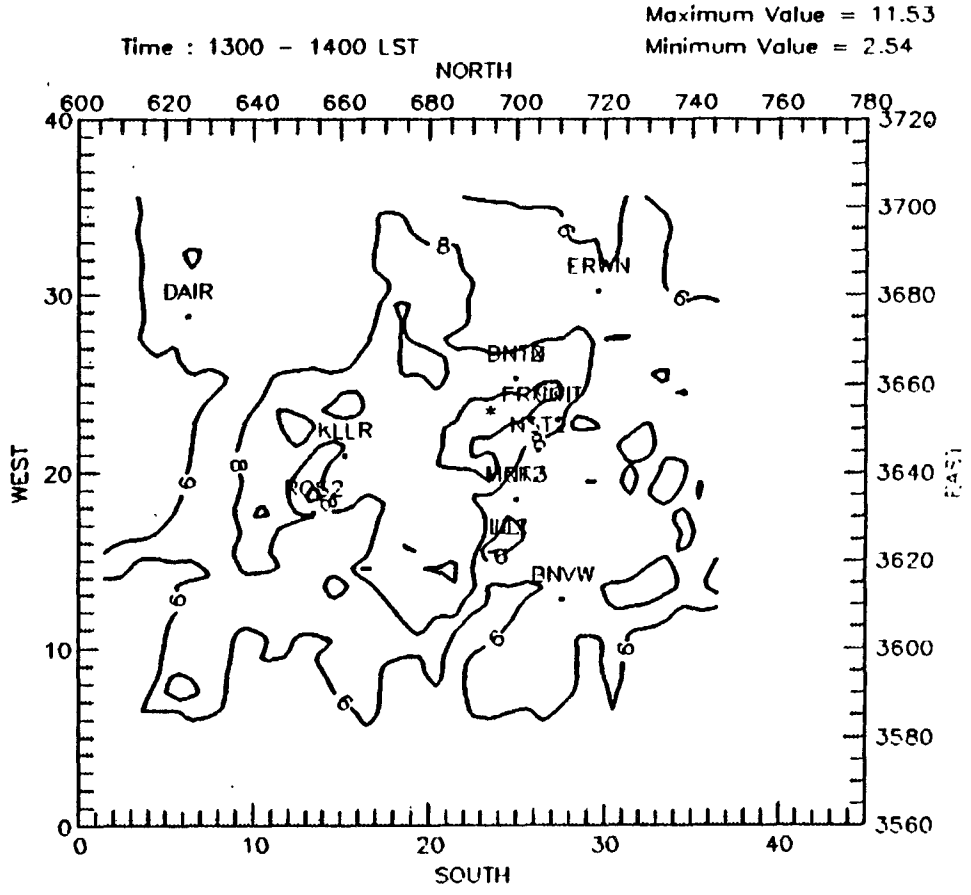

Ozone (pphm), 85 base emissions, August 31, 1985

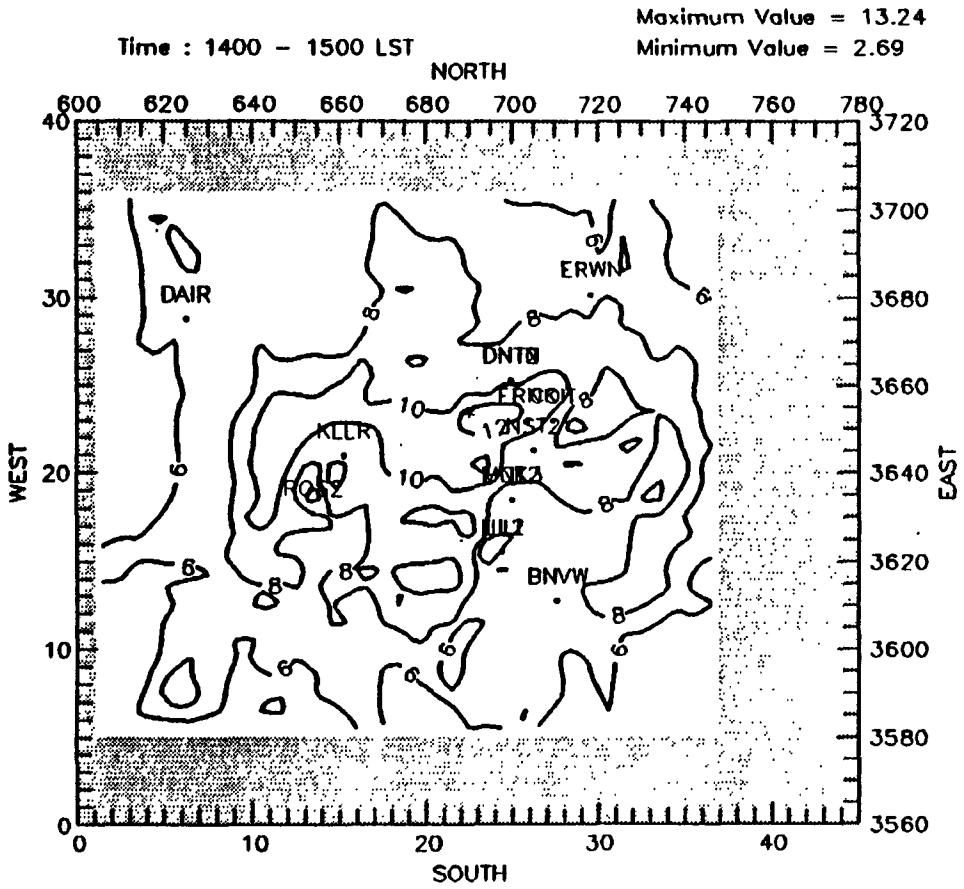

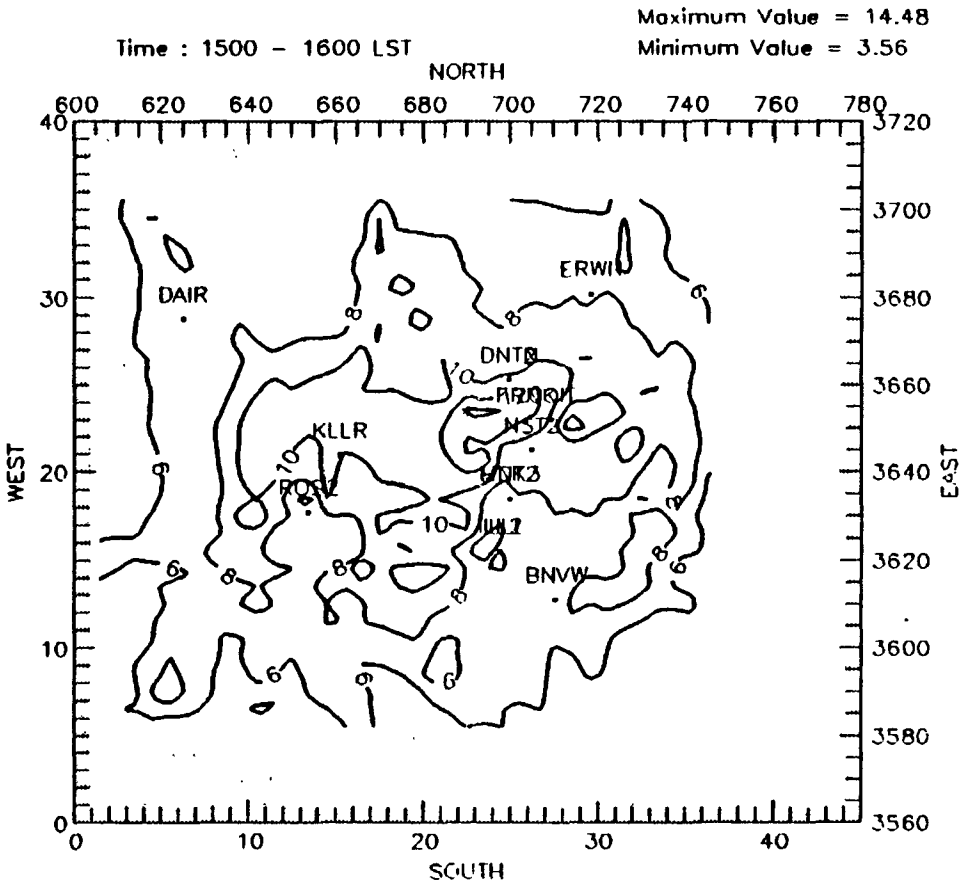

Ozone (pphm), 85 base emissions, August 31, 1985

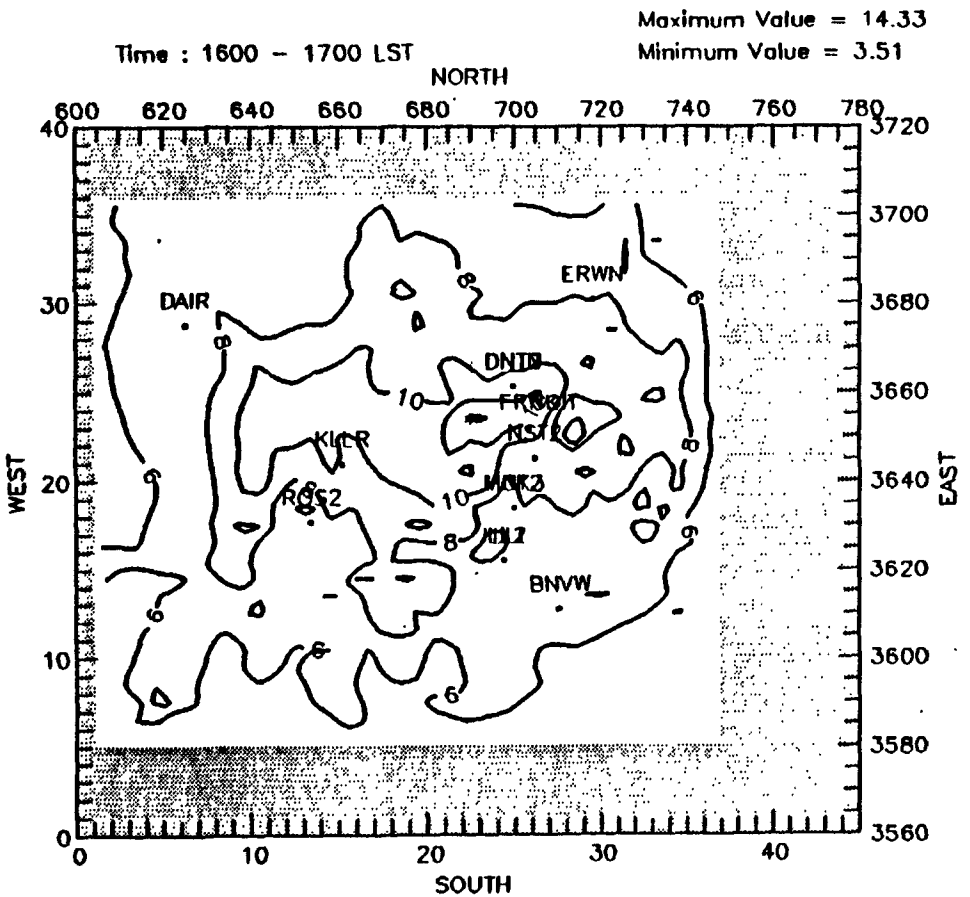

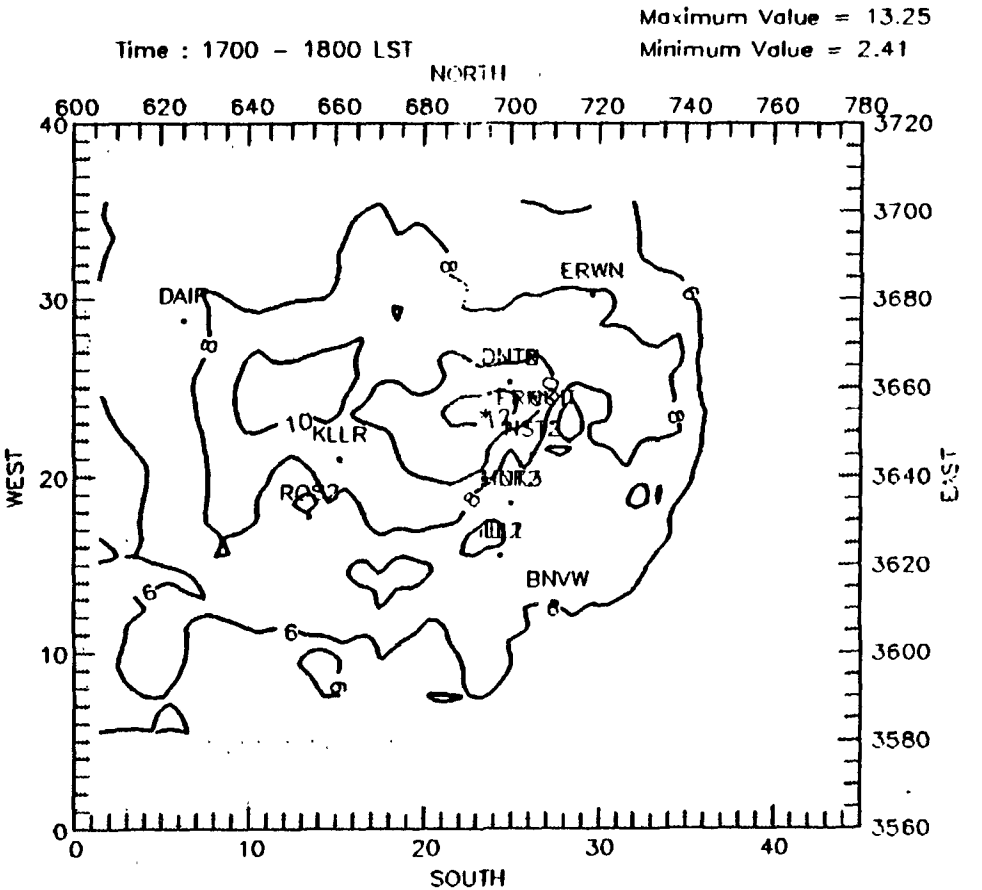

Ozone (pphm), 85 base emissions, August 31, 1985

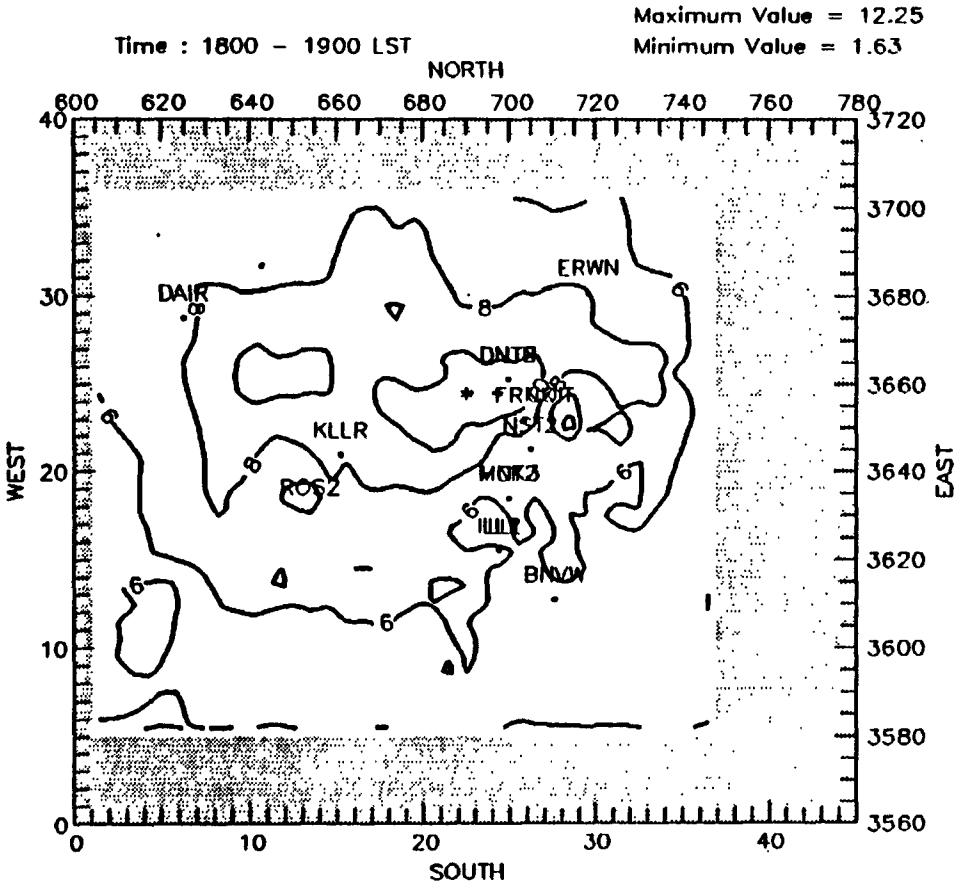

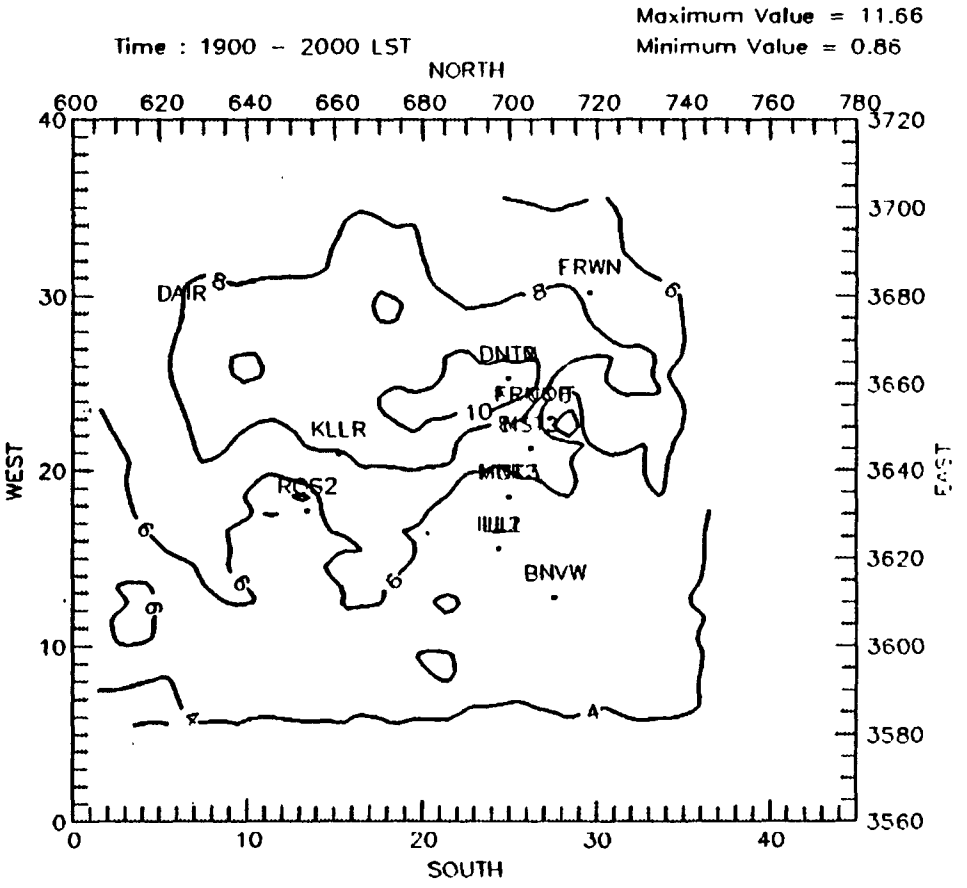

Ozone (pphm), 85 base emissions, August 31, 1985

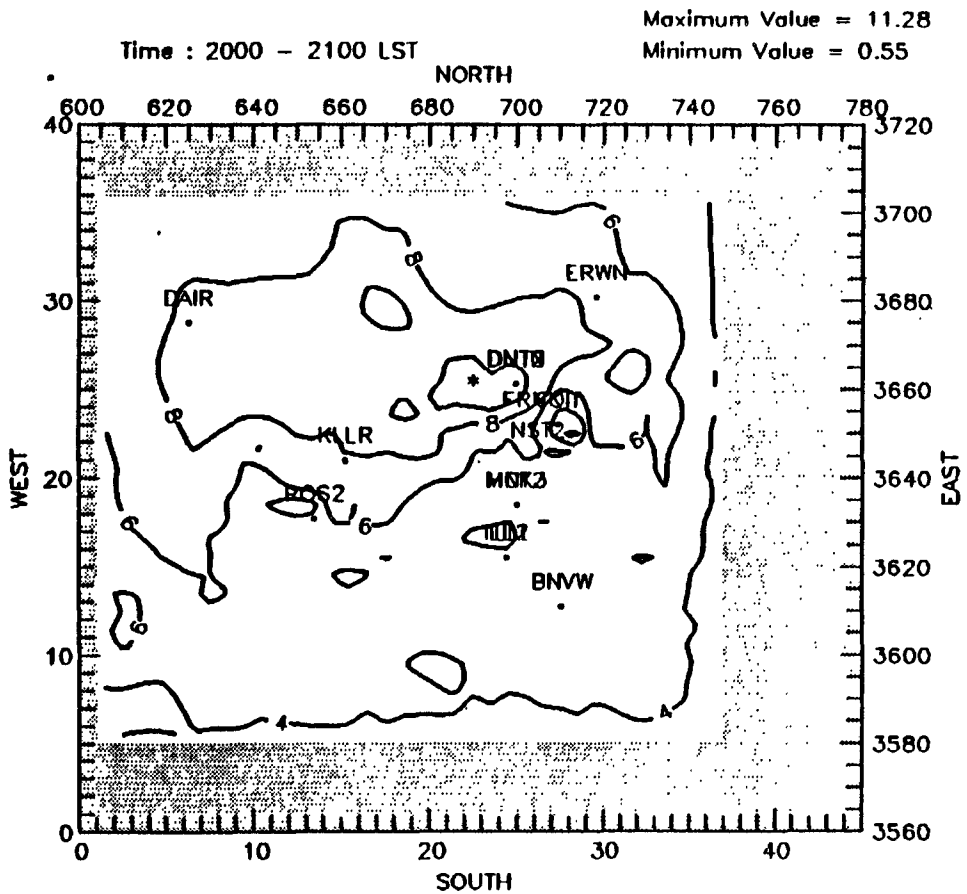

Ozone (pphm), 85 base emissions, August 31, 1985

Appendix H

PREDICTED HOURLY OZONE CONCENTRATIONS (pphm) FOR DALLAS-FORT WORTH DIAGNOSTIC RUN 2

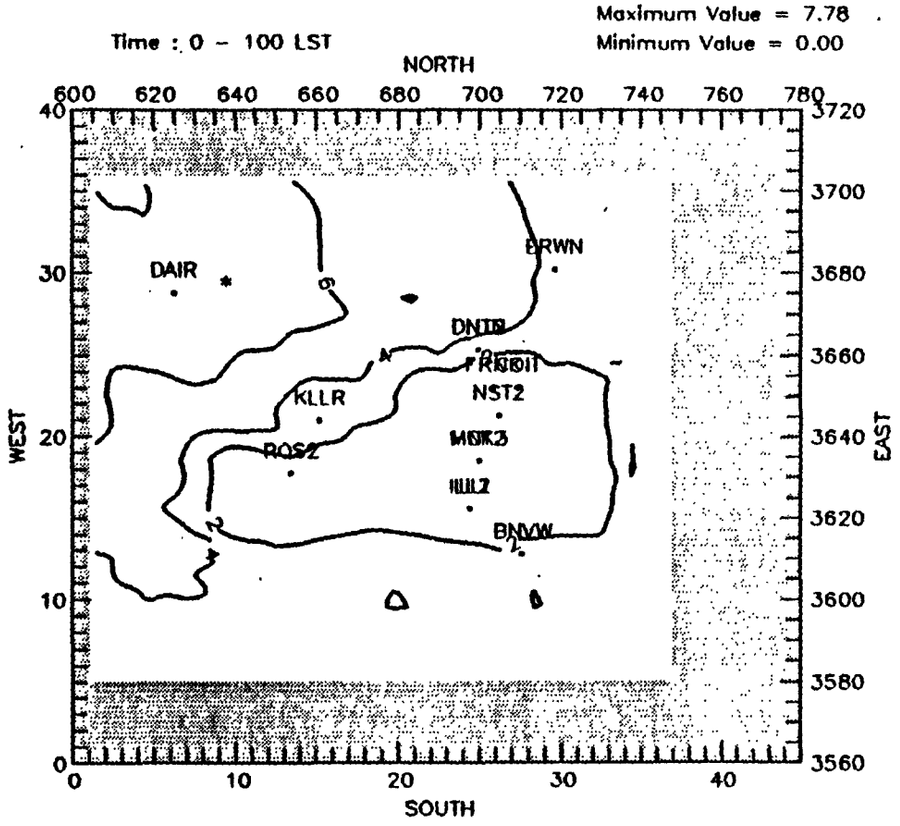

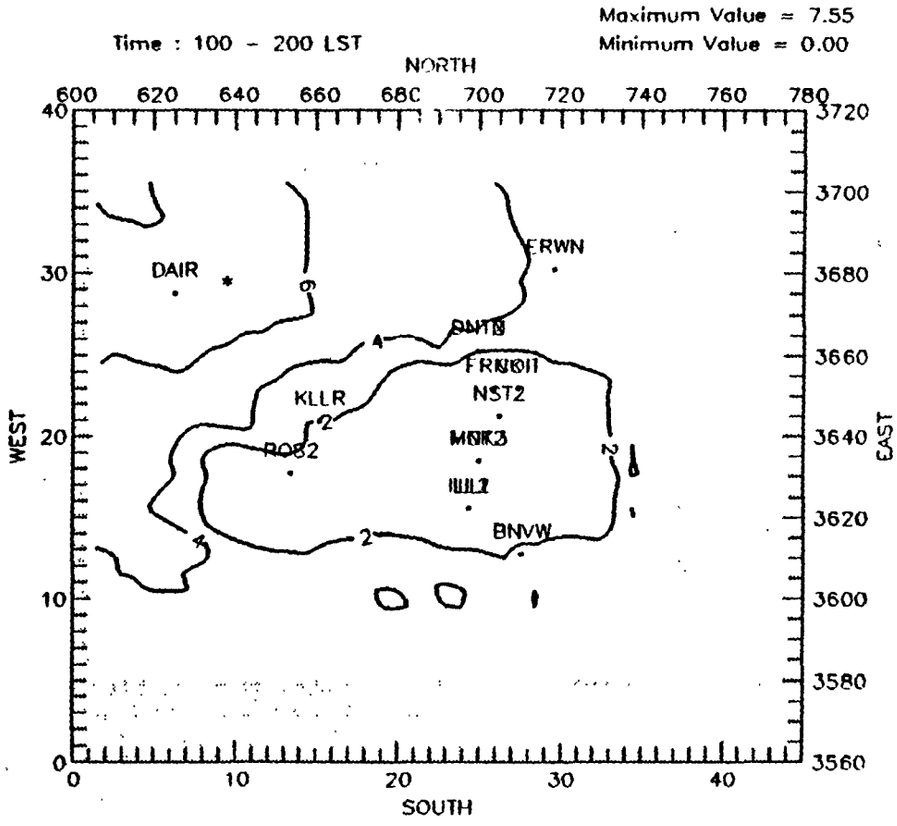

Ozone (pphm), 85 base emissions (Eval. run#2), August 30, 1985

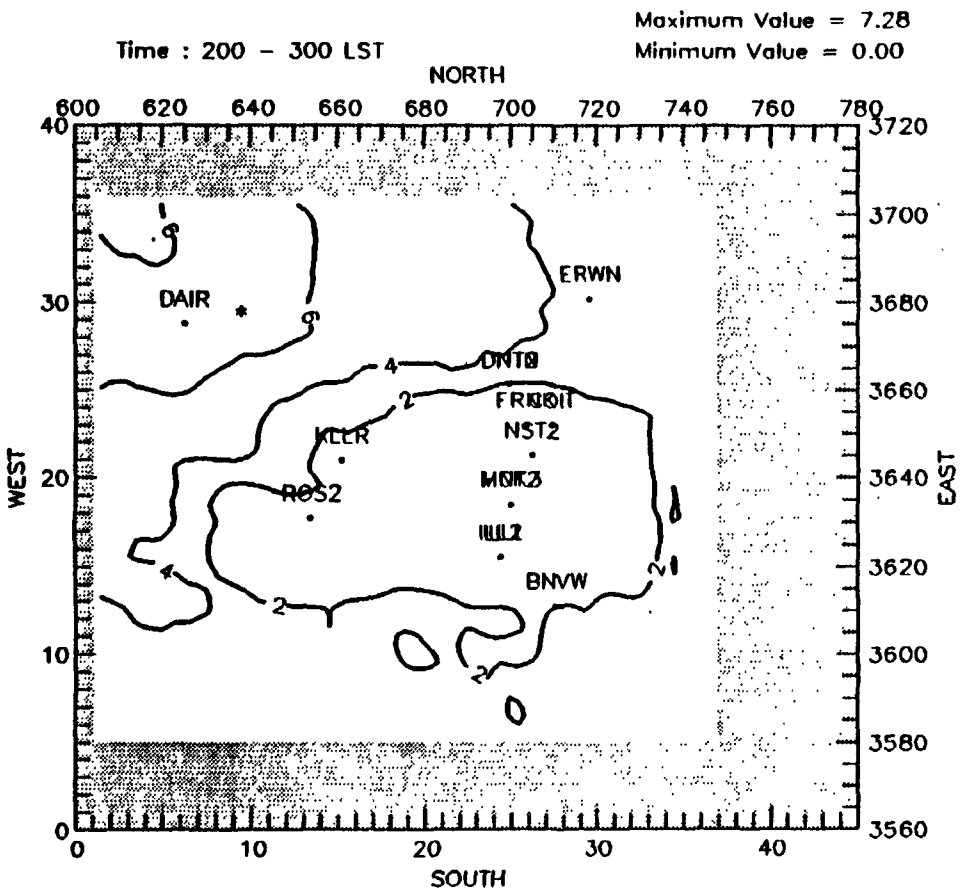

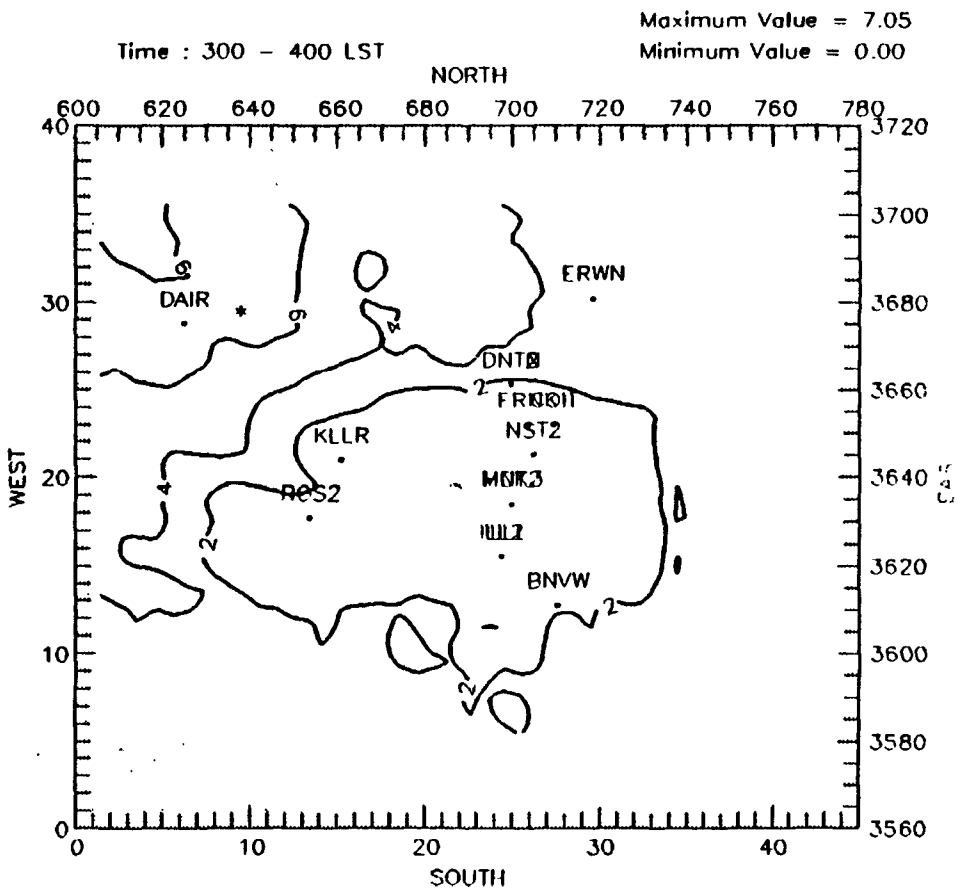

Ozone (pphm), 85 base emissions (Eval. run#2), August 30, 1985

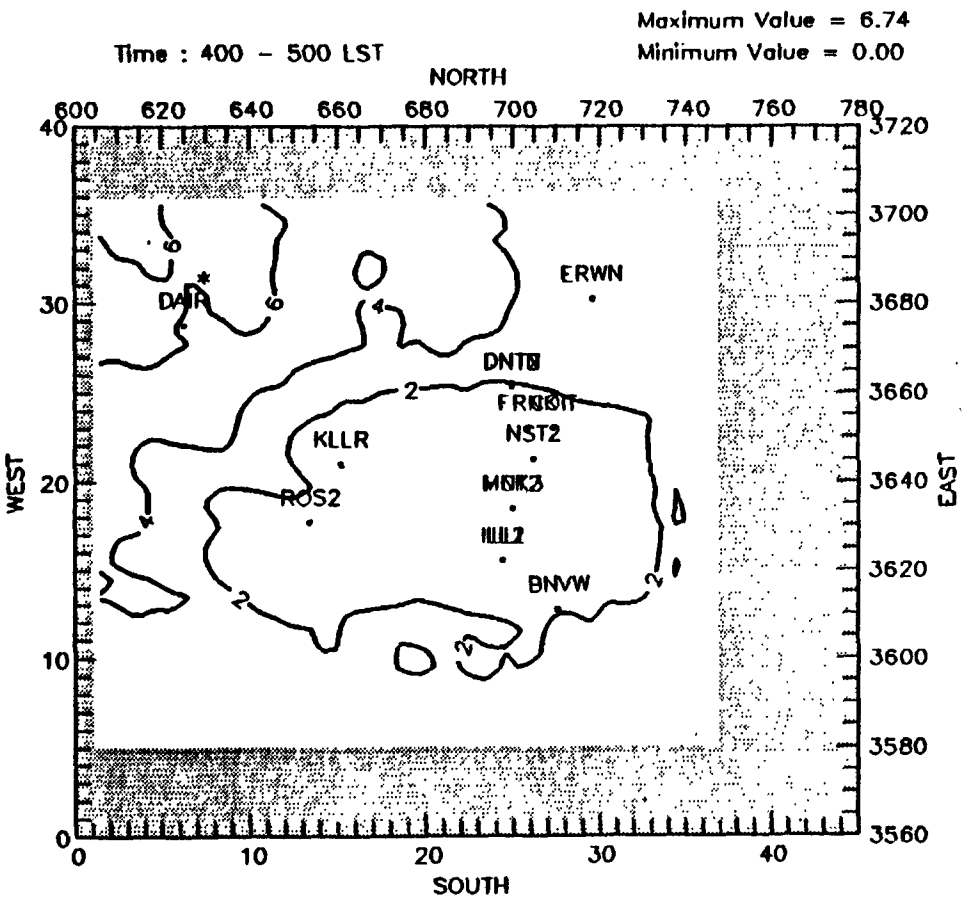

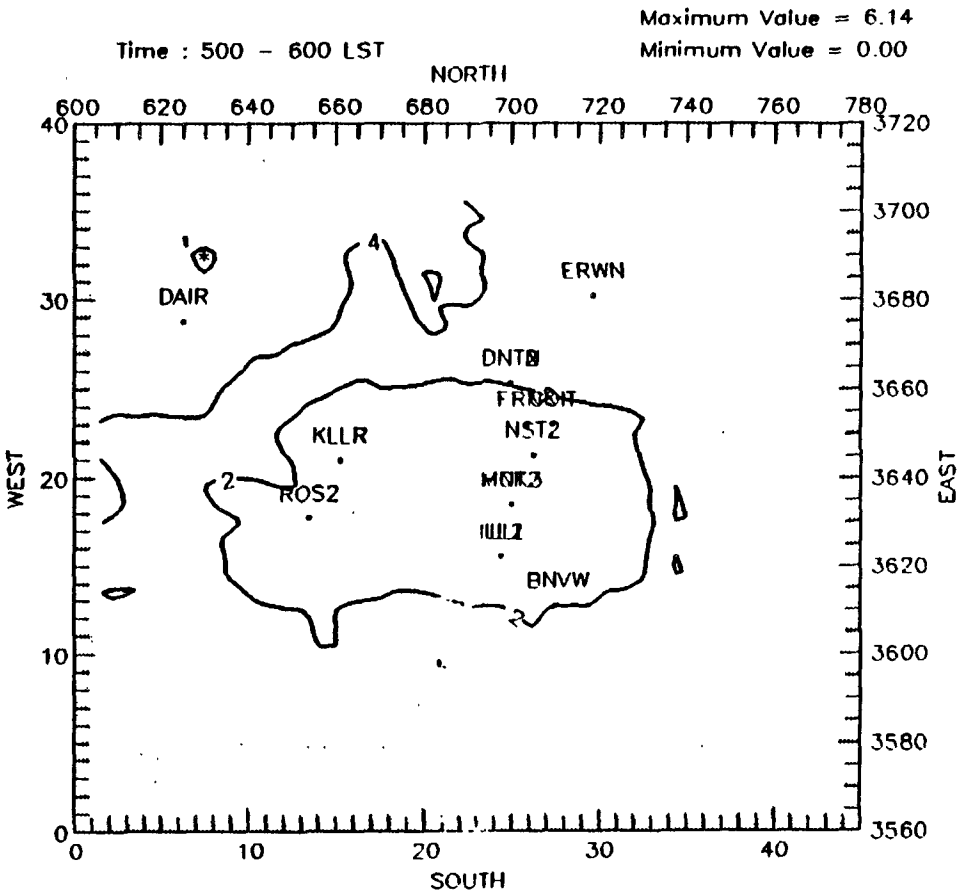

Ozone (pphm), 85 base emissions (Eval. run#2), August 30, 1985

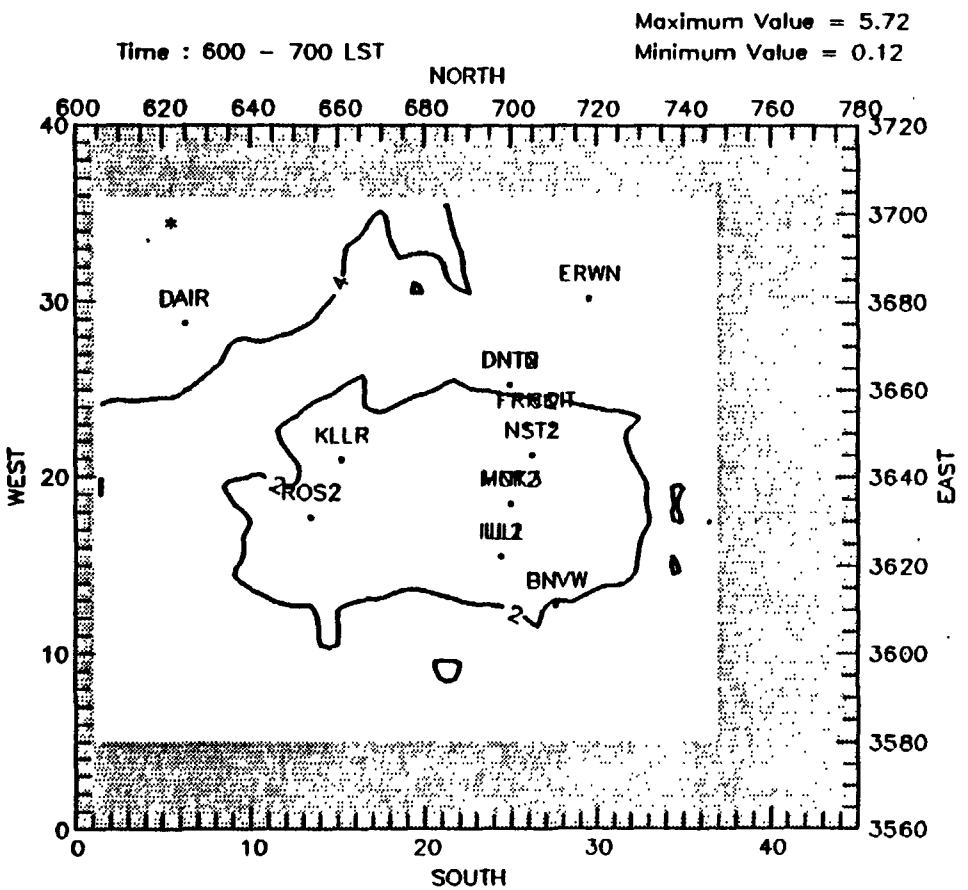

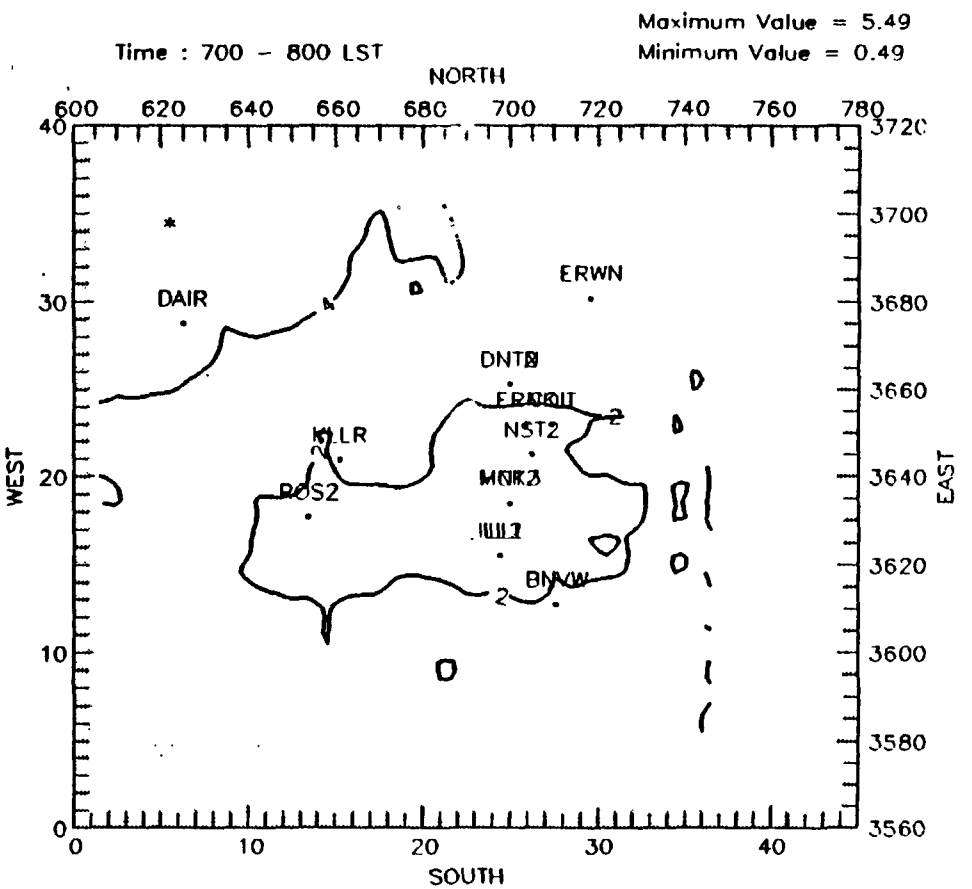

Ozone (pphm), 85 base emissions (Eval. run#2), August 30, 1985

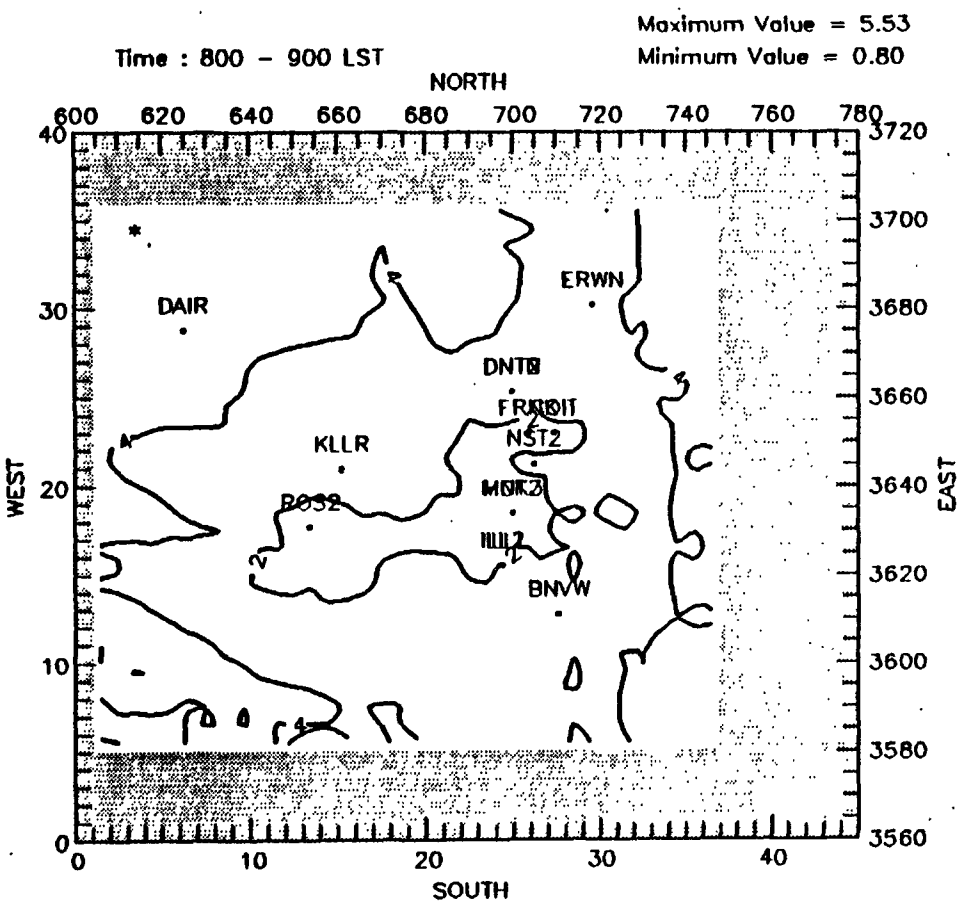

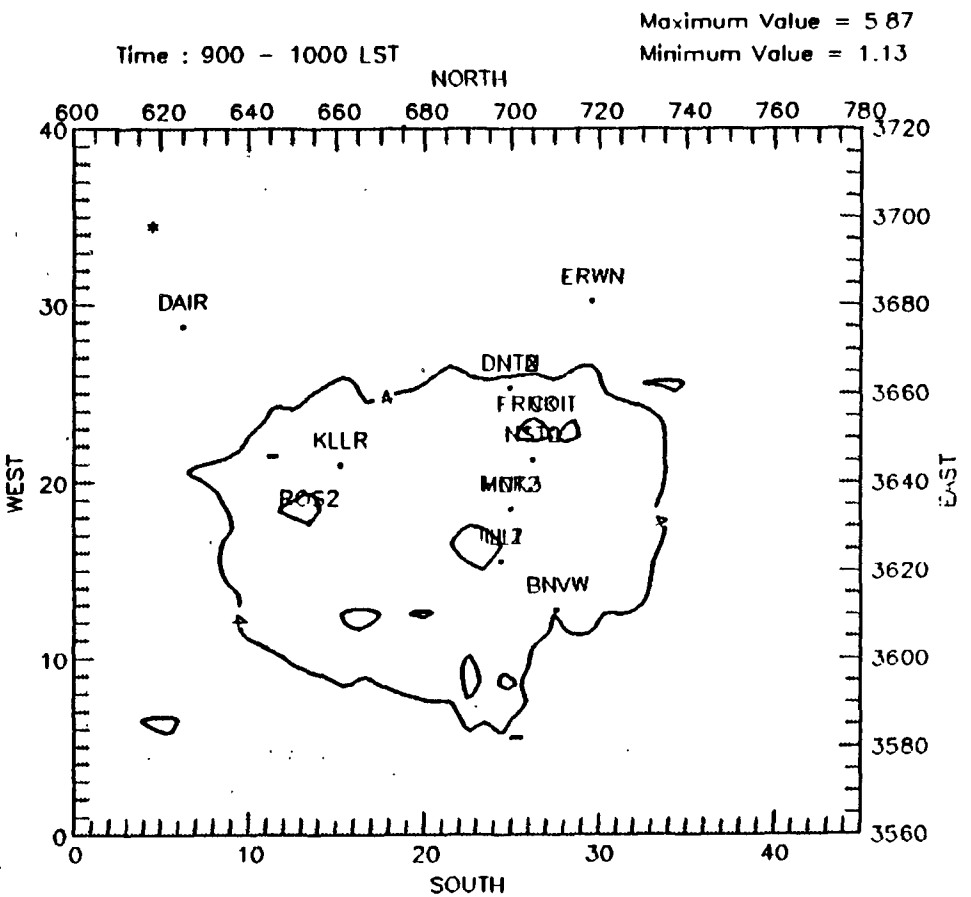

Ozone (pphm), 85 base emissions (Eval. run#2), August 30, 1985

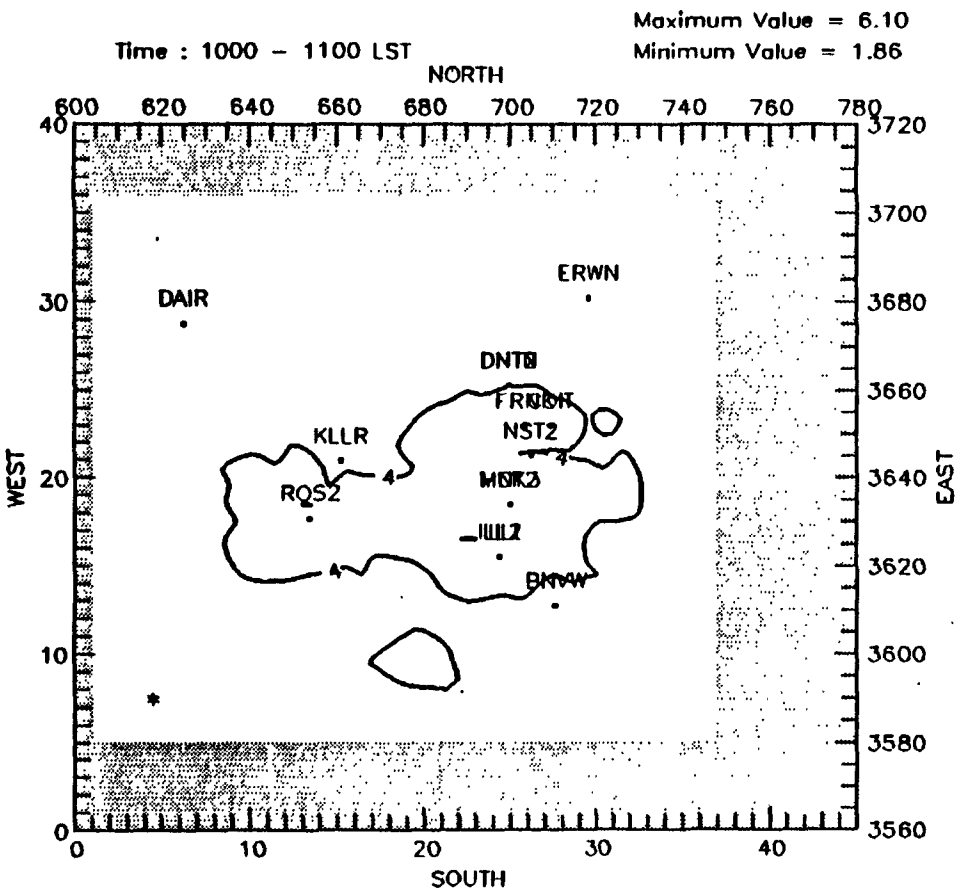

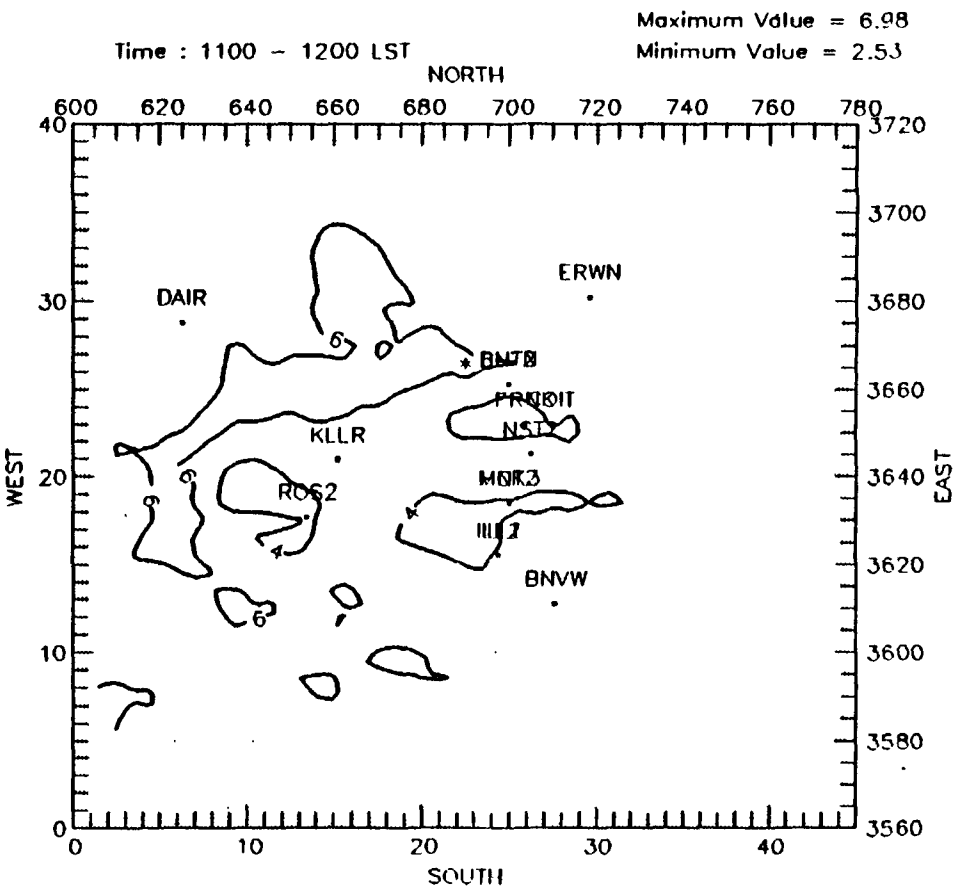

Ozone (pphm), 85 base emissions (Eval. run#2), August 30, 1985

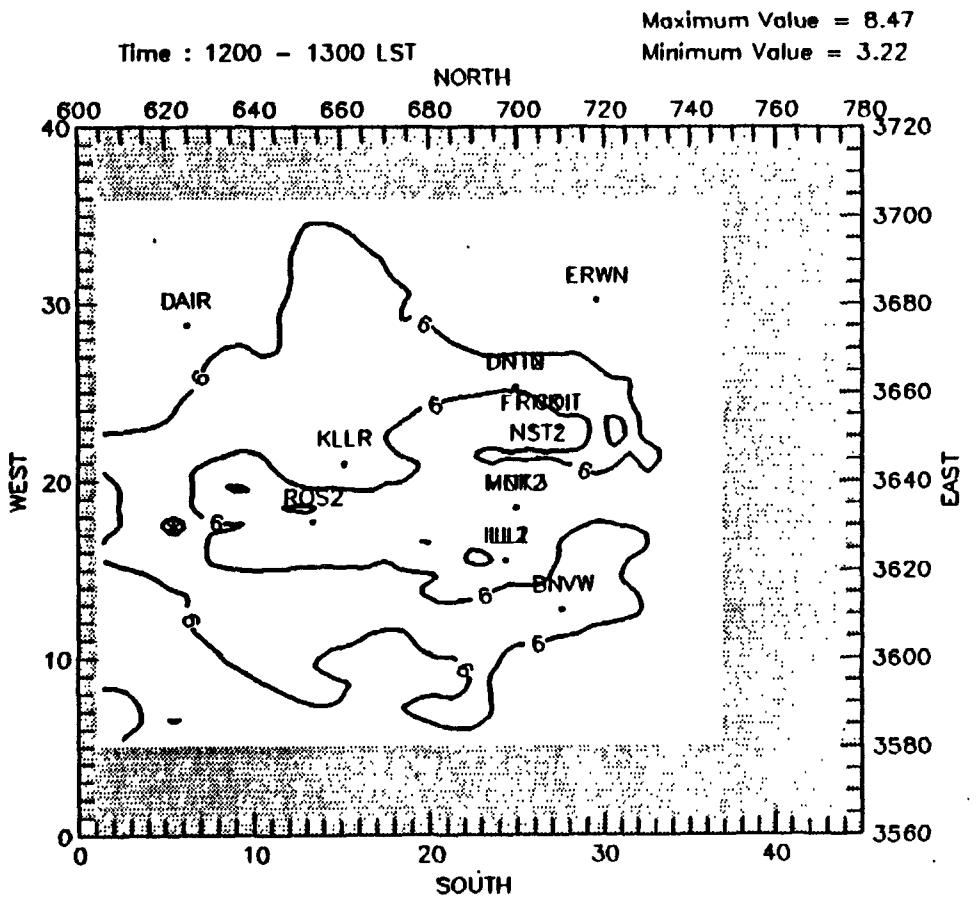

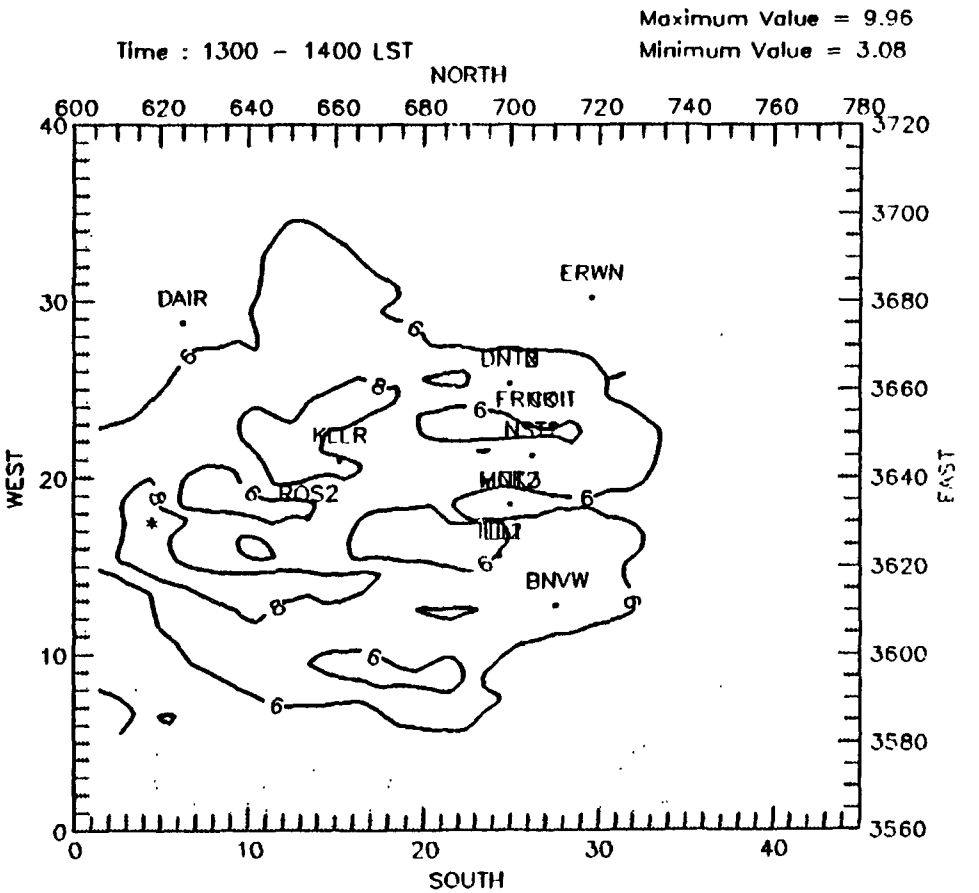

Ozone (pphm), 85 base emissions (Eval. run#2), August 30, 1985

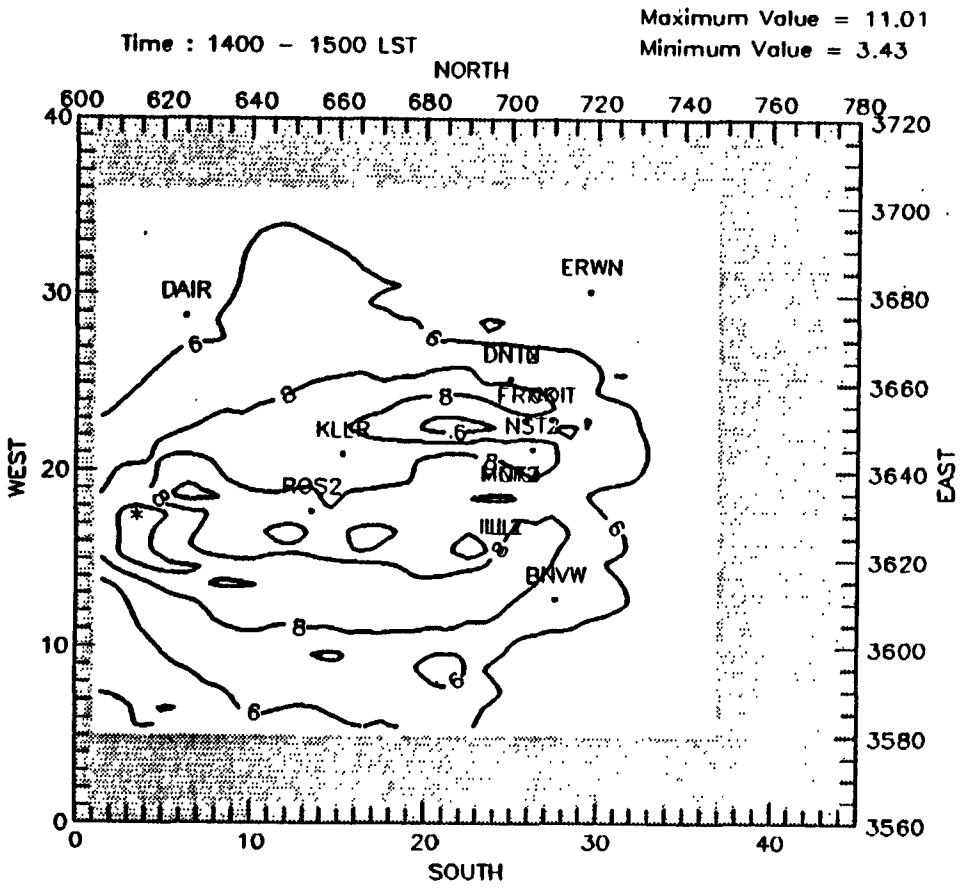

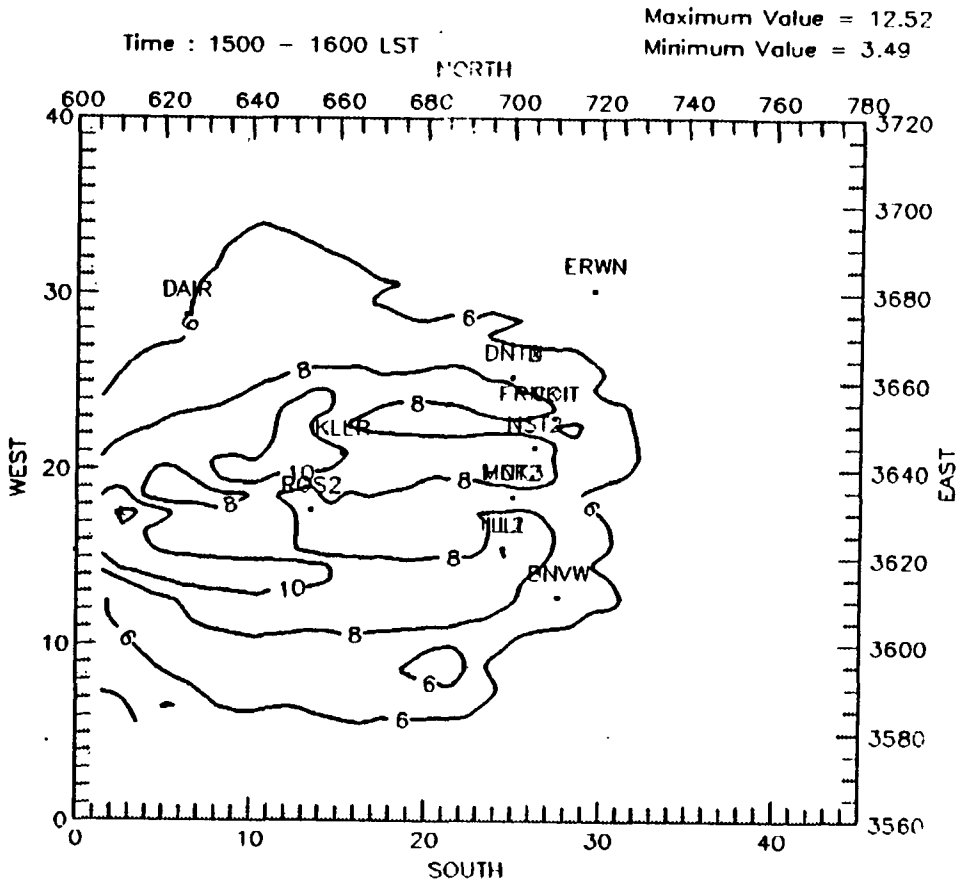

Ozone (pphm), 85 base emissions (Eval. run#2), August 30, 1985

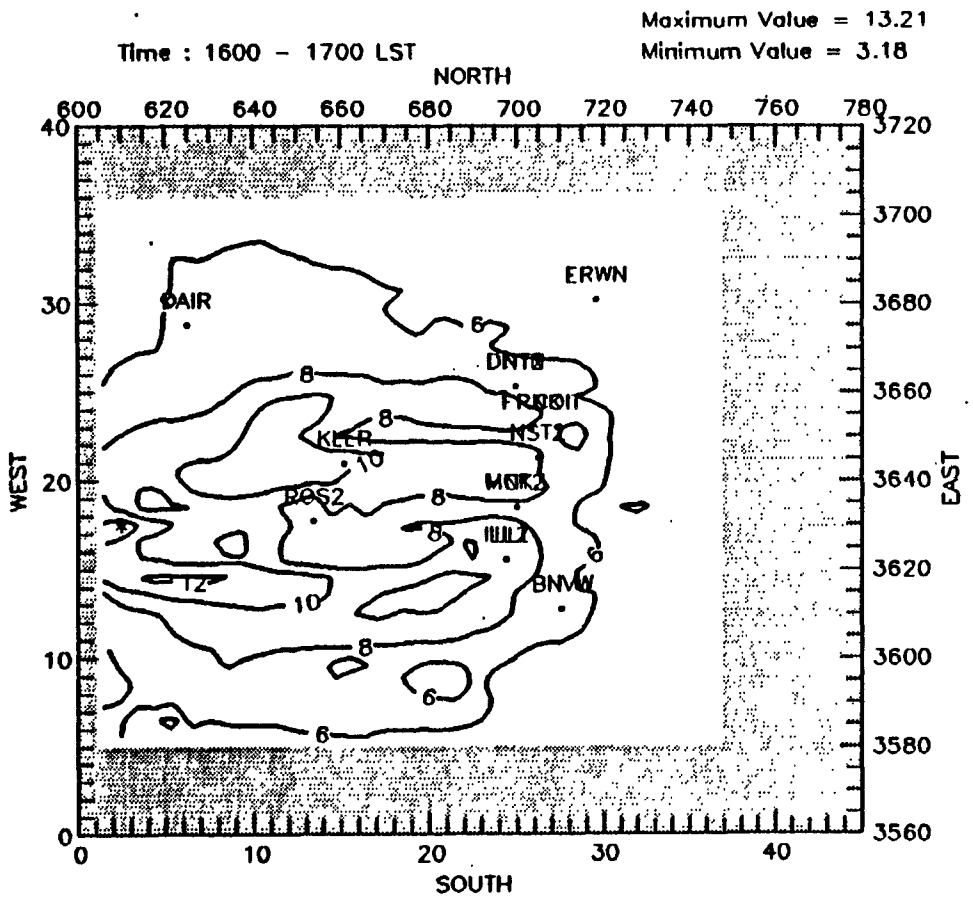

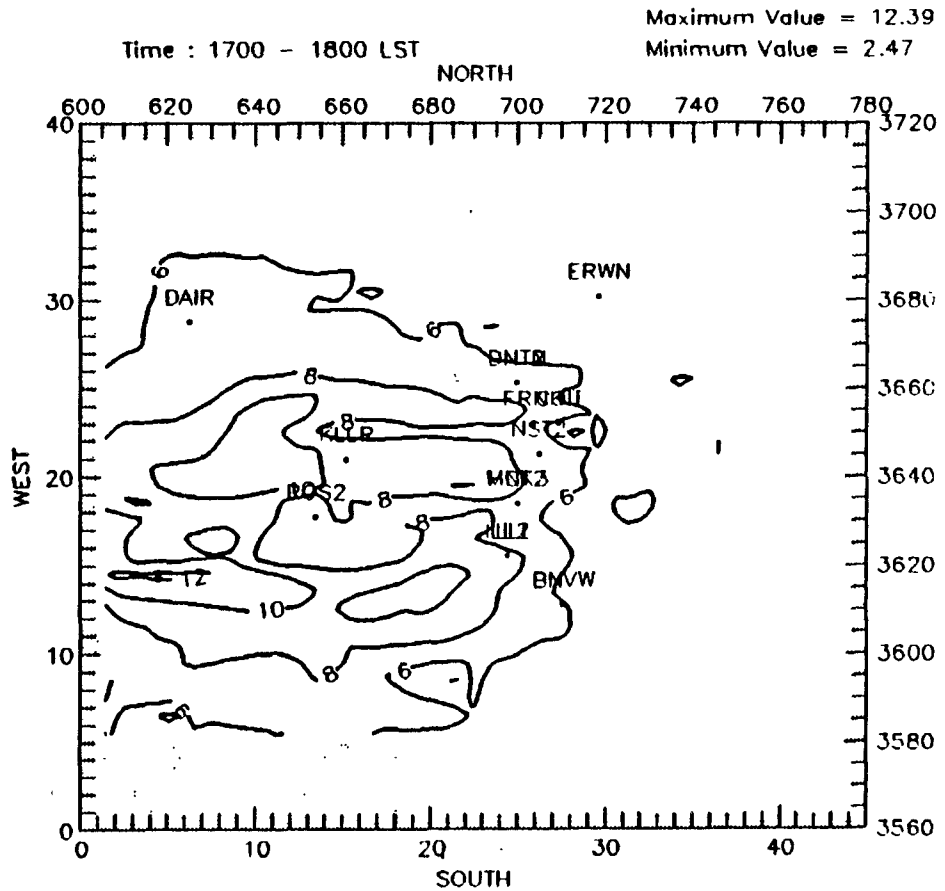

Ozone (pphm), 85 base emissions (Eval. run#2), August 30, 1985

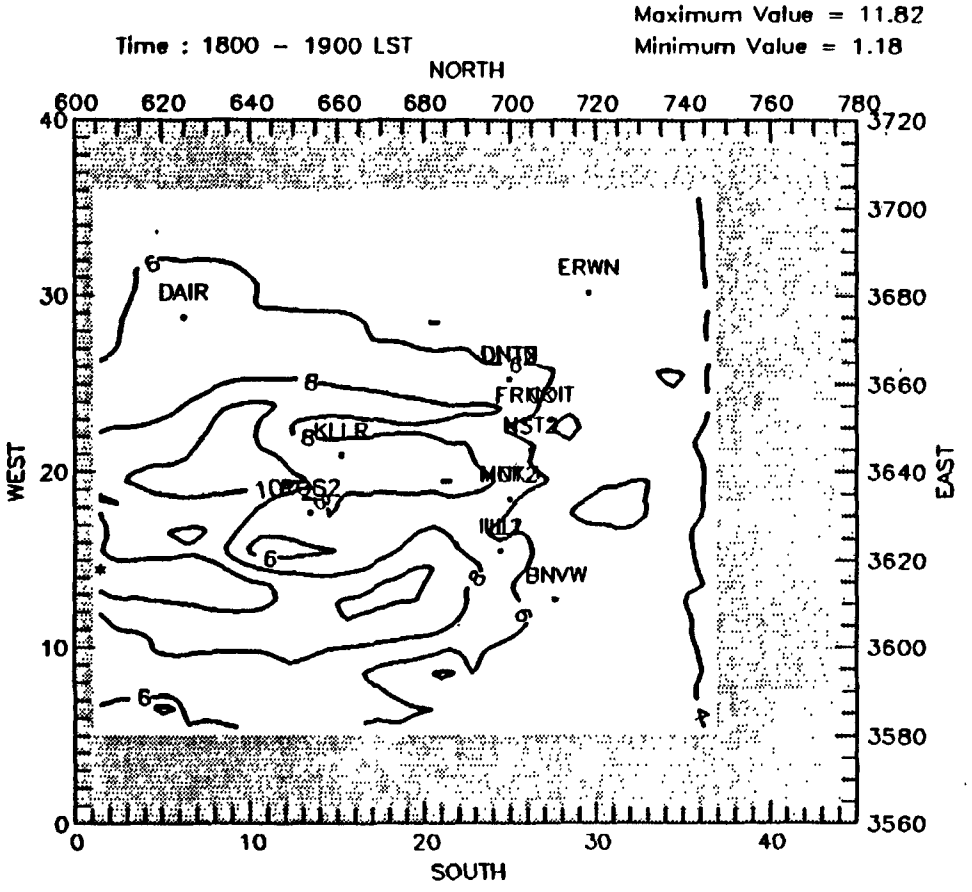

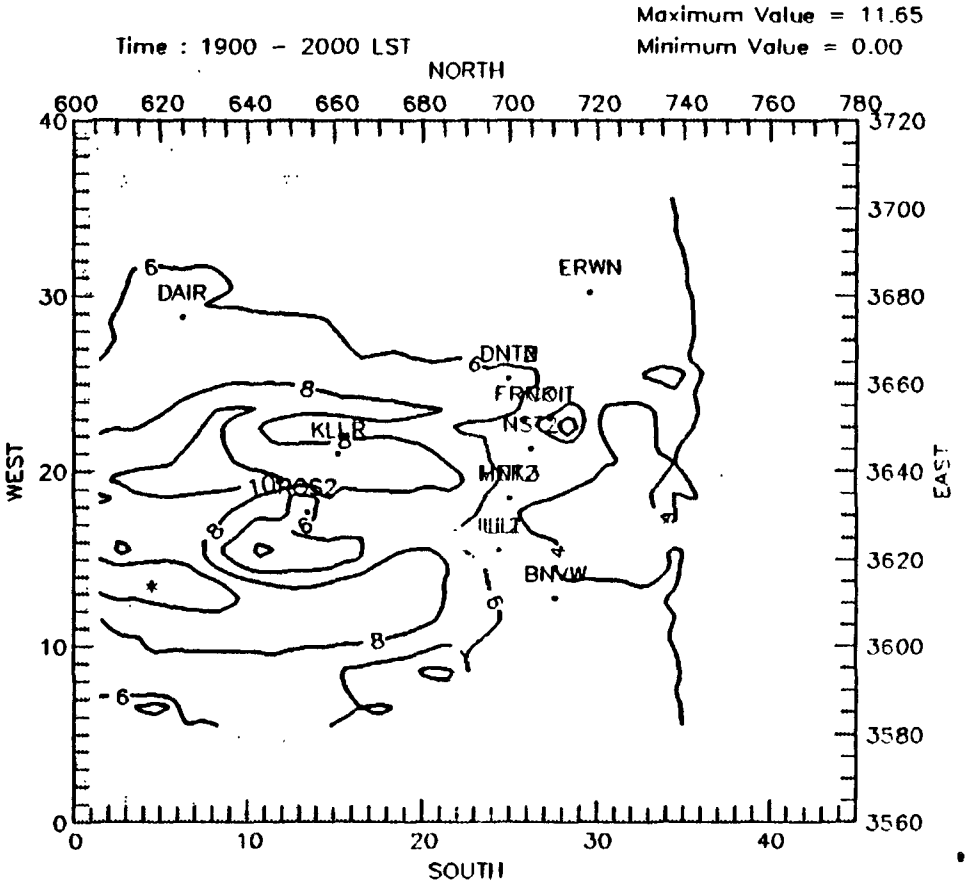

Ozone (pphm), 85 base emissions (Eval. run#2), August 30, 1985

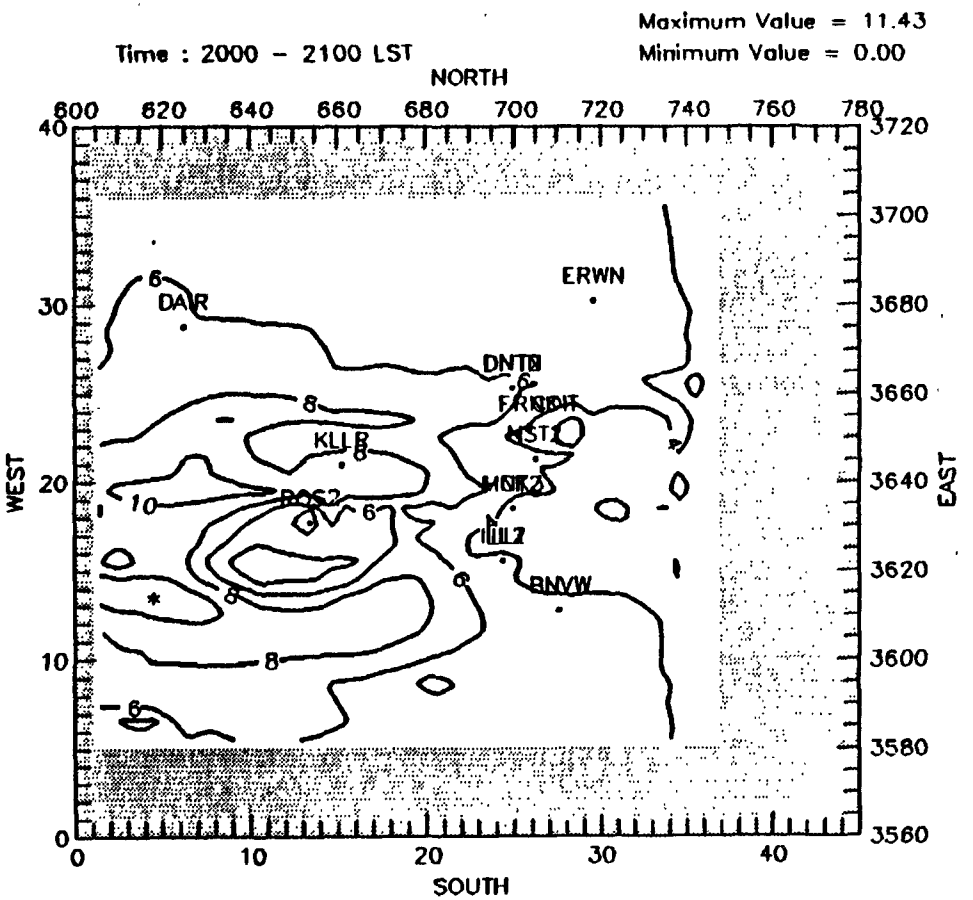

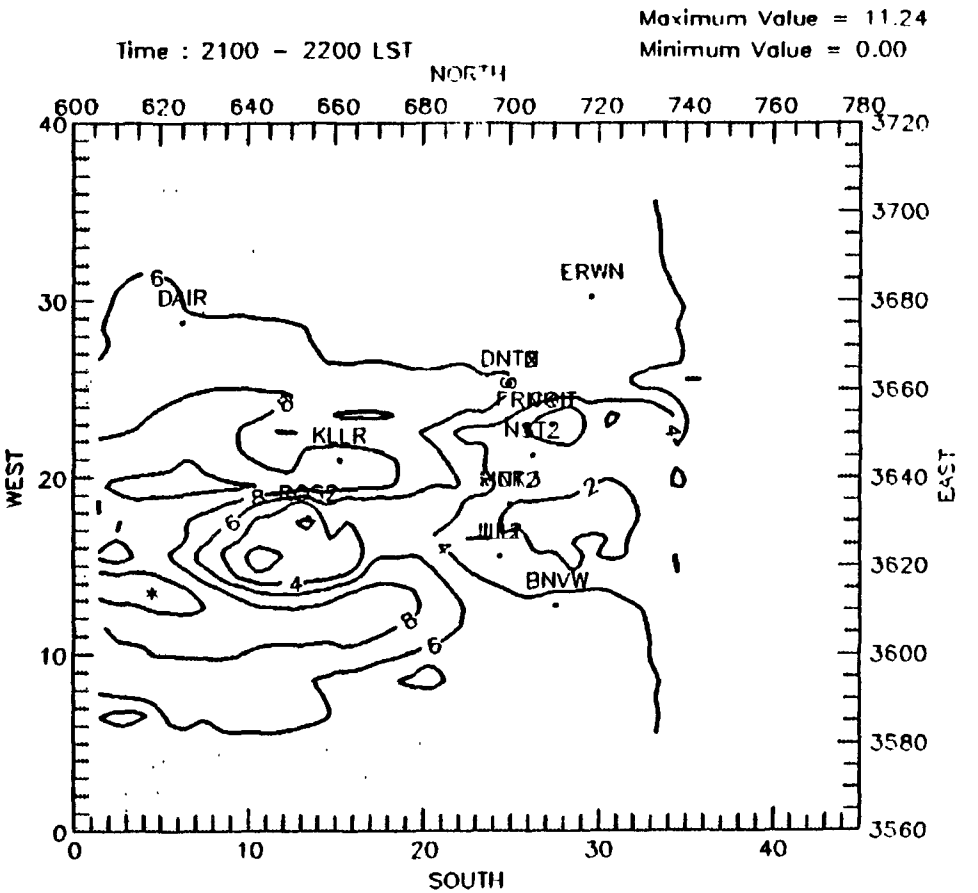

Ozone (pphm), 85 base emissions (Eval. run#2), August 30, 1985

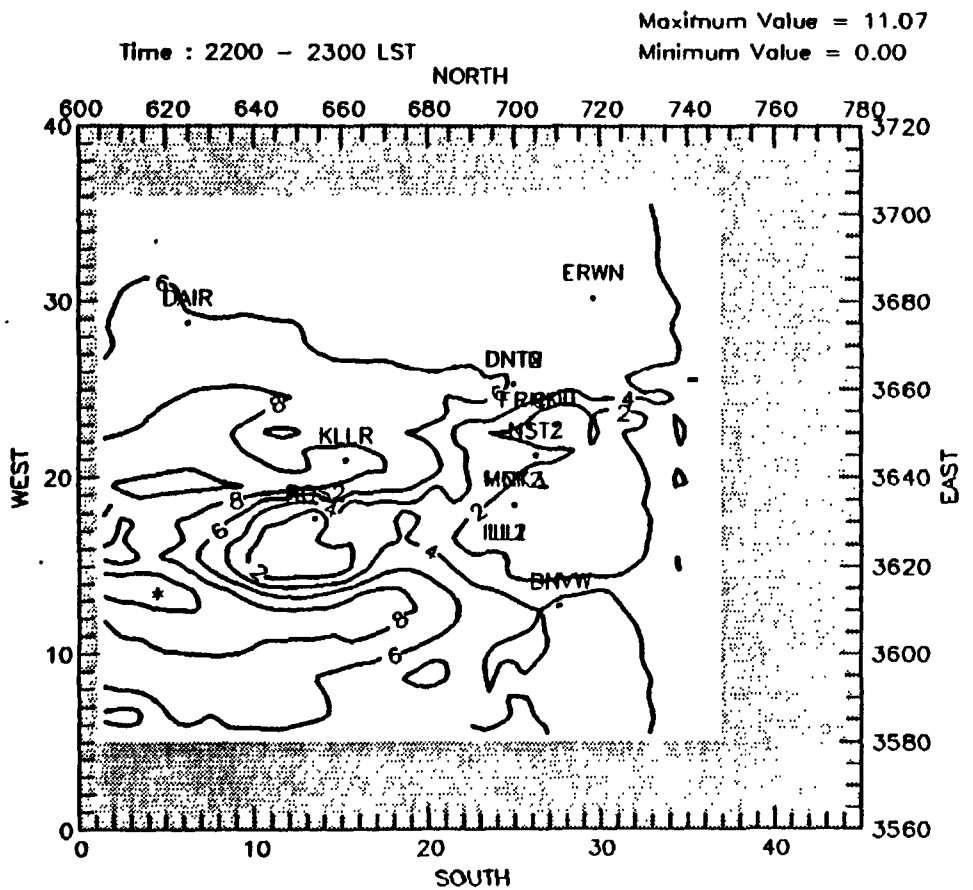

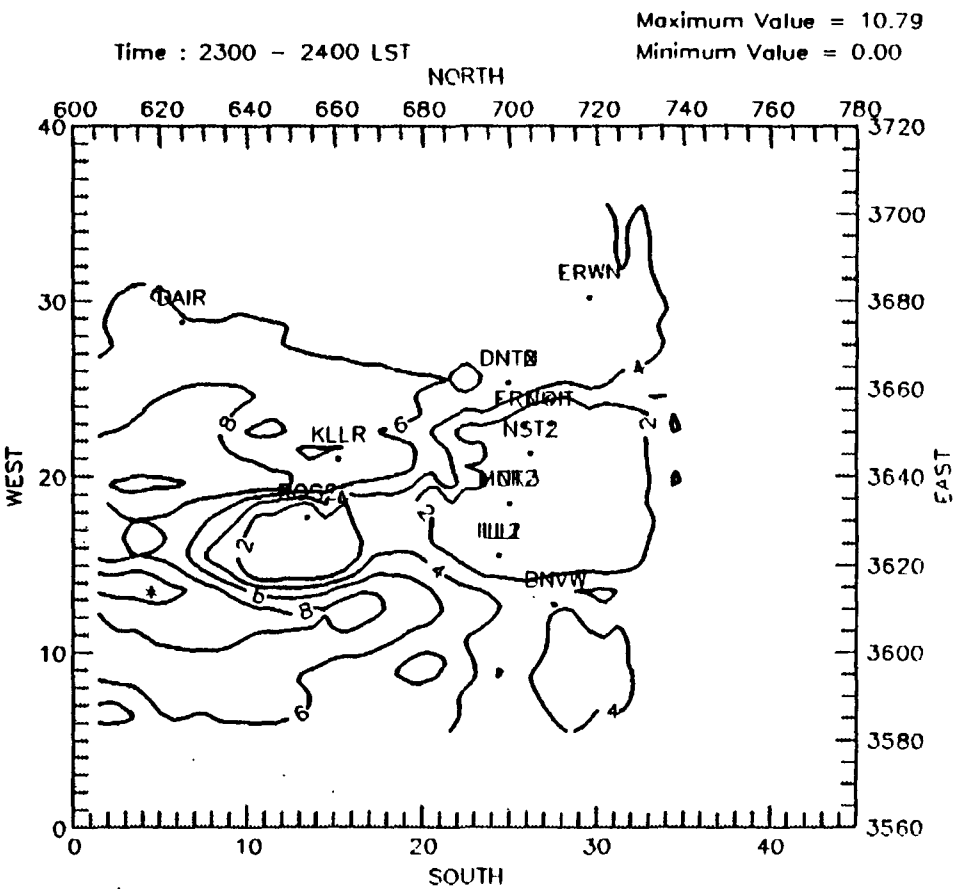

Ozone (pphm), 85 base emissions (Eval. run#2), August 30, 1985

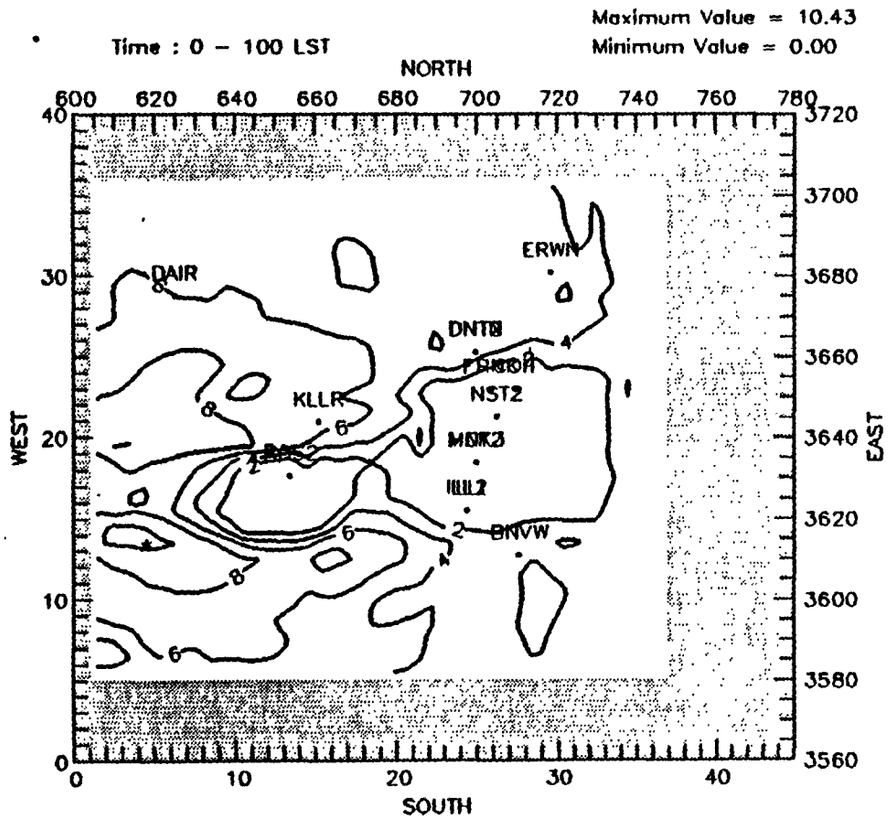

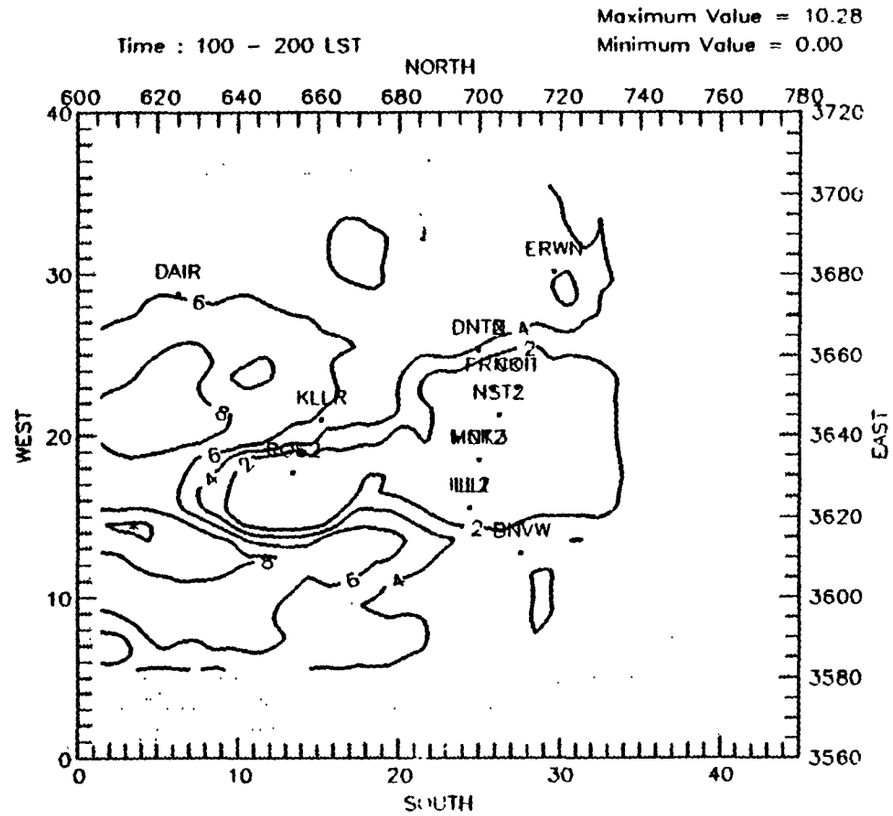

Ozone (pphm), 85 base emissions (Eval. run#2), August 31, 1985

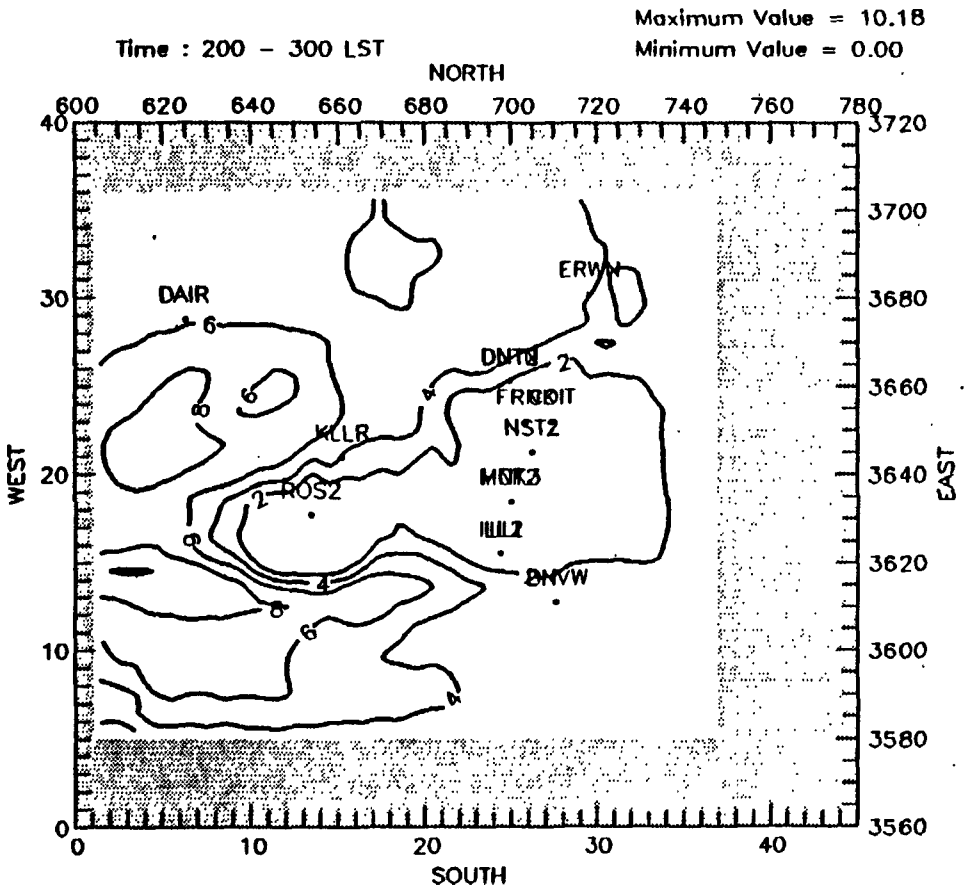

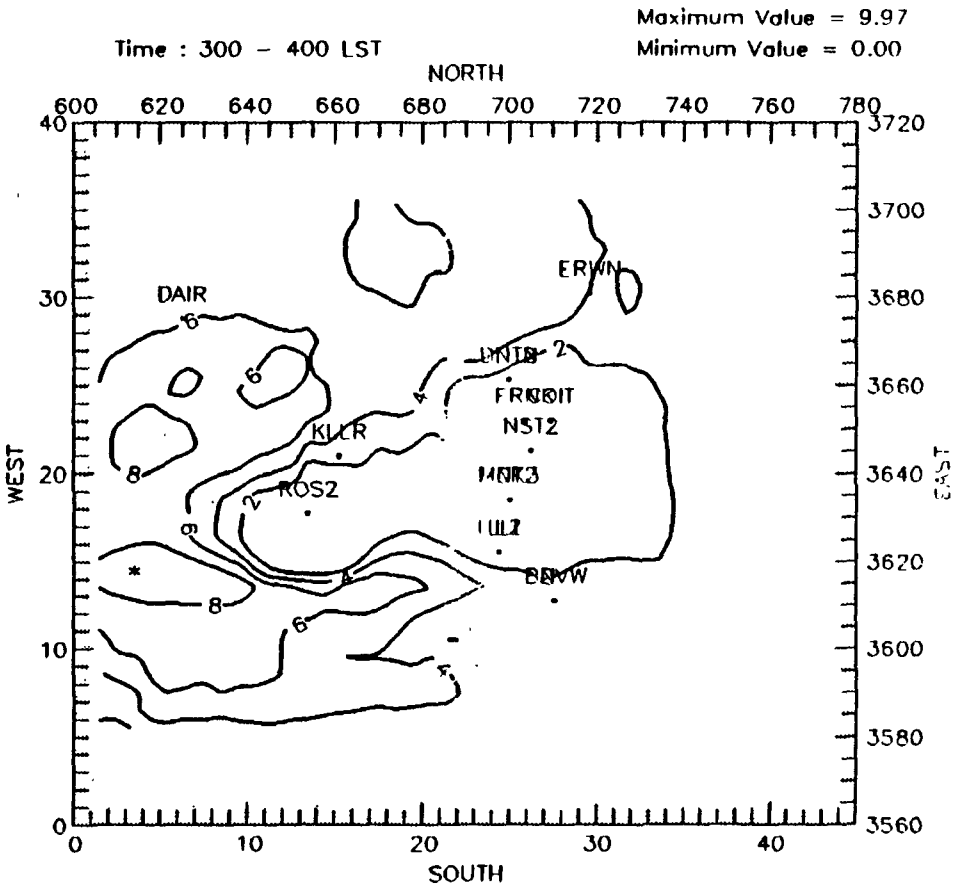

Ozone (pphm), 85 base emissions (Eval. run#2), August 31, 1985

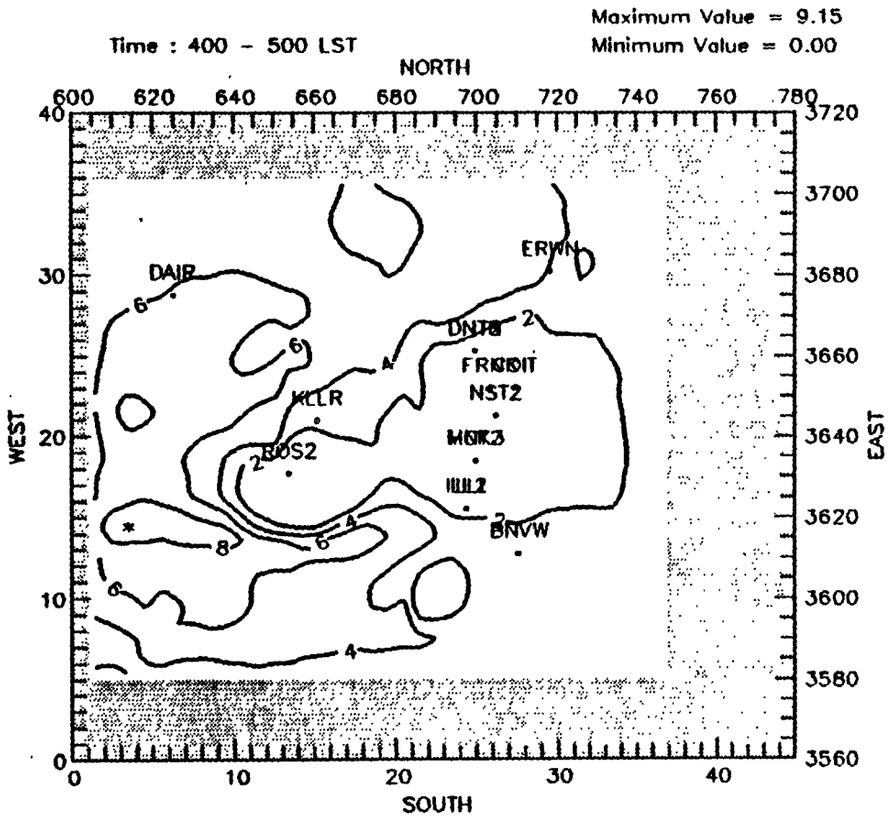

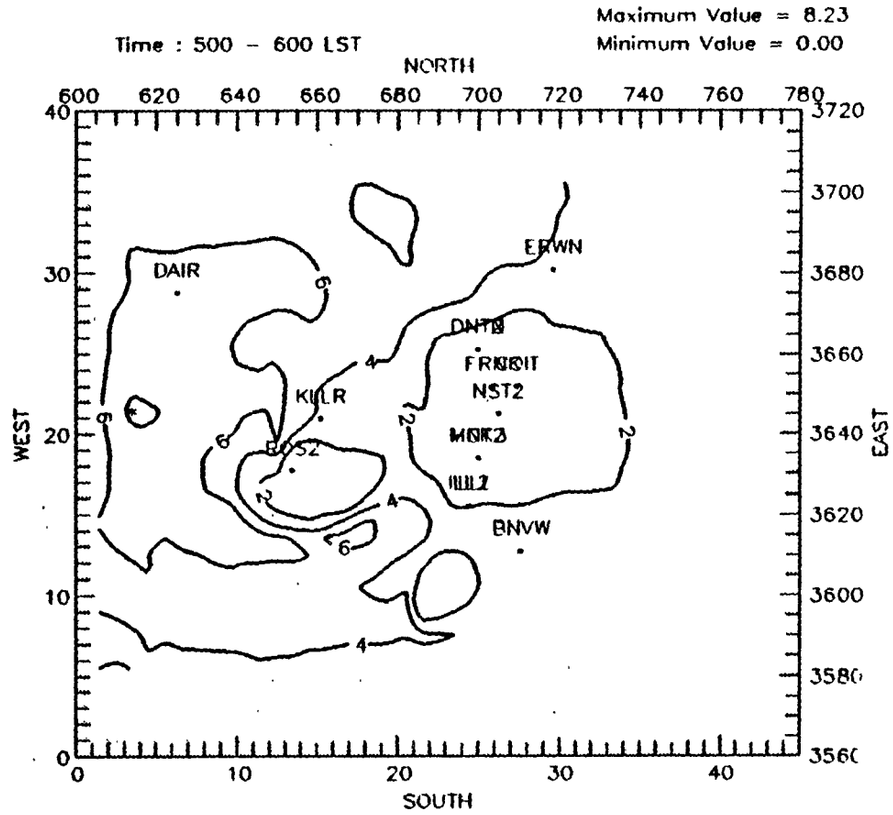

Ozone (pphm), 85 base emissions (Eval. run#2), August 31, 1985

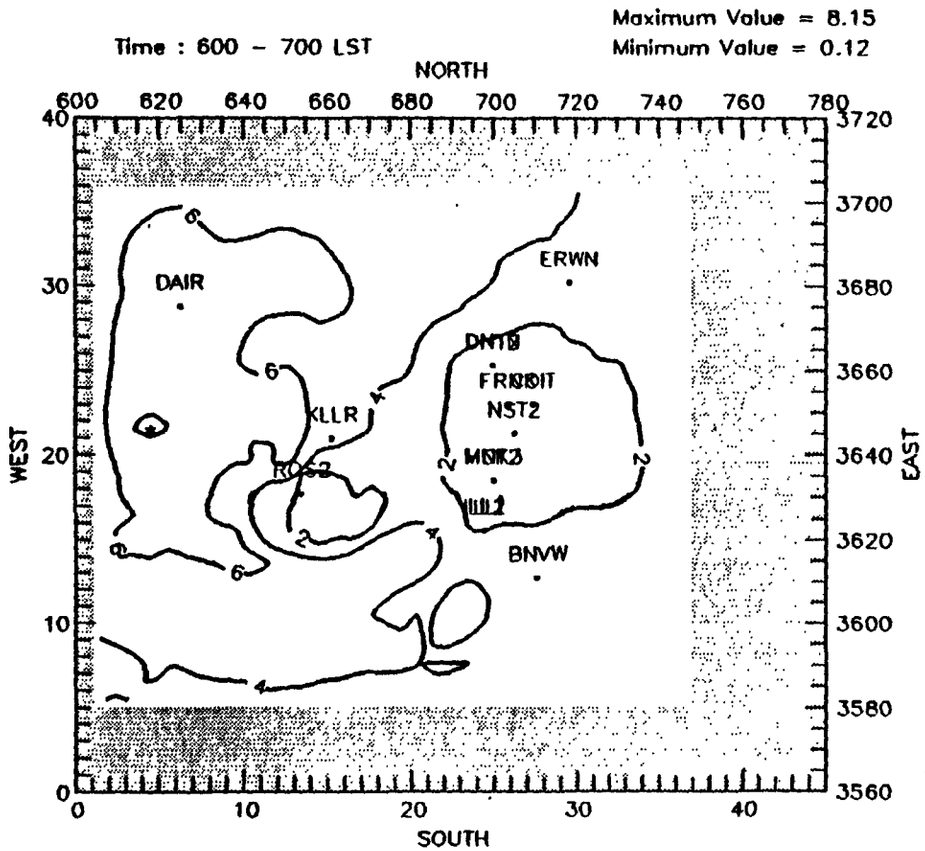

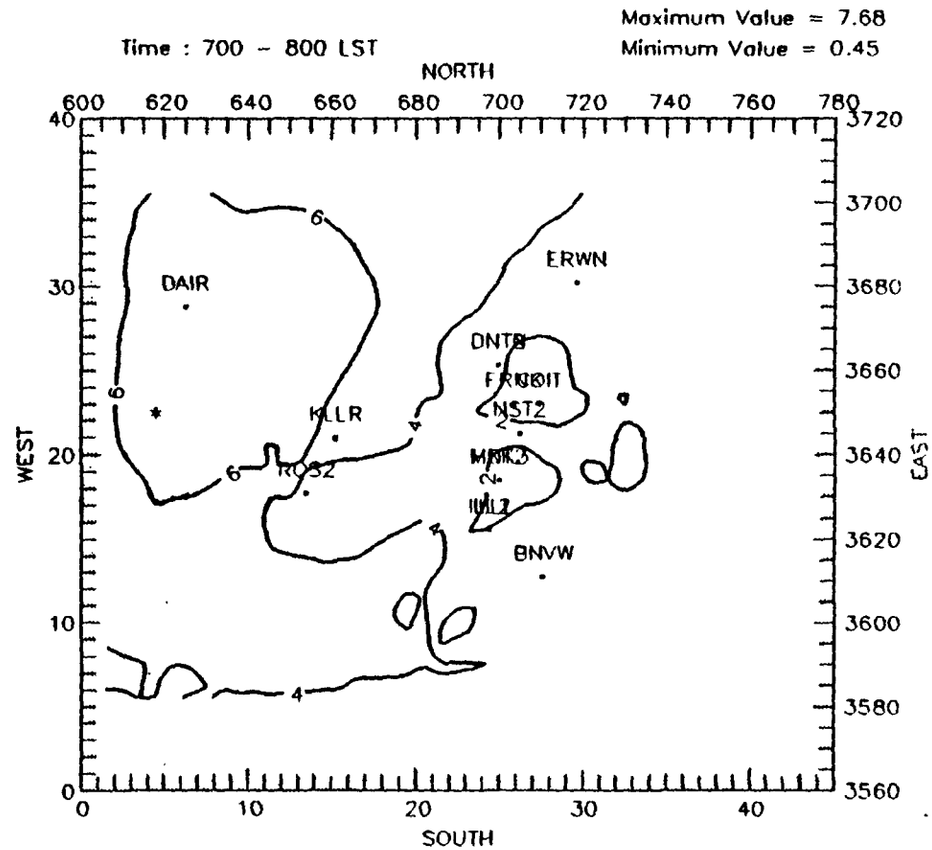

Ozone (pphm), 85 base emissions (Eval. run#2), August 31, 1985

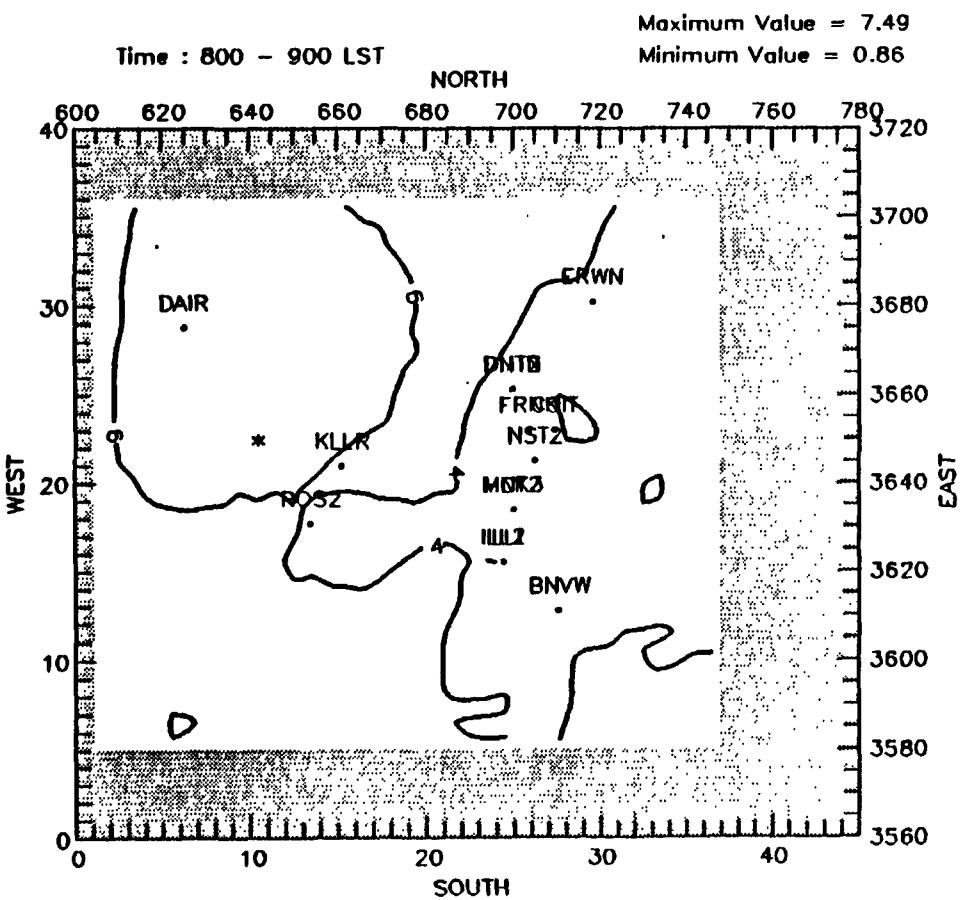

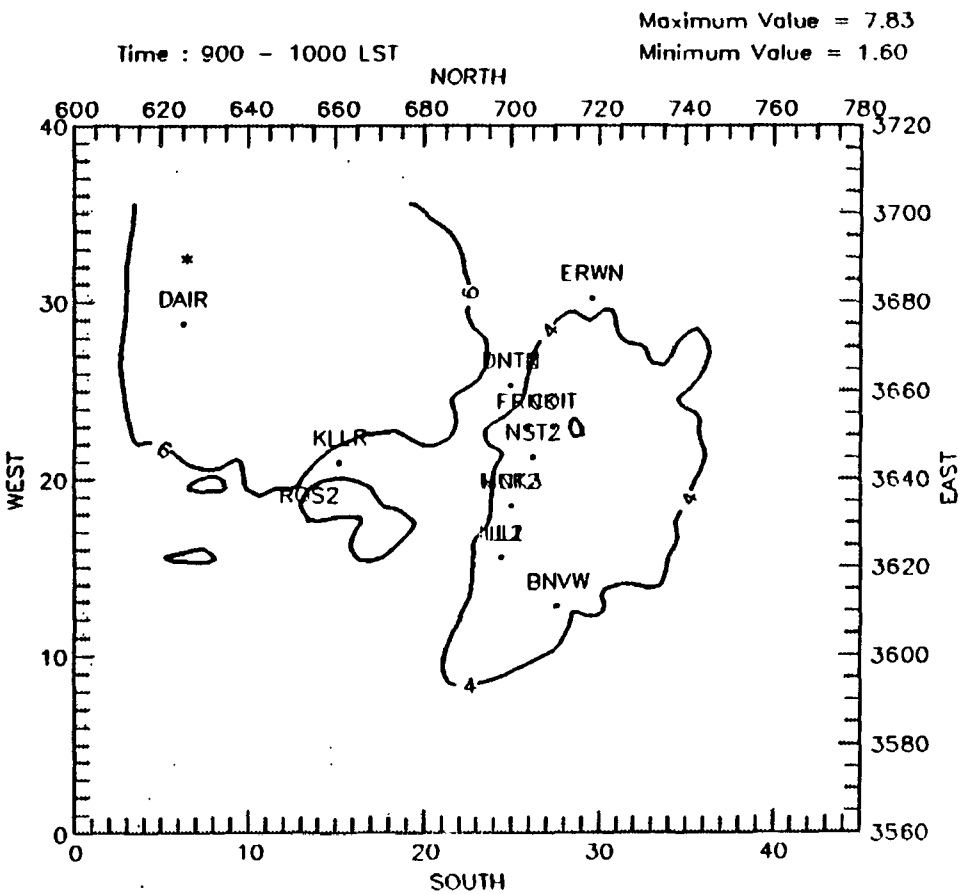

Ozone (pphm), 85 base emissions (Eval. run#2), August 31, 1985

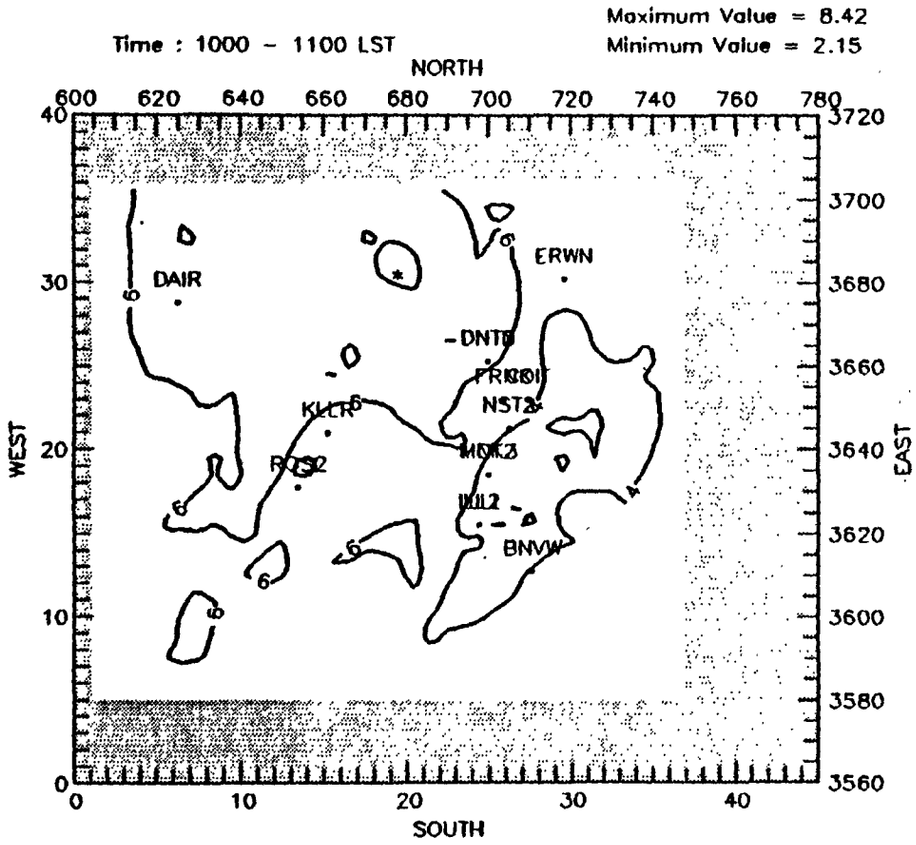

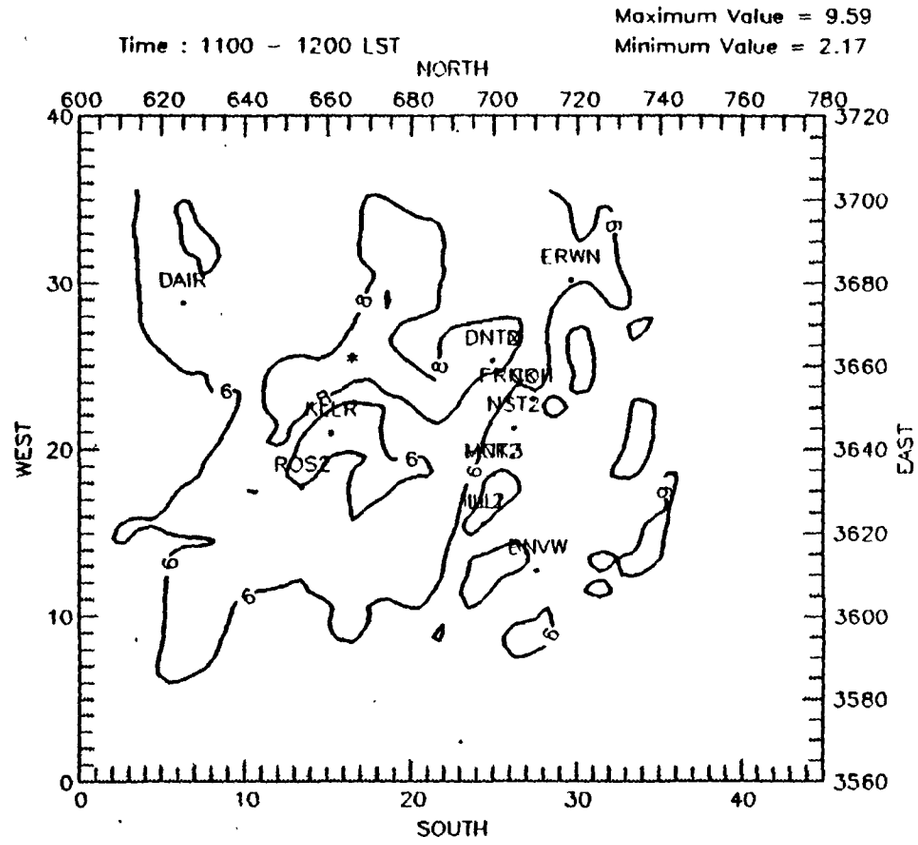

Ozone (pphm), 85 base emissions (Eval. run#2), August 31, 1985

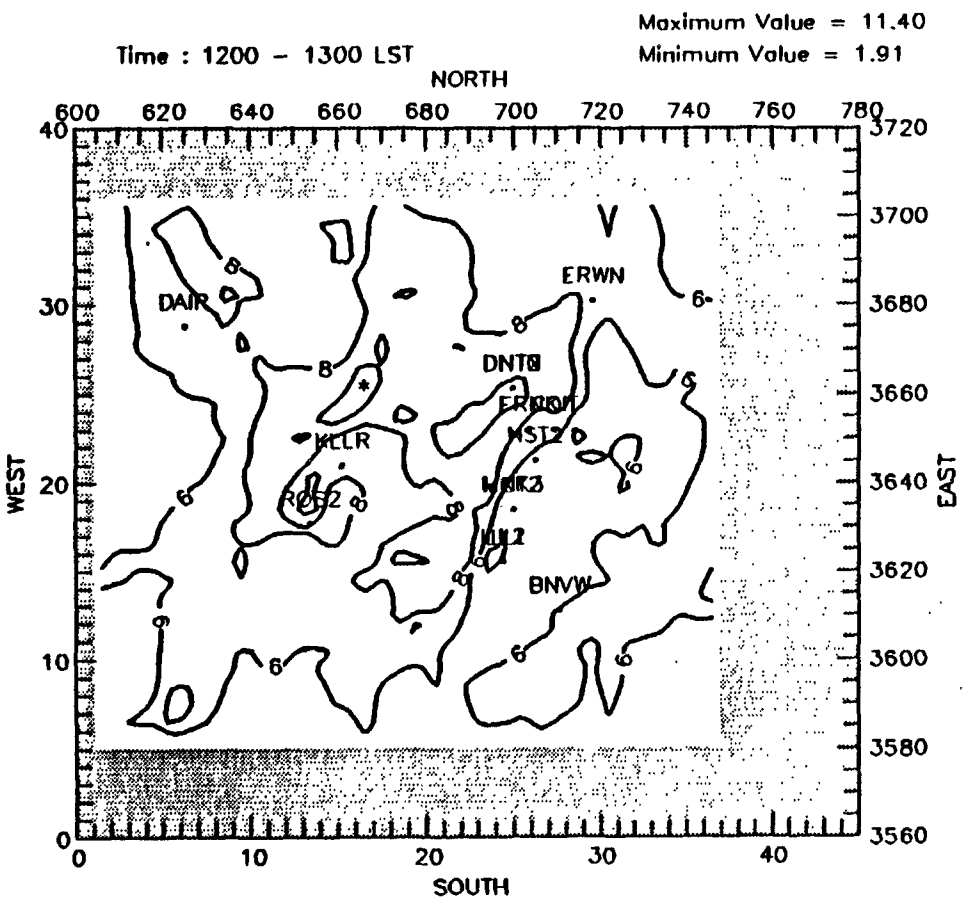

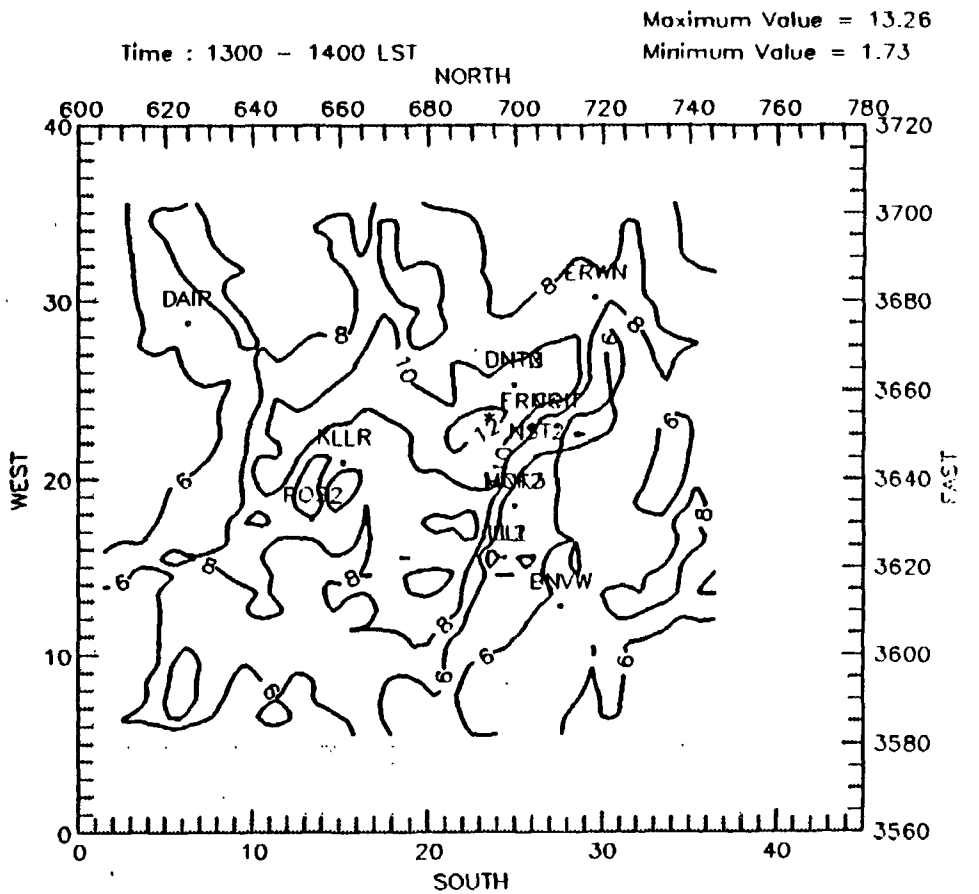

Ozone (pphm), 85 base emissions (Eval. run#2), August 31, 1985

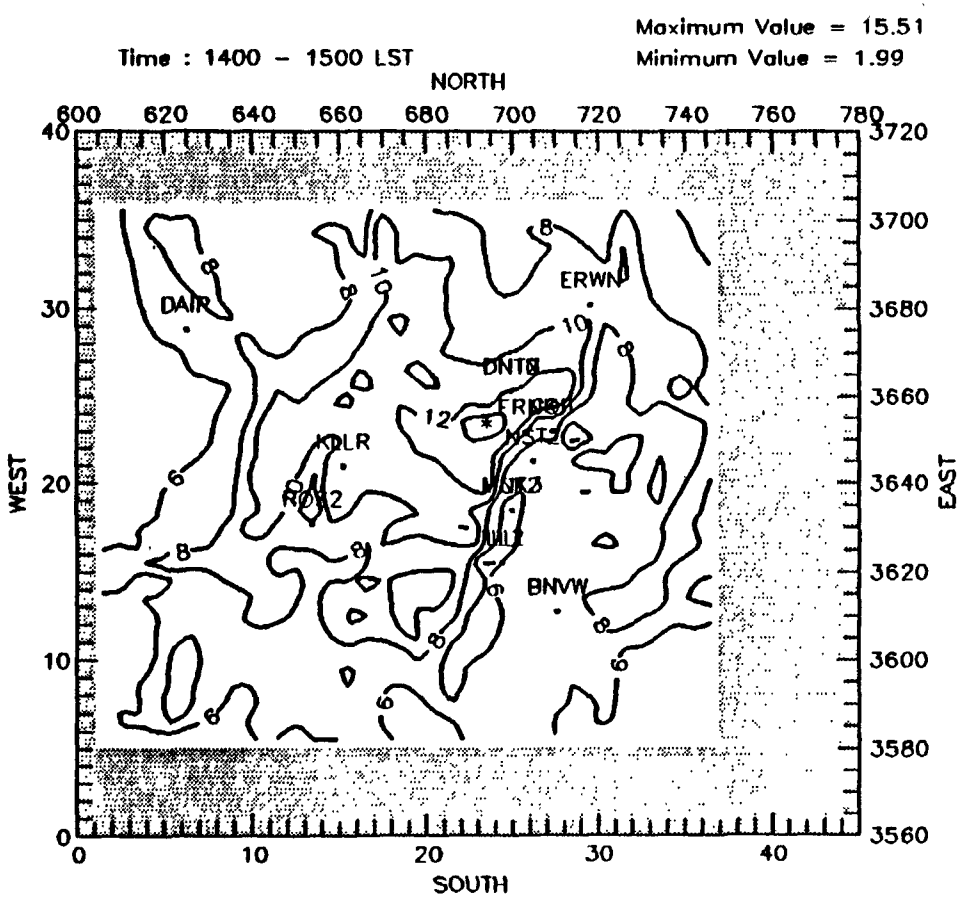

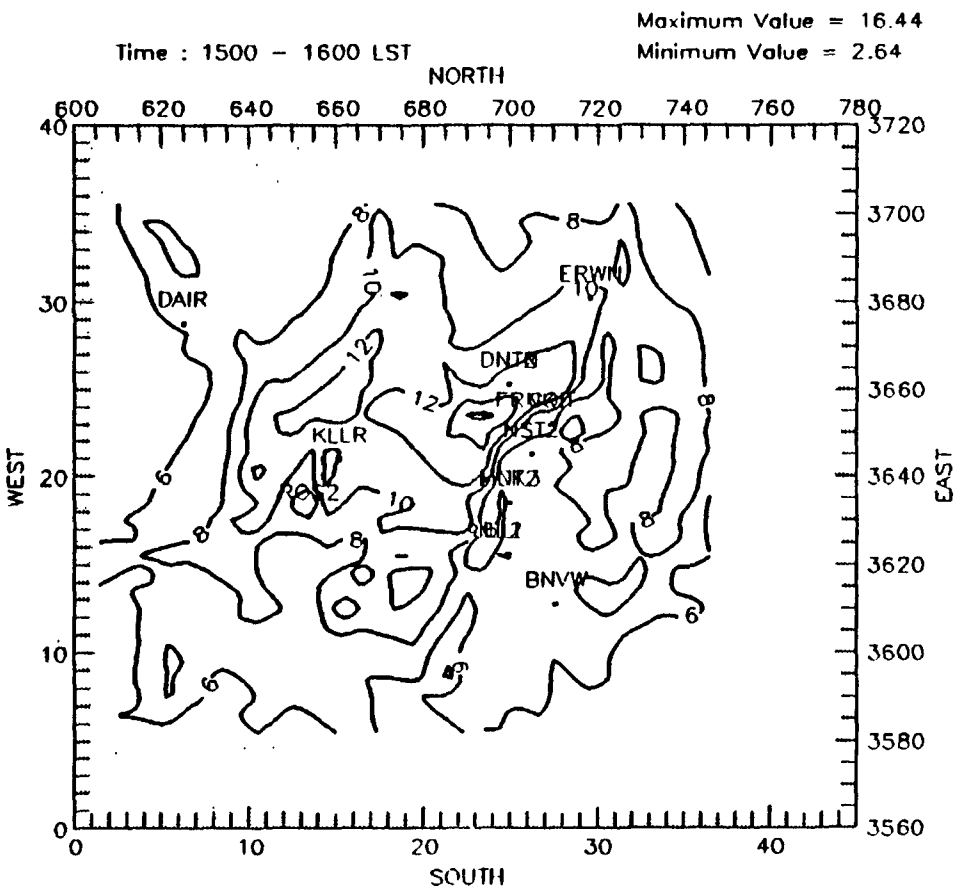

Ozone (pphm), 85 base emissions (Eval. run#2), August 31, 1985

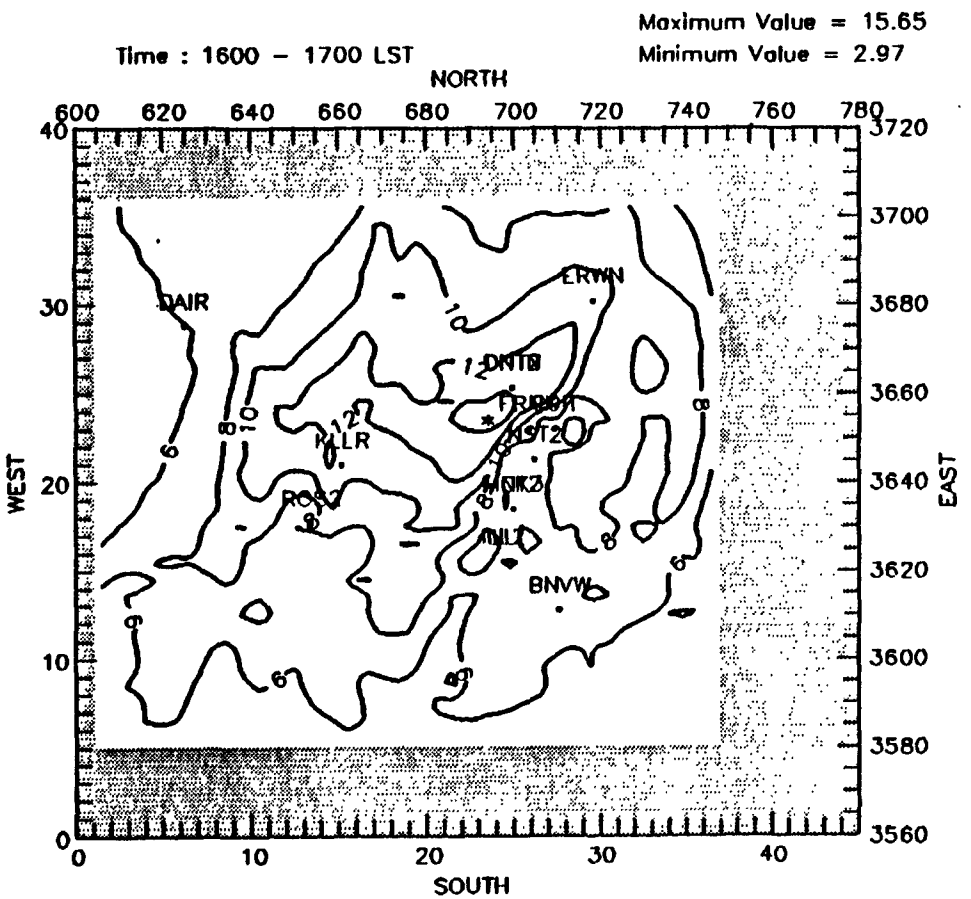

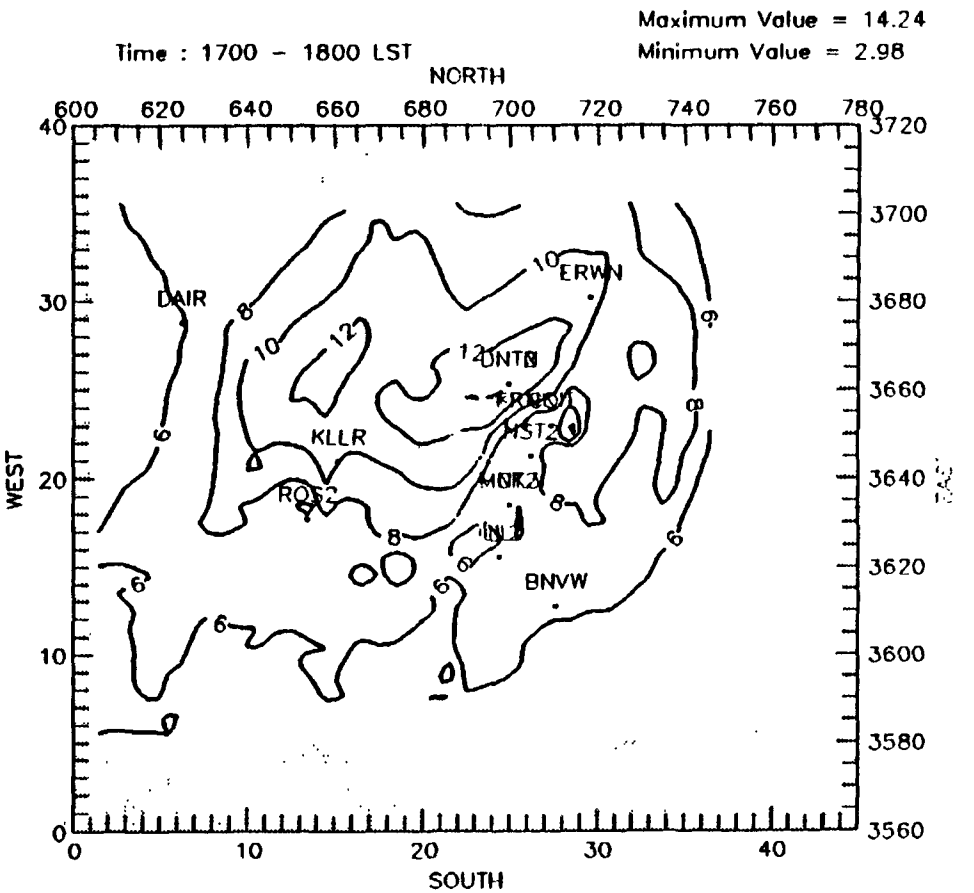

Ozone (pphm), 85 base emissions (Eval. run#2), August 31, 1985

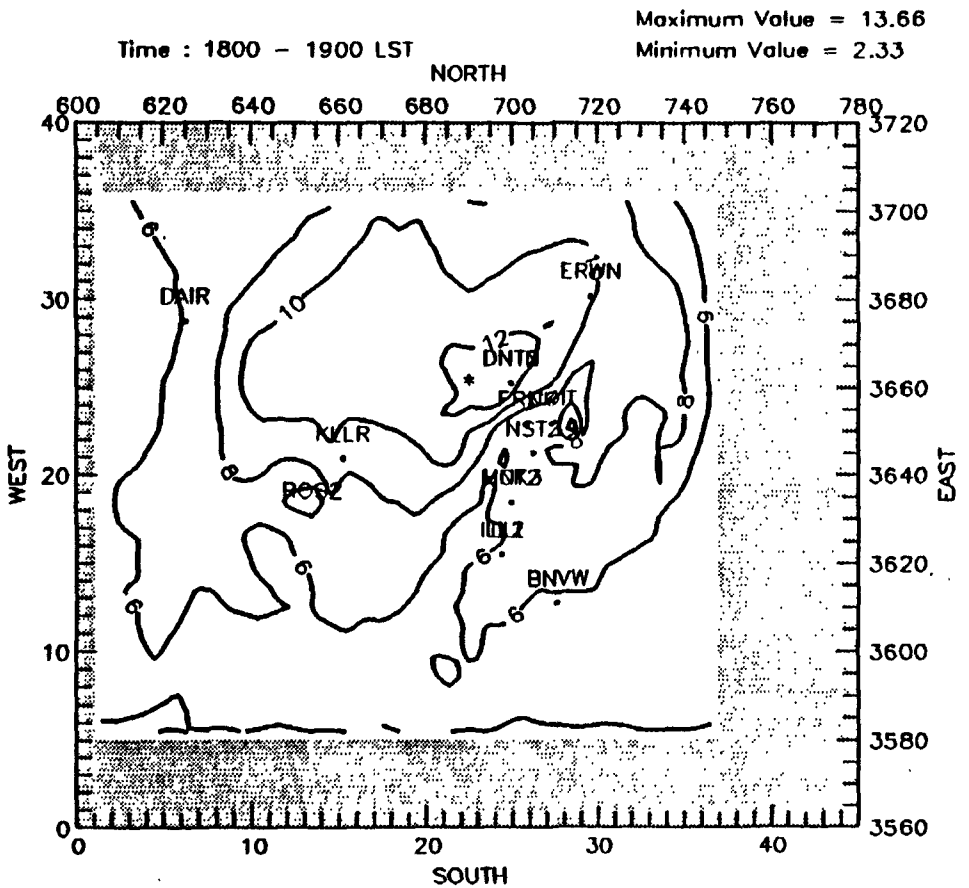

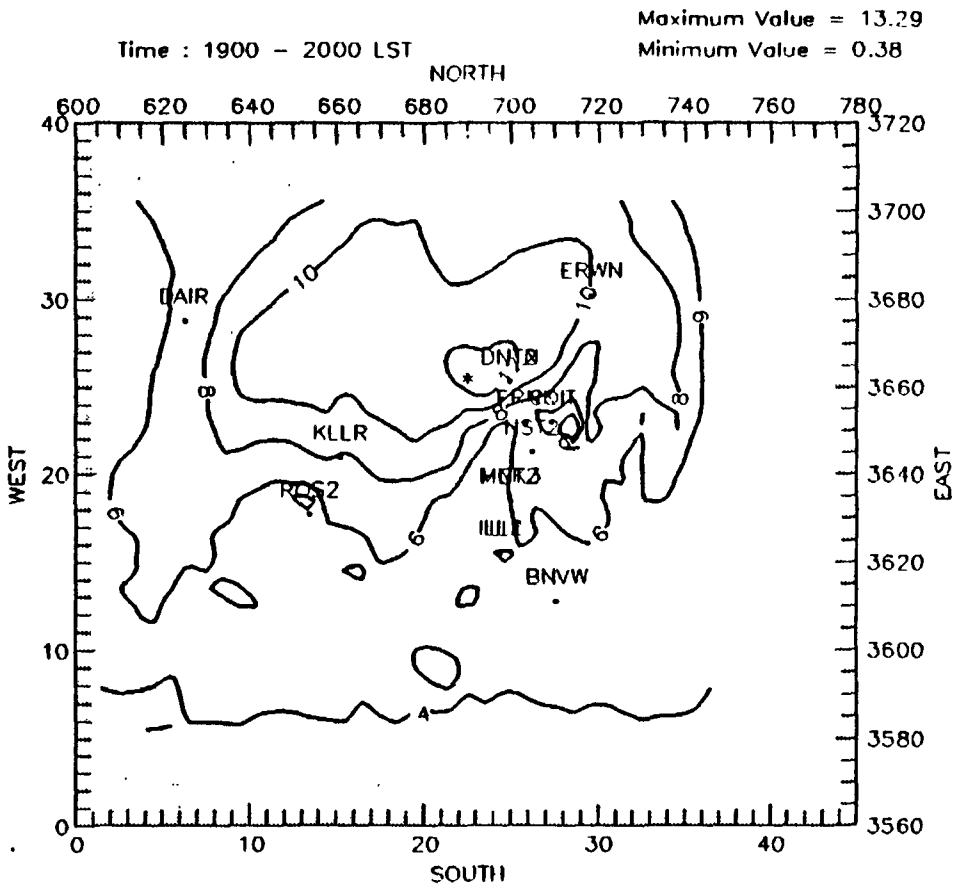

Ozone (pphm), 85 base emissions (Eval. run#2), August 31, 1985

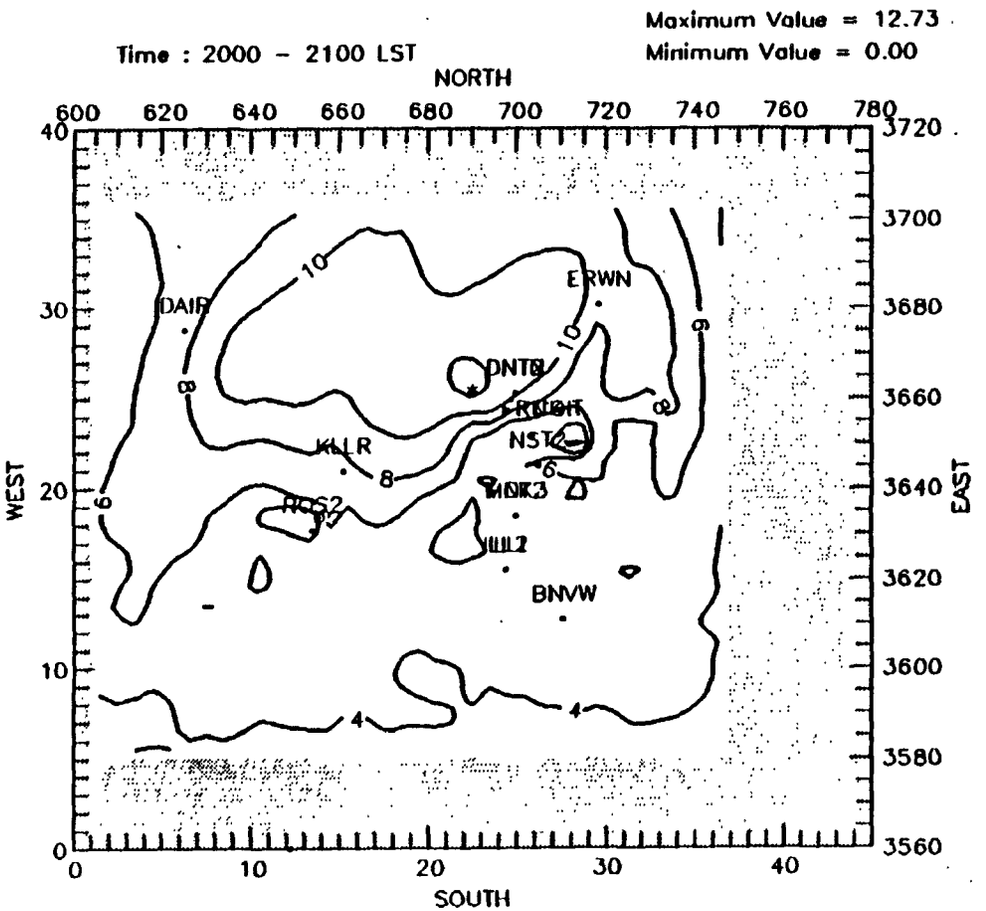

Ozone (pphm), 85 base emissions (Eval. run#2), August 31, 1985

TECHNICAL REPORT DATA
(Please read Instructions on the reverse before completing)

1. REPORT NO. EPA 450/4-90-006B	2.	3. RECIPIENT'S ACCESSION NO.
4. TITLE AND SUBTITLE URBAN AIRSHED MODEL STUDY OF FIVE CITIES - Demonstration of Low-Cost Application of the Model to the City of Atlanta and the Dallas-Fort Worth Metroplex Region		5. REPORT DATE April 1990
		6. PERFORMING ORGANIZATION CODE
7. AUTHOR(S) Ralph E. Morris, Thomas C. Myers, Edward L. Carr, Marianne C. Causley		8. PERFORMING ORGANIZATION REPORT NO.
9. PERFORMING ORGANIZATION NAME AND ADDRESS Systems Applications, Inc. 101 Lucas Valley Road San Rafael, CA 94903		10. PROGRAM ELEMENT NO.
		11. CONTRACT/GRANT NO.
12. SPONSORING AGENCY NAME AND ADDRESS U.S. Environmental Protection Agency Office of Air Quality Plannning and Standards Research Triangle Park, NC 27711		13. TYPE OF REPORT AND PERIOD COVERED
		14. SPONSORING AGENCY CODE

15. SUPPLEMENTARY NOTES

16. ABSTRACT

This document presents methodology for low-cost base case Urban Airshed model application to Atlanta and Dallas-Fort Worth.

17. KEY WORDS AND DOCUMENT ANALYSIS

DESCRIPTORS	b. IDENTIFIERS/OPEN ENDED TERMS	c. COSATI Field/Group
Ozone Urban Airshed Model Photochemistry		

18. DISTRIBUTION STATEMENT	19. SECURITY CLASS *(This Report)*	21. NO. OF PAGES 320
	20. SECURITY CLASS *(This page)*	22. PRICE

EPA Form 2220-1 (Rev. 4-77) PREVIOUS EDITION IS OBSOLETE